Resistance mechanisms to *Didymascella thujina* (Durand) Maire in *Thuja plicata* Donn ex D. Don, *Thuja standishii* (Gord.) Carrière and *Thuja standishii* × *plicata*

by

Juan Andres Aldana
B.Sc., Universidad Nacional de Colombia, 2003
M.Sc., Universidad de los Andes, 2007

A Dissertation Submitted in Partial Fulfillment of the
Requirements for the Degree of

DOCTOR OF PHILOSOPHY

in the Department of Biology

Resistance mechanisms to *Didymascella thujina* (Durand) Maire in *Thuja plicata* Donn ex D. Don, *Thuja standishii* (Gord.) Carrière and *Thuja standishii* × *plicata*

by

Juan Andres Aldana
B.Sc., Universidad Nacional de Colombia, 2003
M.Sc., Universidad de los Andes, 2007

Supervisory Committee

Dr. Barbara J. Hawkins, Co-Supervisor
(Department of Biology)

Dr. John H. Russell, Co-Supervisor
(Department of Biology)

Dr. C. Peter Constabel, Departmental Member
(Department of Biology)

Dr. Jim Mattsson, Departmental Member
(Department of Biology)

Dr. Olaf Niemann, Outside Member
(Department of Geography)

Supervisory Committee

Dr. Barbara J. Hawkins, Co-Supervisor
(Department of Biology)

Dr. John H. Russell, Co-Supervisor
(Department of Biology)

Dr. C. Peter Constabel, Departmental Member
(Department of Biology)

Dr. Jim Mattsson, Departmental Member
(Department of Biology)

Dr. Olaf Niemann, Outside Member
(Department of Geography)

ABSTRACT

Plants and microorganisms interact with each other constantly, with some interactions being mutually beneficial and others being detrimental to the plants. The features of the organisms involved in such interactions will determine the characteristics of individual pathosystems. Plants respond readily to pathogen attacks, regardless of the pathosystem; furthermore, variation in the resistance to pathogens within species is common and well documented in many plant species. The variability in pathogen resistance is at the core of genetic improvement programs for disease resistance. True resistance to pathogens in plants is a genetically determined and complex trait that can involve both constitutive and induced mechanisms at different levels of organization. The complexity of this phenomenon makes the study of compatible plant -

pathogen interactions challenging, and typically, disease resistance studies focus on specific aspects of a pathosystem, such as field resistance, anatomical or physiological features of resistant plants, or molecular mechanisms of resistance.

The *Thuja* sp. - *Didymascella thujina* (E.J. Durand) Maire interaction is an important pathosystem in western North America, which has been studied for more than five decades. Western redcedar (*Thuja plicata* Donn ex D. Don) is very susceptible to cedar leaf blight (*D. thujina*), a biotroph that affects the tree at all stages, although seedlings are the most sensitive to the pathogen. The characteristics of the *Thuja* sp. - *D. thujina* interaction, the wealth of information on the pathosystem and the excellent *Thuja* sp. genetic resources available from the British Columbia Ministry of Forests, Lands, Natural Resource Operations and Rural Development make this interaction an ideal system to advance the study of disease resistance mechanisms in conifers. This Doctoral project presents a comprehensive investigation of the constitutive and induced resistance mechanisms against *D. thujina* in *T. plicata*, *Thuja standishii* (Gord.) Carrière and a *Thuja standishii* × *plicata* hybrid at the phenotypic and gene expression levels, undertaken with the objective of exploring the resistance mechanisms against the biotroph in these conifers. The project also aimed to establish base knowledge for the future development of markers for marker-assisted breeding of *T. plicata*.

The investigations included a combination of histological, chemical and next generation sequencing (NGS) methodologies. NGS data were analyzed, in addition to the traditional clustering analyses, with cutting edge machine learning methods, including grade of membership analysis, dynamic topic modelling and stability selection analysis. The studies were progressively more controlled to narrow the focus on the resistance mechanisms to *D. thujina* in *Thuja* sp. Histological characteristics related to *D. thujina* resistance in *Thuja* sp. were studied first, along with the relationship between climate of origin and disease resistance. The virulence of *D. thujina* was also documented early in this project. Chemical and gene expression constitutive and induced responses to *D. thujina* infection in *T. plicata* seedlings were studied next. *T. plicata* clonal lines were then comprehensively studied to shed light on the mechanisms behind known physiologically determined resistance. A holistic investigation of the resistance mechanisms to *D. thujina* in *T. standishii*, *T. plicata* and a *T. standishii* × *plicata* hybrid explored the possibility of a gene-for-gene resistance

model.

Thirty-five *T. plicata* families were screened during the four field seasons carried out between 2012 and 2015, totalling more than 1,400 seedlings scored for *D. thujina* severity. Thirteen of those families were used in the five studies performed during the program, along with two *T. plicata* seedling lines self-pollinated for five generations and three *T. plicata* clonal lines. One *T. standishii* clonal line, and one *T. standishii* × *plicata* clone were also investigated during the program. A total of 16 histological and anatomical characteristics were studied in more than 750 samples, and more than 270 foliar samples were analyzed for 60 chemical and nutritional compounds. Almost one million transcriptomic sequences in four individually assembled reference transcriptomes were examined during the program.

The results of the project support the variability in the resistance to *D. thujina* in *T. plicata*, as well as the higher resistance to the pathogen in plants originating from cooler and wetter environments. The data collected also depicted the existence of age-related resistance in *T. plicata*, and confirmed the full resistance to the disease in *T. standishii*. Western redcedar plants resistant and susceptible to *D. thujina* showed constitutive differences at the phenotypic and gene expression levels. Resistant *T. plicata* seedlings had thicker cuticles, constitutively higher concentrations of sabinene, α-thujene, and higher levels of expression of NBS-LRR disease resistance proteins. Resistant clones of *T. plicata* and *T. standishii* had higher expression levels of bark storage proteins and of dirigent proteins. Plants from all ages, species and resistance classes studied that were infected with *D. thujina* showed the accumulation of aluminum in the foliage, and increased levels of sequences involved in cell wall reinforcement. Additional responses to *D. thujina* infection in *T. plicata* seedlings included the downregulation of some secondary metabolic pathways, whereas pathogenesis-related proteins were upregulated in clonal lines of *T. plicata*. The comprehensive approach used here to study the *Thuja* sp. - *D. thujina* pathosystem could be applied to other compatible plant-pathogen interactions.

Contents

List of Tables

List of Figures

ABBREVIATIONS

7OMT	7-O-Methyltransferase
AMOC	At most one change
ANOVA	Analysis of variance
ARR	Age-related resistance
avr gene	Pathogen's avirulence gene
BC	British Columbia
BIA	Benzylisoquinoline alkaloid
BSP	Bark storage protein
BXL	β-D-xylosidase
CC	Controlled conditions experiment (Chapter 4)
CG	Cyanogenic glycoside
CHS	Chalcone synthase
CLB	Cedar leaf blight (i.e. *Didymascella thujina* (Durand) Maire)
CRK	Cysteine-rich receptor-like protein kinase
CSP41B	Chloroplast stem-loop binding protein of 41 kDa b
CTAB	Cetyltrimethylammonium bromide
DE	Differential expression
DEPC	Diethyl pyrocarbonate
DHN	Dehydrin
DHQD/SD	Dehydroquinate dehydratase/shikimate dehydrogenase
DIR	Dirigent protein
DIR4	Dirigent protein 4
DOXP	1-Deoxy-D-xylulose-5-phosphate
dpd	Days post deployment
dpi	Days post infection
DRR206	Disease resistance response protein 206
DTM	Dynamic topic modelling
EDR2	Protein enhanced disease resistance 2
eIF2	Eukaryotic translation initiation factor 2 γ subunit
ELIP1	Early light-induced protein 1
FPKM	Fragments per kilobase of transcript per million mapped
GAPDH	Glyceraldehyde-3-phosphate dehydrogenase
Gbp	Giga base pairs (i.e. $\times 10^9$ base pairs)
GMT	Glucomannan 4-β-mannosyltransferase

GoM	Grade of membership analysis
GWAS	Genome-wide association study
HPC	High performance computing
HR	Hypersensitive response
HY5	Long hypocotyl 5
IP_3	Inositol-1,4,5-trisphosphate
ITS2	Internal transcribed spacer 2
JA	Jasmonic acid
LEA	Late embryogenesis abundant protein
LRR	Leucine-rich repeat
LSD	Least significant difference
MIPS	*myo*-inositol-1-phosphate synthase
mi*RNA*	micro*RNA*
MoFLNRORD	Ministry of Forests, Lands, Natural Resource Operations and Rural Development
*n*BGE	*n*-butyl glycidyl ether
NBS	Nucleotide-binding site
NBS-LRR	Nucleotide binding site-leucine-rich repeat
NC	Natural conditions experiment (Chapter 4)
NGS	Next generation sequencing
NHR	Nonhost resistance
PAL	Phenylalanine ammonia lyase
PC	Principal Component (see also PCA)
PCA	Principal Component Analysis
PCR	Polymerase chain reaction
PPD4	PsbP domain-containing protein 4
ppm	Parts per million
PR protein	Pathogenesis-related protein
Pth	Peptidyl-t*RNA* hydrolase
PVPP	Polyvinylpolypyrrolidone
qPCR	Quantitative PCR (see also PCR)
QTL	Quantitative trait loci
R gene	Plant's disease resistance gene
RCD	Root collar diameter
RH	Relative humidity

RhoGAP	Rho GTPase-activiting protein
RIP	Ribosome inactivating protein
RLK	Receptor-like protein kinase
RNA-Seq	*RNA* sequencing
ROS	Reactive oxygen species
RT	Room temperature
SA	Salicylic acid
SEM	Scanning electron microscopy
si*RNA*	Short interfering *RNA*
SNP	Single nucleotide polymorphism
STS	(S)-Stylopine synthase
TF	Transcription factor
TFCC	Tubulin-folding cofactor C
TMM	Trimmed mean of M-values
TPM	Transcripts per million
VSP	Vegetative storage protein
WGCNA	Weighted gene co-expression network analysis
WRC	Western redcedar (i.e. *Thuja plicata* Donn ex D. Don)
XTH	Xyloglucan endotransglucosylase/hydrolase

ACKNOWLEDGEMENTS

I would like to thank my supervisors Dr. Barbara J. Hawkins and Dr. John H. Russell for their guidance, advising and support through the program. I also thank the members of the supervisory committee, Dr. C. Peter Constabel, Dr. Olaf Niemann and Dr. Jim Mattsson for their suggestions that helped improve the project.

I express my gratitude to the Natural Sciences and Engineering Research Council of Canada (NSERC) and to the Centre for Forest Biology at the University of Victoria for funding of the Doctoral program through the CREATE Training Program in Forests and Climate Change. I thank the Tree Improvement Branch of the British Columbia Ministry of Forests, Lands, Natural Resource Operations and Rural Development for the plant material provided to perform each of the studies that make part of this project, and for the funding granted to complete the chemical and next generation sequencing analyses, and part of the scanning electron microscopy imaging.

I would like to thank the Analytical Laboratory of the British Columbia Ministry of Environment and Climate Change Strategy for the analytical chemistry services provided, Genome Quebec Innovation Centre (Montreal, Canada) for the HiSeq 2000 paired end *RNA*-Seq sequencing services provided, as well as Compute Canada (www.computecanada.ca) and its regional partner WestGrid (www.westgrid.ca) for their support with the bioinformatics analyses.

Special acknowledgement is given to Dr. Belaid Moa for his thorough help with the metagenomic analyses carried out with the *RNA*-Seq data. I also thank Dr. Brian J. Haas at the Broad Institute for troubleshooting parts of the Trinity pipeline, Peter Ott for his insights on parametric statistical methods used to analyze the histological and chemical data, and Dr. Juergen Ehlting and Dr. Harry Kope for their scientific advice.

I would like to thank Craig Ferguson, Brad Binges, Samantha Robbins, Brent Gowen, Heather Down and the summer and work students of Dr. Barbara J. Hawkins' lab for their technical assistance during in the lab and field work, and James Tyrwhitt-Drake for colouring the SEM image in Fig. 2.4a of Chapter 2.

I also acknowledge Dr. Stephanie Willerth and Andrew Agbay for the access granted and help provided with the Bioanalyzer, and Loren Perraton and the Pacheedaht First Nation for the access given to the western redcedar progeny trial in Jordan River (British Columbia) that was used as source of cedar leaf blight inoculum.

Finally, I thank my wife, family and friends for their patience and emotional support during the years in the Doctoral program.

DEDICATION

To my wife Yamile Y. Ortega, and to my mother Ana R. Aldana.

Chapter 1

Introduction

Plants interact with other species on a daily basis, with some interactions being beneficial (Klironomos et al., 2000, Ronsheim and Anderson, 2001, Vance et al., 1979, Zahran, 1999) and others harmful (Ji et al., 2016, Joshi et al., 2016, Teixeira et al., 2014, Tichtinsky et al., 2003). Interactions between plants and pathogens that result in plant diseases are studied by plant pathologists (Agrios 2005, p. 5; Sharma 2006, p. 1.4). The field of phytopathology has become especially relevant in recent years due to the effects of changing climates on the life cycles, and range of plant diseases (Boland et al., 2004, Dukes et al., 2009, Ghini et al., 2008, Katsaruware-Chapoto et al., 2017, Pautasso et al., 2012, Sturrock et al., 2011).

An important pathosystem in western North America is the *Thuja plicata* Donn ex D. Don - *Didymascella thujina* (Durand) Maire interaction (Durand, 1913, Frankel, 1990, 1991, 1992, Kope and Trotter, 1998a, Kope, 2000, Kope and Dennis, 1992, Kope et al., 1996a, Porter, 1957, Russell et al., 2007). *T. plicata* is an economically and culturally important species of the region (Barnes, 2016, Gonzalez, 2004, Gregory et al., 2018, Hebda and Mathewes, 1984, Stewart, 1984, Western Red Cedar Export Association, 2004) that can be severely and negatively affected by *D. thujina* (Kope 2000; Minore 1983, p. 27; Minore 1990; Pawsey 1960; Russell et al. 2007; Søegaard 1956, 1966, 1969) especially at young ages when the infection can be devastating (Burdekin and Phillips 1971; Dennis and Sutherland 1989; Pawsey 1960; Søegaard 1969, p. 373). Resistance to *D. thujina* in *T. plicata* is a quantitative trait (Lines, 1988, Russell et al., 2007) that is currently being incorporated into breeding programs (Russell and Yanchuk, 2012); however, no resistance markers for breeding have been developed to date. Furthermore, the resistance mechanisms against the pathogen in *T. plicata* are

unknown, except for the gene-for-gene model of resistance that Søegaard proposed may take place when *Thuja standishii* (Gord.) Carrière and *T. plicata* are crossed (Søegaard, 1956, 1966, 1969).

This Doctoral project explored the resistance mechanisms to *D. thujina* in *Thuja* sp., with particular emphasis on *T. plicata*, to set the basis for the development of markers associated with *D. thujina* resistance. In this chapter, basic plant pathology concepts are described, followed by an introduction to the pathosystem investigated. The rationale, objectives of the project, and organization of the dissertation are then presented. The chapter closes by providing the contributions of the project to the field of plant pathology.

1.1 General aspects of plant pathology

Plant disease is defined as the disruption of a plant's normal function by a pathogen (Agrios 2005, p. 5; Holliday 1989, p. 93; Sharma 2006, p. 1.6), normal function referring to the growth and development of a plant according to its genetic potential as influenced by the environment (Agrios 2005, p. 5). Plant diseases have negative effects on the integrity, physiology and/or form of the plant and/or its parts, and may even lead to death of the whole plant (Agrios 2005, p. 5; Holliday 1989, p. 93; Sharma 2006, p. 1.6). Diseases can be non-infectious or infectious (Agrios 2005, p. 8; Holliday 1989, p. 93). Non-infectious diseases are caused by abiotic factors (Agrios 2005, p. 8), hence are not transmittable from plant to plant. That kind of disease is also known as a disorder (Holliday 1989, p. 93). Infectious diseases, on the contrary, are transmittable and are caused by biotic agents like prokaryotes, fungi, protozoa, nematodes, viruses and viroids (Agrios 2005, p. 134; Sharma 2006, p. 1.10). In infectious diseases, the term "disease" relates to the whole plant-pathogen system, not just to the pathogen (Holliday 1989, p. 93).

Plant-pathogen interactions can be incompatible or compatible. Incompatible interactions take place when the pathogen does not result in a diseased plant (Holliday 1989, p. 149), whereas compatible interactions are those where the pathogen disrupts the physiological functioning of the plant, leading to the development of disease symptoms (Holliday 1989, p. 71). The complex interactions between plant, pathogen, and the abiotic (i.e. environmental) factors that can result in plant disease develop-

ment are represented in plant pathology by the disease triangle (Agrios 2005, p. 79; Jones 1998; Scholthof 2007), although the role of a fourth element in plant health, the microbiota, is gaining attention recently (Feau and Hamelin, 2017). In the case of fungi, the pathogen side of the triangle includes species with dissimilar trophic strategies like saprophytes, necrotrophs, biotrophs and hemibiotrophs (Agrios 2005, p. 78; Duplessis et al. 2011; Sharma 2006, p. 4.9; Spanu 2012). Saprophytes grow on decaying matter (Holliday 1989, p. 286; Sharma 2006, p. 4.9), and necrotrophs, also known as perthophytes (Holliday 1989, p. 197), slowly kill living plants that they colonize as the infection progresses (Agrios 2005, p. 78; Holliday 1989, p. 197). Biotrophic fungi are also called obligate parasites (Agrios 2005, p. 78) and grow only on living hosts (Agrios 2005, p. 78; Sharma 2006, p. 4.9) whose metabolic machinery they reprogram for their own benefit (Berger et al., 2007, Duplessis et al., 2011, Lapin and Van den Ackerveken, 2013, Spanu, 2012). Biotrophs cannot be grown on axenic media (Sharma 2006, p. 4.9). Hemibiotrophs, also called semibiotrophs (Agrios 2005, p. 78), share characteristics of the previous two categories, and require that part of their life cycle be completed in a living host (Agrios 2005, p. 78; Lapin and Van den Ackerveken 2013).

Fungal pathogens complete their life phases in a cyclic manner called the disease cycle (Agrios 2005, p. 80; De Wolf and Isard 2007; Hamelin 2000; Lieberei 2007; Sharma 2006, p. 1.36). The stages of the cycle are inoculation, prepenetration, penetration, infection and dissemination of the pathogen (Agrios 2005, p. 80; Sharma 2006, p. 1.36). Inoculation takes place when the pathogen first encounters the host, and is closely related to prepenetration, given that it involves the processes prior to pathogen entry to the plant (Agrios 2005, pp. 80-82; Sharma 2006, p. 1.37). Penetration can be direct or through natural openings depending on the pathogen (Agrios 2005, p. 88; Sharma 2006, p. 4.6). The infection stage of the disease cycle includes tissue invasion by the pathogen to obtain nutrients from the host plant, as well as to grow and reproduce (Agrios 2005, pp. 89-91; Sharma 2006, pp. 1.38-1.39). The penetration and the early infection are the most critical phases of the disease cycle (Agrios 2005, p. 213; Vidhyasekaran 2008, p. 55) and can either lead to symptom development in compatible plant-pathogen interactions, or to disease resistance in incompatible interactions. The dissemination is the last phase of the cycle, which refers to the spread of the pathogen to start the cycle all over again, and can be achieved via primary or secondary inocula (Agrios 2005, p. 96; Sharma 2006, p. 1.40). Pri-

mary inoculum is that responsible for infection after a pathogen has overseasoned and usually results in severe infections (Agrios 2005, p. 80; Sharma 2006, p. 1.37), while secondary inocula are produced without overwintering or oversummering, and are released by tissues that were infected by the primary inoculum (Agrios 2005, p. 80; Sharma 2006, p. 1.37).

1.1.1 Disease resistance

Plants can be resistant to pathogens when they are not the hosts, a phenomenon known as nonhost resistance (NHR; Agrios 2005, p. 134, Sharma 2006, p. 3.4, Westerink et al. 2004). NHR is the most common type of disease resistance (Agrios 2005, p. 208), and although the phenomenon is not well understood (Agrios 2005, p. 158), NHR appears to be related to the basal immune defenses that are always in place in plants (Fan and Doerner, 2012, Uma et al., 2011). It has also been proposed that NHR may be the result of the lack of host recognition factors in the plant (Agrios 2005, p. 158). True resistance takes place when a plant is the host of a pathogen but withstands penetration and/or infection; such resistance is genetically determined (Agrios 2005, p. 136; Holliday 1989, p. 274; Sharma 2006, p. 3.5; Westerink et al. 2004). True disease resistance against pathogens can be either quantitative or qualitative (Agrios 2005, p. 136; Sharma 2006, p. 3.5; Vidhyasekaran 2008, p. 193). Quantitative resistance is the result of many genes, and produces a continuous range of resistances to the pathogen of interest within a plant species (Agrios 2005, p. 136; Sharma 2006, p. 3.6). This type of resistance is also known as polygenic, partial or horizontal resistance (Agrios 2005, p. 136; Sharma 2006, p. 3.6), and is not easily broken down due to its polygenic nature (Holliday 1989, p. 274) making it the best type of resistance for genetic improvement programs (Grattapaglia and Resende, 2011, Neale and Kremer, 2011, Rostoks et al., 2005, White et al., 2007).

Qualitative resistance confers strong resistance or susceptibility to a pathogen race (Agrios 2005, p. 136; Sharma 2006, p. 3.6). Unlike quantitative resistance, qualitative resistance is due to one or few major genes, and can be easily broken down when resistant plants cross with susceptible plants (Holliday 1989, p. 274; Rouxel and Balesdent 2010). Qualitative resistance is also known as monogenic, race-specific or vertical resistance, and usually involves disease resistance (R) genes (Agrios 2005, p. 136; Sharma 2006, p. 3.6). R-gene resistance is at the heart of the gene-for-gene

model of disease resistance (Agrios 2005, p. 140; Hammond-Kosack and Jones 1997; Sharma 2006, p. 3.9; Vidhyasekaran 2008, p. 193), which states that plants with an *R* gene will be resistant to a pathogen when in the presence of the pathogen's avirulence (*avr*) counterpart (Agrios 2005, p. 140; Hammond-Kosack and Jones 1997; Sharma 2006, p. 3.9; Vidhyasekaran 2008, p. 193). Hypersensitive responses (HR) are the best-studied phenomena related to *R*-genes (Agrios 2005, p. 151; Sharma 2006, p. 5.10). HR is the programmed death of cells that are being infected to contain the pathogen and prevent further colonization of the infected tissues (Stakman, 1915). HR usually takes place during the early stages of infection (Brown et al., 1966, Gees and Hohl, 1988, Lauvergeat et al., 2001). Plant resistance to pathogens can also be the product of *R*-gene "pyramids", which refers to cases where more than one *R* gene is present in a host plant making it fully resistant to a pathogen's race (Agrios 2005, p. 137; Sharma 2006, p. 3.6).

1.1.2 Resistance mechanisms against plant diseases

Resistance mechanisms against pathogens can be classified according to the organizational level at which they occur, or by the type of response elicited by the pathogen. Plants can develop pubescent surfaces, thorns, or other structures at the organ level to deter herbivorous arthropods and mammals (Cooper and Owen-Smith, 1986, Fernandes, 1994, Levin, 1973), but they can also have anatomical defenses at the cellular level like suberin layers (Pawsey, 1960, Smith et al., 2006, Yoshida, 1998) or abscission layers (Agrios 2005, p. 216; Sharma 2006, p. 5.8) to fight pathogens. At the molecular level, leucine-rich repeat (LRR) receptor-like proteins, cysteine-rich receptor-like protein kinases (CRKs), and receptor-like protein kinases (RLKs) in general, play important roles in plant defense (Afzal et al. 2008; Ederli et al. 2011; Goff and Ramonell 2007; Morris and Walker 2003; Tichtinsky et al. 2003; Vidhyasekaran 2008, p. 78; Yeh et al. 2015).

At the chemical level, a wide range of compounds are also involved in plant defense (Aharoni and Galili 2011; Hartmann 1996; Heldt 2005, p. 403; Heldt and Piechulla 2010, p. 399), including sulfur/nitrogen containing compounds, phenolics and terpenes (Aharoni and Galili, 2011). Sulfur-containing compounds include metabolites like glucosinolates (Heldt 2005, p. 409; Heldt and Piechulla 2010, p. 405), while nitrogen-containing compounds comprise metabolites like alkaloids (Heldt 2005,

p. 406; Heldt and Piechulla 2010, p. 402). Phenolics have phenyl rings and include simple phenols or complex phenylpropanoid molecules like cutin, suberin, lignans, lignin, flavonoids, tannins, stilbenes and coumarins (Heldt 2005, p. 435; Heldt and Piechulla 2010, p. 431). Terpenes, also called terpenoids or isoprenoids, are hydrocarbons built from isoprene and classified according to the number of isoprene units (Heldt 2005, p. 413; Heldt and Piechulla 2010, p. 409). Terpenes are the most studied compounds in conifer defense (see e.g. Keeling and Bohlmann 2006, Lewinsohn et al. 1991a, Shalev et al. 2018, Vourc'h et al. 2002).

In relation to the type of response elicited by the pathogen, defense mechanisms can be constitutive or induced. Constitutive defenses are always present regardless of the infection status of the plant (Agrios 2005, p. 210; Sharma 2006, p. 5.2) and can be found at different organizational levels. For example, thick cuticles are a well-known constitutive defense against pathogens that perform direct penetration (Agrios 2005, p. 88; Gees and Hohl 1988; Roundhill et al. 1995; Sherwood 1981), lignified structures are documented to impede pathogen propagation in infected tissues (Smith et al., 2006, Yoshida, 1998), and chemical compounds, like hydroxamic acids, are commonly and consistently found at higher amounts in cereal plants resistant to fungal pathogens (Ahmad et al., 2011, Erb et al., 2011, Kumar et al., 1994, Leighton et al., 1994, Song et al., 2011). Constitutive resistance mechanisms in conifers involve structural defenses like sclereids (Franceschi et al., 2005) or calcium oxalate crystals (Hudgins et al., 2003), and high relative amounts of compounds like phenolics (Franceschi et al., 1998, 2000), resins (Franceschi et al., 2005, Phillips and Croteau, 1999), or terpenes (Huber and Bohlmann, 2005, Keeling and Bohlmann, 2006, Litvak and Monson, 1998).

Induced resistance mechanisms are those triggered by elicitors after the initial plant-pathogen interaction (Agrios 2005, p. 213; Sharma 2006, p. 5.5), and can take place within minutes (Vidhyasekaran 2008, p. 55) to hours (Agrios 2005, p. 215) or even days (e.g. Yoshida 1998). Chemical responses like the production of phytoalexins are rapidly induced responses (Agrios 2005, p. 235; Heldt 2005, p. 404; Heldt and Piechulla 2010, p. 400; Sharma 2006, p. 5.14; Vidhyasekaran 2008, p. 411), as are the production of well-known defenses like the pathogenesis-related proteins (PR proteins). PR proteins are induced in plants only in in response to compatible interactions with pathogens (Antoniw et al., 1980, Jayaraj et al., 2004, van Loon, 1999,

van Loon and van Strien, 1999, van Loon et al., 1994), and include proteins like chitinases (Galindo-González and Deyholos 2016; Neuhaus 1999; Sharma et al. 2011; Vidhyasekaran 2008, p. 55), peroxidases (Chittoor et al., 1999, Ghosh, 2006, Hemetsberger et al., 2012), thaumatin-like proteins (Velazhahan et al., 1999) and β-1,3-glucanases (Beffa et al. 1993; Leubner-Metzger and Meins Jr. 1999; Vidhyasekaran 2008, p. 55). The production of structural defenses like lignin deposition usually take longer (e.g. Xu et al. 2011). Induced defenses in conifers include hypersensitive response, callus deposition and lignification (Franceschi et al., 2005), as well as an increased production of resins (Franceschi et al., 2005, McKay et al., 2003, Phillips and Croteau, 1999) and terpenes (Huber and Bohlmann, 2005, Litvak and Monson, 1998, Miller et al., 2005). The upregulation of genes involved in secondary metabolism, transport, ethylene signalling and transcription in response to pest attacks has also been reported in conifers (Ralph et al., 2006b).

1.2 The *Thuja plicata* - *Didymascella thujina* pathosystem

1.2.1 *Thuja plicata*

Western redcedar (*Thuja plicata*) is a conifer native to western North America (Fan et al. 2008; Glaubitz et al. 2000; Minore 1983, p. 1; Minore 1990; O'Connell and Ritland 2000), and the provincial tree of British Columbia (Provincial Symbols and Honours Act, RSBC 1996, c 380, s 5). The species also occurs in Europe, having been introduced in Denmark in the 1860's (Søegaard, 1956, 1966). *T. plicata* is also known as Pacific redcedar, giant cedar, tree of life, giant arborvitae, western arborvitae, arborvitae, shinglewood and canoe cedar (Gregory et al., 2018). The tree is linked to the cultural heritage of the First Nations of western North America, and was used to produce ritual and everyday products including boxes, masks, canoes and poles as long as 5,000 years ago (Hebda and Mathewes, 1984, Stewart, 1984). *T. plicata* is not considered a true cedar because it does not belong to the *Cedrus* genus, but to the Cupressoideae subfamily of the Cupressaceae, which includes economically important genera like *Thuja*, *Cupressus*, *Calocedrus* and *Chamaecyparis* (Gadek and Quinn, 1993, Qu et al., 2017, Ze-ping and Huo-ran, 1997). Western redcedars are long-lived trees that can reach up to 1,000 years, and grow taller than 50 m, with

diameters at breast height of more than 5 m and crown spreads larger than 16.5 m (Minore 1983, p. 1; Minore 1990). The branches of young *T. plicata* tend to be curved upward, while they swing downward and then upward at the ends in mature trees (Minore 1983, p. 12). The species' foliage is comprised of small, scale-like leaves (Figs. 1.1a - 1.1f) that make up a high fraction of the live crown (Minore 1983, p. 12).

The species occurs in costal and interior regions of western North America. Coastal populations range from northern California to southern Alaska and interior populations from northern Idaho to interior British Columbia (Fan et al. 2008; Glaubitz et al. 2000; Minore 1983, p. 1; Minore 1990; O'Connell and Ritland 2000). The species' altitudinal range varies from sea level to 1,200 m in coastal regions (Minore 1983, p. 2; Minore 1990), and between 300 and 2,100 m in interior areas (Minore 1983, p. 2; Minore 1990). The latitudinal and elevation upper limits are probably due to low winter temperatures (Grossnickle and Russell 2006; Klinka and Brisco 2009, p. 17) because *T. plicata* is not resistant to extreme cold (Minore, 1990) although it has moderate cold hardiness (Fan et al., 2008, Minore, 1990). Western redcedar is a species tolerant to many stressors, which allows it to grow in different habitats, but usually in a mix of several species (Antos et al., 2016). It grows in a range of moisture environments, but the growth rate is the highest in humid habitats (Antos et al., 2016).

Thuja plicata is a monoecious species (Minore, 1990), with 11 chromosomes (Hizume and Fujiwara, 2016, Li et al., 1996), an estimated genome size of 12.6 Gbp (based on the C-value in Williams 2009, p. 43, and the conversion to base pairs in Doležel et al. 2003), and whose chloroplast genome has recently been sequenced (Adelalu et al., 2017). The sexual reproduction process in western redcedar has been described by Owens and Molder (1980), which includes high self-pollination and low outcrossing rates (O'Connell et al., 2004) that might have resulted in the low genetic variability seen in the taxon (Fan et al., 2008, Glaubitz et al., 2000, O'Connell and Ritland, 2000, Yeh, 1988). Despite that, deleterious inbreeding depression appears to have been purged in the species (Russell and Ferguson, 2008, Russell et al., 2003). Little genetic structure has been reported within interior and coastal populations (Bower and Dunsworth, 1987, von Rudloff and Lapp, 1979, von Rudloff et al., 1988, Yeh, 1988), although southern populations appear to be genetically different from northern ones (O'Connell et al., 2008). A phylogenetic study suggests that the species

probably spread from a southern refuge to the current coastal and interior regions of British Columbia after the last ice age (O'Connell et al., 2008). The differences in drought resistance between interior and coastal populations (Fan et al., 2008, Grossnickle and Russell, 2010) can be related to the divergence in range after expansion.

Western redcedar is an economically important species. About 10 million seedlings are planted every year across British Columbia, with most seed produced in managed orchards (Daniels and Russell, 2007). *T. plicata* represents between 18% and 19% of the costal timber harvest (Barnes, 2016, Gregory et al., 2018), nearly 3% of the interior harvest (Barnes, 2016), and about 7% of the total provincial harvest (Gregory et al., 2018). The yearly volumes harvested range between four and five million m^3 that render annual revenues of more than one billion dollars for the province (Barnes, 2016, Gregory et al., 2018). It is estimated that almost 1,900 people are employed across British Columbia in jobs directly related to the manufacture of primary and secondary western redcedar products (Gregory et al., 2018). Primary products of the species include logs, pulp and timber, while secondary products range from shakes and shingles to furniture and instruments (Gonzalez, 2004, Gregory et al., 2018). The species is one of the preferred softwoods for outdoor applications because of its dimension stability and durability characteristics, as well as its beautiful appearance (Daniels et al., 1997, Gonzalez, 2004, Western Red Cedar Export Association, 2004). The weathering and decay resistance of *T. plicata*'s heartwood is attributed to its extractives (Chedgy et al., 2007b, Lim et al., 2007, Morris and Stirling, 2012, Stirling et al., 2017), which include the lignan (-)-plicatic acid (Morris and Stirling, 2012), and the tropolones thujic acid, methyl thujate, γ-thujaplicin, β-thujaplicin and β-thujaplicinol (Chedgy et al., 2007a,b). The most abundant extractives in its wood are β-thujaplicin, γ-thujaplicin, thujic acid and plicatic acid, the last compound giving the wood its characteristic red coloration (Chedgy et al., 2007a, Lim et al., 2007).

The profile of the foliar compounds in *T. plicata* is different from that of the heartwood. Terpenes are prevalent in leaves (Shalev et al., 2018, von Rudloff and Lapp, 1979, von Rudloff et al., 1988, Vourc'h et al., 2001, 2002), and have deer deterrence (Vourc'h et al., 2001, 2002) and antimicrobial properties (Castillo et al., 2012, Mohanraj, 2014, Sarup et al., 2015, Tsiri et al., 2009). The most abundant terpenes in western redcedar foliage are β-thujone, α-thujone and sabinene (Shalev et al., 2018, Tsiri et al., 2009, von Rudloff et al., 1988, Vourc'h et al., 2001, 2002). To date,

the only characterized enzymes associated with the production of foliar secondary metabolites in *T. plicata* are a (+)-sabinene synthase (Foster et al., 2013) and a (+)-sabinene-3-hydroxylase (Gesell et al., 2015), both of which are believed to be involved in the synthesis of α- thujone and β-thujone (Foster et al., 2013, Gesell et al., 2015). Shalev et al. (2018) have identified 33 additional putative terpene synthases in western redcedar. *T. plicata* foliage is also known to contain relatively high amounts of calcium (Daubenmire, 1953). Many species of fungi have been reported on the foliage of *T. plicata* (more than 200; Fernando et al. 1999, Minore 1983, p. 27, Minore 1990), with most of them being non-pathogenic (Minore 1983, p. 27; Minore 1990). Several bacterial species have also been reported in western redcedar leaves, some of which may be beneficial (Bal et al., 2012).

1.2.2 *Didymascella thujina*

Didymascella thujina (cedar leaf blight, CLB) is the most important foliar pathogen of *T. plicata* (Kope 2000; Minore 1983, p. 27; Minore 1990; Pawsey 1960; Russell et al. 2007; Søegaard 1956, 1966, 1969). The species is a biotrophic fungus (Durand 1913; Korf 1962; Søegaard 1956; Søegaard 1969, p. 294) from the Hemiphacidiaceae family of the Helotiales (Korf, 1962) that causes leaf blight disease on *Thuja* species (Figs. 1.1a - 1.1f; Burdekin 1968, 1969, Durand 1913, Kope 2000, Kope and Sutherland 1994b). *D. thujina* infects young plants primarily (Burdekin and Phillips 1971; Dennis and Sutherland 1989; Pawsey 1960; Søegaard 1969, p. 373), and it can be fatal in nurseries (Peace, 1958) although all plant ages are affected (Kope, 2000). The pathogen has been recorded in Europe (Boudier, 1983, Boudru, 1945, Buchwald, 1936, Forbes, 1920, 1921, Loder, 1919, Miles, 1922, Vegni and Ferro, 1964) where it was responsible for nursery loses (Alcock, 1928, Fernández-Magan, 1974), and also in North America, especially in nurseries (Dennis and Sutherland, 1989, Frankel, 1990, 1991, 1992, Kope and Trotter, 1998a, Kope, 1992, Kope and Dennis, 1992, Kope and Sutherland, 1994a, Kope et al., 1996a, Trotter et al., 1994). Diagnosis methods for the disease include host and symptom recognition (Durand, 1913, Kope, 2000, Pawsey, 1960, Søegaard, 1969), as well as molecular biology tools that use the two internal transcribed spacer 2 sequences (ITS2) that have been developed for *D. thujina* (GenBank accessions KT875766 and KT875767). The ITS region was proposed by the Fungal Barcoding Consortium as the universal fungal barcode maker (Schoch et al., 2012).

Figure 1.1. Progression of *Didymascella thujina* symptoms and ascocarp development on foliage of *Thuja plicata* trees more than 10 years old. The pictures shown were taken between April 20 and July 9, 2015 on trees planted in the progeny trial that was used as source of inoculum for the studies presented in Chapters 2 to 6 (Jordan River, British Columbia; 48° 25' 24.52" N, 124° 1' 27.69" W, elev. 76 m). Note how the ascocarps become conspicuous after June 9 (d). See also Appendix A.14, which shows the spore load being released as *D. thujina* ascocarps developed in the progeny trial that year. (a) April 20, (b) May 4, (c) May 18, (d) June 9, (e) June 25, (f) July 9. Scale bars = 1.0 cm.

Cedar leaf blight was observed for the first time on *Thuja occidentalis* in Wisconsin in 1908 (Durand, 1913, Pawsey, 1960, Søegaard, 1956), and it was formally described in 1913 (Durand, 1913, Pawsey, 1960). The species was then seen on *T. plicata* foliage in Idaho in 1912 by Weir (Søegaard 1969, p. 294; Weir 1916), later observed in Ireland in 1918 (Søegaard, 1956), and formally reported there in 1919 by Pethybridge (Forbes, 1920, 1921, Pawsey, 1960). Durand originally classified this leaf blight under the genus *Keithia* (Durand, 1913, Kope, 2000, Korf, 1962, Pawsey, 1960), but it was latter reclassified as *Didymascella* by Maire (Kope, 2000, Korf, 1962, Maire, 1927, Pawsey, 1960) to avoid synonymity with a genus from the Lamiaceae that had been named *Keithia* in 1834 (Kope, 2000, Pawsey, 1960). The disease is therefore known as *Keithia* leaf blight, *Keithia* blight or simply *Keithia* because of that (Durand, 1913, Kope, 2000, Korf, 1962, Maire, 1927, Pawsey, 1960). No anamorph of *D. thujina* has ever been observed (Pawsey, 1960). Known hosts of *D. thujina* are *T. plicata*, *Thuja plicata* var. *atrovirens* (R. Smith) Sudworth and *T. occidentalis* (Durand, 1913, Kope, 2000, Kope et al., 1998, Søegaard, 1966). In Canada, the disease has been observed in Prince Edward Island, New Brunswick, Quebec, Newfoundland and Ontario on *T. occidentalis*, and in British Columbia on *T. plicata* and on *T. plicata* var. *atrovirens* (Kope, 2000).

Cedar leaf blight can be recognized by the scattered pattern of light-brown infected *Thuja* leaves with an oval-shaped dark brown 0.6-1.5 × 0.4-0.8 mm ascocarp in the leaf centre (Figs. 1.1a - 1.1f; Durand 1913, Kope 2000). *D. thujina* ascospores (Figs. 2.1a, 2.1d, 2.2 and 2.4) range from 15-25 × 11.5-18 µm (Kope, 2000) to 22-25 × 15-16 µm (Durand, 1913), are olive-brown in colour (Durand, 1913, Kope, 2000) and have a transversal septum close to one of the ends that results in a two-celled spore with cells of very dissimilar sizes (Durand, 1913, Kope, 2000). Spores that have recently landed have smooth surfaces that turn verrucose and ornamented after releasing the adhesive extracellular matrix that attach them to their host or to any surface (Fig. 2.2b; Kope 2000). The disease cycle of *D. thujina* can take from a few months to several growing seasons to complete depending on the age of the plants and the environmental conditions. For instance, seedlings maintained in growth chambers at 19°C can show symptoms after 77 days when at least 1,071 degree-days have accumulated (Kope and Trotter, 1998a), whereas plants of the same age in the nursery will take one growing season and the accumulation of more than 1,185 degree-days to show

symptoms (Kope and Trotter, 1998a, Kope, 2000). In contrast, *T. plicata* trees older than 20 years may take up to two growing seasons to develop *D. thujina* symptoms in forested environments (Kope and Trotter, 1998a, Kope, 2000, 2004, Kope and Sutherland, 1994b, Pawsey, 1960).

Germ tube germination of *D. thujina* ascospores has been reported at temperatures between 13℃ and 15℃ (Pawsey, 1960), although the highest and lowest limits recorded for germination are 28℃ and 5℃, respectively (Kope and Trotter 1998a; Pawsey 1960; Søegaard 1969, p. 309). *D. thujina* performs direct penetration into *T. plicata* leaves (Søegaard 1969, p. 299), and grows intercellular mycelia that penetrate mesophyll cells to develop intracellular bi- and tri-furcated haustoria (Pawsey 1960; Søegaard 1969, p. 310). Ascocarp development takes place at temperatures between 13℃ and 20℃ (Søegaard 1966; Søegaard 1969, p. 309). Ascocarps have clavate asci that are unitunicate and contain two ascospores each (Durand, 1913, Kope, 2000). Paraphyses are also present in the ascocarps, being hyaline, filiform and sometimes with clavate ends (Durand, 1913, Kope, 2000). At maturity, ascospore discharge takes place at temperatures between 10℃ and 16℃ (Søegaard, 1966) in highly humid environments ($\geq$90%; Søegaard 1966; Søegaard 1969, p. 295). The lowest and highest temperatures reported for ascospore discharge are 5℃ and 28℃, respectively (Kope and Trotter, 1998a). *D. thujina* ascospores are dispersed by air and spore production takes place in two periods over the summer (Porter 1957; Søegaard 1969, p. 305). The first sporulation period occurs between June and July (Figs. 1.1a - 1.1f; see also Appendices A.13 and A.14), while the second season occurs between late August to late September (Porter 1957; Søegaard 1969, p. 305). The spores have been documented to be viable after overwintering for as long as five months at temperatures as low as 5℃ (Pawsey 1957a; Pawsey 1960; Søegaard 1969, p. 309).

Common control methods for *D. thujina* include phytosanitary measures like growing *T. plicata* seedlings in isolated nurseries (Peace, 1955, 1958) or rotating *T. plicata* sowing among nurseries (Pawsey, 1962b), and the use of chemical compounds. In the last category, compounds such as cycloheximide (Burdekin and Phillips, 1971, Pawsey, 1962a, 1965), cycloheximide derivates (Pawsey, 1962a), propiconazole (Kope and Trotter, 1998b), mancozeb (Kope and Trotter, 1998b, Kope et al., 1996a), among others (Frankel, 1990, 1991, 1992) have been used in the past to control the blight in nurseries. An alternative to sanitation or the use of pesticides is breeding for *D.*

thujina resistance in *T. plicata*, which is currently under way (Russell and Yanchuk, 2012).

1.2.3 Resistance to *D. thujina* in *Thuja* sp.

Research on the resistance to *D. thujina* in *Thuja* species was pioneered by Søegaard, and dates back to the 1950's when a hybrid between the Japanese arborvitae (*T. standishii*) and *T. plicata* was found to be resistant to *D. thujina* (Søegaard 1956, 1966; Søegaard 1969, p. 311). *T. standishii* is a species native to Honshū (Japan), where it grows at elevations between 1,000 to 2,300 m (Søegaard 1969, p. 321). The species was introduced to Europe in 1861 (Veitch, 1892), and is less vigorous (Søegaard, 1956), and shorter than *T. plicata* (Søegaard 1969, p. 321), growing between 16 and 36 m tall (Petersen, 1916, Schneck, 1939). *T. standishii* does not have glands in the foliage (Søegaard 1969, p. 321) and has been reported as fully resistant to *D. thujina* (Søegaard, 1956, 1966, 1969).

The *T. standishii* × *plicata* clone identified as resistant to *D. thujina* by Søegaard had been selected from a progeny trial planted in 1938 (clone V. 1625 from sowing No. 259, No. 1; Søegaard 1969, p. 313), and was initially believed to be *T. standishii*, but was later determined to be a hybrid based on breeding records (Søegaard 1966; Søegaard 1969, p. 314). Clone V. 1625 was used in investigations between 1951 (Søegaard, 1956, 1966) and 1963 (Søegaard 1969, p. 343), and reciprocal *T. plicata* × *standishii* hybrids were also produced between 1951 and 1965 (Søegaard 1956, 1966; Søegaard 1969, pp. 329-344). The studies carried out by Søegaard led to the proposition of a gene-for-gene model of resistance (*R*-gene resistance) to *D. thujina* in the *Thuja* species studied (Søegaard 1956, 1966; Søegaard 1969, p. 366). Søegaard's model states that when *T. plicata* and *T. standishii* hybridize, an *R* gene against *D. thujina* from *T. standishii* is passed to the offspring rendering them resistant to the disease (Søegaard, 1956, 1966, 1969). Under such a model, F_2s from self-pollinated hybrid offspring were anticipated to segregate in a 3 (resistant) : 1 (susceptible) proportion, and F_1 hybrids backcrossed to *T. plicata* to segregate in a 1 (resistant) : 1 (susceptible) proportion. F_2s from hybrid F_1s backcrossed to *T. standishii* are predicted to be resistant to *D. thujina* according to the model.

Within *T. plicata*, variability among individuals in their resistance to *D. thujina* was

first observed in the 1950's. Søegaard noticed such variation in adult *T. plicata* trees planted in Denmark, which set the basis for the preliminary studies carried out on seedlings in 1951 (Søegaard, 1954, 1956, 1966). Søegaard's results were presented in 1954 (Søegaard, 1954, 1966), and published in 1956 (Søegaard, 1956, 1966). Porter (1957) also reported genetic variation in the resistance to *D. thujina* in *T. plicata* trees from nurseries in British Columbia at the time. Further studies by Søegaard involved the use of *T. plicata* trees planted in Denmark as far back as 1868, as well as trees sampled in North America since 1951 (Søegaard, 1969). Søegaard's studies revealed that *T. plicata* did not show full resistance to *D. thujina* (Søegaard, 1954, 1956, 1966, 1969), so later investigations focused on "*physiologically determined resistance*" (Søegaard 1969, p. 366) rather than *R*-gene resistance suggested to take place only when *T. standishii* was involved (Søegaard 1956, 1966; Søegaard 1969, p. 366). In the published literature to date, there are no reports of a hypersensitive response to *D. thujina* infection in *T. plicata*, which is an important resistance mechanism associated with *R*-gene resistance (Agrios 2005, p. 151). The studies carried out by Søegaard between 1952 and 1959, comparing disease resistance of seedlings and cuttings, however, showed that seedlings were very susceptible to the disease while cuttings were generally resistant (Søegaard 1969, p. 373). Physiological resistance referred to age-related changes in *T. plicata* trees that resulted in enhanced resistance to *D. thujina* (Søegaard 1969, p. 373), a phenomenon widely documented nowadays and known as age-related resistance (Carella et al., 2015, Kus et al., 2002, Panter and Jones, 2002, Shibata et al., 2010).

Besides seedlings, variation in the resistance to *D. thujina* among western redcedar populations has also been reported in field studies, first in Britain (Lines, 1988) and more recently in Canada (Russell et al., 2007). The investigation by Russell et al. (2007) indicated that trees from coastal and low elevation populations in British Columbia are more resistant to the disease than interior populations at high elevations. Such variability is thought to be the result of natural selection for resistance in the populations that have historically co-existed with *D. thujina* (Russell et al., 2007). Furthermore, it has been predicted that coastal regions will continue to favour the prevalence of *D. thujina* under future climates (Gray et al., 2013), which may drive future natural selection for resistance. Russell et al. (2007)'s study also revealed that *D. thujina* has a negative impact on *T. plicata* growth as shown by the significant negative correlation between disease severity and *T. plicata* diameter at

6 years of age (Russell et al., 2007). The variability in the resistance to *D. thujina* among populations of *T. plicata* in British Columbia is at the core of the current genetic improvement program for the species for resistance against the disease (Russell and Yanchuk, 2012).

1.3 Project rationale

Conifers are long-lived species that are thought to take longer to evolve adaptations in comparison to angiosperms, whose generation spans are generally shorter (Buschiazzo et al., 2012, De La Torre et al., 2017, Kusumi et al., 2015, Prunier et al., 2016). This can be problematic in fast changing scenarios, where long life cycles may reduce the ability of a species to adapt to the rapid changes (Aitken et al., 2008, Shang et al., 2015, Wang et al., 2016b). Climate change poses new challenges to tree species at both the physiological and evolutionary levels (Allen et al., 2010, Garrett et al., 2006, Hogg and Bernier, 2005, Lindner et al., 2010, Spittlehouse and Stewart, 2003). It has been estimated that the global average temperature will increase between 0.3℃ and 0.7℃ in the next 20 years (IPCC [Intergovernmental Panel on Climate Change], 2013). Climate change has already affected the disease cycle of some plant pathogens (Dukes et al., 2009, Katsaruware-Chapoto et al., 2017, Sturrock et al., 2011) and pests (Bentz et al., 2010, Chakraborty and Newton, 2011, Musolin, 2007, Taylor et al., 2018). Climate has both direct and indirect effects on pathogens (Sturrock et al., 2011), and some plant diseases are predicted to expand their current range, enabling the pathogens to reach hosts not previously encountered (Boland et al., 2004, Ghini et al., 2008, Pautasso et al., 2012, Sturrock et al., 2011). In *T. plicata* populations across British Columbia, the risk of *D. thujina* incidence is predicted to increase over the next decade, especially in coastal populations at low elevations (Gray et al., 2013).

Genetic selection of *T. plicata* for increased resistance to *D. thujina* is the best alternative to date to reduce the future impact of the disease on western redcedar populations across British Columbia (Gray et al., 2013). Breeding cycles consists of selection of base populations and desirable traits, breeding, screening (or testing), production, and the repetition of the cycle for advanced generation breeding (White et al., 2007). The longest phase of the breeding cycle is usually the screening phase, which may take up to several decades depending on the trait of interest (White et al., 2007). In the case of resistance to *D. thujina*, *T. plicata* seedlings can be planted in

the field when they are one-year-old, but it takes a few growing seasons before they can be screened for disease severity (Porter, 1957, Søegaard, 1954, 1956, 1966, 1969, Trotter et al., 1994). Longer time spans are required to screen *D. thujina* resistance in adult *T. plicata* trees (Russell et al., 2007). Moreover, phenotype screening is a logistically intense process that can become expensive due to the labour involved, especially in field trials.

In order to accelerate the breeding cycle, the screening phase could be shortened by using markers (genotypic or phenotypic) associated with the traits of interest, but appropriate markers must be first developed before being used. Promising genetic makers for *D. thujina* resistance in *T. plicata* could be based on Søegaard's studies, especially when considering the potential existence of an *R* gene against the blight in *T. standishii*. Yet, the *R*-gene resistance model has never been tested beyond Søegaard's studies. Furthermore, some of Søegaard's studies had resistance screening results that deviated from the anticipated proportions under the gene-for-gene model, and one of the crosses between *T. plicata* and *T. standishii* was more difficult to produce than the other (see Søegaard 1956, 1966, 1969). The genetic basis of the resistance to *D. thujina* in *T. plicata*, *T. standishii* and hybrids between both species appears to be more complex than the *R*-gene model proposed by Søegaard.

In relation to *T. plicata* only, the variability that exists among adult populations (Lines 1988; Russell et al. 2007; Russell and Yanchuk 2012; Søegaard 1969, p. 323) makes it possible that polygenic resistance to the disease is present in the species, in agreement with the quantitative nature of the trait (Agrios 2005, p. 136; Holliday 1989, p. 274; Vidhyasekaran 2008, p. 193). Additionally, the susceptibility to the disease in seedlings and the higher resistance in older plants (Søegaard 1969, p. 373) suggests potential differences between age groups in the resistance mechanisms to the pathogen.

The information currently available on the *Thuja* sp. - *D. thujina* pathosystem highlights the need to understand the resistance mechanisms to the disease in *T. plicata* in order to develop adequate markers associated with *D. thujina* resistance. It is important to discern whether the *T. plicata* plants resistant and susceptible to *D. thujina* are different simply at the constitutive level, or if there is an induced response to *D. thujina* infection that explains such differences. It is equally important to determine

if juvenile and adult *T. plicata* plants use the same or different resistance mechanisms against the pathogen, especially considering the need to screen young plants for breeding. It also is worth exploring the molecular basis of the full resistance to *D. thujina* in *T. standishii* to determine if such mechanisms can be useful to breed for resistance to *D. thujina* in *T. plicata*. This project addressed all of these aspects.

1.4 Objectives

The objectives of this Doctoral project were as follows:

General objective

To investigate the resistance mechanisms to *Didymascella thujina* (Durand) Maire in *Thuja* sp., with special emphasis on *Thuja plicata* Donn ex D. Don, by comparing plants resistant and susceptible to *D. thujina* using histological, chemical and next generation sequencing techniques.

Specific objectives

1. To study the relationship between resistance of young *T. plicata* plants to *D. thujina* and their climate of origin.

2. To examine the constitutive mechanisms of resistance to *D. thujina* in *T. plicata*, *T. standishii* and *T. standishii* × *plicata* plants at the anatomical, chemical and gene expression levels.

3. To analyze the induced defense responses of juvenile and adult *T. plicata* plants to *D. thujina* infection at the chemical and gene expression levels.

4. To explore the induced defense responses of older *T. standishii* and *T. standishii* × *plicata* plants to *D. thujina* infection at the chemical and gene expression levels.

1.5 Organization of this dissertation

This thesis is organized in five content chapters (2 to 6), and a closing chapter. Both seedlings and clonal lines were used through the studies carried out during the

program, and the investigations became more controlled as the project progressed. Chapter 2 describes the anatomical characteristics of the foliage of *T. plicata* seedlings and how they relate to resistance to *D. thujina*. The chapter then discusses the virulence of *D. thujina*, and closes by exploring the relationship between resistance to the pathogen in *T. plicata* seedlings and their climate of origin.

The third chapter explores the chemical and gene expression differences between seedlings of a full-sib *T. plicata* family resistant to *D. thujina* and seedlings of a full-sib family susceptible to the pathogen. Comparisons between symptomless plants and seedlings with symptoms that had been infected in the field are made as well. Chapter 3 focuses on foliar terpenes due to their high prevalence in leaves of *T. plicata*.

Chapter 4 further explores the induced chemical and gene expression responses to *D. thujina* infection in *T. plicata* seedlings from three resistant and three susceptible full-sib families. Field and growth chamber experiments were carried out, with gene expression responses being evaluated only in the controlled conditions experiment.

The fifth chapter is a comprehensive study of the resistance mechanisms of *T. plicata* cuttings against *D. thujina*. The anatomical differences in the foliar anatomy of *T. plicata* clones resistant and susceptible to *D. thujina* were studied, as well as their constitutive chemical and gene expression differences. The study in Chapter 5 also investigated the induced chemical and gene expression responses to controlled *D. thujina* infections in the clones.

Chapter 6 relates to clonal lines of *T. standishii*, *T. standishii* × *plicata* and two single-seed lines of *T. plicata* that had been self-pollinated for five generations. That investigation studied the constitutive differences among the *Thuja* species analyzed at the histological, chemical and gene expression levels. The chapter also investigated the induced chemical and gene expression responses to *D. thujina* infections performed under controlled conditions. Chapter 6 ends by discussing the *R*-gene resistance model proposed by Søegaard in light of the molecular information produced through next generation sequencing.

The closing chapter presents a summary of the differences in *D. thujina* resistance among the various species and age groups studied. It recapitulates the constitutive

resistance mechanisms to *D. thujina* common to both resistance classes as well as to the species and age groups analyzed at the three levels studied (anatomical, chemical and gene expression). The chapter also discusses the general induced responses to *D. thujina* infection in the *Thuja* species investigated, and the differential responses to pathogen infection, especially in *T. standishii*. Chapter 7 presents the conclusions of the project, and suggests future avenues of investigation.

1.6 Contribution of this project to the field of plant pathology

Comprehensive investigations such as those completed during this Doctoral program, which included simultaneous analyses of both phenotypic and genotypic aspects of a plant-pathogen interaction, are not commonly found in the plant pathology literature. Indeed, the study of individual aspects of a pathosystem is the norm in phytopathology. For example, it is usual to find studies devoted mostly to the histopathological aspect of a plant disease (e.g. Anker and Niks 2001, De Luna et al. 2002, Dushnicky et al. 1998, Ramos et al. 1992, Szwacka et al. 2009, Zinsou et al. 2006), the chemical defenses against pathogens (Chen, 2008, Erb et al., 2011, Wen et al., 2006), or the field variability in disease resistance (e.g. Hamilton et al. 2013, Russell et al. 2007, Zhang et al. 1997). Nowadays, it is also common to find next generation sequencing experiments using *RNA*-Seq that study defense responses to pathogen infections (e.g. Ji et al. 2016, Joshi et al. 2016, Kamitani et al. 2016, Krizek et al. 2016, Orshinsky et al. 2012, Petre et al. 2012, Wang et al. 2016c), but those rarely combine other types of data, such as measurements of phenotypic variables.

It is also usual these days to find literature where both plant and pathogen gene expression data are analyzed concomitantly. These so-called "dual *RNA*-Seq" studies (e.g. Camilios-Neto et al. 2014, Hayden et al. 2014, Howard et al. 2013, Kawahara et al. 2012, Meyer et al. 2016, Rodrigues et al. 2013, Westermann et al. 2012) are becoming more prevalent in the scientific phytopathology literature, but many lack the phenotypic aspect of the host's defense mechanisms. Gene expression studies of compatible plant-pathogen interactions that also examine the histological (Galindo-González and Deyholos, 2016, McNeil et al., 2018, Xu et al., 2011, Ye et al., 2017) or chemical aspects (Oates et al., 2015) of a disease are found, but they are less fre-

quent. A common approach to study the relationship between gene expression and phenotypic data in plant pathology is the use of weighted gene co-expression network analysis (WGCNA; e.g. Amrine et al. 2015, Harper et al. 2016, Lanver et al. 2018, Massonnet et al. 2018, Zhang et al. 2016). The methodology first builds a gene network based on the correlations amongst gene expression data that is then used to group genes in modules (Zhang and Horvath, 2005). The relationship between gene modules and phenotypic data is then analyzed to find the modules and "drivers" that can explain the phenotypic data (Zhang and Horvath, 2005). Drawbacks of the technique are that the network analysis is usually limited to a subset of genes due to computational limitations (Zhang and Horvath, 2005), and that the methodology is based on calculations of parametric correlations between genes, which is not ideal to analyze the discrete (count) data produced by *RNA*-Seq experiments.

In this project, a different approach to identify clusters of co-expressed genes was used. I chose a cutting-edge machine learning methodology called grade of membership (GoM; Dey et al. 2017), which is based on the latent Dirichlet allocation method used in topic modelling (Blei, 2012, Blei and Lafferty, 2009). The method uses discrete data as input and has commonly been used to mine and analyze text data from document collections (Blei, 2012, Blei and Lafferty, 2009), but its use has been extended to other fields (Liu et al., 2016a), including gene expression data in toxicology (Yu et al., 2014). GoM was a powerful methodology to detect sequences at similar levels of expression in each transcriptomic sample analyzed here, and therefore was also very useful in the detection of constitutive gene expression differences between *Thuja* sp. plants resistant and susceptible to *D. thujina*. I also used dynamic topic modelling (DTM; Blei 2012, Blei and Lafferty 2006), which is an extension of topic modelling, and is used to analyze how topics change over time (Blei, 2012, Blei and Lafferty, 2006). DTM has also been used on toxicogenomics data (Lee et al., 2016), and here, it allowed me to find common gene expression responses over time in the various plant materials studied in the time-course experiments presented in Chapters 4-6.

In addition to the GoM and DTM analyses, I also used a variable selection methodology called stability selection to study the relationships between the gene expression and the phenotypic data of the project. This methodology was developed to analyze high dimensional datasets, and has been used on transcriptomics data from *Bacillus subtilis* (Meinshausen and Bühlmann, 2010). Here, the technique allowed the de-

tection of the best predictor variables (either chemical or nucleotide sequences) that explained the differences between infection conditions in Chapters 3-6. The method was also very useful to find what nucleotide sequences were related to the accumulation over time of specific chemicals in Chapters 4 and 6.

To my knowledge, and based on the extensive literature reviewed over the years during the program, no plant-pathogen interaction has been so comprehensively investigated in a Doctoral project using a combination of phenotypic and *RNA*-Seq data, and analyzed with state-of-the-art machine learning and high dimensional variable selection techniques altogether. The studies presented in this dissertation provide a holistic view of the *Thuja* sp. - *D. thujina* pathosystem that builds upon the studies by Søegaard (Søegaard, 1954, 1956, 1966, 1969), Porter (Porter, 1957), Peace (Peace, 1955, 1958), Pawsey (Pawsey, 1957a,b,c, 1959, 1960, 1962a,b, 1964, 1965), Phillips (Phillips, 1965, 1966, 1967), Burdekin (Burdekin, 1968, 1969, Burdekin and Phillips, 1971), Kope (Kope and Trotter, 1998a,b, Kope, 1992, 2000, 2004, Kope and Dennis, 1992, Kope and Sutherland, 1994a,b, Kope et al., 1996a,b, 1998), Russell (Russell et al., 2007, Russell and Yanchuk, 2012), among others. This thesis provides a multidimensional framework to study plant-pathogen interactions that could be applied to other pathosystems.

Chapter 2

Histological and climatic aspects of the *Thuja plicata* - *Didymascella thujina* interaction in seedlings

2.1 Introduction

Organisms from several taxa interact with plants on a daily basis (Agrios 2005, p. 134; Sharma 2006, p. 4.6), including viruses (Kamitani et al., 2016, Zvereva and Pooggin, 2012), bacteria (Rodrigues et al., 2013, Tichtinsky et al., 2003), other plants (Rodrigues et al., 2013, Tichtinsky et al., 2003), nematodes (Hussey, 1989, Wallace, 1973) and fungi (Doehlemann et al., 2008, Ji et al., 2016, Kang et al., 2016, Parrott et al., 2016). Some organisms can be pathogenic to some plants, but harmless to others. For example, *Phoma sorghina* (Sacc.) Boerema is a rice endophyte (Fisher and Petrini, 1992) that is pathogenic to several Poaceae (Goswami et al., 2008). *P. sorghina* also causes root diseases in several legumes (Goswami et al., 2008), and leaf spot disease to tobacco (Yuan et al., 2016) and *Oxalis debilis* (Chen et al., 2017), but is innocuous to plants like pepper, tomato, cucumber or carrot (Goswami et al., 2008). Pathogens are characterized by the disruption of the normal physiology/metabolism of the host, which leads to impairment and disease development (Agrios 2005, p. 5; Sharma 2006, p. 1.6; Holliday 1989, p. 93).

The biological characteristics of the pathogen determine the optimal environmental factors associated with its pathogenicity (Agrios 2005, p. 270; Sharma 2006, p. 7.6).

For instance, airborne pathogens are highly sensitive to climate-related variables like humidity or rain (Colhoun, 1973, Hardwick, 2002). Furthermore, humid environments are best suited for bacterial infection and colonization (Hirano and Upper, 1983, Leben, 1981, Schwartz et al., 2003, Underwood et al., 2007), and many airborne pathogens depend on factors like wind (Nussbaum, 1990, Pawsey, 1964) or water (Agrios 2005, p. 97; Sharma 2006, p. 1.42) for their dispersal. The environmental element of the disease triangle (Agrios 2005, p. 79; Jones 1998; Scholthof 2007) is of particular interest in disease escape, which is a type of apparent resistance that can be caused by environmental factors (Agrios 2005, p. 137; Sharma 2006, p. 3.7).

Plants are hosts to many organisms, both benign (Klironomos et al., 2000, Ronsheim and Anderson, 2001, Vance et al., 1979, Zahran, 1999) and pathogenic (Álvarez-Yepes et al., 2016, Joshi et al., 2016, Kimmons et al., 1990, Parrott et al., 2016, Rodrigues et al., 2013, Teixeira et al., 2014, Tichtinsky et al., 2003). Host plants evolve defense systems against pathogenic organisms (Burdon and Thrall, 2009, Frank, 1993, 1992, Occhipinti, 2013) that lead to genetically-based resistance mechanisms, referred to as true resistance (Agrios 2005, p. 136; Holliday 1989, p. 274; Sharma 2006, p. 3.5). True resistance can be due to constitutive mechanisms, such as preexisting defenses (Agrios 2005, p. 210; Sharma 2006, p. 5.2). Constitutive defense mechanisms to pathogens exist at different organizational levels, and range from chemical (Heldt and Piechulla 2010, p. 400; Wang et al. 2016c) and molecular (Agrios 2005, p. 140; Sharma 2006, p. 3.9; Scheel and Nuernberger 2004; Vidhyasekaran 2008, p. 195; Westerink et al. 2004), to structural (Anker and Niks, 2001, Donofrio and Delaney, 2001, Gees and Hohl, 1988, Hau and Rush, 1982, Roundhill et al., 1995, Sherwood, 1996, Voigt, 2014).

The first and most conspicuous constitutive structural defense mechanism against pathogens is the cuticle (Agrios 2005, p. 210; Gees and Hohl 1988; Hau and Rush 1982; Roundhill et al. 1995; Yoshida 1998), which is made of waxes and cutin (Yeats and Rose, 2013). The specific composition of the cuticle determines its physical characteristics (Domínguez et al., 2011, Zinsou et al., 2006), and cuticle thickness is usually related to pathogen resistance (Agrios 2005, p. 210; Zinsou et al. 2006). Cuticles are commonly penetrated by hemibiotrophs and obligate parasites to access their hosts (Agrios 2005, p. 88; Gees and Hohl 1988; Roundhill et al. 1995; Sherwood 1981), so resistant plants tend to have thicker cuticles than susceptible plants (Rhouma et al., 2013, Smith et al., 2006). Stomata can be a structural vulnerability given they are

entry points of microorganisms that do not perform direct penetration (Agrios 2005, p. 88; Dickinson 2003; Sharma 2006, p. 4.6). Stomatal density (McKown et al., 2014, Ramos et al., 1992) and closure (Arnaud and Hwang, 2015, Gudesblat et al., 2009, Underwood et al., 2007) are commonly related to defense against pathogens that penetrate through the stomata. A third constitutive mechanism of defense against pathogens is the presence of suberized (Pawsey, 1960, Smith et al., 2006) or lignified (Xu et al., 2011, Yoshida, 1998) structures that such microorganisms cannot pass.

Many aspects related to the pathogen of the *Thuja plicata* - *Didymascella thujina* system have been studied in the past, including the fungus' morphology (Durand, 1913, Korf, 1962), spore ultrastructure (Kope, 2000), life cycle (Kope and Trotter, 1998a, Kope, 2000, Pawsey, 1957a, 1960), nutrition mode (Durand 1913; Søegaard 1956; Søegaard 1969, p. 294), host range (Durand, 1913, Kope, 2000, Kope et al., 1998, Søegaard, 1966), environmental variables that limit viability and disease development (Kope and Trotter 1998a; Søegaard 1969, p. 299), and even the ability to overwinter (Pawsey 1957a; Pawsey 1960; Søegaard 1969, p. 299). The progress of the disease inside the foliage of *T. plicata* has also been described at the histological level (Pawsey 1960; Søegaard 1969, p. 309), and it is known that variability in the resistance to *D. thujina* exists among adult *T. plicata* populations in British Columbia (Russell et al. 2007; Russell and Yanchuk 2012; Søegaard 1969, p. 323), and that such variability is associated with climate (Russell et al., 2007, Russell and Yanchuk, 2012). However, there is no information to date on the characteristics of the foliage of *T. plicata* seedlings that may be responsible for resistance to *D. thujina*, nor on the relationship between the climate of seed origin and *D. thujina* resistance in western redcedar seedlings; this chapter examines those aspects. Firstly, anatomical features of the host were studied at the histological level to explore what foliar characteristics of young *T. plicata* plants may be related to resistance against *D. thujina*. And secondly, the relationship between climate of origin and *D. thujina* resistance in *T. plicata* seedlings was investigated to shed light on the effect of the environment on *D. thujina* resistance in seedlings.

2.2 Methodology

2.2.1 Assessment of histological traits from *T. plicata* seedlings associated with resistance to *D. thujina*

2.2.1.1 Plant material

One-year-old seedlings from eight full-sib *T. plicata* families with varying resistances to *D. thujina* were used in this experiment (families 399, 525, 528, 582, 583, 685, 687 and 689; see Appendix A.1). The families were chosen based on *D. thujina* screening information provided by the British Columbia Ministry of Forests, Lands, Natural Resource Operations and Rural Development. The seedlings were grown under standard greenhouse conditions in Beaver Styroblock containers 45/340 (Stuewe and Sons., Tangent, OR, USA) from seeds planted the spring of 2012 at the Cowichan Lake Research Station (Mesachie Lake, British Columbia). The plants were maintained in Sunshine Professional Growing Mix 2 (Sun Gro® Horticulture, Vilna AB, Canada).

2.2.1.2 Screening of *T. plicata* seedlings for resistance to *D. thujina*

A set of seedlings from each of the eight families mentioned in section 2.2.1.1 was assessed for resistance to *D. thujina* by exposing them to the disease and scoring its severity: the fewer the symptoms, the more resistant the family. To infect the plants, they were taken to a *T. plicata* progeny trial that showed severe symptoms of *D. thujina* (near Jordan River, British Columbia; 48° 25' 24.52" N, 124° 1' 27.69" W, elev. 76 m). The progeny trial is in the CWHxm2 zone of the Biogeoclimatic Ecosystem Classification System (Green and Klinka, 1994). Twenty seedlings per family were placed under the sporulating trees in spring 2013. Airborne spores present at the site were monitored by placing two microscope slides covered with petroleum jelly next to the seedlings, and replacing them upon every visit to the site (twice a week). All spores collected were identified based on their morphology and counted using a Zeiss light microscope. The plants were checked every 3-4 days while in the field and did not need to be watered given the prevalent rainy weather at the infection site during the inoculation process. The seedlings were taken to the Bev Glover Growth Facility (University of Victoria, Victoria, British Columbia) after two months of exposure in the field, where they remained until *D. thujina* symptoms developed nearly 9 months

later. The plants were watered weekly and fertilized monthly with 100 ppm nitrogen from Peter's 20-7-19 Conifer Grower fertilizer (Jr. Peters Inc, Allentown PA, USA) while in the greenhouse.

Confirmation of D. thujina infection

Infection was confirmed using three methods: 1) scanning electron microscopy examination of foliage that was exposed to *D. thujina* to determine if spores of the pathogen had landed, 2) analysis of the severity of the disease after symptoms developed using colour analysis, and 3) study of the anatomy of the foliage with symptoms using leaf clearing, fungal staining and light microscopy techniques.

Samples used for the scanning electron microscopy (SEM) analyses were collected from four ∼3 mm leaf sections (two from the uppermost branch, one from the middlemost branch and one from the lowermost branch) of five seedlings per family on the fourth day of field deployment. The samples were fixed overnight in 2.5% glutaraldehyde (prepared in Sörensen buffer pH 7.2; Ruzin 1999, pp. 227). The following day, the fixative was washed out of the samples by two consecutive changes of 30 min each in Sörensen buffer. The samples were then dehydrated by 30 min changes in an ascending ethanol series (50%, 70%, 80%, 90% and twice in 100%) and critical point dried in a Leica EM CPD300 system (Leica Microsystems Inc., Richmond Hill ON, Canada). The dried samples were then gold coated in an Edwards S150B Sputter Coater (Edwards Canada, Quebec QC, Canada), and photographed at 1000X in a Hitachi S-3500N Scanning Electron Microscope (Hitachi High-Technologies Canada Inc., Toronto ON, Canada). The length and width of the photographed spores were measured in ImageJ v. 1.46 (Schneider et al., 2012) and those measurements as well as the general morphology of the spores were compared to the published description of *D. thujina* (Durand, 1913, Kope, 2000). The dimensions of the spores that landed on the seedlings of each family were also compared using one-way non-parametric Kruskal-Wallis Analysis of Variance (ANOVA) in R (R Core Team, 2015) because raw measurements could not be normalized with standard transformations.

Disease symptoms were macroscopically examined after symptoms developed (∼ 9 months later) in all plants that were inoculated to verify the general aspect and colour of the symptoms using a dissecting microscope. After examination, the abax-

ial surface of the middlemost branch of each seedling was scanned using an Epson Perfection v750 scanner (Epson Canada Ltd., Markham ON, Canada). Severity of the disease was quantified as percentage of foliar area blighted, and was recorded using the colour analysis mode of WinRHIZO Pro v. 2009c (Regent Instruments Inc., QC, Canada). Severity data per family were compared using non-parametric one-way Kruskal-Wallis ANOVA given that the data could not be normalized using standard transformations. Homogeneous groups were determined using the Kruskal-Wallis all-pairwise comparisons test. The families were then classified as resistant or susceptible based on the results of the ANOVA (see section 2.3.1.1).

The anatomy of the foliage with symptoms was studied using the modified clearing and staining technique of McLean and Byth (1981) used by Liberato et al. (2005). In brief, leaf samples of the same size as those used for SEM, but this time with lesions present, were cleared for 24 h in a 1:1 v/v mix of anhydrous ethanol and 100% acetic acid at room temperature (RT). The cleared samples were then washed with three 5-min changes in distilled water. Free-hand sections were cut and mounted on microscope slides with 0.1% w/v aniline blue prepared in 85% lactic acid. The sections were examined and photographed at 63X and 400X magnification using a Zeiss microscope fitted with a RTKE SPOT camera (SPOT Imaging, Sterling Heights MI, USA) and SPOT v. 4.6 software.

2.2.1.3 Histological characterization of *T. plicata* seedlings

Another set of seedlings belonging to the same families in section 2.2.1.1, but that had never been exposed to *D. thujina* were used for the histological characterization. A total of 13 variables (10 measured and three derived) were studied. The variables included thickness of the cuticle, epidermis, leaf, whole mesophyll, palisade mesophyll and leaf width; cross section areas of the leaf and whole mesophyll; ratios of mesophyll to leaf thickness, mesophyll to leaf cross sectional area and spongy to whole mesophyll cross sectional area; stomatal density; and percentage of epidermal cells with lignified walls. The variables were measured in two branch sections (proximal and distal) from three branches (third from top, middlemost and lowermost) from five seedlings per family. Epidermis and cuticle thickness were measured in the same branches and sections, but both leaf surfaces were included. Stomatal density was also measured on both surfaces, but three branch sections instead of two were included (proximal,

middle and distal).

Samples collected for all histological analyses, except those for the stomatal density measurements, were fixed using the same procedure as described for the SEM preparations. The following day, the fixative was washed out of the samples with two changes of 20 min each in Sörensen buffer. The samples were then dehydrated in the same ethanol series used for the SEM procedures, but changing solutions every 20 min. After the last 100% ethanol step, the samples were changed to a 1:1 v/v ethanol-*n*BGE (*n*-butyl glycidyl ether) solution for 30 min, then to 100% *n*BGE for 30 min, next to a 1:1 v/v *n*BGE-Quetol 651 for 2 h, and lastly to 100% Quetol 651 overnight. The next day, the samples were polymerized in fresh 100% Quetol 651 (Takagi and Sato, 1979) for 24 h at 60℃. Embedded samples were sectioned at 5 µm using a Sorvall JB-4 Microtome and fixed to microscope slides on a hot plate for further processing. Two sets of sections per sample were produced, one for general histology staining with Toluidine Blue O, and another to quantify lignification of epidermal cell walls stained with phloroglucinol.

Samples for general histology were covered for 5 min with 1.0 % w/v Toluidine Blue O (dissolved in 1% aqueous sodium borate), rinsed with distilled water, and then washed for 50 s in 70% ethanol and for 1 min in 100% ethanol. The stained samples were dried at RT and mounted using Permount™ (Fisher Chemical™, Ottawa ON, Canada). Sections were photographed at 100X and 1000X magnifications in the same microscope and with the same camera mentioned in section 2.2.1.2. Digitized images were analyzed with the same program used to measure *D. thujina* spores on the SEM images.

For staining lignification of epidermal cell walls, microscope slides with sections were flooded for 5 min with 1% w/v phloroglucinol (prepared in 70% ethanol). Excess phloroglucinol was removed and the slides covered for 1 min with hydrochloric acid (HCl). The excess HCl was removed and the sections dried at RT. The samples were then mounted as before and photographed within 3 h using the same equipment used to capture light microscopy images (see section 2.2.1.2).

Stomatal densities were studied on leaf impressions produced using transparent nail polish. Two coats were applied to the area of interest and let to dry for 30 min at RT.

The impressions were then removed with transparent tape, mounted on microscope slides and covered with coverslips. The impressions were next photographed at 100X magnification with the equipment mentioned before.

Histological data were explored with Principal Component Analysis (PCA) based on correlation using FactoMineR (Lê et al., 2008). The dataset of the continuous variables was also explored using Pearson correlation analysis in R (R Core Team, 2015). Disease severity values of the families screened in section 2.2.1.2 were included in the Pearson correlation analysis. ANOVA of the individual continuous histological variables was carried out using a fixed-effects split-plot design (Appendix A.2) in R (R Core Team, 2015). Raw data from each variable was checked for normality using the Shapiro-Wilk test, and non-normal variables were transformed prior performing the ANOVA tests (square root for leaf width, and $\log_{10}$ for cuticle thickness, cross section leaf area, leaf thickness, whole mesophyll area and whole mesophyll thickness). Given that the stomatal density was a discrete variable, it was analyzed using non-parametric Kruskal-Wallis one-way ANOVA to detect differences between resistance classes, and differences among families.

2.2.2 Evaluation of the relationship between resistance to *D. thujina* and *T. plicata* climate of origin

2.2.2.1 Plant material and screening for resistance to *D. thujina*

One-year-old seedlings from all families used in section 2.2.1.1, as well as another five families (398, 8182, 8255, 8258 and 8265) were included in this experiment (see Appendix A.1 for parent information of each family). These families were chosen based on a pilot study of *D. thujina* severity executed in 2013, and on information from the British Columbia Ministry of Forests, Lands, Natural Resource Operations and Rural Development. The plant material was grown from seed at Cowichan Lake Research Station (Mesachie Lake, British Columbia) as described in section 2.2.1.1.

Between May and June 2014, 20 one-year-old seedlings from each of the families mentioned were infected in the same *T. plicata* progeny trial used in 2013 (section 2.2.1.2) using the same methodology. The plants were watered 1-2 times a week while in the field due to the dry summer of that year. The seedlings were returned to the Bev Glover Growth Facility (University of Victoria, Victoria, British Columbia) after one

month in the field and maintained until symptoms developed. Watering and fertilization regimes were the same as those used in the experiment of the previous year. *D. thujina* severity was assessed in the foliage of all exposed material as described in section 2.2.1.2.

2.2.2.2 Relationship between disease resistance and climate variables

The relationship between climate of origin and resistance to *D. thujina* in *T. plicata* was studied using correlation and random forest analyses of the disease severity and climate variables from the places of origin of the 13 families and their parents. Given that the families used in this investigation were the result of crosses between plants grown from seed collected in natural populations, the climate variables of each of the 13 families were calculated as the average of the climate variables of the place of origin of the parents. For instance, the mean annual temperature (MAT) of family 8182 (7.3℃) was the average between the MAT of its female parent (6.8℃, seed ID 261), and that of its male parent (7.8℃, seed ID 415).

Climate normal data of the parents (1961-1990) was retrieved from ClimateBC (Wang et al., 2016a) using the coordinates and elevation information in Appendix A.1. Thirty-two climate variables per parent, the same number of calculated variables per family, and the average disease severities screened in section 2.2.2.1 were used in the analyses. For each parent and family, the selected climate variables included temperatures (17 variables), precipitations (10 variables), degree days above or below 5℃ (4 variables), and summer heat-moisture index (1 variable; see Appendix A.11 for the full list). These variables were chosen based on evidence that *T. plicata* populations resistant to *D. thujina* occur in cooler and wetter areas across British Columbia (Russell et al., 2007), and on reports that temperature (average summer temperature, and maximum July and August temperatures), precipitation (May, July, spring and summer precipitations), and summer climate moisture index are good descriptors of the relationship between *D. thujina* intensity and *T. plicata* field site environments (Gray et al., 2013).

The Pearson correlation analyses were completed in R (R Core Team, 2015). All variables were checked for normality before the analysis with the Shapiro-Wilk test, and non-normal variables were transformed to meet the assumption (Appendix A.17

shows the variables that were transformed). Regression random forest analysis was conducted with disease severity as a response variable using the R package randomForest (Liaw and Wiener, 2002) set to grow 2000 trees and to assess the importance of the predictors. The criterion used to rank the predictors of disease severity (i.e. the climate variables) was the increase in node purity score. Change point detection analysis on those scores was used to determine the number of predictors to retain for further analysis. The R package changepoint was used for this purpose with the AMOC method on mean and variance (Killick and Eckley, 2014).

2.3 Results

2.3.1 Histological traits from *T. plicata* seedlings associated with resistance to *D. thujina*

Two main pathogens were present in the *T. plicata* progeny trial where the seedlings were inoculated as surveyed using microscope slides (section 2.2.1.2): *D. thujina* accounted for 32.01% of the spores counted during the inoculation period and *Pestalotiopsis funerea* (synonym *Pestalotia funerea*; Desmazières 1843, Steyaert 1949) for 62.73%. The remaining 5.26% of spores were from other species. The average *D. thujina* spore density in the site during the 2013 infection season was 1.72×10^3 spores$\cdot m^{-2}\cdot h^{-1}$. Germination of *D. thujina* spores on the microscope slides (Fig. 2.1a) was high within three days when rain was present (65.42%), and low when rain was absent (7.39%).

2.3.1.1 Screening for resistance to *D. thujina*

None of the plants retrieved from the inoculation site developed the foliar tip blight symptoms caused by *P. funerea* (Ivanová, 2016, Judith-Hertz, 2016, Mordue, 1976, Steyaert, 1949) despite the high amount of conidiospores present in the site. *P. funerea* conidiospores were fusiform, straight, with three to four medium brown cells and two peripheral hyaline cells. The basal hyaline cell had one appendage, while the apical hyaline cell had three to four appendages. The conidiospore characteristics recorded here corresponded to those published elsewhere (Ivanová, 2016, Madar et al., 1991, Mordue, 1976, Steyaert, 1949).

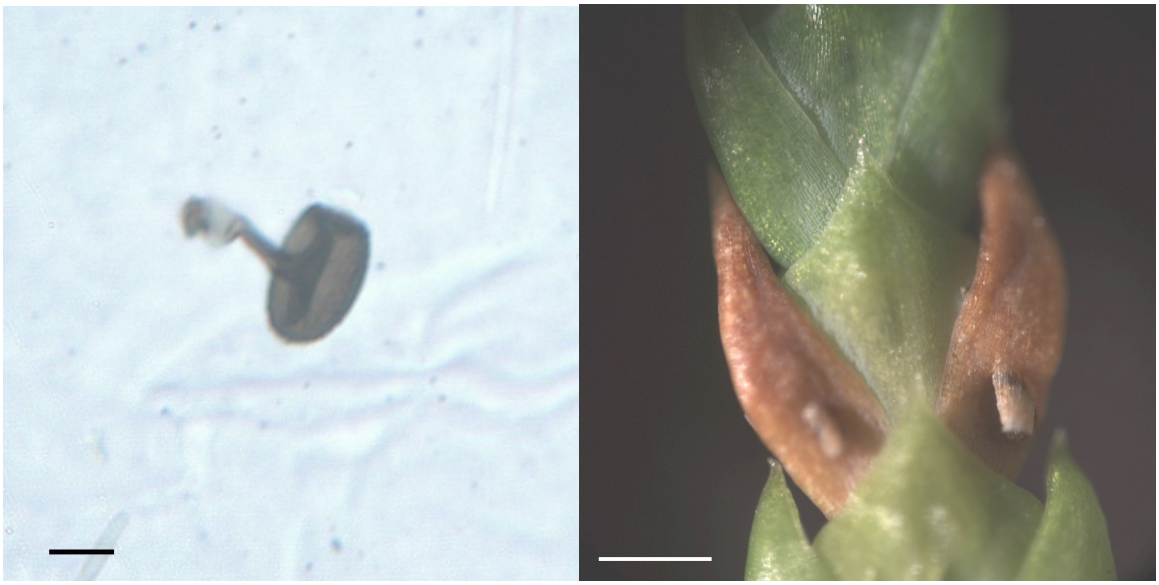

(a) (b)

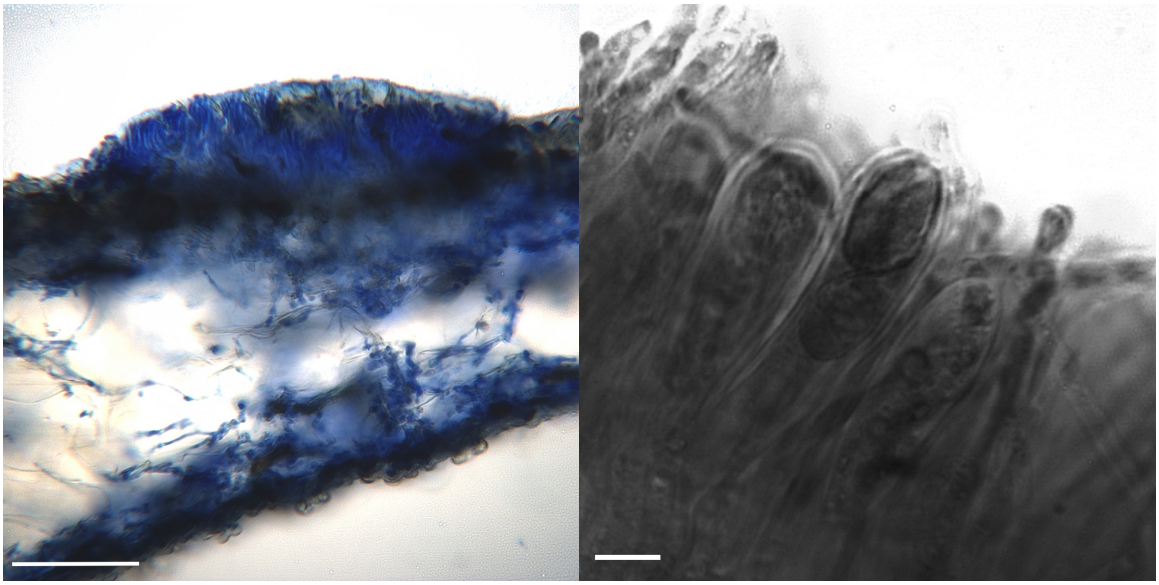

(c) (d)

Figure 2.1. Morphology of the spores and symptoms of *Didymascella thujina* in the plants screened. a) Ascospore with germination tube (19.2 µm long). Notice the characteristic olive-brown colour. The spore was photographed on a glass microscope slide covered with petroleum jelly that was in the inoculation site for three days. Scale bar = 10.0 µm. b) Leaves of *T. plicata* with symptoms of *D. thujina* after sporulation. Individual infected leaves (light brown) developed *D. thujina* ascocarps and released spores within nine months of inoculation. Ascocarps shown have already burst. Scale bar = 1.0 mm. c) Cross section of a *T. plicata* leaf that was showing symptoms as in Fig. 2.1b. The leaf was cleared for 24 h in a 1:1 v/v mix of 100% acetic acid and anhydrous ethanol at room temperature, hand-free sectioned, and mounted in 0.1% w/v aniline blue (prepared in 85% lactic acid). d) Asci of *D. thujina* from a leaf that was cleared and stained as in Fig. 2.1c. The image was a colour photograph filtered to black and white to visualize the histological details of the ascus. Notice the two ascospores per ascus as described in Durand (1913). Scale bar = 10.0 µm. Images captured by Juan A. Aldana using a Zeiss microscope (a, c and d), and a dissecting microscope (b) fitted with a RTKE SPOT camera.

In contrast to *P. funerea*, seedlings from all families developed symptoms of *D. thujina* after ∼9 months. The symptoms of the disease (Fig. 2.1b) were as those described in Durand (1913) and Kope (2000). The mesophyll of symptomatic leaves were full of *D. thujina* hyphae (Fig. 2.1c). Cross section study of the apothecia showed that their anatomy, as well as that of the ascus and ascospores within them (Fig. 2.1d), were the same as those described and shown in Durand (1913). The severity of the disease was significantly different among families ($p < 0.0000$, Table 2.1). Based on the severity results in Table 2.1, families 525, 528, 582 and 583 were categorized as susceptible and families 399, 685, 687 and 689 as resistant.

Table 2.1. Mean severity of *Didymascella thujina* symptoms in eight full-sib *T. plicata* families, and mean ascospore dimensions (± standard error) of the spores that landed on seedlings from the same families. The plants were infected naturally in a *T. plicata* progeny trial in Jordan River (British Columbia) in spring 2013. Severity was recorded as the percentage of foliar area that was blighted after symptoms developed ∼9 months later. Spores were measured on scanning electron micrographs produced from samples collected from five seedlings per family after 4 days of deployment. Superscripts in the severities indicate homogeneous groups from the Kruskal-Wallis all-pairwise comparisons test.

		Ascospore dimensions	
Family	**Severity (%)**	**Length (µm)**	**Width (µm)**
525	45.23^{a}	17.16 ± 0.37	13.18 ± 0.21
528	$42.45^{a,b}$	17.40 ± 0.30	13.02 ± 0.20
582	50.95^{a}	17.31 ± 0.31	13.20 ± 0.19
583	57.11^{a}	17.20 ± 0.30	13.46 ± 0.21
399	$25.09^{b,c}$	17.77 ± 0.28	13.58 ± 0.18
685	$23.39^{b,c}$	17.61 ± 0.27	13.33 ± 0.20
687	20.03^{c}	17.69 ± 0.21	13.49 ± 0.14
689	22.14^{c}	17.41 ± 0.19	13.50 ± 0.14

Ultrastructural analysis of the leaf samples collected after four days of seedling deployment in the field revealed that the mean *D. thujina* spore size was $17.43 \pm 0.10 \times 13.37 \pm 0.06$ µm. There were no significant differences in the sizes of the spores that landed on the different families ($p = 0.8399$ for length, and $p = 0.4105$ for width; Table 2.1). Recently landed spores had smooth surfaces (Fig. 2.2a) that turned into ornamented and verrucose surfaces after their adhesive extracellular matrixes had been released to attach them to the host (Fig. 2.2b; Agrios 2005, p. 82; Vidhyasekaran 2008, p. 2). Only one of the 302 *D. thujina* spores photographed on *T.*

plicata leaves had a conspicuous germination tube. That spore had landed on the abaxial surface of a seedling belonging to family 685, and the 32.12 µm-long germ tube was not penetrating the surface directly nor growing over it, but was instead in a perpendicular orientation in relation to the surface (Figs. 2.4a-2.4c).

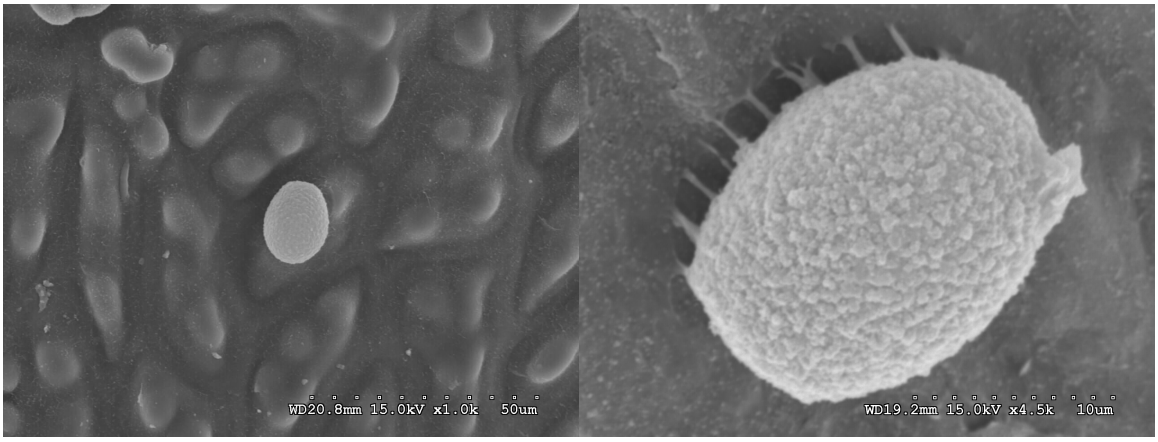

(a) **(b)**

Figure 2.2. Ultrastructural characteristics of the ascospores of *Didymascella thujina*. a) *D. thujina* spore that recently landed on a *Thuja plicata* leaf and has not released the adhesive extracellular matrix yet. b) Spore of *D. thujina* at high magnification (4,500X) showing the ornamented surface and the extracellular matrix that attaches it to its host after landing. Scanning electron micrographs captured by Juan A. Aldana in a Hitachi S-3500N Scanning Electron Microscope.

2.3.1.2 Histological characteristics of *T. plicata* seedlings related to resistance to *D. thujina*

Principal component analysis of the histological variables studied showed that resistant and susceptible plants grouped in overlapping clusters (Fig. 2.3). The first three principal components accounted for 59.85% of the variance. Principal component 1 explained 33.70% of the variance, principal component 2 accounted for 17.48%, and principal component 3 explained 8.73% of the variance. Variables with the highest contributions to component 1 were related to the whole leaf (whole mesophyll cross section area, whole mesophyll thickness, leaf cross section area, and leaf thickness). Variables with the highest contributions to component 2 were related to the leaf strata (spongy to whole mesophyll thickness ratio, palisade mesophyll thickness, and leaf width), and the variable with the highest contribution to component 3 was cuticle thickness. The second and third principal components appear to discriminate between resistance classes (Fig. 2.3).

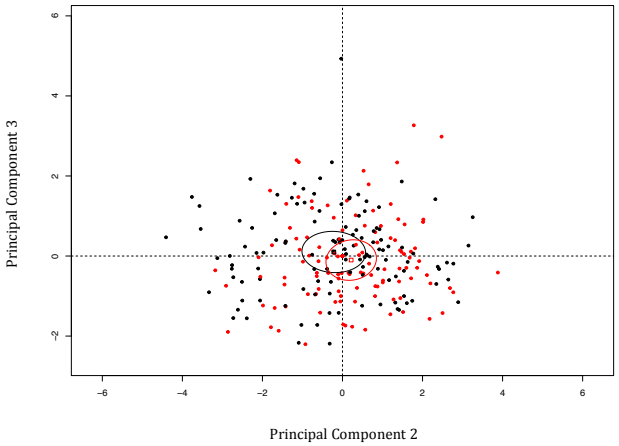

Figure 2.3. Principal component analysis bi-plot of thirteen histological variables recorded in eight *Thuja plicata* full-sib families that differed in resistance to *Didymascella thujina*. Four families were categorized as resistant (black) and four as susceptible (red) according to the severity of the disease measured in a different set of plants (see section 2.3.1.1 and Table 2.1). Confidence level of the ellipses is 99%.

Correlation analysis of the continuous histological variables and severity revealed that 36 of the 78 possible correlations were significantly different from zero, and that most of them were positive (32 out of 36, Table 2.2). Most of the variables were significantly correlated with at least six of the other variables, and all of the positive significant correlations referred to allometric relationships (e.g. bigger cross-section leaf area in thicker leaves $r = 0.6682$, $p > 0.0000$). Spongy to whole mesophyll thickness ratio was the only variable that had correlations significantly different from zero with the rest of the variables, except with severity and leaf width. Cuticle thickness was the only variable with a significant correlation with disease severity (r = -0.1703, p = 0.0090).

Individual analysis of the histological variables showed that there were significant differences among families (within class) in epidermal thickness, leaf thickness, palisade mesophyll thickness, whole mesophyll thickness and in the percentage of epidermal cells with lignified cell walls (Table 2.3). There were also significant differences among crown positions for most variables, except for leaf width, mesophyll to leaf cross section areas ratio, and in the percentage of epidermal cells with lignified cell walls. Cuticle thickness was the only continuous variable where significant differences between resistant and susceptible seedlings existed ($p = 0.0130$, Tables 2.3 and 2.4), with thicker cuticles in the resistant families (2.32 $\pm$ 0.02 µm, Fig. 2.5a) and thinner in the susceptible ones (2.23 $\pm$ 0.02 µm, Fig. 2.5b). Stomatal densities were also

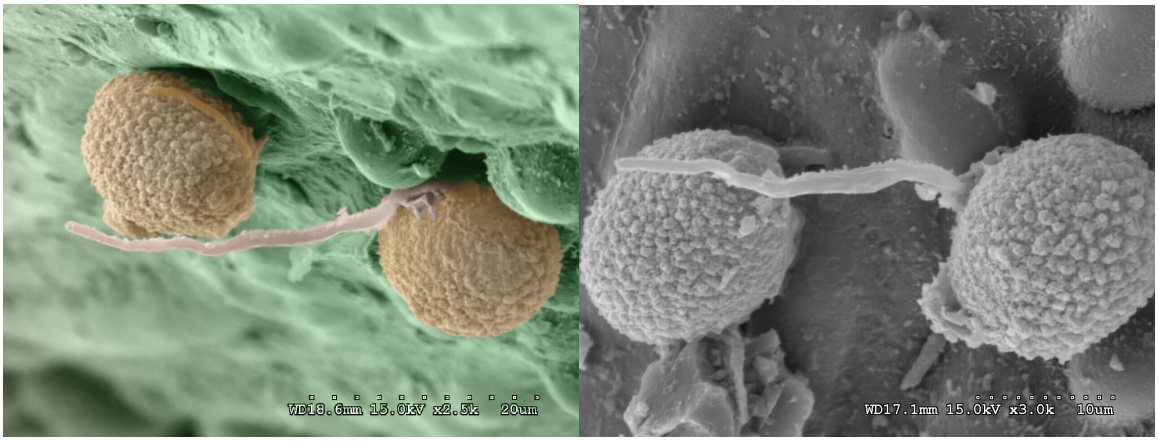

(a) **(b)**

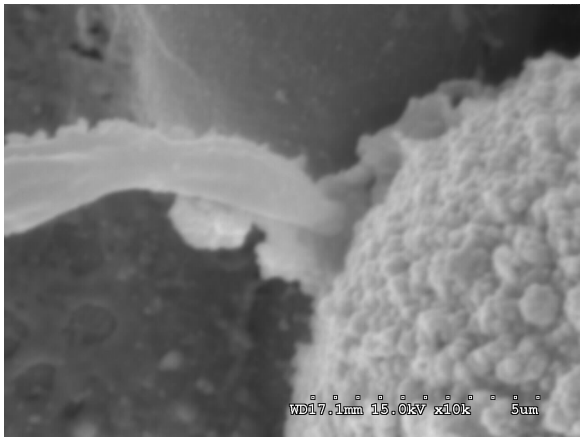

(c)

Figure 2.4. Ultrastructure of the only *D. thujina* spore found with a conspicuous germ tube (out of 302 studied), and which was growing away from the *T. plicata* leaf surface. The ascospore landed on the abaxial surface of a seedling from family 685 within four days of being deployed to a *T. plicata* progeny trial in Jordan River (British Columbia, Canada) where the pathogen had high prevalence. a) *D. thujina* spores photographed at 2,500X magnification and coloured to better visualize them, the leaf surface and a germ tube emerging from the right spore (32.12 µm long). b) *D. thujina* spores in a) photographed from a different angle and at 3,000X magnification to visualize the place of emergence of the germ tube of the spore. c) Place of emergence of the germ tube at 10,000X magnification. Scanning electron micrographs captured by Juan A. Aldana in a Hitachi S-3500N Scanning Electron Microscope. Image a) was kindly coloured from a black and white original by James Tyrwhitt-Drake.

Table 2.2. Correlation matrix (r) of the 12 continuous histological variables and disease severity studied in seedlings of 8 *Thuja plicata* full- sib families inoculated with *Didymascella thujina*. The variables included thicknesses, cross section areas, ratios and percentage of epidermal cells with lignified walls. Pal. mes. = palisade mesophyll; wh. mes. = whole mesophyll. Values within parenthesis in italics are p-values. * = significant at $\alpha = 0.05$. ** = significant at $\alpha = 0.01$.

		Thicknesses						Thickness ratios		Cross section areas		Cross section area ratio
	Severity	**Cuticle**	**Epidermis**	**Leaf**	**Leaf width**	**Wh. mes.**	**Pal. mes.**	**Spongy to Wh. mes.**	**Wh. mes. to leaf**	**Leaf**	**Wh. mes.**	**Wh. mes. to leaf**
Cuticle thickness	-0.1703 *(0.0090**)*											
Epidermal thickness	-0.0460 *(0.4842)*	-0.1044 *(0.1113)*										
Leaf thickness	-0.0834 *(0.2037)*	0.2451 *(0.0002**)*	-0.1004 *(0.1257)*									
Leaf width	0.0516 *(0.4318)*	-0.0467 *(0.4770)*	0.0720 *(0.2729)*	0.0651 *(0.3212)*								
Wh. mes. thickness	-0.0814 *(0.2146)*	0.2233 *(0.0006**)*	-0.0960 *(0.1431)*	0.9930 *(<0.0000**)*	0.0719 *(0.2737)*							
Pal. mes. thickness	-0.0504 *(0.4427)*	-0.0544 *(0.4078)*	0.0705 *(0.2826)*	0.1106 *(0.0915)*	0.2033 *(0.0018**)*	0.1133 *(0.0837)*						
Spongy to wh. mes. thickness ratio	0.0045 *(0.9449)*	0.2166 *(0.0009**)*	-0.1560 *(0.0170*)*	0.6567 *(<0.0000**)*	-0.0948 *(0.1483)*	0.6609 *(<0.0000**)*	-0.6191 *(<0.0000**)*					
Wh. mes. to leaf thickness ratio	-0.0370 *(0.5736)*	-0.0699 *(0.2869)*	-0.0217 *(0.7410)*	0.3347 *(<0.0000**)*	0.0527 *(0.4219)*	0.4407 *(<0.0000**)*	0.1057 *(0.1069)*	0.2908 *(<0.0000**)*				
Cross section leaf area	0.0216 *(0.7419)*	0.1120 *(0.0873)*	-0.0261 *(0.6916)*	0.6682 *(<0.0000**)*	0.7116 *(<0.0000**)*	0.6750 *(<0.0000**)*	0.2658 *(<0.0000**)*	0.3038 *(<0.0000**)*	0.2857 *(<0.0000**)*			
Wh. mes. area	0.0200 *(0.7608)*	0.1045 *(0.1107)*	-0.0243 *(0.7112)*	0.6687 *(<0.0000**)*	0.7101 *(<0.0000**)*	0.6767 *(<0.0000**)*	0.2624 *(<0.0000**)*	0.3071 *(<0.0000**)*	0.2968 *(<0.0000**)*	0.9968 *(<0.0000**)*		
Wh. mes. to leaf area ratio	0.0159 *(0.8088)*	-0.0314 *(0.6330)*	0.0287 *(0.6619)*	0.2922 *(<0.0000**)*	0.3493 *(<0.0000**)*	0.3046 *(<0.0000**)*	0.1250 *(0.0563)*	0.1711 *(0.0087**)*	0.2519 *(0.0001**)*	0.4028 *(<0.0000**)*	0.4669 *(<0.0000**)*	
Lignified cell walls in epidermis	-0.0292 *(0.6566)*	0.0105 *(0.8725)*	0.1692 *(0.0095**)*	-0.0939 *(0.1524)*	0.1253 *(0.0557)*	-0.0942 *(0.1510)*	0.1698 *(0.0092**)*	-0.1856 *(0.0044**)*	-0.0395 *(0.5475)*	0.0518 *(0.4305)*	0.0452 *(0.4917)*	-0.0658 *(0.3164)*

significantly different among families ($p = 0.0178$), and between resistance classes ($p = 0.0076$) according to the Kruskal-Wallis ANOVA. Resistant families had lower stomatal densities (102 ± 4 stomata·mm^{-2}, Table 2.4 and Fig. 2.6a) in comparison to the susceptible families (116 ± 4 stomata·mm^{-2}, Table 2.4 and Fig. 2.6b).

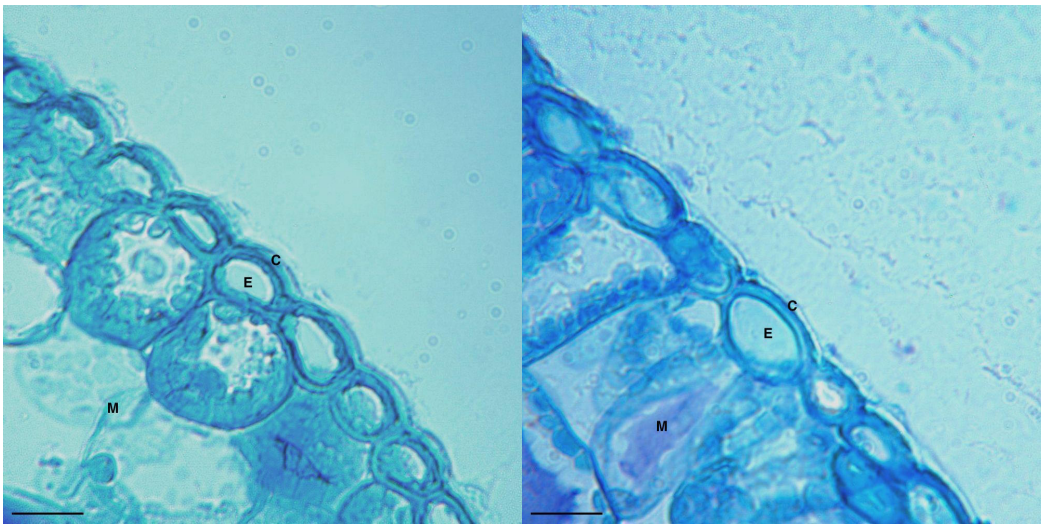

(a) **(b)**

Figure 2.5. Cuticle of seedlings of *Thuja plicata* fill-sib families with different resistance to *Didymascella thujina*. Cross sections of the adaxial surface of samples collected from the distal portion of the lowermost branch are shown. a) Resistant family 399 with a cuticle of 2.33 µm. b) Susceptible family 528 with a cuticle of 2.24 µm. The foliar samples were embedded in Quetol 651, and 5 µm sections were stained with Toluidine Blue O and photographed in a Zeiss microscope fitted with a RTKE SPOT camera. Images captured by Juan A. Aldana. C = cuticle, E = epidermal cell, M = mesophyll. Scale bars = 20 µm.

2.3.2 Climate variables of *T. plicata* site of origin associated with resistance to *D. thujina*

Seedlings from all families developed symptoms of *D. thujina* but not of *P. funerea* after nearly nine months. This result is similar to that of the seedlings screened in section 2.2.1.2. *D. thujina* severity was used as a proxy for disease resistance in the Pearson correlation and random forest analyses with climate variables. Lower severity values were associated with resistance to *D. thujina*, and higher values with susceptibility.

Table 2.3. Statistical significance (p-values) of the factors of the split-plot ANOVAs carried out on the 12 continuous histological variables studied (see also Appendix A.2). Pal. mes. = palisade mesophyll; wh. mes. = whole mesophyll; cr. pos. = crown position. * = significant factors at $\alpha = 0.05$; ** = significant factors at $\alpha = 0.01$.

	Thicknesses						Cross section areas		Thickness ratios		Cross section area ratio	Lignified cell walls
	Cuticle	Epidemis	Leaf	Leaf width	Pal. mes.	Wh. mes.	Leaf	Wh. mes.	Wh. mes. to leaf	Spongy to wh. mes.	Wh. mes. to leaf	In epidermis
Subplots												
Class	0.0130*	0.5552	0.1474	0.1290	0.4580	0.1441	0.1974	0.2338	0.3680	0.2350	0.9700	0.5133
Family(Class)	0.0797	0.0011**	0.0002**	0.8240	0.0001**	0.0004**	0.0517	0.0824	0.3000	0.1390	0.8920	0.0048**
Plot												
Crown position	0.0055**	<0.0000**	<0.0000**	0.0596	0.0018**	<0.0000**	0.0003**	0.0004**	0.0117*	<0.0000**	0.2370	0.1680
Class × cr. pos.	0.9421	0.7457	0.2978	0.3842	0.8091	0.3063	0.7269	0.7039	0.6068	0.3470	0.2520	0.8450
Family(Class) × cr. pos.	0.1200	0.0097**	0.0317*	0.3276	0.1054	0.0222*	0.8081	0.8286	0.4101	0.0430*	0.7400	0.9510

Table 2.4. Mean and standard errors, per family and resistance class, of the 13 variables studied in the histological characterization of the plant material used in this investigation. ANOVAs of the individual continuous histological variables were completed using a fixed-effects split-plot design. Kruskal-Wallis one-way ANOVAs by class and family were done on the the stomatal density data. Similar superscripts in the means of a variable refer to homogeneous groups according to the Tukey HSD all-pairwise comparisons test for the continuous variables, and to homogeneous groups from the Kruskal-Wallis all-pairwise comparisons test for stomatal density.

		Susceptible families				Resistant families				Average	
Trait	**Variable**	**525**	**528**	**582**	**583**	**399**	**685**	**687**	**689**	**Susceptible families**	**Resistant families**
Thickness	Cuticle (µm)	2.21 ± 0.05	2.33 ± 0.05	2.24 ± 0.05	2.15 ± 0.04	2.40 ± 0.06	2.37 ± 0.04	2.25 ± 0.04	2.28 ± 0.04	$2.23^{b} \pm 0.02$	$2.32^{a} \pm 0.02$
	Epidermis (µm)	$13.03^{cd} \pm 0.20$	$13.89^{abc} \pm 0.18$	$13.28^{bcd} \pm 0.22$	$14.31^{a} \pm 0.20$	$12.77^{d} \pm 0.24$	$13.83^{abc} \pm 0.30$	$13.99^{ab} \pm 0.20$	$13.56^{abcd} \pm 0.25$	13.65 ± 0.11	13.54 ± 0.13
	Leaf (µm)	$420^{d} \pm 14$	$526^{abc} \pm 16$	$500^{abcd} \pm 19$	$456^{bcd} \pm 21$	$453^{cd} \pm 22$	$547^{a} \pm 27$	$467^{abcd} \pm 16$	$537^{ab} \pm 35$	474 ± 9	501 ± 13
	Leaf width (µm)	644 ± 31	677 ± 25	673 ± 30	715 ± 50	635 ± 36	619 ± 43	617 ± 37	688 ± 46	677 ± 18	640 ± 20
	Palisade mesophyll (µm)	$39^{bc} \pm 1$	$47^{a} \pm 2$	$42^{abc} \pm 2$	$43^{abc} \pm 1$	$36^{c} \pm 1$	$45^{ab} \pm 1$	$43^{abc} \pm 2$	$44^{abc} \pm 2$	43 ± 1	42 ± 1
	Whole mesophyll (µm)	$390^{c} \pm 14$	$493^{ab} \pm 15$	$467^{abc} \pm 18$	$422^{bc} \pm 21$	$423^{bc} \pm 22$	$508^{a} \pm 26$	$439^{abc} \pm 16$	$505^{a} \pm 34$	442 ± 9	469 ± 13
Cross section area	Leaf (mm^2)	0.2675 ± 0.0147	0.3441 ± 0.0141	0.3232 ± 0.0234	0.3177 ± 0.0291	0.2758 ± 0.0201	0.2995 ± 0.0197	0.2794 ± 0.0188	0.3534 ± 0.0387	0.3126 ± 0.0108	0.3020 ± 0.0130
	Whole mesophyll (mm^2)	0.2424 ± 0.0143	0.3106 ± 0.0137	0.2929 ± 0.0223	0.2879 ± 0.0276	0.2502 ± 0.0189	0.2697 ± 0.0187	0.2532 ± 0.0183	0.3236 ± 0.0367	0.2830 ± 0.0102	0.2742 ± 0.0124
Thickness ratio	Whole mesophyll to leaf	0.9257 ± 0.0050	0.9378 ± 0.0032	0.9326 ± 0.0049	0.9212 ± 0.0067	0.9299 ± 0.0040	0.9264 ± 0.0096	0.9393 ± 0.0028	0.9361 ± 0.0039	0.9291 ± 0.0026	0.9329 ± 0.0029
	Spongy to whole mesophyll	0.8976 ± 0.0044	0.9018 ± 0.0053	0.9085 ± 0.0051	0.8934 ± 0.0047	0.9097 ± 0.0047	0.9051 ± 0.0052	0.8981 ± 0.0063	0.9013 ± 0.0072	0.8999 ± 0.0025	0.9035 ± 0.0030
Cross section area ratio	Whole mesophyll to leaf	0.9006 ± 0.0072	0.9003 ± 0.0063	0.9007 ± 0.0058	0.8983 ± 0.0098	0.9032 ± 0.0059	0.8929 ± 0.0071	0.8985 ± 0.0058	0.9061 ± 0.0069	0.9000 ± 0.0038	0.9002 ± 0.0032
Lignified cell walls	In epidermis (%)	$44^{ab} \pm 4$	$45^{ab} \pm 4$	$53^{a} \pm 4$	$49^{ab} \pm 3$	$44^{ab} \pm 4$	$54^{a} \pm 4$	$43^{b} \pm 4$	$44^{ab} \pm 3$	47 ± 2	46 ± 2
Stomata	Stomatal density (stomata·mm^{-2})	$117^{ab} \pm 10$	$112^{abc} \pm 8$	$116^{ab} \pm 7$	$121^{a} \pm 6$	$102^{abc} \pm 9$	$90^{c} \pm 7$	$95^{bc} \pm 7$	$120^{a} \pm 7$	$116^{a} \pm 4$	$102^{b} \pm 4$

2.3.2.1 Pearson correlation analysis

Twenty-nine of all climate variables studied had significant correlations with *D. thujina* disease severity at $\alpha = 0.01$ (Table 2.5). Thirteen of those 29 variables were related to the climates of the families, 11 to the climate of origin of the male parent, and five to the climate of origin of the female parent. Twelve of the 29 variables were temperature-related, 10 precipitation-related, five degree-day related, and two were summer heat-moisture indices. The five variables most highly correlated with mean family disease severity (i.e. those with the lowest significance values) were autumn precipitation (r = -0.79107, p = 0.00128), July and August maximum mean temperatures for the male parent (r = 0.84725, p = 0.00026; and r = 0.81053, p = 0.00078; respectively), winter mean minimum temperature for the female parent (r = -0.83416, p = 0.00039), and July maximum mean temperature for the family (r = 0.78801, p = 0.00138).

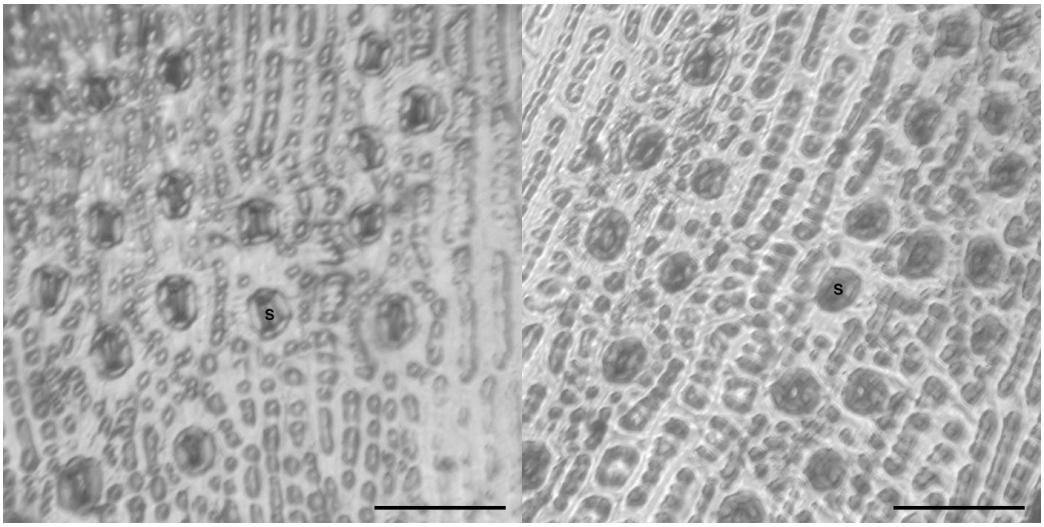

(a) **(b)**

Figure 2.6. Stomata of seedlings of *Thuja plicata* full-sib families with different resistance to *Didymascella thujina*. Impressions of the adaxial surface of samples collected from the middle portion of the lowermost branch are shown. a) Resistant family 685 with stomatal density of 105 stomata·mm^{-2}. b) Susceptible family 525 with stomatal density of 118 stomata·mm^{-2}. Stomatal impressions were produced using transparent nail polish, mounted on microscope slides and photographed in a Zeiss microscope fitted with a RTKE SPOT camera. Images taken by Juan A. Aldana. S = stoma. Scale bars = 100 µm.

2.3.2.2 Random forest analysis

Change point detection analysis on the increase in node purity scores output by random forest showed that 23 of the 96 climate variables studied were strong predictors

Table 2.5. Pearson correlations (r) and significance values (p) of the 29 variables that were significantly correlated with *D. thujina* severity at $\alpha = 0.01$ (organized by increasing probability value). Climate data for the period 1961-1990 was retrieved for each parent from ClimateBC (Wang et al., 2016a), and the family climates were calculated as the average of their parents (see also Appendix A.1). Disease severity data used were the family average of the plants screened in section 2.2.2.1.

Source	Climate variable	r	p
Male parent	July maximum mean temperature	0.84725	0.00026
Female parent	Winter mean minimum temperature	-0.83416	0.00039
Male parent	August maximum mean temperature	0.81053	0.00078
Male parent	Autumn precipitation	-0.79107	0.00128
Seedling family	July maximum mean temperature	0.78801	0.00138
Male parent	June maximum mean temperature	0.78603	0.00144
Seedling family	Autumn precipitation	-0.77676	0.00179
Seedling family	August maximum mean temperature	0.77634	0.00180
Seedling family	Autumn degree-days above 5℃	-0.76182	0.00247
Female parent	Mean annual temperature	-0.75782	0.00269
Male parent	Mean annual precipitation	-0.75499	0.00285
Seedling family	June maximum mean temperature	0.75422	0.00289
Seedling family	Winter mean minimum temperature	-0.75201	0.00303
Male parent	Spring precipitation	-0.75153	0.00306
Seedling family	Mean annual precipitation	-0.74843	0.00325
Seedling family	Spring precipitation	-0.74569	0.00343
Male parent	April precipitation	-0.74274	0.00363
Seedling family	April precipitation	-0.73844	0.00394
Seedling family	Winter degree-days below 5℃	-0.73211	0.00444
Seedling family	September precipitation	-0.72547	0.00501
Male parent	May precipitation	-0.72429	0.00511
Female parent	Autumn degree-days above 5℃	-0.72081	0.00544
Seedling family	September mean temperature	-0.71987	0.00553
Female parent	June maximum mean temperature	-0.70236	0.00743
Male parent	Summer heat-moisture index	0.69178	0.00880
Female parent	July maximum mean temperature	0.69098	0.00891
Seedling family	Summer heat-moisture index	0.69029	0.00901
Male parent	Winter degree-days below 5℃	-0.68800	0.00934
Male parent	Autumn degree-days above 5℃	-0.68523	0.00974

Table 2.6. Top 23 variables selected by change point analysis using the increase in node purity score output by random forest on 96 climate variables studied as predictors for *D. thujina* severity in seedlings of 13 *T. plicata* families. Disease severity data used were the family average of the plants screened in section 2.2.2.1, and climate data corresponded to the period 1961- 1990 and was retrieved for each parent from ClimateBC (Wang et al., 2016a). Family climates were calculated as the average of their parents (see also Appendix A.1).

Source	Climate variable	Increase in node purity score
Seedling family	June maximum mean temperature	54.62806
Male parent	June maximum mean temperature	49.88064
Male parent	July maximum mean temperature	40.45630
Seedling family	July maximum mean temperature	27.94759
Seedling family	Winter mean minimum temperature	26.78182
Female parent	Winter mean minimum temperature	25.68643
Seedling family	Winter degree-days below 5℃	23.10955
Female parent	Winter degree-days below 5℃	18.10865
Male parent	Spring precipitation	16.01758
Male parent	Autumn precipitation	12.93521
Male parent	Mean annual precipitation	12.08463
Seedling family	Autumn mean temperature	11.28917
Seedling family	Autumn degree-days above 5℃	8.84046
Male parent	May precipitation	8.73694
Seedling family	Summer degree-days above 5℃	7.98965
Seedling family	Mean annual temperature	7.72464
Male parent	Summer heat-moisture index	7.10568
Male parent	April precipitation	7.04252
Seedling family	Summer mean temperature	6.91692
Male parent	Mean annual temperature	6.79715
Male parent	Autumn mean temperature	6.71299
Female parent	Summer heat-moisture index	6.58257
Seedling family	June mean temperature	6.40409

Table 2.7. Variables common to the Pearson correlation and random forest analyses that explored the relationship between climate of origin and *Didymascella thujina* severity in 13 *Thuja plicata* families. The variables shown were significant in the correlation analysis at $\alpha = 0.01$ and were among the top 23 of the random forest analysis according to their increase in node purity scores. Climate variables related to the place of origin of the female parent, the male parent, and the average between them (i.e. the seedling family).

	Seedling family			Female parent			Male parent		
	Pearson correlation		Random forest	Pearson correlation		Random forest	Pearson correlation		Random forest
Climate variable	r	p	Increase in node purity score	r	p	Increase in node purity score	r	p	Increase in node purity score
Temperatures									
June maximum mean temperature	0.75422	0.00289	54.62806	-	-	-	0.78603	0.00144	49.88064
July maximum mean temperature	0.78801	0.00138	27.94759	-	-	-	0.84725	0.00026	40.45630
Winter mean minimum temperature	-0.75201	0.00303	26.78182	-0.83416	0.00039	25.68643	-	-	-
Precipitations									
April precipitation	-	-	-	-	-	-	-0.74274	0.00363	7.04252
May precipitation	-	-	-	-	-	-	-0.72429	0.00511	8.73694
Spring precipitation	-	-	-	-	-	-	-0.75153	0.00306	16.01758
Autumn precipitation	-	-	-	-	-	-	-0.79107	0.00128	12.93521
Mean annual precipitation	-	-	-	-	-	-	-0.75499	0.00285	12.08463
Degree-days variables									
Autumn degree-days above 5°C	-0.76182	0.00247	8.84046	-	-	-	-	-	-
Winter degree-days below 5°C	-0.73211	0.00444	23.10955	-	-	-	-	-	-
Summer heat-moisture index									
Summer heat-moisture index	-	-	-	-	-	-	0.69178	0.00880	7.10568

of the disease severity (Appendix A.18). Ten of those variables were related to the climates of the families, another 10 to the climate of origin of the male parent, and three to the climate of origin of the female parent (Table 2.6). Twelve of the 23 variables were temperature-related, five precipitation-related, four degree-day related, and two were summer heat-moisture indices (Table 2.6). The top five predictors of the disease severity (i.e. those with the highest increase in node purity scores) were winter mean minimum temperature and June-July maximum mean temperatures for the family, and June-July maximum mean temperatures for male parent (Table 2.6).

Fourteen variables were common to both the Pearson correlation and random forest analyses, nine were exclusive to the random forest output and 15 unique to the correlation analysis. Six of the 14 shared variables were temperature-related, five were precipitation-related, two were degree day variables, and one was the summer heat-moisture index (Table 2.7). June and July maximum mean temperatures, and summer heat-moisture index of the place of origin were positively correlated with *D. thujina* severity in both analyses. Precipitation variables, winter mean minimum temperature, autumn degree days above 5℃ and winter degree-days below 5℃ in the location of origin had significant, negative correlations with severity in both analyses. It is worth noting that eight of the 14 variables common to both analyses were associated with the paternal location of origin. Those variables were June and July maximum mean temperatures, summer heat-moisture index and all precipitation variables (Table 2.7). On the contrary, only one maternal variable, winter mean minimum temperature, appeared to be related to *D. thujina* severity (Table 2.7).

2.4 Discussion

This investigation explored the histological characteristics of young *T. plicata* plants related to resistance against *D. thujina*, as well as the climatic aspects of the *T. plicata* - *D. thujina* interaction in seedlings. *D. thujina* was highly virulent in the field site where the inoculations took place, and significant differences at the histological level existed between *T. plicata* seedlings resistant and susceptible to *D. thujina*. Few climate variables of family origin were associated with *D. thujina* severity and some of them showed parental kinship. All of those aspects and their relationship with *D. thujina* resistance in western redcedar seedlings are discussed below.

2.4.1 Virulence of the *D. thujina* inoculum used

The results of the screening for *D. thujina* resistance of the *T. plicata* families studied in 2013 highlight the virulence of the ascomycete. Although the average *D. thujina* spore count per hour is similar to values reported in other field studies where airborne spores from fungal species were collected (Nussbaum, 1990, Pawsey, 1964), the abundance of recorded ascospores from *D. thujina* were almost half of *P. funerea* conidiospores' counts. It is interesting that despite such abundance of conidiospores, the seedlings exposed to both pathogens developed only symptoms of *D. thujina*. The development of symptoms of *D. thujina* but not of *P. funerea* after exposure to both pathogens was also seen in the seedlings used to analyze the relationship between *D. thujina* resistance and climate variables in section 2.2.2.1, in the study presented in Chapter 3, in the seedlings of the natural conditions experiment in Chapter 4, as well as in the plants used to quantify *D. thujina* severity in Chapters 5 and 6. *D. thujina* inoculations of all those plants were completed using the same methodology and carried out in the same *T. plicata* progeny trial.

Pestalotiopsis is a species-rich clade of generalist saprophytic (Maharachchikumbura et al., 2014) and endophytic fungi (Photita et al., 2004, Strobel et al., 2000, Wei et al., 2007) with no known teleomorphs in many cases (Maharachchikumbura et al., 2014). *P. funerea* has been shown to be an endophyte of *Catharanthus roseus* (Srinivasan and Muthumary, 2009), a saprobe of dead conifer foliage (Dennis 1995, p. 217; Ellis and Ellis 1997, p. 115), a necrotroph of conifers (Bajo et al., 2008), and the causative agent of silky *Hakea*'s leaf spots (Sousa et al., 2004). *P. funerea* has also been reported to be present on the foliage of *Thuja* sp. in France (Maharachchikumbura et al., 2011), and on leaves of *T. plicata* in North America (Fernando et al. 1999; Minore 1983, p. 27), where it was associated with a dieback in the mid 1900's (Minore 1983, p. 27). The lack of symptoms of *P. funerea* in the foliage of *T. plicata* exposed to the field inoculum can be explained by the fact that *Pestalotiopsis* species are weak opportunistic pathogens that usually cause little damage (Maharachchikumbura et al., 2011) and gain access to their hosts mostly through wounds (Elliott et al. 2004, p. 28; Keith et al. 2006; McQuilken and Hopkins 2004; Wright et al. 1998). The good health of the *T. plicata* seedlings that were taken to the *D. thujina* inoculation site in Jordan River, and the care provided to them during the inoculation phase in the field, as well as during the *D. thujina* colonization phase in the Bev Glover Growth Facility, may

have impeded the initial infection by *P. funerea* and the subsequent development of the disease symptoms.

Unlike *P. funerea*, the symptoms of *D. thujina* infection were evident nine months after inoculation. The characteristic light-brown leaves with oval-shaped dark-brown *D. thujina* ascocarps in the middle were visible to the naked eye, and those symptomatic leaves were scattered through the foliage as described in Durand (1913) and Kope (2000). The asci of symptomatic leaves were clavate in shape and unitunicate, with two spores per ascus as reported (Durand, 1913, Kope, 2000). The ascospores that were collected on microscopes slides, and those that landed on foliage of *T. plicata* both had the characteristic ovoid shape and olive-brown colour reported by Durand (1913) and Kope (2000), and were within the size-range reported by Kope (2000). At the ultrastructural level, ascospores that had landed on foliage and had released the adhesive extracellular matrix showed the typical ornamented surface described by Kope (2000).

The absence of germination tubes within four days in the *D. thujina* ascospores that landed on *T. plicata* foliage, and their presence in microscope slides within three days, suggests that the ascospores might perform direct penetration to access the host. Pawsey (1960) reported similar observations of germination tubes being produced by *D. thujina* ascospores on microscope slides, and Søegaard (1969, p. 298) showed that under specific conditions, *D. thujina* spores could be germinated in bean agar. Porter (1957) and Pawsey (1960) also reported the absence of *D. thujina* germination tubes on *T. plicata* foliage and all evidence led both Pawsey (1960) and Søegaard (1966) to suggest that direct penetration of the host by the pathogen might take place. Visualization of direct penetration of *T. plicata* foliage by *D. thujina*'s germination tube was eventually achieved by studying transverse cuticular sections of infected *T. plicata* foliage stained with cotton blue in lactophenol, and was reported by Søegaard (1969, p. 299).

2.4.2 Histological traits of *T. plicata* associated with resistance to *D. thujina*

Although there are no published studies on the variability of *D. thujina* resistance in seedlings of *T. plicata*, the variation in the disease severity of the eight families

screened in 2013 and that of the 13 families used to analyze the relationship between climate and *D. thujina* resistance (section 2.2.2.1) agrees with reports on the variability of that trait in adult trees (Russell et al. 2007; Russell and Yanchuk 2012; Søegaard 1969, p. 323). Variation in the resistance to *D. thujina* among adult *T. plicata* trees was first observed last century (Søegaard, 1969, p. 323), and formally reported by Russell et al. in the 2000's, when it was shown that *T. plicata* populations of British Columbia occurring in wetter and milder environments had lower *D. thujina* severity than populations from drier and warmer environments (Russell et al., 2007, Russell and Yanchuk, 2012). Quantitative variation in the resistance to fungal diseases is common in plants (Burdon, 2001, Carson and Carson, 1989, Sniezko and Koch, 2017, Telford et al., 2015) and has also been reported in pathosystems like *Pinus taeda* - *Fusarium circinatum* (Quesada et al., 2010), *Juniperus* sp. - *Pseudocercospora juniperi* (Zhang et al., 1997), *P. taeda* - *Cronartium quercuum* (Wilcox et al., 1996) and *Pinus monticola* - *Cronartium ribicola* (Liu et al., 2013). Quantitative variation is at the core of breeding for improved pathogen resistance (Burdon, 2001, Carson and Carson, 1989, Sniezko and Koch, 2017, Telford et al., 2015, White et al., 2007), and the quantitative nature of the resistance to *D. thujina* in *T. plicata* (Russell et al., 2007) makes it a suitable trait for genetic improvement (Grattapaglia and Resende, 2011, Neale and Kremer, 2011, Rostoks et al., 2005, White et al., 2007). Breeding for *D. thujina* would have potential long-term benefits to British Columbia's forests given the predicted risk of increased *D. thujina* intensity under future climate change scenarios (Gray et al., 2013).

To date, there are no reports on *T. plicata* traits associated with variability in the resistance to *D. thujina*. However, the histological analyses carried out on the families investigated in section 2.2.1.3 showed that the cuticles of the families resistant to *D. thujina* were significantly thicker than those of the susceptible families. The cuticle is the first barrier that biotrophic fungi must pass before getting access to the host (Agrios 2005, p. 210; Anker and Niks 2001; Gees and Hohl 1988; Hau and Rush 1982; Roundhill et al. 1995; Sherwood 1996; Zinsou et al. 2006), and its damage releases elicitors (Serrano et al., 2014), which lead to prompt defense responses by the host (Agrios 2005, p. 213; Vidhyasekaran 2008, p. 55). Thicker cuticles are commonly associated with increased resistance to pathogens that perform direct penetration (Agrios 2005, p. 210), and have been reported in pathosystems like olive plants resistant to *Fusicladium oleagineum* (Rhouma et al., 2013), or *Eucalyptus nitens* trees resistant to

Mycosphaerella spp. (Smith et al., 2006). Thick cuticles were also recorded in the only species fully resistant to *D. thujina* investigated in this thesis, the *Thuja standishii* clonal line studied in Chapter 6. Given that *D. thujina* performs direct penetration to infect *T. plicata*'s leaves (Søegaard, 1969, p. 299), it is possible that thick cuticles play an important role in the defense against this pathogen in *T. plicata*, either as a physical barrier, as a system that triggers fast defense responses by the host, or both.

The other anatomical variable that rendered significant differences between *T. plicata* seedlings resistant and susceptible to *D. thujina* was the stomatal density, with susceptible families having higher densities than resistant plants. Natural openings are common entry points for pathogens like bacteria and viruses (Agrios 2005, p. 88; Dickinson 2003; Huang 1986; Ramos et al. 1992; Sharma 2006, p. 4.6; Zinsou et al. 2006), and stomatal densities have been reported to be lower in some species resistant to those kinds of diseases (McKown et al., 2014, Ramos et al., 1992). Obligate parasitic fungi, like *D. thujina* (Durand 1913; Søegaard 1956; Søegaard 1969, p. 294), do not enter their host through natural openings or wounds, but by performing direct penetration (Agrios 2005, p. 88; Gees and Hohl 1988; Roundhill et al. 1995; Sharma 2006, p. 4.6; Sherwood 1981; Søegaard 1969, p. 299). In this investigation, no germination tubes growing towards stomata or wounds as entry points were observed on the SEM micrographs of the *D. thujina* ascospores examined, and earlier histopathology studies on the compatible *T. plicata* - *D. thujina* interaction reported similar findings (Pawsey 1960; Porter 1957; Søegaard 1969, p. 299). Stomatal densities tend to be lower in plants from humid environments (Abrams et al., 1994, Bakker, 1991), so the lower densities of the families resistant to *D. thujina* studied in section 2.2.1.3 may be a sign of adaptation of their resistant parents to humid environments as *T. plicata* populations resistant to *D. thujina* originate from cooler and wetter environments (Russell et al., 2007, Russell and Yanchuk, 2012). Low stomatal density may contribute to defense against attacks by pathogens other than *D. thujina*, which might be present in humid climates, given that those environments are ideal for microorganisms like bacteria to infect and colonize their hosts (Hirano and Upper, 1983, Leben, 1981, Schwartz et al., 2003, Underwood et al., 2007). High stomatal density was also found in the *T. plicata* seedling line 124 studied in Chapter 6, which was susceptible to *D. thujina*, in comparison with the more resistant *T. plicata* seedling line 129 analyzed in that chapter. The relationship between *T. plicata* stomatal density and climate, and between stomatal density and resistance to foliar pathogens that penetrate through

natural openings should be investigated in future studies.

2.4.3 Climate variables associated with resistance to *D. thujina*

The analyses conducted to determine the relationship between *D. thujina* severity, and the climate of origin of the full-sib families and their parents', revealed that only a few variables were related to the disease severity. Those variables included temperature, precipitation, summer heat-moisture index, and degree-day variables. Temperature and precipitation are climate variables commonly related to the pathogenicity and virulence of foliar diseases, with wet regions that have cool temperatures being more suitable for pathogens to flourish than drier and hotter places (Agrios 2005, p. 249; Elad and Pertot 2014; Hardwick 2002; Rosenzweig et al. 2001; Salinari et al. 2006; Sharma 2006, p. 6.2; Talley et al. 2002). Favourable temperature and precipitation accelerate the development of diseases like leaf blotch, brown rust, yellow rust and eyespot in wheat (Wiik and Ewaldz, 2009), *Pantoea* and *Xanthomonas* leaf blights in onion (Schwartz et al., 2003), *Phytophthora infestans* in potato (Hannukkala et al., 2007), *Cylindrocladium quinqueseptatum* in *Eucalyptus camaldulensis* (Booth et al., 2000), and *Dothistroma* needle blight in pines (Woods et al., 2016). July maximum mean temperature, summer heat-moisture index, May precipitation and spring precipitation were significantly correlated with *D. thujina* severity in this investigation, and were also amongst the top disease severity predictors output by the random forest analysis. Those variables had previously been shown to be good descriptors of the best linear unbiased estimators of *D. thujina* intensity in field environments (Gray et al., 2013), and furthermore, spring precipitation has also been reported as an important contributor variable to the model developed by Gray et al. (2013) to predict the future risk of *D. thujina* intensity in British Columbia.

Some of the climate variables related to *D. thujina* severity that were found in this investigation, such as June and July maximum mean temperatures and summer heat-moisture index, had significantly positive correlation with disease severity. June maximum mean temperatures of the places of origin of the seedlings and parents studied ranged between 14.7℃ - 19.9℃, while July's maximum mean temperatures were between 16.8℃ - 22.8℃. Plants with low disease severity scores occurred in climates within the optimal temperature ranges reported for *D. thujina* ascospore discharge

(10℃ -16℃; Søegaard 1966), and germ tube germination (13℃ -15℃; Pawsey 1960), whereas susceptible plants were from ecosystems with ideal temperatures for ascocarp development (13℃ - 20℃; Søegaard 1966 and Søegaard 1969, p. 309). Summer heat-moisture index of the place of origin of the male parent, which is a measure of summer dryness (Wang et al., 2016a), ranged between 13.9℃·mm^{-1} and 68.0℃·mm^{-1}, and *D. thujina* severity was higher in plants coming from drier locations with higher indices. The above data suggest that susceptible plants are associated with warmer and drier climates, where *D. thujina* ascospores cannot survive; however, these plants can be successfully infected if exposed to *D. thujina* inoculum. The highest temperature limit for the germination of *D. thujina* ascospores is 28℃ (Kope and Trotter, 1998a), so *T. plicata* populations that occur in regions with high temperatures in June and July may have not evolved resistance mechanisms to the fungus because high temperatures will render the spores non-viable. Similarly, populations in dry regions will not need to evolve defense systems against *D. thujina* given that high levels of humidity are needed for ascospore discharge (Søegaard 1966 and Søegaard 1969, p. 295).

In contrast to the summer heat-moisture index and temperature variables mentioned above, variables like precipitation and winter minimum mean temperature were negatively correlated with *D. thujina* severity. The male parents' annual mean precipitation ranged between 793 mm and 4,039 mm, and the spring precipitation between 151 mm and 873 mm. Disease severity was lower in plants coming from wetter environments, which are regions where the prevalence of *D. thujina* is high. Gray et al. (2013) showed that sites in British Columbia where *D. thujina* is present have an average mean annual precipitation of 2,772 mm and an average mean spring precipitation of 620 mm, while sites with absence of *D. thujina* had an average mean annual precipitation of 1,699 mm and an average mean spring precipitation of 335 mm. The precipitation of the places of origin of the resistant families and parents studied here were higher than those reported in Gray et al. (2013), while those values in regions where the susceptible families and parents originated were lower than in Gray et al. (2013). Winter minimum mean temperatures in the places of origin of the seedling families and their female parents were between -9.8℃ and 0.5℃. The reported mean minimum winter temperature in places associated with *D. thujina* is -1.1℃, but it is -4.0℃ in places where the blight is absent (Gray et al., 2013). The low temperature threshold for *D. thujina* ascospore discharge of and germination is 5℃ (Kope and Trotter 1998a; Pawsey 1960; Søegaard 1969, p. 309), and spores landing on *T. plicata*

foliage can remain viable for five months at that temperature (Pawsey 1960; Søegaard 1969, p. 309). The higher disease severities in plants coming from places with freezing winters may be due to the environment rendering the ascospores non-viable, so that plants in those locations may have not evolved defense mechanisms against *D. thujina*.

Other variables negatively correlated with *D. thujina* severity were winter degree-days below 5℃ and autumn degree-days above 5℃. The values of those variables in the places of origin of the families ranged between 3 - 61 and 214 - 415, respectively. Degree-days are a common measure of heat accumulation used to describe the amount of time necessary for completion of specific biological processes (McMaster and Wilhelm, 1997). The number of degree-days needed for *D. thujina* ascocarp development and ascospore release after successful infection varies depending on the conditions. For example, these processes take 1,071 degree-days in 77 days in *T. plicata* seedlings maintained at 19℃ in incubators, while they take 1,185 degree-days in one growing season in nursery-grown seedlings, and 1,476 degree-days accumulated in two growing seasons in forest areas (Kope and Trotter, 1998a, Kope, 2000). The negative correlation between *D. thujina* severity and degree-day accumulation (especially above 5℃ in autumn) suggests that plants in milder environments, where degree-days accumulate more quickly, are more resistant to the disease than plants occurring in cold locations. As spores of *D. thujina* are viable at temperatures higher than 5℃ (Kope and Trotter 1998a; Pawsey 1960; Søegaard 1969, p. 309), plants from milder environments may have coexisted with the blight long enough to evolve resistance mechanisms to the pathogen.

In general, both the positive and negative correlations between disease severity and climate variables show that, *T. plicata* parents and families that come from areas with optimal climatic conditions for the infection and development of *D. thujina* had lower disease severities than plants that originate in regions with unfavourable conditions for the biotroph. This may be a sign of co-evolution between host and pathogen, and natural selection for resistance to the pathogen appears to have occurred in those populations. The evolution of resistance mechanisms against diseases is common in populations under selection pressure by pathogens, and the absence of such evolutionary force usually leads to a lack of resistance mechanisms against pathogens in populations that have not contacted the pathogen (Barrett and Heil, 2012, Burdon and Thrall, 2009, Frank, 1993, 1992, Karasov et al., 2014, Occhipinti, 2013).

Plant-pathogen co-evolution appears to be taking place in the *T. plicata* - *D. thujina* pathosystem based on the results of this study, and other reports showing that *D. thujina*-resistant populations occur in wetter and milder areas than susceptible populations (Russell et al., 2007).

2.5 Conclusions

This investigation examined the relationships between 1) *T. plicata* foliar histology and resistance to *D. thujina*, and 2) climate of origin of *T. plicata*'s young plants and pathogen resistance. The inoculations carried out in the field in a *T. plicata* progeny trial in Jordan River showed the high virulence of *D. thujina* in comparison to *P. funerea*, although the latter had the most abundant propagules on the site.

T. plicata seedlings from families resistant to *D. thujina* had significantly thicker cuticles in relation to the susceptible families, which may resist penetration by *D. thujina*. Resistant plants also had significantly lower stomatal densities, but it is unknown whether stomata are involved in *D. thujina* defense. Lower stomatal densities in the resistant plants may be related to adaptation to the humid environments where they originate or to the presence of foliar pathogens that enter through natural openings in such environments. The relationship between humid environments and stomatal density in western redcedar, as well as that between *T. plicata* bacterial foliar pathogens and stomatal density should be studied in future investigations.

Few of the climate variables studied had a strong relationship with *D. thujina* severity. The Pearson correlation and random forest analyses showed that families and parents that occur in humid and cool areas, suitable for *D. thujina*, had lower disease severities than families originating from dry and warm environments, which are unsuitable for *D. thujina* infection and development. Such results agree with previous reports, and suggest a possible co-evolution between *T. plicata* and *D. thujina*.

Chapter 3

Constitutive chemical and gene expression differences between *Thuja plicata* seedlings resistant and susceptible to *Didymascella thujina*

3.1 Introduction

Metabolism is defined as the sum of all anabolic and catabolic reactions that take place within an organism (Beattie 2006; Berg et al. 2007, p. 409; Miller and Tanner 2008, p. 385; Voet and Voet 2004, p. 549), and is commonly divided into primary and secondary in plants (Aharoni and Galili 2011; Hartmann 1996; Heldt 2005, p. 403; Heldt and Piechulla 2010, p. 399). Primary metabolism refers to the basic functions that any plant must complete in order to survive, such as photosynthesis, respiration, reproduction, growth and development, which leads to the production of metabolites that are commonly found across all plants (Aharoni and Galili 2011; Hartmann 1996; Heldt 2005, p. 403; Heldt and Piechulla 2010, p. 399). Secondary metabolism, in contrast, results in the production of specialized compounds that tend to occur in specific taxa (Aharoni and Galili 2011; Hartmann 1996; Heldt 2005, p. 403; Heldt and Piechulla 2010, p. 399). Those secondary compounds have ecological roles that include protection against environmental factors and signalling, among others (Aharoni and Galili 2011; Hartmann 1996; Heldt 2005, p. 403; Heldt and Piechulla 2010, p. 399). Plant secondary metabolites are produced from branches of well-know pri-

mary metabolism pathways and are usually divided in three main categories: phenolics, terpenes/isoprenoids and nitrogen/sulfur containing compounds (Aharoni and Galili, 2011).

An important role of secondary metabolites is plant defense (Aharoni and Galili 2011; Hartmann 1996; Heldt 2005, p. 403; Heldt and Piechulla 2010, p. 399). Plants are resistant to most pathogens due to nonhost resistance (Agrios 2005, p. 134; Sharma 2006, p. 3.4; Westerink et al. 2004). However, plants from different taxa can be susceptible to various unspecialized pathogens, but they can also be infected by very specialized pathogens (Agrios 2005, p. 134; Holliday 1989, p. 274). Different plant clades have evolved to produce specific metabolites to defend themselves against pathogens (Aharoni and Galili 2011; Bednarek 2012; Hartmann 1996; Heldt 2005, p. 403; Heldt and Piechulla 2010, p. 399). For example, grapevines produce fungicidal stilbene derivates like viniferin (Heldt 2005, p. 447; Heldt and Piechulla 2010, p. 443), and monocots like wheat, rye and corn produce hydroxamic acids (Ahmad et al., 2011, Kumar et al., 1994, Leighton et al., 1994), which confer protection against some fungi (Erb et al., 2011, Song et al., 2011). Besides defense, the preferred synthesis of specific secondary metabolites in certain taxa can be due to other factors like nutrient availability. For instance, nitrogen-fixing legumes tend to produce more nitrogen-containing metabolites like alkaloids, amines, non-protein amino acids and glucosinolates than plants that do not fix nitrogen (Wink, 2013).

Thuja plicata (western redcedar) is well known for its heartwood extractives, which confer weathering protection (Chedgy et al., 2007a, Lim et al., 2007, Morris and Stirling, 2012, Stirling et al., 2017). They include γ-thujaplicin, β-thujaplicin, β-thujaplicinol, (-)-plicatic acid, methyl thujate and thujic acid (Chedgy et al., 2007a,b, Morris and Stirling, 2012, Stirling et al., 2017). β-Thujaplicin and γ-thujaplicin inhibit some fungi (Lim et al., 2007, Stirling et al., 2017), and their antimicrobial properties have been compared to those of commercial products (Arima et al., 2003, Barton and MacDonald, 1971, Inamori et al., 1999, 2000, Morita et al., 2004, Sakagami et al., 2000) like pentachlorophenol (Barton and MacDonald, 1971, Daniels and Russell, 2007). Plicatic acid has also been compared to the commercial product zinc chloride (Barton and MacDonald, 1971, Daniels and Russell, 2007). The most prevalent compounds in *T. plicata* heartwood are plicatic acid, which gives the timber its distinctive coloration, and the tropolones β-thujaplicin, γ-thujaplicin and thujic

acid (Chedgy et al., 2007a, Lim et al., 2007). The combination of all those extractives in the species' wood results in the durability and beautiful appearance that make *T. plicata* one of the preferred softwoods for outdoor applications (Daniels et al., 1997, Gonzalez, 2004, Western Red Cedar Export Association, 2004).

The profile of secondary metabolites in *T. plicata* foliage differs from that of the heartwood, leaves having high concentrations of terpenes (Shalev et al., 2018, von Rudloff and Lapp, 1979, von Rudloff et al., 1988, Vourc'h et al., 2001, 2002). However, the variability in the foliar terpene profiles of adult *T. plicata* trees is low among British Columbian populations, even between those in interior and costal regions (von Rudloff and Lapp, 1979, von Rudloff et al., 1988). The terpenes with the highest relative concentrations in adult trees are α- thujone, β-thujone, sabinene and terpinen-4-ol (Tsiri et al., 2009, von Rudloff et al., 1988), although small amounts of β-pinene, myrcene, α-terpinene, α-terpineol α-thujene, *p*-cymene, β-phellandrene, fenchone and geranyl acetate have been reported (von Rudloff and Lapp, 1979). In *T. plicata* seedlings, monoterpenes occur at higher concentrations than other terpenes (Foster et al., 2016, Vourc'h et al., 2001, 2002). The terpenes most frequently found in seedlings are α-thujone, β-thujone and sabinene as well, but also myrcene, α-pinene and limonene (Foster et al., 2016, Shalev et al., 2018, Vourc'h et al., 2001, 2002). Terpene profiles also differ depending on the type of foliage in seedlings, scales having more monoterpenes than needles (Foster et al., 2016). Needles have higher content of sabinene and α-pinene, while scales have higher levels of α- and β-thujone (Foster et al., 2016). Western redcedar terpenes have been shown to have antimicrobial (Castillo et al., 2012, Mohanraj, 2014, Sarup et al., 2015, Tsiri et al., 2009) and deer browsing deterrence properties (Vourc'h et al., 2001, 2002). Other chemicals reported in *T. plicata*'s foliage are dilignol rhamnosides (Manners and Swan, 1971, 1977), biflavonyl pigments (Rahman et al., 1972), and high amounts of calcium (Daubenmire, 1953), although the functions of these are not clear.

Didymascella thujina (cedar leaf blight) is the most virulent foliar pathogen of *T. plicata* (Kope 2000; Minore 1983, p. 27; Minore 1990; Pawsey 1960; Russell et al. 2007; Søegaard 1956). The ascomycete is an obligate parasite (biotroph), responsible for nursery diebacks in North America (Dennis and Sutherland, 1989, Frankel, 1990, 1991, 1992, Kope and Trotter, 1998a, Kope, 1992, Kope and Dennis, 1992, Kope and Sutherland, 1994a, Kope et al., 1996a, Trotter et al., 1994), and losses in Eu-

rope in the last century (Alcock, 1928, Fernández-Magan, 1974). *D. thujina* attacks preferentially the youngest foliage of the current growing season (Kope and Trotter, 1998a, Kope, 2004, Kope and Sutherland, 1994a), and symptoms develop during the second season when apothecia mature and spores are released (Kope and Trotter, 1998a, Kope, 2000, Pawsey, 1957a, 1960, Søegaard, 1969). The most common control method for *D. thujina* infections is the use of pesticides like mancozeb (Kope and Trotter, 1998b, Kope et al., 1996a), propiconazole (Kope and Trotter, 1998b), cycloheximide (Burdekin and Phillips, 1971), cycloheximide derivates (Pawsey, 1962a), among others (Frankel, 1990, 1991, 1992).

T. plicata essential oil foliar extracts are known to inhibit several fungi (*Candida tropicalis*, *Candida albicans* and *Candida glabrata*) and bacteria (*Escherichia coli*, *Klebsiella pneumoniae*, *Enterobacter cloacae*, *Pseudomonas aeruginosa*, *Staphylococcus epidermidis* and *Staphylococcus aureus*) at minimal inhibitory concentrations of 0.87-1.12 $mg{\cdot}mL^{-1}$ and 0.50-1.25 $mg{\cdot}mL^{-1}$, respectively (Tsiri et al., 2009). α-Thujone and β-thujone have also been shown to be the strongest antimicrobial compounds of the *T. plicata*'s essential oils given their inhibiting properties at lower minimal inhibitory concentrations (0.09-0.83 $mg{\cdot}mL^{-1}$; Tsiri et al. 2009). To date, it is unknown whether leaf terpenes and/or other leaf compounds/elements play any roles in *T. plicata* defense against foliar pathogens. In order to understand the relationship between foliar elements/compounds and resistance against *D. thujina* in *T. plicata*, the chemical composition differences between *T. plicata* seedlings resistant and susceptible to *D. thujina* were investigated, with special emphasis on terpenes. *RNA*-Seq analysis was also carried out on the same plant material to detect general constitutive gene expression differences between the two resistance classes, as well as constitutive differences in the expression levels of selected sequences involved in terpene synthesis.

3.2 Methodology

3.2.1 Experimental design

Two *T. plicata* full-sib families (685 and 583, see Appendix A.1), with dissimilar resistance to *D. thujina* (high and low, respectively), were used in this investigation. The families were selected based on a pilot *D. thujina* severity screening study carried out on seedlings infected between May 2 and July 18, 2012 in a *T. plicata* progeny

trial in Jordan River (see below). Seed from each of the two chosen families was sown into Beaver Styroblock containers 45/340 (Stuewe and Sons., Tangent, OR, USA) in a fibreglass house at the Cowichan Lake Research Station (Mesachie Lake, British Columbia) in spring 2012, and the seedlings were grown for a year under standard greenhouse growing procedures. The one-year-old seedlings were then exposed to natural *D. thujina* inoculum between May 8 and June 28, 2013 by placing the styroblocks under 10-year-old trees in a *T. plicata* progeny trial at Jordan River BC (48° 25' 24.52" N, 124° 1' 27.69" W, elev. 76 m) that showed severe *D. thujina* disease symptoms and ongoing sporulation. The site is located in the CWHxm2 zone of the Biogeoclimatic Ecosystem Classification System (Green and Klinka, 1994). The plants, designated as the "exposed to *D. thujina*" treatment (CLB^+), were then taken to the Bev Glover Growth Facility (University of Victoria, Victoria, British Columbia) and maintained in a glasshouse until they developed *D. thujina* symptoms. While in the glasshouse, the plants were watered weekly and fertilized monthly with 100 ppm N from Peter's 20-7-19 Conifer Grower fertilizer (Jr. Peters Inc, Allentown PA, USA). There were also "never-exposed to *D. thujina*" seedlings (CLB^-), which were additional seedlings from the same two families not taken to the infection site, but kept at the Bev Glover Growth Facility while seedlings of the "exposed to *D. thujina*" treatment were being infected. These plants were maintained under the same conditions at the Bev Glover Growth Facility and for the same length of time as the exposed seedlings.

Three seedlings from each family × infection treatment were sampled after symptoms had developed in the plants exposed to *D. thujina* (spring 2014, see Appendix A.6). Foliage from each seedling was collected quickly from the two midmost branches. The material was immediately cut in smaller pieces (∼5 mm-long) and bulked before splitting it in two: one half for *RNA*-Seq analysis, and the other half for chemical analysis. The foliage for both analyses was flash frozen, placed immediately in dry ice and stored at -80℃ until further processing.

Confirmation of the disease

Infection with *D. thujina* was confirmed in three ways: 1) visual quantification of the severity of the disease on seedling foliage, 2) spore identification of *D. thujina* on seedling foliage using scanning electron microscopy, and 3) BLASTn search in the assembled transcriptome (see below) for the two internal transcribed spacer 2 (ITS2)

sequences from *D. thujina* available on GenBank (IDs KT875766 and KT875767). Severity was measured as the percentage of foliar area blighted (brown or black) using colour analysis in WinRHIZO Pro v. 2009c (Regent Instruments Inc., QC, Canada) Leaf images were digitized in an Epson Perfection v750 scanner (Epson Canada Ltd., Markham ON, Canada). Severity data were analyzed using one-way Analysis of Variance (ANOVA) with family as factor in R (R Core Team, 2015). The families were then classified as resistant or as susceptible (see section 3.3).

Identification of *D. thujina*'s spores was done in ∼3 mm-long sections of *T. plicata* foliage collected from the aforementioned branches. The samples were fixed overnight in 2.5% glutaraldehyde (diluted in 0.1 M Sörensen's phosphate buffer pH 7.2; Ruzin, 1999, pp. 227), and then washed twice in the buffer, dehydrated in an ascending ethanol series (50%, 70%, 80% and 90%), and changed twice in anhydrous ethanol (30 min each step). Critical point drying was done in a Leica EM CPD300 system (Leica Microsystems Inc., Richmond Hill ON, Canada), and gold coating in an Edwards S150B Sputter Coater (Edwards Canada, Quebec QC, Canada). Samples were examined and photographed in a Hitachi S-3500N Scanning Electron Microscope (Hitachi High-Technologies Canada Inc., Toronto ON, Canada).

3.2.2 Chemical composition

The following compounds and elements were measured from the foliage sampled: carbon, nitrogen, cellulose, lignin, fibre, starch, sugars, terpenes and mineral nutrients (see Appendix A.19 for the full list). Carbon and nitrogen were quantified by the Nutrient Analysis Laboratory at the Centre for Forest Biology (University of Victoria, Victoria BC, Canada). Samples for carbon and nitrogen analyses were dried at 60℃ for 48 h, and then ground with a Wig-L-Bug grinding mill (International Crystal Laboratories, NJ USA). The samples were then dried overnight before being packaged. The packaging was done in tin pans (10×10mm; Elemental Microanalysis Ltd., Devon UK) and the measurements were carried out in a FlashEA® 1112 Nitrogen and Carbon Analyzer (Thermo Scientific™ Wilmington DE, USA).

The rest of the analyses were carried out by the Analytical Laboratory of the Ministry of Environment and Climate Change Strategy (Victoria BC, Canada). Cellulose,

lignin and fibre were analyzed with the acid detergent fibre and acid detergent cellulose methods developed for forage fibre analysis (Goering and Van Soest, 1970). Starch was quantified with the third enzyme method in Rose et al. (1991), and sugars with the anthrone reagent procedure by Ebell (1969). Terpenes were quantified from foliage samples ground in liquid nitrogen with a chilled pestle and mortar. Four millilitres of methanol were mixed with 0.25-0.50 g of ground material for 48 h to extract the terpenes. *T. plicata* extractive standards were prepared mixing 0.05-0.50 g of the respective standard with 100 mL of methanol. The amount per standard varied depending on the anticipated concentrations in the samples analyzed. Samples and standards were analyzed using 30 m $\times$ 0.25 mm, d_f 0.25 µm capillary GC columns in a Clarus Gas Chromatograph (PerkinElmer Inc., Waltham MA, USA) following the manufacturer's instructions.

Mineral analyses were completed by mixing 0.25 g of fine milled foliage with 4.0 mL digestion reagent (150 µg scandium$\cdot L^{-1}$ prepared in 70% nitric acid) in 15 mL quartz tubes. The digestion was carried out in an Ultrawave Microwave Digestion System (Milestone Inc., Shelton CT, USA) following the manufacturer instructions, and elements were measured with inductively coupled plasma optical emission spectroscopy analysis using the scandium from the digestion step as standard.

Statistical analyses

Principal Components Analysis (PCA) on the correlation matrix was performed to explore the whole dataset using FactoMineR (Lê et al., 2008). Categorical stability selection (Meinshausen and Bühlmann, 2010) was used to select chemical variables that differentiated between 1) families and 2) infection treatment, and regression stability selection was carried out to detect chemical variables that best explained *D. thujina* severity (disease severity was the response variable). Stability selection is a variable selection technique that allows detection of the best variables that explain a response variable arbitrarily chosen by the researcher (either continuous or categorical), and produces an organized list of predictors based on a decreasing score output by the analysis (Meinshausen and Bühlmann, 2010). Stability selections were completed using the randomized lasso algorithm (provided in the Python scikit-learn package). Changepoint with the AMOC criterion on variance (Killick and Eckley, 2014) was used to determine the number of ranked variables to keep from each of

the three stability selection analyses. Changepoint is a methodology that detects the point where a time series changes. In the case of stability selection, it was used to detect the variable with the steepest drop in score. Variables that were kept by changepoint from each stability selection analysis above were used in further analyses (i.e. ANOVAs or Pearson correlations completed in R; R Core Team 2015). Two-way ANOVAs with family and infection treatment as factors and their interaction were conducted on the chemical variables that were kept from each of the categorical stability selections (see Appendix A.22 for the statistical model). Pearson correlation analyses were completed between the severity result from each sampled seedling and the chemical variables chosen by the regression stability selection using package Hmisc (Harrell Jr. and Dupont, 2016).

3.2.3 Gene expression

RNA extraction

RNA extraction was done using a modified version of the protocol by Rajakani et al. (2013). One-and-a-half grams of the sampled foliage were ground in a pre-chilled mortar and pestle using liquid nitrogen. The ground material was transferred to a 50 mL Nalgene™ Oak Ridge high-speed centrifuge tube (Life Technologies Inc., Burlington ON, Canada) and the mortar rinsed with liquid nitrogen. Ground foliage with liquid nitrogen was then placed in a -20℃ freezer to let the nitrogen evaporate. Once the material was dry, 20 mL of preheated 2% CTAB with activated charcoal were added to each sample (200 mM Tris-Cl pH 8.0, 50 mM EDTA pH 8.0 and 2.5 M NaCl, 0.05% activated charcoal, 1.5% PVPP, 3% β-mercaptoethanol; the last three components were added just before using the extraction buffer). The samples were thoroughly vortexed and incubated at 65℃ for 15 min with intermittent shaking. The mixture was then cooled to room temperature (RT) and centrifuged at 17,211 $\times$ g for 20 min at 4℃. The supernatant was recovered in a new 50 mL tube and combined with an equal volume of chloroform, mixed by inversion and centrifuged at 17,211 $\times$ g for 20 min at 4℃. The previous purification step was repeated once more (for a total of two chloroform extractions). The supernatant from the last extraction was then transferred to a new 50 mL tube, mixed with 1/4 volume of 10M lithium chloride and incubated overnight at 4℃.

The next day, samples were centrifuged at 20,199 $\times$ g for 30 min at 4℃. The su-

pernatant was discarded while the pellet was re-suspended in a mixture of 500 µL SSTE (1M NaCl, 0.5% SDS, 10mM Tris HCl pH 8.0, 1mM EDTA pH 8.0) and 400 µL phenol (pH 8.0). The suspension was transferred to a 1.5 mL Eppendorf® tube to which 100 µL of chloroform were added. The solution was vortexed and centrifuged at 18,407 × g for five min at RT. The supernatant was transferred to a new 1.5 mL tube, mixed with 300 µL of chloroform, vortexed and centrifuged again for 5 min at 18,407 × g at RT. The supernatant from the last extraction was placed in a new 1.5 mL tube to which 1/10 volume of 3M sodium acetate and an equal volume of 100% isopropanol were added. The solution was incubated for 25 min at -20℃, and then centrifuged at 20,626 × g at 4℃ for 33 min. The supernatant was discarded, 1.0 mL of 75% chilled ethanol was added to the pellet and mixed by inversion. The mixture was centrifuged for 5 min at 20,626 × g at 4℃, the supernatant was discarded once more to ensure that no ethanol remained (so that the pellet dried at RT). The total extracted *RNA* was suspended in 50 µL of DEPC-treated water, quantified in a NanoDrop™ 2000 Spectrophotometer (Thermo Scientific™ Wilmington DE, USA), and checked for integrity in a 1X MOPs, 1.0% formaldehyde-agarose gel.

m*RNA* enrichment, library production and sequencing

m*RNA* enrichment was done using protocol C of the Thermo Scientific™ MagJET m*RNA* Enrichment Kit (Life Technologies Inc., Burlington ON, Canada). Libraries were made using the NEB Next® Ultra™ *RNA* Library Prep Kit for Illumina® v. 1.2. (New England BioLabs® Inc., Ipswich MA, USA). *DNA* was purified as required using the Thermo Scientific GeneJET NGS Cleanup Kit (Life Technologies Inc.), and size selection (∼450 bp fragment size) was completed with the Thermo Scientific MagJET NGS Cleanup and Size Selection Kit (Life Technologies Inc.). Libraries were barcoded using the NEB Next® Multiplex Oligos for Illumina® - Index Primers Set 1 (New England BioLabs® Inc.). Quality control and quantification of the individual libraries was done with a *DNA* 1K Analysis Kit (Bio-Rad Laboratories, Mississauga ON, Canada) in an Experion™ Automated Electrophoresis Station (Bio-Rad Laboratories). The final pool consisted of 40 ng of *DNA* per library. 100 bp pair-end sequencing was completed in a single lane of an Illumina® HiSeq 2000 sequencer at Genome Quebec Innovation Centre (Montreal QC, Canada).

Bioinformatics

Appendix A.27 outlines the pipeline used for the bioinformatics analyses. All of the processes described below were completed on the WestGrid Hermes cluster hosted at the University of Victoria using customized shell, Python and R scripts. HPC GridRunner was used to enhance annotation searches such as BLAST and HMMER.

Assembling and annotation of the reference transcriptome

Paired-end FASTQ Illumina® 1.9 (Phred-33 ASCII) compressed files were produced for each sample after sequencing. Each file was checked for quality before and after trimming using FastQC v. 0.11.2 (Andrews, 2014). Trimming was done in Trimmomatic v. 0.33 (Bolger et al., 2014) with the following settings: ILLUMINACLIP: TruSeq2-PE-v2.fa:2:30:10 HEADCROP:14 SLIDINGWINDOW:4:15 MINLEN:36 TOPHRED33. The TruSeq2-PE-v2.fa was a custom-made version of the TruSeq2-PE.fa of Trimmomatic produced by adding over-represented sequences reported by FastQC. The reference transcriptome was built using Trinity v. 2.0.6 (Grabherr et al., 2011) with the default settings for paired-end data, and its statistics were calculated in PRINSEQ v. 0.20.1 (Schmieder and Edwards, 2011). Annotation was completed using Trinotate v. 2.0.2 (http://trinotate.github.io). The annotation consisted of: 1) prediction of coding regions with TransDecoder v. 2.0.1. (http://transdecoder.github.io), 2) search for annotations for those predicted coding regions (including Gene Ontology term enrichment, Ashburner et al. 2000, The Gene Ontology Consortium 2015; and EggNOG annotation, Huerta-Cepas et al. 2016) in the Swiss-Prot/TrEMBL and UniRef90 (The UniProt Consortium, 2015, 2017) companion databases of Trinotate using BLAST+ v. 2.2.28 (Camacho et al., 2009), 3) search for protein domains in Pfam (Finn et al., 2016) using HMMER v. 3.1b1 (http://hmmer.org), and 4) search for signal peptides with SignalP v. 4.0 (Petersen et al., 2011), transmembrane regions with TMHMM v. 2.0 (http://www.cbs.dtu.dk /services/TMHMM/) and r*RNA* transcripts with RNAmmer v. 1.2 (Lagesen et al., 2007).

Differential expression analyses

The downstream analyses (Haas et al., 2013) were conducted using the assembled

contigs and contig variants from Trinity v. 2.0.6 (Grabherr et al., 2011) instead of the smaller number of corresponding deduced genes. Trinity refers to the contigs and variants as "transcripts", a term that is used through this document although they may not correspond to transcripts *sensu stricto*. Reads were mapped to the assembly with RSEM v. 1.2.20 (Li and Dewey, 2011) and fragments per kilobase of transcript per million mapped (FPKMs, Trapnell et al. 2010) were calculated. Normalization was achieved in edgeR (Robinson et al., 2010) by computing the trimmed mean of M-values (TMM; Dillies et al. 2013, Robinson and Oshlack 2010). The differential expression (DE) analysis was completed by comparing all samples in pairs using the default settings in edgeR, and then extracting and merging the sequences that had a minimum fold change of four and a maximum false discovery rate of 0.001 from all the samples into a single matrix. A correlation heat map of the expression profile of each sample was then produced. qPCR was not performed to confirm any of the DE transcripts because of the high specificity, sensitivity and overall agreement that has been reported between qPCR and edgeR in comparison to other DE methods like DESeq2, Cuffdiff2 and TSPM (Rajkumar et al., 2015). Additionally, it has been documented that there is a high level of agreement in the relative expression levels among different gene expression platforms, including qPCR and HiSeq 2000 (SEQC/MAQC-III Consortium, 2014).

Data exploration and selection of sequences of interest

For easier browsing and exploration of the processed data, clustering and annotation information of the DE data was ingested into a SQLite database, which was uploaded to a local TrinotateWeb server. TrinotateWeb was downloaded from http://trinotate.github.io, and installed on the Compute Canada's West Cloud (https://west.cloud.computecanada.ca). Data mining for transcripts of interest was achieved using three methodologies: 1) hierarchical clustering, 2) stability selection analysis, and 3) grade of membership modelling.

Hierarchical clustering was used to produce a heat map based on Euclidean distances. The transcripts were then categorized into expression clusters by cutting the transcripts' tree at 45% of its maximum height, and categorical stability selection (Meinshausen and Bühlmann, 2010) by family was executed using the DE matrix to select transcripts that discriminated between families. Changepoint on variance

with the AMOC method (Killick and Eckley, 2014) was used to decide the number of transcripts to report from the stability selection analysis.

Grade of Membership (GoM) modeling (Dey et al., 2017, Yu et al., 2014) was completed using the *CountClust* R package (Dey et al., 2016, 2017) to topic-model expression levels of the transcripts into $K = 20$ clusters with a tolerance of 0.1. GoM is based on the latent Dirichlet allocation method (Blei, 2012, Blei and Lafferty, 2009, Liu et al., 2016a), and from that perspective, each *CountClust* cluster is a topic defined as a probability distribution over the transcripts (denoted by θ), and each sample is viewed as a probability distribution over the topics (denoted by ω). GoM was used to detect transcripts that co-occurred in each seedling analyzed. The top topics from each sample were chosen according to their decreasing ω values, and the top transcripts from each topic were selected using their decreasing θ values and keeping only the first 5. In topic modelling, it is common practise to retain only the top 5-10 "words" from a topic (see e.g. Blei 2012, Blei and Lafferty 2009, Dey et al. 2016, Liu et al. 2016a).

In addition to the three methodologies used to explore the transcriptomic data, the expression levels of sequences related to terpene synthesis in *T. plicata* were also investigated given the importance of sabinene and α-thujene in differentiating plants resistant and susceptible to *D. thujina* at the chemical level (see section 3.3.1). The analysis included enzymes involved in 1) the DOXP (1-deoxy-D-xylulose-5-phosphate) pathway, 2) the α- and β-thujone biosynthesis pathway (see Appendix A.45 for the full list); and 3) the *T. plicata* (+)-sabinene-3-hydroxylase characterized by Gesell et al. (2015).

3.3 Results

As seen in the scanning electron microscope screening, all seedlings in the CLB^+ condition tested positive for presence of *D. thujina* spores during the inoculation phase and developed *D. thujina* symptoms. Disease severity was significantly higher in family 583 as compared to family 685 (3.78% and 1.25%, respectively; $p = 0.0003$). Hereafter, family 583 will be referred to as susceptible, and family 685 as resistant.

3.3.1 Chemical composition

Principal components analysis showed that resistant and susceptible families as well as their infection treatment were clustered separately (Fig. 3.1). Component 1 accounted for differences in infection treatment regardless of the family studied, while component 2 differentiated families without regard to their infection treatment. Component 1 explained 31.54% of the variance in the data, while components 2 and 3 explained 17.31% and 15.00% of the variance, respectively. Variables that contributed most to component 1 were mostly terpenes (R-limonene, mono-terpenes, α-thujone, myrcene, geranyl acetate) and phosphorus. Variables with the greatest contribution to component 2 were also terpenes (sabinene, α-thujene, bornyl acetate and citronellyl acetate) plus boron and potassium.

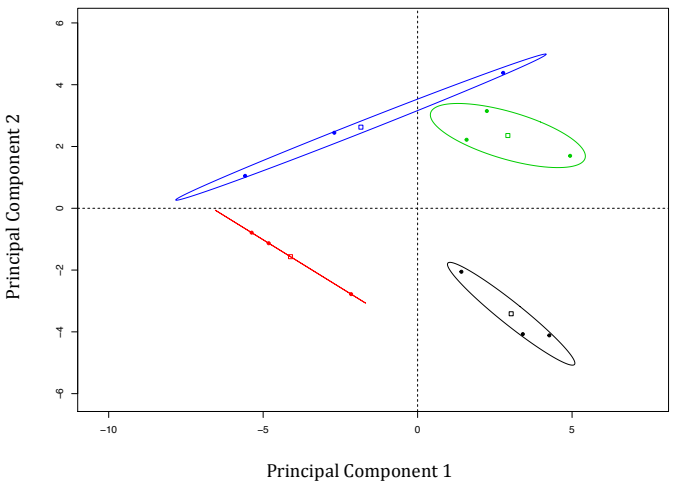

Figure 3.1. Bi-plot of the principal components analysis (correlation matrix-based) of the elements and compounds studied in two *Thuja plicata* families that had been exposed (CLB^+) and never exposed (CLB^-) to *Didymascella thujina*. Fifty-four compounds and elements were quantified from samples taken at the time symptoms had developed in the infected plants. Confidence levels of the ellipses shown is 95%. Treatments have been colour coded as follows: family 685 in the CLB^- treatment in black, family 685 in the CLB^+ treatment in red, family 583 in the CLB^- treatment in green, and family 583 in the CLB^+ treatment in blue.

Stability selection analysis revealed that sabinene and boron were the top variables that distinguished between families as chosen by changepoint. Table 3.1 shows the top four variables as ranked by stability selection. Analysis of variance of those variables showed significantly higher concentrations of sabinene and α-thujene in family 685, and significantly higher concentrations of boron in family 583 (Table 3.1).

The top two elements that discriminated between infected and uninfected seedlings (i.e. by infection treatment) were copper and sulphur as ranked by categorical stability selection and kept by changepoint. Molybdenum and phosphorus ranked third

Table 3.1. Concentrations (mean and standard error) of the top compounds and elements selected by stability selection when discriminating by family and by infection treatment. The selected variables were subsequently analyzed using two-way ANOVA with family and infection treatment as factors; significance values of each factor and the interaction are reported (see also Appendix A.22).

			Never infected		Infected		Statistical significance (two-way ANOVA)		
	Stability selection score	**Compound/element**	**Family 685**	**Family 583**	**Family 685**	**Family 583**	**Infection treatment**	**Family**	**Infection treatment × family interaction**
By family	0.0064	Sabinene ($\mu g \cdot g^{-1}$)	6,694.65 ± 482.94	3,189.00 ± 112.74	5,599.50 ± 389.82	3,474.23 ± 243.12	0.2652	≤ 0.0000	0.0754
	0.0008	Boron ($\mu g \cdot g^{-1}$)	9.69 ± 0.31	11.24 ± 0.32	8.89 ± 0.37	12.49 ± 0.86	0.6719	0.0011	0.0826
	0.0002	α-Thujene ($\mu g \cdot g^{-1}$)	264.94 ± 23.74	167.58 ± 11.60	204.45 ± 16.37	172.92 ± 15.94	0.1530	0.0061	0.0962
	0.0002	Iron ($\mu g \cdot g^{-1}$)	34.02 ± 3.43	50.15 ± 6.59	36.95 ± 4.49	50.05 ± 11.68	0.8510	0.0795	0.8403
By infection treatment	0.1400	Copper ($\mu g \cdot g^{-1}$)	9.85± 0.34	11.69 ± 0.38	16.33 ± 0.44	17.06 ± 0.51	≤ 0.0000	0.0156	0.2239
	0.0276	Sulfur (%)	0.204 ± 0.036	0.179 ± 0.018	0.063 ± 0.007	0.088 ± 0.014	0.0006	0.9991	0.2713
	0.0095	Molybdenum ($\mu g \cdot g^{-1}$)	0.36 ± 0.23	0.28 ± 0.16	2.21 ± 0.43	2.99 ± 0.86	0.0018	0.4989	0.4182
	0.0087	Phosphorus (%)	0.178 ± 0.016	0.196 ± 0.008	0.126 ± 0.004	0.147 ± 0.014	0.0023	0.1272	0.8773

Table 3.2. Concentrations (mean and standard error) of the top compounds and elements as ranked using regression stability selection with severity as the response variable. Pearson correlations between severity and the respective variables are shown as well as their significance values.

		Never infected		Infected		Pearson correlation	
Stability selection score	**Compound/element**	**Family 685**	**Family 583**	**Family 685**	**Family 583**	***r***	***p***
0.1923	Sesqui-, di-terpenes ($\mu g \cdot g^{-1}$)	32,788.18 ± 2,461.88	33,907.30 ± 2,638.90	29,013.40 ± 2,191.32	20,217.01 ± 1,971.41	-0.8947	0.0001
0.0468	Molybdenum ($\mu g \cdot g^{-1}$)	0.36 ± 0.23	0.28 ± 0.16	2.21 ± 0.43	2.99 ± 0.86	0.7505	0.0049
0.0296	Carbon (%)	49.687 ± 0.353	49.617 ± 0.281	50.161 ± 0.278	50.551 ± 0.397	0.6130	0.0341
0.0110	Aluminum ($\mu g \cdot g^{-1}$)	7.87 ± 0.46	8.02 ± 0.32	8.58 ± 0.64	10.92 ± 0.67	0.8041	0.0016

and fourth according to stability selection (Table 3.1). Analysis of variance showed that copper and molybdenum were at significantly higher concentrations in the infected plants, and sulphur and phosphorus at significantly lower concentrations in the infected seedlings (Table 3.1).

Regression stability selection ranked the sesqui- and di-terpenes, plus molybdenum, carbon and aluminum as the top four variables that were related to the disease severity (Table 3.2). The sesqui- and di-terpenes as a group had a significant, negative correlation with severity, while molybdenum, carbon and aluminum had a significant, positive correlation with severity (Table 3.2). Analysis of variance of those variables showed that there were significant differences between infected and uninfected seedlings in the concentration of sesqui- and di-terpenes (lower in infected, Table 3.2; $p = 0.0056$), molybdenum (higher in infected, Table 3.1), and aluminum (higher in infected, Table 3.2; $p = 0.0104$). There were no significant differences between families ($p = 0.6417$) or infection treatment ($p = 0.0663$) for carbon.

3.3.2 Gene expression

The assembled transcriptome consisted of 173,924 transcripts with a mean length of 772 bp, and a N50 contig size of 1,315 bp; 71,746 of the transcripts had annotation hits (see Appendix A.30). The overall alignment rate was 96.77% (Appendix A.31 reports the overall alignment rate of each sample). Only 2,304 of the transcripts were differentially expressed (DE). Samples belonging to family 685 had a similar expression profile regardless of the *D. thujina* treatment (i.e. CLB^+, CLB^-) in comparison to the samples from family 583 (Fig. 3.2).

The BLASTn searches for the two ITS2 sequences of *D. thujina* resulted in the identification of 10 transcripts in the assembled transcriptome, with identities above 90.00% and E-values between 2×10^{-120} and 4×10^{-12}. The top two transcripts were *TR8530|c0_g1_i1* and *TR57876|c6_g1_i5*. The added normalized fragment counts (FPKM-TMM values) of those two transcripts had a significant 85.07% correlation with disease severity ($p = 0.0005$).

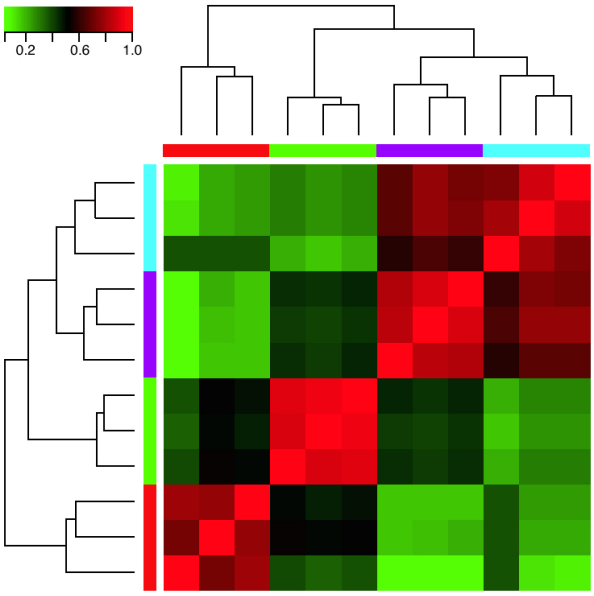

Figure 3.2. Correlation heat map of the expression profiles of all samples used in this study. Samples were grouped using hierarchical clustering with Euclidean distance. Correlation values were colour coded according to the top left bar (green = low correlation, red = high correlation). Family × infection treatment combinations were colour-coded as follows: 583 CLB^+ in red, 583 CLB^- in green, 685 CLB^- in purple, and 685 CLB^+ in cyan. Note that seedlings from family 685 are more correlated with each other, regardless of the *D. thujina* exposure treatment, than to family 583.

3.3.2.1 Hierarchical clustering

Eleven clusters of transcripts, with a minimum fold change of four and a maximum false discovery rate of 0.001, were identified after performing the hierarchical clustering analysis with Euclidean distance and cutting the transcripts' tree at 45% of its maximum height. (Fig. 3.3). More than 90% of the DE transcripts belonged to clusters 1 to 5 (Table 3.3), and the remaining to clusters 6 to 11. There were 674 transcripts at significantly higher expression levels in family 685, regardless of the infection treatment, in comparison to family 583 (cluster 1). In contrast, 437 transcripts had higher expression in family 583 regardless of the infection treatment than in family 685 (cluster 4). Interestingly, there were 121 transcripts that were expressed at the lowest levels in the 583 CLB^- plants, compared to all other family × infection treatment combinations (cluster 3).

Table 3.3. Distribution per cluster of the differentially expressed transcripts shown in Fig. 3.3. Expression patterns per cluster are included.

Cluster	No. of transcripts	Pattern
1	647	High expression in family 685 regardless of the infection treatment
2	798	High expression in 583 CLB^+
3	121	Low expression in 583 CLB^-
4	437	High expression in family 583 regardless of the infection treatment
5	129	High expression in the CLB^- treatment regardless of the family
6 to 11	172	Other expression patterns

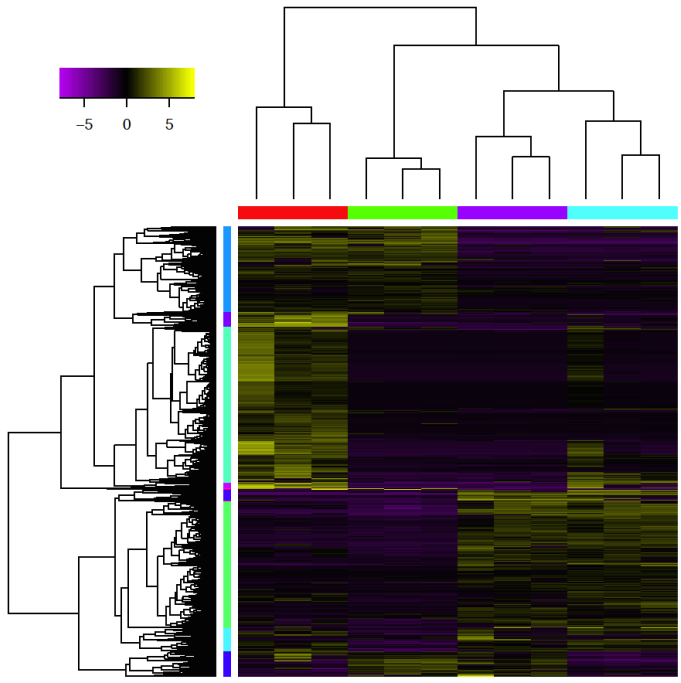

Figure 3.3. Heat map of 2,304 differentially expressed (DE) transcripts in two *Thuja plicata* families (685 and 583) that had been exposed (+) and not exposed (-) to cedar leaf blight (CLB, *Didymascella thujina*). The top tree clustered the seedlings used in this investigation, and the lef-hand tree the DE transcripts. Both clustering trees were produced using hierarchical clustering with Euclidean distance. Eleven expression clusters were produced after cutting the transcripts tree at 45% of its maximum height. The clusters with most transcripts in the left-hand tree were cluster 2 (light green), 1 (green), and 4 (blue), followed by clusters 5 (dark blue) and 3 (cyan). The remaining six clusters totalled to less than 10% of the DE transcripts. Expression levels refer to $\log_2$-transformed and centred FPKM values as calculated by the Trinity pipeline. Expression values were colour coded according to the top left bar (purple = low expression, yellow = high expression). Family × infection treatment combinations were colour-coded as follows: 583 CLB^+ in red, 583 CLB^- in green, 685 CLB^- in purple, and 685 CLB^+ in cyan.

3.3.2.2 Stability selection

There were 62 transcripts with stability selection scores higher than zero that were differentially expressed between resistant and susceptible plants as chosen by changepoint. Table 3.4 shows the top 50 sequences. Most of the transcripts belonged to clusters 1 and 4 of the hierarchical clustering analysis, with a few in cluster 6, and only one in cluster 7. Half of the sequences in Table 3.4 did not have a known function, 21 of them being uncharacterized and four with no hits for annotation.

Sequences selected by stability selection that belonged to clusters 1 and 6 were more highly expressed in family 685 than in family 583. Annotated sequences in those clusters were involved in very specific processes including response to stress (*TR20053/c0_g1_i1*), defense (*TR58144/c0_g2_i5*), signal transduction (*TR5780-4/c2_g1_i2*), protein transport (*TR5811/c0_g1_i1*), cell differentiation (*TR5843-7/c7_g1_i3*, *TR58437/c7_g1_i6*), furaneol biosynthesis (*TR57210/c8_g1_i8*), and alkaloid biosynthesis (*TR55613/c7_g3_i3*).

Sequences in cluster 4 were at higher levels of expression in family 583, but unlike those in cluster 1, these related mostly to primary metabolism and housekeeping activities, including: translation (*TR20781/c1_g2_i1*, *TR58279/c6_g2_i1*, *TR58578/c0_g1_i9*

Table 3.4. Top 50 predictors (transcripts) of the family categories (583 and 685), organized by expression cluster (see Fig. 3.3) and decreasing stability selection score. All annotations are based on BLASTX searches done on the Swiss-Prot database (see methods for details).

Transcript	Stability selection score	Cluster	E-value	Organism	Annotation	Process	Cellular component
TR53913/c1_g1_i4	0.0440	1	5×10^{-74}	*Arabidopsis* sp.	UBP1-associated protein 2A	Nucleic acid binding	
TR59400/c2_g5_i2	0.0350	1	2×10^{-64}	*Physcomitrella* sp.	Predicted protein		
TR57589/c7_g6_i2	0.0350	1	3×10^{-9}	*Picea* sp.	Putative uncharacterized protein		
TR58902/c0_g1_i2	0.0310	1	0	*Amborella* sp.	Uncharacterized protein	mRNA processing (*RNA* splicing)	
TR57804/c2_g1_i2	0.0310	1	2×10^{-135}	*Theobroma* sp.	Small G protein family protein / RhoGAP family protein isoform 1	Signal transduction	Intracellular
TR22003/c0_g3_i1	0.0300	1	0	*Oryza* sp.	Probable potassium transporter 2	Potassium ion transmembrane transporter activity	Integral component of membrane
TR58437/c7_g1_i3	0.0290	1	7×10^{-121}	*Arabidopsis* sp.	Zinc finger CCCH domain-containing protein 37		
TR47725/c0_g1_i1	0.0260	1	0	*Selaginella* sp.	Putative uncharacterized protein		
TR6396/c0_g1_i1	0.0250	1	7×10^{-53}	*Picea* sp.	Putative uncharacterized protein		
TR58437/c7_g1_i6	0.0240	1	3×10^{-121}	*Arabidopsis* sp.	Zinc finger CCCH domain-containing protein 37		
TR56381/c0_g2_i2	0.0230	1	8×10^{-70}	*Beta* sp.	Putative uncharacterized protein		
TR41770/c0_g1_i2	0.0230	1	6×10^{-97}	*Theobroma* sp.	Soul heme-binding family protein isoform 1		
TR58144/c0_g2_i5	0.0220	1	2×10^{-31}	*Arabidopsis* sp.	Probable leucine-rich repeat receptor-like protein kinase At1g35710		
TR59944/c4_g1_i3	0.0210	1	3×10^{-24}	*Pinus* sp.	Gibberellin 2-oxidase12		
TR51798/c1_g3_i1	0.0210	1	5×10^{-55}	*Picea* sp.	Putative uncharacterized protein		
TR48323/c0_g1_i1	0.0210	1	0	*Picea* sp.	Putative uncharacterized protein	Protein folding	
TR8434/c0_g2_i1	0.0200	1	3×10^{-15}	*Picea* sp.	Putative uncharacterized protein		
TR58308/c0_g1_i4	0.0200	1	2×10^{-77}	*Amborella* sp.	Uncharacterized protein		
TR57210/c8_g1_i8	0.0200	1	3×10^{-37}	*Fragaria* sp.	2-methylene-furan-3-one reductase		
TR45175/c0_g2_i1	0.0200	1	1×10^{-84}	*Picea* sp.	Putative uncharacterized protein		Cysteamine dioxygenase activity
TR20781/c1_g2_i1	0.0370	4	0	*Zea* sp.	Eukaryotic translation initiation factor 2 gamma subunit	Translation initiation factor activity	
TR3907/c0_g2_i1	0.0360	4	1×10^{-55}	*Arabidopsis* sp.	Protein Enhanced Disease Resistance 2		
TR52836/c0_g1_i6	0.0330	4	0	*Glycine* sp.	Uncharacterized protein	Regulation of signal transduction	
TR59333/c0_g1_i3	0.0290	4	3×10^{-86}	*Arabidopsis* sp.	Tubulin-folding cofactor C	Microtubule cytoskeleton organization	Cytoplasm
TR58279/c6_g2_i1	0.0290	4	1×10^{-158}	*Amborella* sp.	Uncharacterized protein	tRNA processing	
TR47725/c0_g1_i2	0.0280	4	0	*Selaginella* sp.	Putative uncharacterized protein		
TR58578/c0_g1_i9	0.0270	4	6×10^{-77}	*Arabidopsis* sp.	Peptidyl-tRNA hydrolase	mRNA processing (*RNA* splicing)	Mitochondrion
TR59409/c0_g1_i2	0.0260	4	NA	No hits	No hits		
TR58902/c0_g1_i1	0.0260	4	0	*Amborella* sp.	Uncharacterized protein	mRNA processing (*RNA* splicing)	Spliceosomal complex
TR58836/c0_g1_i2	0.0260	4	1×10^{-101}	*Glycine* sp.	Uncharacterized protein		
TR55562/c0_g1_i1	0.0260	4	0	*Oryza* sp.	ATP-dependent zinc metalloprotease FTSH 7		Chloroplast (thylakoid membrane)
TR52074/c0_g1_i1	0.0240	4	2×10^{-19}	*Capsella* sp.	Uncharacterized protein	Protein binding	
TR59363/c1_g3_i2	0.0230	4	NA	No hits	No hits		
TR48323/c0_g1_i2	0.0230	4	0	*Picea* sp.	Putative uncharacterized protein	Protein folding	
TR59228/c6_g3_i1	0.0220	4	3×10^{-6}	*Arabidopsis* sp.	Probable tyrosine-protein phosphatase At1g05000		
TR31863/c0_g1_i1	0.0220	4	NA	No hits	No hits		
TR52448/c0_g2_i1	0.0210	4	2×10^{-61}	*Selaginella* sp.	Putative uncharacterized protein	Spindle assembly	Centrosome
TR59490/c6_g2_i1	0.0200	4	NA	No hits	No hits		
TR54163/c0_g1_i1	0.0200	4	8×10^{-98}	*Oryza* sp.	Dephospho-CoA kinase	Coenzyme A biosynthetic process	Chloroplast, peroxisome, vacuole
TR52106/c0_g1_i2	0.0200	4	1×10^{-93}	*Arabidopsis* sp.	PsbP domain-containing protein 4	Photosynthesis	Photosystem II oxygen evolving complex
TR51510/c0_g1_i4	0.0200	4	2×10^{-177}	*Arabidopsis* sp.	Pentatricopeptide repeat-containing protein At3g62470		Mitochondrion
TR55998/c0_g1_i2	0.0190	4	2×10^{-163}	*Picea* sp.	Alpha-amylase	Carbohydrate metabolic process	
TR22350/c0_g1_i1	0.0190	4	2×10^{-82}	*Picea* sp.	Putative uncharacterized protein		
TR55562/c0_g1_i2	0.0380	6	0	*Oryza* sp.	ATP-dependent zinc metalloprotease FTSH 7		Chloroplast (thylakoid membrane)
TR5811/c0_g1_i1	0.0280	6	1×10^{-139}	*Oryza* sp.	Secretory carrier-associated membrane protein 1	Protein transport	Integral component of membrane
TR55613/c7_g3_i3	0.0270	6	2×10^{-94}	*Papaver* sp.	(R,S)-reticuline 7-O-methyltransferase		
TR20053/c0_g1_i1	0.0250	6	3×10^{-32}	*Zea* sp.	Uncharacterized protein	Response to stress	
TR33366/c0_g2_i1	0.0230	6	4×10^{-8}	*Picea* sp.	Putative uncharacterized protein		
TR27783/c0_g2_i1	0.0210	6	0	*Arabidopsis* sp.	Probable voltage-gated potassium channel subunit beta;	Potassium ion transport	Plasma membrane, plasmodesma
TR44368/c0_g2_i1	0.0260	7	1×10^{-48}	*Arabidopsis* sp.	Ycf20-like protein	Nonphotochemical quenching	Chloroplast

and *TR58902/c0_g1_i1*), photosynthesis (*TR52106/c0_g1_i2*), carbohydrate metabolism (*TR55998/c0_g1_i2*), and cytoskeleton (*TR59333/c0_g1_i3*, *TR52448-/c0_g2_i1*). An interesting sequence from cluster 4 is the protein Enhanced Disease Resistance 2 (*TR3907/c0_g2_i1*), which was not expressed in family 685.

3.3.2.3 Grade of membership analysis

Each of the 12 seedlings sampled in this study had a different topic that ranked first (Table 3.5). In spite of that, some of those topics had transcripts with similar annotations, and there were clear differences between the topics belonging to family 685 in relation to those in family 583 as seen on the transcript annotations.

Galactinol synthase 1 (*TR57187/c3_g1_i3*) was present in the topics from all uninfected seedlings (CLB^-), while the peroxiredoxin Q (*TR33201/c0_g2_i1*) was present in five of the plants in that category regardless of the family. In contrast, a bark storage protein A (*TR43930/c1_g1_i1*) was present only in two of the resistant seedlings (685-24 and 685-27), phenylalanine ammonia-lyase (PAL, *TR26208/c0_g1_i1*) was present in two of the susceptible seedlings (583-27 and 583-33), and chalcone synthases (*TR59130/c4_g1_i2* and *TR59130/c4_g2_i3*) were in the top topics of two susceptible plants (583-23 and 583-33).

In relation to the CLB^+ treatment, cinnamoyl-CoA reductase 1 (*TR9374/c0_g1_i1*) was present only in the top topics from the resistant plants, but not in any of those from the susceptible seedlings. Early light-induced protein 1's (*TR65408/c0_g1_i1* and *TR9335/c0_g1_i1*) and tricin synthase 1 (*TR19072/c0_g1_i1*) were also present in the top topics of all of the resistant seedlings in this treatment, as well as in that of seedling 583-17. Susceptible plants did not display any pattern, although there were pathogenesis-related (PR) proteins (*TR53697/c0_g2_i1*, *TR59043/c3_g1_i*1 and *TR59043/c3_g1_i2*) that were present in the top topics from seedlings 583-2 and 583-12.

Other sequences present only in the top topics from resistant seedlings were a cysteine-rich receptor-like protein kinase 2 (*TR59000/c3_g2_i1*; present in seedlings 685-4, 685-18 and 685-34), and a linoleate 9S-lipoxygenase A (*TR54665/c5_g1_i2*, important in seedling 685-24).

Table 3.5. Representative transcripts (top 5) of the most important topic of each seedling studied in this investigation. The transcripts within each topic were selected based on their decreasing θ values. All annotations are based on BLASTX searches done on the Swiss-Prot database (see methods for details).

Treatment	Seedling ID	Severity	Topic	θ within topic	Transcript	Cluster	E-value	Organism	Annotation	Process	Cellular component
CLB$^-$	685-24	0.0000	3	0.046603901	*TR54916/c0_g2_i1*	5	NA	No hits	No hits		
				0.042521569	*TR43930/c1_g1_i1*	5	3×10^{-42}	*Populus* sp.	Bark storage protein A	Nucleoside metabolic process	
				0.041166356	*TR54665/c5_g1_i2*	3	0	*Lycopersicon* sp.	Linoleate 9S-lipoxygenase A	Oxylipin biosynthetic process	Cytoplasm
				0.024264453	*TR33201/c0_g2_i1*	5	1×10^{-89}	*Sedum* sp.	Peroxiredoxin Q	Antioxidant activity	Chloroplast
				0.021249167	*TR57187/c3_g1_i3*	5	3×10^{-168}	*Ajuga* sp.	Galactinol synthase 1	Carbohydrate storage	Cytoplasm
	685-27	0.0000	4	0.040455998	*TR54916/c0_g2_i1*	5	NA	No hits	No hits		
				0.039085152	*TR57187/c3_g1_i1*	5	1×10^{-165}	*Ajuga* sp.	Galactinol synthase 1	Carbohydrate storage	Cytoplasm
				0.03230091	*TR33201/c0_g2_i1*	5	1×10^{-90}	*Sedum* sp.	Peroxiredoxin Q	Antioxidant activity	Chloroplast
				0.032146653	*TR43930/c1_g1_i1*	5	3×10^{-42}	*Populus* sp.	Bark storage protein A	Nucleoside metabolic process	
				0.027273501	*TR11549/c0_g1_i1*	5	1×10^{-56}	*Pseudotsuga* sp.	Lea protein	Response to osmotic stress	
	685-34	0.0000	10	0.035844732	*TR57187/c3_g1_i1*	5	1×10^{-165}	*Ajuga* sp.	Galactinol synthase 1	Carbohydrate storage	Cytoplasm
				0.031706454	*TR59000/c3_g2_i1*	1	3×10^{-126}	*Arabidopsis* sp.	Cysteine-rich receptor-like protein kinase 2		
				0.03165305	*TR54916/c0_g2_i1*	5	NA	No hits	No hits		
				0.029320371	*TR56218/c1_g1_i1*	6	2×10^{-163}	*Triticum* sp.	RuBisCO large subunit-binding protein subunit alpha	Photosynthesis	Chloroplast
				0.028221122	*TR33201/c0_g2_i1*	5	1×10^{-94}	*Sedum* sp.	Peroxiredoxin Q	Antioxidant activity	Chloroplast
	583-23	0.0000	5	0.063724072	*TR54916/c0_g2_i1*	5	NA	No hits	No hits		
				0.047493443	*TR33201/c0_g2_i1*	5	1×10^{-91}	*Sedum* sp.	Peroxiredoxin Q	Antioxidant activity	Chloroplast
				0.044820366	*TR59130/c4_g1_i2*	9	2×10^{-60}	*Juniperus* sp.	Chalcone synthase	Flavonoid biosynthetic process	
				0.041464839	*TR57187/c3_g1_i1*	5	1×10^{-165}	*Ajuga* sp.	Galactinol synthase 1	Carbohydrate storage	Cytoplasm
				0.039524442	*TR59130/c4_g2_i3*	4	0	*Pinus* sp.	Chalcone synthase	Flavonoid biosynthetic process	
	583-33	0.0000	6	0.081216729	*TR26208/c0_g1_i1*	9	0	*Pinus* sp.	Phenylalanine ammonia-lyase	Phenyl propanoid pathway	Cytoplasm
				0.043380799	*TR54916/c0_g2_i1*	5	NA	No hits	No hits		
				0.042004155	*TR59130/c4_g2_i3*	4	0	*Pinus* sp.	Chalcone synthase	Flavonoid biosynthetic process	
				0.040125028	*TR59130/c4_g1_i2*	9	2×10^{-60}	*Juniperus* sp.	Chalcone synthase	Flavonoid biosynthetic process	
				0.0372881	*TR57187/c3_g1_i1*	5	1×10^{-165}	*Ajuga* sp.	Galactinol synthase 1	Carbohydrate storage	Cytoplasm
	583-27	0.0000	7	0.054058741	*TR54916/c0_g2_i1*	5	NA	No hits	No hits		
				0.046281105	*TR33201/c0_g2_i1*	5	1×10^{-93}	*Sedum* sp.	Peroxiredoxin Q	Antioxidant activity	Chloroplast
				0.044402383	*TR57187/c3_g1_i1*	5	1×10^{-165}	*Ajuga* sp.	Galactinol synthase 1	Carbohydrate storage	Cytoplasm
				0.038447621	*TR26208/c0_g1_i1*	9	0	*Pinus* sp.	Phenylalanine ammonia-lyase	Phenyl propanoid pathway	Cytoplasm
				0.030467396	*TR59236/c4_g1_i4*	5	NA	No hits	No hits		
CLB$^+$	685-18	2.0463	1	0.081751137	*TR65408/c0_g1_i1*	2	9×10^{-43}	*Arabidopsis* sp.	Early light-induced protein 1		Chloroplast
				0.064815572	*TR9335/c0_g1_i1*	2	1×10^{-45}	*Arabidopsis* sp.	Early light-induced protein 1		Chloroplast
				0.042225173	*TR19072/c0_g1_i1*	2	9×10^{-55}	*Oryza* sp.	Tricin synthase 1	Biosynthesis of secondary metabolites	Nucleus
				0.035711716	*TR59000/c3_g2_i1*	1	3×10^{-123}	*Arabidopsis* sp.	Cysteine-rich receptor-like protein kinase 2		
				0.028796717	*TR9374/c0_g1_i1*	2	3×10^{-82}	*Arabidopsis* sp.	Cinnamoyl-CoA reductase 1	Phenylpropanoid pathway	
	685-4	0.6789	8	0.067591526	*TR65408/c0_g1_i1*	2	9×10^{-43}	*Arabidopsis* sp.	Early light-induced protein 1		Chloroplast
				0.055552706	*TR9335/c0_g1_i1*	2	1×10^{-45}	*Arabidopsis* sp.	Early light-induced protein 1		Chloroplast
				0.041974572	*TR19072/c0_g1_i1*	2	9×10^{-55}	*Oryza* sp.	Tricin synthase 1	Biosynthesis of secondary metabolites	Nucleus
				0.032156825	*TR9374/c0_g1_i1*	2	3×10^{-84}	*Arabidopsis* sp.	Cinnamoyl-CoA reductase 1	Phenylpropanoid pathway	
				0.014753053	*TR59000/c3_g2_i1*	1	3×10^{-125}	*Arabidopsis* sp.	Cysteine-rich receptor-like protein kinase 2		
	685-1	1.0326	12	0.072317276	*TR65408/c0_g1_i1*	2	9×10^{-43}	*Arabidopsis* sp.	Early light-induced protein 1		Chloroplast
				0.044026819	*TR9335/c0_g1_i1*	2	1×10^{-45}	*Arabidopsis* sp.	Early light-induced protein 1		Chloroplast
				0.040247343	*TR19072/c0_g1_i1*	2	9×10^{-55}	*Oryza* sp.	Tricin synthase 1	Biosynthesis of secondary metabolites	Nucleus
				0.029319831	*TR9374/c0_g1_i1*	2	3×10^{-86}	*Arabidopsis* sp.	Cinnamoyl-CoA reductase 1	Phenylpropanoid pathway	
				0.017502319	*TR56218/c1_g1_i1*	6	2×10^{-163}	*Triticum* sp.	RuBisCO large subunit-binding protein subunit alpha	Photosynthesis	Chloroplast
	583-17	3.5383	9	0.051165284	*TR49492/c0_g1_i1*	8	3×10^{-35}	*Neurospora* sp.	Uncharacterized protein		
				0.047667562	*TR65408/c0_g1_i1*	2	9×10^{-43}	*Arabidopsis* sp.	Early light-induced protein 1		Chloroplast
				0.036443332	*TR19072/c0_g1_i1*	2	9×10^{-55}	*Oryza* sp.	Tricin synthase 1	Biosynthesis of secondary metabolites	Nucleus
				0.027368645	*TR9335/c0_g1_i1*	2	1×10^{-45}	*Arabidopsis* sp.	Early light-induced protein 1		Chloroplast
				0.025274788	*TR59130/c4_g1_i2*	9	2×10^{-60}	*Juniperus* sp.	Chalcone synthase	Flavonoid biosynthetic process	
	583-12	4.3511	11	0.052234732	*TR65408/c0_g1_i1*	2	9×10^{-43}	*Arabidopsis* sp.	Early light-induced protein 1		Chloroplast
				0.050508529	*TR26208/c0_g1_i1*	9	0	*Pinus* sp.	Phenylalanine ammonia-lyase	Phenyl propanoid pathway	Cytoplasm
				0.045791771	*TR53697/c0_g2_i1*	7	2×10^{-129}	*Cryptomeria* sp.	Thaumatin-like protein		
				0.041779946	*TR59130/c4_g2_i3*	4	0	*Pinus* sp.	Chalcone synthase	Flavonoid biosynthetic process	
				0.039400874	*TR58068/c0_g1_i1*	8	4×10^{-127}	*Cryptomeria* sp.	Pollen allergen CJP38	Hydrolase activity, hydrolyzing O-glycosyl compounds	
	583-2	3.4456	13	0.125856284	*TR54916/c0_g2_i1*	5	NA	No hits	No hits		
				0.059133626	*TR59043/c3_g1_i2*	8	2×10^{-124}	*Juniperus* sp.	Pathogenesis-related protein	Defense response	
				0.049384925	*TR59043/c3_g1_i1*	8	9×10^{-138}	*Juniperus* sp.	Pathogenesis-related protein	Defense response	
				0.030879161	*TR43930/c1_g1_i1*	5	3×10^{-42}	*Populus* sp.	Bark storage protein A	Nucleoside metabolic process	
				0.028219645	*TR11549/c0_g1_i1*	5	1×10^{-56}	*Pseudotsuga* sp.	Lea protein	Response to osmotic stress	

3.3.2.4 Analysis of sequences related to terpene synthesis in *Thuja plicata*

The expression levels of selected *T. plicata* genes involved in the production of specific terpenes were investigated further given the results of the categorical and regression stability analyses which showed 1) the importance of sabinene to differentiate between resistant and susceptible families, and 2) the relevance of sesqui- and di-terpenes in relation to the disease severity (see section 3.3.1).

Table 3.6 shows the *T. plicata* transcripts of putative DOXP pathway enzymes, and of putative α- and β-thujone biosynthesis pathway enzymes that were found in the assembled transcriptome of this study. Most of the sequences had similar expression levels in both families regardless of the infection treatment, except for four transcripts. Three sequences were at higher levels of expression in the CLB^- condition in family 685 (Fig. 3.4a): *TR52851/c1_g1_i2* (putative short-chain alcohol dehydrogenase-like mRNA), *TR57126/c5_g1_i6* (aldehyde dehydrogenase family 2 member C4, involved in phenylpropanoid biosynthesis) and *TR57111/c2_g1_i1* (a cytochrome P450). Only transcript *TR56505/c0_g1_i1* (a cytochrome P450 71A1) was expressed exclusively in the CLB^+ condition in that same family (Fig. 3.4b).

3.4 Discussion

This investigation studied the constitutive chemical and gene expression (*RNA*-Seq) differences between *T. plicata* seedlings of one full-sib family resistant to *D. thujina* (685) and one full-sib family susceptible to the disease (583). Healthy and diseased seedlings from both families were analyzed, and resistance was determined using the severity of the disease: family 583 had significantly higher severity than family 685 although both values were low (3.78% and 1.25%, respectively). These severities may look uninformative at first sight, however, they are consistent with the pilot investigation carried out in 2012, which rendered greater severities, with family 685 having an average of 9.28% of the foliage blighted, and family 583 an average of 25.07% of the foliage with disease symptoms.

Several factors may be responsible for the differences in the severities between 2012 and 2013, temperature, humidity and rain being very important as they are limiting factors for pathogen infection (Agrios, 2005, Colhoun, 1973, Hardwick, 2002, Sharma,

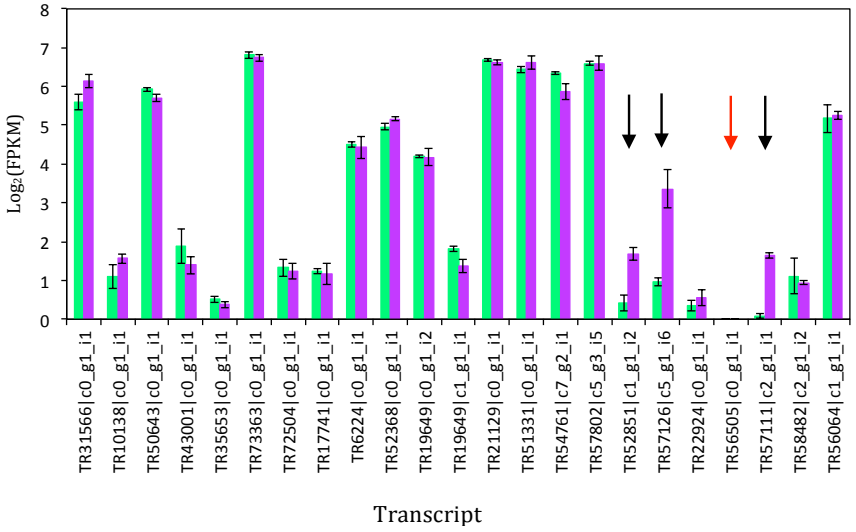

(a)

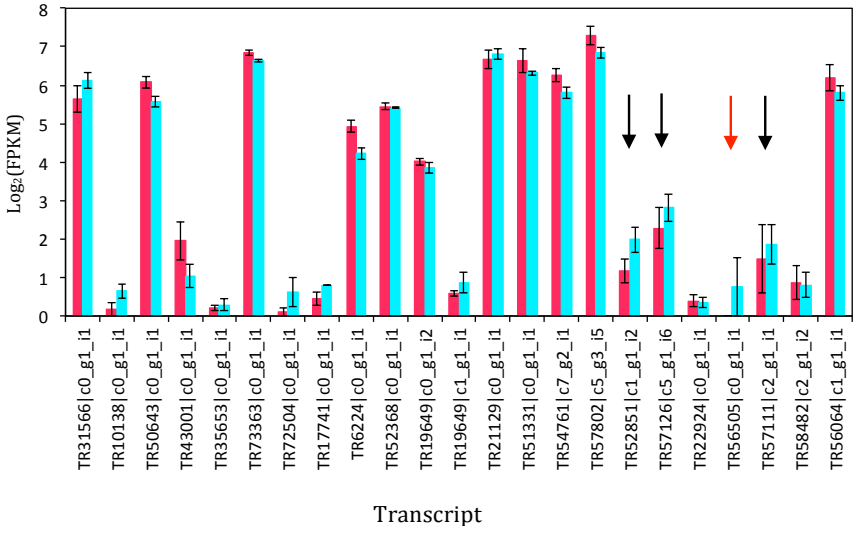

(b)

Figure 3.4. Average expression levels of putative *Thuja plicata* enzymes in the DOXP (1-deoxy-D-xylulose-5-phosphate) pathway, the α- and β-thujone biosynthesis pathway, and (+)-sabinene-3-hydroxylase characterized by Gesell et al. (2015) (see also Table 3.6). The expression profiles of all sequences were very similar regardless of the infection treatment, except for four transcripts (shown by the arrows). A cytochrome P450 71A1 (sequence *TR56505/c0_g1_i1*) was the only transcript to be expressed exclusively in the resistant family (685) in the CLB^+ condition (red arrows). (a) CLB^- treatment, (b) CLB^+ treatment. Family $\times$ *D. thujina* treatment combinations were colour-coded as follows: 583 CLB^- in green, 685 CLB^- in purple, 583 CLB^+ in red, 685 CLB^+ in cyan. Transcripts in the X-axis correspond to those on Table 3.6. Error bars are standard errors.

Table 3.6. Transcripts of putative enzymes in the DOXP (1-deoxy-D-xylulose-5-phosphate) pathway, and in the α- and β-thujone biosynthesis pathway of *Thuja plicata* that were found in the assembled transcriptome of this study. Annotations with an asterisk were based on unpublished sequences kindly provided by Dr. Jim Mattsson (see also Appendix A.45)

Pathway	Transcript	E-value	Organism	Annotation	Process	Cellular component
DOXP pathway	*TR31566/c0_g1_i1*	0	*Oryza* sp.	Probable 1-deoxy-D-xylulose-5-phosphate synthase 2	Terpenoid biosynthetic process	Chloroplast
	TR10138/c0_g1_i1	0	NA	Putative 1-deoxy-D-xylulose-5-phosphate synthase*		
	TR50643/c0_g1_i1	0	*Capsicum* sp.	Probable 1-deoxy-D-xylulose-5-phosphate synthase	Terpenoid biosynthetic process	Chloroplast
	TR43001/c0_g1_i1	0	NA	Putative 1-deoxy-D-xylulose-5-phosphate synthase*		
	TR35653/c0_g1_i1	0	NA	Putative 1-deoxy-D-xylulose-5-phosphate synthase*		
	TR73363/c0_g1_i1	0	*Oryza* sp.	1-deoxy-D-xylulose 5-phosphate reductoisomerase	Isopentenyl diphosphate biosynthetic process	Chloroplast
	TR72504/c0_g1_i1	0	NA	Putative 1-deoxy-D-xylulose 5-phosphate reductoisomerase*		
	TR17741/c0_g1_i1	2×10^{-148}	NA	Putative 1-deoxy-D-xylulose 5-phosphate reductoisomerase*		
	TR6224/c0_g1_i1	1×10^{-146}	*Taxus* sp.	2-C-methyl-D-erythritol 4-phosphate cytidyltransferase	Isoprenoid biosynthetic process	
	TR52368/c0_g1_i1	0	*Ginkgo* sp.	Type 1 4-diphosphocytidyl-2C-methyl-D-erythritol kinase	Terpenoid biosynthetic process	
	TR19649/c0_g1_i2	5×10^{-115}	*Taxus* sp.	2-C-methyl-D-erythritol 2,4-cyclodiphosphate synthase	Terpenoid biosynthetic process	
	TR19649/c1_g1_i1	2×10^{-89}	NA	Putative 2-C-methyl-D-erythritol 2,4-cyclodiphosphate synthase*		
	TR21129/c0_g1_i1	0	*Oryza* sp.	4-hydroxy-3-methylbut-2-en-1-yl diphosphate synthase	Isopentenyl diphosphate biosynthetic process	Chloroplast
	TR51331/c0_g1_i1	0	*Oryza* sp.	4-hydroxy-3-methylbut-2-enyl diphosphate reductase	Isopentenyl diphosphate biosynthetic process	Chloroplast
	TR54761/c7_g2_i1	0	*Oryza* sp.	4-hydroxy-3-methylbut-2-enyl diphosphate reductase	Isopentenyl diphosphate biosynthetic process	Chloroplast
Biosynthesis of α- and β-thujone	*TR57802/c5_g3_i5*	0	*Thuja plicata*	Putative aldo-keto reductase-like mRNA, complete sequence	Candidate in thujone biosynthesis	
	TR52851/c1_g1_i2	0	*Thuja plicata*	Putative short-chain alcohol dehydrogenase-like mRNA,partial sequence		
	TR57126/c5_g1_i6	0	*Arabidopsis* sp.	Aldehyde dehydrogenase family 2 member C4	Phenylpropanoid biosynthetic process	
	TR22924/c0_g1_i1	0	*Pinus* sp.	Cytochrome P450 720B2		Integral component of membrane
	TR56505/c0_g1_i1	6×10^{-40}	*Persea* sp.	Cytochrome P450 71A1		Integral component of membrane
	TR57111/c2_g1_i1	1×10^{-91}	*Eschscholzia* sp.	Cytochrome P450		
	TR58482/c2_g1_i2	0	*Thuja plicata*	Sabinene synthase	Terpene synthase activity	
	TR56064/c1_g1_i1	0	*Thuja plicata*	(+)-Sabinene-3-hydroxylase	Terpene synthase activity	

2006). The estimated mean temperature, relative humidity and total rain during the time the seedlings were exposed to *D. thujina* were 11.4°C, 82.16% and 150.1 mm in 2012, and 12.1°C, 86.05% and 155.8 mm in 2013 (see Appendix A.12). Although 2013 was warmer, more humid and rainier than 2012, the weather conditions of both years were optimal for *D. thujina* spore discharge and infection (Søegaard 1966; Søegaard 1969, p. 295). The key difference between the pilot study and the current investigation was the length of time that the plants were exposed to *D. thujina*. The seedlings remained in the inoculation site about 50% longer in 2012 compared to 2013 (77 and 51 days of exposure, respectively), which might have resulted in a higher cumulative spore load in 2012. Spore load and disease severity are directly related (Agrios, 2005, Sharma, 2006). Interestingly, the susceptible family 583 had about three times greater disease severity than the resistant family 685 in both years. These results and the screening of the families' parents by the BC MoFLNRORD (Appendix A.1) support the categorization of family 685 as resistant to *D. thujina*, and of family 583 as susceptible to the disease.

The chemical and gene expression analyses completed in this investigation showed constitutive differences between family 685 and family 583, despite the fact that none of the enzymes of the DOXP pathway studied were differentially expressed between families. Differences were also seen between infection treatments in each family as well. Each of those aspects is discussed in the following sections.

3.4.1 Characteristics of *T. plicata* seedlings from the family resistant to *D. thujina*

At the chemical level, the key difference between the families studied was the significantly higher concentrations of sabinene and α-thujene in the resistant family 685. Sabinene is a monoterpene (Foster et al., 2013, Gesell et al., 2015, Karp and Croteau, 1982, Karp et al., 1987) produced from geranyl diphosphate by (+)-sabinene synthase (Foster et al., 2013), and thought to be the precursor of α- and β-thujone (Foster et al., 2013, Gesell et al., 2015). α- and β-thujone have fungicidal properties (Tsiri et al., 2009), and are deterrents to deer browsing (Vourc'h et al., 2001, 2002). α-thujene is an isomer of sabinene (Acharya et al., 1969), which may explain the high concentration of that compound in plants with elevated sabinene content. Sabinene and α-thujene have antimicrobial properties as well. They have been shown to inhibit fungal growth

of *Seiridium cardinale* both *in vitro* and *in vivo* in other Cupressaceae (*Cupressus sempervirens*, Achotegui-Castells et al. 2016). Sabinene and α-thujene may then play a role in resistance to *D. thujina* in *T. plicata* seedlings, but the fungicidal activity of both compounds on *D. thujina* should be tested.

The concentrations of sabinene and α-thujene in family 685 might be related to the high expression levels of the enzymes involved in their production. Among the terpene synthesis sequences of interest from the transcriptomic data, four were at higher expression levels in seedlings from family 685: *TR52851/c1_g1_i2*, *TR57126/c5_g1_i6*, *TR57111/c2_g1_i1* and *TR56505/c0_g1_i1*. Of special interest is sequence *TR52851/c1_g1_i2*, the top subject of query KC767270 (Appendix A.45) which was identified as a potential sabinol dehydrogenase in the study by Foster et al. (2013). Another interesting sequence is transcript *TR56505/c0_g1_i1*, the top subject of query KC767279 (Appendix A.45), which is thought to be involved in terpene and probably flavonoid syntheses (Foster et al., 2013). The top UniProt annotation of *TR56505/c0_g1_i1* supports its role in the flavonoid pathway (UniProt accession P24465; The UniProt Consortium 2015, 2017). Transcript *TR57126/c5_g1_i6*, annotated as an aldehyde dehydrogenase, may be involved in the synthesis of ferulic acid (UniProt accession Q56YU0; The UniProt Consortium 2015, 2017) which is the precursor of many phenylpropanoids (Heldt, 2005). Transcript *TR57111/c2_g1_i1* was annotated as a cytochrome P450, but there are no further details. In spite of the annotation information, none of the above sequences have been characterized in *T. plicata*. Biochemical and *in-vivo* characterization of those four enzymes will be required in future studies to determine their exact role in the synthesis of sabinene, α-thujene and/or other terpenes as well as their role in resistance to *D. thujina*.

Besides sabinene, α-thujene and transcripts related to their synthesis, sequences involved in defense, alkaloid biosynthesis, cell differentiation and signal transduction were also at higher expression levels in family 685 in comparison to family 583. Transcripts *TR58144/c0_g2_i5* and *TR59000/c3_g2_i1* were related to defense, the former annotated as a probable leucine-rich repeat receptor-like protein kinase and the latter as a cysteine-rich receptor-like protein kinase. Leucine-rich repeats are common in disease resistance proteins of other pathosystems (LRR; Scheel and Nuernberger 2004; Vidhyasekaran 2008, p. 195), and cysteine-rich receptor-like proteins have been documented in plant defense as well (Ederli et al., 2011, Yeh et al., 2015,

Zhang et al., 2013). Those sequences may be involved in the resistance to *D. thujina* in family 685. Transcript *TR55613/c7_g3_i3* was annotated as a (R,S)-reticuline 7-O-methyltransferase (7OMT). 7OMTs catalyse the production of laudanine from reticuline (Ounaroon et al., 2003), both benzylisoquinoline alkaloids (BIAs, Liscombe and Facchini 2008; Mishra et al. 2013). Although foliar alkaloids have not been reported in *T. plicata* foliage, alkaloids have been found in another Cupressaceae (Zhang et al., 2007). BIAs have antimicrobial activity (Villar et al., 1987), play important roles in plant defense (Dembitsky et al., 2015, Hagel and Facchini, 2013), and may be involved in resistance against *D. thujina*, especially considering the fact that another sequence related to to BIA synthesis was found in the experiment presented in Chapter 4. Sequences *TR58437/c7_g1_i3* and *TR58437/c7_g1_i6*, both annotated as zinc finger CCCH domain-containing proteins 37 (gene HUA1; UniProt accession Q941Q3, The UniProt Consortium 2015, 2017), are involved in flower development (Cheng et al., 2003, Li et al., 2001), but they may also play a role in defense. Zinc finger proteins have been shown to play roles in disease resistance in other pathosystems (Gupta et al., 2012) and may have a similar function in the *T. plicata* - *D. thujina* interaction. The function of proteins with zinc-finger domains in the pathosystem studied here should be further investigated. The signal transduction sequence *TR57804/c2_g1_i2* that was overexpressed in family 685 was annotated as a small G protein family protein / RhoGAP family protein isoform 1. Rho GTPases are involved in internal cellular traffic via cytoskeleton signalling and are regulated by Rho GTPase-activating proteins (RhoGAPs; Nagawa et al. 2010). Besides cellular trafficking, Rho GTPases have been shown to be part of the defense system against pathogens in tobacco (Fujiwara et al., 2006, Moeder et al., 2005). *T. plicata* RhoGAPs may be indirectly involved in defense against *D. thujina* via regulation of Rho GTPases, but such a mechanism has to be investigated in western redcedar.

Other sequences of interest in family 685 were those at high expression levels in each of the infection treatments. Transcript *TR43930/c1_g1_i1*, annotated as bark storage protein A, had high expression levels only in the CLB^- treatment. Bark storage proteins (BSPs), also known as vegetative storage proteins (VSPs; Pettengill et al. 2013), respond to jasmonic acid (Stein et al., 2008) and have been shown to be upregulated in response to pathogen attack (Mulema and Denby, 2012). BSPs were also seen to be at higher levels of expression in plants resistant to *D. thujina* in the studies presented in Chapters 5 and 6. Although their mechanism of action is still unknown,

BSPs appear to be an important constitutive defense mechanism against *D. thujina*, however, future investigations should study their specific role in this pathosystem.

Sequences *TR9374/c0_g1_i1*, *TR19072/c0_g1_i1*, *TR65408/c0_g1_i1* and *TR9335/c0_g1_i1* were highly expressed only in seedlings from family 685 in the CLB^+ treatment. Transcript *TR9374/c0_g1_i1* was annotated as a cinnamoyl-CoA reductase 1, an enzyme involved in the production of lignin (Heldt, 2005, Ruel et al., 2009), but also shown to be upregulated in response to bacteria and probably related to hypersensitive responses (Lauvergeat et al., 2001). Hypersensitivity has not been reported in *T. plicata* as a defense mechanism, but it is possible that the cinnamoyl-CoA reductase acts along with *TR57126/c5_g1_i6* (see above) to reinforce *T. plicata* cell walls via lignification during the colonization of *D. thujina*. Sequence *TR19072/c0_g1_i1* may also be involved in the host's cell wall reinforcement. That transcript is a tricin synthase 1, an enzyme that methylates tricetin to produce tricin (Lee et al., 2008), the latter being a flavone recently shown to conjugate with lignin in monocots (Li et al., 2016). Cell wall reinforcement during compatible interactions is a common defense mechanism (Agrios 2005, p. 232) and lignification is an important response to pathogen infections in other plants like *Cryptomeria japonica* (Yoshida, 1998), eucalyptus (Smith et al., 2006) or wheat (Dushnicky et al., 1998). Transcripts *TR65408/c0_g1_i1* and *TR9335/c0_g1_i1* were annotated as early light-induced protein 1 (ELIP1), which is involved in protection against photooxidative stress (Casazza et al., 2005, Hutin et al., 2003). ELIP1s have not been documented to respond to pathogen attacks, however, the cross talk between light stress defense and pathogen defense signalling via transcription factor HY5 (long hypocotyl 5; Gangappa and Botto 2016, Kleine et al. 2007) may explain the elevated expression of ELIP1s here. In this study, only seven of the 2,304 DE transcripts were annotated as HY5s and four of them were at higher expression levels in family 685 (*TR53680/c0_g1_i1*, *TR53680/c0_g1_i4*, *TR53680/c0_g1_i5* and *TR53680/c0_g1_i6*). The relationship between ELIP1s, HY5s and resistance to *D. thujina* in *T. plicata* should be further investigated.

3.4.2 Characteristics of *T. plicata* seedlings from the family susceptible to *D. thujina*

Unlike family 685, susceptible family 583 did not have constitutively high concentrations of any compounds with apparent defense properties. Only boron was at significantly higher concentration in that family. Boron is an essential plant micronutrient, necessary for normal growth and development (Ahmad et al., 2009, González-Fontes et al., 2014, Tariq and Mott, 2007) and a component of the cell wall (Blevins and Lukaszewski, 1998, Matoh, 1997, Tariq and Mott, 2007). Boron has been little studied in the context of plant-pathogen interactions although some investigations on its role in pest resistance exist (e.g. Ruuhola et al. 2011). The function of boron in the susceptible family studied here is possibly related to primary metabolism (i.e. growth and development) given the functions attributed to this element and the gene expression characteristics of family 583 (see below).

Besides boron, family 583 also showed higher expression levels than family 685 of sequences that are related to primary metabolism. Those sequences were involved in translation, photosynthesis, carbohydrate metabolism and cytoskeleton organization. Transcripts *TR58279/c6_g2_i1*, *TR58902/c0_g1_i1*, *TR58578/c0_g1_i9* and *TR20781/c1_g2_i1* were at high expression levels in family 583 and are all involved in translation. The last two sequences are annotated as mitochondrial peptidyl-t*RNA* hydrolase (Pth), and eukaryotic translation initiation factor 2 gamma subunit (eIF2), respectively. Pth plays a central role in protein translation (Das and Varshney, 2006), and eIF2 is crucial in the initiation of transcription by binding to methionyl-tRNA_i (Kimball, 1999). The γ subunit of eIF2 is also very important as it binds to guanine and tRNA_i during translation (Erickson and Hannig, 1996). A photosynthesis-related transcript (*TR52106/c0_g1_i2*), annotated as a chloroplastic PsbP domain-containing protein 4 (PPD4), was also at higher levels of expression in family 583 in comparison to family 685. Several PPDs have been characterized (see. e.g. Liu et al. 2012 or Roose et al. 2011) and most are essential for photosynthesis (Ifuku et al., 2008). Another sequence with high expression levels, clearly involved in primary metabolism, was transcript *TR55998/c0_g1_i2* (an α-amylase). Amylases are carbohydrate metabolism enzymes that catalyze the cleavage of glycosidic bonds for various cellular processes (Heldt and Piechulla 2010, p. 248). Transcript *TR59333/c0_g1_i3* was also highly expressed in the susceptible family and is involved

in cytoskeleton organization. That sequence was annotated as tubulin-folding cofactor C (TFCC), which is essential for microtubule function *in planta* (Kirik et al., 2002), and required for cytoskeleton organization, cellular division and cytokinesis (Steinborn et al., 2002). The role of *TR59333/c0_g1_i3* is then central for normal growth and development.

An interesting sequence that was at constitutively higher expression levels in family 583 in comparison to family 685 was transcript *TR3907/c0_g2_i1*, annotated as protein enhanced disease resistance 2 (EDR2). This protein is involved in the resistance against the biotroph *Erysiphe cichoracearum* in *Arabidopsis* (Tang et al., 2005, Vorwerk et al., 2007). EDR2 is a negative regulator of the salicylic acid pathway and occurs in the plasma membrane, endosomes and endoplasmic reticulum (Vorwerk et al., 2007). EDR2 also limits the spread of programmed cell death (Vorwerk et al., 2007), a key aspect of hypersensitive response to pathogen attacks (Agrios 2005, p. 151). This gene encodes a protein with a pleckstrin homology domain that binds phosphatidylinositol-4-phosphate *in vitro*, and may be a link between lipid signalling and programmed cell death activated by mitochondria (Tang et al., 2005). The fact that EDR2 was expressed only in family 583 is puzzling, however, there is a possible explanation for such observation. EDR2 limits programmed cell death (Vorwerk et al., 2007), but the *Arabidopsis* mutant *edr2*, which does not express EDR2, is resistant to *E. cichoracearum* and develops necrotic lesions after infection with the pathogen, a probable hypersensitive response. Being fully expressed in family 585, EDR2 could make *T. plicata* seedlings more susceptible to *D. thujina* because programmed cell death in response to infection would be limited if it occurred. Although there is no known literature on hypersensitive response to *D. thujina* infection in *T. plicata* published to date, it is feasible that EDR2 could be more of a marker for susceptibility to *D. thujina* than for resistance to that disease. Further investigations on the role of EDR2 in the susceptibility to *D. thujina* in *T. plicata* will be required.

Family 583 also depicted differences between infection treatments, with sequences like *TR26208/c0_g1_i1*, *TR59130/c4_g1_i2* and *TR59130/c4_g2_i3* found at higher expression levels in seedlings in the CLB^- infection treatment. No plant sequences of interest were captured by the analyses from susceptible seedlings in the CLB^+ treatment. Transcript *TR26208/c0_g1_i1* is a phenylalanine ammonia-lyase (PAL), and sequences *TR59130/c4_g1_i2* and *TR59130/c4_g2_i3* are both chalcone synthases

(CHS). Both enzymes are part of the phenylpropanoid pathway, PAL being the initial step of the pathway, producing *trans*-cinnamic acid from phenylalanine (Heldt and Piechulla 2010, p. 433), and CHS acting downstream as the first step in the production of flavonoids (Tohge et al., 2013). Flavonoids are phenolic compounds (Heldt and Piechulla 2010, p. 431; Sulaiman and Balachandran 2012) with diverse functions in plants, including antioxidants, symbiont signalling, herbivore protection and UV protection (Heldt and Piechulla 2010, p. 445). The high expression levels of PAL and CHS in the seedlings from family 583 that were in the CLB^- treatment may be unrelated to pathogen defense, but may instead be related to UV protection or some other function.

3.4.3 Summary and conclusions

The chemical and gene expression differences between a *T. plicata* family resistant to *D. thujina* and one susceptible to that disease were studied. The resistant seedlings had significantly higher concentrations of sabinene and α-thujene, as well as higher levels of four transcripts that are thought to be part of the pathway leading to the biosynthesis of those compounds. The products of such transcripts need to be characterized in future studies.

The resistant family had higher expression levels of transcripts related to defense functions. Of special interest are a leucine-rich repeat receptor-like protein kinase and a cysteine-rich receptor-like protein, both of which may be involved in the resistance to *D. thujina* in *T. plicata*. Other interesting proteins in family 685 were the zinc finger CCCH domain-containing proteins and the bark storage proteins. Both may play key roles in defense against *D. thujina*, even though their mechanisms of action are still unknown.

Seedlings from the susceptible family studied did not have high concentrations of defense related compounds, nor elevated expression levels of defense-related transcripts. On the contrary, the family appeared to have a strong primary metabolism devoted mostly to growth and development. An interesting sequence found only in the susceptible family was protein EDR2, a protein that may increase the susceptibility to *D. thujina* by limiting programmed cell death, a key process in plant defense. The role of EDR2 in increased susceptibility to *D. thujina* should be further studied.

Chapter 4

Chemical and gene expression (*RNA*-Seq) responses to *Didymascella thujina* infection in *Thuja plicata* seedlings

4.1 Introduction

Plants are in continuing contact with organisms like fungi (Achotegui-Castells et al., 2016, de Cremer et al., 2013, Galindo-González and Deyholos, 2016, Kang et al., 2016, Parrott et al., 2016), bacteria (Mersmann et al., 2010, Tichtinsky et al., 2003), other plants (Olsen et al., 2016), viruses (Álvarez-Yepes et al., 2016, Parrott et al., 2016), nematodes (Sharma 2006, p. 4.6), and other herbivores (Ghaffar et al., 2016, Ruuhola et al., 2011, Vourc'h et al., 2002). The early interactions determine the type of relationship to be established, with some relationships being benign and others being detrimental to one or both of the species involved. Beneficial relationships include mutualisms like seed dispersal (Herrera, 2002), pollination by insects (Bronstein et al., 2006) and animals (Pellmyr, 2002), protection by ants (Bronstein et al., 2006), nodule formation in legumes for nitrogen fixation (Ott et al., 2005, Vance et al., 1979, Vasse et al., 1990, Zahran, 1999), and mycorrhizae formation (Janos, 1980, Klironomos et al., 2000, Plenchette et al., 1983, Ronsheim and Anderson, 2001). Harmful relationships usually result in the deployment of plant defenses against the attacker.

Microorganisms use different strategies to access their hosts. Viruses and bacteria, for instance, tend to enter through wounds and natural openings (Agrios 2005, p. 88; Dickinson 2003; Ramos et al. 1992; Sharma 2006, p. 4.6; Zinsou et al. 2006), while many pathogenic fungi gain access to their host via direct penetration (Agrios 2005, p. 88; Gees and Hohl 1988; Roundhill et al. 1995; Sharma 2006, p. 4.6; Sherwood 1981; Søegaard 1969, p. 299) resulting from the chemical interactions and the release of enzymes like cutinases (Agrios 2005, p. 82; Vidhyasekaran 2008, p. 14; Sharma 2006, p. 4.10), pectinases, cellulases, hemicellulases, ligninases and several proteases (Sharma 2006, p. 4.11). Plant responses to pathogen attacks take place promptly and frequently lead to the release of elicitors (Agrios 2005, p. 213; Heldt 2005, p. 405; Heldt and Piechulla 2010, p. 401; Sharma 2006, p. 3.16; Vidhyasekaran 2008, p. 56) that then induce the production of phytoalexins (Agrios 2005, p. 235; Heldt 2005, p. 404; Heldt and Piechulla 2010, p. 400; Sharma 2006, p. 5.14; Vidhyasekaran 2008, p. 411), as well as structural defenses. Common defense mechanisms include the production of antimicrobial molecules like alkaloids (Bednarek and Osbourn, 2009, Dembitsky et al., 2015, Hagel and Facchini, 2013), flavonoids (Bednarek and Osbourn, 2009, Falcone-Ferreyra et al., 2012, Liu et al., 2006), storage proteins (de Souza Cândido et al., 2011), as well as the accumulation of callose (Donofrio and Delaney, 2001, Voigt, 2014), suberin (Agrios 2005, p. 187; Smith et al. 2006; Yoshida 1998), and lignin (Agrios 2005, p. 187; Smith et al. 2006; Xu et al. 2011; Yoshida 1998). Other common responses to pathogen infection include the induction of pathogenesis related proteins like β-1,3-glucanases (Beffa et al. 1993; Leubner-Metzger and Meins Jr. 1999; Vidhyasekaran 2008, p. 55), chitinases (Galindo-González and Deyholos 2016; Neuhaus 1999; Sharma et al. 2011; Vidhyasekaran 2008, p. 55), thaumatin-like proteins (Velazhahan et al., 1999) and peroxidases (Chittoor et al., 1999, Ghosh, 2006, Hemetsberger et al., 2012).

Plant pathogens reproduce in their hosts and spread in a cyclic manner (Agrios 2005, p. 80; De Wolf and Isard 2007; Lieberei 2007; Sharma 2006, p. 1.36). In general, this disease cycle consists of the following phases (Agrios 2005, p. 80; Sharma 2006, p. 1.36): inoculation, prepenetration, penetration, infection and dissemination. Inoculation refers to the first contact between a plant and a pathogen in a place where infection may occur (Agrios 2005, p. 80; Sharma 2006, p. 1.37). The prepenetration phase includes a series of events, from the attachment of the pathogen and recognition of both organisms by each other, to the germination and formation of appressoria

(Agrios 2005, p. 82; Sharma 2006, p. 1.37). Penetration takes place next (Agrios 2005, p. 87; Sharma 2006, p. 1.37), and can be direct (Gees and Hohl, 1988, Pawsey, 1960, Roundhill et al., 1995, Sherwood, 1981, Søegaard, 1966) or take place through natural openings (Dickinson, 2003, Ramos et al., 1992, Zinsou et al., 2006) or wounds (Agrios 2005, p. 88; Sharma 2006, p. 4.6). Infection is the parasitic phase when the pathogen gets established and obtains the necessary nutrients for its survival (Agrios 2005, p. 89; Sharma 2006, p. 1.38). Successful pathogen infections result in the invasion and colonization of the host and the development of symptoms (Agrios 2005, p. 91; Sharma 2006, p. 1.39). Full invasion and colonization can take from days (De Luna et al., 2002, Roundhill et al., 1995) to months (Orshinsky et al., 2012, Rhouma et al., 2013, Viruega et al., 2011, Zhou et al., 2011). Dissemination is the last stage of the disease cycle and is the spread of the pathogen once the disease cycle has been completed (Agrios 2005, p. 96; Sharma 2006, p. 1.40). The means of dispersal vary from pathogen to pathogen, but they include air, water or biotic vectors (Agrios 2005, p. 96; Sharma 2006, p. 1.41).

The most important phase of the disease cycle for fungal pathogenicity is the infection stage despite the fact that the disease incubation may take months (Agrios 2005, p. 89). The early interactions between plant and pathogens take place within minutes of contact: fungal spores release their adhesive extracellular matrix within seconds to minutes after landing on their hosts (Agrios 2005, p. 82; Vidhyasekaran 2008, p. 2), and plants start inducing defense responses within minutes as well (Vidhyasekaran 2008, p. 55). Once the infection process has successfully begun, fungal mycelia can be visualized inside the host within days (Pawsey 1960; Søegaard 1969, p. 310; Yoshida 1998). Plants resistant to specific diseases tend to defend themselves at early stages (Bestwick et al., 1997, Lindgren et al., 1986, Thordal-Christensen et al., 1997), making it impossible for the pathogen to colonize, reproduce and disperse to the next host. Hypersensitive response (HR) is probably the best-known example of an early resistance mechanism. HR is the controlled necrosis of mesophyll cells in order to block the spread of a pathogenic attack (Stakman, 1915). HR is common in diseases caused by bacteria, nematodes, biotrophic fungi and viruses (Agrios 2005, p. 217; Sharma 2006, p. 5.10), and is a very effective qualitative disease resistance mechanism (Agrios 2005, p. 137; Sharma 2006, p. 5.10). Plants like wheat, potato and *Arabidopsis* induce HR when attacked by certain pathogens (Brown et al., 1966, Gees and Hohl, 1988, Lauvergeat et al., 2001). HR has been shown to be the prod-

uct of gene-for-gene interactions between plant and pathogen (Agrios 2005, p. 151; Sharma 2006, p. 5.10). The gene-for-gene model of disease resistance postulates that resistance (*R*) genes in plants confer full resistance against pathogens that have the complementary avirulence (*avr*) genes (Agrios 2005, p. 140; Hammond-Kosack and Jones 1997; Sharma 2006, p. 3.9; Vidhyasekaran 2008, p. 193).

An important pathosystem in North America is the *Thuja plicata* (western redcedar, WRC) - *Didymascella thujina* (cedar leaf blight, CLB) interaction (Frankel, 1990, 1991, 1992, Kope and Trotter, 1998a, Kope and Dennis, 1992, Kope et al., 1996a). The colonization of *T. plicata* foliage by *D. thujina* is achieved via intercellular mycelia growth in the leaf mesophyll followed by penetration of the cells where intracellular bi- and tri-furcated haustoria develop within days of inoculation (Pawsey 1960; Søegaard 1969, p. 310). Despite the fact that this initial infection process is well understood in this pathosystem, there is no information to date on the initial defense responses to *D. thujina* infection in *T. plicata*. Furthermore, it is also unknown if differences in the early defense responses to *D. thujina* exist between seedlings coming from resistant and susceptible populations. This kind of information is very valuable, especially for seedlings given their high susceptibility to the pathogen (Alcock, 1928, Burdekin and Phillips, 1971, Kope and Trotter, 1998b, Kope, 2000, Kope et al., 1996a). As mentioned earlier, the early stages of the infection process are crucial in the establishment and development of a disease (Agrios 2005, p. 82; Vidhyasekaran 2008, p. 2), and the interplay between plant and pathogen signals during that early interaction results in either resistance or susceptibility of the host (Vidhyasekaran 2008, p. 1). In order to shed light on the initial defense mechanisms against *D. thujina* that result in disease resistance in *T. plicata* seedlings, the early chemical responses to *D. thujina* infection in seedlings from six full-sib *T. plicata* families were studied in both natural and controlled conditions. The gene expression (*RNA*-Seq) responses to pathogen infection from seedlings inoculated under controlled conditions were also investigated, with especial emphasis on their relationship with the chemical responses.

4.2 Methodology

4.2.1 Experimental design

In summer 2014, one-year-old seedlings from six full-sib families (398, 525, 583, 685, 8255 and 8265; see Appendix A.1) were real and mock infected with *D. thujina* under both controlled and natural conditions (see below and Appendix A.7 for details). The seedlings were grown from seed sown in March 2013 in Beaver Styroblock containers 45/340 (Stuewe and Sons., Tangent, OR, USA) in a fibreglass house at the Cowichan Lake Research Station (Mesachie Lake, British Columbia). The plants were maintained under natural light for one season using standard growing procedures.

4.2.1.1 Natural conditions experiment

The natural conditions (NC) experiment took place between May 26th and June 19th 2014, in two progeny trials in Jordan River (British Columbia). The two sites were approximately one kilometer from each other and had similar climates (Appendices A.13 and A.15). *D. thujina* was present in one site (hereafter referred to as "real infection", NC-CLB^{+}; western redcedar progeny trial located on Black Creek road at 48° 25' 24.52" N, 124° 1' 27.69" W, elev. 76 m), but absent in the other (hereafter referred to as "mock infection", NC-CLB^{-}; Douglas fir trial located on East Main road at 48° 25' 51.08" N, 124° 1' 49.12" W, elev. 156 m). Sampling of *T. plicata* seedlings for chemical composition was done just before the seedlings were deployed to the sites (day 0), and 11, 18, 21 and 24 days post deployment (dpd; Appendix A.7). Foliage from the midmost branches from three seedlings per date × family × infection treatment combination were sampled. New seedlings were sampled at each date to avoid any potential induced effects from sampling. The foliage was pooled, flash frozen and placed on dry ice immediately after harvesting, and then stored at -80℃ until further processing.

The seedlings were watered twice a week while in the field, and after the last sampling date, were placed in the Bev Glover Growth Facility (University of Victoria, Victoria, British Columbia). The plants were kept in a glasshouse for nine months until symptoms of *D. thujina* infection developed. In the glasshouse, the seedlings were watered twice a week in summer, and once a week in other seasons and were fertilized once a month using Peter's 20-7-19 Conifer Grower fertilizer (Jr. Peters Inc, Allentown PA,

USA) at 100 parts per million (ppm) nitrogen. Infection was confirmed in two ways: 1) evaluation of the presence of *D. thujina* spores on the plant foliage sampled in the field at each collection date, and 2) assessment of the disease severity after symptoms developed.

Presence or absence of *D. thujina* spores in the foliage that was sampled on each date was assessed in ∼3mm foliar samples that were processed for scanning electron microscopy (SEM). The samples were fixed overnight in 2.5% glutaraldehyde prepared with Sörensen's buffer (pH 7.2; Ruzin, 1999, pp. 227), and then changed two times in Sörensen's buffer alone, before dehydration in an ethanol series (50%, 70%, 80% and 90%). Two final changes were done in 100% ethanol. All changes lasted 30 min. The samples were then critical point dried in a Leica EM CPD300 system (Leica Microsystems Inc., Richmond Hill ON, Canada), gold coated in an Edwards S150B Sputter Coater (Edwards Canada, Quebec QC, Canada), and photographed in a Hitachi S-3500N Scanning Electron Microscope (Hitachi High-Technologies Canada Inc., Toronto ON, Canada). Disease severity was quantified as the percentage of foliar area blighted (brown or black) and was measured in all plants that were exposed to infection using the colour analysis mode of WinRHIZO Pro v. 2009c (Regent Instruments Inc., QC, Canada). Leaves used in this analysis were scanned in an Epson Perfection v750 scanner (Epson Canada Ltd., Markham ON, Canada). Raw severity data were square-root transformed to meet the normality assumption, and analyzed with a one-way analysis of variance (ANOVA) with family as a factor. LSD all-pairwise comparisons test of the disease severity was conducted when the ANOVA was significant, and the families were classified as resistant or susceptible to *D. thujina* based on the results of that test (see section 4.3).

4.2.1.2 Controlled conditions experiment

The controlled conditions (CC) experiment was carried out in one Conviron growth chamber (Conviron, Winnipeg MB, Canada) at the Bev Glover Growth Facility between June 17th and 26th, 2014. The chamber was set for 12 h of darkness at 10℃ and 12 h of light at 14℃ with relative humidity (RH) ∼90%. High humidity was achieved by building a custom-made cage for the plants and placing it inside the growth chamber (Appendix A.10). The cage was made of PVC pipes covered with transparent plastic. Ultrasonic foggers were placed inside the cage to produce and

maintain the desired humidity. The foggers ran for two days before the ∼90% RH was achieved. Analog temperature and humidity meters were placed in the cage to monitor the conditions within the cage during the experiment. The seedlings were acclimated to those conditions for two weeks prior to the start of the experiment.

The experiment consisted of both real (CC-CLB$^+$) and mock (CC-CLB$^-$) infections. Foliar samples for chemical composition analyses were taken just before setting up the inoculation (day 0), and three, six and nine days post infection (dpi, see Appendix A.7). Pooled foliage samples came from inoculated branches (see below) from three seedlings per date × family × infection combination, with no seedling being re-sampled. Small leaf samples (∼3mm) were fixed in 2.5% glutaraldehyde prepared with Sörensen's buffer (pH 7.2) to confirm infection using SEM, Additional foliage harvested was immediately flash frozen, placed on dry ice and stored at -80℃ until further processing. The samples from four of the families (398, 583, 685 and 8265) in the CC-CLB$^+$ treatment were also used for gene expression analysis (*RNA*-Seq). The foliage from these families was promptly cut in smaller pieces, mixed and split in two: one half for chemical analyses, and the other half for *RNA*-Seq analysis. Small fragments from each sample were also fixed in 2.5% glutaraldehyde prepared with Sörensen's buffer for SEM infection confirmation, and the rest of the foliage was flash frozen, placed on dry ice and stored at -80℃ as before.

Inoculations were done using a modified version of the method described in Søegaard (1969, pp. 310). Cuttings with sporulating ascocarps of *D. thujina* were collected from the western redcedar progeny trial site in Jordan River (48° 25' 24.52" N, 124° 1' 27.69" W) at the peak of the sporulation season (June 16th, 2014; spore production was monitored from May 2nd 2014; Appendix A.13). At the time of collection, the cuttings were placed individually in 10 mL floral water pick tubes filled with a general nutrient solution (per 100 L of solution: 0.90 g Chelated Micronutrient Mix [Master Plant-Prod Inc., Brampton ON, Canada], 5.24 g KCl, 12.37 g K_2HPO_4, 28.59 g NH_4NO, 4.05 g $MgSO_4{\cdot}7H_2O$ and 2.15 g $CaSO_4{\cdot}2H_2O$; final N:P:K ratio 100:22:83), and were subsequently taken to a growth chamber set for 12℃, 12 h of light and 12 h of darkness with 80% RH for one day to promote spore release. The infection (CC-CLB$^+$ treatment) was carried out the following day: each pick tube with its respective cutting was planted in the Styroblock cavity of the seedling to be infected and the adaxial surface of the cutting infected with *D. thujina* was placed facing the same

surface of the midmost branch of the seedling to be infected. The two branches were then fastened together with masking tape to ensure that spores released by the cuttings came in contact with the seedling. The mock infections (CC-CLB$^-$ treatment) were set up the same way as the real infections, except that cuttings with no disease symptoms were used. Infection was verified using three methods: 1) evaluation of the presence of *D. thujina* spores using SEM, 2) assessment of the disease incidence after symptoms developed (i.e. ∼9 months), and 3) BLASTn searches for the publicly available internal transcribed spacer 2 (ITS2) sequences of *D. thujina* (GenBank accessions KT875766 and KT875767) in the assembled reference transcriptome (see section 4.2.3). Incidence was measured by counting the number of plants with and without *D. thujina* symptoms, and an independence test (family vs. plants with and without *D. thujina*) was performed on that dataset.

4.2.2 Chemical composition

Fifty-four chemical variables, including sugars, starch, lignin, cellulose, fibre, mineral nutrients, terpenes, carbon and nitrogen were quantified in foliage from both the natural and controlled conditions experiments (see Appendix A.20). All analyses, except carbon and nitrogen, were done at the Analytical Laboratory of the Ministry of Environment and Climate Change Strategy (Victoria BC, Canada). Sugars were quantified using the anthrone reagent procedure by Ebell (1969), starch was measured using the third enzyme method in Rose et al. (1991), and lignin, cellulose and fibre were analyzed using the acid detergent cellulose and acid detergent fibre procedures used in forage fibre analysis (Goering and Van Soest, 1970).

Mineral nutrients were analyzed by digesting 0.25 g of fine milled foliage in 4.0 mL of digestion reagent (150 µg scandium·L^{-1} prepared in 70% nitric acid) using 15 mL quartz tubes. The digestion was carried out in an Ultrawave Microwave Digestion System (Milestone Inc., Shelton CT, USA) according to the manufacturer guidelines, and elements were measured using inductively coupled plasma optical emission spectroscopy analysis with the scandium from the digestion step as the standard. Terpenes were analyzed using 0.25-0.50 g of foliage ground in liquid nitrogen. The terpenes were extracted by mixing the ground foliage with 4 mL of methanol for 48 h, and then quantified using 30 m × 0.25 mm, d_f 0.25 µm capillary GC columns in a Clarus Gas Chromatograph (PerkinElmer Inc., Waltham MA, USA) following the manufac-

turer instructions. Terpene standards for *T. plicata* extractives were prepared mixing 0.05-0.50 g of the extractive in 100 mL methanol at a concentration appropriate for the amount expected to be present in the foliage.

Carbon and nitrogen samples were processed at the Nutrient Analysis Laboratory at the Centre for Forest Biology (University of Victoria, Victoria BC, Canada) as follows: the samples were dried for 48 h at 60℃ ground in a Wig-L-Bug grinding mill (International Crystal Laboratories, NJ USA), and dried again overnight at the same temperature. They were then packed in tin capsules (pressed, standard weight - 10×10mm; Elemental Microanalysis Ltd., Devon UK), and the elements quantified in a FlashEA® 1112 Nitrogen and Carbon Analyzer (Thermo Scientific™ Wilmington DE, USA).

Statistical analyses

Each experiment was analyzed separately although the analyses were the same for both. Datasets with all chemical variables were first explored with principal component analysis (PCA; correlation matrix) using package FactoMineR (Lê et al., 2008) in R (R Core Team, 2015). Chemical variables were then analyzed using categorical stability selection (Meinshausen and Bühlmann, 2010) to select the variables that discriminated between real and mock infections in resistant and susceptible families. Stability selection is a variable selection methodology that detects the best variables that might explain a response variable (categorical or continuous) chosen by the investigator. The technique outputs a sorted list of variables based on a decreasing score determined by the method (Meinshausen and Bühlmann, 2010). The categories were as follows for the NC experiment: CLB^- and all 0 dpd samples in one category, samples from resistant families collected at 11-24 dpd from the CLB^+ treatment in another, and samples belonging to susceptible families collected at 11-24 dpd from the CLB^+ treatment in a third category. For the CC experiment, samples from the CLB^- treatment and all 0 dpi samples were in one category, samples from resistant families collected at 3-9 dpi from the CLB^+ treatment were in another, and samples belonging to susceptible families collected at 3-9 dpi from the CLB^+ treatment were in a third category. The stability selections were executed using the randomized lasso algorithm implemented in the scikit-learn package (Python). Change point analysis with the AMOC method on variance (Killick and Eckley, 2014) was then used on

the scores output by the stability selection to determine which chemical variables to keep from the stability selections to then analyze with ANOVAs. Change point is a procedure that finds the changing point of a time series, and was used to detect the variable with the steepest drop in score. It is assumed that variables that ranked below those chosen have lesser contribution to the categories used as response variable in the stability selections. The selected variables were then analyzed using a statistical mixed-effects factorial model (see Appendix A.23).

Graphs from selected chemical variables shown in this document corresponded to relative concentrations in the real infections normalized against mock infections (see e.g. Figs. 4.2a-4.2f and Appendix A.25). For each family × time combination, the absolute value of the variable of interest (e.g. aluminum) in CLB^+ was divided by its respective value in CLB^-, and ratios by resistance class were then averaged, standard errors calculated and the plots generated.

4.2.3 Gene expression - controlled conditions experiment

RNA extraction

An activated charcoal - cetyltrimethylammonium bromide (CTAB) method modified from Rajakani et al. (2013) was used for the *RNA* extraction from the *RNA*-Seq samples referred to in section 4.2.1.2. All glassware and water was treated with diethyl pyrocarbonate (DEPC) before the extraction. Briefly, 1.5 g of foliage were ground in liquid nitrogen in a pre-chilled mortar and pestle. Using liquid nitrogen, the samples were poured into 50 mL Nalgene™ Oak Ridge high-speed centrifuge tubes (Life Technologies Inc., Burlington ON, Canada) and left to dry in a -20℃ freezer. Once dry, the samples were taken from the freezer, and 20 mL of preheated (to 65℃) 2% CTAB with activated charcoal was added (200 mM Tris-Cl pH 8.0, 50 mM EDTA pH 8.0, 2.5 M NaCl, 0.05% activated charcoal, 1.5% polyvinylpolypyrrolidone [PVPP] and 3% β-mercaptoethanol; the last three compounds were added immediately before use). The samples were then vortexed and incubated with intermittent shaking for 15 min at 65℃, cooled down to room temperature (RT), and centrifuged at 17,211 × g for 20 min at 4℃. The supernatant was transferred to a new 50 mL tube, mixed with chloroform in a 1:1 proportion, mixed by inversion and centrifuged again for 20 min at 4℃ at 17,211 × g. The last step was repeated once more for a total of two chloroform extractions. The final supernatant was transferred to a clean 50 mL tube,

mixed with 10M lithium chloride in a 4:1 proportion and incubated at 4℃ overnight.

The next morning, the samples were centrifuged for 30 min at 20,199 × *g* at 4℃. The supernatant was poured out and the pellet suspended in a mixture of 400 µL phenol (pH 8.0) and 500 µL SSTE (1M NaCl, 0.5% SDS, 10mM Tris HCl pH 8.0, 1mM EDTA pH 8.0). The solution was then placed in a 1.5 mL Eppendorf® tube, 100 µL of chloroform were added, and the solution was vortexed and centrifuged for 5 min at 18,407 × *g* at RT. The supernatant was moved into a new 1.5 mL tube, mixed with 300 µL of chloroform, vortexed and centrifuged at 18,407 × *g* at RT for 5 min. The last supernatant was mixed with 100% isopropanol and 3M sodium acetate in a 10:10:1 proportion. The mixture was incubated at -20℃ for 25 min and centrifuged for 33 min at 20,626 × *g* at 4℃. The supernatant was discarded, and the pellet combined with 1.0 mL of 75% chilled ethanol, mixed by inversion and centrifuged at 20,626 × *g* at 4℃ for 5 min. The final supernatant (ethanol) was removed and the pellet was let to dry fully at RT. Final elution of the total *RNA* extracted was done in 50 µL of DEPC-treated water. *RNA* was quantified using a NanoDrop™ 2000 Spectrophotometer (Thermo Scientific™ Wilmington DE, USA), and integrity was checked using 1X MOPs, 1.0% formaldehyde-agarose gel.

Messenger *RNA* enrichment, c*DNA* library production and sequencing

The Thermo Scientific™ MagJET m*RNA* Enrichment Kit, protocol C (Life Technologies Inc., Burlington ON, Canada) was used for messenger *RNA* enrichment, and the NEB Next® Ultra™ *RNA* Library Prep Kit for Illumina® v. 1.2. (New England BioLabs® Inc., Ipswich MA, USA) was used for all library production procedures except the *DNA* purifications and size selection. *DNA* purifications were completed with the Thermo Scientific GeneJET NGS Cleanup Kit (Life Technologies Inc.), and size selections (∼500 bp) with the Thermo Scientific MagJET NGS Cleanup and Size Selection Kit (Life Technologies Inc.). Barcoding was done with the NEB Next® Multiplex Oligos for Illumina® - Index Primers Set 1 (New England BioLabs® Inc.). Individual libraries were quality controlled in an Experion™ Automated Electrophoresis Station (Bio-Rad Laboratories) using a *DNA* 1K Analysis Kit (Bio-Rad Laboratories, Mississauga ON, Canada). The samples were then pooled in two separate batches ensuring no index primer was repeated in each batch. The two final batches consisted of 40 ng per library, and were outsourced for sequencing to Genome Que-

bec Innovation Centre (Montreal QC, Canada). Two 100 bp paired-end lanes were sequenced in an Illumina® HiSeq 2000 sequencer.

Bioinformatics

The pipeline outlined in Appendix A.28 was used for the bioinformatics analyses. Customized shell, Python and R scripts were used on the WestGrid Hermes cluster, hosted at the University of Victoria, to complete the analyses outlined below. HPC GridRunner was used to speed up annotation searches like BLAST and HMMER because of Hermes' low capabilities for such tasks ($\sim$ 240 nodes, each with 16 cores and 128GB of RAM).

Assembling of a reference transcriptome and annotation

The compressed, paired-end FASTQ Illumina® 1.9 (Phred-33 ASCII) files produced after sequencing were retrieved from Genome Quebec Innovation Centre, and were quality checked before and after trimming using FastQC v. 0.11.2 (Andrews, 2014). The files were trimmed with Trimmomatic v. 0.33 (Bolger et al., 2014) using the following settings: ILLUMINACLIP:TruSeq2-PE-v2.fa:2:30:10 HEADCROP:14 SLIDINGWINDOW:4:15 MINLEN:36 TOPHRED33. The TruSeq2-PE-v2.fa was produced by adding over-represented sequences reported by FastQC into Trimmomatic' TrueSeq2-PE.fa. Trinity v. 2.0.6 (Grabherr et al., 2011) was used to build the reference transcriptome using the default settings. The assembly's statistics were calculated with PRINSEQ v. 0.20.1 (Schmieder and Edwards, 2011), and the sequences were annotated in Trinotate v. 2.0.2 (http://trinotate.github.io). The annotation process was as follows: coding regions were predicted with TransDecoder v. 2.0.1. (http://transdecoder.github.io), and the Swiss-Prot/TrEMBL and UniRef90 (The UniProt Consortium, 2015, 2017) databases, as well as Gene Ontology (Ashburner et al., 2000, The Gene Ontology Consortium, 2015), and EggNOG (Huerta-Cepas et al., 2016) were searched using BLAST+ v. 2.2.28 (Camacho et al., 2009). Additionally, protein domains were searched in the Pfam database (Finn et al., 2016) using HMMER v. 3.1b1 (http://hmmer.org). RNAmmer v. 1.2 (Lagesen et al., 2007), TMHMM v. 2.0 (http://www.cbs.dtu.dk/services/TMHMM/), and SignalP v. 4.0 (Petersen et al., 2011) were executed as part of the annotation process as well.

Differential expression analyses

The Trinity pipeline (Haas et al., 2013) was used in downstream analysis using the read counts of the assembler's transcripts. Although Trinity's "transcripts" may not correspond to real transcripts, but to contigs or contig variants of Trinity's "genes", the term "transcript" is used in this document for simplicity. RSEM v. 1.2.20 (Li and Dewey, 2011) was used to map raw reads to the assembled transcriptome, and FPKMs (Trapnell et al., 2010) and trimmed mean of M-values (TMM) (Dillies et al., 2013, Robinson and Oshlack, 2010) were calculated for normalization. Differential expression (DE) analysis was done by performing pair comparisons between all samples using edgeR (Robinson et al. 2010; with a dispersion value of 0.1), and then grouping all transcripts that had a minimum fold change of 4 and maximum false discovery rate of 0.001. A Pearson correlation heat map of all samples using all DE transcripts was produced as well. No qPCR confirmation was done to any of the DE sequences as the method used (edgeR) has high sensitivity and specificity as well as high overall agreement with qPCR measurements when compared to other DE methods, such as Cuffdiff2, TSPM or DESeq2 (Rajkumar et al., 2015). Furthermore, it has been reported that relative expression levels agree across different gene expression platforms, including HiSeq 2000 and qPCR (SEQC/MAQC-III Consortium, 2014).

Data mining and detection of sequences of interest

Selection of sequences of interest was done using the following procedures: 1) hierarchical clustering, 2) stability selection and, 3) dynamic topic modelling. Euclidean distance-based hierarchical clustering was used to produce a heat map of the DE transcripts. Clusters were produced by cutting the tree at 68.5% of its height. To ease the inspection of the processed data, the annotations and clustering information of the DE data were ingested into a SQLite database that was uploaded into a local TrinotateWeb server. TrinotateWeb was installed on Compute Canada's West Cloud (https://west.cloud.computecanada.ca), and was obtained from http://trinotate.github.io .

The randomized lasso algorithm for continuous (regression) and categorical response variables, provided in the Python scikit-learn package, was used to complete the stability selection analyses (Meinshausen and Bühlmann, 2010). Regression analysis was

carried out using the family disease severity after symptoms developed in the NC-CLB$^+$ treatment as the response variable. Regression stability selection was also done using the aluminum concentrations of the samples used for *RNA*-Seq analysis as the response variable because of the importance of that element in the CLB$^+$ treatments of both experiments (see section 4.3.1). Categorical stability selection was completed by resistance class and infection status combination to detect transcripts that showed differential responses between resistant and susceptible families. More specifically, categories were as follows: 0 dpi samples of both resistant and susceptible families in one category, 3-9 dpi samples of the resistant families in another category, and 3-9 dpi samples of the susceptible families in a third category. changepoint with the mean and variance AMOC method was used on the top 100 transcripts ranked by the stability selection analyses in order to decide the number of sequences to report from each.

Dynamic topic modelling (DTM, Blei and Lafferty, 2006, Lee et al., 2016) was used to model the expression levels after infection of transcripts that co-occurred at 0 dpi. Dynamic topics were modelled using the Dynamic Topic Models software (https://github.com/blei-lab/dtm) with K (number of topics) = 20 . Dynamic topics of interest were the most frequent topics among the transcripts retained by the stability selection analyses. The top dynamic topic per transcript retained (k) was that with the highest β value before infection (i.e. the topic with the highest $\beta_{0,k}$). The representative transcripts within each dynamic topic chosen were selected using the decreasing inferred posterior expression distribution scores of all differentially expressed transcripts at 0 dpi ($\beta_{0,k}$) and keeping the first 10. In dynamic topic modelling, it is common practise to use the top 5-10 "words" per topic to analyze them (see e.g. Blei 2012, Blei and Lafferty 2009, Liu et al. 2016a).

4.3 Results

All plants sampled in the NC-CLB$^+$ and CC-CLB$^+$ treatments had *D. thujina* spores present on their foliage after infections took place (11-24 dpd and 3-9 dpi, respectively) as assessed by SEM. Seedlings in the NC-CLB$^+$ treatment developed *D. thujina* symptoms within nine months of infection, and there were significant differences in the severity of the disease among families ($p < 0.0000$, Table 4.1). Based on the homogeneous groups that resulted from the LSD all-pairwise comparisons test on the

disease severity values, three families were classified as resistant (families 398, 685 and 8255) and three as susceptible (families 525, 583 and 8265). This classification is consistent with *D. thujina* severity screening data from the families' parents in progeny trials established by the British Columbia Ministry of Forests, Lands, Natural Resource Operations and Rural Development (see Appendix A.1).

Table 4.1. Severity and incidence of *D. thujina* symptoms in six *T. plicata* families in the natural (NC) and controlled conditions (CC) experiments. Severity was measured in the natural conditions-real infection treatment (NC-CLB$^+$), and incidence in the controlled conditions-real infection treatment (CC-CLB$^+$). Both variables were assessed once *D. thujina* symptoms were conspicuous.

Family	**Severity (%)[1]**	**Incidence (%)[2]**
525	22.93^{A}	69.23
583	24.17^{A}	62.50
8265	25.61^{A}	75.00
398	13.12^{B}	12.50
685	4.10^{C}	25.00
8255	$8.04^{B,C}$	50.00

[1] A-C: homogeneous groups in the NC-CLB$^+$ treatment based on the LSD all-pairwise comparisons test with $\alpha = 0.05$.

[2] Measured in the CC-CLB$^+$ treatment. Test of independence of family vs. presence/absence of *D. thujina* symptoms was significant ($p = 0.002$).

Plants in the CC-CLB$^+$ treatment developed *D. thujina* symptoms within nine months as did those in the NC-CLB$^+$ treatment. Independence test of family vs. presence/absence of *D. thujina* symptoms (used to calculate incidence) was significant ($p = 0.002$, Table 4.1).

4.3.1 Chemical composition

Principal component analysis showed before-infection (0 dpd/dpi) and after-infection samples to group separately in both the NC and CC experiments (Figs. 4.1a and 4.1b). In the natural conditions experiment, principal component 1 accounted for 21.18% of the data's variance, component 2 for 12.38%, and component 3 for 9.45%. The cumulative percentage of variance explained by the first three principal components was 43.02%. Variables with the highest contributions to component 1 were terpenes (e.g. myrcene, monoterpenes, R-limonene, α-pinene, α-thujene and α-thujone),

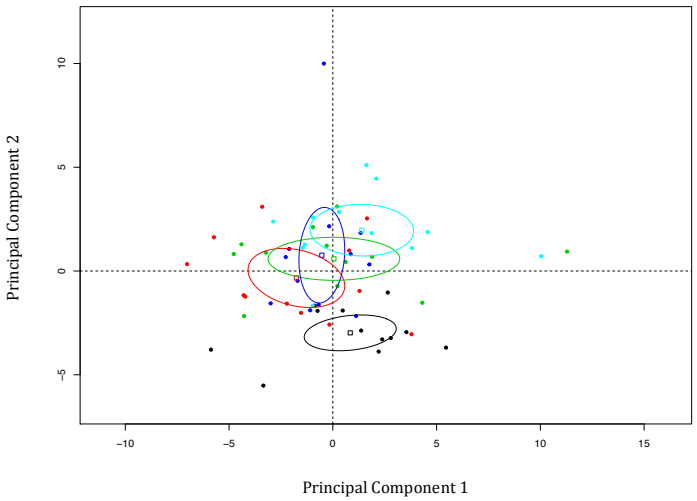

(a)

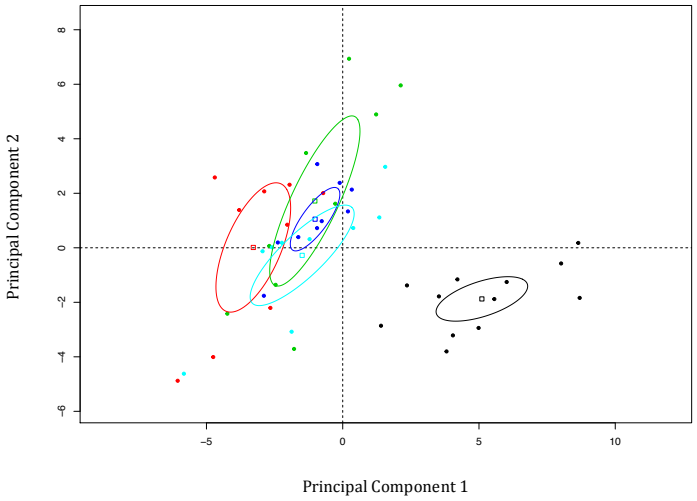

(b)

Figure 4.1. Bi-plot of the principal component analyses of the chemical variables studied in both the natural conditions (a), and controlled conditions (b), experiments. Fifty-four elements and compounds were analyzed in six *Thuja plicata* families (three resistant and three susceptible) that were real (CLB^+) and mock-infected (CLB^-) with *Didymascella thujina* in (a) Jordan River (British Columbia, Canada), and (b) growth chambers in the spring of 2014. For the natural conditions experiment (a), samples were taken just before the plants were deployed to the study field (0), and 11, 18, 21 and 24 dpd. Sampling was done 0, 3, 6 and 9 dpi in the controlled conditions experiment (b). Both analyses were correlation matrix-based; the confidence level of the ellipses shown is 95%. Samples and centroid ellipses are colour-coded as follows: 0 dpd/dpi samples in black, resistant families in the CLB^- treatment in red, resistant families in the CLB^+ treatment in green, susceptible families in the CLB^- treatment in blue, and susceptible families in the CLB^+ treatment in cyan.

while the greatest contributions to component 2 were from elements (sulfur, magnesium, phosphorus, sodium, iron and aluminum).

In the controlled conditions experiment, components 1, 2 and 3 explained 24.37%, 13.21% and 11.34% of the variance, respectively. The cumulative variance of those three components was 48.92%. Variables with the highest contributions to component 1 were terpenes (e.g. fenchone and terpinolene, geranyl acetate and myrcene) and elements (magnesium, potassium and nitrogen). Variables with the highest contributions to component 2 were also terpenes (R-limonene, α-pinene, monoterpenes and α-thujene) and elements (iron and zinc). Appendix A.20 lists variable contributions to the first three components of the PCA for each experiment.

In both experiments, there were only six chemical variables that discriminated between real and mock infections in resistant versus susceptible families as detected by the changepoint algorithm used on the categorical stability selection scores (Table 4.2). Aluminum ranked first in both experiments and showed significant differences in time, infection status, and the time × infection status interaction in the ANOVAs ($p < 0.05$ in all cases; Table 4.2). In both experiments, aluminum concentration increased over time and was significantly higher in susceptible families compared to resistant families (see Figs. 4.2a and 4.2b). Given that aluminum was the only chemical variable that showed the same trend in both experiments, it was used as response variable in one of the regression stability selections to detect predictor transcripts that explained such a response (see section 4.3.1).

Fenchone and terpinolene were top-ranked in both experiments as well, being third in the natural conditions experiment and fourth in the controlled conditions (see Table 4.2). However, there were differences between experiments. Concentrations of fenchone and terpinolene dropped over time in the natural conditions experiment (Fig. 4.2c). In contrast, their concentrations increased over time in the controlled conditions experiment, but the resistance category × time interaction was significant because resistant families had higher concentrations at 6 dpi than susceptible families (Fig. 4.2d). Carbon ranked second according to the categorical stability selection in the natural conditions experiment, and most factors and their interactions were significant except for resistance category and resistance category × time (Table 4.2). Carbon concentrations dropped dramatically in the susceptible families and increased

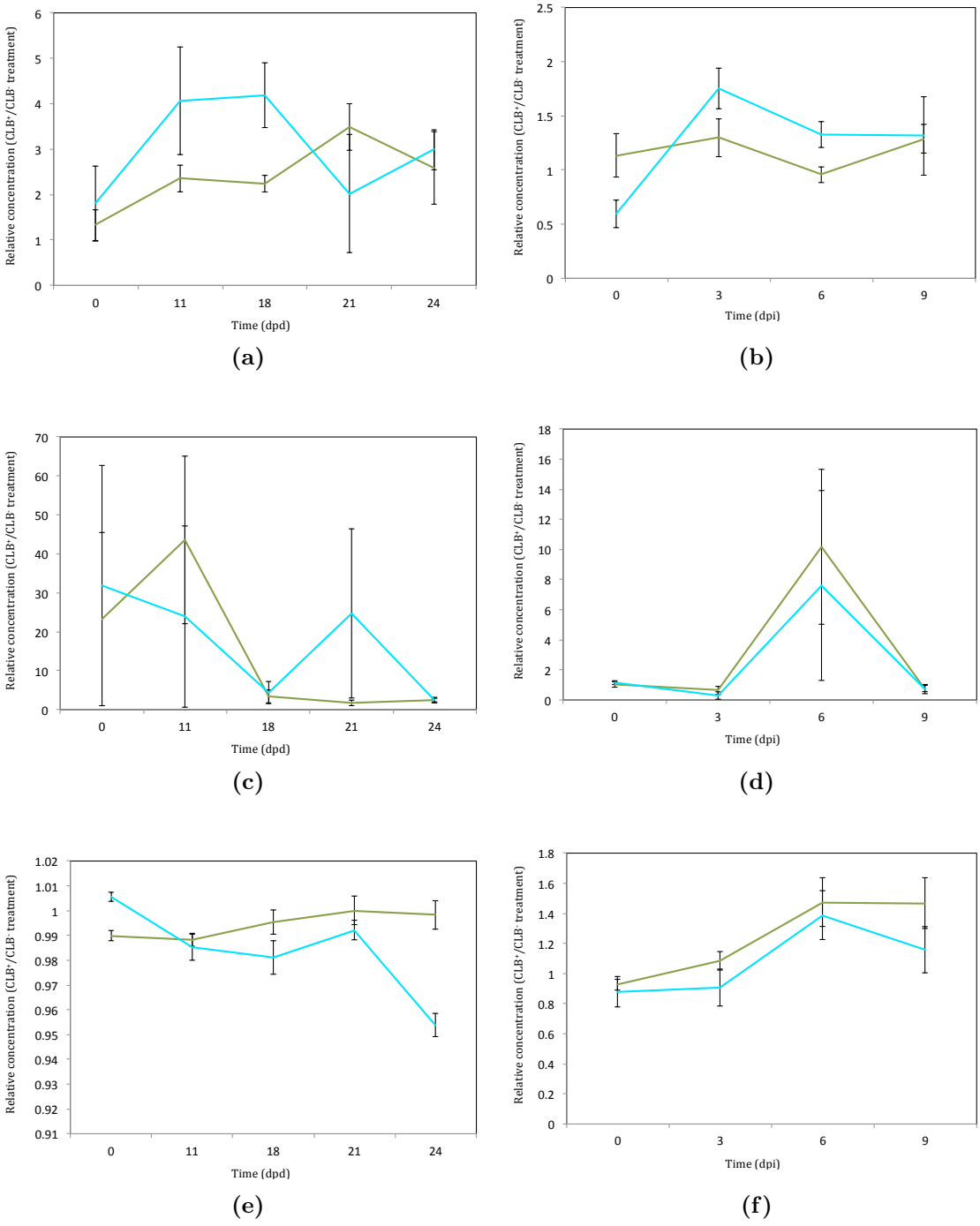

Figure 4.2. Temporal variation of the relative concentrations of selected chemical variables in the real infections normalized against mock infections in both experiments. Variables from the natural conditions experiment: (a) aluminum, (c) fenchone and terpinolene, (e) carbon. Variables from the controlled conditions experiment: (b) aluminum, (d) fenchone and terpinolene, (f) sesqui- and di-terpenes. Resistant families in green, susceptible families in cyan. Concentrations are higher in the real infections if the relative concentration (CLB^+/CLB^-) is >1, and higher in the mock infections if <1. dpd = days post deployment, dpi = days post infection.

Table 4.2. Statistical significance (p-values) from the ANOVAs of the top six chemical variables in the natural and controlled conditions experiments that differentiated between real and mock infections according to categorical stability selections (see also Figs. 4.2a-4.2f and Appendix A.25). Stability selection scores of the ranked variables are included. The variables were analyzed using a mixed-effects factorial model (see Appendix A.23). The "resistance category" factor refers to resistant versus susceptible plants, and the "infection status" factor to real and mock infections. *= significant factors at $\alpha = 0.05$; **= significant factors at $\alpha = 0.01$.

Natural conditions experiment							
Element/compound		Aluminum	Carbon	Fenchone + Terpinolene	Starch	Bornyl Acetate	Camphor
Stability selection score		0.5446	0.4689	0.4283	0.3202	0.2103	0.1802
Factor	Resistance category	0.6383	0.1491	0.4061	0.9265	0.2762	0.3510
	Time	$\leq$ 0.0000**	$\leq$ 0.0000**	0.0158*	0.0237*	0.4197	0.0082**
	Infection status	$\leq$ 0.0000**	$\leq$ 0.0000**	$\leq$ 0.0000**	$\leq$ 0.0000**	0.0259*	0.0240*
	Resistance category × Time	0.9390	0.1312	0.9238	0.3027	0.9716	0.1303
	Time × Infection status	0.0322*	0.0028**	0.6126	0.1622	0.8733	0.2750
	Resistance category × Infection status	0.8098	0.0039**	0.7451	0.6060	0.2613	0.3229
	Resistance category × Time × Infection status	0.1530	$\leq$ 0.0000**	0.6656	0.8633	0.4658	0.4909
Controlled conditions experiment							
Element/compound		Aluminum	Copper	Molybdenum	Fenchone + Terpinolene	Sesqui- and Di-terpenes	Iron
Stability selection score		0.4927	0.3177	0.1843	0.1718	0.1463	0.1398
Factor	Resistance category	0.8086	0.0040**	0.1946	0.1712	0.2523	0.6478
	Time	$\leq$ 0.0000**	0.6506	$\leq$ 0.0000**	$\leq$ 0.0000**	0.0189*	$\leq$ 0.0000**
	Infection status	0.0022**	$\leq$ 0.0000**	0.7827	0.3174	0.0261*	0.1262
	Resistance category × Time	0.3652	0.9496	0.0583	0.2529	0.8735	0.6458
	Time × Infection status	0.0302*	0.0069**	0.7535	0.1101	0.0096**	0.1464
	Resistance category × Infection status	0.3646	0.7085	0.0976	0.4422	0.2136	0.7509
	Resistance category × Time × Infection status	0.2813	0.7942	0.0301*	0.5125	0.9317	0.9287

slightly in the resistant families as the infection progressed in the natural conditions experiment (Fig. 4.2e). In the controlled conditions experiment, the sesqui- and di-terpenes ranked fourth as discriminants between resistance categories, with higher levels in the resistant infected families, although this difference was not significant (Table 4.2). Sesqui- and di-terpene concentrations increased in response to infection (Fig. 4.2f). The remaining variables selected by changepoint in both the natural conditions experiment (bornyl acetate, camphor and starch; Appendix A.25) and the control conditions experiment (copper, iron and molybdenum; Appendix A.25) had broad variances in spite of the significant differences that resulted from the ANOVAs.

4.3.2 Gene expression - controlled conditions experiment

There were 122,588 transcripts in the assembled reference transcriptome, with 51,656 of them with annotation hits (see Appendix A.30 for additional assembly statistics). The overall alignment rate was 97.10% (Appendix A.32 shows the overall alignment rates per sample). Among the annotated sequences, almost all belonged to plant species (93.89%), while 3.48% were fungal. About 15% of all transcripts were differentially expressed (18,867). Before infection samples (0 dpi) had similar expression profiles as did after infection samples (3, 6 and 9 dpi; Appendix A.36). All infected samples used in the gene expression analyses tested positive for the two ITS2 sequences of *D. thujina*. The top two *D. thujina* transcripts from the BLASTn searches were *TR35196/c4_g1_i4* (95.71% identity, E-value: 7×10^{-24}) and *TR35196/c4_g1_i6* (94.29% identity, E-value: 3×10^{-22}).

4.3.2.1 Hierarchical clustering

Ten clusters of sequences that had a maximum false discovery rate of 0.001 and a minimum fold change of four were identified after clustering the transcripts and cutting the tree at 68.5% of the tree's maximum height (Fig. 4.3). Three of the clusters identified included almost 95% of all transcripts. The cluster with the most transcripts (10,809) corresponded to sequences with high levels of expression at 0 dpi and different responses after infection. The second cluster in size had 5,753 transcripts with expression levels that were low at 0 dpi and varied at 3-9 dpi. The third cluster included 1,337 transcripts which had high levels of expression at 0 dpi and low levels thereafter.

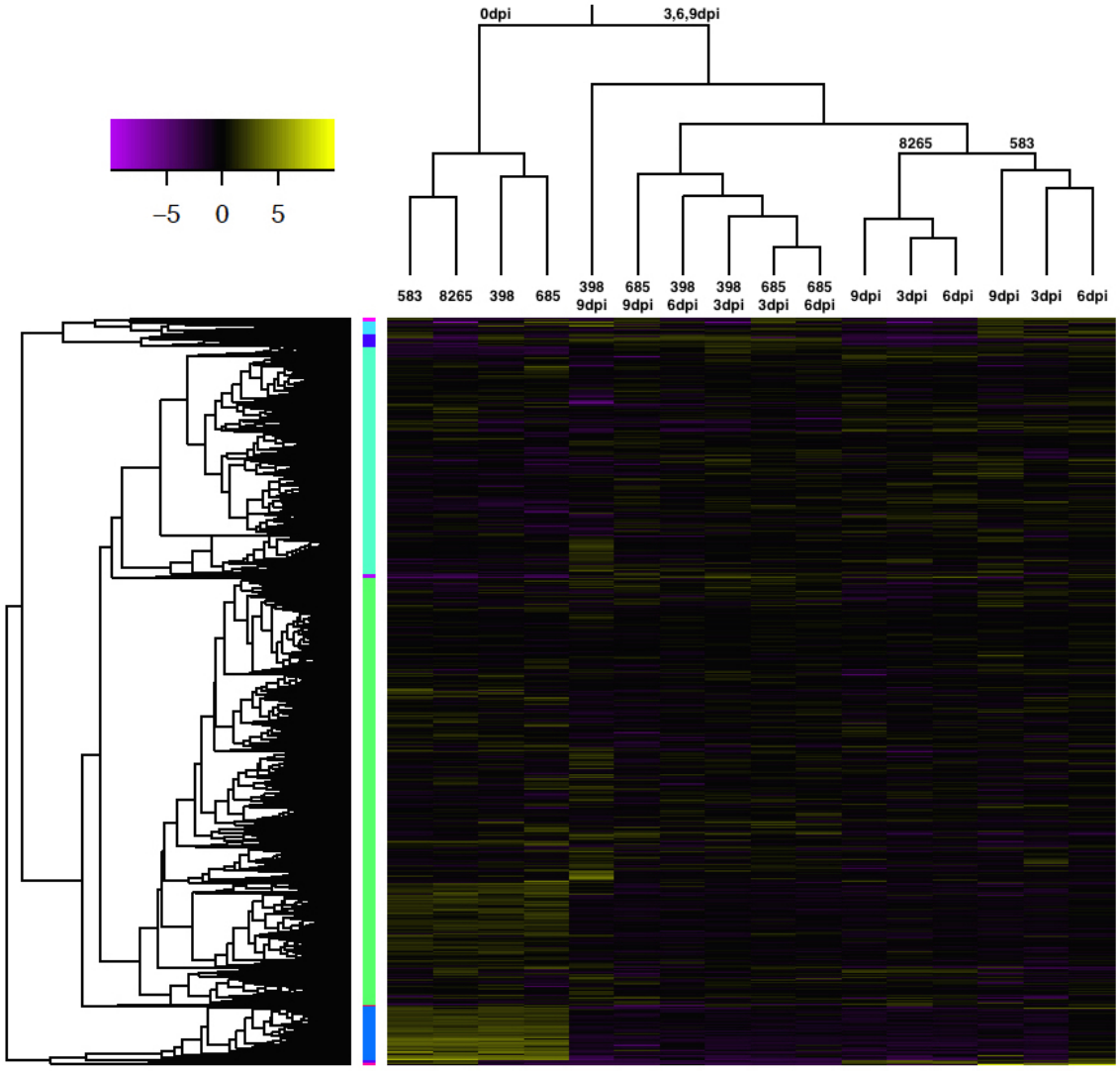

Figure 4.3. Heat map of 18,867 differentially expressed (DE) transcripts from the samples in the CC-CLB^{+} treatment that were used in gene expression analyses. Samples are clustered in the top tree (by sampling time × family combination), and DE transcripts are clustered in the left-hand tree. Ten clusters of transcripts were produced after cutting the clustering tree at 68.5% of its maximum height. The cluster in green had the most sequences (10,809 transcripts), followed by the one in light green (5,753 transcripts) and that in blue (1,337 transcripts). The remaining 7 clusters accounted for 5.13% of the DE transcripts. Log_2-transformed and centered FPKM were used as expression levels as calculated by the Trinity pipeline. The top left bar shows the expression colour code (yellow = high expression, purple = low expression). Labels on the branches of the top tree refer to specific family × time combination samples.

4.3.2.2 Stability selection analyses

Regression stability selection using severity as a response variable

Thirty-nine transcripts were identified as the best predictors of the disease severity according to the changepoint analysis on the rank of transcripts produced by stability selection (Table 4.3). Ten of the transcripts listed in Table 4.3 were upregulated in response to *D. thujina* infection in the susceptible families but not in the resistant families (*TR9242/c0_g1_i1*, *TR17372/c0_g1_i1*, *TR19991/c0_g2_i1*, *TR36416/c1_g1_i1*, *TR36804/c2_g2_i2*, *TR30640/c1_g1_i1*, *TR36155/c4_g2_i4*, *TR33294/c2_g2_i3*, *TR36700/c5_g1_i1*, *TR36321/c5_g1_i1*), and the remaining transcripts were more highly expressed in the resistant families. All of the transcripts upregulated in the susceptible families ranked first (i.e. top $\beta_{0,k}$) to dynamic topic (k) 19 (see section 4.3.2.3), and most of the transcripts that responded in the resistant families ranked first to dynamic topic 11 (28 out of 29 transcripts).

There were only three disease resistance protein transcripts (*TR37382/c2_g1_i1*, *TR36626/c4_g2_i1*, *TR34618/c8_g1_i1*) and one TMV resistance protein transcript (*TR31269/c1_g1_i1*) present in Table 4.3, and all were expressed at higher levels in the resistant plants in comparison to the susceptible plants after *D. thujina* infection (Figs. 4.4a, 4.4b, 4.4c and 4.4d, respectively). The only transcript with "defense response" as a process annotation (*TR9242/c0_g1_i1*) was at higher levels of expression in susceptible seedlings than resistant after infection (Fig. 4.4f). Interestingly, a metal tolerance protein (*TR34816/c1_g2_i2*) was found to be at higher levels of expression in the resistant trees (Fig. 4.4e). "Membrane" and "chloroplast" were the cellular component annotations of several of the transcripts listed in Table 4.3.

Categorical stability selection

Changepoint analysis of the scores of the ranked transcripts produced by categorical stability selection showed that only 20 transcripts were the best predictors to differentiate the responses between resistant and susceptible families in the CC-CLB^{+} treatment (Table 4.4). Eight of the transcripts showed higher levels of expression in the resistant families after infection (*TR34128/c3_g1_i4*, *TR31465/c0_g1_i2*, *TR23620/c0_g2_i1*, *TR37258/c6_g1_i6*, *TR35088/c2_g1_i3*, *TR36742/c3_g1_i2*,

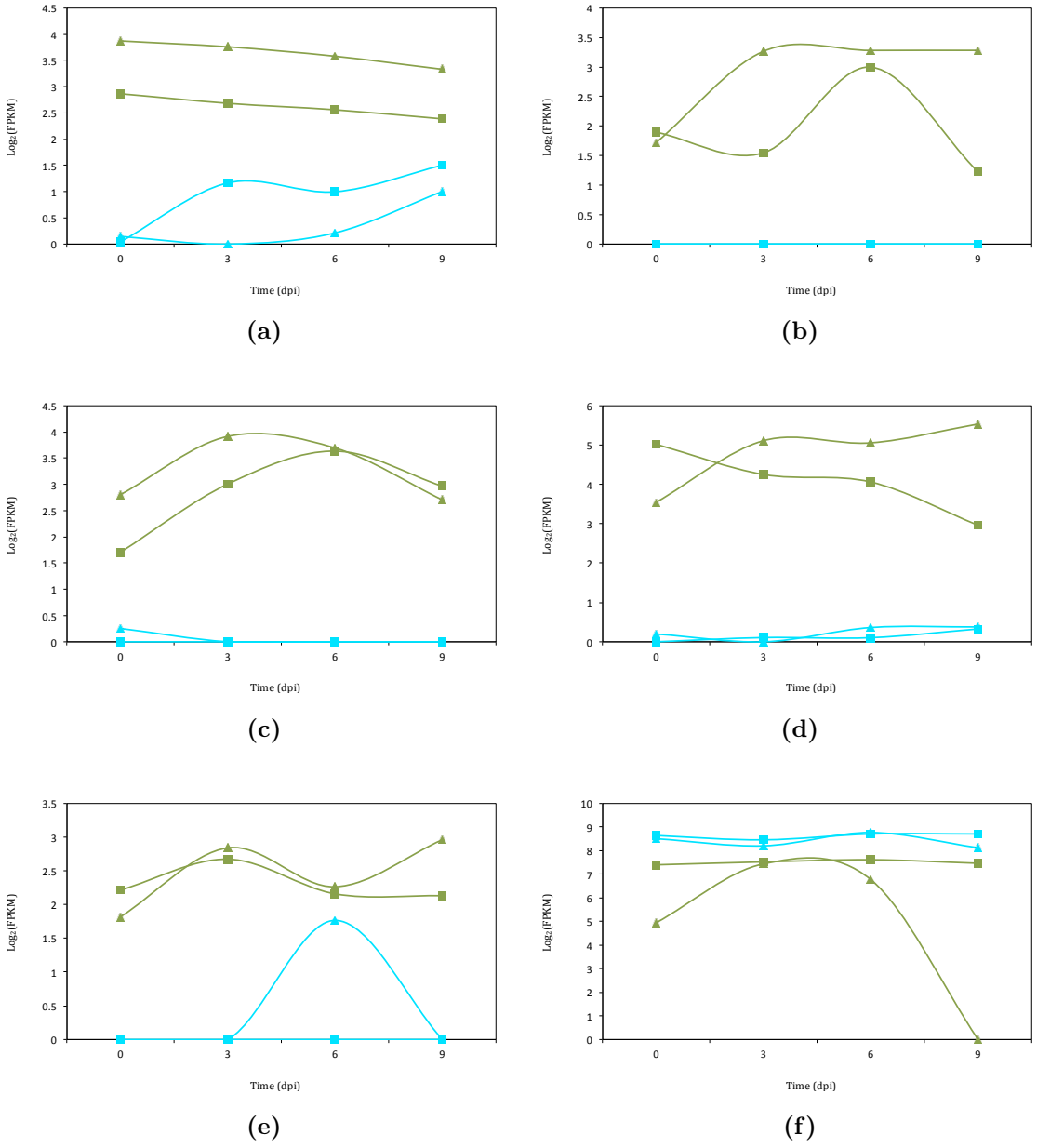

Figure 4.4. Expression over time of selected transcripts detected by the regression stability selection analysis using severity as a response variable in the CC-CLB^{+} samples collected for gene expression (see also section 4.2.1.2). (a) *TR37382/c2_g1_i1* (disease resistance protein RPM1), (b) *TR36626/c4_g2_i1* (putative disease resistance protein RGA4), (c) *TR34618/c8_g1_i1* (disease resistance RPP13-like protein 4), (d) *TR31269/c1_g1_i1* (TMV resistance protein N), (e) *TR34816/c1_g2_i2* (metal tolerance protein 12), (f) *TR9242/c0_g1_i1* (chloroplast stem-loop binding protein of 41 kDa b). Susceptible families were plotted in cyan (8265 with squares, 583 with triangles), and resistant families in green (398 with squares, 685 with triangles). dpi = days post infection.

Table 4.3. Top 39 predictors (transcripts) of the disease severity according to the change point analysis on the ranked stability selection scores (see also section 4.2.3). The dynamic topic to which the transcripts ranked first is included (based on their top $\beta_{0,k}$). Annotations are based on BLASTX searches done on the Swiss-Prot database.

Transcript	Stability selection (score)	E-value	Organism	Annotation	Process	Cellular component	Dynamic topic per transcript
TR37382/c2_g1_i1	0.2498	3×10^{-41}	*Arabidopsis* sp.	Disease resistance protein RPM1			11
TR33827/c11_g1_i1	0.1649	NA	No hits	No hits			11
TR9242/c0_g1_i1	0.1645	0	*Arabidopsis* sp.	Chloroplast stem-loop binding protein of 41 kDa b	Defense response	Chloroplast	19
TR17372/c0_g1_i1	0.1636	2×10^{-102}	*Vitis* sp.	Putative uncharacterized protein	Oxidoreductase activity	Chloroplast	19
TR36525/c2_g4_i1	0.1521	NA	No hits	No hits			11
TR36870/c3_g1_i1	0.1499	3×10^{-49}	*Picea* sp.	Putative uncharacterized protein			11
TR36555/c3_g1_i1	0.1421	NA	No hits	No hits			11
TR32566/c0_g1_i2	0.1368	2×10^{-91}	*Amborella* sp.	Uncharacterized protein			11
TR29119/c0_g1_i3	0.1284	3×10^{-24}	*Arabidopsis* sp.	Trihelix transcription factor GT-3a	Transcription, *DNA*-templated	Nucleus	11
TR34419/c1_g1_i2	0.1207	6×10^{-61}	*Arabidopsis* sp.	Protein STRICTOSIDINE SYNTHASE-LIKE 4	Strictosidine synthase activity		11
TR33665/c0_g1_i2	0.1129	2×10^{-48}	*Arabidopsis* sp.	UDP-glycosyltransferase 91C1			11
TR28254/c1_g2_i1	0.1108	3×10^{-159}	*Arabidopsis* sp.	Protein trichome birefringence-like 16			11
TR19991/c0_g2_i1	0.1059	0	*Oryza* sp.	Protein argonaute 1A	Gene silencing by *RNA*		19
TR36626/c4_g2_i1	0.0833	1×10^{-15}	*Solanum* sp.	Putative disease resistance protein RGA4	ADP binding		11
TR19991/c0_g1_i1	0.0825	0	*Oryza* sp.	Protein argonaute 1A	Gene silencing by *RNA*		11
TR35137/c1_g3_i2	0.0821	NA	No hits	No hits			11
TR22016/c1_g1_i1	0.0794	NA	No hits	No hits			16
TR36416/c1_g1_i1	0.0787	3×10^{-80}	*Arabidopsis* sp.	*DNA* mismatch repair protein MLH3	Reciprocal meiotic recombination	Mismatch repair complex	19
TR33528/c7_g2_i3	0.0786	NA	No hits	No hits			11
TR36818/c1_g1_i3	0.0762	1×10^{-48}	*Physcomitrella* sp.	Predicted protein			11
TR35140/c0_g1_i1	0.073	2×10^{-45}	*Picea* sp.	Auxin-responsive protein	Transcription, *DNA*-templated	Nucleus	11
TR36804/c2_g2_i2	0.0729	3×10^{-13}	*Theobroma* sp.	Hydroxyproline-rich glycoprotein family protein, putative isoform 1			19
TR37043/c4_g3_i1	0.0703	NA	No hits	No hits			11
TR34268/c0_g1_i2	0.0697	5×10^{-130}	*Arabidopsis* sp.	Probable hydroxyacylglutathione hydrolase 2	Glutathione biosynthetic process	Chloroplast	11
TR28503/c0_g2_i1	0.0679	4×10^{-67}	*Beta* sp.	Putative uncharacterized protein			11
TR30640/c1_g1_i2	0.0664	0	*Arabidopsis* sp.	UDP-glucuronic acid decarboxylase 2	UDP-D-xylose biosynthetic process	Membrane	11
TR34618/c8_g1_i1	0.066	3×10^{-30}	*Arabidopsis* sp.	Disease resistance RPP13-like protein 4			11
TR30640/c1_g1_i1	0.0651	0	*Arabidopsis* sp.	UDP-glucuronic acid decarboxylase 2	UDP-D-xylose biosynthetic process	Membrane	19
TR22119/c1_g2_i1	0.0642	2×10^{-26}	*Theobroma* sp.	UPF0481 protein, putative			11
TR28958/c0_g1_i1	0.0623	2×10^{-40}	*Picea* sp.	Putative uncharacterized protein	Sequence-specific *DNA* binding	Nucleus	11
TR36155/c4_g2_i4	0.0623	2×10^{-83}	*Papaver* sp.	Non-functional NADPH-dependent codeinone reductase 2			19
TR32437/c0_g1_i3	0.0609	2×10^{-29}	*Cryptomeria* sp.	Uncharacterized protein	Protein binding		11
TR33294/c2_g2_i3	0.0573	8×10^{-103}	*Arabidopsis* sp.	GDT1-like protein 5		Membrane	19
TR36254/c0_g1_i4	0.0565	7×10^{-79}	*Amborella* sp.	Uncharacterized protein			11
TR35657/c0_g2_i3	0.0552	9×10^{-37}	*Arabidopsis* sp.	Serine/threonine-protein kinase SRK2C		Integral component of membrane	11
TR36700/c5_g1_i1	0.0546	4×10^{-57}	*Picea* sp.	Putative uncharacterized protein			19
TR36321/c5_g1_i1	0.0534	NA	No hits	No hits			19
TR34816/c1_g2_i2	0.0533	6×10^{-81}	*Morus* sp.	Metal tolerance protein 12	Cation transmembrane transporter activity	Integral component of membrane	11
TR31269/c1_g1_i1	0.0519	9×10^{-23}	*Nicotiana* sp.	TMV resistance protein N			11

Table 4.4. Top 20 predictors (transcripts) detected by the categorical stability selection analysis that discriminated between resistant and susceptible families infected with *D. thujina* (CC-CLB^{+} treatment) according to the changepoint detection analysis carried out on the ranked stability selection scores (see also section 4.2.3). The dynamic topic to which the transcripts ranked first is included (based on their top $\beta_{0,k}$). Annotations are based on BLASTX searches done on the Swiss-Prot database.

Transcript	Stability selection (score)	E-value	Organism	Annotation	Process	Cellular component	Dynamic topic per transcript
TR17615/c0_g1_i1	0.2361	7×10^{-39}	*Pinus* sp.	Cytochrome P450 750A1			1
TR30822/c0_g1_i1	0.1691	1×10^{-39}	*Cupressus* sp.	Putative oleosin		Monolayer-surrounded lipid storage body	19
TR25584/c1_g1_i2	0.1409	2×10^{-10}	*Oryza* sp.	Os05g0414400 protein	Nucleic acid binding		19
TR34128/c3_g1_i4	0.1279	NA	No hits	No hits			11
TR36859/c1_g1_i1	0.1071	NA	No hits	No hits			1
TR36979/c2_g1_i1	0.1036	2×10^{-81}	*Arabidopsis* sp.	LRR receptor-like serine/threonine-protein kinase GSO1			19
TR31465/c0_g1_i2	0.1015	NA	No hits	No hits			11
TR20625/c0_g1_i1	0.0987	2×10^{-87}	*Arabidopsis* sp.	Probable complex I intermediate-associated protein 30			19
TR23620/c0_g2_i1	0.0981	1×10^{-19}	*Picea* sp.	Putative uncharacterized protein			11
TR37258/c6_g1_i6	0.084	NA	No hits	No hits			11
TR36742/c3_g1_i1	0.0818	4×10^{-10}	*Pisum* sp.	Pyruvate decarboxylase 1			19
TR29481/c0_g1_i2	0.0815	NA	No hits	No hits			1
TR37054/c2_g2_i1	0.0782	NA	No hits	No hits			5
TR35088/c2_g1_i3	0.0777	0	*Arabidopsis* sp.	Oligopeptide transporter 3	Peptide transport	Integral component of membrane	11
TR36742/c3_g1_i2	0.0708	5×10^{-10}	*Pisum* sp.	Pyruvate decarboxylase 1			11
TR20324/c0_g1_i1	0.0689	1×10^{-98}	*Oryza* sp.	Peroxisomal membrane protein 11-4	Peroxisome fission	Integral component of peroxisomal membrane	19
TR27129/c2_g1_i1	0.0601	3×10^{-98}	*Physcomitrella* sp.	Predicted protein			19
TR21734/c0_g1_i1	0.056	1×10^{-69}	*Papaver* sp.	Salutaridine reductase			11
TR37054/c2_g1_i1	0.0485	7×10^{-27}	*Nicotiana* sp.	TMV resistance protein N			18
TR34272/c1_g1_i1	0.0454	0	*Arabidopsis* sp.	4-coumarate–CoA ligase-like 5	Jasmonic acid biosynthetic	Peroxisome	11

TR21734/c0_g1_i1 and *TR34272/c1_g1_i1*), while the remaining 12 were higher in the susceptible families. Figures 4.5a-4.5f show the expression levels of selected transcripts from Table 4.4.

Defense related transcripts like cytochrome P450 (*TR17615/c0_g1_i1*, Fig. 4.5a) and the LRR receptor-like serine/threonineprotein kinase GSO1 (*TR36979/c2_g1_i1*, Fig. 4.5b) were at high levels of expression in the susceptible families after infection. Most of the transcripts with high levels of expression in the resistant families after infection were either unknown (*TR34128/c3_g1_i4*, *TR31465/c0_g1_i2*, *TR37258/c6_g1_i6*) or uncharacterized (*TR23620/c0_g2_i1*, Fig. 4.5c). Some of the few transcripts with annotations in this last category were related to peptide transport (*TR35088/c2_g1_i3*, Fig. 4.5d), alkaloid biosynthesis (*TR21734/c0_g1_i1*, Fig. 4.5e), or jasmonic acid (JA) biosynthesis (*TR34272/c1_g1_i1*, Fig. 4.5f). All of the transcripts upregulated in response to *D. thujina* infection in the resistant families ranked first to dynamic topic 11 (Table 4.4), whereas most of the transcripts overexpressed in the susceptible families ranked first to dynamic topic 19.

Regression stability selection using aluminum as a response variable

Regression stability selection analysis on the differential expression matrix of the controlled conditions experiment using aluminum as response variable was completed because aluminum concentration was the only variable that rendered similar results in both experiments (see section 4.3.1 and Table 4.2). Forty-three transcripts were identified as the best predictors of the aluminum concentrations in the CC-CLB$^+$ treatment as chosen by changepoint analysis on the stability selection ranked scores (Table 4.5). In general, the expression pattern of each of those sequences was similar in all families in the CC-CLB$^+$ treatment.

The top two sequences were related to regulation of gene expression (*TR29879-/c2_g1_i2*, Fig. 4.6c; and *TR31316/c0_g1_i7*, Table 4.5). Several transcripts were involved in metal ion binding (*TR34581/c8_g1_i2*, *TR36010/c6_g1_i7*, *TR3622-2/c1_g1_i4*, *TR36842/c2_g1_i1*, *TR20490/c0_g1_i3* and *TR35271/c5_g1_i5*) or calmodulin binding (*TR36118/c2_g1_i1*, Fig. 4.6d), while others were involved in defense (*TR11555/c1_g1_i1*; *TR36619/c5_g1_i1*; *TR33482/c0_g1_i1*, Fig. 4.6b; and *TR29996/c0_g6_i1*, 4.6a). Few sequences were associated with the outside of the

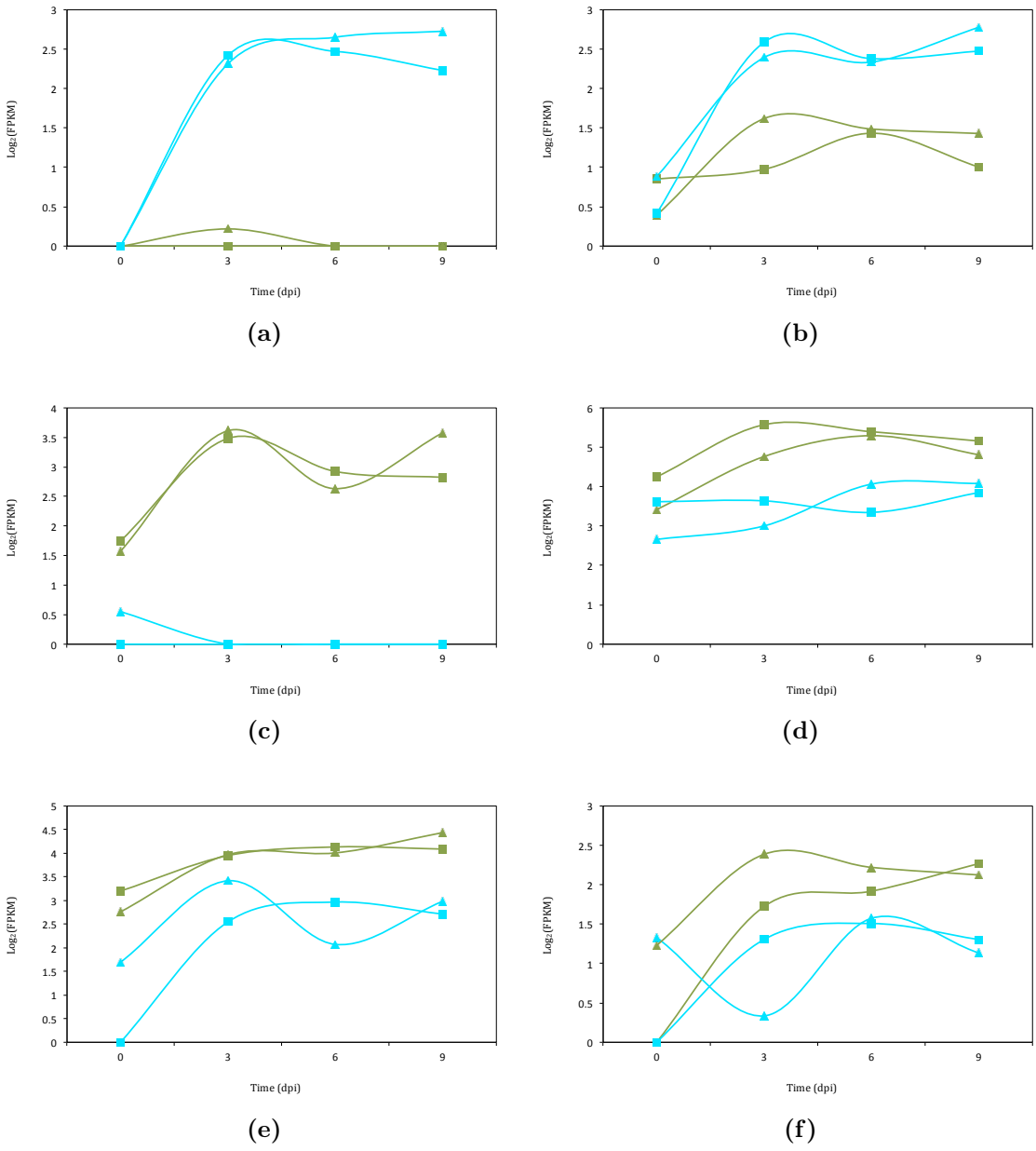

Figure 4.5. Expression over time of selected transcripts detected by the categorical stability selection analysis that discriminated between resistant and susceptible families in the CC-CLB^{+} treatment. (a) *TR17615/c0_g1_i1* (cytochrome P450 750A1), (b) *TR36979/c2_g1_i1* (LRR receptor-like serine/threonine-protein kinase GSO1), (c) *TR23620/c0_g2_i1* (putative uncharacterized protein), (d) *TR35088/c2_g1_i3* (oligopeptide transporter 3), (e) *TR21734/c0_g1_i1* (salutaridine reductase), (f) *TR34272/c1_g1_i1* (4-coumarate-CoA ligase-like 5). Susceptible families are plotted in cyan (8265 with squares, 583 with triangles), and resistant families in green (398 with squares, 685 with triangles). dpi = days post infection.

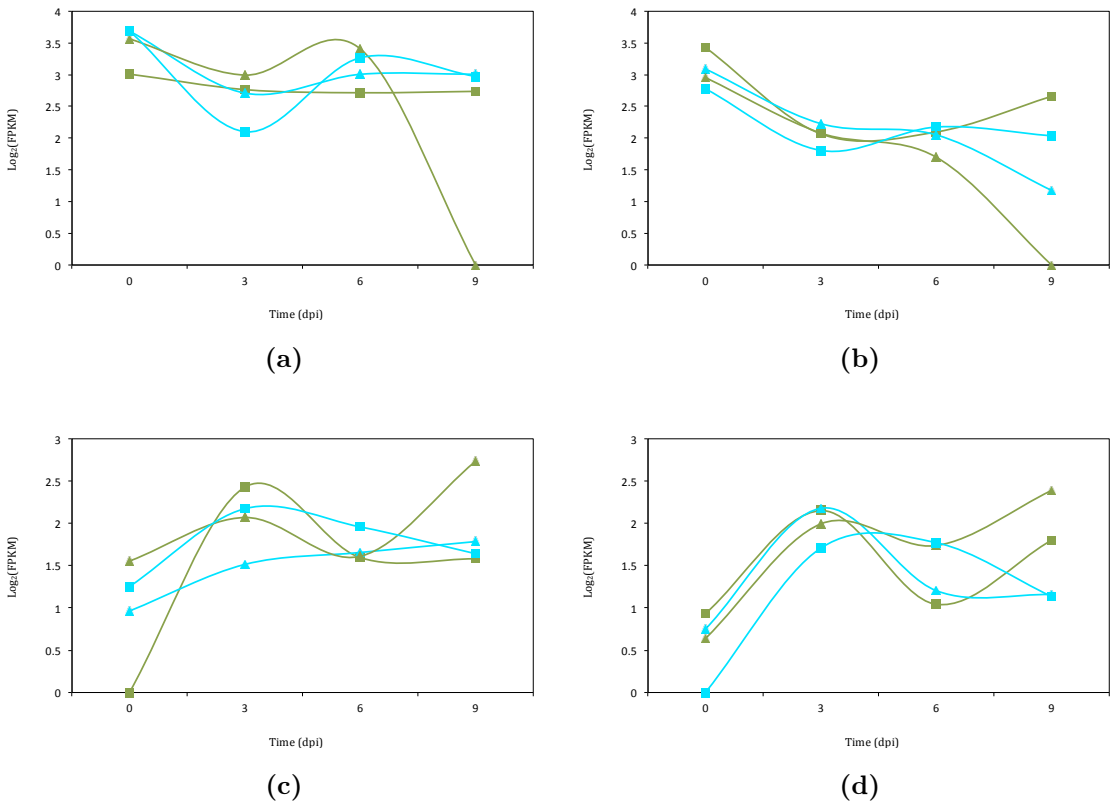

Figure 4.6. Expression over time of selected transcripts detected by the regression stability selection using aluminum concentrations as a response variable in the CC-CLB^{+} treatment. (a) *TR29996|c0_g6_i1* (probable receptor-like protein kinase At1g30570), (b) *TR33482|c0_g1_i1* (probable LRR receptor-like serine/threonine-protein kinase At2g24230), (c) *TR29879|c2_g1_i2* (serine/arginine-rich splicing factor RS31A), (d) *TR36118|c2_g1_i1* (G-type lectin S-receptor-like serine/threonine-protein kinase At1g34300). Susceptible families are plotted in cyan (8265 with squares, 583 with triangles), and resistant families in green (398 with squares, 685 with triangles). dpi = days post infection.

Table 4.5. Top 43 predictors (transcripts) of the aluminum concentrations in the CC-CLB^{+} samples collected for gene expression, according to the change point analysis on the ranked stability selection scores (see also section 4.2.3). The dynamic topic to which the transcripts ranked first is included (based on their top $\beta_{0,k}$). Annotations are based on BLASTX searches done on the Swiss-Prot database.

Transcript	Stability selection (score)	E-value	Organism	Annotation	Process	Cellular component	Dynamic topic per transcript
TR29879/c2_g1_i2	0.2346	3×10^{-55}	*Arabidopsis* sp.	Serine/arginine-rich splicing factor RS31A	Nucleic acid binding		14
TR31316/c0_g1_i7	0.2116	3×10^{-38}	*Vitis* sp.	PHD finger protein ING	Chromatin modification	Nucleus	18
TR9904/c0_g2_i1	0.1805	NA	No hits	No hits			14
TR9578/c0_g2_i1	0.1499	0	*Arabidopsis* sp.	GPCR-type G protein 2	Response to abscisic acid	Intracellular membrane-bounded organelle	8
TR39372/c0_g1_i1	0.1469	NA	No hits	No hits			3
TR36118/c2_g1_i1	0.1426	0	*Arabidopsis* sp.	G-type lectin S-receptor-like serine/threonine-protein kinase At1g34300	Calmodulin binding	Plasma membrane	14
TR11555/c1_g1_i1	0.1344	5×10^{-26}	*Arabidopsis* sp.	Glucan endo-1,3-beta-glucosidase 2	Carbohydrate metabolic process		8
TR7516/c0_g2_i1	0.1211	2×10^{-35}	*Coffea* sp.	Coffea canephora DH200=94 genomic scaffold, scaffold_3			3
TR31326/c0_g1_i5	0.1144	4×10^{-109}	*Arabidopsis* sp.	Probable ADP-ribosylation factor GTPase-activating protein AGD8	Regulation of ARF GTPase activity		18
TR33495/c0_g1_i4	0.109	0	*Eucalyptus* sp.	Uncharacterized protein			14
TR33526/c1_g1_i2	0.1083	6×10^{-21}	*Arabidopsis* sp.	Nuclear pore complex protein NUP98A	Transport	Nuclear pore	18
TR36619/c5_g1_i1	0.1039	2×10^{-44}	*Arabidopsis* sp.	Leucine-rich repeat receptor-like serine/threonine-protein kinase At1g17230			11
TR28212/c0_g1_i2	0.0946	0	*Arabidopsis* sp.	Bifunctional 3-dehydroquinate dehydratase/shikimate dehydrogenase	Shikimate metabolic process	Chloroplast	13
TR32315/c0_g2_i3	0.0933	2×10^{-42}	*Petunia* sp.	Anthocyanidin 3-O-glucosyltransferase	Transferase activity		6
TR29996/c0_g6_i1	0.0927	6×10^{-150}	*Arabidopsis* sp.	Probable receptor-like protein kinase At1g30570			3
TR450/c0_g1_i1	0.0869	7×10^{-100}	*Arabidopsis* sp.	Expansin-A13	Plant-type cell wall organization	Cell wall	8
TR33998/c5_g1_i5	0.0867	3×10^{-101}	*Arabidopsis* sp.	Polyubiquitin 11	Ubiquitin-dependent protein catabolic process	Cytoplasm	13
TR33482/c0_g1_i1	0.0817	9×10^{-85}	*Arabidopsis* sp.	Probable LRR receptor-like serine/threonine-protein kinase At2g24230	Regulation of defense response		3
TR32780/c1_g2_i1	0.0773	1×10^{-13}	*Arabidopsis* sp.	F-box/kelch-repeat protein At2g44130			13
TR25343/c1_g1_i2	0.0761	6×10^{-83}	*Selaginella* sp.	Putative uncharacterized protein	Base-excision repair		15
TR34581/c8_g1_i2	0.0745	0	*Arabidopsis* sp.	Laccase-5	Response to copper ion	Apoplast	14
TR26078/c0_g4_i1	0.0737	NA	No hits	No hits			3
TR30054/c0_g2_i1	0.0735	NA	No hits	No hits			13
TR8534/c0_g2_i1	0.0711	NA	No hits	No hits			13
TR30658/c1_g1_i2	0.0664	0	*Prunus* sp.	Uncharacterized protein			19
TR36010/c6_g1_i7	0.0624	2×10^{-82}	*Picea* sp.	Putative uncharacterized protein	Iron ion binding		3
TR33998/c5_g1_i12	0.0621	0	*Arabidopsis* sp.	Polyubiquitin 14	Ubiquitin-dependent protein catabolic process	Vacuole	19
TR34828/c1_g2_i2	0.059	9×10^{-153}	*Arabidopsis* sp.	Galacturonokinase	Galactose metabolic process	Cytoplasm	8
TR28233/c0_g1_i2	0.0584	NA	No hits	No hits			18
TR1717l/c0_g1_i1	0.056	1×10^{-64}	*Prunus* sp.	Uncharacterized protein	Chloroplast organization		3
TR36222/c1_g1_i4	0.0554	8×10^{-148}	*Arabidopsis* sp.	Cytochrome P450 734A1	Iron ion binding		14
TR15760/c0_g1_i1	0.055	NA	No hits	No hits			10
TR36513/c4_g2_i3	0.0541	5×10^{-124}	*Cryptomeria* sp.	Cold acclimation protein COR413-TM1			19
TR32004/c0_g1_i2	0.0541	6×10^{-81}	*Arabidopsis* sp.	Glucuronoxylan 4-O-methyltransferase 1			16
TR36842/c2_g1_i1	0.0539	1×10^{-5}	*Eustoma* sp.	Flavonoid 3',5'-hydroxylase	Iron ion binding		14
TR36146/c3_g1_i1	0.0478	NA	No hits	No hits			10
TR33827/c10_g1_i1	0.0476	0	*Prunus* sp.	Uncharacterized protein			14
TR37384/c3_g3_i1	0.0471	3×10^{-19}	*Arabidopsis* sp.	Cysteine-rich repeat secretory protein 55			10
TR24194/c0_g1_i1	0.0459	3×10^{-159}	*Ricinus* sp.	Putative uncharacterized protein			13
TR20490/c0_g1_i3	0.0431	1×10^{-90}	*Glycine* sp.	Uncharacterized protein	Metal ion binding		8
TR36916/c1_g2_i1	0.0419	8×10^{-120}	*Arabidopsis* sp.	G-type lectin S-receptor-like serine/threonine-protein kinase SD2-5	Protein serine/threonine kinase activity		18
TR35271/c5_g1_i5	0.0417	2×10^{-156}	*Pinus* sp.	Cytochrome P450 720B2	Iron ion binding	Integral component of membrane	13
TR10543/c0_g2_i1	0.0394	NA	No hits	No hits			16

cell (*TR36118/c2_g1_i1*, *TR450/c0_g1_i1* and *TR34581/c8_g1_i2*), only two of the transcripts were cytochromes P450s (*TR36222/c1_g1_i4* and *TR35271/c5_g1_i50*), one was connected to the shikimate pathway (*TR28212/c0_g1_i2*), one to the flavonoids pathway (*TR36842/c2_g1_i1*), and one to response to abscisic acid (*TR9578/c0_g2_i1*).

Twenty-two of the 43 transcripts in Table 4.5 ranked first to dynamic topics 3, 13 and 14; three to dynamic topic 19 (*TR30658/c1_g1_i2*, *TR33998/c5_g1_i12*, *TR36513/c4_g2_i3*); and one to dynamic topic 11 (*TR36619/c5_g1_i1*, Table 4.5). Transcripts in dynamic topic 13 showed increased expression levels at 3 dpi with decreasing expressions afterwards in all families (see Fig. 4.8a) On the contrary, sequences in dynamic topic 3 tended to be at high levels of expression from 0 to 6 dpi to then drop at 9 dpi (see e.g. *TR29996/c0_g6_i1* and *TR33482/c0_g1_i1*, Figs. 4.6a and 4.6b, respectively). Transcripts in dynamic topic 14 did not depict a specific pattern although some of them were upregulated in response to infection in all families (see e.g. *TR29879/c2_g1_i2* and *TR36118/c2_g1_i1*, Figs. 4.6c and 4.6d, respectively).

4.3.2.3 Dynamic topic modelling

Dynamic topic modelling was carried out to model how groups of transcripts that co-occurred at 0 dpi changed over time in response to infection. The most frequent topics among the transcripts ranked by the stability selection analyses and chosen by the changepoint analyses were dynamic topics 11, 13, 14 and 19 (see section 4.3.2.2 and Tables 4.3, 4.3 and 4.5). Dynamic topic 11 (Fig. 4.7a) and dynamic topic 19 (Fig. 4.7b) emerged consistently among the transcripts from the categorical and regression stability selection analysis using severity as a response variable. In relation to the stability selection using aluminum as a response variable, more than one-third of the transcripts belonged to dynamic topics 13 (Fig. 4.8a) and 14 (Fig. 4.8b).

Dynamic topic 11 included sequences that were usually at higher levels of expression in *D. thujina*-resistant families than susceptible families regardless of their pattern after infection (see e.g. Figs. 4.4a, 4.4b, 4.4c, 4.4d, 4.4e, 4.5c, 4.5d, 4.5e and 4.5f). All of the top ten transcripts modelled in dynamic topic 11 (selected according to the $\beta_{0,11}$ scores; Table 4.6) depicted downregulation in response to *D. thujina* infection, except

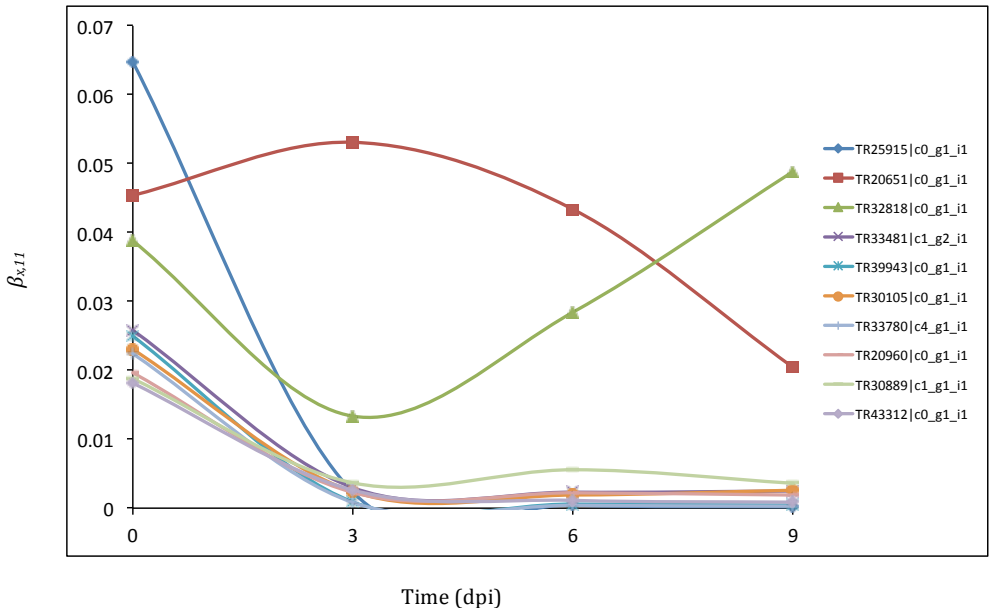

(a)

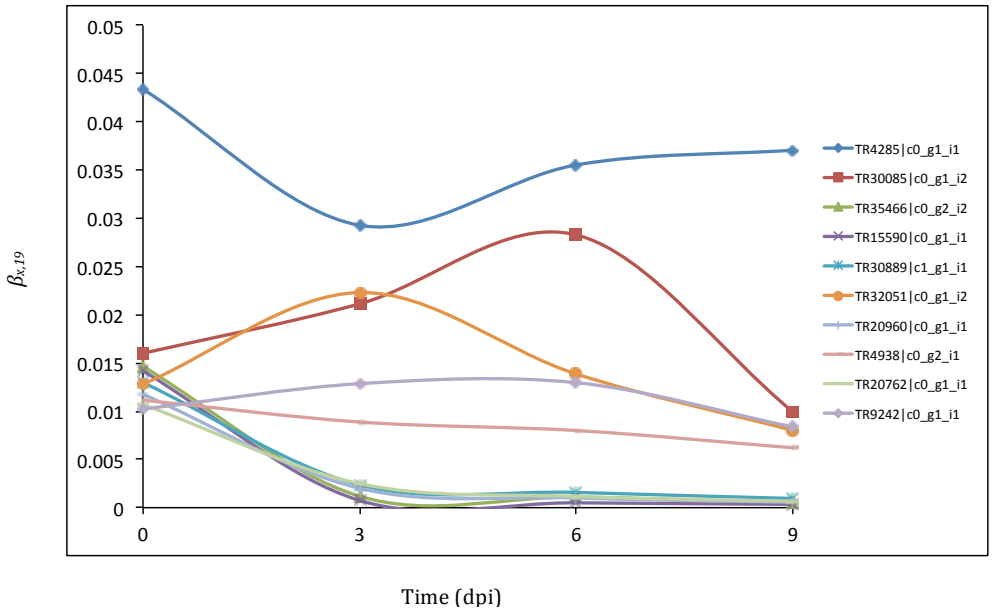

(b)

Figure 4.7. Two of the most frequent dynamic topics (11 and 19) among the transcripts ranked by the stability selection analyses performed on the differentially expressed sequences from the CC-CLB^{+} treatment. Count data were fitted into 20 topics (i.e. $k = 20$) using the Dynamic Topic Models software (https://github.com/blei-lab/dtm ; see methods). Inferred posterior expression distributions per date ($\beta_{x,k}$) of the top 10 transcripts of topics 11 and 19 are plotted. (a) Dynamic topic 11, (b) dynamic topic 19. x = dpi = days post infection.

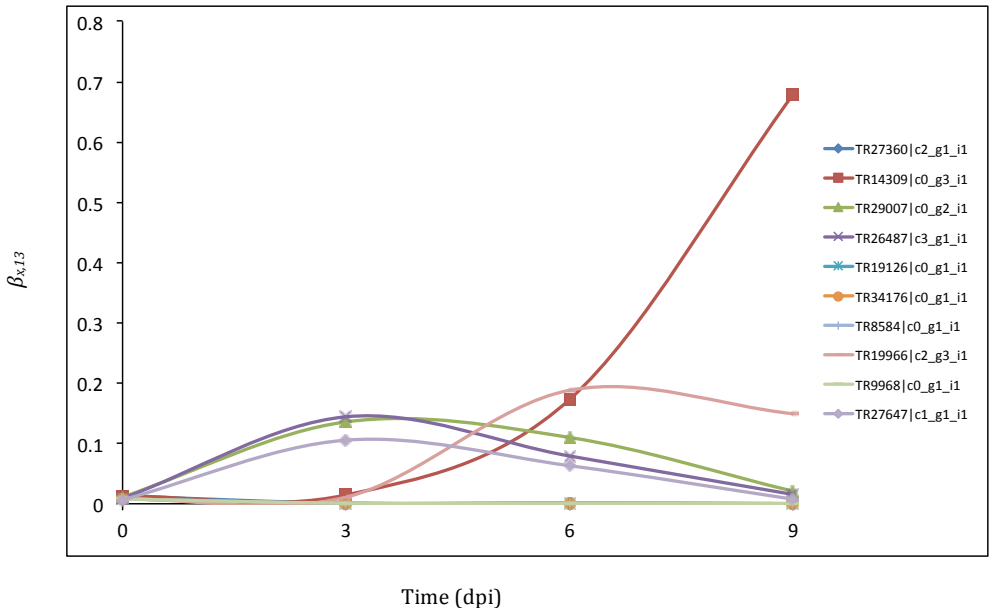

(a)

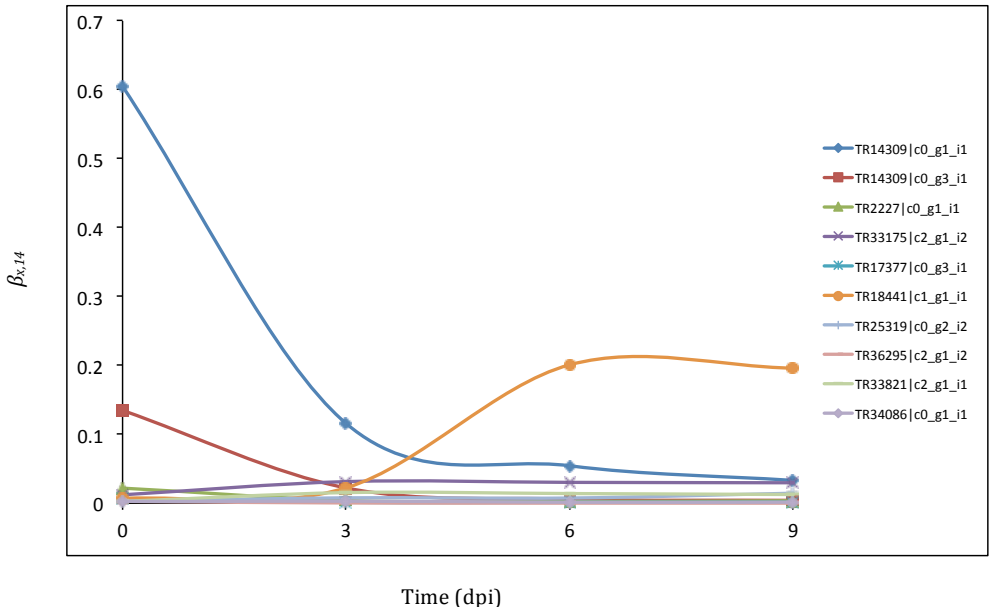

(b)

Figure 4.8. Two of the most frequent dynamic topics (13 and 14) among the transcripts ranked by the stability selection analyses performed on the differentially expressed sequences from the CC-CLB^{+} treatment. Count data were fitted into 20 topics (i.e. $k = 20$) using the Dynamic Topic Models software (https://github.com/blei-lab/dtm ; see methods). Inferred posterior expression distributions per date ($\beta_{x,k}$) of the top 10 transcripts of topics 13 and 14 are plotted. (a) Dynamic topic 13, (b) dynamic topic 14. x = dpi = days post infection.

Table 4.6. Representative (top 10) transcripts per dynamic topic of the four most frequent topics among the transcripts ranked by the stability selection analyses. Count transcriptomic data were fitted into 20 topics (i.e. $K = 20$) using the Dynamic Topic Models software (https://github.com/blei-lab/dtm), and transcripts were ranked within each topic based on their inferred posterior expression distributions at 0 dpi ($\beta_{0,k}$). Annotations were completed with BLASTX searches on the Swiss-Prot database.

Dynamic topic (k)	Transcript	$\beta_{0,k}$	E-value	Organism	Annotation	Process	Cellular component
11	*TR25915/c0_g1_i1*	0.06483728	8×10^{-16}	*Pinus* sp.	Non-specific lipid-transfer protein	Lipid binding	
	TR20651/c0_g1_i1	0.04550166	0	*Arabidopsis* sp.	Peroxisomal (S)-2-hydroxy-acid oxidase GLO1	Defense response	Peroxisome
	TR32818/c0_g1_i1	0.03873375	1×10^{-70}	*Arabidopsis* sp.	Dehydration-responsive protein RD22		
	TR33481/c1_g2_i1	0.02572755	0	*Pinus* sp.	Flavanone 3-hydroxylase	Flavonoid biosynthetic process	
	TR39943/c0_g1_i1	0.02491045	0	*Petunia* sp.	Flavonoid 3',5'-hydroxylase 2	Anthocyanin-containing compound biosynthetic process	Endoplasmic reticulum
	TR30105/c0_g1_i1	0.02312838	0	*Helianthus* sp.	Trans-cinnamate 4-monooxygenase		
	TR33780/c4_g1_i1	0.02239168	2×10^{-132}	*Arabidopsis* sp.	BAHD acyltransferase DCR		
	TR20960/c0_g1_i1	0.01958449	2×10^{-127}	*Arabidopsis* sp.	Fasciclin-like arabinogalactan protein 17		
	TR30889/c1_g1_i1	0.01871365	0	*Arabidopsis* sp.	Beta-galactosidase 1		Cell wall
	TR43312/c0_g1_i1	0.01806637	3×10^{-46}	*Pisum* sp.	Early light-induced protein		Chloroplast
13	*TR27360/c2_g1_i1*	0.01254971	6×10^{-180}	*Arabidopsis* sp.	Sorbitol dehydrogenase		Cytoplasm
	TR14309/c0_g3_i1	0.01228608	NA	No hits	No hits		
	TR29007/c0_g2_i1	0.01125583	7×10^{-71}	*Picea* sp.	Putative uncharacterized protein	Adenyl nucleotide binding	
	TR26487/c3_g1_i1	0.00896099	0	*Nicotiana* sp.	Pleiotropic drug resistance protein 2	Transport	Integral component of membrane
	TR19126/c0_g1_i1	0.00829734	4×10^{-83}	*Argemone* sp.	(S)-stylopine synthase	Isoquinoline alkaloid biosynthetic process	Integral component of membrane
	TR34176/c0_g1_i1	0.00823115	4×10^{-135}	*Ricinus* sp.	Putative zinc finger protein		
	TR8584/c0_g1_i1	0.00785437	2×10^{-140}	*Ricinus* sp.	Putative zinc finger protein		
	TR19966/c2_g3_i1	0.00737035	1×10^{-92}	*Brassica* sp.	BnaC09g29270D protein		
	TR9968/c0_g1_i1	0.00698595	0	*Arabidopsis* sp.	Glucomannan 4-beta-mannosyltransferase 9	Defense response	Cell wall organization
	TR27647/c1_g1_i1	0.00664175	0	*Oryza* sp.	Cellulose synthase-like protein H1	Cell wall organization	Integral component of membrane
14	*TR14309/c0_g1_i1*	0.60572914	3×10^{-133}	*Medicago* sp.	Putative uncharacterized protein		
	TR14309/c0_g3_i1	0.13456751	NA	No hits	No hits		
	TR2227/c0_g1_i1	0.02266061	1×10^{-53}	*Oryza* sp.	Tricin synthase 1		
	TR33175/c2_g1_i2	0.01227038	0	*Arabidopsis* sp.	Chaperonin 60 subunit alpha 1	Protein refolding	Chloroplast
	TR17377/c0_g3_i1	0.00753754	NA	No hits	No hits		
	TR18441/c1_g1_i1	0.00607363	6×10^{-93}	*Medicago* sp.	Putative signal anchor		
	TR25319/c0_g2_i2	0.00271735	0	*Arabidopsis* sp.	Adenosylhomocysteinase 1		
	TR36295/c2_g1_i2	0.00261196	2×10^{-131}	*Pinus* sp.	Cytochrome P450 720B2		
	TR33821/c2_g1_i1	0.00242023	0	*Arabidopsis* sp.	Probable inositol transporter 2	Signaling	Plasma membrane
	TR34086/c0_g1_i1	0.00190376	0	*Arabidopsis* sp.	Beta-amylase 3	Starch catabolic process	Chloroplast
19	*TR4285/c0_g1_i1*	0.04334234	3×10^{-25}	*Lens* sp.	Non-specific lipid-transfer protein 5	Lipid transport	
	TR30085/c0_g1_i2	0.0160039	3×10^{-47}	*Picea* sp.	Putative uncharacterized protein		
	TR35466/c0_g2_i2	0.0146392	1×10^{-89}	*Arabidopsis* sp.	Leucoanthocyanidin dioxygenase		
	TR15590/c0_g1_i1	0.01411896	2×10^{-105}	*Arabidopsis* sp.	Glucan endo-1,3-beta-glucosidase 13	Carbohydrate metabolic process	
	TR30889/c1_g1_i1	0.01300649	0	*Arabidopsis* sp.	Beta-galactosidase 1		Cell wall
	TR32051/c0_g1_i2	0.01283214	0	*Pisum* sp.	Glyceraldehyde-3-phosphate dehydrogenase B	Glucose metabolic process	Chloroplast
	TR20960/c0_g1_i1	0.01172682	2×10^{-127}	*Arabidopsis* sp.	Fasciclin-like arabinogalactan protein 17		
	TR4938/c0_g2_i1	0.01116556	3×10^{-89}	*Pinus* sp.	Mitochondrial glycine decarboxylase complex H-protein		
	TR20762/c0_g1_i1	0.01071276	9×10^{-84}	*Arabidopsis* sp.	Protein Senescence-Related Gene 1		
	TR9242/c0_g1_i1	0.01018747	0	*Arabidopsis* sp.	Chloroplast stem-loop binding protein of 41 kDa b	Defense response	Chloroplast

for the third transcript (*TR32818/c0_g1_i1*; Fig. 4.7a). Transcripts in this group were related mostly to cutin synthesis (*TR33780/c4_g1_i1*) and compounds from secondary metabolic pathways like flavonoids (*TR33481/c1_g2_i1*), anthocyanins (*TR39943/c0_g1_i1*) and phenylpropanoids (*TR30105/c0_g1_i1*).

The top 10 sequences in dynamic topic 19 (selected according to the $\beta_{0,19}$ scores; Table 4.6) were usually expressed at higher levels in the susceptible families (see e.g. Figs. 4.4f and 4.5b). Three of the sequences modelled in this dynamic topic (Table 4.6) showed higher expression levels than the rest (*TR4285/c0_g1_i1*, *TR30085/c0_g1_i2* and *TR32051/c0_g1_i2*), two depicted steady levels as the infection progressed (*TR9242/c0_g1_i1* and *TR4938/c0_g2_i1*), and the remaining sequences were at lower expression levels than those at 0 dpi as infection progressed (Fig. 4.7b). Most sequences in this topic are related to primary metabolism: lipid transport (*TR4285/c0_g1_i1*), glycine decarboxylation (*TR4938/c0_g2_i1*), and metabolism of carbohydrates (*TR15590/c0_g1_i1*) and glucose (*TR32051/c0_g1_i2*).

The transcripts modelled in dynamic topic 13 (selected according to the $\beta_{0,13}$ scores; Table 4.6) generally depicted increased expression levels at 3 dpi with decreasing values later on regardless of the resistance class (Fig. 4.8a). Two of the sequences modelled in this topic exhibited a different behaviour however: transcript *TR14309/c0_g3_i1* had a steep increase through infection that continued until 9 dpi, and transcript *TR19966/c2_g3_i1* peaked at 6 dpi with the expression levels remaining high in relation to the rest of the transcripts at 9 dpi (Fig. 4.8a). Sequences of dynamic topic 13 were involved in early responses to infection (of different kinds), like gene expression regulation (*TR34176/c0_g1_i1* and *TR8584/c0_g1_i1*), defense (*TR9968/c0_g1_i1*), resistance (*TR26487/c3_g1_i1*), and alkaloid synthesis (*TR19126/c0_g1_i1*).

Seven of the top 10 transcripts modelled in dynamic topic 14 (selected according to the $\beta_{0,14}$ scores; Table 4.6) depicted low and steady expression levels in general (Fig. 4.8b). The remaining transcripts showed a different pattern: transcripts *TR14309/c0_g1_i1* and *TR14309/c0_g3_i1* showed decreases in their expression levels as the infection progressed, while transcript *TR18441/c1_g1_i1* was upregulated at 6-9 dpi. Transcripts in this topic seemed to be related to housekeeping functions such as amino-acid synthesis (*TR25319/c0_g2_i2*), signalling/transport (*TR33821/c2_g1_i1*), protein

folding (*TR33175/c2_g1_i2*), methylation (*TR2227/c0_g1_i1*) and carbohydrate catabolism (*TR34086/c0_g1_i1*).

4.4 Discussion

The results, as a whole, depict two main aspects of the *T. plicata* - *D. thujina* interaction: 1) differences between resistant and susceptible families in the gene expression responses to infection, and 2) general responses to infection regardless of the resistance class of the seedlings. Both aspects are discussed below.

4.4.1 Differential gene expression responses to *D. thujina* infection between resistant and susceptible *T. plicata* families

The main difference between *T. plicata* seedlings that were resistant and susceptible to *D. thujina* was apparent constitutive defenses in the resistant families, and the absence of pre-existing defenses in the susceptible families. Resistant families had constitutively higher expression levels of a disease resistance protein RPM1 (*TR37382/c2_g1_i1*), a disease resistance RPP13-like protein 4 (*TR34618/c8_g1_i1*), a putative disease resistance protein RGA4 (*TR36626/c4_g2_i1*), as well as a TMV resistance protein N (*TR31269/c1_g1_i1*). Resistant families also exhibited higher expression levels of transcripts involved in cutin synthesis (*TR33780/c4_g1_i1*), flavonoids (*TR33481/c1_g2_i1*), anthocyanins (*TR39943/c0_g1_i1*) and phenylpropanoids (*TR30105/c0_g1_i1*) as modelled in dynamic topic 11.

Many disease resistance proteins have been shown to be involved in signal perception, which triggers the defense response and resistance mechanisms against pathogen infection (Vidhyasekaran 2008, p. 195). Predominant motifs of many *R* genes are leucine-rich repeats (LRR; Scheel and Nuernberger 2004; Vidhyasekaran 2008, p. 195) and nucleotide-binding sites (NBS; Vidhyasekaran 2008, p. 195). All of the disease resistance proteins found in this investigation belonged to the NBS-LRR family (UniProt accessions Q39214, Q38834, Q7XA39 and Q40392; The UniProt Consortium 2015, 2017). Two of those resistance proteins have been documented to confer resistance to bacterial infections (Q39214 and Q38834), one to an oomycete (Q7XA39) and one to a virus (Q40392). The presence of several disease resistance proteins and the vari-

ability in the disease severity among the resistant families raise the possibility that *T. plicata* displays quantitative (or polygenic), but not qualitative (or monogenic) resistance to *D. thujina* (Agrios 2005, p. 136; Holliday 1989, p. 274; Vidhyasekaran 2008, p. 193). If so, this may explain the lack of a few major genes responsible for *D. thujina* resistance, and the presence of several defense responses. Quantitative disease resistance cannot be easily broken by pathogen adaptation and therefore is beneficial although challenging for long term breeding for resistance (Holliday 1989, p. 274). Characterization of those *T. plicata* disease resistance proteins and investigation into their molecular roles in the defense against *D. thujina* will be required in future studies.

The transcripts related to the phenylpropanoid (*TR30105/c0_g1_i1*), flavonoid (*TR33481/c1_g2_i1*), anthocyanin (*TR39943/c0_g1_i1*) and cutin synthesis (*TR33780/c4_g1_i1*) pathways, that were upregulated in the resistant families, are all related and might be involved in detoxification processes as well as defense. Transcript *TR30105/c0_g1_i1* was annotated as *trans*-cinnamate 4-monooxygenase (also known as cinnamate 4-hydroxylase; Schomburg and Stephan 1994), an enzyme that catalyzes the production of *p*-coumarate from *trans*-cinnamate, the latter being the upstream precursor of phenylpropanoids like flavonoids, anthocyanin and cutin (Heldt 2005, p. 435; Tohge et al. 2013). Transcript *TR33481/c1_g2_i1* was annotated as flavanone 3-hydroxylase, an enzyme that catalyses the production of dihydroflavonols from flavanones (e.g. dihydrokaempferol from naringenin; Menting et al. 1994, Shimada et al. 1999, Tu et al. 2016). Transcript *TR39943/c0_g1_i1* was annotated as flavonoid 3′,5′-hydroxylase 2 and is responsible for the production of dihydroxyflavanones from flavanone (UniProt accession P48419; The UniProt Consortium 2015, 2017) which are precursors of other flavonols, flavones and anthocyanins (Shimada et al., 1999). Flavonoids are metal chelators (Falcone-Ferreyra et al., 2012, Williams et al., 2004), and known to respond to increased aluminum levels (Falcone-Ferreyra et al., 2012, Smirnov et al., 2015). In this study, aluminum concentration increased in infected plants in both the CC and NC experiments. Transcript *TR33780/c4_g1_i1* was annotated as BAHD acyltransferase DCR, an enzyme proposed to transfer 9(10),16-dihydroxy-hexadecanoic acid into cutin (Panikashvili et al., 2009, Yeats and Rose, 2013). Cutin and waxes are the primary constituents of the cuticle (Yeats and Rose, 2013), and the cuticle is the first barrier to be overcome by pathogens of any pathosystem (Agrios 2005, p. 210; Anker and Niks 2001; Gees and Hohl 1988; Hau and Rush

1982; Roundhill et al. 1995; Sherwood 1996; Zinsou et al. 2006).

The gene expression profile of the families susceptible to *D. thujina* was different from that of the resistant families. Susceptible families had higher expression levels of the transcripts modelled in dynamic topic 19, which were related to primary metabolism (e.g. carbohydrate metabolism, glycine decarboxylation and lipid transport). These families also had higher expression levels of a defense-related transcript (*TR9242|c0_g1_i1*; a chloroplast stem-loop binding protein of 41 kDa b, CSP41B). CSP41B binds to *RNA* molecules (UniProt accession Q9SA52; The UniProt Consortium 2015, 2017) and is involved in transcription and translation of chloroplast *RNA*s (Bollenbach et al., 2009), which can be regarded as a primary metabolic function. Biotrophs are known to reprogram the primary metabolism of the host so that it provides the attacker with substrates the pathogen cannot produce by itself (Berger et al., 2007, Duplessis et al., 2011, Kogovšek et al., 2016, Lapin and Van den Ackerveken, 2013, Spanu, 2012). The lack of constitutive molecular mechanisms of disease resistance and the presence of a vigorous primary metabolism in susceptible *T. plicata* seedlings may explain why they are prone to infection and establishment of *D. thujina*. Plants with such characteristics will likely occur in areas where pathogens cannot thrive (Russell et al., 2007), so that minimal energy is spent in defense (via secondary metabolism) and more in growth and development (via primary metabolism).

In relation to the responses to *D. thujina* infection, susceptible families upregulated defense-related transcripts like the LRR receptor-like serine/threonine-protein kinase GSO1 (*TR36979|c2_g1_i1*) and the cytochrome P450 750A1 (*TR17615|c0_g1_i1*), the latter not being expressed at all in the resistant families studied. The LRR receptor-like serine/threonine-protein kinase GSO1 is involved in epidermis development in aerial organs (Tsuwamoto et al., 2008) and has the gene ontology annotation "response to wounding" (UniProt accession C0LGQ5; The UniProt Consortium 2015, 2017). The cytochrome P450 750A1 has been annotated as having a monooxygenase function, more specifically as the enzyme EC 1.14.13.109 (UniProt accession Q50EK4; The UniProt Consortium 2015, 2017). This enzyme is involved in the synthesis of diterpene resin acids (Placzek et al., 2017, Ro and Bohlmann, 2006, Ro et al., 2005, Scheer et al., 2011). The annotations of both transcripts appear to depict a wounding response rather than defense against pathogens. However, considering that no plants were re-sampled during the experiments carried out in this study, the upregulation of

those sequences cannot be explained by the wounding that took place during the sampling process. Instead, such a reaction could be the response to the direct penetration by *D. thujina* during the infection (Søegaard 1969, p. 299).

4.4.2 General responses to *D. thujina* infection in seedlings of *T. plicata* full-sib families

4.4.2.1 Chemical responses

Aluminum was the only chemical variable that displayed significantly increased levels over time in the real-infected plants in relation to the mock-infected, especially in the susceptible families. Aluminum is a well-known plant toxin (see e.g. Duressa et al. 2011, Hamel et al. 1998, Jiang et al. 2015, Mossor-Pietraszewska 2001, Poot-Poot and Hernandez-Sotomayor 2011) that interferes with growth in plants (Hamel et al., 1998, Mossor-Pietraszewska, 2001, Yuan et al., 2017). Soil aluminum toxicity has been well-studied in different plant species (see e.g. Duressa et al. 2011, Hamel et al. 1998, Jiang et al. 2015, Poot-Poot and Hernandez-Sotomayor 2011), and it is documented that the trivalent Al^{3+} is the most toxic form (Fichtner, 2003, Hamel et al., 1998). Aluminum resistance is a well-studied topic, especially in crop species that grow in acidic soils (Firestone et al., 1983, Hamel et al., 1998, Yuan et al., 2017), but based on the extensive literature reviewed, no reports on increased foliar aluminum concentrations in response to obligate leaf pathogens exist in plants.

Despite the widely reported toxic effects of soil aluminum in plants, it has also been shown that increased aluminum concentrations can result in similar responses as those triggered by pathogen infection (Hamel et al., 1998). Such responses include lignification, hypersensitive response, upregulation of pathogenesis-related proteins as well as proteins related to cell wall synthesis (Hamel et al., 1998), and disruption of Ca^{2+} signalling (Hamel et al., 1998, Mossor-Pietraszewska, 2001, Silva, 2012). None of those responses were seen in the *T. plicata* families studied here, except possibly for the disruption of Ca^{2+} signalling given the upregulation of transcript *TR36118/c2_g1_i1* (G-type lectin S-receptor-like serine/threonine-protein kinase At1g34300), a calmodulin binding protein. Nevertheless, aluminum is not only toxic to plants but also to fungi (Avis et al., 2007, Fichtner, 2003, Firestone et al., 1983). Aluminum in leachates at high concentrations of 500 µM have been shown to inhibit growth of *Aspergillus flavus* in bioassays (Firestone et al., 1983), and low concentrations have also been

reported to be toxic to soilborne fungi like *Thielaviopsis basicola* ($\geq$ 20 µM Al) and *Phytophthora parasitica* ($<$ 1.0 µM, Fichtner 2003). Aluminum salts, such as aluminum chloride, have also been documented as toxic to phytopathogenic fungi like *Fusarium sambucinum*, *Phytophthora infestans*, *Helminthosporium solani* and *Rhizoctonia solani* where they limit fungal growth (Avis et al., 2007). It is plausible that aluminum may play a role in the defense against *D. thujina* in *T. plicata*, but it is unknown whether it is used directly or indirectly by the plant to defend itself. Further investigation will be required to elucidate if there is a direct link between increased aluminum levels and defense against this foliar pathogen in *T. plicata* seedlings.

4.4.2.2 Gene expression responses

The general gene expression responses to *D. thujina* infection in the *T. plicata* seedlings studied here were those modelled in dynamic topic 13. Sequences there were predicted to upregulate at 3 dpi and downregulate at later time points. The top representative transcripts of dynamic topic 13 included transcripts that were involved in cell wall organization (*TR27647/c1_g1_i1*, cellulose synthase-like protein H1; and *TR9968/c0_g1_i1*, glucomannan 4-β-mannosyltransferase, GMT) and alkaloid synthesis (*TR19126/c0_g1_i1*, [S]-stylopine synthase, STS). Cellulose synthases and GMT are part of cell wall synthesis (Heldt 2005, p. 4, Liepman and Cavalier 2012, Wojtasik et al. 2016), the former being responsible for the synthesis of cellulose (Heldt 2005, p. 269, Liepman and Cavalier 2012) and the latter being involved in hemicellulose biosynthesis (Wojtasik et al., 2016). Both cellulose and hemicellulose are targets of fungal enzymes during colonization (Mortaji 2011, Vidhyasekaran 2008, pp. 294-295, Wojtasik et al. 2016). Cell wall reinforcement is a common response to pathogen attack (Vidhyasekaran 2008, p. 298), and increased levels of cellulose synthases and GMT transcripts at 3 dpi in *D. thujina*-infected *T. plicata* seedlings might be related to such a response. STS catalyzes the production of (S)-stylopine from (S)-cheilanthifoline (Desgagné-Penix et al., 2010), an intermediate step in the production of benzylisoquinoline alkaloids (BIAs; Diamond and Desgagné-Penix 2016). To my knowledge, and based on the extensive literature reviewed, alkaloids of *T. plicata* foliage have not been widely studied. However, chamobtusin A (an alkaloid) is known to be present in the foliage of at least another Cupressaceae (*Chamaecyparis obtusa* cv. *tetragon*; Zhang et al. 2007). BIAs play an important role in plant defense (Dembitsky et al., 2015, Hagel and Facchini, 2013) because of their antibacterial activity

(Villar et al., 1987). Interestingly, another sequence related to BIAs' synthesis was also found in the experiment presented in Chapter 3. It then seems plausible that *T. plicata* seedlings may use alkaloids as secondary/supporting defense mechanism in addition to other compounds mentioned earlier.

Stability selection analysis on the differentially expressed transcripts using aluminum as the target variable showed that other gene expression responses associated with increased aluminum concentration took place in the plants. Sequences related to copper ion response, iron binding, metal ion binding proteins, receptor-like proteins, the shikimate pathway, and the flavonoid pathway as well as the abscisic acid pathway were among the top 43 predictors of the aluminum concentrations of the plants used for the *RNA*-Seq analysis. Most metal binding proteins (iron and metal) and a copper ion response sequence were upregulated with increased levels of aluminum, while many of the receptor-like proteins were downregulated. The transcripts that related to the shikimate pathway and to the abscisic acid pathway were downregulated while that of the flavonoid pathway was upregulated with increased aluminum concentrations. In general, the expression pattern of those sequences was similar in all families in the CC-CLB$^+$ treatment regardless of the resistance class, suggesting a common response mechanism associated with increased levels of aluminum, to *D. thujina* infection.

The upregulation of metal binding proteins may be related to the stress caused by the increased levels of aluminum. Metal binding amino acids, and derived molecules like oligopeptides, play important roles in plant adaptation to heavy metal stress including antioxidant activity, signalling and metal chelation with phytochelatins (Sharma and Dietz, 2006). Plant iron binding proteins, on the contrary, may be involved in iron homeostasis in response to oxidative stress (Briat et al., 2010). It is known that increased aluminum concentrations result in oxidative stress and the production of reactive oxygen species (Silva, 2012). Interestingly, the increased iron levels in the CLB$^+$ treatment of the controlled conditions experiment support the idea that iron may play a role in homeostasis responses to oxidative stress. The copper ion response transcript (*TR34581/c8_g1_i2*), upregulated in response to *D. thujina* infection, was annotated as laccase-5. Because of its localization (apoplast) and the documented role of this enzyme in cell wall lignification (Wang et al., 2015), *TR34581/c8_g1_i2* is probably involved in cell-wall reinforcement in response to pathogen attack. This

can be further supported by the increased levels of copper in the CLB^{+} treatment of the controlled conditions experiment.

Downregulation of receptor-like proteins was seen in response to the invading attacker. Receptor-like protein kinases (RLKs) are a superfamily of proteins that consist of an extracellular domain, a membrane domain, and an intracellular domain (Morris and Walker 2003; Tichtinsky et al. 2003; Vidhyasekaran 2008, p. 78). RLKs are involved in processes like growth, development, differentiation, hormonal response and pathogen response (Afzal et al., 2008, Goff and Ramonell, 2007, Morris and Walker, 2003, Tichtinsky et al., 2003, Vidhyasekaran, 2008). Many of the characterized RLKs belong to the leucine-rich repeat (LRR) subfamily (Afzal et al., 2008, Goff and Ramonell, 2007, Tichtinsky et al., 2003), and their downregulation can result in reduction of defense related genes (Parrott et al., 2016). Little information exists on the mechanisms of plant RLKs downregulation in response to fungal attacks, but gene silencing by the attacker is a possibility. *RNA* silencing is a common defense mechanism in viral and bacterial pathosystems where the foreign sequences are silenced by micro*RNA*s (mi*RNA*) and short interfering *RNA*s (si*RNA*; Zvereva and Pooggin 2012). The existence of NB-LRR genes silenced by mi*RNA*s that can be indirectly suppressed by bacteria (Zvereva and Pooggin, 2012), of LRR-RLK genes downregulated by viruses (e.g. Parrott et al. 2016), and the fact that *RNA* silencing may contribute to pathogenesis of other non-viral pathogens (Zvereva and Pooggin, 2012) suggest a possibility where *D. thujina* may be involved in the downregulation of the *T. plicata* receptor-like proteins reported here.

According to the regression stability selection using aluminum as response variable, transcripts related to the shikimate pathway and to the abscisic acid pathway were downregulated, while one in the flavonoid pathway was upregulated with increased aluminum levels. The bifunctional 3-dehydroquinate dehydratase/shikimate dehydrogenase (DHQD/SD; transcript *TR28212|c0_g1_i2*) was the shikimate pathway transcript downregulated. The DHQD/SD produces shikimate from 3-dehydroquinate, and is a key regulator of phenolic secondary metabolite pathways (Tohge et al., 2013). Downregulation of this gene may be the result of the host reprogramming by *D. thujina* so that the defense responses of *T. plicata* are repressed and the carbon metabolism diverted for the benefit of the invading pathogen. Transcriptomic analysis of the responses of rice, *Brachypodium distachyon* and barley to *Magnaporthe*

grisea infection has shown that *M. grisea* infection leads to decreased production of shikimate and to increased quinate in its host (Parker et al., 2009). The latter can be used a as carbon source by the pathogen (Soanes et al., 2012, Taniguti et al., 2015). This host reprogramming also resulted in the repression of defense-related compounds produced downstream in the shikimate pathway (Soanes et al., 2012, Taniguti et al., 2015). The decreased levels of transcripts of the abscisic acid pathway can be explained by the interference between that pathway and the signalling of plant responses to biotic stressors. This interference seems to repress the abscisic acid pathway as the host plant defends against pathogen attacks (Mauch-Mani and Mauch, 2005). In fact, it has been shown that increased levels of abscisic acid or genes from that pathway result in enhanced susceptibility to pathogens like viruses (Alazem and Lin, 2015), bacteria (Fan et al., 2009), fungi (Ulferts et al., 2015) and even nematodes (Moosavi, 2017). The flavonoid pathway transcript that was upregulated (*TR36842/c2_g1_i1*; annotated as flavonoid 3′,5′-hydroxylase, F3′5′H) may be related to the detoxification of aluminum rather than to pathogen defense itself. The F3′5′H hydroxylates dihydroflavonols (de Vetten et al., 1999, Shimada et al., 1999), as well as hydroxyflavanones and dihydroquercetin (Menting et al., 1994). As mentioned earlier, flavonoids are involved in chelating metals (Falcone-Ferreyra et al., 2012, Williams et al., 2004) and have been shown to increase in response to aluminum toxicity (Barceló and Poschenrieder, 2002, Falcone-Ferreyra et al., 2012, Smirnov et al., 2015). Indeed, specific flavonoids like quercetin have been reported to be exuded with increased aluminum levels in maize (Falcone-Ferreyra et al., 2012, Kidd et al., 2001). It is then plausible that flavonoids may be produced to mitigate increased aluminum levels in *T. plicata* seedlings infected by *D. thujina*.

4.4.3 Summary and conclusions

This study explored the chemical and gene expression responses to *D. thujina* infection in seedlings of six full-sib *T. plicata* families. Two time-course experiments were set up, one where natural infections took place, and another where infections were carried out in a controlled environment. Seedlings from all families in both environments had increased concentrations of aluminum in the real infection treatments; no other chemical responses were common to both experiments. Gene expression analysis showed that increased aluminum concentrations were also related to changes in transcripts involved in metal biding, receptor-like proteins and the shikimate, abscisic

acid and flavonoid pathways. The role of aluminum in the *T. plicata* - *D. thujina* interaction studied is intriguing, and it is unknown whether the seedlings are using this element as a defense or if the change is a by-product of some other defense response. Further investigations on the role of aluminum in defense against *D. thujina* are required to clarify its role in this pathosystem. *RNA*-Seq analysis revealed differences between resistant and susceptible families as well, the most important finding being the constitutively higher expression levels of several disease resistance proteins of the NBS-LRR family in seedlings of the resistant families. This may partly explain the qualitative nature of the resistance to *D. thujina* in *T. plicata*. Characterization of those disease resistance proteins will be needed to better understand their roles in the defense against *D. thujina*.

Chapter 5

Phenotypic and gene expression constitutive differences between *Thuja plicata* clones resistant and susceptible to *Didymascella thujina*, and their induced responses to pathogen infection

5.1 Introduction

Plants are constantly challenged by both biotic and abiotic factors. Biotic stressors are often detrimental to their hosts and include dissimilar organisms like fungi (Achotegui-Castells et al., 2016, de Cremer et al., 2013, Doehlemann et al., 2008, Galindo-González and Deyholos, 2016, Ji et al., 2016, Joshi et al., 2016, Kang et al., 2016, Parrott et al., 2016, Teixeira et al., 2014), other plants (Olsen et al., 2016), or arthropods (Ghaffar et al., 2016, Köllner et al., 2008, Major and Constabel, 2006, Ruuhola et al., 2011, Wang et al., 2016c). Each taxon has evolved different mechanisms to attack/access its host; for instance, obligate parasitic fungi perform direct penetration (Agrios 2005, p. 88; Gees and Hohl 1988; Roundhill et al. 1995; Sharma 2006, p. 4.6; Sherwood 1981; Søegaard 1969, p. 299). Different attackers also use plant resources differently. Many insects use plants mainly as food source (Vourc'h

et al., 2001, 2002), while obligate parasites depend on the cellular machinery of their hosts to survive (Berger et al., 2007, Doehlemann et al., 2008, Duplessis et al., 2011, Kogovšek et al., 2016, Lapin and Van den Ackerveken, 2013, Spanu, 2012). The wide range of strategies that pests and pathogens use against their hosts has resulted in the evolution of an extensive array of defense mechanisms in plants.

Defense mechanisms are diverse in plants and vary across the different levels of organization. At the organ level, constitutive mechanical defenses like thorns, trichomes and pubescent surfaces deter mammals (Cooper and Owen-Smith, 1986) and protect against arthropods (Fernandes, 1994, Levin, 1973). Cellular and tissue defenses like hypersensitive response (Agrios 2005, p. 217; Brown et al. 1966; Gees and Hohl 1988; Lauvergeat et al. 2001), the development of papillae (Agrios 2005, p. 214), and the deposition of lignin (Agrios 2005, p. 187; Smith et al. 2006; Xu et al. 2011; Yoshida 1998) and suberin (Agrios 2005, p. 187; Smith et al. 2006; Yoshida 1998) are commonly induced in compatible plant-pathogen interactions. Chemical compounds also play important roles in plant protection against pests (Köllner et al., 2008) and pathogens (Castillo et al. 2012; Heldt 2005, p. 404; Heldt and Piechulla 2010, p. 400; Wang et al. 2016c) through several mechanisms. For example, terpenes like α-thujene and sabinene accumulate in *Cupressus sempervirens* in response to *Seiridium cardinale* infection (Achotegui-Castells et al., 2016).

At the molecular level, plants have a collection of both constitutive and induced defenses, the best example being the resistance (R) genes. R genes confer full resistance to a plant pathogen when in the presence of their pathogen avirulence (avr) counterparts (Agrios 2005, p. 140; Hammond-Kosack and Jones 1997; Sharma 2006, p. 3.9; Vidhyasekaran 2008, p. 193). Many R genes encode proteins with nucleotide-binding sites (NBS; Vidhyasekaran 2008, p. 195; Westerink et al. 2004) and leucine-rich repeats (LRR; Scheel and Nuernberger 2004; Vidhyasekaran 2008, p. 195; Westerink et al. 2004), which trigger defense cascade reactions in response to pathogen infection (Ghaffar et al. 2016; Vidhyasekaran 2008, p. 195; Westerink et al. 2004). An interesting *R-Avr* interaction is that of the *Zea mays* - *Ustilago maydis* pathosystem (Doehlemann et al., 2008, 2009, Duplessis et al., 2011, Hemetsberger et al., 2012, Sonah et al., 2016, Spanu, 2012). *U. maydis* is a biotrophic fungi that causes tumours on aerial organs of *Euchlaena mexicana* and *Z. mays* (Doehlemann et al., 2008). Although genomic studies of the compatible interaction shows a complex re-

programming of the host's cells by the pathogen (Doehlemann et al., 2008) there is a probable *Avr* gene (*Pep1*) responsible for the inhibition of the host's cell responses to infection (Doehlemann et al., 2009, Hemetsberger et al., 2012, Sonah et al., 2016).

Besides full pathogen resistance in plants due to *R* genes, plants can also have several to many genes with small effects that result in quantitative disease resistance (Agrios 2005, p. 136; Sharma 2006, p. 3.5; Vidhyasekaran 2008, p. 193). Unlike *R*-genes, quantitative resistance is not full, and infected plants may show few symptoms of the disease (Agrios 2005, p. 136; Sharma 2006, p. 3.6). The traditional approach to detect minor resistance genes involved in quantitative resistance has been through quantitative trait loci (QTL) studies (Bhadauria et al., 2017, Christensen et al., 2004, Liu et al., 2016b, Nzuki et al., 2017, Simko et al., 2013, Young, 1996, Zyprian et al., 2016). QTL discovery requires a large number of known genetic markers as well as high numbers of both parents and offspring in order to be able to produce the linkage maps (Collard et al., 2005, White et al., 2007, Young, 1996). Those are usually drawbacks in non-commercial and non-model plant species. The declining costs of next generation sequencing (NGS) tools, like *RNA*-Seq, are providing new insights into the multiplicity of genes responsible for quantitative resistance in different pathosystems (Ji et al., 2016, Rodrigues et al., 2013, Teixeira et al., 2014, Wang et al., 2016c). NGS technology is being used for SNP discovery and genotyping (Bhadauria et al., 2017, Liu et al., 2016b, Lopez-Maestre et al., 2016, Nzuki et al., 2017), as well as to study plant responses to pathogen infections (Álvarez-Yepes et al., 2016, Galindo-González and Deyholos, 2016, Joshi et al., 2016, Krizek et al., 2016). In many cases, *RNA*-Seq studies have shown that complex gene interactions that involve many defense pathways and mechanisms take place during compatible plant-pathogen interactions (de Cremer et al., 2013, Kamitani et al., 2016, Parrott et al., 2016). Dual *RNA*-Seq analyses are also being used to study simultaneously the expression profiles of plant and pathogen during compatible interactions in order to determine the dynamics of the infection and the defense processes (Camilios-Neto et al., 2014, Hayden et al., 2014, Kawahara et al., 2012, Meyer et al., 2016).

The vast range of defense mechanisms that exist in plants comes at both energetic and evolutionary costs (Barrett and Heil, 2012, Brown and Rant, 2013, Bruns, 2016, Burdon and Thrall, 2009, Frank, 1993, 1992, Karasov et al., 2014, Mitchell-Olds et al., 1996, Occhipinti, 2013, Susi and Laine, 2015, Züst and Agrawal, 2017). When plants

allocate more energy to defenses, they have less energy available for primary metabolic functions like growth and development, so trade-offs between intrinsic and extrinsic factors determine whether defense or growth and development get priority (Brown and Rant, 2013, Bruns, 2016, Mitchell-Olds et al., 1996, Susi and Laine, 2015, Züst and Agrawal, 2017). The complex interactions between the pathways involved in defense as well as in growth and development usually result in the co-evolution of plant and pathogen systems where defense mechanisms in the host are selected in response to pathogenic characteristics being selected in the attacker (Barrett and Heil, 2012, Burdon and Thrall, 2009, Frank, 1993, 1992, Karasov et al., 2014, Occhipinti, 2013). A consequence of that co-evolutionary process, however, is that plant populations that have been isolated from their pathogens for millennia may not evolve defense mechanisms against them, and can be susceptible upon encountering the pathogen (Barrett and Heil, 2012, Burdon and Thrall, 2009, Frank, 1992, Occhipinti, 2013).

Variation in the resistance to *D. thujina* has been reported (Søegaard 1969, p. 323) and studied in *T. plicata* in the past (Russell et al., 2007, Russell and Yanchuk, 2012). "Physiologically determined resistance" to *D. thujina* has also been reported in *T. plicata* (Søegaard 1969, p. 366), the term having been used by Søegaard in the 1960's to refer to the increased resistance to *D. thujina* in *T. plicata* plants as they aged (Søegaard 1969, p. 373). Nowadays, the phenomenon is known as age related resistance (ARR) and takes place in plants commonly (Carella et al., 2015, Kus et al., 2002, Panter and Jones, 2002, Shibata et al., 2010). Understanding the basis of *D. thujina* resistance in foliage from mature *T. plicata* trees may help to guide the identification of phenotypic and/or genotypic markers for resistance to *D. thujina* in seedlings, which may have been overlooked when studying *T. plicata* seedlings exclusively. In this chapter, the constitutive phenotypic and genotypic differences among *T. plicata* clonal lines with different susceptibilities to *D. thujina* were studied in order to shed light on the potential resistance mechanisms to *D. thujina* in *T. plicata* mature foliage. The chemical and gene expression responses to *D. thujina* infection were also investigated in those lines to establish if differential responses between resistant and susceptible plants account for the variability.

5.2 Methodology

5.2.1 Plant material

Three *T. plicata* clonal lines with contrasting resistances to *D. thujina* were used in this experiment (lines 5382, 5398 and 5412; see Appendix A.1). Each of the three clones was propagated from individual plants from three different, unrelated full-sib families. The clones were selected based on data from a common garden *T. plicata* genetic trial on Vancouver Island (Russell, J.H.; unpublished data) that indicated significant clonal differences in *D. thujina* severity after three years in the field. Cuttings were collected from the donor plants and propagated in a greenhouse using Beaver Styroblock containers 45/340 (Stuewe and Sons., Tangent, OR, USA) with Sunshine Professional Growing Mix 2 (Sun Gro® Horticulture, Vilna AB, Canada) at Cowichan Lake Research Station (Mesachie Lake, British Columbia). Plants were grown under these conditions for one year prior to the experiment.

5.2.2 Morphological and histological characterization of the plant material

A total of 16 variables (13 measured and three derived), were studied to characterize the plant material used (see also Appendix A.8). The variables were related to plant size, leaf toughness and leaf anatomy. Plant size variables were plant height, root collar diameter (RCD) and the ratio of height to RCD (18 plants per line). Leaf toughness was measured in both young and old foliage (nine plants per line), using a custom-made penetrometer. Young foliage corresponded to the youngest leaves in the third branch counting from the top of the plant (i.e. from the current year), while older foliage referred to leaves from first-order branchlets of the middlemost branch of the plant. Toughness was calculated as in Graça and Zimmer (2005) and Quinn et al. (2000).

Leaf anatomy variables included width, thicknesses (leaf, cuticle, epidermis, whole mesophyll, palisade mesophyll and spongy mesophyll), thickness ratios (palisade to spongy mesophyll and whole mesophyll to leaf), percentage of epidermal cells with lignified walls, and stomatal density. These variables were measured on samples taken from the middle section of each of three branches (lowermost, mid-crown, and third from the top) from three plants per line. Leaf epidermis, cuticle thickness and stom-

atal densities were measured on the same three branches, but both leaf surfaces were included.

Samples for all anatomical analyses (∼3.5 mm-long), except stomatal density, were fixed overnight in 2.5% glutaraldehyde (0.1 M Sörensen phosphate buffer pH 7.2 used as diluent; Ruzin, 1999, pp. 227). Fixed sections were washed for 20 min in Sörensen's buffer two times, dehydrated in an ascending ethanol sequence (50%, 70%, 80% and 90%, 20 min each), and changed twice in 100% ethanol (20 min each step). The samples were then embedded in Quetol 651 (Takagi and Sato, 1979) as follows: 30 min change in a 1:1 volume mixture of ethanol-*n*BGE (*n*-butyl glycidyl ether), 30 min change 100% *n*BGE, 2 h change *n*BGE-Quetol 651 (1:1 volume), and overnight change in 100% Quetol 651. The following day, the samples were hardened for 24 h at 60℃. Sections from the embedded samples were cut in a Sorvall JB-4 Microtome and fixed to microscope slides on a hot plate. Two sets of 5 µm-thick sections were produced per sample, one to measure thicknesses (stained with Toluidine Blue O), and another to count lignified epidermal cells (stained with phloroglucinol).

For the thickness measurements, microscope slides with the sections were flooded with 1.0 % w/v Toluidine Blue O (dissolved in 1% aqueous sodium borate) for five min, rinsed, and then washed in 70% ethanol for 50 s and in 100% ethanol for 1 min. The slides were left to dry at room temperature (RT) and mounted semi-permanently with Permount™ (Fisher Chemical™, Ottawa ON, Canada). Mounted samples were photographed at 100X and 1000X magnifications using a Zeiss microscope fitted with a RTKE SPOT camera (SPOT Imaging, Sterling Heights MI, USA) and SPOT v. 4.6 software. The digital images were analyzed using ImageJ v. 1.46 (Schneider et al., 2012).

Phloroglucinol was used to stain the set of samples used to count epidermal cells with lignified walls. Microscope slides with sections were covered with 1% w/v phloroglucinol (diluted in 70% ethanol) for 5 min, the excess was removed and the sections covered with hydrochloric acid (HCl) for 1 min. Excess HCl was removed and the slides let to dry at RT. The samples were then mounted using Permount™ as before, and pictures were taken within 3 h using the same equipment and software described above.

Stomatal density was quantified from leaf impressions taken using commercial transparent nail polish. Two coats were applied to the areas of interest, let to dry for 30 min at RT, and impressions were removed using transparent packing tape. The impressions were then mounted on microscope slides, covered with cover slips, and photographed at 100X magnification using the same equipment and software used for the other traits studied.

The continuous variables recorded were checked for normality with the Shapiro-Wilk test, and non-normal variables were transformed to meet the assumption ($\log_{10}$ for cuticle thickness, and height to RCD ratio). Plant size and toughness variables were analyzed in R using one-way analyses of variance (ANOVA) with clonal line as a fixed effect (R Core Team, 2015). The anatomical variables were analyzed with a fixed-effects split-plot design (Appendix A.3) in R. Homogeneous groups for variables with significant differences among lines were obtained using the Tukey HSD all-pairwise comparisons test. Stomatal densities were analyzed using Kruskal-Wallis one-way ANOVAs in R.

5.2.3 Time-course responses to infection with *D. thujina*

The three *T. plicata* lines (5382, 5398 and 5412) were mock- (CLB^-) and real-infected (CLB^+) in a controlled environment. Three leaf samples per type of infection treatment × line combination were taken just before inoculation (0 days post-infection, dpi), and 4, 8 and 12 dpi (Appendix A.8). The samples were used for the following purposes: 1) gene expression analyses (*RNA*-Seq), 2) chemical composition, and, 3) confirmation of the infection. Samples for 1) and 2) were flash frozen in liquid nitrogen and those for 3) were fixed in glutaraldehyde prepared in Sörensen's buffer (see previous section).

The experiment took place in a Conviron growth chamber (Conviron, Winnipeg MB, Canada) at the Bev Glover Growth Facility (University of Victoria, Victoria, British Columbia) that was set up to an average temperature of 16℃, 12 h light - 12 h darkness, and relative humidity ≥90%. Humidity levels were achieved using the same chamber used in Chapter 4 (Appendix A.10), except that HOBO U23 Pro v2 data loggers (Onset, Bourne MA, USA) were used to track the temperature and humidity inside the chamber this time. The plants were acclimated inside that chamber for

two weeks before the start of the experiment.

Inoculation and infection confirmation procedures

An adapted version of the technique described in Søegaard (1969, pp. 310) was used to inoculate the plants that were real-infected. *D. thujina* inoculum was collected in the field from a *T. plicata* progeny trial in Jordan River (British Columbia; 48° 25' 24.52" N, 124° 1' 27.69" W, elev. 76 m) during the sporulation season (Appendix A.14). *T. plicata* foliage with *D. thujina* ascocarps releasing spores were collected in floral water pick vials containing a general nutrient solution with a N:P:K ratio of 100:22:83 (per 100 L: 2.15 g $CaSO_4{\cdot}2H_2O$, 12.37 g K_2HPO_4, 5.24 g KCl, 28.59 g NH_4NO, 4.05 g $MgSO_4{\cdot}7H_2O$ and 0.90 g Chelated Micronutrient Mix [Master Plant-Prod Inc., Brampton ON, Canada]). The collected cuttings were taken to the Bev Glover Growth Facility and kept in a high humidity chamber ($\geq$90%,) for one day before setting up the infections. On the day of the infection, each vial was placed in the cavity of the plant to be infected, and the adaxial surface of a branch from the plant to be infected was placed against the cutting's leaf surface with the most sporulating ascocarps. The two branches were subsequently held together with masking tape to ensure the spores being released landed directly on the branches of interest. The mock infections were set up in a similar way as the real infections, but branches from seedlings that had never been infected were used instead of the infected cuttings. After the last sampling point, the plants were transferred to a glasshouse where they remained for nine months until the development of *D. thujina* symptoms. All plants were fertilized monthly using Peters' 20-7-19 Conifer Grower fertilizer (100 parts-per-million of N; Jr. Peters Inc, Allentown PA, USA), and watered three times a week during the summer (June-September), bi-weekly in fall (October-November), and weekly in winter (December-February).

Three methodologies were used to confirm the infection of the inoculated plants: 1) incidence assessment of the disease after symptom development (recorded as the number of plants per line that showed *D. thujina* symptoms), 2) BLASTn searches in the assembled reference transcriptome (see section 5.2.3.2) for the two *D. thujina* internal transcribed spacer 2 (ITS2) sequences available in GenBank (accessions KT875766 and KT875767), and 3) detection of *D. thujina* spores (Kope, 2000) using Scanning Electron Microscopy (SEM). For the SEM, *T. plicata* samples were fixed, washed

and dehydrated as were the samples processed in the histological characterization, except that they were changed every 30 min. After the last 100% ethanol change, the samples were critical point dried using a Leica EM CPD300 system (Leica Microsystems Inc., Richmond Hill ON, Canada). Dry samples were gold-coated in an Edwards S150B Sputter Coater (Edwards Canada, Quebec QC, Canada), and then studied and photographed at 900X magnification using a Hitachi S-3500N Scanning Electron Microscope (Hitachi High-Technologies Canada Inc., Toronto ON, Canada).

In addition to the infection assessments mentioned above, variation of the resistance to *D. thujina* among lines was quantified by measuring the severity of the disease. A similar set of plants as those in section 5.2.1 were taken to the progeny trial used as source of inoculum (mentioned in section 5.2.3), where the plants remained from late May to mid July. The plants were watered twice a week while they were in the field, and were later taken to a glasshouse inside the Bev Glover Growth Facility where they remained until symptoms developed nearly nine months later. Severity referred to the percentage of foliar area with *D. thujina* symptoms, and was quantified by scanning the adaxial surface of the middlemost branch in an Epson Perfection v750 scanner (Epson Canada Ltd., Markham ON, Canada) and doing colour analysis in WinRHIZO Pro v. 2009c (Regent Instruments Inc., QC, Canada). Severity data was analyzed using Kruskal-Wallis one-way analysis of variance (ANOVA) with line as factor since neither the raw data nor the transformed data met the normality assumption.

5.2.3.1 Chemical composition analyses

Seventy-two foliar samples (3 *T. plicata* clonal lines × 2 infection conditions × 4 time points × 3 replicates) were sent for analysis to the Analytical Laboratory of the Ministry of Environment and Climate Change Strategy Branch (Victoria BC, Canada). Sixty chemical variables that included fibre, cellulose, lignin, terpenes, and mineral nutrients were quantified (see Appendix A.21 for full list). Mineral nutrients were measured at 0 and 8 dpi only, and the rest at all time points. Fibre, cellulose and lignin were quantified with the acid detergent fibre and acid detergent cellulose procedures used for forage fibre analysis (Goering and Van Soest, 1970). Samples for terpene analyses were ground in liquid nitrogen using a chilled mortar and pestle. Approximately 0.25-0.50 g of ground foliage was extracted for 48 h in

4 mL of methanol. *T. plicata* terpene standards were prepared by mixing, in 100 mL of methanol, 0.05-0.50 g of the respective extractive (the amount depended on the expected relative abundance in the samples). Terpenes were quantified using 30 m $\times$ 0.25 mm, d_f 0.25 µm capillary GC columns in a Clarus Gas Chromatograph (PerkinElmer Inc., Waltham MA, USA) according to the manufacturer's guidelines. The samples for mineral analysis (0.25 g) were digested with 4.0 mL digestion reagent (150 µg scandium$\cdot L^{-1}$ prepared in 70% nitric acid) using 15 mL quartz tubes in an Ultrawave Microwave Digestion System (Milestone Inc., Shelton CT, USA) according to the manufacturer's recommendations. Elements were quantified via inductively coupled plasma optical emission spectroscopy analysis using the scandium from the digestion reagent as an internal standard.

Data were analyzed using Principal Component Analysis (PCA) on the correlation matrix using FactoMineR (Lê et al., 2008) in R (R Core Team, 2015). Selection of variables of interest was done using stability selection (Meinshausen and Bühlmann, 2010). Stability selection is a variable selection methodology that detects the best predictor of a variable of interest arbitrarily chosen by the investigator. The method produces an organized list of variables using a decreasing score calculated for each variable. Two categorical stability selection analyses were performed: 1) based on categories that grouped samples according to plant lines, regardless of the infection condition, to establish the chemical variables that differentiated the lines; and 2) based on categories that grouped samples according to the infection condition and sampling time points to detect the compounds that changed in response to *D. thujina* infection. Variables to analyze further from each stability selection analysis were chosen with change point analysis on the sorted stability selection scores. This was done using changepoint with the AMOC method on variance (Killick and Eckley, 2014) in R. Variables retained by changepoint were then analyzed using three-way factorial ANOVA, with clone line, time point, infection status (CLB^+ or CLB^-) and their interactions as fixed effects (see Appendix A.24). For the variables that did not meet the normality assumption, each factor was analyzed individually using non-parametric Kruskal-Wallis one-way ANOVAs. Given the high variability of the magnesium and phosphorus measurements, those were analyzed by normalizing their values in the real infected plants (CLB^+) with those in the mock infections (CLB^-) and then performing two-sample proportion tests per pair of clonal lines at 8 dpi.

Selected chemical variables were plotted as the relative concentrations of their values in the real infections (CLB^+) in relation to the mock infections (CLB^-; see e.g. Figs. 5.3a- 5.3c and Appendix A.26). For every line × time combination, the value of the variable of interest (e.g. *p*-cymene) in the CLB^+ condition was divided by the value in CLB^- condition. Means and standard errors of the ratios by line and time point were then calculated and the plots generated.

5.2.3.2 Gene expression analyses

Extraction of total RNA

RNA extraction was done using a modified version of the protocol in Rajakani et al. (2013). All plastic-ware and distilled deionized water had previously been DEPC-treated. In brief, one gram of foliage was ground in liquid nitrogen using chilled pestle and mortar. The powdered foliage was poured into 50 mL Falcon™ centrifuge tubes (Fisher Scientific, Ottawa ON, Canada) using liquid nitrogen, and the nitrogen was let to evaporate in a freezer at -20℃. Once dry, the samples were mixed with 10 mL of warm 2% CTAB extraction buffer with activated charcoal (2.5 M NaCl, 50 mM EDTA pH 8.0, 200 mM Tris-Cl pH 8.0, 3% β-mercaptoethanol, 1.5% PVPP and 0.05% activated charcoal; the last three components added just before use). The mixture was incubated with intermittent shaking for 15 min at 65℃, cooled down to RT, and centrifuged at 18,514 × *g* for 20 min at 4℃. The supernatant was transferred to a 15 mL Falcon™ tube, mixed by inversion with an equal volume of chloroform and centrifuged at 4℃ for 20 min at 18,514 × *g*. The supernatant was kept, and a second chloroform cleaning step was performed. The latest supernatant was placed in 2 mL centrifuge tubes, and a 1/4 volume of lithium chloride (10M) was added. The mixtures were incubated overnight at 4℃.

The next morning, the samples were centrifuged at 4℃ for 30 min at 21,728 × *g*. Supernatants were discarded, and the pellets suspended by pipetting in 500 µL SSTE (0.5% SDS, 1M NaCl, 1mM EDTA pH 8.0, 10mM Tris HCl pH 8.0) and 400 µL phenol (pH 8.0). One-hundred microliters of chloroform were added to the mixture before vortexing and centrifuging at 18,407 × *g* for 5 min at RT. The supernatant was then transferred to a 1.5 mL Eppendorf® tube, mixed with 300 µL of chloroform, vortexed and centrifuged at RT for 5 min at 18,407 × *g*. The last supernatant was placed in a

new 1.5 mL Eppendorf® tube, and 1/10 volume of 3M NaOAC and an equal volume of chilled 100% isopropanol were added. The solution was incubated at -20℃ for 25 min. After incubation, the samples were centrifuged at 16,168 × *g* for 33 min at 4℃, the supernatants were discarded and 1 mL of chilled 75% ethanol was added to the pellets. The samples were mixed by inversion and centrifuged at 4℃ for 5 min at 16,168 × *g*. Supernatants were discarded and the cleaned pellets let to dry. The final pellet, total *RNA*, was re-suspended in DEPC-treated deionized distilled water, quantified in a NanoDrop™ 2000 Spectrophotometer (Thermo Scientific™ Wilmington DE, USA), and checked for integrity in a 1X MOPs, 1.0% formaldehyde-agarose gel.

mRNA enrichment, cDNA production and sequencing

The total *RNA* samples were processed *in-house* for m*RNA* enrichment and c*DNA* library production, while sequencing was outsourced to Genome Quebec Innovation Centre (Montreal QC, Canada) for Illumina® HiSeq 2000 100bp paired-end sequencing. m*RNA* enrichment was completed using protocol C of the Thermo Scientific™ MagJET m*RNA* Enrichment Kit (Life Technologies Inc., Burlington ON, Canada). Library production was done with the NEB Next® Ultra™ *RNA* Library Prep Kit for Illumina® v. 2.1. (New England BioLabs® Inc., Ipswich MA, USA) except for the *DNA* purification and size selection (∼400 bp) procedures. The Thermo Scientific GeneJET NGS Cleanup Kit (Life Technologies Inc.) and the Thermo Scientific MagJET NGS Cleanup and Size Selection Kit (Life Technologies Inc.) were used for those steps. Samples were barcoded with the NEB Next® Multiplex Oligos for Illumina® - Index Primers Sets 1 and 2 (New England BioLabs® Inc.). Individual libraries were quality controlled in an Agilent 2100 Bioanalyzer (Agilent Technologies, Santa Clara CA, USA) with the Agilent *DNA* 1000 Kit (Agilent Technologies). The final libraries were pooled in five batches (40 ng of *DNA* per library), and each batch was sequenced in a single lane. The samples were barcoded and pooled so that all treatments were present in all sequencing lanes. Sequencing was done using an Illumina® HiSeq 2000 sequencer that produced 100 bp paired-end reads.

Bioinformatics

The pipeline shown in Appendix A.29 was used for the bioinformatics analyses. Batch job scripts and PBS shell scripts were used to complete the analyses below on the

Hermes cluster (University of Victoria) of Westgrid (www.westgrid.ca).

Reference transcriptome assembling and annotation

Two FASTQ Illumina® 1.9 (Phred-33 ASCII) compressed files per sample were downloaded from Genome Quebec Innovation Centre to Hermes using wget. The files were quality checked in FastQC v. 0.11.4 (Andrews, 2014) and trimmed with Trimmomatic v. 0.36 (Bolger et al., 2014) set up as follows: Illumina® clip TruSeq v2 paired-end 2:30:10, head crop 14bp, sliding window 4:15, minimum length 36bp, convert quality scores to Phred-33. A reference transcriptome was built on Westgrid's cloud system using Trinity v. 2.2.0 (Grabherr et al., 2011). The assembly's statistics were computed in PRINSEQ v. 0.20.4 (Schmieder and Edwards, 2011).

The assembly was annotated in Trinotate v. 3.0.1 (http://trinotate.github.io). TransDecoder v. 2.1.0. was used to predict coding regions (http://transdecoder.github.io) , and protein-coding transcripts were blasted with BLAST+ v. 2.2.28 (Camacho et al., 2009) using HPC GridRunner. The following databases were searched for annotations: EggNOG v. 4.5 (Huerta-Cepas et al., 2016), Swiss-Prot/TrEMBL and UniRef90 release 2016_03 (The UniProt Consortium, 2017), KEGG release 78.1 (Kanehisa et al., 2017) and Gene Ontology (Ashburner et al., 2000, The Gene Ontology Consortium, 2015). HMMER v. 3.1b2 (http://hmmer.org) was used to search protein domains in Pfam 29.0 (Finn et al., 2016). Trans-membrane domains were predicted using TMHMM v. 2.0 (http://www.cbs.dtu.dk/services/TMHMM/), signal peptide sites were predicted using SignalP v. 4.0 (Petersen et al., 2011) and ribosomal *RNA*s were searched with RNAmmer v. 1.2 (Lagesen et al., 2007).

Differential expression analyses

Reads were mapped to the assembly with RSEM v. 1.3.0 (Li and Dewey, 2011), and counts normalized by calculating transcripts per million (TPMs; Li and Dewey 2011, Li et al. 2010, Wagner et al. 2012) and the trimmed mean of M-values (TMM; Dillies et al. 2013, Robinson and Oshlack 2010). Downstream analyses were completed using the Trinity pipeline (Haas et al., 2013) on the transcript expression matrix. The term "transcript" is used through this document for simplicity despite the fact that the sequences may not necessarily correspond to real transcripts.

edgeR (Robinson et al., 2010) was used to calculate differentially expressed (DE) transcripts between pairs of samples. The transcripts with a maximum false discovery rate of 0.001 and minimum fold-change of 4 were compiled in a final DE matrix. The DE data were then explored using PCA (based on correlation) using FactoMineR as in section 5.2.3.1, and were also used to produce a Pearson's correlation heat-map of the expression profile of all samples and a hierarchical clustering map of differentially expressed transcripts versus samples using Euclidean distance. The transcripts' tree was cut at 49% of its maximum height to produce clusters of differentially expressed transcripts. The annotation report and DE matrix were ingested into a SQLite database and uploaded to a local TrinotateWeb server for data exploration. TrinotateWeb was obtained from http://trinotate.github.io/TrinotateWeb.html, and installed on Compute Canada's West Cloud (https://west.cloud.computecanada.ca).

No qPCR confirmation was performed on any of the DE sequences as it has been shown that the DE method used (*edgeR*) has high sensitivity and specificity, as well as high overall agreement with qPCR measurements when compared to other methods, such as Cuffdiff2, TSPM or DESeq2 (Rajkumar et al., 2015). Furthermore, it has been reported that relative expression levels agree across different gene expression platforms, including HiSeq 2000 and qPCR (SEQC/MAQC-III Consortium, 2014).

Search for transcripts of interest

Sequences of interest were found using three methodologies: 1) categorical stability selection analysis, 2) grade of membership (GoM) analysis, and 3) dynamic topic modelling. Stability selection was completed with the randomized lasso algorithm (Meinshausen and Bühlmann, 2010) in Python (scikit-learn package). That analysis was completed to find predictors (transcripts) of plant infection by selecting sequences that were differentially expressed among lines in the real- versus mock-infections. Specifically, the categories used in the stability selection analysis were as follows: a) all plants in the CLB^- and in the 0 dpi CLB^+ conditions were grouped into one category; and b) the remaining plants (4-8 dpi CLB^+) were categorized according to their line (i.e. three extra categories). The number of transcripts to be retained from the analysis was decided using changepoint with the AMOC method on mean and variance (Killick and Eckley, 2014).

GoM is a dimension reduction technique that was used to detect transcripts that co-occurred in each plant line regardless of their infection status or time point. GoM was carried out using the latent Dirichlet allocation method (Blei, 2012, Blei and Lafferty, 2009, Liu et al., 2016a) implemented in *CountClust* (Dey et al., 2016, 2017) with K (number of clusters) = 25. From a Dirichlet allocation perspective, each *CountClust* cluster is a topic (hereafter referred to as static topic). Each of the 25 topics corresponds to a probability distribution over the counts of the DE transcripts (θ matrix in *CountClust*), and each of the 72 samples (3 *T. plicata* clonal lines $\times$ 2 infection conditions $\times$ 4 time points $\times$ 3 replicates) is a probability distribution over the 25 topics (ω matrix in *CountClust*). A hierarchical, Euclidean distance-based heat-map of samples versus static topics was produced using the ω matrix, and topics of interest per line were chosen from that heat-map. Representative transcripts per selected static topic were chosen by sorting in decreasing order the θ scores of all DE transcripts and retaining the top 10. In topic modelling, it is common practice to interpret the topics based on 5-10 "words" (see e.g. Blei 2012, Blei and Lafferty 2009, Dey et al. 2016, Liu et al. 2016a).

Dynamic topic modelling (Blei and Lafferty, 2006, Lee et al., 2016) was used to model the expression over time of transcripts that co-occurred just before the infection with *D. thujina* took place (0 dpi). Dynamic topic modelling was performed with K = 25 (i.e. 25 dynamic topics) using Dynamic Topic Models (https://github.com/blei-lab/dtm). Dynamic topics of interest were chosen based on the frequency of the top dynamic topics of the transcripts that were retained in the stability selection analysis. The top dynamic topic of each transcript (k) selected by stability selection was the topic with the highest β score at 0 dpi (i.e. the topic with the highest $\beta_{0,k}$ per transcript retained in the stability selection analysis). The representative transcripts of the chosen dynamic topics were then determined using the decreasing $\beta_{0,k}$ scores of all DE transcripts and keeping the top 10. It is common practice to retain 5-10 "words" per dynamic topic to analyze the function of the topic (see e.g. Blei 2012, Blei and Lafferty 2009, Dey et al. 2016, Liu et al. 2016a).

5.3 Results

5.3.1 Characterization of the plant material

There were no significant differences among lines in the toughness of young or old foliage (p =0.3011 and p =0.7604, respectively), nor in the stomatal density (p = 0.9621). The thicknesses of most leaf strata were not significantly different among lines (Appendix A.4). Lignification of the epidermal cells was not significantly different among lines (Appendix A.4). The only leaf anatomy variables that rendered significant differences among lines were the spongy mesophyll thickness ($p = 0.0107$), and the palisade to spongy mesophyll thickness ratio ($p = 0.0147$). Spongy mesophyll was significantly thicker in lines 5398 and 5412, and the palisade to spongy mesophyll thickness ratio was significantly higher in lines 5382 and 5412 (Table 5.1).

Table 5.1. Mean and standard errors for *Thuja plicata* clonal lines, of the 16 variables recorded for the morphological and histological characterization of the plant material used in this study. The variables relate to plant size, leaf anatomy and leaf toughness. One-way analyses of variance were carried out for the plant size and leaf toughness variables, while a split-plot statistical model was used for all leaf anatomy variables except stomatal density, which was analyzed using Kruskal-Wallis analysis of variance. Similar superscripts on the means refer to homogeneous groups according to the Tukey HSD all-pairwise comparisons test. RCD = root collar diameter.

		***Thuja plicata* clonal line**		
Trait	**Variable**	**5382**	**5412**	**5398**
Plant size	RCD (mm)	$4.50^{a} \pm 0.16$	$3.50^{b} \pm 0.17$	$3.28^{b} \pm 0.14$
	Height (cm)	$47.29^{a} \pm 1.10$	$37.79^{b} \pm 1.59$	$41.21^{b} \pm 0.98$
	Height to RCD ratio	$106.3^{b} \pm 2.9$	$110.1^{b} \pm 4.6$	$128.3^{a} \pm 4.3$
Leaf anatomy	Epidermal thickness (µm)	11.35 ± 0.37	10.18 ± 0.30	11.10 ± 0.35
	Cuticle thickness (µm)	2.44 ± 0.19	1.97 ± 0.14	2.24 ± 0.13
	Palisade mesophyll thickness (µm)	75 ± 9	61 ± 19	37 ± 10
	Spongy mesophyll thickness (µm)	$368^{a} \pm 24$	$457^{b} \pm 28$	$455^{b} \pm 43$
	Whole mesophyll thickness (µm)	442 ± 6	518 ± 12	491 ± 16
	Leaf thickness (µm)	482 ± 17	543 ± 33	527 ± 44
	Leaf width (µm)	885 ± 36	888 ± 51	1047 ± 68
	Palisade to spongy mesophyll ratio	$0.22^{b} \pm 0.03$	$0.13^{a,b} \pm 0.04$	$0.08^{a} \pm 0.02$
	Whole mesophyll to leaf thickness ratio	0.92 ± 0.02	0.95 ± 0.02	0.93 ± 0.02
	Epidermal cells with lignified walls (%)	61 ± 6	52 ± 8	51 ± 6
	Stom. density (stomata·mm^{-2})	124 ± 12	127 ± 19	131 ± 24
Leaf toughness	Young foliage (kPa)	$1{,}200.7 \pm 33.4$	$1{,}165.2 \pm 62.5$	$1{,}092.7 \pm 46.7$
	Old foliage (kPa)	$1{,}900.6 \pm 85.3$	$1{,}991.8 \pm 107.2$	$1{,}896.9 \pm 111.9$

Plant size variables were significantly different among lines ($p < 0.0000$ for height and RCD, and $p = 0.0010$ for the ratio of height to RCD). Line 5382 was the tallest, and lines 5412 and 5398 were shorter and not significantly different from each other (see homogeneous groups in Table 5.1). Similarly, line 5382 had the greatest RCD, with

smaller RCDs in lines 5412 and 5398. The height to RCD ratio was the highest in line 5398, and lines 5382 and 5412 had lower ratios that were not significantly different from each other.

5.3.2 Time-course responses to infection

Didymascella thujina symptoms developed in most of the inoculated plants. Incidence was high with no differences among lines (Table 5.2). Only samples from 4-12 dpi in the CLB^+ treatment tested positive for the presence of *D. thujina* spores as seen in the SEM screening. The severity of the disease was significantly different among plant lines ($p = 0.0039$; Table 5.2). Line 5382 had the highest severity (6.51%), while lines 5398 and 5412 had similar and lower severities (1.63% and 1.57%, respectively). Line 5382 will be referred to as susceptible through the rest of this document, and lines 5398 and 5412 as resistant.

Table 5.2: Incidence and severity of *Didymascella thujina* symptoms per clonal line. Incidence was assessed in the plants that were used in the time-course experiment performed in growth chambers, and severity was measured in a set of plants that were infected in the field (see methods for details). Both variables were evaluated at the time *D. thujina* symptoms were present.

Clone line	Incidence (%)[1]	Severity (%)[2]
5382	88.89	6.51^{A}
5398	77.78	1.63^{B}
5412	88.89	1.57^{B}

[1] The test of independence of line vs. presence/absence of *D. thujina* symptoms was not significant ($p = 0.7457$).

[2] A-B: homogeneous groups based on the Kruskal-Wallis all-pairwise comparisons test at $\alpha = 0.05$.

5.3.2.1 Chemical composition

Principal components analysis showed that samples from lines 5398 and 5412 grouped closer to each other than to line 5382, and that CLB^+ samples separated from CLB^- samples in lines 5382 and 5412, but not in line 5398 (Fig. 5.1). The first three principal components (PC) explained 47.84% of the variance. PC1 accounted for 31.80% of the variance, PC2 for 8.95% and PC3 for 7.10%. PC1 appeared to be related

to the responses to infection, while PC2 seemed to refer to the differences between the more susceptible line (5382) and the resistant lines (5398 and 5412). Chemical variables that had the highest contributions to PC 1 were terpenes (monoterpenes, α-pinene, myrcene, α-thujene, β-pinene, R-limonene and α-thujone), while those with the highest contributions to PC 2 were different terpenes (citronellyl acetate, cembrene, *trans*-ferruginol, *cis*-ferruginol, 3-carene) phosphorus, and zinc.

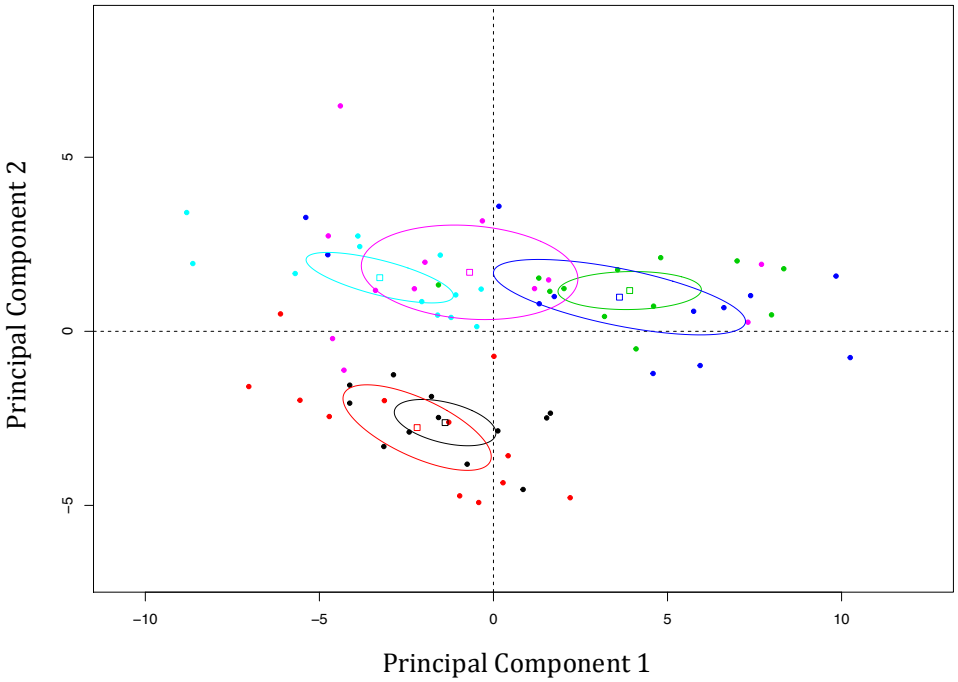

Figure 5.1. Principal components analysis bi-plot (correlation matrix-based) of sixty chemical variables studied in three *Thuja plicata* clonal lines with dissimilar resistances to *Didymascella thujina* (cedar leaf blight, CLB). The three lines were real- (CLB^+) and mock-infected (CLB^-) under controlled conditions, and samples collected just before infection (0 days post inoculation), and 4, 8 and 12 dpi. Samples and centroid ellipses were colour-coded as follows: line 5382 in the CLB^- treatment in black, line 5382 in the CLB^+ treatment in red, line 5412 in the CLB^- treatment in cyan, line 5412 in the CLB^+ treatment in magenta, line 5398 in the CLB^- treatment in green, and line 5398 in the CLB^+ treatment in blue. The confidence level of the ellipses is 95%. Note that lines 5398 and 5412 are closer to each other than to line 5382.

According to the change point analysis of the ranked categorical stability selection scores, there was only one terpene (citronellyl acetate) and two minerals (calcium and zinc) that discriminated between the susceptible line (5382) and the resistant lines

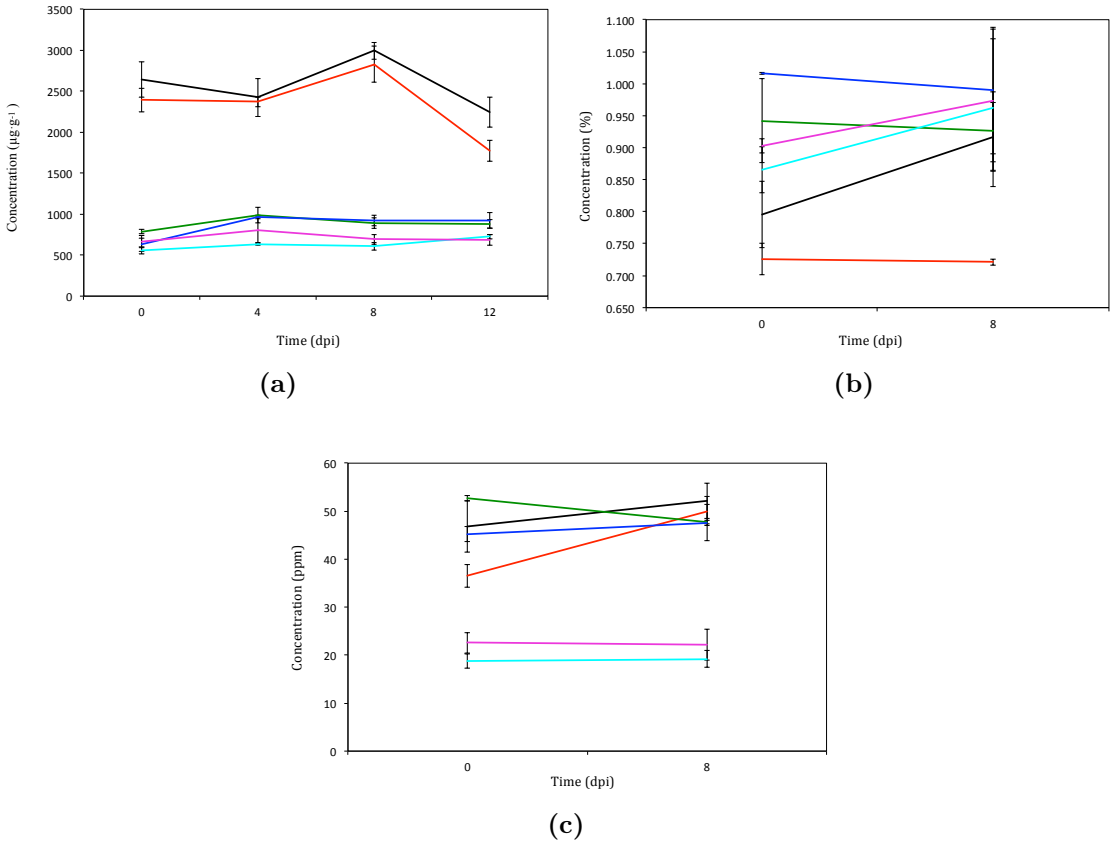

Figure 5.2. Chemical variables that discriminated among *Thuja plicata* clonal lines according to categorical stability selection. Samples were grouped per plant line regardless of the infection condition, and then, the chemical variables were ranked using categorical stability selection (see methods). (a) Citronellyl acetate, (b) calcium, (c) zinc. Treatments were colour-coded as follows: 5382 CLB$^-$ in black, 5382 CLB$^+$ in red, 5412 CLB$^-$ in cyan, 5412 CLB$^+$ in magenta, 5398 CLB$^-$ in green and 5398 CLB$^+$ in blue. Error bars are standard errors.

(5398 and 5412). There were significant differences in the concentration of citronellyl acetate among lines ($p < 0.0000$), with line 5382 having the highest concentration (2,459 $\pm$ 89 µg·g^{-1}), and lines 5398 and 5412 having lower concentrations (874 $\pm$ 30 and 672 $\pm$ 26 µg·g^{-1}, respectively; Fig. 5.2a). Calcium concentration was significantly different among the three clonal lines ($p = 0.0023$, Fig. 5.2b). Line 5382 had the lowest calcium concentration (0.79 $\pm$ 0.03 %), while lines 5398 and 5412 had similar values (0.97 $\pm$ 0.03 % for line 5398, and 0.93 $\pm$ 0.04 % for line 5412). Zinc was significantly lower in line 5412 (20.7 $\pm$ 1.1 ppm; $p < 0.0000$) in relation to the other two lines (46.4 $\pm$ 2.4 ppm for line 5382, and 48.3 $\pm$ 1.3 ppm for line 5398; Fig. 5.2c).

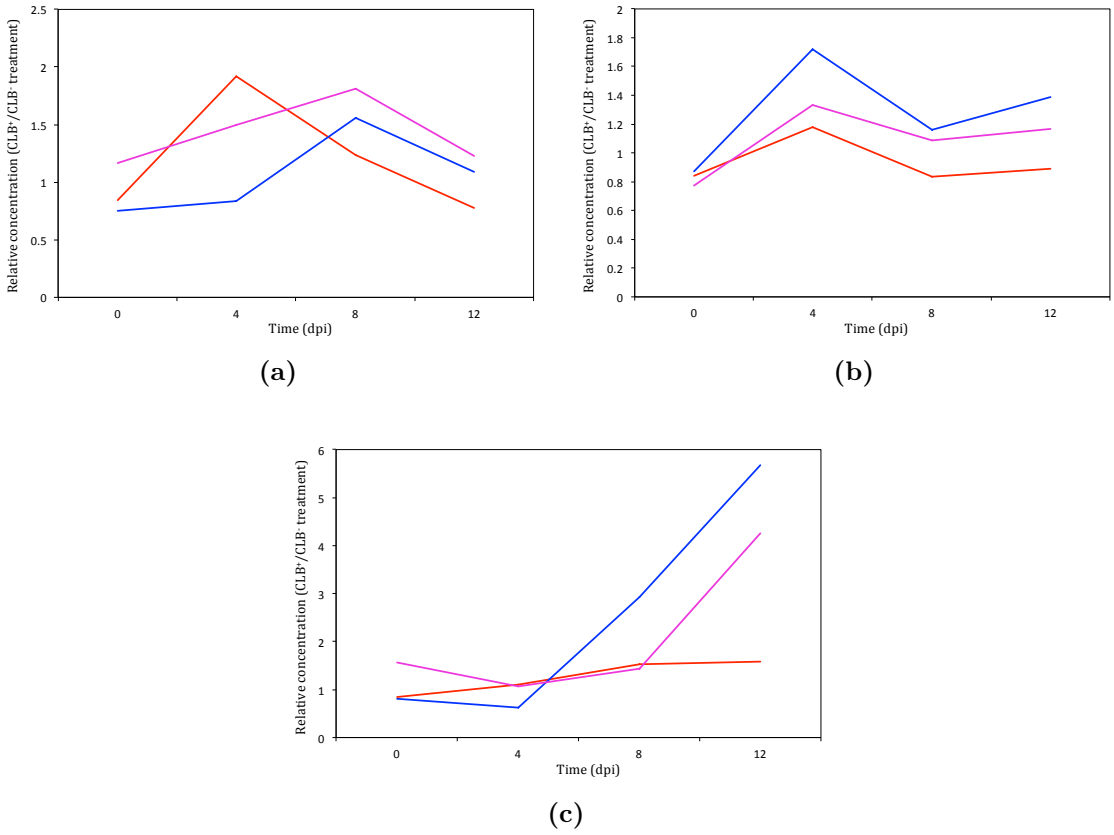

Figure 5.3. Temporal variation in response to *Didymascella thujina* of the relative concentrations of selected *Thuja plicata* terpenes in the real infections normalized against the values in mock infections. Each variable shown was among the top predictors of the infection categories according to the stability selection analysis. Clone lines were colour-coded as follows: 5382 in red, 5412 in magenta, and 5398 in blue. (a) Sandaracopimarinol, (b) *p*-cymene, (c) germacrene-D-4-ol. Concentrations were higher in the real infections if the relative concentration (CLB^+/CLB^-) was >1, and they were higher in the mock infections if that ratio was <1.

Five chemical variables showed temporal variation among lines in the CLB^+ treatments as detected by change point analysis on the ranked stability selection scores. Three of them were the terpenes sandaracopimarinol, *p*-cymene and germacrene-D-4-ol. There were significant differences among lines ($p = 0.0033$), time points ($p < 0.0000$), infection status ($p = 0.0057$), the interaction of infection status × time ($p = 0.0059$), and the interaction among all factors ($p = 0.0422$) for sandaracopimarinol. The levels of that compound in infected plants, relative to uninfected plants, had a steep increase in line 5382 at 4 dpi, followed by an abrupt decline afterwards, while

it increased steadily in lines 5398 and 5412 until 8 dpi, after which levels dropped (Fig. 5.3a). *p*-Cymene levels depicted a similar response to *D. thujina* infection in all lines ($p = 0.1467$ for the interaction line × time), peaking at 4 dpi and again at 12 dpi (Fig. 5.3b). There were differences among lines, however ($p = 0.0089$), with line 5398 having significantly higher levels of this compound (161 ± 10 $\mu g \cdot g^{-1}$) than the other two lines (139 ± 5 $\mu g \cdot g^{-1}$ for line 5412, and 127 ± 5 $\mu g \cdot g^{-1}$ for line 5382). The concentration of germacrene-D-4-ol was significantly different among time points ($p = 0.0033$), and between infection statuses ($p = 0.0171$). Although there were not significant differences among lines ($p = 0.4107$), the steep increase in the concentration of this compound in lines 5398 and 5412 after 8 dpi is notable(Fig. 5.3c).

The two other chemical variables with temporal variation among lines were phosphorus and magnesium. Both elements had significantly lower concentrations at 8 dpi ($p = 0.0269$ and $p = 0.0157$, respectively). The ratio of phosphorus in infected vs. uninfected plants (CLB^+/CLB^-) was significantly different among lines ($p < 0.000$ for all pairs of proportion tests), being lowest in line 5412 (0.867; Appendix A.26). In contrast, that ratio for magnesium was significantly higher in line 5398 (1.090, Appendix A.26; $p < 0.000$ for proportion tests between line 5398 and the other two lines).

5.3.2.2 Gene expression

The reference transcriptome consisted of 339,748 transcripts, with an overall alignment rate of 97.00% (overall alignment rates per sample are presented in Appendixes A.33 and A.34). 64,889 of the transcripts resulted in annotation hits. Among the annotated sequences, 72.55% belonged to plants, 13.42% were annotated as fungal, and 14.03% belonged to other taxa (Appendix A.30 includes additional assembly statistics).

BLASTn searches for the two ITS2 sequences of *D. thujina* in the assembled transcriptome resulted in 12 Trinity genes for KT875766 and 13 Trinity genes for KT875767. Hits for KT875766 had E-values between 5×10^{-33} and 1×10^{-13}, and identity percentages between 87.20% and 97.22%. E-values for the KT875767 hits ranged from 2×10^{-52} to 1×10^{-13} with identities between 88.00% and 97.22%. For both *D. thujina* ITS2 queries, *TRINITY_DN124702_c3_g4_i1* was the hit with the highest identity

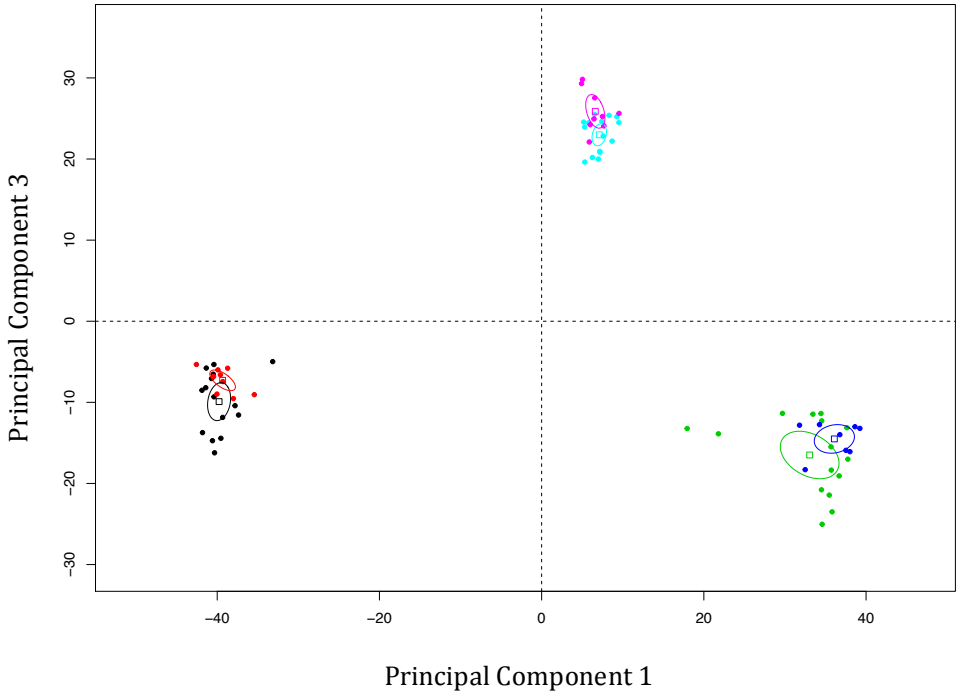

Figure 5.4. Principal component analysis bi-plot (correlation matrix-based) of 9,551 differentially expressed transcripts in three *Thuja plicata* clonal lines. The lines were real- (CLB^+) and mock-infected (CLB^-) with *D. thujina* under controlled conditions. Samples were collected just before infection (0 dpi), and 4, 8 and 12 dpi. The first three components explained 65.29% of the samples' variance (33.84%, 20.05% and 11.40% for components 1, 2 and 3, respectively). The two principal components plotted discriminated among the clonal lines, but component 3 also differentiated between CLB^- and CLB^+ conditions. The confidence level of the ellipses is 95%. Samples and centroid ellipses were colour-coded as follows: 5382 CLB^- in black, 5382 CLB^+ in red, 5412 CLB^- in cyan, 5412 CLB^+ in magenta, 5398 CLB^- in green and 5398 CLB^+ in blue. Note that CLB^- and CLB^+ samples group separately within each clonal line.

value (97.22% in both cases) and low E-value (2×10^{-26} in both instances). No reads from samples in the CLB^- treatments mapped to *TRINITY_DN124702_c3_g4_i1*.

There were 9,551 sequences that were differentially expressed among all samples (2.81% of the assembly), 56.87% of them were annotated as plant sequences, 34.09% had no annotation hits, and 9.04% belonged to other taxa. Principal component analysis of the DE data revealed that the *T. plicata* lines studied were genetically different from each other, and that the infected samples grouped separately from the uninfected within each line (Fig. 5.4). In spite of that, DE data from lines 5398 and 5412 were more closely correlated with each other than with line 5382 (Appendix A.37).

Hierarchical clustering

There were 11 clusters of transcripts with a minimum 4-fold change and maximum 0.001 false discovery rate that were identified after cutting the hierarchical tree at 49% of its height, six clusters accounting for more than 95% of the DE sequences (Fig. 5.5). The biggest cluster had 3,657 sequences and the smallest had just 6 transcripts. 1,216 sequences were at low expression levels in line 5382 but highly expressed in the other two lines (light green cluster in Fig. 5.5). 956 sequences were at high expression levels in line 5382 and at low levels of expression in the other two lines (cyan cluster). 571 transcripts were highly expressed in line 5398 but low in the other two lines (blue cluster), and 388 sequences had low expression in line 5398 and high expression in the other two lines (purple cluster). The green cluster in Fig. 5.5 refers to general responses to *D. thujina* infection, and included 3,657 transcripts with high expression levels in all lines at 0 dpi (in both CLB^- and CLB^+ conditions) but at low expression levels in the CLB^+ treatment. The remaining clusters had more complex expression patterns that were difficult to discern from the heat-map.

Grade of Membership Analysis

Clustering of samples and static topics using the ω matrix revealed that, in general, two topics per clonal line had higher ω values than the rest (Fig. 5.6). Topics 2 and 6 had the highest ω values for line 5382, topics 4 and 12 for line 5412, and topics 1 and 7 for line 5398. Table 5.3 shows the representative 10 transcripts per topic, ranked

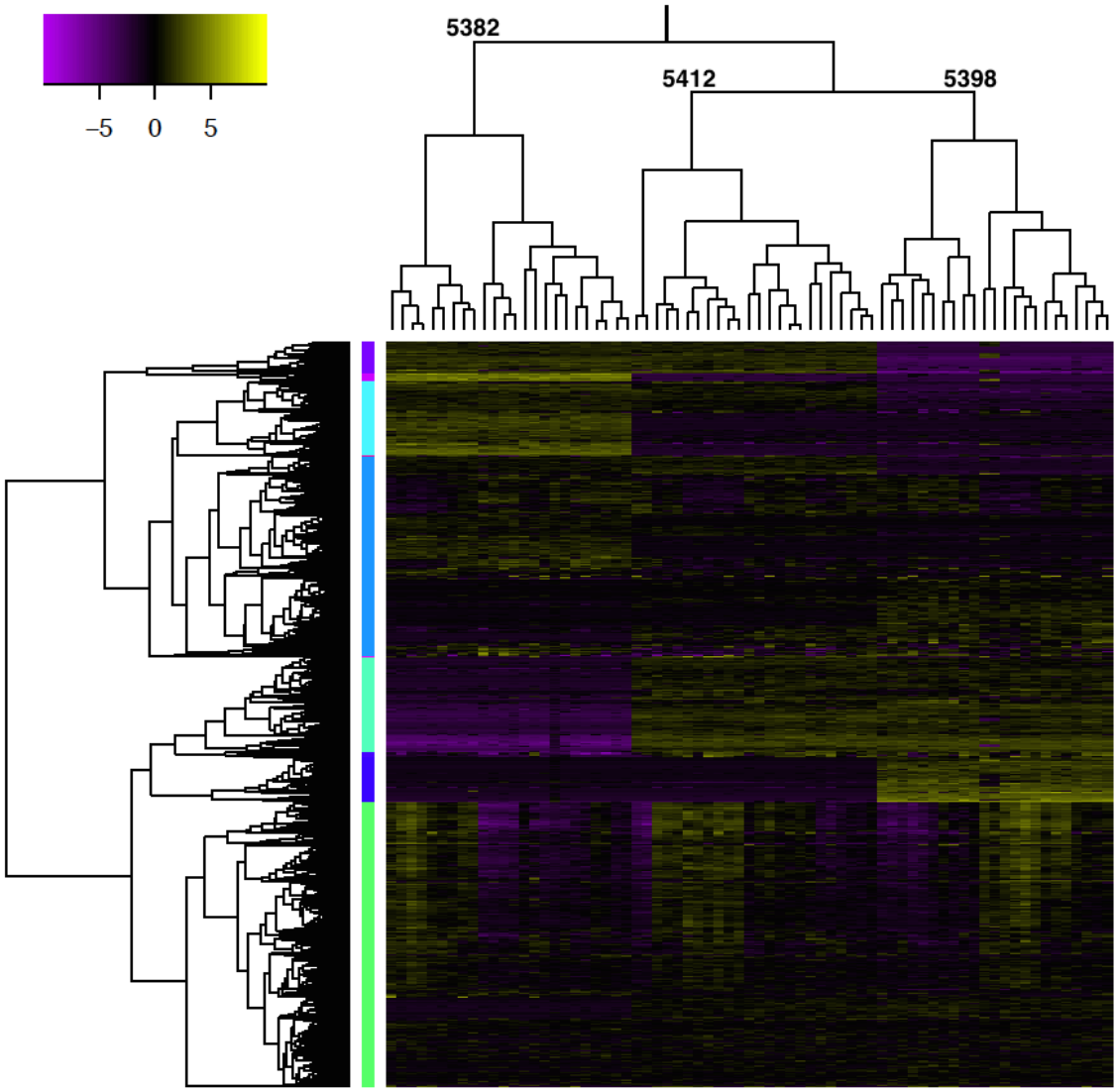

Figure 5.5. Heat map of 9,551 differentially expressed transcripts from three *Thuja plicata* clonal lines with differing resistances to *Didymascella thujina* (cedar leaf blight, CLB). All lines were real- and mock-inoculated in growth chambers, and samples collected at 0, 4, 8 and 12 days post infection. Eleven clusters of transcripts were produced after cutting the tree at 49% of its height. Most of the transcripts were in the following clusters: green (3,657 transcripts), light blue (2,556 transcripts), light green (1,216 transcripts), cyan (956 transcripts), blue (571 transcripts), and purple (388 transcripts). The rest of the clusters accounted for the remaining sequences (2.17% of the total). Expression levels shown are $\log_2$-transformed and centred TPMs calculated by the Trinity pipeline. Labels on the tree's clusters refer to the clonal lines used. Notice how the resistant lines (5398 and 5412) are grouped closer to each other than to the susceptible line (5382, see also section 5.3.2). Expression values were colour-coded according to the top left bar (purple = low expression, yellow = high expression).

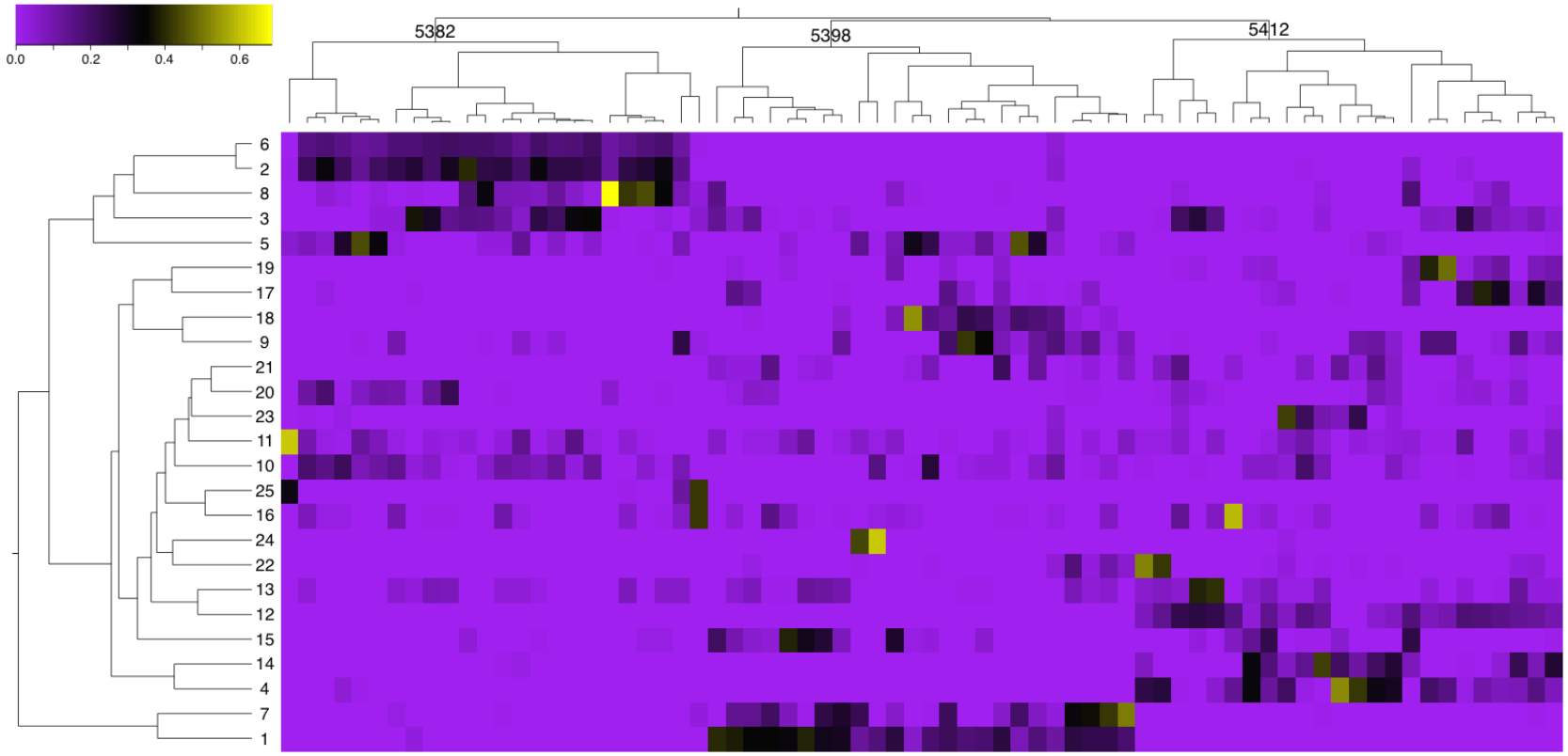

Figure 5.6. Heat-map of samples versus static topics used in the grade of membership (GoM) analysis. GoM is a dimension reduction technique based on the latent Dirichlet allocation method that, in this case, groups transcripts based on their co-occurrences. Each of the 25 topics is a probability distribution over the 9,551 differentially expressed transcripts (θ matrix in *CountClust*), and each of the 72 samples is a probability distribution over the 25 topics (ω matrix in *CountClust*). The ω matrix was used as input to generate the above map using hierarchical clustering with Euclidean distance (the higher the ω value, the more important the topic is in a respective sample). Samples from each clonal line in this study clustered "monophyletically" (top tree). The vertical tree on the left shows the topics. Notice that topics 1 and 7 had higher ω values in line 5398, topics 4 and 12 in line 5412, and topics 2 and 6 in line 5382. Omega values were colour-coded according to the top left bar (yellow = high, purple = low).

according to their decreasing θ values.

Inspection of the top transcripts within each of the aforementioned topics (Table 5.3) revealed that the protein translation factor SUI1 homolog 1 (transcripts *TRINITY_DN110415_c1_g1_i1* and *TRINITY_DN110415_c1_g1_i2*) and the catalase-3 (sequence *TRINITY_DN115787_c0_g2_i1*, Appendix A.39) were present in five of the six topics that were most strongly identified with the three *T. plicata* lines (Table 5.3). The uncharacterized protein ORF91 (transcript *TRINITY_DN121192_c6_g1-0_i1*), the sedoheptulose-1,7-bisphosphatase (sequences *TRINITY_DN76933_c0_g-4_i1* and *TRINITY_DN76933_c0_g5_i1*), and the probable mediator of *RNA* polymerase II transcription subunit 37c (transcripts *TRINITY_DN121468_c0_g2_i1* and *TRINITY_DN121468_c0_g1_i1*) were also present in all lines, but had high θ values only in one topic per line. The only ethylene-responsive transcription factor, RAP2-4 (sequence *TRINITY_DN4933_c0_g3_i1*, Appendix A.40), was present in the susceptible line (topic 6 in line 5382). Bark storage proteins A (transcripts *TRINITY_DN123991_c13_g1_i1*, *TRINITY_DN123991_c13_g1_i2*, *TRINITY_DN123991_c13_g2_i1* and *TRINITY_DN129016_c13_g2_i1*; Figs. 5.7a-5.7d) were present only in the resistant lines, 5398 and 5412 (topics 1, 4, 7 and 12), as were dehydrin Xero 1 (sequence *TRINITY_DN119739_c4_g1_i4* in topics 4 and 7) and glyceraldehyde-3-phosphate dehydrogenase B (transcript *TRINITY_DN122568_c0_g1_i3* in topics 1 and 12, Appendix A.41). It is worth noticing that transcripts shared between/among clonal lines had similar expression levels in the lines involved (e.g. sequence *TRINITY_DN115787_c0_g2_i1*, Appendix A.39), while sequences that were present only in one of the lines, had higher levels of expression in the respective line in relation to the others (e.g. transcript *TRINITY_DN122568_c0_g1_i3*, Appendix A.41).

Stability Selection Analysis

Change point analysis on the ranked stability selection scores showed that 53 transcripts were the best predictors of *D. thujina* infection (Table 5.4). Twenty-six of those sequences had cellular component annotations, 16 of them being to membranes, the extracellular region or the apoplast. Six sequences were related to defense responses (*TRINITY_DN110577_c1_g1_i3*, *TRINITY_DN126040_c5_g1_i6*, *TRINITY_DN120721_c4_g1_i1*, *TRINITY_DN129144_c3_g2_i2*, *TRINITY_DN127515_c7_g-*

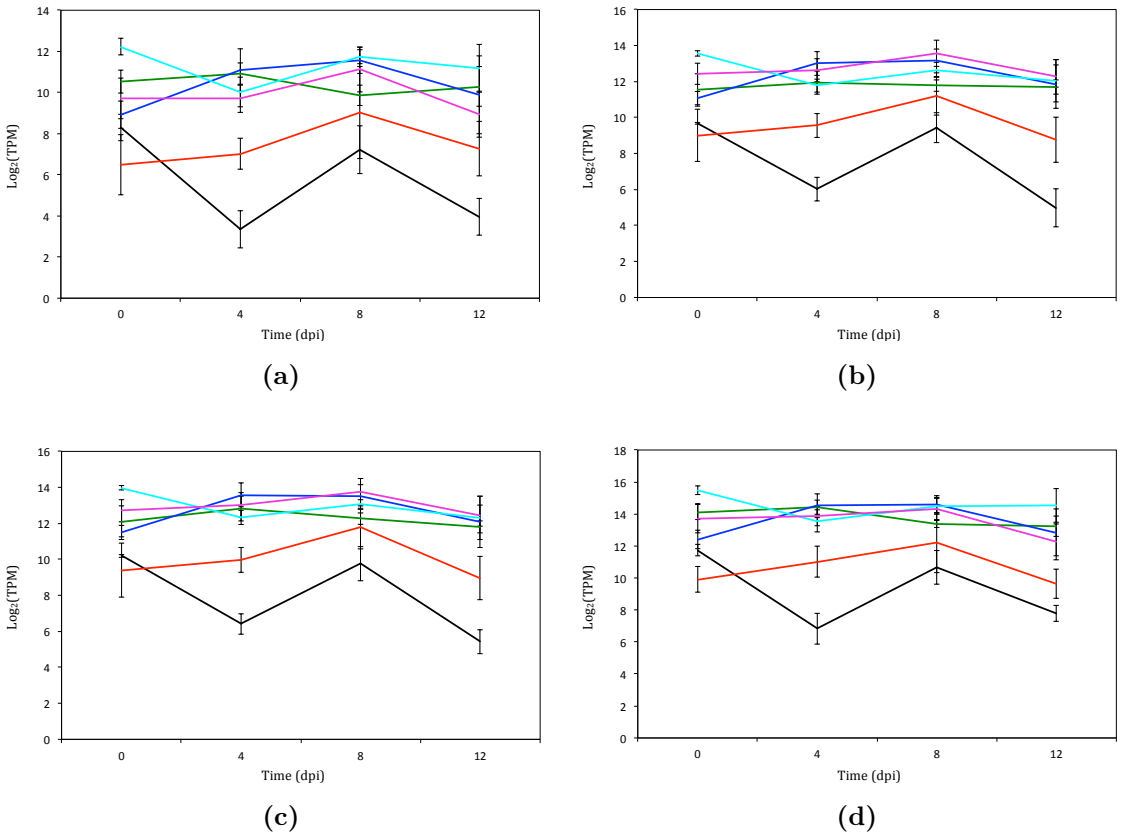

Figure 5.7. Expression levels of transcripts of the bark storage protein A from the *Thuja plicata* lines used in this investigation. Three *T. plicata* clonal lines (5382, 5398 and 5412) were real (+) and mock (-) infected with *Didymascella thujina* (cedar leaf blight, CLB) under controlled conditions, and foliar samples taken 0, 4, 8 and 12 days post infection (dpi). The samples were processed for gene expression using the Illumina HiSeq 2000 paired-end technology. Only four sequences annotated as bark storage protein A were shared among the top 10 sequences of topics 1, 4, 7 and 12 (see Table 5.3): (a) *TRINITY_DN123991_c13_g1_i1*, (b) *TRINITY_DN123991_c13_g1_i2*, (c) *TRINITY_DN123991_c13_g2_i1*, (d) *TRINITY_DN129016_c13_g2_i1*. Treatments were colour coded as follows: 5382 CLB^- in black, 5382 CLB^+ in red, 5412 CLB^- in cyan, 5412 CLB^+ in magenta, 5398 CLB^- in green and 5398 CLB^+ in blue. Notice that expression levels of the bark storage protein A's were lower in the susceptible line 5382 in comparison to the other two lines.

Table 5.3. Top ten transcripts of the representative static topics per clonal line in Fig. 5.6. Theta values refer to the latent Dirichlet allocation distribution of the 25 topics modelled over the 9,551 differentially expressed Trinity transcripts. The higher the θ value of a sequence, the more important it is in a respective topic. Transcripts per topic shown were ranked in a descending order according to those probabilities. All annotations are based on BLASTX searches done on the Swiss-Prot database. Annotations with asterisk were based on BLASTP searches on the same database.

Clone line	Topic	Transcript	θ	E-value	Organism	Annotation	Process	Cellular component
5382	2	*TRINITY_DN122791_c1_g1_i1*	0.09509	0	*Lycopersicon* sp.	Linoleate 9S-lipoxygenase A	Oxylipin biosynthetic process	Cytoplasm
		TRINITY_DN110415_c1_g1_i1	0.03840	2.0×10^{-47}	*Arabidopsis* sp.	Protein translation factor SUI1 homolog 1	Translation initiation factor activity	
		TRINITY_DN121921_c0_g1_i3	0.02579	5.0×10^{-149}	*Arabidopsis* sp.	Probable xyloglucan endotransglucosylase/hydrolase protein 7	Cell wall organization	Cell wall
		TRINITY_DN32788_c0_g2_i1	0.02071	0	*Phaseolus* sp.	Vacuolar-processing enzyme	Cysteine-type peptidase activity	
		TRINITY_DN160191_c0_g1_i1	0.02020	5.0×10^{-07}	*Picea* sp.	Metallothionein-like protein EMB30	Metal ion binding	
		TRINITY_DN115787_c0_g2_i1	0.01951	0	*Glycine* sp.	Catalase-3	Response to hydrogen peroxide	Cytoplasm
		TRINITY_DN121192_c6_g10_i1	0.01310	5.0×10^{-50}	*Phalaenopsis* sp.	Uncharacterized protein ORF91		Chloroplast
		TRINITY_DN43781_c0_g1_i1	0.00908	2.0×10^{-116}	*Oryza* sp.	Thioredoxin-like protein CDSP32		Chloroplast
		TRINITY_DN96674_c0_g1_i1	0.00900	0	*Antirrhinum* sp.	Granule-bound starch synthase 1	Starch biosynthetic process	Chloroplast, amyloplast
		TRINITY_DN69800_c0_g1_i1	0.00889	3.0×10^{-88}	*Nepenthes* sp.	Aspartic proteinase nepenthesin-2	Aspartic-type endopeptidase activity	Extracellular region
	6	*TRINITY_DN110415_c1_g1_i2*	0.07515	2.0×10^{-47}	*Arabidopsis* sp.	Protein translation factor SUI1 homolog 1	Translation initiation factor activity	
		TRINITY_DN46638_c0_g3_i1	0.01915	0	*Arabidopsis* sp.	Beta-amylase 1	Starch catabolic process	Chloroplast, cytosol, nucleous
		TRINITY_DN4933_c0_g3_i1	0.01774	2.0×10^{-32}	*Arabidopsis* sp.	Ethylene-responsive transcription factor RAP2-4	Ethylene-activated signaling pathway	Nucleus
		TRINITY_DN51305_c0_g1_i1	0.01344	NA	No hits	No hits		
		TRINITY_DN76933_c0_g4_i1	0.01102	0	*Triticum* sp.	Sedoheptulose-1,7-bisphosphatase	Reductive pentose-phosphate cycle	Chloroplast
		TRINITY_DN126209_c0_g1_i2	0.01081	1.0×10^{-166}	*Arabidopsis* sp.	Pectin acetylesterase 8	Cell wall organization	Cell wall, extracellular region
		TRINITY_DN121468_c0_g1_i1	0.01055	1.0×10^{-172}	*Arabidopsis* sp.	Probable mediator of *RNA* polymerase II transcription subunit 37c		
		TRINITY_DN124815_c24_g1_i1	0.00934	3.0×10^{-163}	*Lycopersicon* sp.	Chlorophyll a-b binding protein 1B	Protein-chromophore linkage	Chloroplast
		TRINITY_DN34147_c0_g2_i1	0.00753	9.0×10^{-99}	*Arabidopsis* sp.	Ubiquitin-conjugating enzyme E2 35	Protein ubiquitination	Cytoplasm, nucleus
		TRINITY_DN66528_c0_g2_i1	0.00708	3.0×10^{-27}	*Arabidopsis* sp.	MLP-like protein 423	Defense response	Membrane
5412	4	*TRINITY_DN129016_c13_g2_i1*	0.30615	2.0×10^{-42}	*Populus* sp.	Bark storage protein A	Nucleoside metabolic process	
		TRINITY_DN123991_c13_g2_i1	0.12068	8.0×10^{-23}	*Populus* sp.	Bark storage protein A	Nucleoside metabolic process	
		TRINITY_DN110415_c1_g1_i1	0.02835	2.0×10^{-47}	*Arabidopsis* sp.	Protein translation factor SUI1 homolog 1	Translation initiation factor activity	
		TRINITY_DN123991_c13_g1_i2	0.02552	3.0×10^{-11}	*Populus* sp.	Bark storage protein A	Nucleoside metabolic process	
		TRINITY_DN129016_c13_g1_i1	0.02435	NA	No hits	No hits		
		TRINITY_DN115787_c0_g2_i1	0.01581	0	*Glycine* sp.	Catalase-3	Response to hydrogen peroxide	Cytoplasm
		TRINITY_DN11246_c0_g1_i1	0.01452	NA	No hits	No hits		
		TRINITY_DN123991_c13_g1_i1	0.01053	4.0×10^{-09}	*Populus* sp.	Bark storage protein A	Nucleoside metabolic process	
		TRINITY_DN121192_c6_g10_i1	0.01035	5.0×10^{-50}	*Phalaenopsis* sp.	Uncharacterized protein ORF91		Chloroplast
		TRINITY_DN119739_c4_g1_i4	0.00960	9.0×10^{-08}	*Arabidopsis* sp.	Dehydrin Xero 1*	Response to stress	Cytosol
	12	*TRINITY_DN110415_c1_g1_i1*	0.08396	2.0×10^{-47}	*Arabidopsis* sp.	Protein translation factor SUI1 homolog 1	Translation initiation factor activity	
		TRINITY_DN123991_c13_g2_i1	0.02319	8.0×10^{-23}	*Populus* sp.	Bark storage protein A	Nucleoside metabolic process	
		TRINITY_DN121468_c0_g2_i1	0.01769	1.0×10^{-172}	*Arabidopsis* sp.	Probable mediator of *RNA* polymerase II transcription subunit 37c	ATP binding	
		TRINITY_DN76933_c0_g5_i1	0.01666	0	*Triticum* sp.	Sedoheptulose-1,7-bisphosphatase	Sedoheptulose-bisphosphatase activity	Chloroplast
		TRINITY_DN122568_c0_g1_i3	0.01415	0	*Pisum* sp.	Glyceraldehyde-3-phosphate dehydrogenase B	Reductive pentose-phosphate cycle	Chloroplast
		TRINITY_DN91372_c0_g1_i2	0.01355	6.0×10^{-91}	*Manihot* sp.	Eukaryotic translation initiation factor 5A	Translation initiation factor activity	
		TRINITY_DN152671_c0_g1_i1	0.01277	0	*Arabidopsis* sp.	Subtilisin-like protease SBT1.5	Organ senescence	Apoplast, cell wall, vacuole
		TRINITY_DN115787_c0_g2_i1	0.01231	0	*Glycine* sp.	Catalase-3	Response to hydrogen peroxide	Cytoplasm
		TRINITY_DN111785_c0_g1_i2	0.01116	7.0×10^{-165}	*Arabidopsis* sp.	Cadmium/zinc-transporting ATPase HMA2	Cadmium ion transmembrane transporter activity	Integral component of plasma membrane
		TRINITY_DN51305_c0_g2_i1	0.00875	NA	No hits	No hits		
5398	1	*TRINITY_DN110415_c1_g1_i2*	0.12082	2.0×10^{-47}	*Arabidopsis* sp.	Protein translation factor SUI1 homolog 1	Translation initiation factor activity	
		TRINITY_DN122791_c1_g1_i1	0.09527	0	*Lycopersicon* sp.	Linoleate 9S-lipoxygenase A	Oxylipin biosynthetic process	Cytoplasm
		TRINITY_DN115787_c0_g2_i1	0.02513	0	*Glycine* sp.	Catalase-3	Response to hydrogen peroxide	Cytoplasm
		TRINITY_DN123991_c13_g2_i1	0.01874	8.0×10^{-23}	*Populus* sp.	Bark storage protein A	Nucleoside metabolic process	
		TRINITY_DN129016_c13_g2_i1	0.01832	2.0×10^{-42}	*Populus* sp.	Bark storage protein A	Nucleoside metabolic process	
		TRINITY_DN121192_c6_g10_i1	0.01359	5.0×10^{-50}	*Phalaenopsis* sp.	Uncharacterized protein ORF91		Chloroplast
		TRINITY_DN76933_c0_g4_i1	0.01273	0	*Triticum* sp.	Sedoheptulose-1,7-bisphosphatase	Reductive pentose-phosphate cycle	Chloroplast
		TRINITY_DN121468_c0_g1_i1	0.01244	1.0×10^{-172}	*Arabidopsis* sp.	Probable mediator of *RNA* polymerase II transcription subunit 37c		
		TRINITY_DN122568_c0_g1_i3	0.01122	0	*Pisum* sp.	Glyceraldehyde-3-phosphate dehydrogenase B	Reductive pentose-phosphate cycle	Chloroplast
		TRINITY_DN124815_c24_g1_i4	0.00889	3.0×10^{-161}	*Nicotiana* sp.	Chlorophyll a-b binding protein 21	Protein-chromophore linkage	Chloroplast
	7	*TRINITY_DN129016_c13_g2_i1*	0.25766	2.0×10^{-42}	*Populus* sp.	Bark storage protein A	Nucleoside metabolic process	
		TRINITY_DN123991_c13_g2_i1	0.11391	8.0×10^{-23}	*Populus* sp.	Bark storage protein A	Nucleoside metabolic process	
		TRINITY_DN129016_c13_g1_i1	0.02702	NA	No hits	No hits		
		TRINITY_DN123991_c13_g1_i2	0.02627	3.0×10^{-11}	*Populus* sp.	Bark storage protein A	Nucleoside metabolic process	
		TRINITY_DN119739_c4_g1_i4	0.01520	9.0×10^{-08}	*Arabidopsis* sp.	Dehydrin Xero 1*	Response to stress	Cytosol
		TRINITY_DN40205_c0_g1_i1	0.01453	NA	No hits	No hits		
		TRINITY_DN162113_c1_g1_i1	0.01435	3.0×10^{-07}	*Musa* sp.	Metallothionein-like protein type 3	Metal ion binding	
		TRINITY_DN11246_c0_g1_i1	0.01419	NA	No hits	No hits		
		TRINITY_DN118395_c0_g3_i1	0.01357	NA	No hits	No hits		
		TRINITY_DN115787_c0_g2_i1	0.01290	0	*Glycine* sp.	Catalase-3	Response to hydrogen peroxide	Cytoplasm

1_i4 and *TRINITY_DN124485_c8_g1_i1*). One WRKY transcription factor SUSIBA2 with higher expression levels in infected plants was detected (*TRINITY_DN111124_c0_g1_i1*), as well as a dirigent protein 1 (*TRINITY_DN128247_c1_g2_i1*) that had higher levels of expression in infected plants of lines 5382 and 5412. There were also three leucine-rich repeat receptor-like proteins (*TRINITY_DN129144_c3_g2_i2*, *TRINITY_DN122065_c0_g1_i1* and *TRINITY_DN127477_c1_g1_i4*) whose expression levels were similar in all lines.

Some of the sequences resulting from this analysis were at higher expression levels in the resistant lines (5398 and 5412) regardless of their infection status. Those transcripts included the cell wall-associated receptor kinase 2 (*TRINITY_DN126460_c1_g5_i4*), the protein SRG1 (*TRINITY_DN129699_c0_g1_i3*, related to organ senescence), the senescence-associated carboxylesterase 101 (*TRINITY_DN127515_c7_g1_i4*), and the only two cytochromes P450 750A1 detected by stability selection (*TRINITY_DN109363_c2_g1_i1*, Fig. 5.8a; and *TRINITY_DN69100_c0_g2_i1*, Fig. 5.8b). Infected plants of lines 5398 and 5412 had higher expression levels of the only cysteine-rich receptor-like protein kinase detected by this analysis (*TRINITY_DN124485_c8_g1_i1*, Fig. 5.8c). Two of the transcripts in table 5.4 were not expressed at all in the susceptible line 5382: the EMSY-LIKE 3 sequence (*TRINITY_DN126040_c5_g1_i6*, related to basal defense to fungus; Fig. 5.9a), and a DMR6-like oxygenase 2 (*TRINITY_DN129734_c10_g1_i2*, involved in the salicylic acid pathway; Fig. 5.9b). There was a second DMR6-like oxygenase 2 (*TRINITY_DN115727_c5_g1_i1*; Table 5.4), whose expression levels were lower in line 5382 in comparison to lines 5398 and 5412 (Fig. 5.9c).

The stability selection analysis also detected transcripts that were at higher levels of expression in line 5382 in comparison to the other lines studied, like the TMV resistance protein N (*TRINITY_DN131892_c1_g1_i4*), and two sequences related to nitrate transport (*TRINITY_DN117397_c1_g1_i2*, Fig. 5.9d; and *TRINITY_DN117397_c3_g1_i1* Fig. 5.9e). Interestingly, the only pathogenesis-related protein among the top predictors of *D. thujina* infection (transcript *TRINITY_DN110577_c1_g1_i3* in Table 5.4) was expressed exclusively in the susceptible line 5382 (Fig. 5.9f).

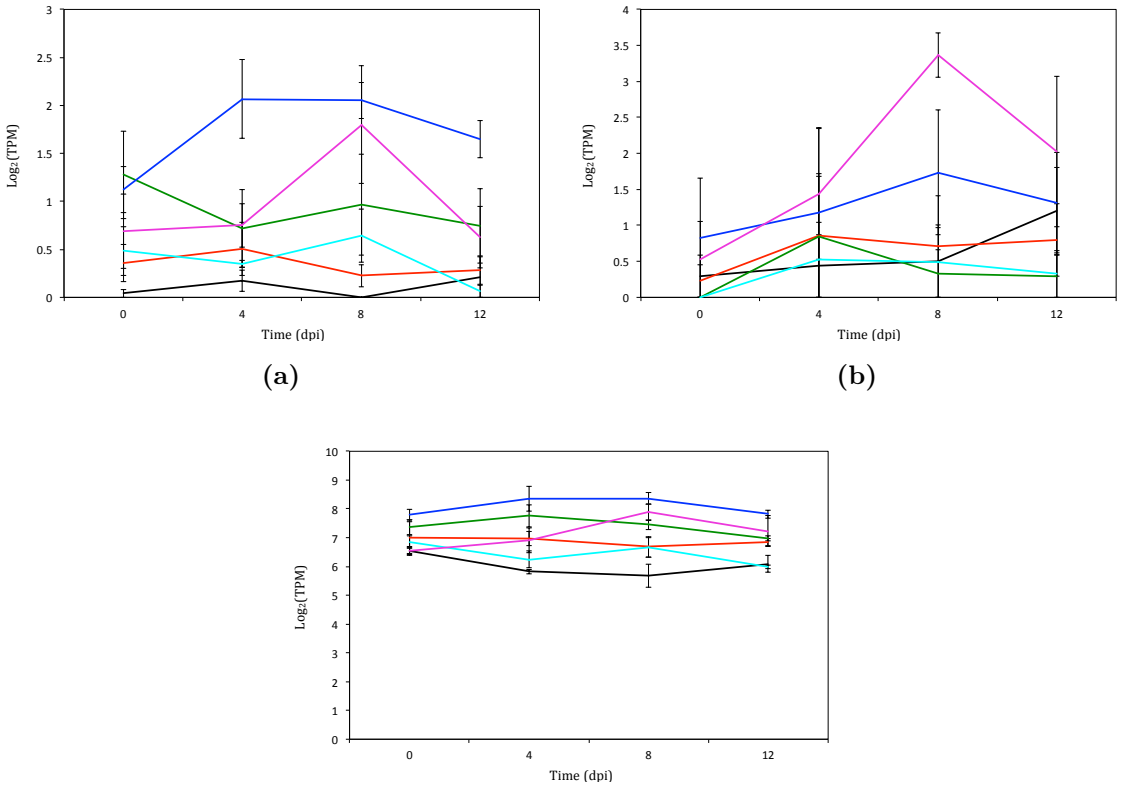

Figure 5.8. Selected predictors (transcripts) of *Didymascella thujina* infection according to the categorical stability selection analysis (see also Table 5.4). (a-b) Cytochrome P450 750A1 (*TRINITY_DN109363_c2_g1_i1* and *TRINITY_DN69100_c0_g2_i1*, respectively), (c) cysteine-rich receptor-like protein kinase 2 (*TRINITY_DN124485_c8_g1_i1*). Treatments were colour-coded as follows: 5382 CLB^- in black, 5382 CLB^+ in red, 5398 CLB^- in green, 5398 CLB^+ in blue, 5412 CLB^- in cyan, 5412 CLB^+ in magenta. Error bars are standard errors.

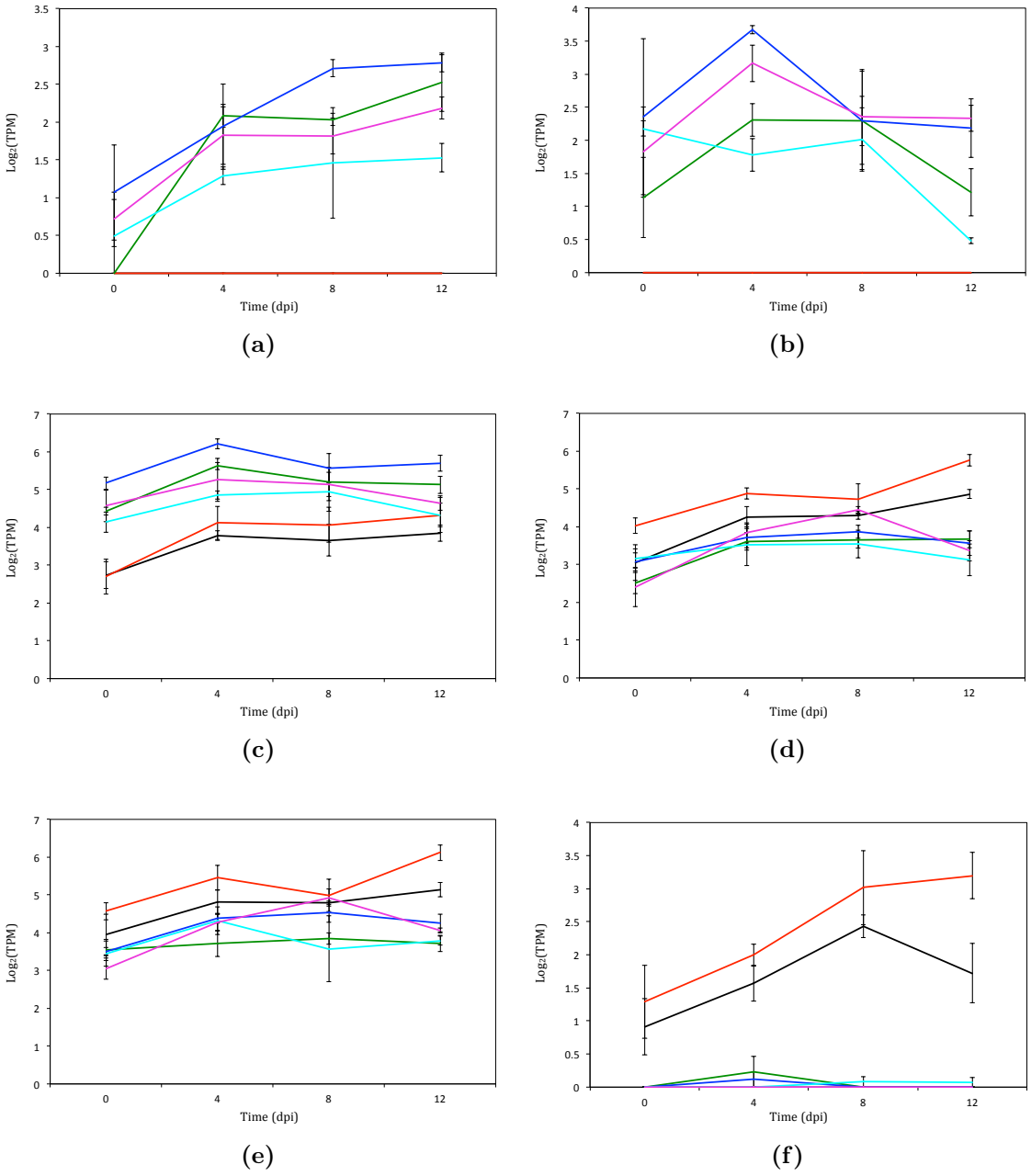

Figure 5.9. Selected predictors (transcripts) of *Didymascella thujina* infection according to the categorical stability selection analysis (see also Table 5.4). (a) EMSY-LIKE 3 (*TRINITY_DN126040_c5_g1_i6*), (b-c) DMR6-like oxygenase 2 (*TRINITY_DN129734_c10_g1_i2* and *TRINITY_DN115727_c5_g1_i1*, respectively), (d) protein NRT1/PTR family 2.13 (*TRINITY_DN117397_c1_g1_i2*), (e) protein NRT1/PTR family 3.1 (*TRINITY_DN117397_c3_g1_i1*), (f) pathogenesis-related protein (*TRINITY_DN110577_c1_g1_i3*). Treatments were colour-coded as follows: 5382 CLB^- in black, 5382 CLB^+ in red, 5398 CLB^- in green, 5398 CLB^+ in blue, 5412 CLB^- in cyan, 5412 CLB^+ in magenta. Error bars are standard errors.

Table 5.4. Top 53 predictors (transcripts) of *Didymascella thujina* infection according to the change point analysis on the ranked scores of the categorical stability selection analysis. The dynamic topic to which the transcripts ranked first is included (based on the top $\beta_{0,k}$) All annotations are based on BLASTX searches done on the Swiss-Prot database. Annotations with asterisk were based on BLASTP searches on the same database.

Transcript	Stability selection (score)	E-value	Organism	Annotation	Process	Cellular component	Dynamic topic per transcript (based on $\beta_{0,k}$)
TRINITY_DN129699_c0_g1_i3	0.3855	7.0×10^{-22}	*Arabidopsis* sp.	Protein SRG1	Organ senescence		23
TRINITY_DN127886_c4_g2_i3	0.3850	6.0×10^{-48}	*Arabidopsis* sp.	AAA-ATPase At3g28610	Response to salt stress		4
TRINITY_DN129672_c0_g1_i1	0.3811	1.0×10^{-159}	*Arabidopsis* sp.	Cytochrome P450 94B3	Jasmonic acid metabolic process	Integral component of membrane	8
TRINITY_DN126547_c4_g2_i1	0.3614	NA	No hits	No hits			23
TRINITY_DN129886_c8_g1_i1	0.3599	9.0×10^{-108}	*Cucurbita* sp.	Nitrate reductase [NADH]	Nitrate assimilation		21
TRINITY_DN103802_c0_g2_i1	0.3255	3.0×10^{-19}	*Triticum* sp.	Histone H1	Nucleosome assembly	Nucleus	22
TRINITY_DN119108_c1_g4_i2	0.3180	4.0×10^{-148}	*Arachis* sp.	Cationic peroxidase 1	Response to oxidative stress	Extracellular region	4
TRINITY_DN126629_c4_g2_i2	0.2941	NA	No hits	No hits			1
TRINITY_DN120561_c0_g1_i2	0.2880	9.0×10^{-47}	*Arabidopsis* sp.	Linoleate 9S-lipoxygenase 5	Oxylipin biosynthetic process	Chloroplast	4
TRINITY_DN126460_c1_g5_i4	0.2714	2.0×10^{-119}	*Arabidopsis* sp.	Wall-associated receptor kinase 2	Calcium ion binding	Integral component of membrane	4
TRINITY_DN109363_c2_g1_i1	0.2584	1.0×10^{-78}	*Pinus* sp.	Cytochrome P450 750A1		Integral component of membrane	4
TRINITY_DN113243_c1_g1_i1	0.2548	NA	No hits	No hits			1
TRINITY_DN48638_c0_g2_i1	0.2524	0	*Arabidopsis* sp.	Methionine gamma-lyase	Methionine catabolic process via 2-oxobutanoate	Cytosol	23
TRINITY_DN127937_c3_g1_i1	0.2372	1.0×10^{-36}	*Arabidopsis* sp.	Galactinol synthase 1	Response to oxidative stress	Cytoplasm	8
TRINITY_DN129734_c10_g1_i2	0.2361	4.0×10^{-34}	*Arabidopsis* sp.	Protein DMR6-LIKE OXYGENASE 2			9
TRINITY_DN110577_c1_g1_i3	0.2292	2.0×10^{-18}	*Juniperus* sp.	Pathogenesis-related protein	Defense response		1
TRINITY_DN121476_c3_g1_i2	0.2164	NA	No hits	No hits			9
TRINITY_DN124607_c2_g1_i3	0.2162	4.0×10^{-85}	*Oryza* sp.	Protein IN2-1 homolog B	Protein glutathionylation	Cytoplasm	8
TRINITY_DN111124_c0_g1_i1	0.2116	1.0×10^{-98}	*Hordeum* sp.	WRKY transcription factor SUSIBA2	Regulation of transcription, *DNA*-templated	Nucleus	14
TRINITY_DN117397_c1_g1_i2	0.2086	2.0×10^{-42}	*Arabidopsis* sp.	Protein NRT1/ PTR FAMILY 2.13	Nitrate transport	Plasma membrane	7
TRINITY_DN131169_c10_g1_i1	0.2009	NA	No hits	No hits			9
TRINITY_DN128247_c0_g1_i1	0.1960	NA	No hits	No hits			23
TRINITY_DN121492_c0_g2_i1	0.1813	NA	No hits	No hits			4
TRINITY_DN117397_c3_g1_i1	0.1774	7.0×10^{-51}	*Arabidopsis* sp.	Protein NRT1/ PTR FAMILY 3.1	Nitrate assimilation	Integral component of membrane	7
TRINITY_DN125323_c2_g1_i10	0.1758	2.0×10^{-83}	*Vigna* sp.	Alpha-amylase	Carbohydrate metabolic process		1
TRINITY_DN126040_c5_g1_i6	0.1751	1.0×10^{-7}	*Arabidopsis* sp.	EMSY-LIKE 3*	Defense response to fungus	Nucleus	9
TRINITY_DN120721_c4_g1_i1	0.1681	2.0×10^{-157}	*Arabidopsis* sp.	MLO-like protein 6	Defense response to fungus	Plasma membrane	23
TRINITY_DN121462_c2_g1_i1	0.1673	NA	No hits	No hits			1
TRINITY_DN128103_c1_g1_i2	0.1647	NA	No hits	No hits			23
TRINITY_DN129144_c3_g2_i2	0.1640	5.0×10^{-118}	*Arabidopsis* sp.	Inactive LRR receptor-like serine/threonine-protein kinase BIR2	Regulation of defense response to fungus	Plasma membrane	1
TRINITY_DN127515_c7_g1_i4	0.1597	1.0×10^{-10}	*Arabidopsis* sp.	Senescence-associated carboxylesterase 101	Defense response	Cytoplasm, nucleus	9
TRINITY_DN106749_c1_g1_i1	0.1486	NA	No hits	No hits			14
TRINITY_DN128247_c1_g2_i1	0.1412	2.0×10^{-13}	*Arabidopsis* sp.	Dirigent protein 1		Apoplast	23
TRINITY_DN109893_c0_g2_i1	0.1411	NA	No hits	No hits			8
TRINITY_DN164157_c0_g1_i1	0.1393	2.0×10^{-135}	*Vitis* sp.	Peroxidase 4	Response to oxidative stress	Extracellular region	2
TRINITY_DN122065_c0_g1_i1	0.1358	7.0×10^{-44}	*Zea* sp.	Leucine-rich repeat receptor-like protein FASCIATED EAR2	Cell differentiation	Integral component of membrane	7
TRINITY_DN122749_c1_g1_i2	0.1356	8.0×10^{-46}	*Glycine* sp.	Histone H4	Nucleosome assembly	Nucleus	14
TRINITY_DN166031_c0_g1_i1	0.1327	NA	No hits	No hits			1
TRINITY_DN107782_c0_g1_i1	0.1258	NA	No hits	No hits			1
TRINITY_DN64258_c0_g2_i1	0.1251	0	*Arabidopsis* sp.	Heat shock 70 kDa protein 8	Response to hydrogen peroxide		8
TRINITY_DN127922_c3_g1_i1	0.1241	NA	No hits	No hits	Protein binding		1
TRINITY_DN69100_c0_g2_i1	0.1235	1.0×10^{-40}	*Pinus* sp.	Cytochrome P450 750A1		Integral component of membrane	23
TRINITY_DN124485_c8_g1_i1	0.1221	8.0×10^{-122}	*Arabidopsis* sp.	Cysteine-rich receptor-like protein kinase 2	Defense response	Plasma membrane, plasmodesma	4
TRINITY_DN129817_c2_g1_i6	0.1221	NA	No hits	No hits			20
TRINITY_DN127477_c1_g1_i4	0.1197	2.0×10^{-46}	*Arabidopsis* sp.	Leucine-rich repeat receptor-like protein kinase PXL2	Cell differentiation	Integral component of membrane	4
TRINITY_DN122629_c0_g1_i3	0.1158	NA	No hits	No hits			23
TRINITY_DN100265_c0_g1_i1	0.1140	4.0×10^{-31}	*Arabidopsis* sp.	Phytolongin Phyl1.1	Protein transport	Plasma membrane	8
TRINITY_DN131892_c1_g1_i4	0.1113	8.0×10^{-11}	*Nicotiana* sp.	TMV resistance protein N			1
TRINITY_DN115727_c5_g1_i1	0.1089	3.0×10^{-6}	*Arabidopsis* sp.	Protein DMR6-LIKE OXYGENASE 2			4
TRINITY_DN102278_c0_g2_i1	0.1072	5.0×10^{-32}	*Oryza* sp.	Peroxisomal membrane protein 11-5	Peroxisome fission	Peroxisomal membrane	1
TRINITY_DN147093_c0_g1_i1	0.1058	NA	No hits	No hits			21
TRINITY_DN131098_c6_g2_i3	0.1019	NA	No hits	No hits			23
TRINITY_DN131803_c1_g1_i1	0.1007	2.0×10^{-20}	*Arabidopsis* sp.	Ankyrin repeat-containing protein At3g12360	Response to salt stress	Plasma membrane	9

Dynamic topic modelling

Dynamic topic modelling was used to model the expression over time of transcripts that co-occurred just before *D. thujina* infection took place (0 dpi). This was done to study groups of transcripts and track how those changed through time. The results of the categorical stability selection analysis allowed the detection of four dynamic topics of interest in this investigation. More than two-thirds of the transcripts in Table 5.4 ranked first to dynamic topics 1, 4, 9 and 23, while 14 of the 25 dynamic topics modelled were not represented at all. Table 5.5 shows the top 10 transcripts of dynamic topics 1, 4, 9 and 23 ranked according to the $\beta_{0,1}$, $\beta_{0,4}$, $\beta_{0,9}$ and $\beta_{0,23}$ scores, respectively.

In general, the top 10 sequences of each topic were not present in the top 10 of the other dynamic topics selected, except for three transcripts. Transcripts *TRINITY_DN11246_c0_g1_i1* and *TRINITY_DN119739_c4_g1_i4* were in dynamic topics 4 and 9, while transcript *TRINITY_DN118395_c0_g3_i1* was in topics 4 and 23. None of the sequences from dynamic topic 1 were present in the other three topics of interest. In relation to the annotations, "dehydrin Xero 1" was present in dynamic topics 4 and 9, while the "pectin acetylesterase 8" and the "ubiquitin-conjugating enzyme E2 35" were in present in dynamic topics 1 and 9. None of the annotations of the top 10 sequences from topic 23 were present in the top 10 sequences of the other topics.

Sequences in dynamic topic 1 were at higher expression levels in line 5382 than in the other two *T. plicata* lines used in this study, regardless of their infection status. One of the top 10 sequences in this topic was involved in defense response (*TRINITY_DN109531_c0_g1_i1*, a MLP-like protein 423), and one was related to cell wall organization (*TRINITY_DN126209_c0_g1_i2*, a pectin acetylesterase 8). Interestingly, the only ethylene pathway-related sequence found in this study was part of this dynamic topic (*TRINITY_DN4933_c0_g3_i1*, the ethylene-responsive transcription factor RAP2-4; see also GoM section), and had expression levels that were slightly higher after infection (Fig. 5.10a). Four of the transcripts modelled in this topic showed interesting responses at 4-12 dpi (Fig. 5.10a): transcript *TRINITY_DN110415_c1_g1_i2* (a protein translation factor SUI1 homolog 1) had a steep and continuous decrease until 12 dpi, sequence *TRINITY_DN46638_c0_g3_i1* (a beta-amylase 1) had a slight decrease at 4 dpi and then an increase to 0 dpi levels'

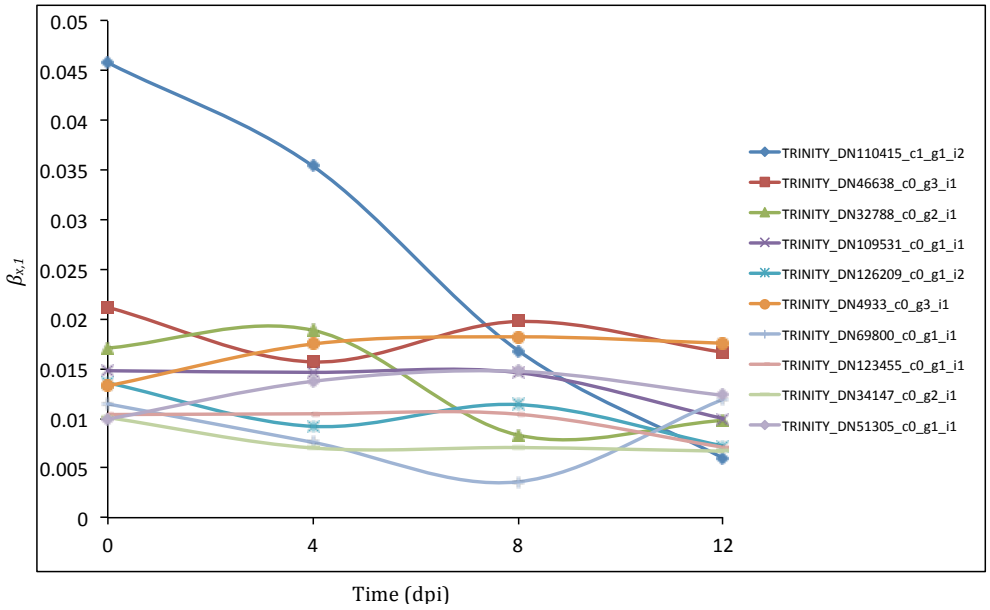

(a)

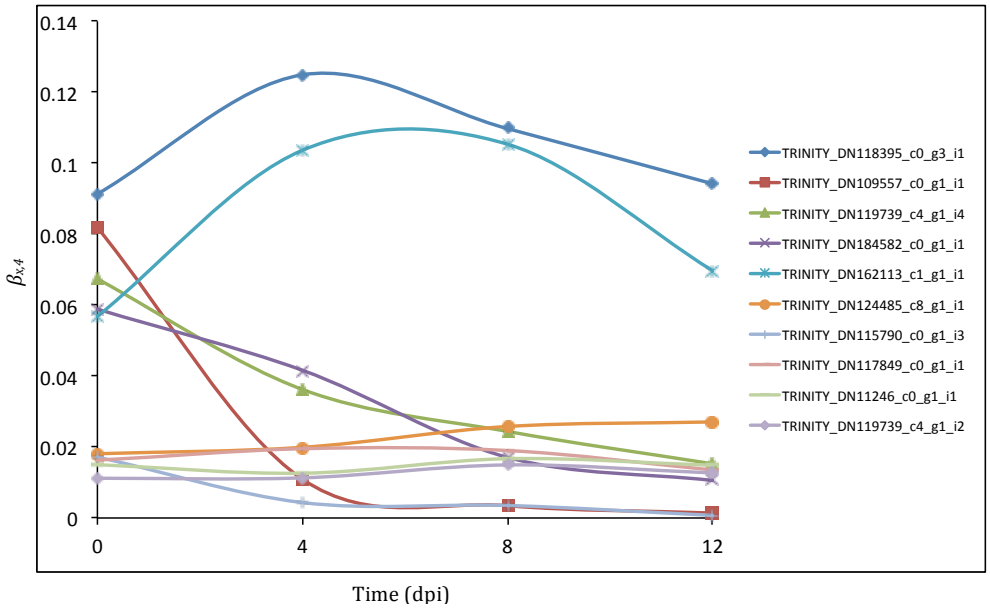

(b)

Figure 5.10. Representative dynamic topics (1 and 4) of this experiment. The topics were chosen based on the annotations of the sequences detected by the categorical stability selection analysis (see last column of Table 5.4). Count data of the differentially expressed transcripts were modelled into 25 dynamic topics ($k = 25$) using the Dynamic Topic Models software (https://github.com/blei-lab/dtm ; see also methods). The graphs show the inferred posterior expression distribution per transcript per time point ($\beta_{x,k}$) of the top 10 transcripts of topics 1 and 4. (a) Dynamic topic 1, (b) dynamic topic 4. x = dpi = days post infection.

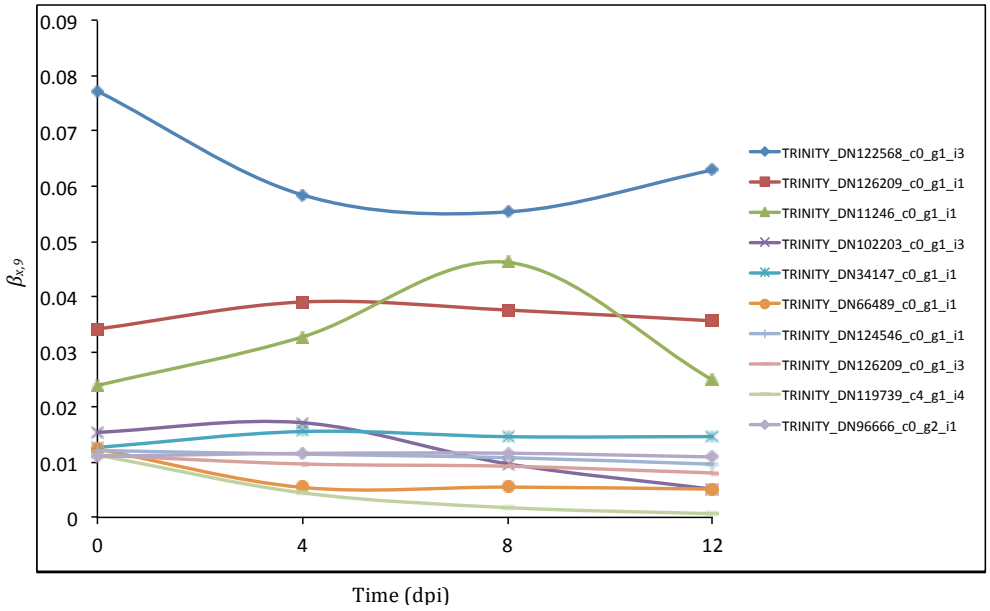

(a)

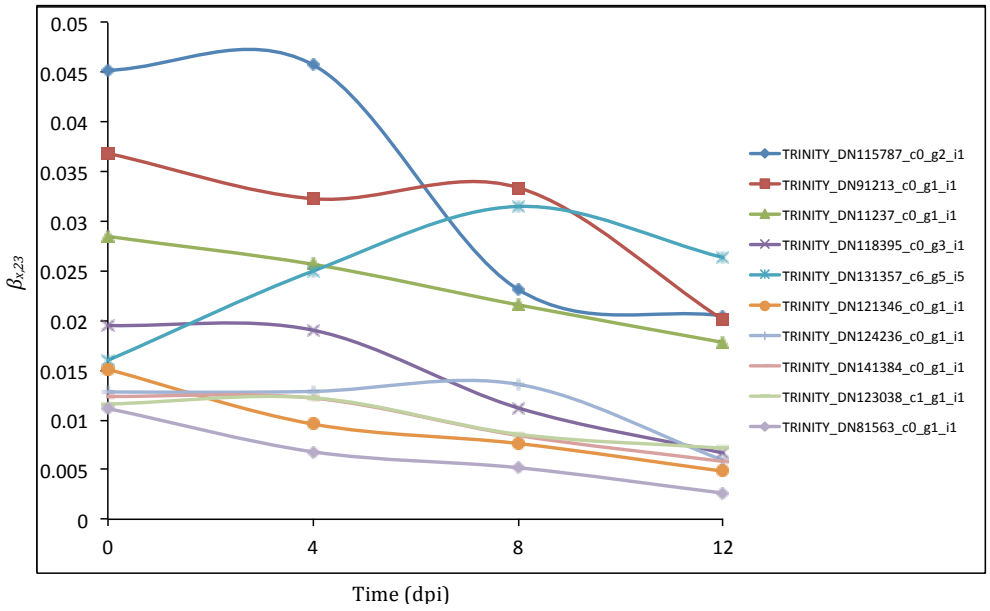

(b)

Figure 5.11. Representative dynamic topics (9 and 23) of this experiment. The topics were chosen based on the annotations of the sequences detected by the categorical stability selection analysis (see last column of Table 5.4). Count data of the differentially expressed transcripts were modelled into 25 dynamic topics ($k = 25$) using the Dynamic Topic Models software (https://github.com/blei-lab/dtm ; see also methods). The graphs show the inferred posterior expression distribution per transcript per time point ($\beta_{x,k}$) of the top 10 transcripts of topics 9 and 23. (a) dynamic topic 9, (b) dynamic topic 23. x = dpi = days post infection.

Table 5.5. Top 10 transcripts per dynamic topic of the four representative dynamic topics of this investigation. The count matrix of the differentially expressed transcripts were modelled into 25 dynamic topics using the Dynamic Topic Models package (https://github.com/blei-lab/dtm). The sequences shown below were chosen based on their decreasing $\beta_{O,k}$ scores. All annotations were based on BLASTX searches done on the Swiss-Prot database. Annotations with asterisk were based on BLASTP searches on the same database.

Dynamic topic (k)	Transcript	$\beta_{o,k}$	E-value	Organism	Annotation	Process	Cellular component
1	*TRINITY_DN110415_c1_g1_i2*	0.045773	2.0×10^{-47}	*Arabidopsis* sp.	Protein translation factor SUI1 homolog 1	Translation initiation factor activity	
	TRINITY_DN46638_c0_g3_i1	0.021113	0	*Arabidopsis* sp.	Beta-amylase 1	Starch catabolic process	Chloroplast, cytosol, nucleus
	TRINITY_DN32788_c0_g2_i1	0.017119	0	*Phaseolus* sp.	Vacuolar-processing enzyme	Cysteine-type peptidase activity	
	TRINITY_DN109531_c0_g1_i1	0.014767	3.0×10^{-29}	*Arabidopsis* sp.	MLP-like protein 423	Defense response	Membrane
	TRINITY_DN126209_c0_g1_i2	0.013518	1.0×10^{-166}	*Arabidopsis* sp.	Pectin acetylesterase 8	Cell wall organization	Cell wall, extracellular region
	TRINITY_DN4933_c0_g3_i1	0.013241	2.0×10^{-32}	*Arabidopsis* sp.	Ethylene-responsive transcription factor RAP2-4	Ethylene-activated signaling pathway	Nucleus
	TRINITY_DN69800_c0_g1_i1	0.011436	3.0×10^{-88}	*Nepenthes* sp.	Aspartic proteinase nepenthesin-2	Aspartic-type endopeptidase activity	Extracellular region
	TRINITY_DN123455_c0_g1_i1	0.010352	3.0×10^{-41}	*Arabidopsis* sp.	3-Dehydrosphinganine reductase TSC10A	Sphingolipid biosynthetic process	Endoplasmic reticulum membrane
	TRINITY_DN34147_c0_g2_i1	0.010082	9.0×10^{-99}	*Arabidopsis* sp.	Ubiquitin-conjugating enzyme E2 35	Protein ubiquitination	Cytoplasm, nucleus
	TRINITY_DN51305_c0_g1_i1	0.009854	NA	No hits	No hits		
4	*TRINITY_DN118395_c0_g3_i1*	0.091326	NA	No hits	No hits		
	TRINITY_DN109557_c0_g1_i1	0.081837	0	*Sesamum* sp.	Inositol-3-phosphate synthase	Phospholipid biosynthetic process	Cytoplasm
	TRINITY_DN119739_c4_g1_i4	0.067357	9.0×10^{-08}	*Arabidopsis* sp.	Dehydrin Xero 1*	Response to stress	
	TRINITY_DN184582_c0_g1_i1	0.058667	4.0×10^{-25}	*Lens* sp.	Non-specific lipid-transfer protein 5	Lipid transport	
	TRINITY_DN162113_c1_g1_i1	0.056824	3.0×10^{-07}	*Musa* sp.	Metallothionein-like protein type 3	Metal ion binding	
	TRINITY_DN124485_c8_g1_i1	0.018110	8.0×10^{-122}	*Arabidopsis* sp.	Cysteine-rich receptor-like protein kinase 2	Defense response	Plasma membrane, plasmodesma
	TRINITY_DN115790_c0_g1_i3	0.017319	7.0×10^{-177}	*Zea* sp.	Polyamine oxidase	N1-acetylspermine:oxygen oxidoreductase activity	
	TRINITY_DN117849_c0_g1_i1	0.016149	1.0×10^{-59}	*Nicotiana* sp.	Pathogenesis-related protein 1C	Defense response	Extracellular region, vacuole
	TRINITY_DN11246_c0_g1_i1	0.015016	NA	No hits	No hits		
	TRINITY_DN119739_c4_g1_i2	0.011164	2.0×10^{-07}	*Arabidopsis* sp.	Dehydrin Xero 1*	Response to stress	
9	*TRINITY_DN122568_c0_g1_i3*	0.077287	0	*Pisum* sp.	Glyceraldehyde-3-phosphate dehydrogenase B	Reductive pentose-phosphate cycle	Chloroplast
	TRINITY_DN126209_c0_g1_i1	0.034138	2.0×10^{-166}	*Arabidopsis* sp.	Pectin acetylesterase 8	Cell wall organization	Cell wall
	TRINITY_DN11246_c0_g1_i1	0.023904	NA	No hits	No hits		
	TRINITY_DN102203_c0_g1_i3	0.015406	NA	No hits	No hits		
	TRINITY_DN34147_c0_g1_i1	0.012672	8.0×10^{-99}	*Arabidopsis* sp.	Ubiquitin-conjugating enzyme E2 35	Ubiquitin-dependent protein catabolic process	Cytoplasm, nucleus
	TRINITY_DN66489_c0_g1_i1	0.012306	6.0×10^{-90}	*Glycine* sp.	Ferritin-3	Cellular iron ion homeostasis	Chloroplast
	TRINITY_DN124546_c0_g1_i1	0.012055	0	*Solanum* sp.	Pyruvate dehydrogenase E1 component subunit alpha	Glycolytic process	Mitochondrial matrix
	TRINITY_DN126209_c0_g1_i3	0.011275	1.0×10^{-165}	*Arabidopsis* sp.	Pectin acetylesterase 8	Cell wall organization	Cell wall
	TRINITY_DN119739_c4_g1_i4	0.011267	9.0×10^{-08}	*Arabidopsis* sp.	Dehydrin Xero 1*	Response to stress	
	TRINITY_DN96666_c0_g2_i1	0.011135	1.0×10^{-100}	*Lycopersicon* sp.	Ubiquitin-conjugating enzyme E2-17 kDa	Protein ubiquitination	
23	*TRINITY_DN115787_c0_g2_i1*	0.045259	0	*Glycine* sp.	Catalase-3	Response to hydrogen peroxide	Cytoplasm
	TRINITY_DN91213_c0_g1_i1	0.036853	1.0×10^{-136}	*Arabidopsis* sp.	Glucan endo-1,3-beta-glucosidase 11	Defense response	Anchored component of plasma membrane
	TRINITY_DN11237_c0_g1_i1	0.028440	NA	No hits	No hits		
	TRINITY_DN118395_c0_g3_i1	0.019548	NA	No hits	No hits		
	TRINITY_DN131357_c6_g5_i5	0.015948	1.0×10^{-22}	*Prunus* sp.	Major allergen *Pru* ar 1	Defense response	
	TRINITY_DN121346_c0_g1_i1	0.015042	0	*Canavalia* sp.	Alpha-mannosidase	Mannose metabolic process	Protein storage vacuole
	TRINITY_DN124236_c0_g1_i1	0.012760	2.0×10^{-137}	*Arabidopsis* sp.	Peroxidase 21	Defense response to fungus	Cytosol
	TRINITY_DN141384_c0_g1_i1	0.012425	0	*Arabidopsis* sp.	Beta-D-xylosidase 4	Systemic acquired resistance	Plant-type cell wall
	TRINITY_DN123038_c1_g1_i1	0.011557	1.0×10^{-89}	*Catharanthus* sp.	Peptidyl-prolyl cis-trans isomerase	Protein folding	Cytoplasm
	TRINITY_DN81563_c0_g1_i1	0.011201	9.0×10^{-159}	*Arabidopsis* sp.	Probable xyloglucan endotransglucosylase/hydrolase protein 6	Cell wall organization	Cell wall

at 8 dpi, and transcripts *TRINITY_DN32788_c0_g2_i1* (a vacuolar-processing enzyme) and *TRINITY_DN69800_c0_g1_i1* (an aspartic proteinase nepenthesin-2) showed decreased expression levels at 8 dpi.

Dynamic topic 4 referred to transcripts that were expressed at slightly higher levels in lines 5398 and 5412 in relation to line 5382, especially in the CLB^{+} treatments. Two of the top 10 sequences in this topic were involved in response to stress (*TRINITY_DN119739_c4_g1_i4* and *TRINITY_DN119739_c4_g1_i2*, both dehydrins Xero 1), two were related to defense response (*TRINITY_DN124485_c8_g1_i1*, a cysteine-rich receptor-like protein kinase 2; and *TRINITY_DN117849_c0_g1_i1* a pathogenesis-related protein 1C), and one was part of the phospholipid biosynthetic process (*TRINITY_DN109557_c0_g1_i1*, an inositol-3-phosphate synthase). Two of the sequences modelled in this group depicted increased levels after infection at 4 dpi and then decreased at 8-12 dpi (*TRINITY_DN118395_c0_g3_i1*, no annotation hits; and *TRINITY_DN162113_c1_g1_i1*, a metallothionein-like protein type 3, Fig. 5.10b). Three other transcripts showed downregulation after infection as early as 4 dpi, and continued decreasing up to 12 dpi (*TRINITY_DN109557_c0_g1_i1*, the inositol-3-phosphate synthase mentioned earlier; *TRINITY_DN119739_c4_g1_i4*, one of the dehydrins Xero 1 in this topic; and *TRINITY_DN184582_c0_g1_i1*, a non-specific lipid-transfer protein 5). Transcript *TRINITY_DN115790_c0_g1_i3* (a polyamine oxidase) also had lower expression levels after 4 dpi, but not as low as the previous sequences (Fig. 5.10b).

Dynamic topic 9 included sequences that were at higher levels of expression in lines 5398 and 5412 in comparison to line 5382 regardless of the infection status. Two of the transcripts in this topic were related to cell wall organization (*TRINITY_DN126209_c0_g1_i1* and *TRINITY_DN126209_c0_g1_i3*, both pectin acetylesterases 8), one of them being fully repressed in line 5382 (*TRINITY_DN126209_c0_g1_i3*). One of the sequences in this dynamic topic was related to response to stress (*TRINITY_DN119739_c4_g1_i4*, a dehydrin Xero 1). Most transcripts modelled in this topic depicted steady expression levels over time, except for sequence *TRINITY_DN122568_c0_g1_i3* (glyceraldehyde-3-phosphate dehydrogenase B) and for transcript *TRINITY_DN11246_c0_g1_i1* (with no annotation hits). The former showed an abrupt decrease of expression at 4-8 dpi followed by a slightly increase at 12 dpi, while the later depicted a steady increase of expression levels that peaked at 8 dpi

and decreased at 12 dpi (Fig. 5.11a).

Dynamic topic 23 was related to transcripts that were at higher levels of expression in CLB^+ treatments in relation to CLB^-, especially in lines 5398 and 5412. Three of the sequences in this group were involved in defense response (*TRINITY_DN91213_c0_g1_i1*, a glucan endo-1,3-beta-glucosidase 11; *TRINITY_DN131357_c6_g5_i5*, a major allergen *Pru* ar 1; and *TRINITY_DN124236_c0_g1_i1*, a peroxidase 21), and two were part of the cell wall (*TRINITY_DN81563_c0_g1_i1*, a probable xyloglucan endotransglucosylase/hydrolase protein 6; and *TRINITY_DN141384_c0_g1_i1*, a beta-D-xylosidase 4); the last one being part of the systemic acquired resistance response. All sequences modelled in this topic showed decreasing expression levels after 4 dpi, except for transcript *TRINITY_DN131357_c6_g5_i5* (the major allergen *Pru* ar 1 aforementioned) which depicted a steady increase in expression until 8 dpi before dropping at 12 dpi (Fig. 5.11b). Interesting as well, was transcript *TRINITY_DN115787_c0_g2_i1* (catalase-3) whose levels of expression were the highest of the topic until 4 dpi, after which the expression decreased (Fig. 5.11b).

5.4 Discussion

This investigation examined the constitutive morphological, anatomical, chemical and gene expression differences among three *T. plicata* clonal lines with dissimilar resistances to *D. thujina*, as well as their induced chemical and gene expression responses when exposed to the pathogen. Differences at both the constitutive and induced levels were seen between resistant and susceptible clones, aspects which are discussed below.

5.4.1 Constitutive differences among the three *T. plicata* lines studied

5.4.1.1 Phenotypic differences

Phenotypic differences existed between resistant and susceptible *T. plicata* clonal lines at the morphological level. Resistant lines 5412 and 5398 were shorter and had smaller RCDs than susceptible line 5382. Differences in size may be related to

resource allocation in that resistant plants may spend more resources in secondary metabolism/defense in relation to the susceptible line. Pathogens are an evolutionary force with an associated fitness cost on their hosts, such that plants susceptible to pathogens have reduced fitness but plants with constitutive resistance mechanisms also have fitness disadvantages when the pathogen is absent (Brown and Rant, 2013, Bruns, 2016, Susi and Laine, 2015). The resistant lines investigated here are likely the product of co-evolution between *T. plicata* and *D. thujina* (Russell et al., 2007), and therefore they may allocate more resources to defense mechanisms than growth. Resistant *T. plicata* lines also had thicker spongy mesophylls and lower palisade to spongy mesophyll thickness ratios than the susceptible line 5382. Thinner palisade mesophyll is associated with shade leaves (Boardman 1977; Jackson 1967; Taiz et al. 2015, p. 250), which captures less light and assimilate less CO_2 than sun leaves (Boardman 1977; Taiz et al. 2015, p. 250). The shade-like leaf anatomy of the resistant trees may be a sign of reduced energy expenditure in light capture.

Besides the differences in growth and leaf anatomy that existed between the resistant and susceptible lines, the chemical and gene expression data also indicate that resistant lines 5398 and 5412 have more constitutive defenses in place than susceptible line 5382. The concentration of citronellyl acetate was on average three times higher in the susceptible line in comparison to the resistant lines. The terpene citronellyl acetate has been shown to have antimicrobial properties against some fungi (*Microsporum gypseum* and *Candida albicans*) and bacteria (*Streptococcus mutans*, *Staphylococcus aureus* and *Staphylococcus epidermidis*; Singh et al. 2012), but its effectiveness against *D. thujina* is unknown. It is plausible that citronellyl acetate has a wide-spectrum defense function in the susceptible line 5382, but it is unknown if this compound is an antimicrobial agent against *D. thujina*.

Differences between resistance classes also existed in foliar calcium concentration as revealed by the stability selection analysis. The element was at significantly higher concentration in lines 5398 and 5412 in comparison to susceptible line 5382. Calcium is an important element of the pectin component of the cell wall (Cosgrove 2005; Heldt 2005, p. 5; Heldt and Piechulla 2010, p. 5), but is also a secondary messenger involved in many cellular processes, including growth and development (Heldt 2005, p. 458; Heldt and Piechulla 2010, p. 454) temperature stress, light stress, hormones, mechanical stimulation (Batistič and Kudla, 2012), osmotic stress (Batistič and Kudla,

2012, Silva, 2012) and boron deficiency (González-Fontes et al., 2014). Calcium has also been shown to be involved in defense responses (Agrios 2005, p. 214; Batistič and Kudla 2012; La Mantia et al. 2018; Sharma 2006, p. 5.6; Scheel and Nuernberger 2004; Vidhyasekaran 2008, p. 79), and to reduce the severity of plant diseases caused by *Fusarium oxysporum*, *Sclerotium* sp., *Rhizoctonia* and *Botrytis* (Agrios 2005, p. 259). At the gene expression level, disruption of calcium signalling in response to *D. thujina* infection was also seen in the experiments of Chapters 4 and 6. Higher levels of calcium in resistant lines 5398 and 5414 could be the result of adaptation to pathogen defense for those lines to respond more quickly to pathogen attacks than susceptible trees. A more extensive screening of *T. plicata* populations resistant and susceptible to *D. thujina* will reveal if higher calcium concentration or faster calcium signalling confers resistance advantages in the resistant populations.

5.4.1.2 Gene expression differences

Genotypic differences between the resistant and susceptible lines investigated were also present. The most interesting difference was the higher expression of bark storage proteins A (BSPs) in the resistant lines 5398 and 5412, as detected by the GoM analysis. Those BSPs had the gene ontology annotation "nucleoside metabolic process", and are expected to have phosphorylase superfamily protein domains according to the HMMER domain searches. BSPs, in general, are known to accumulate in xylem rays and bark parenchyma during the fall and to decrease during the spring (Langheinrich and Tischner, 1991, Sauter and van Cleve, 1991, Wetzel et al., 1989). It is also known that their accumulation is regulated by photoperiod and mediated by phytochromes (Coleman et al., 1991, Zhu and Coleman, 2001). BSPs are related to the Vegetative Storage Proteins (VSPs; Pettengill et al. 2013), and have sequence similarity to purine nucleoside phosphorylases, which play roles in nucleoside metabolism (Pettengill et al., 2013). BSPs are believed to be involved in nitrogen storage in plants (Smith and Atkins, 2002, Werner and Witte, 2011). Both BSPs and VSPs accumulate in response to drought, high nitrogen, wounding (Coleman et al., 1994, Lawrence et al., 2001, Liu et al., 2005, Plomion et al., 2006), and herbivory (Liu et al., 2005, Major and Constabel, 2006); VSPs also increase after pathogen attacks (e.g. gene *At4g24340* in Mulema and Denby 2012). Some VSPs have been reported to be jasmonic acid (JA)-responsive elements involved in pathogen defense (Liu et al., 2005, Stein et al., 2008).

A fascinating aspect of the BSPs found in this experiment is that those transcripts were present in the *T. plicata* resistant lines at a time when they were not expected (summer of 2015); this is because BSP levels were anticipated to decrease during the spring (Langheinrich and Tischner, 1991, Sauter and van Cleve, 1991, Wetzel et al., 1989). Although the study was carried out in growth chambers and the plant material had been acclimated for two weeks before the experiment started, the artificial temperature and humidity were close to those in the field that summer (Appendixes A.14 and A.16, respectively). In spite of that, the findings of the current experiment match the family and function of other reported BSPs, but it is unknown whether the BSPs documented here have any specific role in the defense against *D. thujina* in *T. plicata*. To date, there is only one bark protein-like nucleotide sequence from *Thuja occidentalis* in the GenBank (AY795849). The sequence was used to standardize a fast expression system for secreted recombinant proteins given its thaumatin-like protein ToH1 signal peptide (Baur et al., 2005), but has never been investigated in regards to defense responses or nitrogen reserve-related functions in *T. plicata*. Future work should investigate if there is a relationship between BSPs and defense to *D. thujina* in *T. plicata*, and if so, the mechanism of action in such a compatible interaction.

Other transcripts highly expressed in the resistant lines according to the GoM analysis were the glyceraldehyde-3-phosphate dehydrogenase B (GAPDH) and the dehydrin Xero 1, the latter being captured also by the dynamic topic modelling analysis. The GAPDH found in this investigation is chloroplastic and participates in photosynthesis (UniProt accession P12859, The UniProt Consortium 2015, 2017; Heldt 2005, p. 188; Heldt and Piechulla 2010, p. 186). However, GAPDHs can be also involved in plant defense, not just photosynthesis. Some cytosolic GAPDHs have been shown to play roles in the regulation of reactive oxygen species (ROS) and plant defense against pathogens in other pathosystems (Henry et al., 2015). Interestingly, a transcript with the exact same annotation was found in one of the dynamic topics of the experiment presented in Chapter 4. In relation to the aforementioned dehydrin Xero 1, dehydrins (DHNs), also known as group II of the Late Embryogenesis Abundant proteins, (LEA; Allagulova et al. 2003; Hanin et al. 2011; Rorat 2006), are thermostable proteins (Allagulova et al., 2003) that accumulate in response to abiotic stresses that cause cellular dehydration (Allagulova et al., 2003, Kosová et al., 2010, Rorat, 2006). Although DHNs respond mostly to abiotic stressors, they have also been reported to

accumulate in response to herbivory, probably due to the dehydration effect caused by the physical disruption during pest attacks (Kosová et al., 2010). DHNs have also been shown to play roles in plant defense responses to pathogens, including the activation of pathogenesis-related proteins (Brini et al., 2011). LEA proteins were also present in the GoM analysis performed in the experiment presented in Chapter 3. It is possible that both chloroplastic GAPDHs and dehydrin Xero 1 are part of the constitutive defense mechanisms against *D. thujina* in *T. plicata*. Furthermore, *T. plicata* DHNs may be involved in the upregulation of several of the pathogenesis-related protein families found in this investigation (see below).

Besides the findings of the GoM analysis, the stability selection also captured a transcript of interest that depicted constitutive expression differences between resistant and susceptible lines, an EMSY-like 3 sequence. That sequence was expressed in the resistant lines and fully repressed in the susceptible line 5382. EMSY-like genes have been shown to contribute to resistance against the biotrophic oomycete *Hyaloperonospora arabidopsidis* in *Arabidopsis* via resistance gene *RPP7* (Tsuchiya and Eulgem, 2011); a very interesting finding considering the biotrophic nature of *D. thujina* (Durand 1913; Søegaard 1956; Søegaard 1969, p. 294). A search for *RPP7* transcripts in the assembly built here resulted in no hits in the enriched m*RNA* of this experiment. This suggests that instead of enhanced resistance via *RPP7*, the EMSY-like 3 protein found here may be playing a defense role using a different mechanism. Tsuchiya and Eulgem (2011)'s work showed that, besides the *RPP7*, some of the EMSY-like genes studied appeared to confer basal disease defense via chromatin remodelling/methylation (see also Berr et al. 2012 and Bobadilla and Berr 2016). It is plausible that the same mechanism may be present in the resistant *T. plicata* lines investigated here.

5.4.2 Induced responses to *D. thujina* infection in the *T. plicata* clonal lines

5.4.2.1 Chemical responses

Categorical stability selection analysis of the chemical data showed that all lines had a prompt response to *D. thujina* infection given the differences over time in the concentration of several terpenes in the real infections. The concentration of *p*-cymene increased at 4 dpi in the infected plants of all lines in relation to the controls. *p*-

cymene is a volatile monoterpene with weak antimicrobial properties (Bagamboula et al., 2004, Kordali et al., 2008), which has been shown to be involved in plant signalling (Fujita et al., 2016, Kessler et al., 2006). Increased amounts of *p*-cymene have been reported in response to wounding (Kessler et al., 2006), herbivory (Degenhardt and Lincoln, 2006) and fungal attack (Das et al., 2012). It is thought that *p*-cymene plays a role in plant-to-plant signalling by priming the defense of plants in close proximity (Kessler et al., 2006). In Cupressaceae, *p*-cymene appears to be an inducer of the production of tropolones like β-thujaplicin and of volatile terpenes like sabinene (Fujita et al., 2016), the former being a powerful phytoalexin (Chedgy et al., 2007b, Fujita et al., 2016, Lim et al., 2007). Future studies should investigate whether *p*-cymene has antimicrobial properties or a plant-to-plant priming function in this pathosystem.

Germacrene-D-4-ol was the other terpene that displayed differences over time in the infected plants. Germacrene-D-4-ol is a sesquiterpene volatile (Yoshikuni et al., 2006) with antimicrobial properties (Šarac et al., 2014) that accumulates in response to herbivory (Arimura et al., 2004, Markovic et al., 2016) and touch (Markovic et al., 2016). The compound has been shown to deter *Myzus persicae* and *Macrosiphum euphorbiae* in *Solanum tuberosum* (Markovic et al., 2016), and is the major component of antimicrobial terpenes from *Pinus nigra* var. *banatica* (Šarac et al., 2014). Germacrene-D-4-ol may be playing a direct defense role against *D. thujina* along with sandaracopimarinol, especially in the resistant lines 5398 and 5412 where the two compounds peaked by 8 dpi. Sandaracopimarinol is a diterpene (Cheng and Chang, 2014, Ishikawa et al., 2005) with antibacterial properties against Gram-positive bacteria in *Cryptomeria japonica* (Cheng and Chang, 2014, Matsushita et al., 2006). The relationship between the two compounds is unclear, however, it is possible that they are part of a combination of substances that are induced in response to *D. thujina* infection, given that is common for plants to induce more than one family of defensive compounds in response to pathogen and herbivore attacks (Bednarek and Osbourn, 2009, Fürstenberg-Hägg et al., 2013, Liu et al., 2017, Mason and Singer, 2015, Richards et al., 2016, Sudha and Ravishankar, 2002, Wittstock and Gershenzon, 2002).

5.4.2.2 Gene expression responses

From a gene expression perspective, general responses to pathogen infection were seen in all lines. Many of the sequences captured by the categorical stability selection analysis depicted the extracellular nature of the initial colonization process. Almost one-third of the sequences from stability selection had cellular compartment annotations to the apoplast, the extracellular region or cell membranes, highlighting that the first contact of this plant-pathogen interaction takes place on the surface of the leaf and/or the outside of the cells. Unlike bacterial and viral pathogens that enter their hosts via natural openings or wounds (Agrios 2005, p. 87; Sharma 2006, p. 4.5), biotrophic fungi enter their host by direct penetration (Agrios 2005, p. 88, Sharma 2006, p. 4.6). *D. thujina* must perform direct penetration (Søegaard 1969, p. 299) before gaining access to the mesophyll, to colonize it with intercellular mycelium (Pawsey, 1960). The cell compartment annotations of the infection predictors (transcripts) detected by stability selection support the intercellular type of colonization carried out by *D. thujina*. A similar annotation pattern regarding the initial infection process was seen in the gene expression results of the experiment to be presented in Chapter 6.

The stability selection analysis also showed that all plant lines induced defense-like responses to *D. thujina* infection. The analysis captured several defense-related transcripts that changed over time, including six transcripts with defense response annotations, a WRKY transcription factor, a dirigent protein, and three leucine-rich repeat (LRR) receptor-like proteins. Among the transcripts with defense response annotations, there was a pathogenesis-related protein (pollen allergen Jun a 3), a cysteine-rich receptor-like protein kinase (CRK) and a LRR receptor-like serine/threonine-protein kinase. Although the WRKY transcription factor (TF) found here (SUSIBA2) plays roles in sugar signalling (Sun et al., 2005) and starch synthesis (Sun et al., 2003), WRKY TFs are also involved in plant defense (Pandey and Somssich, 2009, Phukan et al., 2016). Dirigent proteins (DIR) are involved in monolignol coupling leading to lignin formation (Davin and Lewis, 2000, Gang et al., 1999, Hosmani et al., 2013), but have also been shown to play roles in plant defense (Li et al., 2017, Ralph et al., 2006a). Interestingly, another dirigent protein was also found at high expression levels in the resistant lines in Chapter 6. It is possible that both WRKY and DIR are involved in *T. plicata* defense against *D. thujina*.

The pathogenesis-related (PR) protein mentioned before (pollen allergen Jun a 3) very likely plays a role in plant defense. PR proteins are defined as proteins that are "*coded for by the host plant but induced only in pathological or related situations*" (Antoniw et al., 1980, Jayaraj et al., 2004, van Loon, 1999, van Loon and van Strien, 1999, van Loon et al., 1994) and were originally seen to accumulate in hypersensitive responses to tobacco mosaic virus infections in tobacco plants (van Loon, 1999). The pollen allergen Jun a 3 (UniProt accession P81295; The UniProt Consortium 2015, 2017) belongs to the PR-5 family (Midoro-Horiuti et al., 2001). PR-5s are thaumatin-like proteins (Jayaraj et al., 2004, van Loon and van Strien, 1999, van Loon et al., 1994) with membrane-permeabilizing properties specific to fungal pathogens (Velazhahan et al., 1999). The properties of PR-5s suggest that pollen allergen Jun a 3 is a potential defense mechanism against *D. thujina* in *T. plicata*.

LRR receptor-like proteins and CRKs belong to the receptor-like protein kinase (RLK) superfamily (Afzal et al. 2008; Ederli et al. 2011; Goff and Ramonell 2007; Morris and Walker 2003; Tichtinsky et al. 2003; Vidhyasekaran 2008, p. 78; Yeh et al. 2015) and, as mentioned before, were found to be induced in *T. plicata* in response to infection with *D. thujina*. RLKs have extracellular, trans-membrane and intracellular domains, the latter domain being involved in signal transduction (Morris and Walker 2003; Tichtinsky et al. 2003; Vidhyasekaran 2008, p. 78). LRRs are involved in defense responses against pathogens (Afzal et al. 2008; Goff and Ramonell 2007; Morris and Walker 2003; Tichtinsky et al. 2003; Vidhyasekaran 2008, p. 78), and CRKs have been shown to be induced by both pathogens and salicylic acid and may trigger programmed cell death (Ederli et al., 2011, Zhang et al., 2013). CRKs are characterized by the presence of repeats of the DUF26 motif (C-X8-C-X2-C) in the extracellular domain (Ederli et al., 2011, Yeh et al., 2015). Interestingly, CRKs were also highly expressed in the resistant *T. plicata* family studied in Chapter 3, and LRRs were at high levels of expression in the resistant seedlings of Chapters 3 and 4. It is plausible that both RLKs play roles in *T. plicata* defense against *D. thujina*.

The gene expression analyses showed that differential responses to infection existed between resistance classes. Dynamic topic modelling revealed that three sequences, related to defense, had higher levels of expression in the infected resistant lines: glucan endo-1,3-beta-glucosidase 11, major allergen *Pru* ar 1 and peroxidase 21. Glu-

can endo-1,3-β-glucosidases (EC 3.2.1.39, Kanehisa et al. 2017; Beffa et al. 1993, Leubner-Metzger and Meins Jr. 1999) cleave 1,3-β-D-glycosidic linkages of β-glucans (UniProt accession Q8L868, The UniProt Consortium 2015, 2017; Leubner-Metzger and Meins Jr. 1999), which are important components of fungal cell walls (Fesel and Zuccaro, 2016, Free, 2013, Geoghegan et al., 2017). They belong to the PR-2 family (Jayaraj et al., 2004, Leubner-Metzger and Meins Jr., 1999) and are usually upregulated in response to pathogens (Beffa et al., 1993, Leubner-Metzger and Meins Jr., 1999). Glucan endo-1,3-β-glucosidases have been shown to have antifungal activity *in vitro* in *Pisum sativum* L. cv "Dot" (Mauch et al., 1988) and tobacco (Leubner-Metzger and Meins Jr., 1999), and appear to defend the host in two ways: directly by degrading fungal cell walls, and indirectly by releasing elicitors produced by the digested cell walls that then trigger defense responses (Jayaraj et al., 2004, Leubner-Metzger and Meins Jr., 1999). Induction of glucan endo-1,3-β-glucosidases was also seen in the experiments of Chapters 4 and 6, being a predictor of aluminum concentrations in Chapter 4 and one of the top 10 transcripts of dynamic topic 2 in Chapter 6.

The major allergen *Pru* ar 1 is another pathogenesis-related protein (UniProt accession O50001; The UniProt Consortium 2015, 2017). Although little information exists regarding *Pru ar 1*'s, a soy homolog upregulated in response to pathogen infection (*Phytophthora sojae*) has been shown to be a PR-10 protein with *RNA*se activity (Fan et al., 2015). PR-10 proteins are structurally related to ribonucleases (van Loon and van Strien, 1999) and include the ribosome-inactivating proteins (RIPs; Jensen et al. 1999). RIPs cleave a highly conserved 28S r*RNA* sequence in a specific adenine residue that results in blocked translation (Jensen et al., 1999). *Pru* ar 1 may then play a role against *D. thujina* in western redcedar. The third transcript of interest mentioned, peroxidase 21, is a classical class III peroxidase (EC 1.11.1.7, UniProt accession Q42580, The UniProt Consortium 2015, 2017; Kanehisa et al. 2017), which includes plant peroxidases that are mostly extracellular (Chittoor et al., 1999, Ghosh, 2006). Peroxidase 21 has been shown to be induced during systemic acquired resistance (Maleck et al., 2000) as well as in response to wounding in *Arabidopsis* (Cheong et al., 2002). The specific role of peroxidases in pathogen defense is still unclear, but it has been proposed that they defend their host via cell wall reinforcement (Chittoor et al., 1999, Jayaraj et al., 2004, van Loon and van Strien, 1999). Tobacco "lignin-forming peroxidases" have that function and, interestingly, belong to another family of pathogenesis-related proteins: PR-9 (Jayaraj et al., 2004, van Loon, 1999, van Loon

and van Strien, 1999). Peroxidases have also been shown to inhibit hyphal growth of *Trichosporium vesiculosum*, *Macrophomina phaseolina* and *Fusarium moniliforme* in *Acorus calamus* without the presence of H_2O_2 (Ghosh, 2006), which suggests that peroxidases may have other roles besides plant cell wall remodelling. The specific mechanism of action of peroxidase 21 in the *T. plicata* - *D. thujina* pathosystem is unknown, but it may play a role in host defense.

The combination of more than one family of PR proteins being upregulated in response to *D. thujina* infection in *T. plicata* (PR-2, PR-5, PR-10 and a probable PR-9) may be a key resistance mechanism against the disease. Synergistic interactions between PR proteins to defend their hosts have been shown in other pathosystems (Jayaraj et al., 2004, Jensen et al., 1999), like barley - *Trichoderma reesei* and barley - *Fusarium sporotrichioides* (Jensen et al., 1999). In both cases, the combination of RIPs, chitinases and 1,3-β-glucosidases showed increased synergistic inhibition of the pathogen *in vitro* (Jensen et al., 1999). The interactions among and the potential synergistic defense effects of the families of PR proteins found here may be a difference between *T. plicata* plants resistant and susceptible to *D. thujina*, and should be investigated in future studies on this pathosystem.

Dynamic topic modelling also showed higher levels of expression of two sequences involved in cell wall processes in the infected resistant plants: a probable xyloglucan endotransglucosylase/hydrolase protein 6, and a beta-D-xylosidase 4. Xyloglucan endotransglucosylase/hydrolases (XTHs) are involved in cell wall modification of actively growing plant regions and in places where cell wall remodelling is taking place (Cho et al., 2006, Cosgrove, 2005, Hara et al., 2014, Liu et al., 2007, Miedes and Lorences, 2007). XTHs cleave β-1,4 bonds of the xyloglucan backbone and transfer the xyloglucanyl end to an acceptor xyloglucan chain (UniProt accession Q8LF99; The UniProt Consortium 2015, 2017; Cosgrove 2005; Liu et al. 2007). They have been shown to be involved in drought/salt tolerance (Cho et al., 2006), ripening (Saladié et al., 2006), primary root growth (Liu et al., 2007), and plant defense (Divol et al., 2007, Miedes and Lorences, 2007, Olsen et al., 2016, Sharmin et al., 2012). XTHs accumulate in response to infection by *Macrophomina phaseolina* in jute (Sharmin et al., 2012), in response to aphid infestation in *Apium graveolens* (Divol et al., 2007), and also play important roles in the infection process carried out by some parasitic plants (Olsen et al., 2016). The β-D-xylosidase (BXL) found here (EC 3.2.1.37, UniProt ac-

cession Q9FLG1, The UniProt Consortium 2015, 2017; Kanehisa et al. 2017; Placzek et al. 2017; Scheer et al. 2011) is also a hydrolase, specifically a glycoside hydrolase (Minic, 2008). BXLs are known to be involved in both symbiotic (Balestrini and Bonfante, 2014a,b) and pathogenic (Blanco-Ulate et al., 2014a,b, Herrmann et al., 1997, Sharma et al., 2011) plant-fungi interactions even though there is not much information on their role on in plant defense. BXLs are known to make cell wall modifications by digesting β-1,4 bonds of xylan (Hatano and Hamada, 2008, Kanehisa et al., 2017, Placzek et al., 2017, Scheer et al., 2011), which is a key hemicellulose component of plant cell walls (Hatano and Hamada 2008; Heldt 2005, p. 4; Heldt and Piechulla 2010, p. 4). The specific roles of XTHs and BXLs in the compatible *T. plicata* - *D. thujina* interaction are unknown, but they may be indirectly involved in pathogen defense by remodelling the host's cell walls during infection.

5.4.3 Conclusions

The results of this investigation showed the existence of constitutive differences, at both the phenotypic and gene expression levels, among *T. plicata* clones with dissimilar resistances to *D. thujina*. *T. plicata* plants resistant to *D. thujina* were significantly smaller than the susceptible line and had shade-like leaf anatomy. Resistant lines had also higher concentrations of calcium, as well as increased expression levels of several BSPs, a DHN, a EMSY-like 3 and a GAPDH in comparison with the susceptible line. It appears that the resistant lines allocate more resources to secondary metabolism/defense than susceptible lines. Further investigations should establish the role of BSPs in *T. plicata* resistance to *D. thujina*.

In spite of the constitutive differences between resistance classes, all lines showed induced responses to *D. thujina* infection, including the accumulation of *p*-cymene, and the upregulation of a WRKY transcription factor, a dirigent protein, a PR-5 and several LRRs and CRKs. In addition to those responses, plants resistant to *D. thujina* also showed the accumulation of germacrene-D-4-ol and sandaracopimarinol as well as induction of a XTH, a BXL and several PRs (PR-2, PR-10 and a peroxidase). PRs may act in a synergistic way to defend the host and be one of the key defense mechanisms that is absent in the susceptible line.

Chapter 6

Constitutive and induced defense mechanisms against *Didymascella thujina* in *Thuja standishii*, *Thuja plicata* and a *Thuja standishii* × *plicata* hytbrid

6.1 Introduction

Plants are in constant contact with different types of bacteria, fungi, viruses, nematodes and other plants, some interactions being pathogenic. Most pathogens are innocuous to most plants simply because they are not their hosts, a phenomenon known as nonhost resistance (Agrios 2005, p. 134; Sharma 2006, p. 3.4; Westerink et al. 2004). When a plant species is the host of a pathogen, apparent and true resistance can take place. Apparent resistance refers to two phenomena in plants susceptible to a pathogen: disease escape and tolerance (Agrios 2005, p. 137; Sharma 2006, p. 3.7). Susceptible plants "escape" susceptibility when the pathogen load or environmental conditions are not optimal for pathogen infection and establishment. Tolerance is evident when susceptible infected plants can still function normally in the presence of the pathogen and show few symptoms of the disease. True resistance takes place when the host is genetically equipped with defense mechanisms against the disease, which can be either constitutive or induced in the presence of the pathogen

(Agrios 2005, p. 136; Holliday 1989, p. 274; Sharma 2006, p. 3.5; Westerink et al. 2004).

True resistance to plant pathogens has always been at the core of plant breeding for disease resistance (Agrios 2005, p. 136; Holliday 1989, p. 274; Sharma 2006, p. 3.8; Westerink et al. 2004; White et al. 2007). It can be quantitative or qualitative; the former is polygenic in nature and does not confer full resistance against a pathogen, while the latter is either monogenic or oligogenic and usually results in full resistance to the disease (Agrios 2005, p. 136; Sharma 2006, p. 3.5; Vidhyasekaran 2008, p. 193). Although qualitative resistance might be considered better in the short term, it is easily broken down when pathogens evolve, making it unstable for breeding (Holliday 1989, p. 274; Rouxel and Balesdent 2010). An approach to dissect the molecular mechanisms of quantitative pathogen resistance is by the use of quantitative trait loci (QTL; Buerstmayr et al. 2002; Carson et al. 2004; Collard et al. 2005; Pelgas et al. 2011; Welz and Geiger 2000; White et al. 2007), which has been used for more than 20 years in studies of tree defense (Neale and Kremer, 2011). A drawback of the technique, however, is the large number of individuals needed (parents and offspring) and known genetic markers required for linkage map production (Collard et al., 2005, White et al., 2007, Young, 1996), which makes this type of investigation challenging.

The accessibility and declining cost of next generation sequencing (NGS) techniques have resulted in an increase in studies on the molecular mechanisms of defense against pathogens. For example, the technique has been used to study the responses to *Sclerotinia* sp. in canola (Joshi et al., 2016), *Fusarium* sp. in flax (Galindo-González and Deyholos, 2016), *Fusarium* sp. in rice (Ji et al., 2016), *Moniliophthora perniciosa* in cacao (Teixeira et al., 2014), *Botrytis cinerea* in lettuce (de Cremer et al., 2013), among others (e.g. Adhikari et al. 2012; Hulvey et al. 2012; Petre et al. 2012; Tremblay et al. 2011). Those investigations have shown that plants under attack upregulate defense-related genes, like glucanases (Joshi et al., 2016), chitinases (Adhikari et al., 2012, Galindo-González and Deyholos, 2016, Joshi et al., 2016), peroxidases (Adhikari et al., 2012, Joshi et al., 2016), catalases (Adhikari et al., 2012), protein inhibitors (Adhikari et al., 2012) and even transcription factors (including WRKYs; Galindo-González and Deyholos 2016; Ji et al. 2016; Joshi et al. 2016). Genes involved in hormone-signalling pathways like the jasmonic (de Cremer et al., 2013, Joshi et al., 2016), salicylic (de Cremer et al., 2013), and abscisic acids (de Cremer et al., 2013),

as well sequences related to secondary metabolites like flavonoids (Galindo-González and Deyholos, 2016), lignin (de Cremer et al., 2013) and terpenes (de Cremer et al., 2013) are also upregulated in response to pathogen infection. *RNA*-Seq studies have also shown that some pathogens reprogram their hosts' metabolism to their own benefit (Petre et al., 2012, Teixeira et al., 2014, Tremblay et al., 2011). In addition to gene expression studies, NGS techniques like *RNA*-Seq are currently being used for single nucleotide polymorphism (SNP) genotyping when a reference genome is not available (Lopez-Maestre et al., 2016). Those applications of the NGS technology can be very useful for programs interested in marker-assisted breeding for pathogen resistance (Grattapaglia and Resende, 2011, White et al., 2007) when used in combination with more classical methods (Neale and Kremer, 2011, Rostoks et al., 2005, White et al., 2007).

Thuja plicata (western redcedar, WRC) shows genetic variation in the resistance to *Didymascella thujina* (cedar leaf blight, CLB; Russell et al. 2007, Russell and Yanchuk 2012), indicating that this species has true resistance to the pathogen. True resistance against *D. thujina* has also been reported in *Thuja standishii* (Japanese arborvitae) as well as in hybrids between that species and *T. plicata*. *T. standishii* and its hybrid offspring, but not *T. plicata*, have been reported to be fully resistant to *D. thujina* (Søegaard, 1956, 1966, 1969). The studies by Søegaard (1956, 1966, 1969) led to the proposition of a gene-for-gene model for this pathosystem, where resistance to the disease is thought to be due to a single dominant resistance (R) gene in *T. standishii* that is then passed on to the hybrids, rendering them immune to *D. thujina*. Resistance to *D. thujina* in *T. plicata*, on the contrary, appears to be a quantitative trait that involves many genes and confers no full resistance to the disease (Russell et al. 2007; Søegaard 1969, p. 366).

The gene-for-gene model of resistance to *D. thujina* in *T. standishii* and its hybrid offspring has never been put to the test beyond Søegaard's experiments and it is unknown whether alternative explanations to such a phenomenon exist. The model predicts that a single plant R gene is responsible for full resistance when in the presence of the avirulence (avr) counterpart from the pathogen (Agrios 2005, p. 140; Hammond-Kosack and Jones 1997; Sharma 2006, p. 3.9; Vidhyasekaran 2008, p. 193). Full disease resistance can be achieved, alternatively, when a few major genes pyramid to defend their host, which results in qualitative resistance (Agrios 2005, p. 136;

Sharma 2006, p. 3.6; Vidhyasekaran 2008, p. 193). In order to explore whether resistance to *D. thujina* in *T. standishii* and *T. standishii* × *plicata* is a monogenic or a multigenic trait, the gene expression (*RNA*-Seq) profiles of susceptible *T. plicata* inbred seedling lines, and of resistant *T. standishii* and *T. standishii* × *plicata* clonal lines were investigated, as well as their initial gene expression responses to *D. thujina* infection. Differences at the morphological, histological and chemical levels among the lines studied were also investigated to determine if constitutive defense mechanisms other than those that are gene expression-related accounted for differences in *D. thujina* resistance.

6.2 Methodology

The variables measured, methods used, and analyses carried out here were the same as those described in Chapter 5, except for the plant material utilized (section 6.2.1) and the time-course infection sampling points (section 6.2.2). A brief overview of the methodology is given below. Please refer to the previous chapter for details.

6.2.1 Plant material and characterization

Two species (*T. plicata* and *T. standishii*) and a hybrid of the two (*T. standishii* × *plicata*) were used. The hybrid and *T. standishii* were clonal lines, while *T. plicata* plants were single seed descent seedlings from two lines (124 and 129) that had been self-pollinated for five generations (see Appendix A.1; Russell and Ferguson 2008). The *T. standishii* × *plicata* hybrid was a clone of the "Green Giant" Arborvitae (NA 29972; U.S. National Arboretum, Washington, D.C., USA) and was obtained from a local nursery. *T. standishii* clonal lines originated from seedlings germinated from wild stand seed obtained from the Japanese Forest Tree Breeding Centre. The lines were maintained in Beaver Styroblock containers 45/340 (Stuewe and Sons., Tangent, OR, USA) in a fibreglass house at Cowichan Lake Research Station (Mesachie Lake, British Columbia) under standard growing conditions prior the start of the experiment.

The plant material was characterized morphologically and histologically by quantifying 13 original and 3 derived variables that related to leaf toughness, plant size and leaf anatomy (see Appendix A.9). Leaf toughness was measured in young and

older foliage, and plant size measurements included plant height, root collar diameter (RCD) and the ratio between the two. Leaf anatomy variables were studied in Quetol-embedded cross-sections and included leaf width, various thicknesses (cuticle, epidermis, whole mesophyll, palisade mesophyll, spongy mesophyll and leaf), two thickness ratios (whole mesophyll to leaf and palisade to spongy mesophyll), lignification of epidermal cells and stomatal density. Histological variables were analyzed using a fixed-effects split-plot design in R (R Core Team, 2015), except for the palisade mesophyll thickness and the palisade to spongy mesophyll ratio because they could not be normalized. Those variables and stomatal density were analyzed using Kruskal-Wallis one-way Analysis of Variance (ANOVA).

6.2.2 Time-course infection with *D. thujina*

All plant lines were real- (CLB^+) and mock- (CLB^-) inoculated under controlled conditions in Conviron growth chambers (Conviron, Winnipeg MB, Canada), at the Bev Glover Growth Facility (University of Victoria, Victoria, British Columbia). The chambers were set for 12 h light and 12 h darkness, relative humidity $\geq$90% and a constant temperature of 16℃, and the plants were acclimated for two weeks before the experiment started. The real inoculations were done with *D. thujina* collected during the sporulation season (June 1, 2015). The infected cuttings used as inoculum source were collected in a *T. plicata* progeny trial in Jordan River (British Columbia; 48° 25' 24.52" N, 124° 1' 27.69" W, elev. 76 m) and the infections were set up using a variation of the technique used by Søegaard (1969, p. 310).

At the time of the experiment, the plants were sampled just before the infections took place (0 days post infection, dpi), and at 4 and 8 dpi. Two samples per treatment (i.e. type of infection $\times$ line $\times$ time) were collected (see Appendix A.9), and were used to complete the following analyses: 1) infection confirmation, 2) chemical composition, and, 3) gene expression (*RNA*-Seq). Foliage collected for infection confirmation was fixed in 2.5% glutaraldehyde (diluted in 0.1 M Sörensen' buffer, pH 7.2; Ruzin, 1999, pp. 227), and that for the chemical and gene expression analyses was flash-frozen in liquid nitrogen and stored at -80℃ until further processing.

Infections were confirmed by scanning electron microscopy (SEM) visualization of *D. thujina* spores on the inoculated foliage (Kope, 2000). Further verification of the infec-

tion was done using two additional methodologies mentioned in the previous chapter: evaluation of the disease incidence after symptoms developed ∼9 months later in the inoculated plants (scored as the percentage of plants with *D. thujina* symptoms), and BLASTn searches in the reference transcriptome built (see section 6.2.4) for the two internal transcribed spacer 2 (ITS2) sequences of *D. thujina* that are currently in the GenBank (accessions KT875766 and KT875767).

Disease severity was measured in each line, in addition to the incidence, using another set of plants that belonged to the same lines investigated. The plants were taken to the same place where the inoculum was collected (see section 6.2.2) and were exposed to natural infection during the sporulation season of *D. thujina*, between May and July 2015 (see Appendix A.14). Severity was measured ∼9 months later when symptoms were present, and was recorded as the percentage foliage of blighted determined by color analysis in WinRHIZO Pro v. 2009c (Regent Instruments Inc., QC, Canada).

6.2.3 Chemical analyses

Quantification of mineral nutrients, terpenes, lignin, fibre and cellulose in the foliage sampled was outsourced to the Analytical Laboratory of the Ministry of Environment and Climate Change Strategy Branch. A total of 60 variables were measured, mineral nutrients being quantified only at 0 and 8 dpi and the rest of the variables at the three time points. Principal Component Analysis (PCA) using the correlation matrix (Lê et al., 2008) was performed to explore the differences in the chemical profiles among plant lines. Categorical stability selection (Meinshausen and Bühlmann, 2010) and change point analysis (Killick and Eckley, 2014) were used to detect variables that 1) discriminated among plant lines, and 2) were related to *T. plicata* responses to *D. thujina* infection. The detected variables were then analyzed with three-way factorial ANOVAs that had infection status (CLB^+ or CLB^-), clone line, time point, and their interactions as fixed factors. Non-parametric variables were analyzed using Kruskal-Wallis one-way ANOVAs.

6.2.4 Gene expression analyses

Total *RNA* from the foliage sampled was extracted using a customized version of Rajakani et al. (2013), and outsourced to Genome Quebec Innovation Centre (Montreal QC, Canada) for m*RNA* enrichment, library production, and 100 bp paired-end

sequencing in an Illumina® HiSeq 2000 sequencer. The same pipeline of the previous chapter was used to complete the bioinformatics analyses of gene expression. Quality control of the raw paired-end libraries was done in FastQC v. 0.11.4 (Andrews, 2014), trimming was achieved with Trimmomatic v. 0.36 (Bolger et al., 2014), and the reference transcriptome was assembled using Trinity v. 2.2.0 (Grabherr et al., 2011) in WestGrid's Hermes cluster (www.westgrid.ca) . The transcriptome was then annotated using Trinotate v. 3.0.1 (http://trinotate.github.io).

Reads were mapped to the reference transcriptome using RSEM v. 1.3.0 (Li and Dewey, 2011), and differential expression (DE) analysis was done with *edgeR* (Robinson et al., 2010). Sequences with a minimum fold change of 4 and a maximum false discovery rate of 0.001 were kept for downstream analyses. The DE data was then used as input for PCA analysis (on the correlation matrix) to explore the differences in gene expression profiles among plant lines as in section 6.2.3. DE data was also explored using hierarchical clustering of samples versus transcripts. As in Chapter 5, the term "transcript" refers to contig variants of Trinity's "genes", but "transcripts" was used throughout this document for simplicity. The transcript's tree of the heat-map produced was cut at 43.3% of its maximum height to obtain clusters of DE transcripts. To ease the exploration of the transcriptomic data, the annotations and DE matrix were ingested in a SQLite database that was then uploaded to a local TrinotateWeb server. The TrinotateWeb server was installed on Compute Canada's West Cloud (https://west.cloud.computecanada.ca) and was obtained from http://trinotate.github.io/TrinotateWeb.html

Transcripts of interest were detected using 1) categorical and regression stability selections, 2) grade of membership (GoM) analysis (Dey et al., 2016, 2017), and 3) dynamic topic modelling (Blei and Lafferty, 2006, Lee et al., 2016). Categorical stability selection was completed to find predictors (transcripts) of *D. thujina* infection by categorizing the samples according to the plant line and infection condition. Regression stability selection was carried out using aluminum as the response variable given the high concentrations of that element in *T. standishii* plants that were in the CLB^+ condition (see section 6.3.2.1). GoM analysis was completed using $K = 25$, and relevant static topics were chosen from a hierarchical clustering heatmap of samples versus topics produced using the ω matrix (probability distribution of the *RNA*-Seq samples over the 25 static topics from a Dirichlet allocation perspective;

Blei 2012, Blei and Lafferty 2009, Dey et al. 2016, Liu et al. 2016a). Dynamic topic modelling was conducted using $K = 25$ as well, and dynamic topics of interest were the most frequent dynamic topics among the transcripts retained by the stability selection analyses (based on the transcripts' $\beta_{0,k}$ scores).

6.3 Results

6.3.1 Characterization of the plant material

There was significant variation among plant lines for many of the morphological and anatomical traits measured (Table 6.1). All variables related to plant size, one pertaining to toughness and three leaf anatomy traits were significantly different among lines. *T. plicata* line 124 and *T. standishii* × *plicata* were the tallest plants ($p < 0.0000$), and had the largest RCD ($p = 0.0001$; Table 6.1). *T. plicata* line 124 had the greatest height to RCD ratio ($p = 0.0001$), with the other three lines grouping together, based on the Tukey HSD all-pairwise comparisons test at $\alpha = 0.05$ (Table 6.1). Leaf toughness was significantly different among lines only for the young foliage ($p = 0.0323$), with leaves of *T. plicata* line 124 being the toughest and those of *T. plicata* line 129 being the softest (Table 6.1).

Leaf anatomy variables that differed significantly among lines were: epidermal thickness ($p = 0.0004$), spongy mesophyll thickness ($p = 0.0204$), and leaf width ($p = 0.0298$; Table 6.1). *T. standishii* × *plicata* had the thinnest epidermis, followed by *T. standishii*. *T. plicata* line 129 had the thinnest spongy mesophyll, line 124 the thickest, while *T. standishii* and *T. standishii* × *plicata* were intermediate. *T. plicata* line 124 had the narrowest leaves of all, and *T. standishii* and *T. standishii* × *plicata* the widest.

The only variable with significant line × crown position interaction was cuticle thickness (p =0.0080; Appendix A.5). The cuticles of *T. standishii* × *plicata*'s lower branches and those of *T. standishii*'s upper branches were the thickest (Table 6.2). The thinnest cuticles were in the upper and middle branches of *T. plicata* line 129, and in the middle branches of *T. standishii* × *plicata*.

Table 6.1. Mean and standard errors, per line, of the 16 variables measured to characterize the plant material studied. The variables relate to plant size, leaf anatomy and toughness. Leaf toughness and plant size variables were analyzed with parametric one-way analyses of variance. Leaf anatomy variables were analyzed using a split-plot statistical model, except for palisade mesophyll thickness and palisade to spongy mesophyll thickness ratio. Homogeneous groups for statistically significant variables among species were produced with the Tukey HSD all-pairwise comparisons test. Stomatal density, palisade mesophyll thickness and palisade to spongy mesophyll ratio were analyzed using Kruskal-Wallis analysis of variance. Similar letters in the superscripts of the means refer to homogeneous groups within each variable according to the Tukey HSD all-pairwise comparisons test.

Trait	Variable	*Thuja plicata* (line 124)	*Thuja plicata* (line 129)	*Thuja standishii*	*Thuja standishii* × *plicata*
Plant size	Root collar diameter (RCD; mm)	$4.07^{a} \pm 0.13$	$3.39^{b} \pm 0.10$	$3.39^{b} \pm 0.08$	$3.91^{a} \pm 0.15$
	Height (cm)	$40.35^{a} \pm 0.99$	$27.12^{c} \pm 1.21$	$27.48^{c} \pm 1.08$	$33.68^{b} \pm 1.67$
	Height to RCD ratio	$100.0^{a} \pm 2.8$	$80.1^{b} \pm 3.0$	$81.9^{b} \pm 4.1$	$86.5^{b} \pm 3.4$
Leaf anatomy	Epidermal thickness (µm)	$12.11^{b} \pm 0.32$	$12.12^{b} \pm 0.31$	$11.05^{b} \pm 0.33$	$9.48^{a} \pm 0.35$
	Cuticle thickness (µm)	2.23 ± 0.13	1.86 ± 0.13	2.54 ± 0.16	2.56 ± 0.28
	Palisade mesophyll thickness (µm)	65 ± 11	47 ± 7	74 ± 22	51 ± 15
	Spongy mesophyll thickness (µm)	$521^{b} \pm 36$	$399^{a} \pm 43$	$432^{a,b} \pm 36$	$459^{a,b} \pm 44$
	Whole mesophyll thickness (µm)	587 ± 15	446 ± 14	507 ± 12	511 ± 13
	Leaf thickness (µm)	632 ± 48	510 ± 41	574 ± 32	545 ± 38
	Leaf width (µm)	$1044^{b} \pm 50$	$856^{a} \pm 21$	$1137^{b} \pm 62$	$1166^{b} \pm 44$
	Palisade to spongy mesophyll ratio	0.13 ± 0.02	0.13 ± 0.02	0.19 ± 0.06	0.13 ± 0.05
	Whole mesophyll to leaf thickness ratio	0.93 ± 0.01	0.87 ± 0.02	0.88 ± 0.02	0.93 ± 0.01
	Epidermal cells with lignified walls (%)	47 ± 7	54 ± 5	40 ± 5	45 ± 8
	Stom. density (stomata·mm^{-2})	110 ± 23	73 ± 15	112 ± 24	103 ± 24
Leaf toughness	Young foliage (kPa)	$1{,}161.5^{a} \pm 24.9$	$986.8^{b} \pm 69.6$	$1{,}030.2^{a,b} \pm 22.4$	$1{,}108.7^{a,b} \pm 42.3$
	Old foliage (kPa)	$1{,}963.3 \pm 120.5$	$2{,}113.1 \pm 156.7$	$2{,}393.3 \pm 122.5$	$2{,}163.5 \pm 117.4$

Table 6.2. Cuticle thickness per line and crown position (mean and standard error). Similar letters in the superscripts of the means refer to homogeneous groups in each variable across all lines and crown positions according to the Tukey HSD all-pairwise comparisons test.

Line	Crown position	Cuticle (µm)
Thuja plicata (line 124)	Upper	$1.97^{a,b,c} \pm 0.12$
	Middle	$2.16^{a,b,c} \pm 0.12$
	Lower	$2.56^{a,b,c} \pm 0.12$
Thuja plicata (line 129)	Upper	$1.61^{c} \pm 0.08$
	Middle	$1.76^{c} \pm 0.12$
	Lower	$2.22^{a,b,c} \pm 0.16$
Thuja standishii × *plicata*	Upper	$2.40^{a,b,c} \pm 0.12$
	Middle	$1.88^{b,c} \pm 0.09$
	Lower	$3.39^{a} \pm 0.41$
Thuja standishii	Upper	$2.96^{a,b} \pm 0.20$
	Middle	$2.57^{a,b,c} \pm 0.13$
	Lower	$2.09^{a,b,c} \pm 0.09$

6.3.2 Time-course responses to infection

Samples from all plant lines tested positive for the presence of *D. thujina* spores only in the 4-8 dpi CLB^{+} treatments as visualized in the SEM examination. Incidence was significantly different among lines ($p = 0.0021$), *T. plicata* lines had higher incidences of the disease than *T. standishii* × *plicata* or *T. standishii* (Table 6.3). Disease severity was also significantly different among lines ($p = 0.0020$). *T. plicata* lines had the highest disease severity values (33.25% for line 124, and 14.33% for line 129; Table 6.3), and *T. standishii* × *plicata* a very low severity (0.48%). *T. standishii* was fully resistant to *D. thujina*, with 0.00% incidence and severity.

6.3.2.1 Chemical composition

Principal component analysis of the chemical composition data showed that results were clustered by species and hybrid (*T. plicata*, *T. standishii* and *T. standishii* × *plicata*; Fig. 6.1). The first principal component explained 32.63% of the variance, the second 26.74% and the third 7.20%. The cumulative variance explained by those components was 66.58%. Principal component 1 discriminated among the species

Table 6.3. Incidence and severity of *Didymascella thujina* symptoms in the plant material studied assessed approximately nine months after inoculation. Incidence was evaluated in the plants that were used in the time-course experiment carried out in growth chambers. Severity was measured in a set of plants that were infected in a *Thuja plicata* progeny trial for that purpose (see methods for details). Both variables were measured when *D. thujina* symptoms were present (about nine months later).

Plant line	Incidence (%)[1]	Severity (%)[2]
Thuja plicata line 124	50.00	33.25^{A}
Thuja plicata line 129	50.00	14.33^{A}
Thuja standishii	0.00	0.00^{B}
Thuja standishii × *plicata*	16.67	0.48^{B}

[1] The test of independence of plant line vs. presence/absence of *D. thujina* symptoms was significant ($p = 0.0021$).

[2] A-B: homogeneous groups based on the Kruskal-Wallis all-pairwise comparisons test at $\alpha = 0.05$.

and hybrid, while component 2 separated *T. plicata* lines from the rest. The second component also discriminated between CLB^- and CLB^+ treatments in all lines. The five variables with the highest contributions to the first component were terpenes (α-thujone, α-thujene, sabinene and totarol acetate and trans-ferruginol) and the top five variables contributing to component 2 were additional terpenes (citronellyl acetate, fenchone and terpinolene, citronellal, β-pinene and linalool).

Three terpenes (citronellyl acetate, α-gurjunene and 3-carene) discriminated among the two species and the hybrid according to the changepoint algorithm on the stability selection scores. There were significant differences in the concentration of citronellyl acetate among lines ($p < 0.0000$, Fig. 6.2a). *T. standishii* and *T. standishii* × *plicata* had higher concentrations (1,085 ± 39 $\mu g \cdot g^{-1}$ and 951 ± 44 $\mu g \cdot g^{-1}$, respectively) than *T. plicata* lines 124 and 129 (268 ± 13 $\mu g \cdot g^{-1}$ and 231 ± 16 $\mu g \cdot g^{-1}$, respectively). There were significant differences in the concentration of α-gurjunene among lines as well ($p < 0.0000$, Fig. 6.2b). *T. standishii* × *plicata* had higher concentration of that compound (2,388 ± 186 $\mu g \cdot g^{-1}$) in comparison to *T. standishii* (0 $\mu g \cdot g^{-1}$) or *T. plicata* lines (334 ± 69 $\mu g \cdot g^{-1}$ for line 124, and 20 ± 1 $\mu g \cdot g^{-1}$ for line 129). Significant differences among lines also existed for 3-carene ($p < 0.0000$, Fig. 6.2c), which was at high levels in *T. standishii* (370 ± 23 $\mu g \cdot g^{-1}$), and completely absent in both *T. plicata* lines as well as in *T. standishii* × *plicata* (0 $\mu g \cdot g^{-1}$ in all).

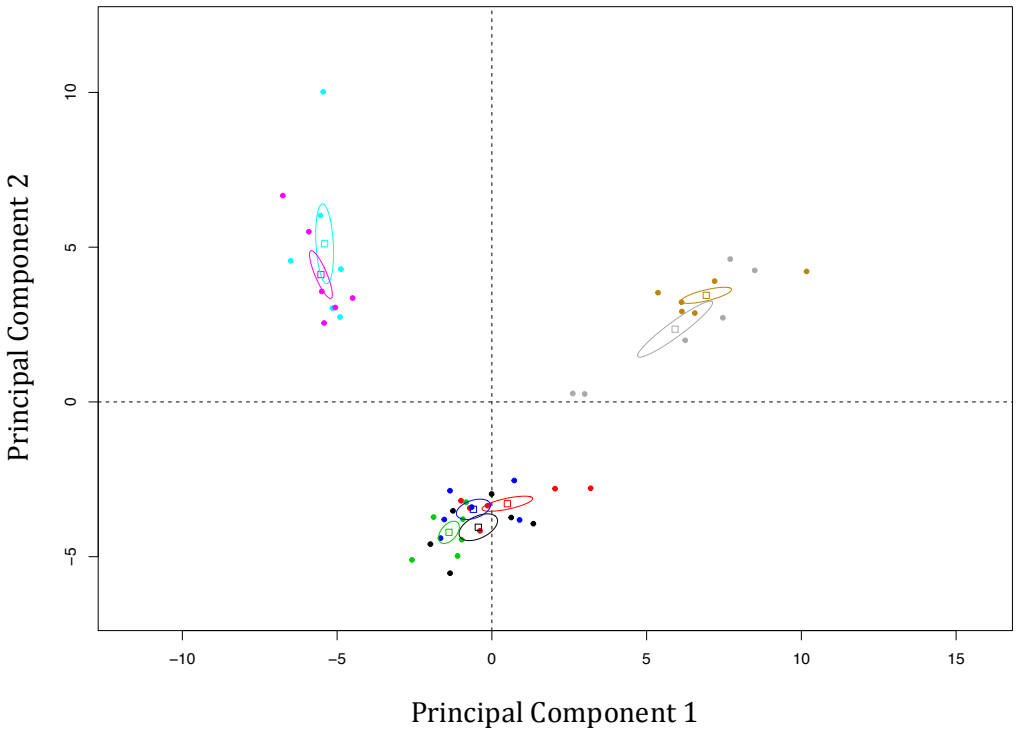

Figure 6.1. Principal component analysis (correlation matrix-based) bi-plot of sixty chemical variables studied in the plant material included in this investigation (compare to Fig. 6.3). Two *Thuja plicata* seedling lines (124 and 129), a clonal line of *Thuja standishii* and a clonal line of *T. standishii* × *plicata* were real- (+) and mock-inoculated (-) with *Didymascella thujina* (cedar leaf blight, CLB) in a controlled conditions environment. Samples from all line × infection status combinations were collected just before the infections were set up (0 days post inoculation, dpi), and 4 and 8 dpi. Confidence interval for the ellipses is 50%. Ellipses and samples were colour-coded as follows: *T. plicata* 124 CLB^- in black, *T. plicata* 124 CLB^+ in red, *T. plicata* 129 CLB^- in green, *T. plicata* 129 CLB^+ in blue, *T. standishii* CLB^- in cyan, *T. standishii* CLB^+ in magenta, *T. standishii* × *plicata* CLB^- in grey, and *T. standishii* × *plicata* CLB^+ in brown.

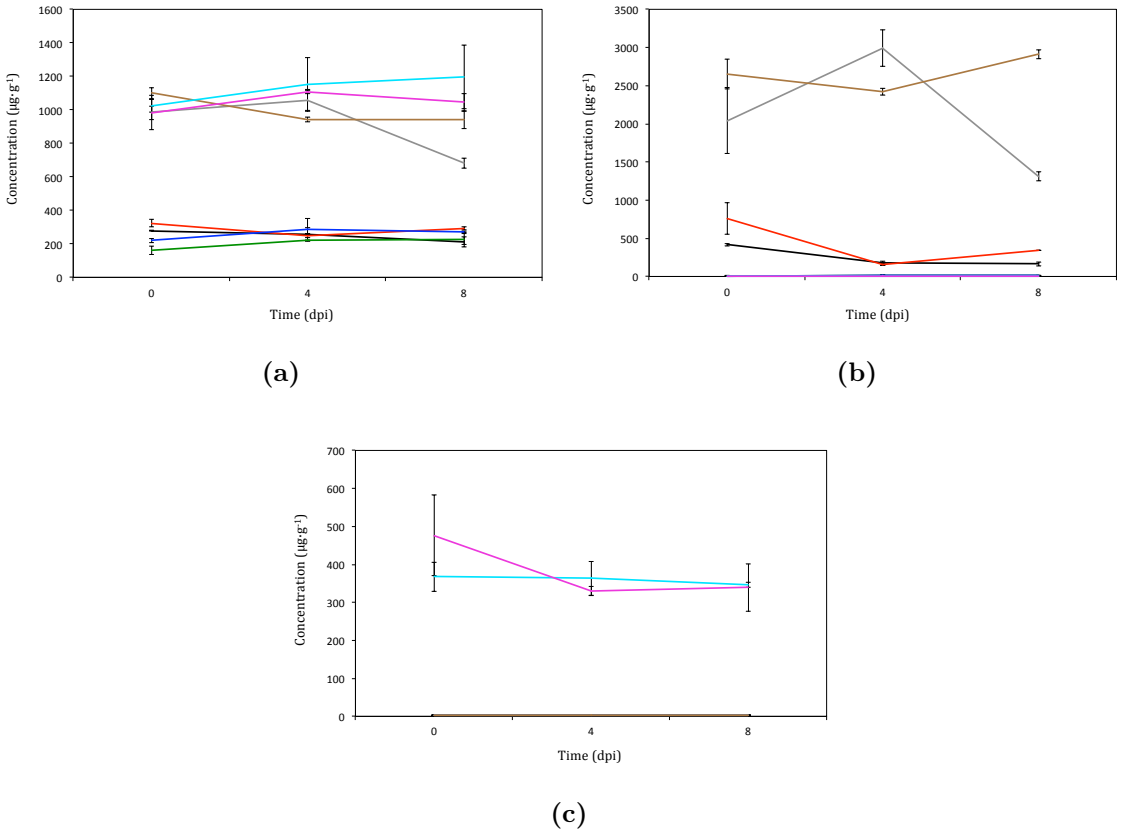

Figure 6.2. Mean concentrations (± standard errors) at three time points of three chemical variables that discriminated among two *Thuja plicata* seedling lines, a *Thuja standishii* clonal line, and a *T. standishii* × *plicata* clonal line according to categorical stability selection: (a) citronellyl acetate, (b) α-gurjunene, (c) 3-carene. Samples were grouped in three categories (*T. standishii*, *T. plicata*, and *T. standishii* × *plicata*) regardless of the infection condition, and then, the chemical variables were ranked using categorical stability selection (see also methods). Treatments were colour-coded as follows: *T. plicata* 124 CLB$^-$ in black, *T. plicata* 124 CLB$^+$ in red, *T. plicata* 129 CLB$^-$ in green, *T. plicata* 129 CLB$^+$ in blue, *T. standishii* CLB$^-$ in cyan, *T. standishii* CLB$^+$ in magenta, *T. standishii* × *plicata* CLB$^-$ in grey, and *T. standishii* × *plicata* CLB$^+$ in brown.

Aluminum was the only variable that displayed temporal variation after infection in the real- vs. mock-infected plants according to changepoint analysis on the ranked stability selection scores of the chemical variables. Analysis of variance revealed significant differences in the concentration of aluminum among plant lines ($p = 0.0008$), infection status ($p < 0.0000$), time points ($p < 0.0000$), and all factor combinations (line×infection status, $p = 0.0030$; line×time, $p = 0.0006$; infection status×time, $p < 0.0000$; and line×infection status×time, $p = 0.0003$). The Tukey HSD all-pairwise comparisons test on the line×infection status×time factor combination also showed that (refer to Table 6.4): i) all 0 dpi samples grouped together regardless of the infection status (i.e. CLB^- and CLB^+; homogeneous group *b*), ii) all samples from 8 dpi in the CLB^- condition grouped together regardless of the plant line (homogeneous group *e*), iii) samples from both *T. plicata* lines and *T. standishii* × *plicata* taken 8 dpi in the CLB^+ condition were grouped together (homogeneous group *c*), and iv) the *T. standishii* mean aluminum concentration from 8 dpi samples in the CLB^+ condition was all alone (homogeneous group *a*). It is worth noting that the mean aluminum concentration of *T. standishii* in the CLB^+ infection condition at 8 dpi was 581.3 $\mu g \cdot g^{-1}$, while the second highest aluminum concentration in this experiment was almost 10 times lower (58.8 $\mu g \cdot g^{-1}$, from samples belonging to *T. plicata* line 124 taken at 0 dpi in the CLB^- infection status).

Table 6.4. Mean aluminum concentrations (in $\mu g \cdot g^{-1}$) in the plant material used in this investigation. Three-way analysis of variance showed significant differences in all factors and factor combinations (data were $\log_{10}$-transformed to meet the normality assumption). Superscripts refer to homogeneous groups in the line×infection status×time factor combination according to the Tukey HSD all-pairwise comparisons test. dpi = days post infection.

		Time (dpi)	
Line	**Infection status**	**0**	**8**
Thuja plicata 124	Mock infection (CLB^-)	58.8^{b}	$1.4^{d,e}$
	Real infection (CLB^+)	55.0^{b}	$19.9^{b,c}$
Thuja plicata 129	Mock infection (CLB^-)	$8.4^{b,c,d}$	$3.3^{c,d,e}$
	Real infection (CLB^+)	54.2^{b}	$15.6^{b,c}$
Thuja standishii × *plicata*	Mock infection (CLB^-)	57.0^{b}	1.0^{e}
	Real infection (CLB^+)	53.5^{b}	$4.4^{c,d,e}$
Thuja standishii	Mock infection (CLB^-)	53.5^{b}	$1.5^{d,e}$
	Real infection (CLB^+)	55.2^{b}	581.3^{a}

6.3.2.2 Gene expression

The transcriptome assembly consisted of 311,664 Trinity transcripts. The overall alignment rate was 98.16% (overall alignment rates per sample are shown in Appendix A.35). 77,886 of the transcripts resulted in annotation hits, 68.31% belonging to plant species, 14.45% to fungi and 17.24% to other taxa (Appendix A.30 includes further assembly statistics). There were 27,432 differentially expressed transcripts among all samples, which accounted for 8.80% of the transcriptome's sequences. More than half of the DE transcripts were plant sequences (52.46%), followed by sequences with no annotation hits (39.15%).

BLASTn searches for the two publicly available ITS2 sequences of *D. thujina* (queries KT875766 and KT875767) in the assembled transcriptome resulted in four hits for KT875766 and the same number of hits for KT875767. E-values of the transcripts ranged between 6×10^{-72} and 3×10^{-70} for the results of query KT875766, and between 4×10^{-73} and 2×10^{-71} for the hits of query KT875767. Percentage of identities of the resulting hits were between 80.32% and 80.59% for query KT875766, and between 80.53% and 80.80% for query KT875767. The top result from both searches for *D. thujina* sequences (transcript *TRINITY_DN93692_c2_g1_i1*) had many more reads mapped in the CLB^+ samples (62.132 transcripts per million [TPM] in total) than in the CLB^- ones (3.664 TPM in total).

Principal component analysis of the DE transcripts showed that each line is genetically different, and that CLB^- samples clustered separately from the CLB^+ treatment within each line, except for *T. standishii* (Fig. 6.3). The expression profiles of *T. plicata* samples from both lines were highly correlated to each other, and to a lesser extent to *T. standishii* × *plicata* (Appendix A.38). The *T. standishii* expression profile had very low correlation to that of either *T. plicata* or *T. standishii* × *plicata*.

Hierarchical clustering

Eighteen clusters of transcripts with minimum 4-fold change and maximum 0.001 false discovery rates were produced after cutting the tree at 43.3% of its height (Fig. 6.4). Six of the clusters accounted for 94.4% of the DE expressed sequences. The biggest cluster was composed of 13,794 sequences, and the smallest had just one.

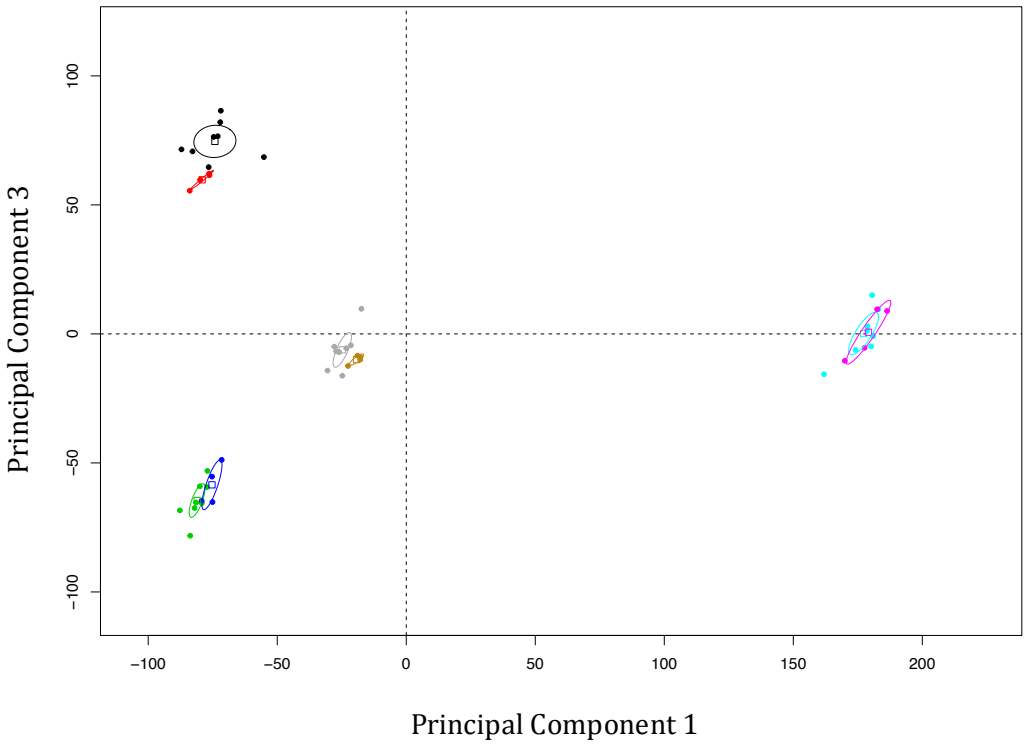

Figure 6.3. Principal component analysis bi-plot (correlation matrix-based) of the 27,432 differentially expressed transcripts found in this investigation (compare to Fig. 6.1). Two *Thuja plicata* seedling lines (124 and 129), one *Thuja standishii* clonal line, and a clonal line of *T. standishii* × *plicata* were exposed to real- (CLB^+) and mock- (CLB^-) infections with *Didymascella thujina* (cedar leaf blight, CLB) in growth chambers at the Bev Glover Growth Facility (University of Victoria). Samples from all treatments were collected just prior to inoculations (0 days post infection, dpi), and 4 and 8 dpi. Principal components (PC) 1-3 explained 62.79% of the samples' variance (40.38%, 14.14% and 8.27% for PC 1, 2 and 3, respectively). PC 1 discriminated among *T. plicata*, *T. standishii* and *T. standishii* × *plicata*, PC 2 clustered *T. standishii* × *plicata* in one group and the rest in another, and PC 3 separated the *T. plicata* lines from each other but reunited the other lines in a single group. Notice that CLB^- and CLB^+ samples group separately within each line except for *T. standishii*. Ellipses have a 95% confidence. Samples and ellipses were colour-coded as follows: *T. plicata* 124 CLB^- in black, *T. plicata* 124 CLB^+ in red, *T. plicata* 129 CLB^- in green, *T. plicata* 129 CLB^+ in blue, *T. standishii* CLB^- in cyan, *T. standishii* CLB^+ in magenta, *T. standishii* × *plicata* CLB^- in grey, and *T. standishii* × *plicata* CLB^+ in brown.

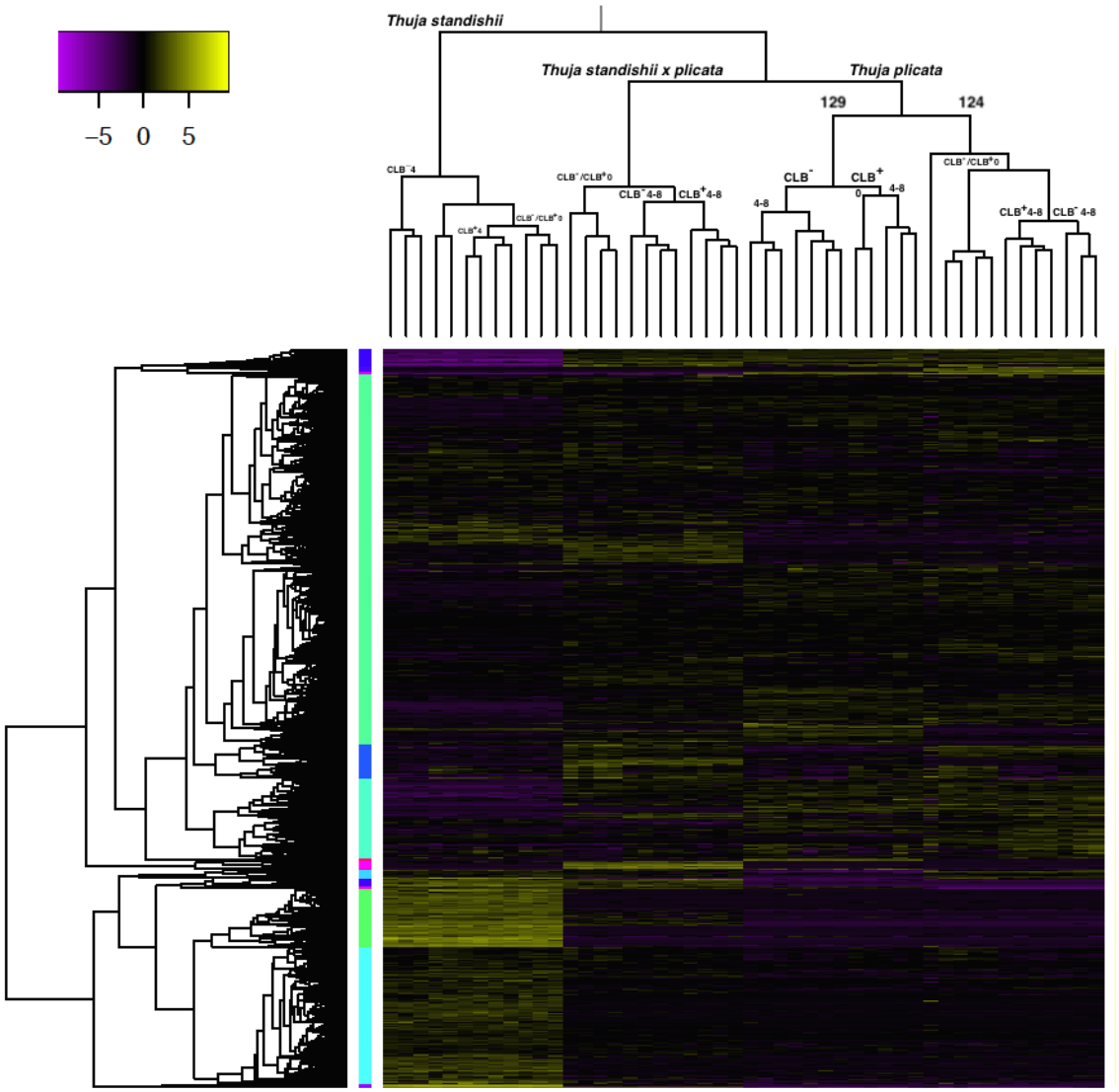

Figure 6.4. Heat-map of 27,432 differentially expressed transcripts among two lines of *Thuja plicata* seedlings (124 and 129), one *Thuja standishii* clonal line, and a *T. standishii* × *plicata* clonal line. All lines were infected (+) and mock-infected (-) with *Didymascella thujina* (cedar leaf blight, CLB) under controlled conditions, and samples collected 0, 4, and 8 days post infection (dpi). Eighteen clusters were produced after cutting the transcripts' tree at 43.3% of its height. The following six clusters included 94.4% of the transcripts: light green (13,794 sequences), cyan (5,086 sequences), dark cyan (2,953 sequences), green (2,197 sequences), blue (1,277 sequences) and dark blue (593 sequences). Important nodes are labeled: each clonal line clustered as an independent "monophyletic" group, and both *T. plicata* lines grouped together, each one being "monophyletic" as well. Numbers refer to dpi, and CLB^-/CLB^+ to mock and real infections, respectively. Expression levels are $\log_2$-transformed and centred TPMs that were colour-coded according to the top left bar (yellow = high expression, purple, low expression).

Seven of the clusters had between 100 and 600 sequences, and 6 included fewer than 100 transcripts. Among all of the DE sequences, 2,197 transcripts were at high expression levels exclusively in *T. standishii* (green cluster in Fig. 6.4), while 593 were at very low levels in that same species (dark blue cluster in Fig. 6.4). 5,086 sequences had high expression levels in *T. standishii* with varying expression levels in the other species and hybrid (cyan cluster in Fig. 6.4). 2,953 transcripts had low expression levels in *T. standishii*, but high expression levels in both *T. plicata* lines (dark cyan cluster in Fig. 6.4). 1,277 sequences had low levels of expression in *T. standishii*, but higher levels in *T. standishii* × *plicata* and *T. plicata* line 124 (blue cluster in Fig. 6.4). The cluster with most sequences (13,794, light green in Fig. 6.4) did not have a specific expression pattern.

Grade of Membership Analysis

Hierarchical clustering of the samples and of the static topics using the ω matrix produced by *CountClust* showed that topic 1 had higher ω values in *Thuja plicata* regardless of the seedling line, that topic 2 had higher values in *Thuja standishii*, and topic 3, and to a lesser extent topic 7, had high ω in *Thuja standishii* × *plicata* (Fig. 6.5). Table 6.5 shows the top 10 transcripts per topic from each plant species according to their θ values.

A closer look at the sequences in Table 6.5 reveals some interesting patterns. Two transcripts were shared among the top ten transcripts of those four static topics (*TRINITY_DN86213_c8_g2_i2* and *TRINITY_DN87363 _c15_g3_i1*). Transcripts *TRINITY_DN188465_c0_g1_i1* (a peptidase vacuolar-processing enzyme), *TRINITY_DN85473_c0_g1_i1* (plastocyanin), *TRINITY_DN65470_c0_g2_i1* (photosystem I reaction center subunit psaK) and *TRINITY_DN79613_c1_g1_i1* (metallothionein-like protein EMB30) were unique to *T. plicata*, whereas transcripts *TRINITY_DN101197_c2_g1_i2* (chlorophyll a-b binding protein 1B), *TRINITY_DN94350_c0_g2_i2* (glutamine synthetase cytosolic isozyme), *TRINITY_DN88193_c0_g1_i2* (oxygen-evolving enhancer protein 1), *TRINITY_DN65470_c0_g1_i1* (photosystem I reaction center subunit psaK), and *TRINITY_DN95836_c2_g1_i3* (a bark storage protein) were exclusive to *T. standishii*. The rest of the transcripts from both *T. plicata* and *T. standishii* were shared with *T. standishii* × *plicata*. Only three sequences were unique to *T. standishii* × *plicata*: *TRIN-*

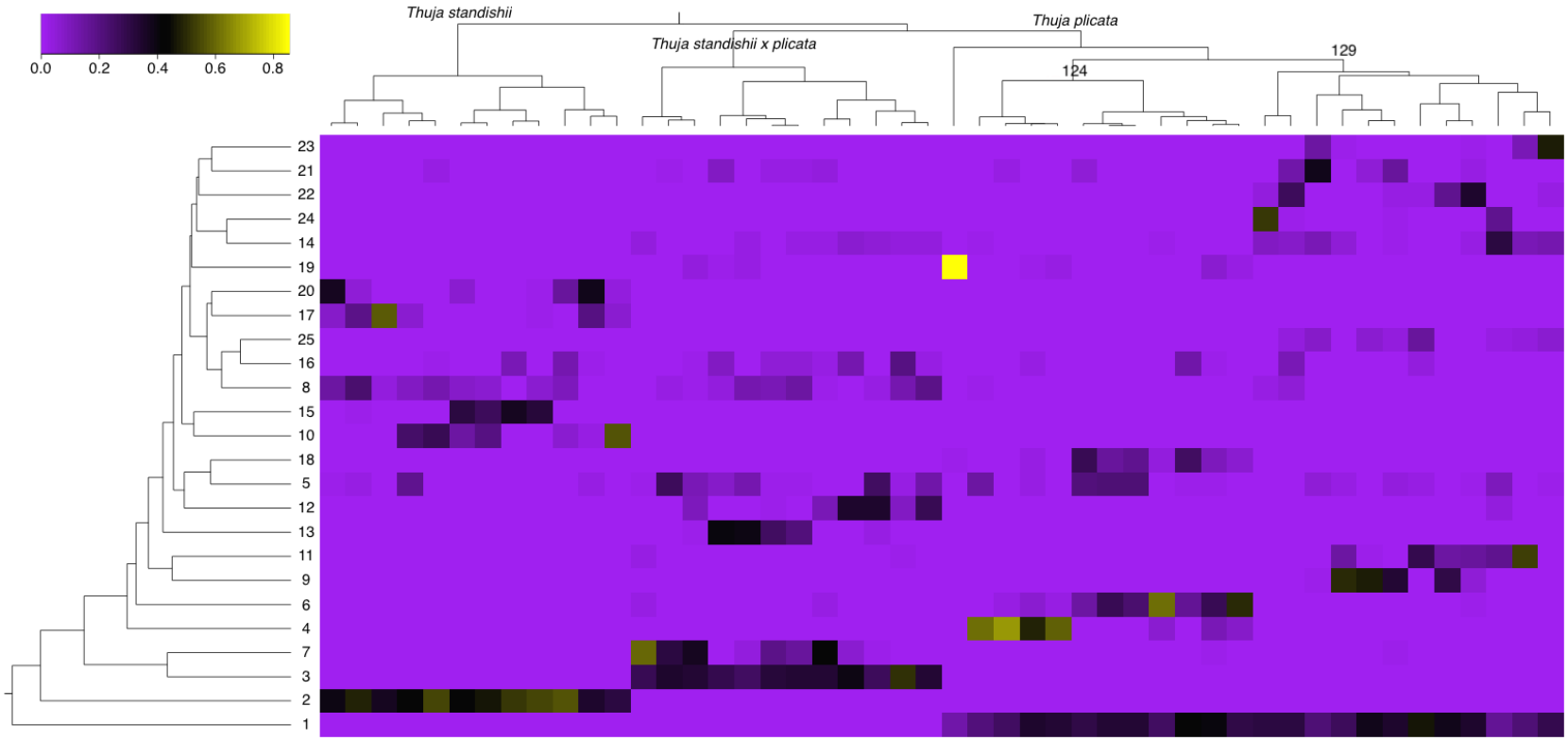

Figure 6.5. Heat-map of samples versus static topics used in the grade of membership (GoM) analysis. GoM analysis is a dimension reduction technique based on the latent Dirichlet allocation method that, in this case, groups transcripts based on their co-occurrences. Each of the 25 topics is a probability distribution over the 27,432 differentially expressed transcripts (θ matrix in *CountClust*), and each of the 48 samples is a probability distribution over the 25 topics (ω matrix in *CountClust*). The ω matrix was used as the input to generate the above map using hierarchical clustering with Euclidean distance (top-ranked static topics per sample/line were those with higher ω values). Samples from each line studied grouped "monophyletically" (top tree). The vertical tree on the left refers to the topic clustering. Notice that topics 1, 2 and 3 had high ω values in *Thuja plicata*, *Thuja standishii*, and *Thuja standishii* $\times$ *plicata*, respectively. Topic 7 also had high ω values in *T. standishii* $\times$ *plicata* (see text for more details). Omega values were colour-coded as per the top left bar (purple = low, yellow = high).

Table 6.5. Top ten transcripts of the representative static topics per species in Fig. 6.5. *CountClust* used the latent Dirichlet allocation method to topic model the transcriptomic data so that each of the 25 topics became a probability distribution over the 27,432 differentially expressed Trinity transcripts (θ matrix). The top 10 driving transcripts per topic were chosen based on their decreasing θ values. Annotations were the result of BLASTX searches carried out on Swiss-Prot.

Species	Static topic	Transcript	θ	E-value	Organism	Annotation	Process	Cellular component
Thuja plicata	1	*TRINITY_DN88193_c0_g1_i1*	0.031515	0	*Nicotiana* sp.	Oxygen-evolving enhancer protein 1	Photosystem II stabilization	Chloroplast thylakoid membrane
		TRINITY_DN101197_c2_g1_i5	0.027770	2.0×10^{-163}	*Lycopersicon* sp.	Chlorophyll a-b binding protein 1B	Chlorophyll binding	Chloroplast thylakoid membrane
		TRINITY_DN75032_c0_g2_i1	0.026541	2.0×10^{-46}	*Arabidopsis* sp.	Protein translation factor SUI1 homolog 1	Translation initiation factor activity	
		TRINITY_DN188465_c0_g1_i1	0.014009	0	*Phaseolus* sp.	Vacuolar-processing enzyme	Cysteine-type peptidase activity	
		TRINITY_DN83144_c0_g1_i1	0.013308	4.0×10^{-150}	*Lycopersicon* sp.	Chlorophyll a-b binding protein 4	Chlorophyll binding	Chloroplast thylakoid membrane
		TRINITY_DN85473_c0_g1_i1	0.013301	2.0×10^{-48}	*Spinacia* sp.	Plastocyanin		Chloroplast
		TRINITY_DN86213_c8_g2_i2	0.012733	6.0×10^{-14}	*Phalaenopsis* sp.	Uncharacterized protein ORF91		Chloroplast
		TRINITY_DN87363_c15_g3_i1	0.011284	NA	No hits	No hits		
		TRINITY_DN65470_c0_g2_i1	0.010763	8.0×10^{-35}	*Hordeum* sp.	Photosystem I reaction center subunit psaK	Chlorophyll binding	Chloroplast thylakoid membrane
		TRINITY_DN79613_c1_g1_i1	0.009533	5.0×10^{-07}	*Picea* sp.	Metallothionein-like protein EMB30	Metal ion binding	
Thuja standishii	2	*TRINITY_DN101197_c2_g1_i2*	0.034676	1.0×10^{-163}	*Lycopersicon* sp.	Chlorophyll a-b binding protein 1B	Chlorophyll binding	Chloroplast
		TRINITY_DN86213_c8_g2_i2	0.024418	6.0×10^{-14}	*Phalaenopsis* sp.	Uncharacterized protein ORF91		Chloroplast
		TRINITY_DN87363_c15_g3_i1	0.021744	NA	No hits	No hits		
		TRINITY_DN96614_c0_g2_i1	0.017587	4.0×10^{-70}	*Larix* sp.	Ribulose bisphosphate carboxylase small chain	Reductive pentose-phosphate cycle	Chloroplast
		TRINITY_DN94350_c0_g2_i2	0.017401	0	*Pinus* sp.	Glutamine synthetase cytosolic isozyme	Glutamine biosynthetic process	Cytoplasm
		TRINITY_DN87363_c15_g1_i1	0.014563	NA	No hits	No hits		
		TRINITY_DN88193_c0_g1_i2	0.014338	0	*Nicotiana* sp.	Oxygen-evolving enhancer protein 1	Photosystem II stabilization	Chloroplast thylakoid membrane
		TRINITY_DN65470_c0_g1_i1	0.014068	8.0×10^{-35}	*Hordeum* sp.	Photosystem I reaction center subunit psaK	Chlorophyll binding	Chloroplast thylakoid membrane
		TRINITY_DN95836_c2_g1_i1	0.010976	3.0×10^{-41}	*Populus* sp.	Bark storage protein A	Nucleoside metabolic process	
		TRINITY_DN95836_c2_g1_i3	0.010646	1.0×10^{-34}	*Populus* sp.	Bark storage protein A	Nucleoside metabolic process	
Thuja standishii × *plicata*	3	*TRINITY_DN96614_c0_g2_i1*	0.026375	4.0×10^{-70}	*Larix* sp.	Ribulose bisphosphate carboxylase small chain	Reductive pentose-phosphate cycle	Chloroplast
		TRINITY_DN86213_c8_g2_i2	0.024902	6.0×10^{-14}	*Phalaenopsis* sp.	Uncharacterized protein ORF91		Chloroplast
		TRINITY_DN87363_c15_g3_i1	0.023113	NA	No hits	No hits		
		TRINITY_DN75032_c0_g2_i1	0.018670	2.0×10^{-46}	*Arabidopsis* sp.	Protein translation factor SUI1 homolog 1	Translation initiation factor activity	
		TRINITY_DN95836_c2_g1_i1	0.015803	3.0×10^{-41}	*Populus* sp.	Bark storage protein A	Nucleoside metabolic process	
		TRINITY_DN87363_c15_g1_i1	0.015746	NA	No hits	No hits		
		TRINITY_DN101197_c2_g1_i5	0.015405	2.0×10^{-163}	*Lycopersicon* sp.	Chlorophyll a-b binding protein 1B	Chlorophyll binding	Chloroplast thylakoid membrane
		TRINITY_DN88193_c0_g1_i1	0.015343	0	*Nicotiana* sp.	Oxygen-evolving enhancer protein 1	Photosystem II stabilization	Chloroplast thylakoid membrane
		TRINITY_DN83144_c0_g1_i1	0.013702	4.0×10^{-150}	*Lycopersicon* sp.	Chlorophyll a-b binding protein 4	Chlorophyll binding	Chloroplast thylakoid membrane
		TRINITY_DN86213_c8_g2_i3	0.013634	4.0×10^{-50}	*Phalaenopsis* sp.	Uncharacterized protein ORF91		Chloroplast
	7	*TRINITY_DN96614_c0_g2_i1*	0.022728	4.0×10^{-70}	*Larix* sp.	Ribulose bisphosphate carboxylase small chain	Reductive pentose-phosphate cycle	Chloroplast
		TRINITY_DN88193_c0_g1_i1	0.019028	0	*Nicotiana* sp.	Oxygen-evolving enhancer protein 1	Photosystem II stabilization	Chloroplast thylakoid membrane
		TRINITY_DN95569_c0_g2_i1	0.017399	0	*Glycine* sp.	Catalase-3	Hydrogen peroxide catabolic process	Cytoplasm
		TRINITY_DN83144_c0_g1_i1	0.015359	4.0×10^{-150}	*Lycopersicon* sp.	Chlorophyll a-b binding protein 4	Chlorophyll binding	Chloroplast thylakoid membrane
		TRINITY_DN84814_c1_g1_i1	0.013753	7.0×10^{-152}	*Arabidopsis* sp.	Probable xyloglucan endotransglucosylase/hydrolase protein 7	Cell wall biogenesis	Apoplast/cell wall
		TRINITY_DN101197_c2_g1_i5	0.012345	2.0×10^{-163}	*Lycopersicon* sp.	Chlorophyll a-b binding protein 1B	Chlorophyll binding	Chloroplast thylakoid membrane
		TRINITY_DN86213_c8_g2_i2	0.012209	6.0×10^{-14}	*Phalaenopsis* sp.	Uncharacterized protein ORF91		Chloroplast
		TRINITY_DN87363_c15_g3_i1	0.011075	NA	No hits	No hits		
		TRINITY_DN75032_c0_g2_i1	0.008907	2.0×10^{-46}	*Arabidopsis* sp.	Protein translation factor SUI1 homolog 1	Translation initiation factor activity	
		TRINITY_DN102033_c1_g1_i2	0.008691	0	*Picea* sp.	Chalcone synthase 7	Flavonoid biosynthetic process	

ITY_DN86213_c8_g2_i3 (an uncharacterized protein), *TRINITY_DN84814_c-1_g1_i1* (probable xyloglucan endotransglucosylase/hydrolase protein 7), and *TRINITY_DN102033_c1_g1_i2* (chalcone synthase 7). Interestingly, bark storage proteins (*TRINITY_DN95836_c2_g1_i1* and *TRINITY_DN95836_c2_g1_i3*) were common only to *T. standishii* and *T. standishii* × *plicata*. It is worth noting that more than half of the sequences in Table 6.5 were located in the chloroplasts. It is equally important to highlight that one of the characteristics of GoM analysis is that sequences shared between/among species are usually at similar expression levels in the taxa involved (e.g. transcripts *TRINITY_DN86213_c8_g2_i2* and *TRINITY_DN87363_c15_g3_i1*, Appendix A.42), while transcripts that are present only in one of the topics/species are at higher expression levels in the relevant species in comparison to the rest (e.g. *TRINITY_DN94350_c0_g2_i2* in *T. standishii*, Appendix A.43).

In relation to the two *T. plicata* seedling lines, topics 4 and 6 had the highest ω values in line 124, and topics 9 and 11 had high ω values in line 129 (Fig. 6.5). Many of the top ten sequences from those topics were also located in the chloroplast (Appendix A.44). The same two transcripts that were shared among topics 1, 2, 3 and 7 (*TRINITY_DN86213_c8_g2_i2* and *TRINITY_DN87363_c15_g3_i1*, Table 6.5) were present in topics 6, 9 and 11 (Appendix A.44). Several sequences from topics 4, 6, and 9 were shared with *T. standishii* × *plicata*, but the only transcripts related to defense response (*TRINITY_DN63359_c0_g1_i1* and *TRINITY_DN76260_c0_g1_i1*) belonged exclusively to the more resistant *T. plicata* line (129, Appendix A.44). Interestingly, catalase-3 (*TRINITY_DN95569_c0_g2_i1*) was present only in *T. plicata* line 129 (Appendix A.44) and in *T. standishii* × *plicata* (Table 6.5).

Stability Selection Analyses

Categorical

There were 60 transcripts that depicted major responses to *D. thujina* infection in the plant lines studied according to the changepoint algorithm (Table 6.6). Almost one-quarter of the transcripts in Table 6.6 had "defense response" as the biological process, and almost half of the sequences were located either in the apoplast, the cell

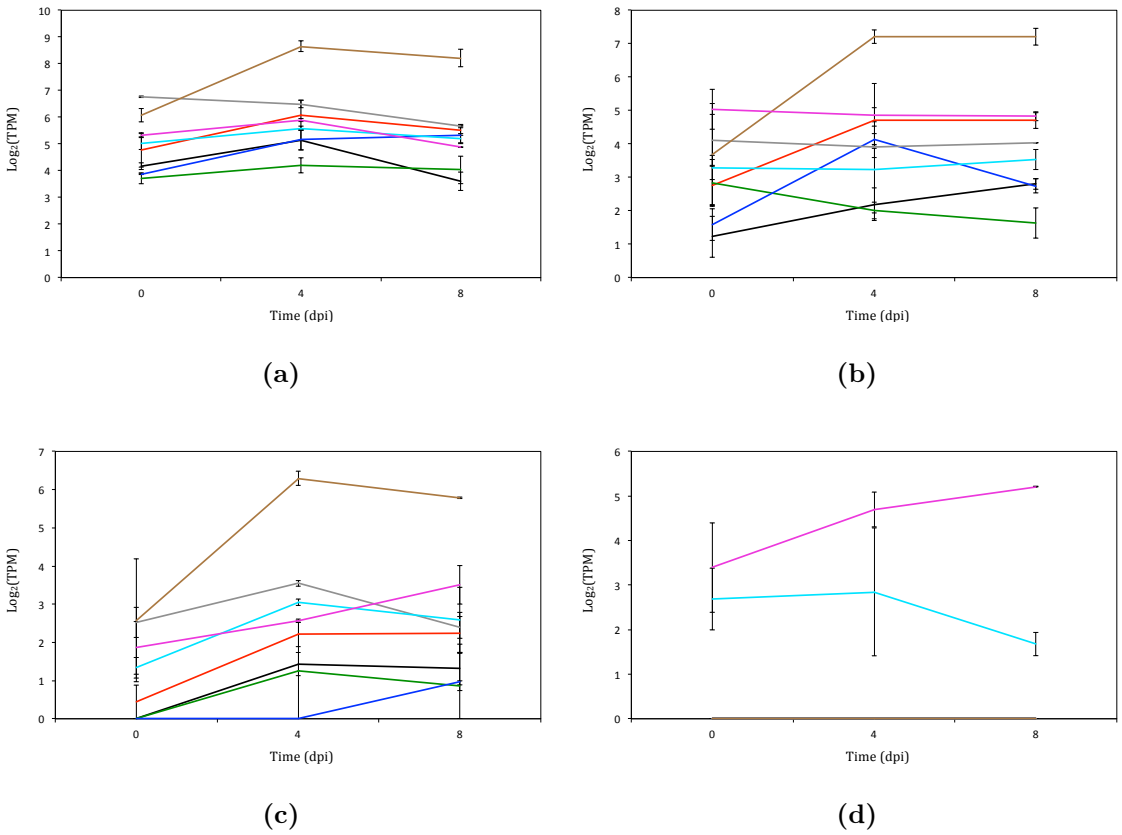

Figure 6.6. Selected predictors (transcripts) of *D. thujina* infection as detected by the categorical stability selection analysis (see also Table 6.6). (a) *TRINITY_DN90538_c2_g1_i2* (pathogenesis-related protein 1C), (b) *TRINITY_DN97888_c0_g1_i1* (endochitinase At2g43610), (c) *TRINITY_DN99675_c1_g1_i5* (disease resistance response protein 206), (d) *TRINITY_DN81079_c0_g2_i1* (cationic peroxidase 1). Note that the expression values of those transcripts tend to be higher in *T. standishii* and *T. standishii* × *plicata* regardless of their infection status in comparison to *T. plicata* lines. Error bars are standard errors. Treatments were colour-coded as follows: *T. plicata* 124 CLB$^-$ in black, *T. plicata* 124 CLB$^+$ in red, *T. plicata* 129 CLB$^-$ in green, *T. plicata* 129 CLB$^+$ in blue, *T. standishii* CLB$^-$ in cyan, *T. standishii* CLB$^+$ in magenta, *T. standishii* × *plicata* CLB$^-$ in grey, and *T. standishii* × *plicata* CLB$^+$ in brown.

Table 6.6. Top 60 predictors (transcripts) of *D. thujina* infection according to the change point analysis on the ranked scores of the categorical stability selection analysis. The dynamic topic to which the transcripts ranked first is included (based on the top $\beta_{0,k}$). All annotations are based on BLASTX searches done on the Swiss-Prot database. Annotations with an asterisk were based on BLASTP searches on the same database.

Transcript	Stability selection (score)	E-value	Organism	Annotation	Process	Cellular component	Dynamic topic per transcript (based on $\beta_{0,k}$)
TRINITY_DN98866_c1_g1_i1	0.3404	6.0×10^{-57}	*Arachis* sp.	Cationic peroxidase 1	Response to oxidative stress	Extracellular region	10
TRINITY_DN88179_c0_g2_i2	0.328	1.0×10^{-64}	*Arabidopsis* sp.	Glutathione S-transferase U23	Response to toxic substance	Cytoplasm	12
TRINITY_DN99675_c1_g1_i3	0.3264	3.0×10^{-34}	*Pisum* sp.	Disease resistance response protein 206	Defense response	Apoplast	23
TRINITY_DN102903_c8_g1_i1	0.3101	1.0×10^{-15}	*Prunus* sp.	Major allergen Pru ar 1	Defense response		23
TRINITY_DN97687_c0_g1_i10	0.2889	3.0×10^{-13}	*Arabidopsis* sp.	Pentatricopeptide repeat-containing protein At5g16860			23
TRINITY_DN97272_c0_g2_i4	0.288	NA	No hits	No hits			23
TRINITY_DN102582_c0_g1_i1	0.2861	0	*Arabidopsis* sp.	Phosphatidylinositol 4-kinase gamma 5			12
TRINITY_DN102737_c2_g2_i1	0.2775	3.0×10^{-28}	*Arabidopsis* sp.	L-gulonolactone oxidase 5	L-ascorbic acid biosynthetic process	Cell wall, membrane	11
TRINITY_DN43626_c0_g3_i1	0.2717	NA	No hits	No hits			11
TRINITY_DN99675_c1_g1_i1	0.2545	1.0×10^{-6}	*Pisum* sp.	Disease resistance response protein 206	Defense response	Apoplast	16
TRINITY_DN98866_c2_g1_i1	0.2423	4.0×10^{-42}	*Arachis* sp.	Cationic peroxidase 1	Response to oxidative stress	Extracellular region	10
TRINITY_DN101901_c4_g1_i1	0.2285	3.0×10^{-71}	*Arabidopsis* sp.	Omega-hydroxypalmitate O-feruloyl transferase	Cell wall pectin biosynthetic process		15
TRINITY_DN74723_c0_g3_i1	0.2273	2.0×10^{-155}	*Picea* sp.	Pinene synthase	Terpene synthase activity	Chloroplast	16
TRINITY_DN97676_c2_g3_i1	0.2209	NA	No hits	No hits			14
TRINITY_DN99675_c1_g1_i5	0.2208	3.0×10^{-37}	*Pisum* sp.	Disease resistance response protein 206	Defense response	Apoplast	16
TRINITY_DN95732_c2_g1_i2	0.1809	2.0×10^{-46}	*Oryza* sp.	B3 domain-containing protein Os04g0581400	Regulation of transcription, *DNA*-templated	Nucleus	21
TRINITY_DN102903_c9_g10_i8	0.1756	NA	No hits	No hits			2
TRINITY_DN94417_c1_g1_i2	0.1717	2.0×10^{-24}	*Alnus* sp.	Major pollen allergen Aln g 1	Defense response	Cytoplasm	18
TRINITY_DN96603_c2_g1_i10	0.1674	1.0×10^{-35}	*Arabidopsis* sp.	Protein EDS1B	Defense response	Cytoplasm, nucleus	23
TRINITY_DN84374_c0_g1_i1	0.1649	5.0×10^{-54}	*Antirrhinum* sp.	Myb-related protein 308	Regulation of transcription, *DNA*-templated	Nucleus	13
TRINITY_DN97489_c1_g2_i2	0.1647	NA	No hits	No hits	Structural constituent of cell wall		13
TRINITY_DN102903_c9_g10_i4	0.1585	NA	No hits	No hits			2
TRINITY_DN93904_c0_g1_i1	0.1501	0	*Arabidopsis* sp.	Methionine gamma-lyase	Methionine catabolic process via 2-oxobutanoate	Cytosol	12
TRINITY_DN98866_c2_g1_i2	0.1489	8.0×10^{-21}	*Arachis* sp.	Cationic peroxidase 1	Response to oxidative stress	Extracellular region	11
TRINITY_DN96424_c0_g1_i1	0.1437	NA	No hits	No hits			24
TRINITY_DN85247_c0_g1_i1	0.1435	NA	No hits	No hits			2
TRINITY_DN99198_c8_g3_i1	0.1373	1.0×10^{-123}	*Arabidopsis* sp.	Cysteine-rich receptor-like protein kinase 2	Defense response	Plasma membrane, plasmodesma	13
TRINITY_DN99675_c1_g1_i4	0.1358	2.0×10^{-31}	*Pisum* sp.	Disease resistance response protein 206	Defense response	Apoplast	16
TRINITY_DN100699_c0_g1_i3	0.1301	7.0×10^{-53}	*Arabidopsis* sp.	LOB domain-containing protein 39			13
TRINITY_DN87161_c4_g3_i5	0.1237	5.0×10^{-45}	*Arabidopsis* sp.	Cytochrome P450 76C1	Secondary metabolite biosynthetic process	Integral component of membrane	12
TRINITY_DN97162_c2_g3_i3	0.1202	4.0×10^{-18}	*rabidopsis* sp.	Phytosulfokine receptor 1	Regulation of defense response	Plasma membrane	18
TRINITY_DN101724_c2_g1_i3	0.1201	6.0×10^{-80}	*Pinus* sp.	Cytochrome P450 750A1		Integral component of membrane	16
TRINITY_DN92947_c0_g1_i1	0.1193	1.0×10^{-23}	*Arabidopsis* sp.	Probable E3 ubiquitin-protein ligase XERICO	Response to chitin	Integral component of membrane	2
TRINITY_DN98289_c7_g1_i1	0.1161	1.0×10^{-12}	*Arabidopsis* sp.	Protein NUCLEAR FUSION DEFECTIVE 4	Karyogamy	Integral component of membrane	2
TRINITY_DN91108_c2_g1_i1	0.1155	1.0×10^{-27}	*Arabidopsis* sp.	Protein C2-DOMAIN ABA-RELATED 3	Abscisic acid-activated signaling pathway	Plasma membrane, nucleus	1
TRINITY_DN95044_c1_g1_i1	0.1132	7.0×10^{-76}	*Arabidopsis* sp.	Glucan endo-1,3-beta-glucosidase 3	Defense response	Anchored component of plasma membrane	17
TRINITY_DN79867_c2_g1_i1	0.1112	5.0×10^{-15}	*Prunus* sp.	Major allergen Pru ar 1	Defense response		12
TRINITY_DN100609_c11_g11_i1	0.1076	NA	No hits	No hits			11
TRINITY_DN81079_c0_g2_i1	0.1063	2.0×10^{-64}	*Arachis* sp.	Cationic peroxidase 1	Response to oxidative stress	Extracellular region	11
TRINITY_DN88249_c0_g1_i2	0.1002	8.0×10^{-101}	*Arabidopsis* sp.	Aquaporin TIP2-1	Water transport	Most organelles	24
TRINITY_DN90538_c2_g1_i4	0.0941	2.0×10^{-58}	*Nicotiana* sp.	Pathogenesis-related protein 1C	Defense response	Extracellular region	2
TRINITY_DN98294_c1_g1_i5	0.0933	2.0×10^{-98}	*Linum* sp.	Allene oxide synthase	Oxylipin biosynthetic process	Chloroplast	13
TRINITY_DN89963_c0_g1_i3	0.0877	1.0×10^{-7}	*Arabidopsis* sp.	Uncharacterized mitochondrial protein AtMg00300*		Mitochondrion	11
TRINITY_DN97162_c1_g2_i2	0.0877	4.0×10^{-76}	*Arabidopsis* sp.	Receptor-like protein kinase 2	Viral process	Plasma membrane	2
TRINITY_DN97482_c0_g1_i3	0.0861	5.0×10^{-58}	*Cannabis* sp.	Tetrahydrocannabinolic acid synthase	Flavin adenine dinucleotide binding	Apoplast	13
TRINITY_DN94333_c1_g1_i2	0.0849	NA	No hits	No hits			10
TRINITY_DN75539_c0_g1_i1	0.0829	NA	No hits	No hits			21
TRINITY_DN97888_c0_g1_i1	0.0819	2.0×10^{-89}	*Arabidopsis* sp.	Endochitinase At2g43610	Defense response	Plasma membrane	16
TRINITY_DN78208_c0_g2_i1	0.0805	0	*Arabidopsis* sp.	Cytochrome P450 734A1	Response to brassinosteroid	Integral component of membrane	13
TRINITY_DN97175_c0_g1_i1	0.0798	NA	No hits	No hits			11
TRINITY_DN96744_c0_g2_i1	0.0759	1.0×10^{-40}	*Arabidopsis* sp.	Homeobox-leucine zipper protein HAT2	Transcription, *DNA*-templated	Nucleus	12
TRINITY_DN97272_c0_g1_i1	0.075	NA	No hits	No hits			23
TRINITY_DN90538_c2_g1_i2	0.074	4.0×10^{-64}	*Nicotiana* sp.	Pathogenesis-related protein 1C	Defense response	Extracellular region	2
TRINITY_DN97272_c0_g2_i3	0.0715	2.0×10^{-12}	*Arabidopsis* sp.	Chaperone protein dnaJ 8		Chloroplast	15
TRINITY_DN88249_c0_g1_i4	0.0711	2.0×10^{-100}	*Antirrhinum* sp.	Probable aquaporin TIP-type	Water transport	Most organelles	4
TRINITY_DN70581_c0_g1_i1	0.0636	4.0×10^{-13}	*Arabidopsis* sp.	G-type lectin S-receptor-like serine/threonine-protein kinase RLK1	Protein serine/threonine kinase activity	Plasma membrane	16
TRINITY_DN94297_c0_g3_i2	0.0623	4.0×10^{-82}	*Arabidopsis* sp.	Wall-associated receptor kinase 5	Protein serine/threonine kinase activity	Integral component of membrane	13
TRINITY_DN11103_c0_g1_i1	0.0615	NA	No hits	No hits			16
TRINITY_DN89168_c0_g2_i7	0.0597	2.0×10^{-25}	*Arabidopsis* sp.	Leucine-rich repeat receptor-like protein kinase PXC2	Protein kinase activity	Plasma membrane	11
TRINITY_DN99198_c8_g3_i2	0.0589	5.0×10^{-40}	*Arabidopsis* sp.	Cysteine-rich receptor-like protein kinase 2	Defense response	Plasma membrane, plasmodesma	4

wall, the plasma membrane or the extracellular region. Four dynamic topics (2, 11, 13 and 16) accounted for more than half of the sequences in Table 6.6.

Fourteen of the sequences in Table 6.6 did not result in annotations to any known protein. There were two major allergens, three cytochrome P450s, two cysteine-rich receptor-like protein kinases, and two pathogenesis-related protein 1C. Transcripts of the pathogenesis-related protein 1C were at higher levels of expression in *T. standishii* × *plicata* in comparison to the other lines regardless of the infection status (e.g. transcript *TRINITY_DN90538_c2_g1_i2*; Fig. 6.6a). Other defense-related proteins included the glucan endo-1,3-beta-glucosidase 3 (sequence *TRINITY_DN95044_c1_g1_i1*), the protein EDS1B (transcript *TRINITY_DN96603_c2_g1_i10*) and the phytosulfokine receptor 1 (sequence *TRINITY_DN97162_c2_g3_i3*). The endochitinase At2g43610 (transcript *TRINITY_DN97888_c0_g1_i1*) was at higher expression levels in the CLB^+ treatments of both *T. standishii* × *plicata* and *T. standishii* (Fig. 6.6b).

It is noteworthy that four sequences were annotated as "disease resistance response protein 206", three of them belonging to dynamic topic 16 (Table 6.6). Their expression levels, in general, were higher in both *T. standishii* and *T. standishii* × *plicata* in comparison to the *T. plicata* lines regardless of the infection status (see e.g. transcript *TRINITY_DN99675_c1_g1_i5*, Fig. 6.6c). Another four transcripts were annotated as "cationic peroxidase 1". Two of those pertained to dynamic topic 10 and two to 11. Transcripts of the cationic peroxidase 1 were higher in infected clones of *T. standishii* and *T. standishii* × *plicata* in general, but in some cases they were present exclusively in *T. standishii* clones, regardless of their infection status (e.g. transcript *TRINITY_DN81079_c0_g2_i1*, Fig. 6.6d).

Regression using aluminum as a response variable

Given that aluminum concentrations were very high in *T. standishii* after infection (see section 6.3.2.1), it was decided to explore what sequences might be predictors of such a response by conducting regression stability selection on the expression values of the DE transcripts using the aluminum concentrations as a response variable. There were 47 transcripts that explained the observed aluminum concentrations as chosen by changepoint (Table 6.7). Near half of the sequences in Table 6.7 belonged to three

dynamic topics. The group with the most sequences was dynamic topic 11, followed by dynamic topics 8 and 12.

Many of the sequences captured by this analysis (Table 6.7) related to: i) growth and development (*TRINITY_DN102384_c2_g1_i2*, *TRINITY_DN94463_c2_g2_i5*, *TRINITY_DN96105_c1_g1_i5*, *TRINITY_DN90757_c0_g1_i3*, *TRINITY_DN102968_c0_g1_i1* and *TRINITY_DN90039_c0_g1_i1*), ii) regulation of gene expression (*TRINITY_DN101864_c0_g1_i5*, *TRINITY_DN98694_c2_g1_i1*, *TRINITY_DN97033_c0_g1_i3*, *TRINITY_DN91331_c1_g1_i8* and *TRINITY_DN86187_c0_g1_i1*), and iii) calcium signalling (*TRINITY_DN102764_c1_g1_i2*, *TRINITY_DN102721_c4_g1_i3*, *TRINITY_DN95987_c1_g2_i4* and *TRINITY_DN88958_c0_g1_i1*). Other sequences of interest detected by the analysis were in the heat shock pathway (*TRINITY_DN95934_c0_g1_i1* and *TRINITY_DN96352_c0_g1_i1*), sulfate transport (*TRINITY_DN73957_c0_g1_i2*), and regulation of the cell cycle (*TRINITY_DN99989_c0_g1_i3*). Interestingly, transcript *TRINITY_DN97175_c0_g1_i1* was shared with the previous analysis (see categorical stability selection, and Table 6.6).

The regression stability selection analysis also detected several transcripts with higher or lower levels of expression in *T. standishii* in relation to the other lines. Those sequences were related to calcium metabolism (e.g. *TRINITY_DN102764_c1_g1_i2* and *TRINITY_DN95987_c1_g2_i4*), and sulfur metabolism (*TRINITY_DN73957_c0_g1_i2*). Transcript *TRINITY_DN102764_c1_g1_i2* (G-type lectin S-receptor-like serine/threonine-protein kinase RLK1), a calmodulin binding protein, was expressed exclusively in *T. standishii* plants that were infected with *D. thujina* (Fig. 6.7a). Transcript *TRINITY_DN95987_c1_g2_i4* (protein QUIRKY), a calcium-dependent phospholipid binding protein, had higher expression levels in *T. standishii* (especially in plants in the CLB^+ condition) in comparison to the other lines (Fig 6.7b). Transcript *TRINITY_DN73957_c0_g1_i2* was the only sulfate transporter detected by stability selection, and was fully repressed in *T. standishii*-CLB^+ clones (Fig. 6.7c). The only sequence with "response to fungus" as a process annotation (*TRINITY_DN81123_c1_g1_i8*) was at higher expression levels in all infected plants except for *T. standishii* × *plicata* (Fig. 6.7d). Furthermore, the expression levels of that transcript were much higher in *D. thujina*-infected *T. standishii* plants in comparison to the other lines.

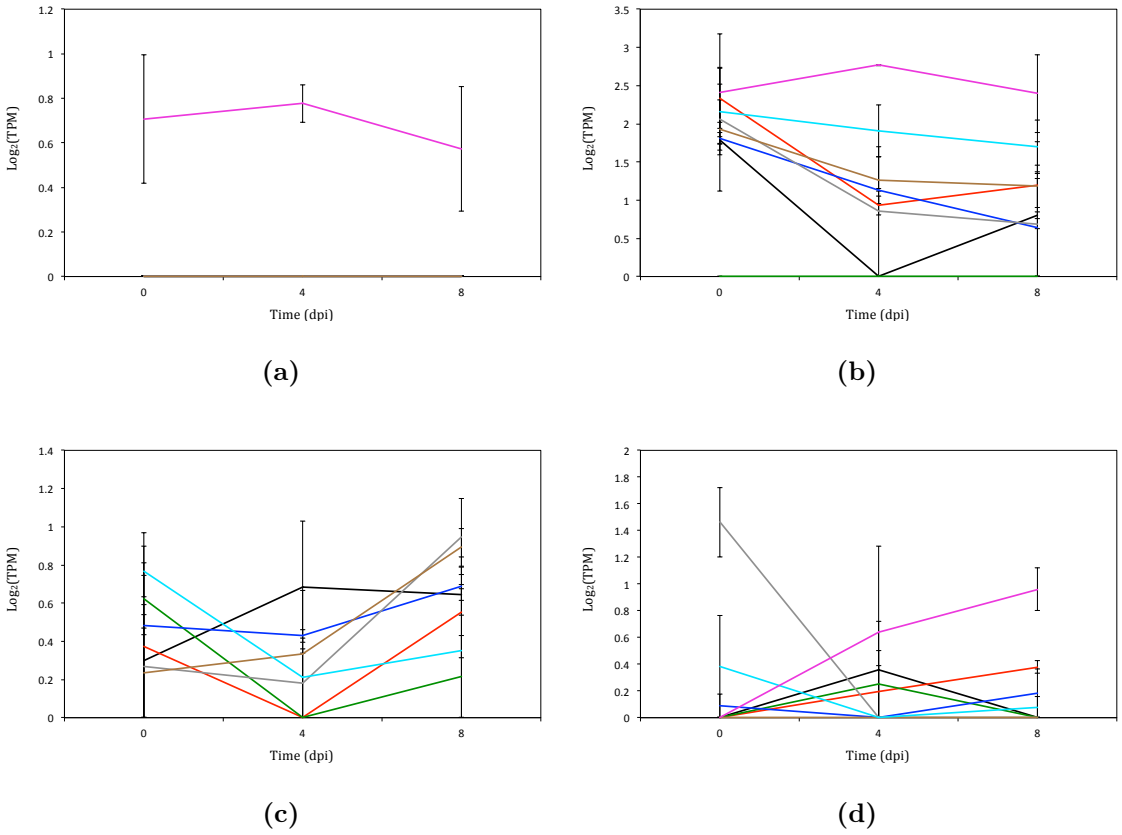

Figure 6.7. Selected predictors of the observed aluminum concentrations as detected by the regression stability selection analysis (see also Table 6.7). (a) *TRINITY_DN102764_c1_g1_i2* (G-type lectin S-receptor-like serine/threonine-protein kinase RLK1), (b) *TRINITY_DN95987_c1_g2_i4* (protein QUIRKY), (c) *TRINITY_DN73957_c0_g1_i2* (sulfate transporter 4.1, chloroplastic), (d) *TRINITY_DN81123_c1_g1_i8* (transcriptional corepressor LEUNIG). Note that the expression values of those transcripts tend to be higher in *T. standishii* and *T. standishii* × *plicata* regardless of their infection status in comparison to *T. plicata* lines. Error bars are standard errors. Treatments were colour-coded as follows: *T. plicata* 124 CLB$^-$ in black, *T. plicata* 124 CLB$^+$ in red, *T. plicata* 129 CLB$^-$ in green, *T. plicata* 129 CLB$^+$ in blue, *T. standishii* CLB$^-$ in cyan, *T. standishii* CLB$^+$ in magenta, *T. standishii* × *plicata* CLB$^-$ in grey, and *T. standishii* × *plicata* CLB$^+$ in brown.

Table 6.7. Top 47 predictors (transcripts) of the aluminum concentration according to the change point analysis on the ranked scores of the regression stability selection analysis. The dynamic topic to which the transcripts ranked first is included (based on the top $\beta_{0,k}$). All annotations are based on BLASTX searches done on the Swiss-Prot database.

Transcript	Stability selection (score)	E-value	Organism	Annotation	Process	Cellular component	Dynamic topic per transcript (based on $\beta_{0,k}$)
TRINITY_DN101864_c0_g1_i5	0.3674	5.0×10^{-144}	*Arabidopsis* sp.	Pentatricopeptide repeat-containing protein At1g71210			11
TRINITY_DN98111_c0_g3_i5	0.3399	4.0×10^{-58}	*Lycopersicon* sp.	Beta-galactosidase	Carbohydrate metabolic process		11
TRINITY_DN102384_c2_g1_i2	0.3141	1.0×10^{-167}	*Arabidopsis* sp.	Serine/threonine-protein kinase Nek5	Epidermal-cell morphogenesis		8
TRINITY_DN102764_c1_g1_i2	0.2717	5.0×10^{-141}	*Arabidopsis* sp.	G-type lectin S-receptor-like serine/threonine-protein kinase RLK1	Calmodulin binding	Plasma membrane	11
TRINITY_DN94477_c0_g1_i1	0.2583	NA	No hits	No hits			23
TRINITY_DN99989_c0_g1_i3	0.2472	2.0×10^{-123}	*Oryza* sp.	Cyclin-T1-4	Cell division/cycle	Nucleus	11
TRINITY_DN94463_c2_g2_i5	0.1921	9.0×10^{-97}	*Arabidopsis* sp.	Protein SHOOT GRAVITROPISM 5	Regulation of transcription, *DNA*-templated		12
TRINITY_DN9534_c0_g1_i1	0.1755	1.0×10^{-31}	*Glycine* sp.	17.9 kDa class II heat shock protein		Cytoplasm	8
TRINITY_DN86699_c0_g1_i3	0.1551	NA	No hits	No hits	Cell cycle, mitotic nuclear division	Nucleus	8
TRINITY_DN87674_c0_g1_i4	0.1515	3.0×10^{-68}	*Arabidopsis* sp.	Probable receptor-like protein kinase At1g33260	Protein serine/threonine kinase activity		17
TRINITY_DN96105_c1_g1_i5	0.1512	5.0×10^{-106}	*Arabidopsis* sp.	AP2-like ethylene-responsive transcription factor ANT	Multicellular organism development	Nucleus	11
TRINITY_DN82714_c0_g1_i1	0.1457	1.0×10^{-176}	*Arabidopsis* sp.	Carboxypeptidase SOL1	Protein processing	Extracellular space	25
TRINITY_DN90039_c0_g1_i1	0.1444	2.0×10^{-84}	*Arabidopsis* sp.	Putative E3 ubiquitin-protein ligase RING1a	Cell fate determination	Nucleus	23
TRINITY_DN99663_c1_g1_i2	0.1431	NA	No hits	No hits			12
TRINITY_DN73957_c0_g1_i2	0.1396	0	*Arabidopsis* sp.	Sulfate transporter 4.1, chloroplastic	Sulfate transmembrane transport	Chloroplast membrane	20
TRINITY_DN102721_c4_g1_i3	0.1339	0	*Arabidopsis* sp.	Glutamate receptor 3.4	Calcium-mediated signaling	Plasma membrane, plastid	16
TRINITY_DN98694_c2_g1_i1	0.1282	6.0×10^{-77}	*Oryza* sp.	Zinc finger CCCH domain-containing protein 24	Metal ion binding		21
TRINITY_DN58163_c0_g1_i1	0.1246	NA	No hits	No hits			11
TRINITY_DN97033_c0_g1_i3	0.1238	0	*Oryza* sp.	Protein argonaute 7	Gene silencing by miRNA	Cytoplasm	8
TRINITY_DN102643_c0_g1_i21	0.1237	NA	No hits	No hits			11
TRINITY_DN81123_c1_g1_i8	0.1183	1.0×10^{-149}	*Arabidopsis* sp.	Transcriptional corepressor LEUNIG	Response to fungus	Nucleus	16
TRINITY_DN96970_c0_g1_i1	0.1152	0	*Arabidopsis* sp.	Probable *DNA* primase large subunit	Primosome complex	*DNA* primase activity	5
TRINITY_DN99793_c0_g1_i2	0.111	NA	No hits	No hits			8
TRINITY_DN91043_c1_g1_i3	0.1019	9.0×10^{-36}	*Arabidopsis* sp.	Putative UPF0481 protein At3g02645		Integral component of membrane	11
TRINITY_DN144112_c0_g1_i1	0.1014	NA	No hits	No hits			2
TRINITY_DN87220_c0_g1_i2	0.0986	NA	No hits	No hits			6
TRINITY_DN95030_c3_g1_i1	0.0979	4.0×10^{-11}	*Arabidopsis* sp.	Chaperone protein dnaJ 49		Integral component of membrane	20
TRINITY_DN90757_c0_g1_i3	0.0954	6.0×10^{-69}	*Arabidopsis* sp.	Protein root UVB sensitive 6			9
TRINITY_DN96507_c0_g1_i6	0.0949	NA	No hits	No hits			16
TRINITY_DN102259_c0_g1_i1	0.0943	7.0×10^{-15}	*Arabidopsis* sp.	*DNA* topoisomerase 3-alpha			20
TRINITY_DN86187_c0_g1_i1	0.0942	2.0×10^{-41}	*Arabidopsis* sp.	B-box zinc finger protein 19	Transcription factor activity	Nucleus	22
TRINITY_DN95987_c1_g2_i4	0.0941	0	*Arabidopsis* sp.	Protein QUIRKY	Calcium-dependent phospholipid binding	Plasma membrane, plasmodesma	8
TRINITY_DN97175_c0_g1_i1	0.0912	NA	No hits	No hits			11
TRINITY_DN102968_c0_g1_i1	0.0894	8.0×10^{-57}	*Oryza* sp.	Two-component response regulator-like PRR73	Phosphorelay signal transduction system	Nucleus	11
TRINITY_DN91331_c1_g1_i8	0.0885	5.0×10^{-37}	*Arabidopsis* sp.	Transcription factor bHLH81	Transcription from *RNA* polymerase II promoter	Nucleus	25
TRINITY_DN93146_c0_g1_i1	0.0861	NA	No hits	No hits			12
TRINITY_DN88590_c0_g2_i3	0.0838	1.0×10^{-140}	*Pinus* sp.	Cytochrome P450 750A1		Integral component of membrane	5
TRINITY_DN97886_c0_g1_i1	0.0818	0	*Arabidopsis* sp.	HIPL1 protein	Carbohydrate metabolic process	Anchored component of plasma membrane	20
TRINITY_DN97762_c0_g1_i4	0.0814	NA	No hits	No hits			13
TRINITY_DN88958_c0_g1_i1	0.0757	0	*Lycopersicon* sp.	Calcium-transporting ATPase, endoplasmic reticulum-type	Calcium ion transmembrane transport	Integral component of endoplasmic reticulum membrane	8
TRINITY_DN100449_c0_g1_i1	0.0752	2.0×10^{-128}	*Arabidopsis* sp.	Pentatricopeptide repeat-containing protein At5g15010, mitochondrial		Mitochondrial	16
TRINITY_DN96352_c0_g1_i1	0.0732	1.0×10^{-45}	*Glycine* sp.	17.9 kDa class II heat shock protein		Cytoplasm	12
TRINITY_DN86276_c0_g1_i1	0.0725	3.0×10^{-14}	*Arabidopsis* sp.	Rhomboid-like protein 14, mitochondrial	Serine-type endopeptidase activity	Mitochondrial membrane	9
TRINITY_DN103015_c2_g4_i1	0.0725	NA	No hits	No hits			11
TRINITY_DN97757_c1_g3_i3	0.0713	0	*Arabidopsis* sp.	Myosin-11	Actin filament-based movement	Cytoplasm	1
TRINITY_DN44694_c0_g2_i1	0.0712	NA	No hits	No hits			9
TRINITY_DN100722_c0_g1_i11	0.0668	NA	No hits	No hits			12

Dynamic topic modelling

Dynamic topic modelling was used to model the expression of transcripts within gene groups (topics) through the three time points sampled in this investigation. The results of the stability selection analyses allowed the detection of the main dynamic topics related to *D. thujina* infection by studying the top topic per transcript at time 0 ($\beta_{0,k}$) in Tables 6.6 and 6.7. Topics 2, 11, 13 and 16 were the most frequent amongst the transcripts chosen by categorical stability selection (see Table 6.6), and topics 8, 11 and 12 were the most prevalent among sequences detected by regression stability selection using aluminum as a response variable (see Table 6.7). In this section, emphasis is given to the most frequent topics from transcripts ranked by categorical stability selection (i.e. topics 2, 11, 13 and 16; Table 6.8 and Figs. 6.8a-6.9b) since this investigation focused on the responses to *D. thujina* infection in *Thuja* sp. plants.

Dynamic topic 2 included transcripts with higher levels of expression in *T. standishii* × *plicata* and both *T. plicata* lines in comparison to *T. standishii*. Among the top 10 sequences in this topic (Table 6.8), two were related to gene expression regulation (*TRINITY_DN75032_c0_g2_i1* and *TRINITY_DN96279_c0_g1_i1*), two to photosynthesis (*TRINITY_DN101197_c2_g1_i5* and *TRINITY_DN88193_c0_g1_i1*), another two to stress response (*TRINITY_DN94654_c1_g2_i1*, *TRINITY_DN100731_c3_g1_i2*), and one was involved in defense response (glucan endo-1,3-beta-glucosidase 1, transcript *TRINITY_DN97934_c0_g1_i1*). Three of the top ten sequences in dynamic topic 2 were also among the top 10 transcripts of static topics 1, 3 and 7 (*TRINITY_DN75032_c0_g2_i1*, *TRINITY_DN101197_c2_g1_i5* and *TRINITY_DN88193_c0_g1_i1*; see also Table 6.5). Most transcripts in this topic depicted relatively steady expression levels over time, except for transcript *TRINITY_DN87437_c1_g2_i2* that showed increased modelled levels at 4 dpi which were maintained until 8 dpi (Fig. 6.8a).

Dynamic topic 11 referred to transcripts that were expressed prominently in *T. standishii* but not in *T. standishii* × *plicata* or either of the *T. plicata* lines. Half of the top 10 sequences of this topic were located in the chloroplast and were involved in photosynthesis (*TRINITY_DN101197_c2_g1_i2*, *TRINITY_DN96614_c0_g2_i1*, *TRINITY_DN88193_c0_g1_i2*, *TRINITY_DN65470_c0_g1_i1* and *TRINITY_-*

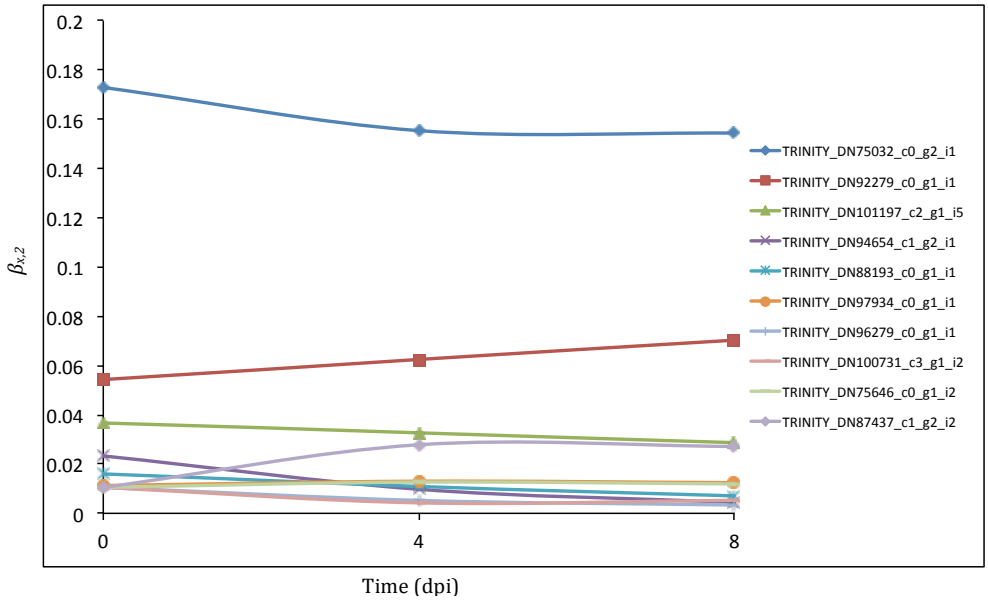

(a)

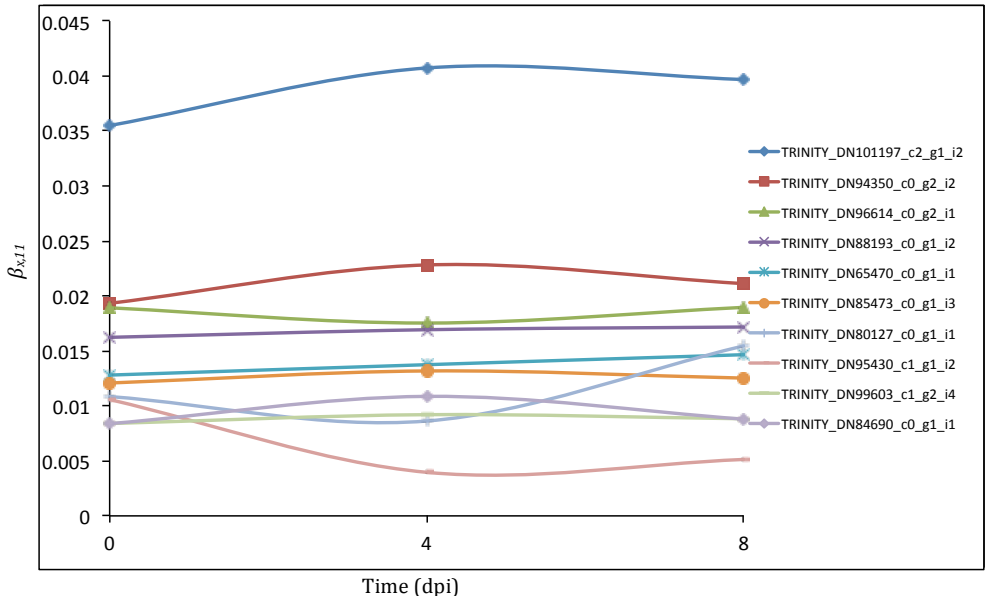

(b)

Figure 6.8. Most frequent dynamic topics (2 and 11) detected in the categorical stability selection analysis. Differential expression count (*RNA*-Seq) data were fitted into 25 dynamic topics ($k = 25$) with the Dynamic Topic Models software (https://github.com/blei-lab/dtm ; see methods). The graphs show the inferred posterior expression distribution per transcript per time point ($\beta_{x,k}$) of the top 10 transcripts of topics 2 and 11. (a) Dynamic topic 2, (b) dynamic topic 11. x = dpi = days post infection.

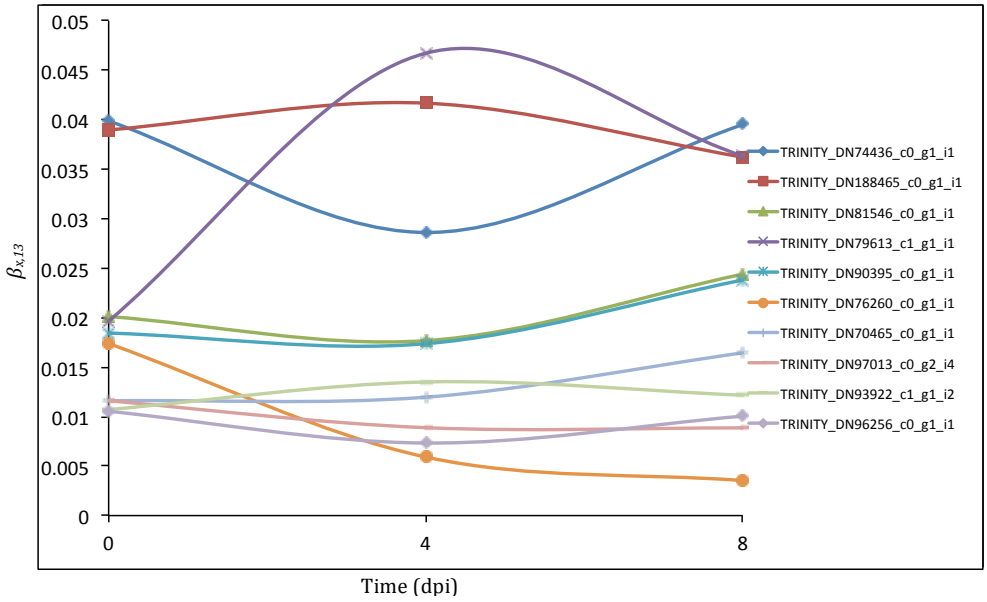

(a)

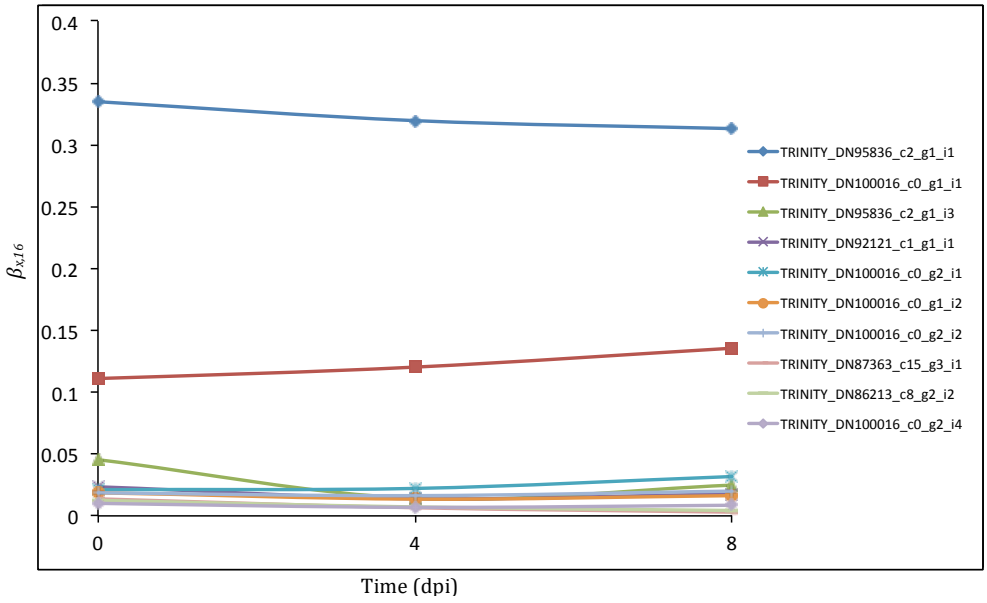

(b)

Figure 6.9. Most frequent dynamic topics (13 and 16) detected in the categorical stability selection analysis. Differential expression count (*RNA*-Seq) data were fitted into 25 dynamic topics ($k = 25$) with the Dynamic Topic Models software (https://github.com/blei-lab/dtm ; see methods). The graphs show the inferred posterior expression distribution per transcript per time point ($\beta_{x,k}$) of the top 10 transcripts of topics 13 and 16. (a) Dynamic topic 13, (b) dynamic topic 16. x = dpi = days post infection.

Table 6.8. Top 10 transcripts per dynamic topic of the four most frequent topics among the transcripts detected in the categorical stability selection analysis used to capture predictor sequences of *Didymascella thujina* infection. Count data of the DE transcripts were modelled into 25 topics using the Dynamic Topic Models software (https://github.com/blei-lab/dtm). The sequences shown were ranked within each topic based on their $\beta_{0,k}$ values. All annotations were the result of BLASTX searches done on the Swiss-Prot database. Annotations with an asterisk resulted from BLASTP searches on the same database.

Dynamic topic (k)	Transcript	$\beta_{0,k}$	E-value	Organism	Annotation	Process	Cellular component
2	*TRINITY_DN75032_c0_g2_i1*	0.17317	2.0×10^{-46}	*Arabidopsis* sp.	Protein translation factor SUI1 homolog 1	Translation initiation factor activity	
	TRINITY_DN92279_c0_g1_i1	0.05407	6.0×10^{-173}	*Ajuga* sp.	Galactinol synthase 1	Galactose metabolic process	Cytoplasm
	TRINITY_DN101197_c2_g1_i5	0.03690	2.0×10^{-163}	*Lycopersicon* sp.	Chlorophyll a-b binding protein 1B	Chlorophyll binding	Chloroplast thylakoid membrane
	TRINITY_DN94654_c1_g2_i1	0.02355	8.0×10^{-8}	*Arabidopsis* sp.	Dehydrin Xero 1*	Response to stress	Cytosol
	TRINITY_DN88193_c0_g1_i1	0.01617	0	*Nicotiana* sp.	Oxygen-evolving enhancer protein 1	Photosystem II stabilization	Chloroplast thylakoid membrane
	TRINITY_DN97934_c0_g1_i1	0.01128	9.0×10^{-137}	*Arabidopsis* sp.	Glucan endo-1,3-beta-glucosidase 11	Defense response	Anchored component of plasma membrane
	TRINITY_DN96279_c0_g1_i1	0.01063	9.0×10^{-13}	*Lycopersicon* sp.	Histone H1	*DNA* binding	Nucleus
	TRINITY_DN100731_c3_g1_i2	0.01057	0	*Oryza* sp.	Chaperone protein ClpB1	Protein metabolic process	Cytosol, nucleus
	TRINITY_DN75646_c0_g1_i2	0.01055	NA	No hits	No hits		
	TRINITY_DN87437_c1_g2_i2	0.01046	NA	No hits	No hits		
11	*TRINITY_DN101197_c2_g1_i2*	0.03550	1.0×10^{-163}	*Lycopersicon* sp.	Chlorophyll a-b binding protein 1B	Chlorophyll binding	Chloroplast
	TRINITY_DN94350_c0_g2_i2	0.01930	0	*Pinus* sp.	Glutamine synthetase cytosolic isozyme	Glutamine biosynthetic process	Cytoplasm
	TRINITY_DN96614_c0_g2_i1	0.01892	4.0×10^{-70}	*Larix* sp.	Ribulose bisphosphate carboxylase small chain	Reductive pentose-phosphate cycle	Chloroplast
	TRINITY_DN88193_c0_g1_i2	0.01624	0	*Nicotiana* sp.	Oxygen-evolving enhancer protein 1	Photosystem II stabilization	Chloroplast thylakoid membrane
	TRINITY_DN65470_c0_g1_i1	0.01281	8.0×10^{-35}	*Hordeum* sp.	Photosystem I reaction center subunit psaK	Chlorophyll binding	Chloroplast thylakoid membrane
	TRINITY_DN85473_c0_g1_i3	0.01207	6.0×10^{-49}	*Lycopersicon* sp.	Plastocyanin		Chloroplast
	TRINITY_DN80127_c0_g1_i1	0.01090	7.0×10^{-54}	*Oryza* sp.	Tricin synthase 1	Methylation	Nucleus
	TRINITY_DN95430_c1_g1_i2	0.01054	0	*Sesamum* sp.	Inositol-3-phosphate synthase	Phospholipid biosynthetic process	Cytoplasm
	TRINITY_DN99603_c1_g2_i4	0.00840	0	*Picea* sp.	S-adenosylmethionine synthase 2	S-adenosylmethionine biosynthetic process	Cytoplasm
	TRINITY_DN84690_c0_g1_i1	0.00833	0	*Zea* sp.	Polyamine oxidase	Spermine oxidase activity	
13	*TRINITY_DN74436_c0_g1_i1*	0.03990	2.0×10^{-88}	*Nepenthes* sp.	Aspartic proteinase nepenthesin-2	Aspartic-type endopeptidase activity	Extracellular region
	TRINITY_DN188465_c0_g1_i1	0.03902	0	*Phaseolus* sp.	Vacuolar-processing enzyme	Cysteine-type peptidase activity	
	TRINITY_DN81546_c0_g1_i1	0.02015	0	*Beta* sp.	Glucose-1-phosphate adenylyltransferase large subunit	Starch biosynthetic process	Chloroplast, amyloplast
	TRINITY_DN79613_c1_g1_i1	0.01967	5.0×10^{-7}	*Picea* sp.	Metallothionein-like protein EMB30	Metal ion binding	
	TRINITY_DN90395_c0_g1_i1	0.01850	0	*Antirrhinum* sp.	Granule-bound starch synthase 1	Starch biosynthetic process	Chloroplast, amyloplast
	TRINITY_DN76260_c0_g1_i1	0.01739	1.0×10^{-29}	*Arabidopsis* sp.	MLP-like protein 423	Defense response	Membrane
	TRINITY_DN70465_c0_g1_i1	0.01161	3.0×10^{-172}	*Arabidopsis* sp.	Cytochrome P450 709B2		Integral component of membrane
	TRINITY_DN97013_c0_g2_i4	0.01154	0	*Oryza* sp.	Galactinol–sucrose galactosyltransferase	Response to abscisic acid	Chloroplast
	TRINITY_DN93922_c1_g1_i2	0.01071	0	*Arabidopsis* sp.	Adenosylhomocysteinase 1	One-carbon metabolic process	
	TRINITY_DN96256_c0_g1_i1	0.01051	3.0×10^{-79}	*Arabidopsis* sp.	Temperature-induced lipocalin-1	Response to heat	All cellular compartments
16	*TRINITY_DN95836_c2_g1_i1*	0.33486	3.0×10^{-41}	*Populus* sp.	Bark storage protein A	Nucleoside metabolic process	
	TRINITY_DN100016_c0_g1_i1	0.11055	2.0×10^{-19}	*Populus* sp.	Bark storage protein A	Nucleoside metabolic process	
	TRINITY_DN95836_c2_g1_i3	0.04576	1.0×10^{-34}	*Populus* sp.	Bark storage protein A	Nucleoside metabolic process	
	TRINITY_DN92121_c1_g1_i1	0.02389	NA	No hits	No hits		
	TRINITY_DN100016_c0_g2_i1	0.02154	2.0×10^{-20}	*Populus* sp.	Bark storage protein A	Nucleoside metabolic process	
	TRINITY_DN100016_c0_g1_i2	0.01904	2.0×10^{-16}	*Populus* sp.	Bark storage protein B	Nucleoside metabolic process	
	TRINITY_DN100016_c0_g2_i2	0.01851	3.0×10^{-19}	*Populus* sp.	Bark storage protein A	Nucleoside metabolic process	
	TRINITY_DN87363_c15_g3_i1	0.01369	NA	No hits	No hits		
	TRINITY_DN86213_c8_g2_i2	0.01246	6.0×10^{-14}	*Phalaenopsis* sp.	Uncharacterized protein ORF91		Chloroplast
	TRINITY_DN100016_c0_g2_i4	0.00990	2.0×10^{-16}	*Populus* sp.	Bark storage protein A	Nucleoside metabolic process	

DN85473_c0_g1_i3), two were involved in the transfer of methyl groups (*TRINITY_DN80127_c0_g1_i1* and *TRINITY_DN99603_c1_g2_i4*), and one was related to phospholipid biosynthesis (*TRINITY_DN95430_c1_g1_i2*; Table 6.8). Five of the sequences in dynamic topic 11 were also among the top 10 of static topic 2 (*TRINITY_DN101197_c2_g1_i2*, *TRINITY_DN94350_c0_g2_i2*, *TRINITY_DN96614_c0_g2_i1*, *TRINITY_DN88193_c0_g1_i2* and *TRINITY_DN65470_c0_g1_i1*; see Table 6.5). Transcripts in this topic depicted steady expression levels as those in dynamic topic 2, except for the tricin synthase 1 (transcript *TRINITY_DN80127_c0_g1_i1*) whose expression levels were higher at 8 dpi in comparison to 0 and 4 dpi (Fig. 6.8b).

Dynamic topic 13 grouped sequences that had higher levels of expression in *T. plicata* (regardless of the line), in comparison to *T. standishii* or *T. standishii* × *plicata*. Three of the sequences in this topic were related to responses to different stimuli (defense response, *TRINITY_DN76260_c0_g1_i1*; response to abscisic acid, *TRINITY_DN97013_c0_g2_i4*; and response to heat, *TRINITY_DN96256_c0_g1_i1*), two were peptidases (*TRINITY_DN74436_c0_g1_i1* and *TRINITY_DN188465_c0_g1_i1*), and two were involved in starch biosynthesis (*TRINITY_DN81546_c0_g1_i1* and *TRINITY_DN90395_c0_g1_i1*). In general, this dynamic topic depicts responses to *D. thujina* infection in both *T. plicata* lines. Figure 6.9a shows the modelled expression levels of the transcripts from dynamic topic 13 in Table 6.8. Expression of the aspartic proteinase nepenthesin-2 (transcript *TRINITY_DN74436_c0_g1_i1*) decreased from 0 dpi to 4 dpi and reached pre-infection levels at 8 dpi. On the contrary, expression of the metallothionein-like protein EMB30 (sequence *TRINITY_DN79613_c1_g1_i1*) increased from 0 dpi to 4 dpi and then decreases at 8 dpi. Interestingly, the only defense-related transcript in this topic, the MLP-like protein 423 (transcript *TRINITY_DN76260_c0_g1_i1*), had a 5-fold decrease in expression levels from 0 dpi to 8 dpi.

Dynamic topic 16 reunited transcripts with higher levels of expression in *T. standishii* and *T. standishii* × *plicata* in relation to either of the *T. plicata* lines. Among the top ten sequences in that dynamic topic (Table 6.8), seven were bark storage proteins A, one was an uncharacterized protein ORF91 located in the chloroplast (transcript *TRINITY_DN86213_c8_g2_i2*), and the remaining two did not result in annotation hits (*TRINITY_DN92121_c1_g1_i1* and *TRINITY_DN87363_c15_g3_i1*). The

expression levels of the top 10 transcripts from dynamic topic 16 were steady over the time points sampled (Figure 6.9b).

6.4 Discussion

This investigation studied the phenotypic and genotypic differences among resistant and susceptible *Thuja* plants, and their early responses to infection with *D. thujina*. The results showed that *T. standishii* was fully resistant to *D. thujina*, and that *T. standishii* × *plicata* was highly resistant to the disease, while both *T. plicata* lines were susceptible to it. There were also important differences at both the phenotypic and genotypic levels among the plant species and the hybrid, which may partly explain differences in their resistances to *D. thujina*. This study also revealed important differences in the early responses to infection amongst the plant materials studied, especially in *T. standishii*. All of the above aspects are discussed in detail below.

6.4.1 Constitutive differences among *T. standishii*, *T. plicata* and *T. standishii* × *plicata*

Differences existed among the species and hybrid studied at the histological level. The cuticles of the upper branches of *T. standishii*, as well as those of the lower branches of *T. standishii* × *plicata* were thicker than the cuticles of either *T. plicata* line. The cuticle is the first barrier that obligate parasitic fungi must overcome in order to get established and propagate inside the host (Agrios 2005, p. 210; Anker and Niks 2001; Gees and Hohl 1988; Hau and Rush 1982; Roundhill et al. 1995; Sherwood 1996; Zinsou et al. 2006). Thicker cuticles increase the resistance to infection only in diseases where the pathogen enters through direct penetration (Agrios 2005, p. 210), a characteristic of biotrophic fungi (Agrios 2005, p. 88). *D. thujina* is a biotroph (Durand 1913; Søegaard 1956; Søegaard 1969, p. 294) that performs direct penetration (Søegaard 1969, p. 299) to infect young leaves from the current growing season (Kope and Trotter, 1998b, Kope, 2004, Kope and Sutherland, 1994a). The fact that the thickest cuticles in *T. standishii* were located in the upper branches is interesting considering that it is the location of the youngest foliage, and this may be related to the resistance to *D. thujina* in that species. Thick cuticles have been reported in other pathosystems like *Eucalyptus nitens* - *Mycosphaerella* spp. (Smith et al., 2006) and olive - *Fusicladium oleagineum* (Rhouma et al., 2013). In both cases, resistant

plants had thicker cuticles in comparison to susceptible plants.

In addition to the cuticle, the epidermal thickness of the plant material studied was also significantly different among plant lines. *T. standishii* and *T. standishii* × *plicata* had a thinner epidermis than the *T. plicata* lines investigated. The epidermis is the next barrier to be overcome after infection before *D. thujina* colonizes the mesophyll with intercellular mycelium and haustoria (Pawsey, 1960). The thickness and toughness of the epidermis cell wall are important in conferring resistance against pathogens (Agrios 2005, p. 210). It is unknown whether the thickness of the epidermis itself determines how resistant a plant will be against a pathogen. The studies by Smith et al. (2006) and Rhouma et al. (2013) showed that trees that were resistant to their respective diseases had a thinner epidermis than susceptible plants. The findings of this investigation match those studies, given that plants resistant to *D. thujina* (*T. standishii* and *T. standishii* × *plicata*) had a significantly thinner epidermis than *T. plicata*. The differences in cuticle and epidermal thickness could also be explained by the nature of plant material used here. *T. standishii* and *T. standishii* × *plicata* were clonal plants while both *T. plicata* lines were seedlings. Although cuticle thickness varies with age among species (Kurtz Jr., 1950), leaf cuticles of woody plants like *Eucalyptus regnans* are thicker in older plants (England and Attiwill, 2005). *Thuja* clonal lines are also ontogenetically older than seedlings, and have been reported to be more resistant to *D. thujina* attack than seedlings (Russell, unpubl. data; Søegaard 1969, p. 373).

At the chemical level, differences existed amongst the three biological entities studied. Both the PCA and the categorical stability selection analyses executed on the chemical variables showed that citronellyl acetate discriminated between the *T. plicata* lines and the other plant lines. This compound was at significantly higher concentrations in *T. standishii* and *T. standishii* × *plicata*. The stability selection analysis also showed that 3-carene was present only in *T. standishii*. The differences in the concentrations of those compounds could also be partly due to the age of the plant material analyzed. The physiology of terpenes and essential oil production change with the ontogeny of the plant so that leaves at different stages have different concentrations and composition of the various terpenes and phenolics produced (Goodger et al., 2013, Sangwan et al., 2001). In *T. plicata*, differences in the chemical profiles of leaves of different ages have been reported in seedlings (Foster et al., 2016). Scales

have more monoterpenes than needles, with α-thujone being the most abundant terpene in the scales of *T. plicata* seedlings (Foster et al., 2016).

Both citronellyl acetate and 3-carene have been shown to have defense properties. Citronellyl acetate has antimicrobial properties against bacteria (*Staphylococcus aureus*, *Staphylococcus epidermidis* and *Streptococcus mutans*) and fungi (*Candida albicans* and *Microsporum gypseum*) at a minimum inhibitory concentration of 1,250 $\mu g \cdot mL^{-1}$ (Singh et al., 2012), while 3-carene has been shown to be involved in weevil resistance in Sitka spruce (Roach et al., 2014, Robert et al., 2010) as well as in pathogen resistance in Norway and white spruce (Alfaro, 1995, Alfaro et al., 2002, Fäldt et al., 2003, Tomlin et al., 2000). In this study, 3-carene was not detected in *T. plicata*, and has not been detected in the past because the species lacks resin-producing tissues, and, instead, has isolated resin cells scattered through the stem (Lewinsohn et al., 1991b). It is intriguing how *T. standishii* produces such a large amount of 3-carene while *T. plicata* and the hybrid do not. This may be one of the resistance mechanisms against *D. thujina* unique to *T. standishii*. Future investigations should examine the anatomical organization of *T. standishii*'s stem to determine if specialized resin structures exist in the Japanese arborvitae.

Intriguing differences between the resistant and susceptible plant lines studied were observed at the gene expression level. Categorical stability selection showed that the disease resistance response protein 206 (DRR206) was at a higher expression level in the most resistant plants (i.e. *T. standishii* and *T. standishii* × *plicata*). DRR206s have been shown to accumulate rapidly in *Pisum sativum* in response to *Fusarium solani* f. sp. *phaseoli* (Culley et al., 1995), in *Brassica napus* after infection with *Leptosphaeria maculans* (Wang et al., 1999) as well as in other hosts after fungal or viral infections (Halls et al., 2004). In response to a compatible plant-pathogen interaction, DDR206s are secreted by the plant into the apoplastic region (UniProt accession P13240, The UniProt Consortium 2015, 2017; Halls et al. 2004). Furthermore, it has been shown that extracts with DDR206 inhibit *L. maculans* germination in vitro (Wang et al., 1999). DRR206s are also known as dirigent proteins, and are involved in the production of 8-8' optically active lignans by the stereoselective coupling of radicals to form single products (Halls et al., 2004). In this investigation, there were 12 Trinity genes annotated as DDR206s, gene *TRINITY_DN99675_c1_g1* being of special interest because four of its 12 transcripts were captured by the categorical sta-

bility selection analysis. To date, there are nine *T. plicata* dirigent genes reported to be involved in the 8-8' coupling process leading to the production of (+)-pinoresinol (Kim et al., 2002). It is possible that some of the 12 transcripts mentioned (*TRINITY_DN99675_c1_g1_i1* - *TRINITY_DN99675_c1_g1_i12*) may be the 9 dirigent genes reported by Kim et al. (2002), however, it is unknown which one of them might be related to defense against *D. thujina* in *Thuja* species. BLASTn searches for the four DRR206s selected by the categorical stability selection performed in this study showed that the top hit for two of them was to *T. plicata*'s dirigent protein 4 (DIR4; Gang et al. 1999, Kim et al. 2002). Future studies should investigate the specific roles of *Thuja* dirigent proteins in the defense against cedar leaf blight.

In addition to DDR206s, both the grade of membership and dynamic topic modelling analyses indicated that bark storage proteins (BSPs) were expressed at high levels only in *T. standishii* and *T. standishii* × *plicata*. BSPs accumulate in the bark during the fall and decrease during the spring in deciduous tree species (Langheinrich and Tischner, 1991, Sauter and van Cleve, 1991, Wetzel et al., 1989), and are thought to play a role in short term storage of nitrogen in plants that have limited access to that nutrient (Smith and Atkins, 2002, Werner and Witte, 2011). It has also been reported that the accumulation of BSPs in poplar during fall is photoperiod-regulated and mediated by phytochromes (Coleman et al., 1991, Zhu and Coleman, 2001). BSPs are evolutionarily related to the Vegetative Storage Proteins (VSPs; Pettengill et al. 2013), and they accumulate in response to drought, high nitrogen, wounding, herbivory, and after pathogen attack (Coleman et al., 1994, Lawrence et al., 2001, Major and Constabel, 2006, Mulema and Denby, 2012, Plomion et al., 2006). Although the findings of the current experiment match the information available on those proteins in regards to their upregulation in response to pathogen infection, little is known about their specific role in the defense against *D. thujina* in *Thuja* species. Future investigations should be carried out to determine if BSPs play a role in defense against *D. thujina* in *Thuja* sp.

Other genes that were differentially expressed among the plant lines studied, regardless of their infection status, were related to light signal transduction and defense. Transcripts *TRINITY_DN101197_c2_g1_i2* (chlorophyll a-b binding protein 1B) and *TRINITY_DN65470_c0_g1_i1* (photosystem I reaction center subunit psaK) had higher levels of expression only in *T. standishii* in comparison to the hybrid or any

of the *T. plicata* lines studied, and are involved in light signal transduction. Although not directly related to pathogen defense, light signal transduction and pathogen defense signals have been reported to cross-talk during pathogen infections (Kleine et al., 2007, Schenk et al., 2000), which may explain the high expression levels of those sequences in *T. standishii*, the only species that was fully resistant to *D. thujina* in this study. Transcript *TRINITY_DN63359_c0_g1_i1* (cysteine proteinase RD21a) has been shown to be involved in plant defense (Shindo et al., 2012) and its expression levels were significantly higher in *T. plicata* line 129 in comparison to the other plant lines analyzed. Cysteine proteinase RD21a is a defense gene reported to confer resistance to *Botrytis cinerea* in *Arabidopsis* (Shindo et al., 2012) and is involved in programmed cell death in *Arabidopsis* as a result of a compatible interaction with the pathogen (Hayashi et al., 2001, Lampl et al., 2013). *T. plicata* line 129 was the most resistant of the two western redcedar seedling lines used in this investigation. Therefore, the cysteine proteinase RD21a reported here could be one of the resistance mechanisms to *D. thujina* in *T. plicata* line 129 despite the lack of reports on hypersensitivity or programmed cell death in *T. plicata* in response to biotrophic infections.

6.4.2 Time-course responses to *D. thujina* infection in *Thuja* sp.

Both the chemical and gene expression analyses depicted time-course responses to *D. thujina* infection in the plants studied. Fourteen of the 60 transcripts detected by the categorical stability selection performed on the DE transcriptomic data had "defense response" as their biological process annotation among the gene ontology enrichment terms, and almost half of the sequences detected by the same analysis were extracellular components (plasma membrane, cell wall, apoplast and extracellular region). The fact that such terms were part of the annotations of the sequences captured by the stability selection analysis, which aimed to detect genes that were up/down regulated in response to *D. thujina* infection, highlights the extracellular nature of the early interaction between the host and the pathogen. Fungal penetration and establishment occur early during the infection process, and may take place immediately after spores land or later, depending on environmental conditions such as temperature and humidity, as well as on the nature of the infecting spores (Agrios 2005, p. 86). The experiment presented here was carried out within 8 days, and samples were collected

for chemical and gene expression analyses as early as 4 dpi. A previous study on *T. plicata* seedlings that were infected under field condition showed that *D. thujina* spores germinated on microscope slides within three days when rain was present (see Chapter 2), and a histological investigation of the infection process indicated that *D. thujina* haustoria can be visualized inside *Thuja* sp. foliage infected with the disease within four days (Søegaard 1969, p. 310). The screening for *D. thujina* spores, as well as the BLASTn searches for the two ITS2 sequences of *D. thujina* in the material studied confirm that infection was in progress at 4-8 dpi in all plant lines that were in the CLB^{+} infection condition.

An interesting induced response to *D. thujina* infection involved aluminum concentrations, which were about 10 times higher at 8 dpi in the *T. standishii* plants that were real infected with *D. thujina*, compared to all plant lines in both infection conditions at 0 dpi. The apparent accumulation of aluminum in response to *D. thujina* infection, although not as high as that reported in this investigation, was also seen in the *T. plicata* seedlings of the study presented in Chapter 4, as well as in the seedlings of the same species with *D. thujina* symptoms in Chapter 3. Aluminum is toxic to plants (Duressa et al., 2011, Hamel et al., 1998, Jiang et al., 2015, Mossor-Pietraszewska, 2001, Poot-Poot and Hernandez-Sotomayor, 2011) and causes growth anomalies when plants are grown in acidic soils (Firestone et al., 1983, Hamel et al., 1998, Mossor-Pietraszewska, 2001, Yuan et al., 2017). The trivalent aluminum cation is the most poisonous form (Fichtner, 2003, Hamel et al., 1998), and resistance to the element's toxicity has been studied in crop species (Firestone et al., 1983, Hamel et al., 1998, Yuan et al., 2017). Organic acids are usually involved in the detoxification and translocation of aluminum *in planta* (Fang-Ma, 2000, Feng-Ma, 2007, Feng-Ma et al., 2001, Guo et al., 2005, Panda et al., 2009), while secretion of organic anions and phenolics (like catechin and quercetin) are common aluminum defense mechanisms outside the roots (Feng-Ma, 2007). Aluminum toxicity is not a plant-exclusive phenomenon however. The element is also toxic to fungi like *Aspergillus flavus* (Firestone et al., 1983), *Phytophthora parasitica*, *Thielaviopsis basicola* (Fichtner, 2003), and the phytopathogens *Helminthosporium solani*, *Phytophthora infestans*, *Fusarium sambucinum* and *Rhizoctonia solani* (Avis et al., 2007).

To date, there is no information available on the role of aluminum as a defense mechanism against foliar biotrophs. However, the element has been shown to induce

defense-like responses in plants exposed to high soil levels of aluminum (Hamel et al., 1998). Those responses include the upregulation of pathogenesis-related proteins, hypersensitive responses, lignification and induction of cell wall synthesis proteins (Hamel et al., 1998). Disruption of calcium metabolism has also been reported as a consequence of aluminum toxicity (Feng-Ma, 2007, Hamel et al., 1998, Jones et al., 1998, Mossor-Pietraszewska, 2001, Rengel, 1992, Silva, 2012), and may have been indicated in this investigation. Regression stability selection on the DE transcriptomic data using aluminum as response variable revealed that a calmodulin-binding protein (*TRINITY_DN102764_c1_g1_i2*; G-type lectin S-receptor-like serine/threonine-protein kinase RLK1), and a calcium-dependent phospholipid binding protein (*TRINITY_DN95987_c1_g2_i4*; protein QUIRKY) were among the best predictors of the foliar aluminum concentrations, and were highly expressed in *T. standishii*, but not in *T. plicata* or the hybrid. Transcript *TRINITY_DN102764_c1_g1_i2* produces a receptor-like protein kinase (RLK) found in the plasma membrane, that has S-locus and G-type lectin regions, and is similar to that reported by Sun et al. (2013) in *Arabidopsis*. They showed that such a protein was involved in tolerance to salt stress, probably by binding to Ca^{2+}/calmodulin to trigger downstream resistance responses. Interestingly, a similar protein (G-type lectin S-receptor-like serine/threonine-protein kinase At1g34300) was found to be among the best predictors in the regression stability selection analysis that used aluminum concentrations as response variable in the experiment presented in Chapter 4. The other transcript aforementioned, sequence *TRINITY_DN95987_c1_g2_i4*, produces the protein QUIRKY, which is thought to be involved in membrane traffic via Ca^{2+} signalling (Fulton et al., 2009). Calcium, in general, is a secondary messenger that triggers plant defenses against pathogens via mobilization of the element itself, membrane trafficking or both (Vidhyasekaran 2008, p. 79). It is possible that a cross-talk between aluminum and calcium signalling exists in *T. standishii*, and both may be related to resistance against *D. thujina*. Further studies should investigate the role of calcium signalling in the defense against *D. thujina* in *Thuja* species.

The stability selection analysis using aluminum also captured a transcript with the gene ontology term "response to fungus" (*TRINITY_DN81123_c1_g1_i8*) that was preferentially expressed in the infected lines, especially in *T. standishii*. The dynamic topic analysis revealed a transcript related to *myo*-inositol (*TRINITY_DN95430_c1_g1_i2*) that was also at higher expression levels in *T. standishii* in comparison

to the other lines studied. Transcript *TRINITY_DN81123_c1_g1_i8*, annotated as transcriptional corepressor LEUNIG, has been shown to have mediator functions and repress transcription via changes in chromatin structure (Gonzalez et al., 2007). LEUNIG is involved in embryo development (Sitaraman et al., 2008), flower development (Franks et al., 2002, Liu and Meyerowitz, 1995, Sitaraman et al., 2008, Sridhar et al., 2004), mucilage extrusion probably through cell wall modification (Bui et al., 2011, Walker et al., 2011), and disease resistance (UniProt accession Q9FUY2; The UniProt Consortium 2015, 2017). Modifications of the plant cell wall, like those likely induced by LEUNIG, are a common defense mechanism during plant-pathogen interactions (Agrios 2005, p. 210; Sharma 2006, p. 5.3; Vidhyasekaran 2008, p. 275), and may take place in the foliage of *Thuja* plants during *D. thujina* infection. Sequence *TRINITY_DN95430_c1_g1_i2* was annotated as inositol-3-phosphate synthase, also known as *myo*-inositol-1-phosphate synthase (MIPS, EC 5.5.1.4; Kanehisa et al. 2017). MIPS catalyzes the first step in the production of *myo*-inositol (UniProt accession Q9FYV1, The UniProt Consortium 2015, 2017; Majumder et al. 1997), the precursor of inositol-containing products including phospholipids (Majumder et al., 1997). Multiple MIPS genes exist in plants and are differentially expressed depending on the tissue (Donahue et al., 2010). This enzyme is involved in the suppression of cell death (Donahue et al., 2010) and appears to play a role in pathogen resistance (e.g. *Fusarium solani* f. sp. *glycines*; Iqbal et al. 2002), but the exact mechanism is still unknown. It is plausible that MIPS contribute to the resistance against *D. thujina* in *T. standishii*.

6.4.3 On the full resistance of *T. standishii* and partial resistance of *T. standishii* × *plicata* to *D. thujina*

Two interesting findings of this study were: 1) the confirmation of full resistance against *D. thujina* in *T. standishii*, and 2) the partial resistance against the disease in the *T. standishii* × *plicata* clonal line investigated here. These results support the findings of Bent Søegaard in regards to *T. standishii*, but contradict his findings on full resistance in offspring from crosses between *T. plicata* and *T. standishii* (Søegaard, 1956, 1966, 1969). Based on his investigations, Søegaard proposed that an *R* gene was responsible for the full resistance to *D. thujina* in *T. standishii*, and that such a gene could be passed on to hybrids between *T. plicata* and *T. standishii*, rendering them fully resistant (Søegaard, 1956, 1966, 1969). The molecular evidence

collected in the current study does not support the gene-for-gene model (Agrios 2005, p. 140; Hammond-Kosack and Jones 1997; Sharma 2006, p. 3.9; Vidhyasekaran 2008, p. 193) proposed by Søegaard to explain compatible *Thuja* sp. - *D. thujina* interactions. Furthermore, the partial resistance of the *T. standishii* × *plicata* hybrid clone analyzed here suggests that *D. thujina* resistance in *T. standishii* could be a multigenic phenomenon rather than a monogenic trait as initially hypothesized by Søegaard. The machine learning analyses carried out here on the transcriptomic data (i.e. stability selection, GoM and dynamic topic modelling) could not relate resistance against the disease to an unique *R* gene from *T. standishii*, and no fungal sequences from *D. thujina* with the characteristics of avirulence (*avr*) genes were found in the incompatible interaction in this investigation either. The presence of both genes is a requirement of the gene-for-gene model of pathogen resistance (Agrios 2005, p. 141, Hammond-Kosack and Jones 1997; Rouxel and Balesdent 2010; Sharma 2006, p. 3.9; Vidhyasekaran 2008, p. 193; Westerink et al. 2004).

A detailed look at Søegaard's studies reveals that several of the F_2s reported had resistance screening results that deviated from the anticipated proportions under the gene-for-gene model, some even rendering dissimilar results in different years (see Søegaard 1956, 1966, 1969). For instance, *T. standishii* × *plicata* hybrids (V. 1625) backcrossed directly and reciprocally to *T. plicata* (V. 335) in 1951 resulted all resistant to *D. thujina* (Søegaard, 1956), but the same *T. standishii* × *plicata* (V. 1625) × *T. plicata* (V. 335) cross carried out in 1962 and tested in 1963 (sow 4398; Søegaard 1969, p. 343) depicted a ~ 2 (resistant) : 1 (susceptible) ratio (Søegaard 1969, p. 354). Other offspring that deviated from the 1:1 proportion (Søegaard 1969, p. 354) were sow 3406 from 1957 (Søegaard 1969, p. 331), sow 4103 from 1960 (Søegaard 1969, p. 335) and sow 4187 from 1961 (Søegaard 1969, p. 341). Søegaard also reported and discussed deviations from the 3 (resistant) : 1 (susceptible) ratios in F_2s from self-pollinated hybrids (see e.g. Søegaard 1969, p. 357).

In addition to the offspring segregation deviations, Søegaard's *T. standishii* × *plicata* hybrids were much more difficult to produce and therefore to test than the reciprocal hybrids. Only three *T. standishii* × *T. plicata* controlled crosses were recorded by Søegaard between 1957 and 1965 (Søegaard 1969, pp. 331-344), two being unsuccessful (sows 3413 and 3414 from 1957; Søegaard 1969, p. 331) and the third one resulting in a very low offspring (only 10 plants, sow 4185 from 1961; Søegaard 1969, p. 341).

In contrast, 26 of the 27 *T. plicata* × *T. standishii* controlled crosses carried out by Søegaard between 1951 (Søegaard, 1956, 1966) and 1965 (Søegaard 1969, pp. 329-344) were successful and rendered high offspring numbers from the beginning in 1952 (1,300 plants; Søegaard 1956), up until the last investigations carried out in 1965 (3,800 plants, sow 4684 from 1965; Søegaard 1969, p. 344). The genetic basis of the resistance to *D. thujina* in *T. plicata*, *T. standishii* and hybrids between both species appears then to be more complex than the *R*-gene model proposed by Søegaard.

All of the above information suggest that full resistance to *D. thujina* in *T. standishii* could potentially be the result of a combination of various resistance mechanisms that neutralize the invading fungus, including a thick cuticle, presence of 3-carene, higher expression levels of DRR206s, BSPs and a very effective early defense response that includes aluminum accumulation, changes in calcium metabolism and upregulation of MIPS as well as the transcriptional corepressor LEUNIG, among other genes. The multigenic nature of the defenses against *D. thujina* displayed by *T. standishii* is puzzling, given that quantitative, and not qualitative, resistance usually results when such a combination of resistance mechanisms exist (Agrios 2005, p. 136; Sharma 2006, p. 3.6; Vidhyasekaran 2008, p. 193). The only *R* gene found in this interaction was *DRR206*, which has been shown to play roles in the resistance to *L. maculans* in *B. napus* (Wang et al., 1999), to *F. solani* f. sp. *phaseoli* in *P. sativum* (Culley et al., 1995), and other pathosystems (Halls et al., 2004). However, its upregulation in response to *D. thujina* infection in the susceptible *T. plicata* line 124 appears to rule out the possibility of *DRR206* as a candidate resistance gene, unless an unknown mechanism is counteracting the gene in that line.

In spite of the probable multigenic nature of the resistance to *D. thujina* in *T. standishii*, the Japanese arborvitae might still show qualitative resistance against the blight if few major resistance genes are part of the defense mechanisms. Indeed, qualitative and monogenic resistances belong to the same resistance category, but qualitative resistance is oligogenic in nature, unlike the monogenic resistance where the gene-for-gene model applies (Agrios 2005, p. 136; Sharma 2006, p. 3.6; Vidhyasekaran 2008, p. 193). Full resistance to plant diseases can also be achieved when resistance genes are pyramided within a plant. In that scenario, one *R* gene (e.g. R_1) would confer resistance to a pathogen strain with the *avr* counterpart (e.g. avr_1), another *R* gene (e.g. R_2) would lead to resistance to a strain with another *avr* gene

(e.g. avr_2), and so forth. The pyramiding model of resistance, with as many as 20-40 *R* genes, has been reported in pathosystems like barley - *Blumeria graminis* f.sp. *hordei* (synonym *Erysiphe graminis* f.sp. *hordei*), cotton - *Xanthomonas citri* pv. *malvacearum* (synonym *Xanthomonas campestris* pv. *malvacearum*), and wheat - *Puccinia recondita* (Agrios 2005, p. 137; Sharma 2006, p. 3.6). The possibility that qualitative resistance is present in *T. standishii* can be additionally supported by the lack of complete resistance in the *T. standishii* × *plicata* hybrid studied here, especially when considering the very low disease severity in that line when compared to the *T. plicata* lines investigated. Alternatively, *T. standishii* may simply display nonhost resistance (NHR), which is thought to be part of the basal defense system in plants (Fan and Doerner, 2012, Uma et al., 2011). Although NHR has not been as widely studied as *R*-gene resistance, it appears to be due to be the result of a combination of resistance mechanisms that include more than *R* genes (Fan and Doerner, 2012, Heath, 2000, Uma et al., 2011). *T. standishii* has not been reported as a host of *D. thujina* (Durand, 1913, Kope, 2000, Kope et al., 1998, Søegaard, 1966), and NHR would explain the lack of symptom development and the multigenic nature of the species' full resistance to *D. thujina*.

6.4.4 Conclusions

Phenotypic and gene expression differences in relation to *D. thujina* resistance between *T. plicata* seedlings and clones of *T. standishii* and *T. standishii* × *plicata* were studied. Both *T. plicata* lines investigated were susceptible to *D. thujina*, while *T. standishii* × *plicata* was highly resistant and *T. standishii* fully resistant to the disease. *T. standishii* and *T. standishii* × *plicata* plants had thicker cuticles and a thinner epidermis than the *T. plicata* lines, and *T. standishii* had higher concentrations of 3-carene. At the genetic level, transcripts of DRR206s and BSPs were at higher expression levels in *T. standishii* and *T. standishii* × *plicata* in comparison to either *T. plicata* line. The roles of 3-carene, DRR206s and BSPs in the defense against *D. thujina* by *T. standishii* and *T. standishii* × *plicata* are unknown and future studies should investigate their mechanisms of action.

The plant lines studied depicted different early responses to infection with *D. thujina*. Aluminum accumulation appeared to be an important response to infection in the Japanese arborvitae. Aluminum had a significant, 10-fold increase in foliar

concentration in *T. standishii* infected with *D. thujina*. This may be related to the defense-like responses induced by the element at high concentrations, possibly via disruption of calcium signalling. Further investigations should search for specific mechanisms of action of aluminum in the defense against *D. thujina* by *T. standishii*.

This research also explored the type of resistance to *D. thujina* shown by *T. standishii* in light of Søegaard's hypothesis. The multigenic nature of the constitutive and induced defense mechanisms against *D. thujina* in the Japanese arborvitae do not support the gene-for-gene resistance hypothesis. In spite of that, the lack of *D. thujina* symptoms in infected *T. standishii* and the presence of several defense mechanisms in that species suggests that either qualitative or nonhost resistance against the disease may exist in *T. standishii*.

Chapter 7

Common potential resistance mechanisms to *Didymascella thujina* in the *Thuja* species studied

In this Doctoral project, the resistance mechanisms to *Didymascella thujina* in *Thuja plicata*, *Thuja standishii* and *Thuja standishii* × *plicata* were investigated. True resistance (Agrios 2005, p. 136; Holliday 1989, p. 274; Sharma 2006, p. 3.5; Westerink et al. 2004) exists in *Thuja* sp. against *D. thujina*, a phenomenon initially observed last century by Søegaard (1956, 1966, 1969), and reported early this century in *T. plicata* by scientists from the British Columbia Ministry of Forests, Lands, Natural Resource Operations and Rural Development (Russell et al., 2007, Russell and Yanchuk, 2012). Five major studies were carried out during the project using seedlings and clonal lines. The seedlings included full-sib families, and single seed descent lines self-pollinated for five generations (Russell and Ferguson, 2008). Four field seasons were carried out where disease incidence and severity screening of more than 100 clones and of more than 1,400 seedlings from 35 families was completed. More than 400 samples were processed for scanning electron microscopy to confirm the presence of the pathogen in the real inoculations of all experiments, by comparing the sampled *D. thujina* ascospores to their ultrastructural characteristics in the published literature (Kope, 2000).

Several aspects of the *Thuja* sp. - *D. thujina* interaction were studied in this project, including the relationship between disease resistance in seedlings of *T. plicata* full-sib

families and their climates of origin, the anatomical differences between *Thuja* sp. plants resistant and susceptible to *D. thujina*, the constitutive phenotypic and gene expression differences between resistance classes of *Thuja* sp. plants, and the induced phenotypic and gene expression responses to infection in the *Thuja* species investigated. The histological studies of *Thuja* sp. leaf anatomy included more than 750 samples (Chapters 2, 5 and 6), and the chemical analyses in Chapters 3-6 included more than 270 foliar samples. One-hundred-and-forty-eight transcriptomic samples were produced for Chapters 3-6 combined, and four *de novo* reference transcriptomes were assembled (one per gene expression study; Chapters 3-6) totalling almost one million Trinity transcripts (Table 7.1; Grabherr et al. 2011, Haas et al. 2013). The bioinformatics analyses resulted in more than 50,000 differentially expressed transcripts combined (Table 7.1).

The investigations completed during the program showed that, on average, 8% of the phenotypic variables studied (leaf anatomy and chemical composition) exhibited significant differences between *Thuja* sp. plants resistant and susceptible to *D. thujina* (Table 7.1). The common features that differentiated between resistance classes at the phenotypic level were two of the leaf anatomy variables in Chapters 2 and 6 and four of the chemical composition variables in Chapter 3 (Table 7.1). The average percentage of chemical variables that discriminated between plants subject to real and mock *D. thujina* infections was 6% (Table 7.1). The two experiments in Chapter 4 had the most chemical variables that showed significant differences between infection status, with six chemicals in the natural conditions experiment, and four in the controlled conditions (Table 7.1). Differential responses to *D. thujina* infection between resistance classes were also seen at the chemical level. However, the percentage of chemical variables that depicted those differences, as assessed by the resistance class $\times$ infection status interaction, were only 2% (Table 7.1). At the gene expression level, the average percentage of overall differentially expressed transcripts among all experiments in Chapters 3-6 was 7%, with the highest percentage in the controlled conditions experiment in Chapter 4 (Table 7.1).

The data collected over the years in this project suggest that the major differences between *Thuja* sp. plants resistant and susceptible to *D. thujina* are constitutive. Such differences are usually found in other pathosystems and tend to include structural defenses like reinforced cell walls and cuticles (Agrios 2005, p. 210; Anker and Niks

Table 7.1. Number of variables per feature studied in *Thuja* sp. plants that rendered significant differences in various comparisons in the experiments carried out during this Doctoral project. * = Controlled conditions experiment in Chapter 4. ** = Natural conditions experiment in Chapter 4.

Feature	Comparison	Chapter	Number of variables studied	Number of variables with significant differences	Percentage of variables with significant differences
Climate of origin	Resistance classes[1]	2	96	5	5
Leaf anatomy	Resistance classes[1]	2	13	2	15
		6	11	2	18
Chemical composition	Resistance classes[1]	3	54	4	7
		4-CC*	54	1	2
		5	60	2	3
		6	60	2	3
	Infection status[2]	3	54	4	7
		4-CC*	54	3	6
		4-NC**	54	6	11
		5	60	3	5
		6	60	1	2
	Resistance class × infection status[3]	4-NC**	54	1	2
		6	60	1	2
Gene expression	Overall differential expression[4]	3	173,924	2,304	1
		4-CC*	122,588	18,867	15
		5	339,748	9,551	3
		6	311,664	27,432	9

[1] Refers to variables that discriminated between plants resistant and susceptible to *Didymascella thujina*.
[2] Relates to variables that were common to both resistance classes, but differed between plants that were mock- and real-infected with *D. thujina*.
[3] Makes reference to variables that showed differential responses to infection between resistance classes.
[4] Includes all possible comparisons among pairs of samples in the gene expression portion of the experiments in Chapters 3-6.

2001; Sherwood 1996; Yoshida 1998; Zinsou et al. 2006), the presence of chemical compounds (e.g. stilbenes; Heldt 2005, p. 447; Heldt and Piechulla 2010, p. 443), or the constitutive expression of defense-related genes like those from the nucleotide binding site-leucine-rich repeats (NBS-LRR) family (Vidhyasekaran 2008, p. 198). The results of this project also showed that plants from both resistance classes responded to *D. thujina* infection, with few differential responses between classes. The only species with a noticeable differential response to *D. thujina* infection at the chemical level was *T. standishii* (section 7.2.2). Induced responses to pathogen infection take place in any compatible plant-pathogen interaction, and include structural changes like the deposition of suberin (Agrios 2005, p. 187; Smith et al. 2006), hypersensitive responses (Agrios 2005, p. 217; Brown et al. 1966; Gees and Hohl 1988), the production of phytoalexins such as flavonoids (Falcone-Ferreyra et al., 2012), and the induction of defense-related genes like cell wall remodelling enzymes (Bellincampi et al., 2014, Krizek et al., 2016, Smit and Dubery, 1997) or pathogenesis related proteins (Chittoor et al., 1999, Ghosh, 2006, Velazhahan et al., 1999). All of these findings are summarized in the following sections.

7.1 Potential constitutive disease resistance mechanisms

In all investigations carried out during the Doctoral program, differences in the severity of *D. thujina* symptoms were seen among the studied *Thuja* sp. plants. The *T. standishii* clone analysed did not develop any symptoms of the disease, while the *T. standishii* × *plicata* clone showed very low disease severity values (Table 7.2). Those results agree with previous reports on the full resistance to *D. thujina* by *T. standishii* and on the high resistance to the pathogen by *T. standishii* × *plicata* (Søegaard, 1956, 1966, 1969). The *T. plicata* plants screened, on the contrary, showed a range of disease severities in both seedlings and clones (Table 7.2). Intraspecific variation to pathogen resistance in field studies is common in conifers (Hattemer, 1966, Hodge and Dvorak, 2000, Hoff, 1966, Wu et al., 1996) and angiosperms (Jokela, 1966, Laine, 2004), and variability in the resistance to *D. thujina* has previously been reported in adult trees of *T. plicata* (Russell and Yanchuk 2012; Russell et al. 2007; Søegaard 1969, p. 323). Furthermore, the severity screenings carried out during the project are supported by the findings in Russell et al. (2007). For instance, the female

parent of susceptible family 528 (parent ID 1428 in Appendix A.1) was grown from seed collected from population 19 (Gilpin High) in Russell et al. (2007), which was a susceptible population in that study.

Analyses in Chapter 2 investigating the relationship between *D. thujina* severity and climate of origin highlighted the potential role of local adaptation in the resistance to the pathogen. *T. plicata* seedlings resistant to *D. thujina* came from parents from areas with milder climates (Table 7.2), which are optimal for pathogen survival (Kope and Trotter 1998a; Pawsey 1960; Søegaard 1969, p. 309), germ tube germination (Pawsey, 1960) and spore discharge (Søegaard, 1966). The association between climate of origin and *D. thujina* resistance is also found in *T. plicata* field trials (Russell et al., 2007). Similar relationships between climate of origin and field disease resistance have been reported by Zhang et al. (1997) in another Cupressaceae, eastern redcedar (*Juniperus virginiana* L.). Zhang showed that trees resistant to *Pseudocercospora juniperi* originated in regions with higher humidity and temperatures than those where susceptible trees originated (Zhang et al., 1997). The climate of origin - disease resistance relationship has also been found in angiosperms. For instance, Tasmanian blue gum populations resistant to *Teratosphaeria cryptica* and *Teratosphaeria nubilosa* occur in areas with higher temperatures and autumn rainfalls than populations susceptible to those pathogens (Hamilton et al., 2013). Like Russell et al. (2007), both Zhang et al. (1997) and Hamilton et al. (2013) argued that the relationship between climate of origin and disease resistance could be due to plant-pathogen co-evolution in those pathosystems. The association between climate of origin and disease resistance has usually been considered a sign of co-evolution between host and pathogen (Hamilton et al., 2013, Russell et al., 2007, Zhang et al., 1997).

Co-evolution between plants and pathogens in places where both are present is common, and is a recurrent topic in evolutionary biology (Barrett and Heil, 2012, de Wit et al., 2012, Dusabenyagasani et al., 2002, Hamelin, 2000, Karasov et al., 2014, Occhipinti, 2013, Ojeda Alayon et al., 2017, Sakalidis et al., 2016, Vialle et al., 2013). The co-evolutionary model predicts that pathogen pressure has an associated fitness cost to the host that will result in selection for resistance, but it also predicts that the evolution of resistance mechanisms against pathogens in plants that do not co-exist with the pathogen will come with a negative fitness cost (Barrett and Heil, 2012, Burdon and Thrall, 2009, Frank, 1992, Occhipinti, 2013). Under this model, it is

Table 7.2. Constitutive phenotypic differences between the *Thuja* sp. plants resistant and susceptible to *Didymascella thujina* that were investigated during this Doctoral project. Values reported are mean ± standard error. #: *T. plicata* = *Thuja plicata*, *T. standishii* = *Thuja standishii*, *T. standishii* × *plicata* = *Thuja standishii* × *plicata*. * = Controlled conditions experiment in Chapter 4.

				Resistance class			
Feature	**Variable**	**Species#**	**Type of plant material**	**Resistant**	**Susceptible**	**Result**	**Chapter**
Susceptibility to CLB	Severity (% foliage blighted)	*T. plicata*	Seedlings (full-sib)	22.71 ± 1.88	48.59 ± 1.80	Lower disease severity in resistant plants.	2
		T. plicata	Seedlings (full-sib)	1.25 ± 0.41	3.78 ± 0.29	Lower disease severity in resistant plants.	3
		T. plicata	Seedlings (full-sib)	9.07 ± 5.74	24.30 ± 2.33	Lower disease severity in resistant plants.	4
		T. plicata	Seedlings (5-gen. selfed)	14.33 ± 7.61	33.25 ± 8.64	Lower disease severity in resistant plants.	6
		T. plicata	Clones	1.60 ± 0.71	6.51 ± 1.42	Lower disease severity in resistant plants.	5
		T. standishi	Clones	-	0.00	Fully resistant to *D. thujina*.	6
		T. standishii × *plicata*	Clones	-	0.48 ± 0.48	Resistant to *D. thujina*.	6
Climate of origin	June maximum mean temperature (°C)	*T. plicata*	Seedlings (full-sib)	16.3 ± 0.1	17.9 ± 0.8	Cooler June temperatures for resistant plants.	2
	July maximum mean temperature (°C)	*T. plicata*	Seedlings (full-sib)	18.9 ± 0.1	21.0 ± 0.9	Cooler July temperatures for resistant plants.	2
	Winter mean minimum temperature (°C)	*T. plicata*	Seedlings (full-sib)	-0.8 ± 0.4	-7.6 ± 1.4	Warmer winter temperatures for resistant plants.	2
	Autumn degree-days above 5°C	*T. plicata*	Seedlings (full-sib)	376.6 ± 12.9	248.8 ± 19.9	More autum degree-days in resistant plants.	2
	Winter degree-days below 5°C	*T. plicata*	Seedlings (full-sib)	41.9 ± 5.2	11.2 ± 5.1	More winter degree-days in resistant plants.	2
Leaf anatomy	Cuticle thickness (µm)	*T. plicata*	Seedlings (full-sib)	2.32 ± 0.02	2.23 ± 0.02	Thicker cuticles in resistant plants.	2
		T. plicata	Seedlings (5-gen. selfed)	-	2.04 ± 0.09	Thin cuticle.	6
		T. standishi	Clones	2.54 ± 0.16	-	Thick cuticle.	6
		T. standishii × *plicata*	Clones	2.56 ± 0.28	-	Thick cuticle.	6
	Epidermal thickness (µm)	*T. plicata*	Seedlings (5-gen. selfed)	-	12.12 ± 0.22	Thick epidermis.	6
		T. standishi	Clones	11.05 ± 0.33	-	Thin epidermis.	6
		T. standishii × *plicata*	Clones	9.48 ± 0.35	-	Thin epidermis.	6
	Stomatal density (stomata·mm^{-2})	*T. plicata*	Seedlings (full-sib)	102 ± 4	116 ± 4	Lower stomatal densities in resistant plants.	2
		T. plicata	Seedlings (5-gen. selfed)	73 ± 15	110 ± 23	Lower stomatal densities in resistant plants.	6
Chemical composition	Citronellyl acetate (µg·g^{-1})	*T. plicata*	Seedlings (5-gen. selfed)	-	250 ± 11	Very low concentration in comparison to *T. plicata* clones	6
		T. plicata	Clones	772 ± 24	2,459 ± 88	Lower concentration in resistant clones.	5
		T. standishi	Clones	1,085 ± 39	-	Similar concentration to resistant *T. plicata* clones.	6
		T. standishii × *plicata*	Clones	951 ± 44	-	Similar concentration to resistant *T. plicata* clones.	6
	α-Thujene (µg·g^{-1})	*T. plicata*	Seedlings (full-sib)	234.69 ± 18.69	170.25 ± 8.90	Higher concentration in resistant plants.	3
	Sabinene (µg·g^{-1})	*T. plicata*	Seedlings (full-sib)	6,147.08 ± 370.14	3,331.68 ± 135.76	Higher concentration in resistant plants.	3
	Boron (µg·g^{-1})	*T. plicata*	Seedlings (full-sib)	9.29 ± 0.28	11.86 ± 0.50	Lower concentration in resistant plants	3
	Calcium (%)	*T. plicata*	Clones	0.948 ± 0.024	0.790 ± 0.029	Higher concentration in resistant plants.	5
	Copper (µg·g^{-1})	*T. plicata*	Seedlings (full-sib)	13.09 ± 1.47	14.37 ± 1.23	Lower concentration in resistant plants	3
		T. plicata	Seedlings (full-sib)	10.22 ± 1.10	16.82 ± 3.83	Lower concentration in resistant plants.	4-CC*

expected that *T. plicata* populations from milder climates, which are optimal for the pathogen, would be more resistant to *D. thujina*. This was confirmed in Chapter 2. The model also anticipates that interior *T. plicata* populations will not be resistant to *D. thujina* given the very cold winters that are unsuitable for *D. thujina* survival (Kope and Trotter 1998a; Pawsey 1960; Søegaard 1969, p. 309). The parental data of the families used in Chapters 2 to 4 support that prediction of the co-evolution model. In the experiments presented there, both parents of *T. plicata* families 582, 583 and 8265 came from high elevation regions in the interior of British Columbia, and they also had high disease scores in comparison to the parents of the resistant coastal families used in the same studies (see Appendix A.1). The parents of the susceptible clonal line used in Chapter 5 were also from high elevation interior locations in British Columbia (see Appendix A.1). The evolution of resistance to *D. thujina* then appears to be based on major constitutive differences between *Thuja* sp. resistance classes evident at the phenotypic and gene expression levels.

7.1.1 Possible constitutive phenotypic resistance mechanisms

The constitutive phenotypic differences between *Thuja* sp. plants resistant and susceptible to *D. thujina* related to leaf anatomy and chemical composition. Cuticle thickness, stomatal density and epidermal thickness were the anatomical variables that discriminated between resistance classes. Thicker cuticles were present in resistant *T. plicata* seedlings as well as in clones of both *T. standishii* and *T. standishii* × *plicata*, but the trait did not render significant differences between resistance classes in *T. plicata* clones (Table 7.2). The cuticle is the first physical barrier to be overcome by fungi that perform direct penetration (Agrios 2005, p. 210; Anker and Niks 2001; Gees and Hohl 1988; Hau and Rush 1982; Roundhill et al. 1995; Sherwood 1996; Zinsou et al. 2006), and thicker cuticles are usually found in plants with higher resistance to pathogens. For instance, *Eucalyptus* trees resistant to *Mycosphaerella* spp. have thicker cuticles than susceptible trees (Smith et al., 2006), as do olive plants resistant to *Fusicladium oleagineum* (Rhouma et al., 2013).

Low stomatal densities were observed in the resistant seedlings of *T. plicata* (Table 7.2), but no relationship between stomatal density and disease resistance was seen on *Thuja* clones of any species. Lower stomatal densities have been associated with resistance to foliar pathogens that enter their host through natural openings (Agrios

2005, p. 88; Huang 1986; Ramos et al. 1992; Sharma 2006, p. 4.6; Zinsou et al. 2006). However, the use of a different route of entrance by *D. thujina* (Søegaard 1969, p. 299) makes it unlikely that stomata play a role in the defense against the biotroph. The epidermis was generally thinner in *Thuja* sp. plants resistant to *D. thujina*. Clones of *T. standishii* and *T. standishii* × *plicata* had significantly thinner epidermis than *T. plicata* seedlings (Table 7.2), and a thinner epidermis was also recorded in the resistant clonal lines of *T. plicata* (Table 5.1) although this difference was not significant. The same was true for the seedlings of the resistant families studied in Chapter 2 (Table 2.4). It is unknown if a thin epidermis is related to plant defense against pathogens despite the fact that they have been recorded in resistant plants of other pathosystems (Rhouma et al., 2013, Smith et al., 2006). On the contrary, the thinner epidermal thickness and the lower stomatal density recorded in resistant *Thuja* sp. plants may have nothing to do with *D. thujina* resistance, but instead to local adaptations to the climates where resistant plants occur. Thin epidermises have been reported in plants grown at high humidity (Torre et al., 2003), while low stomatal densities have been recorded in plants found in humid environments (Abrams et al., 1994, Bakker, 1991). Interestingly, high humidity is one of the characteristics of the locations where *T. plicata* populations resistant to *D. thujina* originate (Russell et al., 2007).

At the chemical level, different variables discriminated between resistance classes in clones in comparison to seedlings, although the main variables were terpenes in both age groups. Resistant *Thuja* sp. clones had lower concentrations of citronellyl acetate compared to susceptible clonal lines, and those concentrations were higher than in self-pollinated seedlings (Table 7.2). In seedlings of full-sib *T. plicata* families, plants resistant to *D. thujina* had significantly higher concentrations of α-thujene and sabinene (Table 7.2). The differences between clones and seedlings may be related to the physiological changes in terpene production that take place as plants age (Sangwan et al., 2001). For instance, it has been reported in *Eucalyptus* that compounds that are energetically inexpensive to synthesize, like phenolics, are usually produced by young plants, while energetically costly compounds like terpenes are present in adult trees (Goodger et al., 2013). The terpene profiles of adult and young *T. plicata* trees differ, in spite of the fact that plants of all ages have high amounts of α- and β-thujone in comparison to other terpenes (Shalev et al., 2018, Tsiri et al., 2009, von Rudloff et al., 1988, Vourc'h et al., 2001, 2002). Adult *T. plicata* trees

have been shown to have high relative concentrations of *p*-cymene, β-phellandrene, terpinen-4-ol, α-terpinene, α-terpineol and α-thujene (von Rudloff and Lapp, 1979), while seedlings have been reported to have high relative amounts of limonene (Vourc'h et al., 2001, 2002). Regardless of the differences in terpene profiles between adult and young *T. plicata* plants, citronellyl acetate, α-thujene and sabinene all have antimicrobial properties (Achotegui-Castells et al., 2016, Singh et al., 2012). Citronellyl acetate inhibits the growth of *Microsporum gypseum* and *Candida albicans in vitro* (Singh et al., 2012), and α-thujene and sabinene inhibit *Seiridium cardinale in vitro* as well as *in planta* in *Cupressus sempervirens* (Achotegui-Castells et al., 2016). Furthermore, α-thujene is a sabinene isomer (Acharya et al., 1969), and sabinene is believed to be an intermediate in the production of α- and β-thujone (Foster et al., 2013, Gesell et al., 2015), the latter two being powerful antimicrobial compounds as well (Tsiri et al., 2009). Citronellyl acetate, α-thujene and sabinene may play roles in the constitutive defense against *D. thujina* in *Thuja* sp. However, it remains to be determined whether or not they have fungicidal or fungistatic properties against *D. thujina*, or if they are intermediates of other defense compounds against the pathogen.

Boron, calcium and copper also exhibited significant differences in concentration between resistance classes (Table 7.2). Boron is a component of the cell wall (Blevins and Lukaszewski, 1998, Matoh, 1997, Tariq and Mott, 2007), and its role in growth and development (Ahmad et al., 2009, González-Fontes et al., 2014, Tariq and Mott, 2007) may explain its higher concentration in susceptible seedlings, which are anticipated to spend less resources in defense than growth according to the plant-pathogen co-evolutionary model (Brown and Rant, 2013, Bruns, 2016, Susi and Laine, 2015). Calcium is a secondary messenger (Heldt 2005, p. 458; Heldt and Piechulla 2010, p. 454), that plays many roles in the plant cell (Batistič and Kudla, 2012, González-Fontes et al., 2014, Silva, 2012), but is also involved in defense responses to pathogen infections (Agrios 2005, p. 214; Scheel and Nuernberger 2004; Vidhyasekaran 2008, p. 79). Calcium signalling appears to have been disrupted in the experiments presented in Chapters 4 and 6 as discussed later (section 7.2.1), and could therefore be involved in the resistance to *D. thujina* by *T. plicata*. The role of copper in the susceptible plants is uncertain, but it is known that the element can limit the growth of pathogens (Fones and Preston, 2013), and copper-based compounds are common in pesticides (Agrios 2005, p. 338; Sharma 2006, p. 8.15).

7.1.2 Probable constitutive genetic resistance mechanisms

Constitutive gene expression differences between resistance classes were found in both seedlings and clones, but seedlings had a different set of constitutive gene expression-related resistance mechanisms against *D. thujina* compared to clones. The most consistent finding in clones was the constitutively higher expression levels of bark storage proteins (BSPs) in the resistant lines from both *Thuja* species and the hybrid (Table 7.3). As discussed in Chapters 5 and 6, BSPs are proteins originally found to accumulate during the fall, but decrease in spring in poplar (Langheinrich and Tischner, 1991, Sauter and van Cleve, 1991, Wetzel et al., 1989). Interestingly, the BSP transcripts documented in this Doctoral project were found in summer, a time when they were not expected to be present according to the literature (Langheinrich and Tischner, 1991, Sauter and van Cleve, 1991, Wetzel et al., 1989), although it is unknown if their protein products were present. The function of BSPs was originally proposed to be storage of nitrogen, especially in plants with limited access to the element (Smith and Atkins, 2002, Werner and Witte, 2011). Now it is known that BSPs also accumulate in wounded poplar leaves (Major and Constabel, 2006), as well as in *Arabidopsis* leaves in response to pathogen infection (e.g. gene *At4g24340* in Mulema and Denby 2012). Some BSPs have indeed been demonstrated to have acid phosphatase activity against *Diabrotica undecimpunctata howardi*, *Callosobruchus maculatus* and *Drosophila* larvae (Liu et al., 2005). The role of BSPs in the defense against *D. thujina* in *Thuja* sp. is unknown, but their consistently higher levels of expression in the resistant plants of all clonal lines studied make them a potential resistance mechanism to the pathogen. To date, only one similar bark protein-like sequence from *Thuja occidentalis* exists in GenBank (AY795849). Sequence AY795849 was investigated along with other sequences as part of a standardization procedure in the production of recombinant secreted proteins (Baur et al., 2005), so it is unknown if the sequence has a defense-related function in *T. occidentalis* considering that species is a known host of *D. thujina* (Durand, 1913, Kope, 2000, Kope et al., 1998, Søegaard, 1966). BSPs may be involved in pathogen resistance via the jasmonic acid (JA) pathway given their reported upregulation in response to JA in *Arabidopsis* (Stein et al., 2008).

Besides BSPs, both *T. standishii* and *T. standishii* × *plicata* clones had higher expression levels than *T. plicata* self-pollinated seedling lines of a dirigent protein (disease resistance protein 206, DRR206; Table 7.3). As discussed in Chapter 6, DRR206s

Table 7.3. Constitutive gene expression differences between the *Thuja* sp. plants resistant and susceptible to *Didymascella thujina* that were investigated during this Doctoral project. Values reported are mean ± standard error. #: The units of the gene expression values shown are $\log_2$(FPKM) for transcripts from Chapters 3 and 4, and $\log_2$(TPM) for transcripts from Chapters 5 and 6. ##: *T. plicata* = *Thuja plicata*, *T. standishii* = *Thuja standishii*, *T. standishii* × *plicata* = *Thuja standishii* × *plicata*. *: Controlled conditions experiment in Chapter 4.

					Resistance class			
Process/function	**Transcript annotation**	**Transcript ID#**	**Species##**	**Type of plant material**	**Resistant**	**Susceptible**	**Result**	**Chapter**
Alkaloids synthesis	(R,S)-reticuline 7-O-methyltransferase	*TR55613/c7_g3_i3*	*T. plicata*	Seedlings (full-sib)	5.46 ± 0.10	0.03 ± 0.03	Higher expression in resistant plants.	3
Bark storage	Bark storage protein A	*TRINITY_DN123991_c13_g1_i1*	*T. plicata*	Clones	10.48 ± 0.23	6.58 ± 0.54	Higher expression in resistant plants.	5
		TRINITY_DN123991_c13_g1_i2	*T. plicata*	Clones	12.31± 0.18	8.58 ± 0.49	Higher expression in resistant plants.	5
		TRINITY_DN123991_c13_g2_i1	*T. plicata*	Clones	12.70 ± 0.18	8.98 ± 0.49	Higher expression in resistant plants.	5
		TRINITY_DN129016_c13_g2_i1	*T. plicata*	Clones	13.86 ± 0.20	9.97 ± 0.47	Higher expression in resistant plants.	5
		TRINITY_DN95836_c2_g1_i1	*T. plicata*	Seedlings (5-gen. selfed)	-	7.59 ± 0.45	Lower expression in comparison to *T. standishii* or *T. standishii* × *plicata*.	6
			T. standishii	Clones	13.02 ± 0.37	-	Higher expression in comparison to *T. plicata*.	6
			T. standishii × *plicata*	Clones	13.02 ± 0.46	-	Higher expression in comparison to *T. plicata*.	6
		TRINITY_DN95836_c2_g1_i3	*T. plicata*	Seedlings (5-gen. selfed)	-	4.52 ± 0.50	Lower expression in comparison to *T. standishii* or *T. standishii* × *plicata*.	6
			T. standishii	Clones	12.00 ± 0.38	-	Higher expression in comparison to *T. plicata*.	6
			T. standishii × *plicata*	Clones	9.52 ± 0.59	-	Intermediate expression in comparison to *T. standishii* and *T. plicata*.	6
Defense to fungus	EMSY-like 3	*TRINITY_DN126040_c5_g1_i6*	*T. plicata*	Clones	1.65 ± 0.13	0.00	Expressed only in resistant plants.	5
Dirigent protein	Disease resistance response protein 206	*TRINITY_DN99675_c1_g1_i1*	*T. plicata*	Seedlings (5-gen. selfed)	-	3.01 ± 0.33	Lower expression in comparison to *T. standishii* or *T. standishii* × *plicata*.	6
			T. standishii	Clones	4.52 ± 0.35	-	Higher expression in comparison to *T. plicata*.	6
			T. standishii × *plicata*	Clones	3.87 ± 0.65	-	Higher expression in comparison to *T. plicata*.	6
		TRINITY_DN99675_c1_g1_i3	*T. plicata*	Seedlings (5-gen. selfed)	-	3.53 ± 0.22	Lower expression in comparison to *T. standishii* or *T. standishii* × *plicata*.	6
			T. standishii	Clones	4.52 ± 0.25	-	Higher expression in comparison to *T. plicata*.	6
			T. standishii × *plicata*	Clones	4.03 ± 0.30	-	Intermediate expression in comparison to *T. standishii* and *T. plicata*.	6
		TRINITY_DN99675_c1_g1_i4	*T. plicata*	Seedlings (5-gen. selfed)	-	2.97 ± 0.32	Lower expression in comparison to *T. standishii* or *T. standishii* × *plicata*.	6
			T. standishii	Clones	4.78 ± 0.32	-	Higher expression in comparison to *T. plicata*.	6
			T. standishii × *plicata*	Clones	3.75 ± 0.63	-	Intermediate expression in comparison to *T. standishii* and *T. plicata*.	6
		TRINITY_DN99675_c1_g1_i5	*T. plicata*	Seedlings (5-gen. selfed)	-	0.90 ± 0.20	Lower expression in comparison to *T. standishii* or *T. standishii* × *plicata*.	6
			T. standishii	Clones	2.49 ± 0.27	-	Higher expression in comparison to *T. plicata*.	6
			T. standishii × *plicata*	Clones	3.85 ± 0.53	-	Higher expression in comparison to *T. plicata*.	6
LEA protein	Dehydrin Xero 1	*TRINITY_DN119739_c4_g1_i4*	*T. plicata*	Clones	10.27 ± 0.11	9.13 ± 0.18	Higher expression in resistant plants.	5
RLK (CRK)	Cysteine-rich receptor-like protein kinase	*TR59000/c3_g2_i1*	*T. plicata*	Seedlings (full-sib)	7.49 ± 0.31	3.85 ± 0.34	Higher expression in resistant plants.	3
RLK (LRR receptor-like protein)	Disease resistance protein RPM1	*TR37382/c2_g1_i1*	*T. plicata*	Seedlings (full-sib)	3.13 ± 0.20	0.63 ± 0.21	Higher expression in resistant plants.	4-CC*
	Disease resistance RPP13-like protein 4	*TR34618/c8_g1_i1*	*T. plicata*	Seedlings (full-sib)	3.06 ± 0.25	0.03 ± 0.03	Higher expression in resistant plants.	4-CC*
	Probable leucine-rich repeat receptor-like protein	*TR58144/c0_g2_i5*	*T. plicata*	Seedlings (full-sib)	1.96 ± 0.21	0.08 ± 0.08	Higher expression in resistant plants.	3
	Putative disease resistance protein RGA4	*TR36626/c4_g2_i1*	*T. plicata*	Seedlings (full-sib)	2.40 ± 0.31	0.00	Expressed only in resistant plants.	4-CC*
	TMV resistance protein N	*TR31269/c1_g1_i1*	*T. plicata*	Seedlings (full-sib)	4.44 ± 0.31	0.19 ± 0.05	Higher expression in resistant plants.	4-CC*
Salicylic acid pathway	DMR6-like oxygenase 2	*TRINITY_DN129734_c10_g1_i2*	*T. plicata*	Clones	2.10 ± 0.15	0.00	Expressed only in resistant plants.	5
Signal transduction	Small G protein family protein/RhoGAP family protein isoform 1	*TR57804/c2_g1_i2*	*T. plicata*	Seedlings (full-sib)	2.63 ± 0.07	0.00	Expressed only in resistant plants.	3
Terpene synthesis	Aldehyde dehydrogenase family 2 member C4	*TR57126/c5_g1_i6*	*T. plicata*	Seedlings (full-sib)	3.09 ± 0.30	1.62 ± 0.39	Higher expression in resistant plants.	3
	Cytochrome P450	*TR57111/c2_g1_i1*	*T. plicata*	Seedlings (full-sib)	1.75 ± 0.24	0.78 ± 0.50	Higher expression in resistant plants.	3
	Putative short-chain alcohol dehydrogenase-like mRNA	*TR52851/c1_g1_i2*	*T. plicata*	Seedlings (full-sib)	1.83 ± 0.18	0.79 ± 0.23	Higher expression in resistant plants.	3
Zinc finger proteins	Zinc finger CCCH domain-containing proteins 37	*TR58437/c7_g1_i3*	*T. plicata*	Seedlings (full-sib)	3.32 ± 0.15	0.03 ± 0.03	Higher expression in resistant plants.	3
		TR58437/c7_g1_i6	*T. plicata*	Seedlings (full-sib)	4.26 ± 0.19	0.12 ± 0.12	Higher expression in resistant plants.	3

take part in the production of 8-8' optically active lignans (Halls et al., 2004), and have been shown to be upregulated in response to *Fusarium solani* f. sp. *phaseoli* infection in pea (Culley et al., 1995), and in genetically modified canola inoculated with *Leptosphaeria maculans* (Wang et al., 1999). There are nine dirigent genes related to the 8-8' coupling process reported in *T. plicata* to date (Kim et al., 2002), and the BLASTn search analysis presented in Chapter 6 suggests that dirigent protein 4 (DIR4; Gang et al. 1999, Kim et al. 2002) may be the gene expressed highly in *T. standishii* and *T. standishii* × *plicata*. In *T. plicata*, in addition to BSPs, resistant clones had higher expression levels of other defense-related transcripts like a dehydrin (Xero 1), as well as sequences related to defense against fungi (EMSY-like 3) and the salicylic acid pathway (DMR6-like oxygenase 2; Table 7.3). Dehydrins have been reported to induce the expression of pathogenesis-related proteins from families PR-3, PR-6, PR-8, PR-11, PR-12, PR-13 and PR-14 in transgenic *Arabidopsis* (Brini et al., 2011), and the expression of EMSY-like genes are needed for basal disease resistance in the same species (Tsuchiya and Eulgem, 2011). The salicylic acid pathway appears to be involved in programmed cell death (Ederli et al., 2011, Vorwerk et al., 2007, Zhang et al., 2013), which is a very important process in hypersensitive responses (Agrios 2005, p. 151). The above gene expression data highlight that *Thuja* sp. clones resistant to *D. thujina* have a number of constitutively expressed defense genes that may act individually or in concert in comparison to susceptible plants.

The constitutive gene expression profiles of *T. plicata* seedlings resistant and susceptible to *D. thujina* were different from those of the clonal lines, in agreement with the differences found between ages at both the anatomical and chemical composition levels, as previously discussed. The most evident difference between resistance classes in seedlings from full-sib families at the gene expression level was the constitutively higher expression of several disease resistance proteins in the resistant families (Table 7.3). Most of those resistance proteins belong to the NBS-LRR family, which are part of the receptor-like protein kinase (RLK) superfamily (Afzal et al. 2008; Goff and Ramonell 2007; Morris and Walker 2003; Tichtinsky et al. 2003; Vidhyasekaran 2008, p. 78). The high expression levels of those sequences in the resistant families is interesting given that several resistance (R) genes to bacterial and fungal pathogens from species like rice, wheat, pepper, tomato and corn are known to belong to the NBS-LRR class (Vidhyasekaran 2008, p. 198). Seedlings of resistant family 685 also had significantly higher expression levels of a cysteine-rich receptor-like protein ki-

nase (CRK), another member of the RLK superfamily (Ederli et al., 2011, Yeh et al., 2015). CRKs have been reported to be involved in defense responses in pathosystems like the *Arabidopsis thaliana* - *Pseudomonas syringae* pv. *tomato* DC3000 (Ederli et al., 2011, Yeh et al., 2015).

Additional sequences of interest, highly expressed in seedlings of the resistant family studied in Chapter 3 were zinc finger proteins and transcripts involved in signal transduction, and terpenes and alkaloids syntheses (Table 7.3). Zinc finger proteins have been shown to be involved in disease resistance (Fujiwara et al., 2006, Moeder et al., 2005), as has been the signal transduction sequence shown in Table 7.3 (Gupta et al., 2012). Terpenes have been reported to inhibit *Candida* sp. fungi and several bacterial species *in vitro* (Tsiri et al., 2009), as well as canker fungi in the Mediterranean cypress *in vivo* (Achotegui-Castells et al., 2016). Terpenes have also been linked to deer deterrence in *T. plicata* (Vourc'h et al., 2001, 2002), and are also the compounds found at highest concentrations in the foliage of western redcedar (Shalev et al., 2018, von Rudloff and Lapp, 1979, von Rudloff et al., 1988, Vourc'h et al., 2001, 2002). The higher expression levels of transcripts *TR52851/c1_g1_i2* and *TR56505/c0_g1_i1* in the resistant seedlings studied in Chapter 3 may be related to the higher concentrations of α-thujene and sabinene in those plants (Table 7.2). Based on the BLASTn searches, *TR52851/c1_g1_i2* was identified as a probable sabinol dehydrogenase (sequence KC767270 in Foster et al. 2013), while sequence *TR56505/c0_g1_i1* appears to be involved in the synthesis of terpenes and flavonoids (sequence KC767279 in Foster et al. 2013).

Foliar alkaloids of *T. plicata* have not been studied much, however, alkaloids have been found in the leaves of another Cupressaceae (Zhang et al., 2007) as discussed in Chapter 3. The sequence in Table 7.3 is involved in the production of benzylisoquinoline alkaloids (BIAs; Liscombe and Facchini 2008, Mishra et al. 2013), which have been shown to inhibit the growth of bacteria and fungi *in vitro* (Villar et al., 1987). The high expression levels of more than one type of disease resistance gene in *T. plicata* seedlings resistant to *D. thujina*, along with other highly expressed defense-related transcripts, supports the polygenic quantitative nature of the species' resistance to the disease (Russell et al., 2007, Russell and Yanchuk, 2012) that is likely the result of natural selection for resistance to the pathogen (Barrett and Heil, 2012, Burdon and Thrall, 2009, Frank, 1993, 1992, Karasov et al., 2014, Occhipinti, 2013) in parental

populations of the seedlings investigated as discussed in section 7.1.

7.2 Induced responses to *Didymascella thujina* infection

7.2.1 Common to both resistant and susceptible plants

The studies carried out during the program showed that all *Thuja* sp. plants analyzed responded to *D. thujina* infection. Although a few mineral nutrients and a terpene showed significant changes in their concentrations after pathogen infection, aluminum was the only chemical variable with a consistent response across all species, age groups, and studies (Table 7.4). Significant increases in aluminum concentrations after inoculation with *D. thujina* were seen in both experiments presented in Chapters 4 and 6, and aluminum concentrations were significantly correlated with disease severity in Chapter 3. Furthermore, the accumulation of aluminum in *Thuja* plants after infection was documented not just in the experiments performed under controlled conditions (Chapters 4 to 6), but also in plants infected under natural conditions (Chapters 3 and 4). Increased amounts of aluminum in infected *T. plicata* clones were also seen in Chapter 5, despite the non-significant difference compared to plants in the mock infections. The accumulation of aluminum in response to *D. thujina* infection was the most common and consistent finding of this Doctoral project.

Aluminum is a toxic element (Duressa et al., 2011, Hamel et al., 1998, Jiang et al., 2015, Mossor-Pietraszewska, 2001, Poot-Poot and Hernandez-Sotomayor, 2011) that causes growth anomalies in plants (Hamel et al., 1998, Mossor-Pietraszewska, 2001, Yuan et al., 2017). High aluminum concentrations are also toxic to other species, including fungi (Avis et al., 2007, Fichtner, 2003, Firestone et al., 1983). The trivalent form of the element is the most poisonous (Fichtner, 2003, Hamel et al., 1998), and is usually found in acidic soils (Firestone et al., 1983, Hamel et al., 1998, Yuan et al., 2017). The fact that aluminum accumulates in the leaves of *Thuja* sp. after infection is puzzling, especially considering that *D. thujina* is a host-specific (Durand, 1913, Kope, 2000, Kope et al., 1998, Søegaard, 1966) obligate foliar parasite (Durand 1913; Søegaard 1956; Søegaard 1969, p. 294) and not a soilborne pathogen. To my knowledge, there is no information on the role of aluminum in plant defense against

Table 7.4. General phenotypic and gene expression induced responses to *Didymascella thujina* infection in the *Thuja* sp. plants studied in this Doctoral project. Values reported are mean ± standard error. #: The units of the gene expression values shown are $\log_2$(FPKM) for transcripts from Chapters 3 and 4, and $\log_2$(TPM) for transcripts from Chapters 5 and 6. ##: *T. plicata* = *Thuja plicata*, *T. standishii* = *Thuja standishii*, *T. standishii* × *plicata* = *Thuja standishii* × *plicata*. *: Controlled conditions experiment in Chapter 4. **: Natural conditions experiment in Chapter 4.

					Infection status			
Process/function	**Variable or transcript annotation**	**Transcript ID#**	**Species##**	**Type of plant material**	**Mock-infected**	**Real-infected**	**Result**	**Chapter**
General phenotypic induced responses to *D. thujina* infection								
Minerals	Aluminum (µg·g^{-1})		*T. plicata*	Seedlings (full-sib)	7.95 ± 0.26	9.75 ± 0.66	Higher concentration in plants with symptoms.	3
			T. plicata	Seedlings (full-sib)	16.89 ± 0.74	21.91 ± 1.36	Higher concentration after infection.	4-CC*
			T. plicata	Seedlings (full-sib)	29.08 ± 3.55	75.50 ± 7.21	Higher concentration after infection.	4-NC**
			T. plicata	Seedlings (5-gen. selfed)	2.05 ± 0.68	17.77 ± 2.15	Higher concentration after infection.	6
			T. plicata	Clones	7.42 ± 2.29	10.67 ± 6.45	Higher concentration after infection.	5
			T. standishii	Clones	1.48 ± 0.48	581.35 ± 251.28	Much higher concentration after infection.	6
			T. standishii × *plicata*	Clones	1.00 ± 0.00	4.45 ± 0.41	Higher concentration after infection.	6
	Carbon (%)		*T. plicata*	Seedlings (full-sib)	50.167 ± 0.120	49.496 ± 0.103	Lower concentration after infection.	4-NC**
	Phosphorus (%)		*T. plicata*	Seedlings (full-sib)	0.187 ± 0.009	0.136 ± 0.008	Lower concentration in plants with symptoms	3
			T. plicata	Clones	0.254 ± 0.014	0.225 ± 0.011	Lower concentration after infection.	5
Terpene	*p*-cymene (µg·g^{-1})		*T. plicata*	Clones	135 ± 5	160 ± 8	Higher concentration after infection.	5
General gene expression induced responses to *D. thujina* infection								
Alkaloids synthesis	(S)-stylopine synthase	*TR19126|c0_g1_i1*	*T. plicata*	Seedlings (full-sib)	7.12 ± 0.18	2.16 ± 0.27	Lower expression after infection.	4-CC*
Calmodulin-binding	G-type lectin S-receptor-like serine/threonine-protein kinase	*TR36118|c2_g1_i1*	*T. plicata*	Seedlings (full-sib)	0.58 ± 0.20	1.69 ± 0.13	HIgher expression in plants with symtoms.	4-CC*
		TRINITY_DN102764_c1_g1_i2	*T. standishii*	Clones	0.00	0.67 ± 0.13	Higher expression in resistant plants.	6
Cell wall organization	Tricin synthase 1	*TR19072|c0_g1_i1*	*T. plicata*	Seedlings (full-sib)	7.40 ± 0.18	10.09 ± 0.12	HIgher expression in plants with symtoms.	3
	Cellulose synthase-like protein H1	*TR27647|c1_g1_i1*	*T. plicata*	Seedlings (full-sib)	5.78 ± 0.23	8.11 ± 0.18	Higher expression after infection.	4-CC*
	Probable xyloglucan endotransglucosylase/hydrolase protein 6	*TRINITY_DN81563_c0_g1_i1*	*T. plicata*	Clones	8.18 ± 0.15	8.65 ± 0.18	Higher expression after infection.	5
	Beta-D-xylosidase 4	*TRINITY_DN141384_c0_g1_i1*	*T. plicata*	Clones	6.62 ± 0.09	7.05 ± 0.14	Higher expression after infection.	5
	Omega-hydroxypalmitate O-feruloyl transferase	*TRINITY_DN101901_c4_g1_i1*	*T. plicata*	Seedlings (5-gen. selfed)	7.86 ± 0.15	8.53 ± 0.11	Higher expression after infection.	6
			T. standishii	Clones	7.95 ± 0.13	8.10 ± 0.13	Higher expression after infection.	6
			T. standishii × *plicata*	Clones	7.98 ± 0.16	8.46 ± 0.10	Higher expression after infection.	6
Dirigent protein	Dirigent protein 1	*TRINITY_DN128247_c1_g2_i1*	*T. plicata*	Clones	0.31 ± 0.06	0.93 ± 0.13	Higher expression after infection.	5
Phenylpropanoids synthesis	*trans*-cinnamate 4-monooxygenase	*TR30105|c0_g1_i1*	*T. plicata*	Seedlings (full-sib)	8.03 ± 0.12	5.76 ± 0.15	Lower expression after infection.	4-CC*
	BAHD acyltransferase DCR (cutin)	*TR33780|c4_g1_i1*	*T. plicata*	Seedlings (full-sib)	8.13 ± 0.14	3.22 ± 0.28	Lower expression after infection.	4-CC*
	Flavanone 3-hydroxylase (flavonoids)	*TR33481|c1_g2_i1*	*T. plicata*	Seedlings (full-sib)	8.30 ± 0.19	6.30 ± 0.21	Lower expression after infection.	4-CC*
	Flavonoid 3',5'-hydroxylase 2 (flavonoids)	*TR39943|c0_g1_i1*	*T. plicata*	Seedlings (full-sib)	8.11 ± 0.06	3.58 ± 0.40	Lower expression after infection.	4-CC*
	Laccase-5 (lignin)	*TR34581|c8_g1_i2*	*T. plicata*	Seedlings (full-sib)	0.81 ± 0.30	2.04 ± 0.20	Higher expression after infection.	4-CC*
Shikimate pathway	Bifunctional 3-dehydroquinate dehydratase/shikimate dehydrogenase	*TR28212|c0_g1_i2*	*T. plicata*	Seedlings (full-sib)	4.36 ± 0.12	2.22 ± 0.23	Lower expression after infection.	4-CC*

foliar pathogens based on the extensive literature reviewed for this dissertation. In spite of that, aluminum toxicity has been shown to trigger defense-like responses in wheat (Hamel et al., 1998), probably through the disruption of calcium homeostasis (Silva, 2012), as well as its effects on the phospholipid signalling system (Poot-Poot and Hernandez-Sotomayor, 2011), both known to play defense roles against pathogens (Vidhyasekaran 2008, pp. 79 and 85).

The stability selection analyses carried out in Chapters 4 and 6 using aluminum as a response variable showed that calcium signalling may have indeed been disrupted as a consequence of increased aluminum concentrations in the foliage of infected *Thuja* sp. plants. In both cases, G-type lectin S-receptor-like serine/threonine-protein kinases (At1g34300 in Chapter 4, and RLK1 in Chapter 6) were among the top predictors of aluminum concentrations, and were upregulated after *D. thujina* infection (Table 7.4). As discussed in the previous chapter, both At1g34300 and RLK1 occur in the plasma membrane and have calmodulin binding functions (UniProt accessions Q39202 and Q9XID3; The UniProt Consortium 2015, 2017). G-type lectin S-receptor-like serine/threonine protein kinases have been associated with salt tolerance in *Glycine soja* through calmodulin/Ca^{2+} signalling (Sun et al., 2013). Such a mechanism suggests possible tolerance to increased levels of aluminum in the infected plants.

The gene expression analyses completed in Chapters 3-6 revealed other common gene expression responses to *D. thujina* infection in *Thuja* sp. plants besides the upregulation of At1g34300 and RLK1. Those analyses suggested that several secondary metabolism pathways were downregulated in response to pathogen inoculation in seedlings, whereas early defense-related transcripts seemed upregulated in both clones and seedlings (Table 7.4). The shikimate pathway appeared to be downregulated via decreased expression of the bifunctional 3-dehydroquinate dehydratase/shikimate dehydrogenase (DHQD/SD; Table 7.4). The lower levels of DHQD/SD after *D. thujina* infection may also be associated with the downregulation of sequences related to the production of phenylpropanoids like lignin, flavonoids and cutin (Table 7.4). This is because DHQD/SD is an upstream enzyme of the pathways that lead to the production of those phenolic secondary metabolites (Tohge et al., 2013). Similarly, the downregulation of transcripts involved in alkaloid production after three days of infection (see also section 4.4.2.2 in Chapter 4) may be related to lower levels of DHQD/SD because the shikimate pathway is upstream in the production of those products as

well (Heldt 2005, p. 302; Heldt and Piechulla 2010, p. 300). It is worth noting that the transcript involved in alkaloid production in Table 7.4 ([S]-stylopine synthase) is related to the production of BIAs (Diamond and Desgagné-Penix, 2016), which are the same type of alkaloid thought to be synthesized by the constitutively highly expressed transcript *TR55613/c7_g3_i3* in the resistant full-sib family 685 (see Table 7.3). The downregulation of secondary metabolism pathways in *T. plicata* seedlings can be related to the reprogramming that the pathogen does to the metabolism of the host plant (Petre et al., 2012, Teixeira et al., 2014, Tremblay et al., 2011), which includes subduing of the plant defenses. For example, rice and barley plants infected with *Magnaporthe grisea*, a pathogen with biotrophic characteristics, have decreased production of shikimate and phenylpropanoids (Parker et al., 2009), the same response reported here in *T. plicata* seedlings infected with *D. thujina*.

Early defense responses to *D. thujina* infection also involved the upregulation of several sequences related to cell wall organization, including lignin synthesis transcripts. The upregulated transcripts involved in the synthesis of lignin were a tricin synthase 1 and a laccase-5 (Table 7.4). Tricin is a flavone that conjugates with lignin (Li et al., 2016), while laccase-5 participates in lignin deposition in cell walls (Wang et al., 2015). Other sequences related to cell-wall organization with increased expressions after infection were a cellulose synthase-like protein H1, a probable xyloglucan endotransglucosylase/hydrolase (XTH) protein 6, a beta-D-xylosidase 4, and an omega-hydroxypalmitate O-feruloyl transferase (Table 7.4). The last four transcripts play roles in cellulose synthesis (Heldt 2005, p. 269; Heldt and Piechulla 2010, p. 268; Liepman and Cavalier 2012), xyloglucan modifications (Cosgrove, 2005, Liu et al., 2007), hemicellulose modification (Hatano and Hamada, 2008), and suberin synthesis (Gou et al., 2009, Molina et al., 2009), respectively. XTHs have been shown to accumulate in the phloem of celery plants attacked by aphids (Divol et al., 2007), in jute plants infected with *Macrophomina phaseolina* (Sharmin et al., 2012), as well as in tomato plants attacked by parasitic *Cuscuta* sp. plants (Olsen et al., 2016). An omega-hydroxypalmitate O-feruloyl transferase has also been reported to be upregulated in tea plants attacked by the biotroph *Exobasidium vexans* (Jayaswall et al., 2016). Plant cell walls are amongst the first targets of pathogenic fungi (Blanco-Ulate et al., 2014b), and cell wall reinforcement in plants is a common early response to pathogen infection (Agrios 2005, p. 232; Vidhyasekaran 2008, p. 298). Based on the gene expression results in Chapters 3 to 6, cell wall remodelling appears to be one

of the early responses to *D. thujina* infection in *Thuja* sp. plants regardless of the species, age or resistance class.

One last interesting general response to *D. thujina* infection was the upregulation of a dirigent protein in the *T. plicata* clones studied in Chapter 5 (Table 7.4). This finding is remarkable considering that another dirigent protein (disease resistance response protein 206) was recorded at constitutively high expression levels in the *T. standishii* and *T. standishii* × *plicata* clonal lines investigated in Chapter 6. Unlike the dirigent protein found in clones of the Japanese arborvitae and the *T. standishii* × *plicata* hybrid (probably a DIR4), the gene of a dirigent protein 1 was upregulated instead in *T. plicata* clones after *D. thujina* inoculation. Dirigent proteins have been shown to be upregulated in response to pathogen infection as discussed previously (see section 7.1.2), and may be important players in *D. thujina* resistance in ontogenetically older *Thuja* plants.

7.2.2 Differentially induced between resistance classes

There were not many differential responses to *D. thujina* infection between *Thuja* sp. plants resistant and susceptible to *D. thujina*. Nevertheless, the differences found occurred mostly in the clonal lines, with resistant plants having stronger responses to infection than susceptible lines, as assessed by the fold change in the concentrations of chemical compounds and the expression levels of the differentially expressed transcripts. The greatest fold change response of all was the foliar accumulation of high amounts of aluminum in *T. standishii* (Table 7.5), the only species studied that was fully resistant to *D. thujina*. The possible role of aluminum as a general defense mechanism against *D. thujina* has been discussed in section 7.2.1. However, the regression stability selection analysis using aluminum as a response variable carried out in Chapter 6, showed that besides the G-type lectin S-receptor-like serine/threonine-protein kinase RLK1 previously mentioned, a calcium-dependent phospholipid binding protein (protein QUIRKY) and an inositol-3-phosphate synthase had increased expression levels with increased aluminum concentrations (Table 7.5).

Aluminum stress has been shown to affect calcium homeostasis (Silva, 2012), and RLK1 and protein QUIRKY are both involved in calcium signalling (Fulton et al., 2009, Sun et al., 2013). Calcium is a general secondary messenger in plants (Batis-

Table 7.5. Differential induced responses to *Didymascella thujina* infection, at the phenotypic and gene expression levels, between the resistant and susceptible *Thuja* sp. plants studied in this Doctoral project. Only values (mean ± standard error) of plants in the real-infection status are presented (e.g. compare the aluminum values below with those shown in Table 7.4). #: The units of the gene expression values shown are $\log_2$(TPM). ##: *T. plicata* = *Thuja plicata*, *T. standishii* = *Thuja standishii*, *T. standishii* × *plicata* = *Thuja standishii* × *plicata*.

					Resistance class			
Process/function	**Variable or transcript annotation**	**Transcript ID#**	**Species##**	**Type of plant material**	**Resistant**	**Susceptible**	**Result**	**Chapter**
Differential induced responses to *D. thujina* infection at the phenotypic level								
Minerals	Aluminum (µg·g^{-1})		*T. plicata*	Seedlings (5-gen. selfed)	-	17.77 ± 2.15	Much lower in infected compared to *T. standishii*.	6
			T. standishii	Clones	581.35 ± 251.28	-	Very high concentration in infected plants.	6
			T. standishii × *plicata*	Clones	4.45 ± 0.41	-	Much lower in infected compared to *T. standishii*.	6
Differential induced responses to *D. thujina* infection at the gene expression level								
Cell wall organization	Beta-D-xylosidase 4	*TRINITY_DN141384_c0_g1_i1*	*T. plicata*	Clones	7.16 ± 0.14	6.85 ± 0.31	Higher expression in resistant plants after infection.	5
	Probable xyloglucan endotransglucosylase/hydrolase protein 6	*TRINITY_DN81563_c0_g1_i1*	*T. plicata*	Clones	8.90 ± 0.16	8.15 ± 0.39	Higher expression in resistant plants after infection.	5
Membrane trafficking	Protein QUIRKY	*TRINITY_DN95987_c1_g2_i4*	*T. plicata*	Seedlings (5-gen. selfed)	-	0.97 ± 0.18	Lower expression in comparison to *T. standishii* or *T. standishii* × *plicata*.	6
			T. standishii	Clones	2.58 ± 0.23	-	Higher expression in comparison to *T. plicata*.	6
			T. standishii × *plicata*	Clones	1.22 ± 0.17	-	Higher expression in comparison to *T. plicata*.	6
PR-protein	Glucan endo-1,3-beta-glucosidase 11	*TRINITY_DN91213_c0_g1_i1*	*T. plicata*	Clones	7.67 ± 0.23	6.68 ± 0.22	Higher expression in resistant plants after infection.	5
	Major allergen *Pru* ar 1	*TRINITY_DN131357_c6_g5_i5*	*T. plicata*	Clones	9.33 ± 0.30	7.34 ± 0.24	Higher expression in resistant plants after infection.	5
	Peroxidase 21	*TRINITY_DN124236_c0_g1_i1*	*T. plicata*	Clones	8.92 ± 0.19	8.05 ± 0.21	Higher expression in resistant plants after infection.	5
Phospholipids synthesis	Inositol-3-phosphate synthase	*TRINITY_DN95430_c1_g1_i2*	*T. plicata*	Seedlings (5-gen. selfed)	-	0.64 ± 0.19	Low expression in comparison to *T. standishii*.	6
			T. standishii	Clones	9.33 ± 0.14	-	Very high expression in comparison to *T. plicata* or *T. standishii* × *plicata*.	6
			T. standishii × *plicata*	Clones	0.86 ± 0.39	-	Low expression in comparison to *T. standishii*.	6

tič and Kudla, 2012) that is also known to be involved in pathogen defense (Vidhyasekaran 2008, p. 79). Aluminum has also been reported to disrupt the phospholipid signalling system (Poot-Poot and Hernandez-Sotomayor, 2011), and the inositol-3-phosphate synthase is related to that pathway (Majumder et al., 1997). Four phospholipases are found in plant cell membranes (PLA1, PLA2, PLC and PLD; Vidhyasekaran 2008, p. 86), PLC being involved in the production of inositol-1,4,5-trisphosphate (IP_3; Vidhyasekaran 2008, p. 87). IP_3 is involved in defense responses triggered by the JA pathway (Mosblech et al., 2008). The gene expression findings related to aluminum accumulation suggest that augmented concentrations of the element, calcium signalling and the phospholipid pathway in leaves may be parts of a complex and effective defense system against *D. thujina* infection in *T. standishii*.

Differential gene expression responses to *D. thujina* between resistance classes were also seen in *T. plicata* clones, and related to pathogenesis-related (PR) proteins and cell wall organization sequences (Table 7.5). Transcripts in the last category were discussed in section 7.2.1. PR proteins are induced as result of plant-pathogen interactions (Antoniw et al., 1980, Jayaraj et al., 2004, van Loon, 1999, van Loon and van Strien, 1999, van Loon et al., 1994), and those mentioned in Table 7.5 have pathogen defense-related functions. For example, glucan endo-1,3-β-glucosidases have been reported to have antimicrobial activity *in vitro* in tobacco (Leubner-Metzger and Meins Jr., 1999) and pea (Mauch et al., 1988), a soy homolog of *Pru ar* 1 has been documented to be a PR-10 protein with *RNA*se activity (Fan et al., 2015), and the peroxidase 21 in Table 7.5 is a class III peroxidase induced during systemic acquired resistance in *Arabidopsis* (Maleck et al., 2000). The production of more than one type of PR protein in response to pathogen infection leads to a synergistic defense response by the host (Jayaraj et al., 2004, Jensen et al., 1999), which is possibly one of the resistance mechanisms to *D. thujina* in resistant *T. plicata* clones.

7.3 Conclusions and future work

In this Doctoral project, the resistance mechanisms to *D. thujina* in *T. plicata*, *T. standishii* and *T. standishii* × *plicata* were investigated. The five main investigations carried out during the program showed that *T. standishii* was fully resistant to the disease, and that *T. standishii* × *plicata* was highly resistant as reported in the past (Søegaard, 1956, 1966, 1969). In contrast, *T. plicata* depicted quantitative resistance

to the pathogen, in agreement with previous reports on variability in the resistance to the disease in that species (Russell and Yanchuk 2012; Russell et al. 2007; Søegaard 1969, p. 323). Furthermore, analyses of the relationship between climate of origin and disease severity in seedlings of *T. plicata* revealed that resistant plants originated from milder climates as has been reported for adults (Russell et al., 2007, Russell and Yanchuk, 2012). In general, the phenotypic and gene expression data collected suggest that major constitutive differences between resistant and susceptible *Thuja* sp. plants account for the resistance to *D. thujina*, and that the resistance mechanisms differ, depending on the age of the plant.

Constitutive resistance mechanisms to *D. thujina* in *T. plicata* seedlings include thicker cuticles, higher concentrations of α-thujene and sabinene, and higher expression levels of disease resistance proteins of the NBS-LRR family. Resistant *T. plicata* seedlings also had significantly lower stomatal densities than susceptible seedlings, but it is unknown if this plays a role in defense against *D. thujina*. In *Thuja* sp. clonal lines, the constitutive resistance to the pathogen was associated with a thinner epidermis, lower citronellyl acetate concentrations than susceptible clones, and higher levels of expression of bark storage proteins. In addition to the aforementioned mechanisms present in resistant clonal lines, *T. standishii* and *T. standishii* $\times$ *plicata* clones had also thicker cuticles and elevated expression levels of a dirigent protein (disease resistance protein 206).

Thuja sp. plants from all lines and ages responded to *D. thujina* infection despite the constitutive differences between resistance classes. The most general response to infection was the foliar accumulation of aluminum, especially in *T. standishii*, where concentrations were much higher in the infected plants in relation to the other species or hybrid. Cell wall reinforcement after *D. thujina* inoculation was also recorded, as well as the downregulation in *T. plicata* seedlings of several pathways involved in secondary metabolite production, including the shikimate, alkaloid, flavonoids and cutin pathways. In addition to those general responses, *T. plicata* clonal lines resistant to the pathogen showed significantly higher expression levels of several PR proteins and of a dirigent protein (dirigent protein 1).

Differences among plants of different ages in the resistance to pathogen infections are common, with older plants generally being more resistant than young plants

(Develey-Rivière and Galiana, 2007, Panter and Jones, 2002). That phenomenon is known as age related resistance (ARR; Carella et al. 2015, Kus et al. 2002, Panter and Jones 2002, Shibata et al. 2010) and although the specific mechanism is not well understood (Kus et al., 2002, Panter and Jones, 2002), it has been reported that the salicylic acid (SA) pathway (Kus et al., 2002, Shibata et al., 2010) and the ethylene pathway (Shibata et al., 2010) may be involved. For instance, it has been shown the SA pathway is triggered in response to pathogen infection in both young and old *Arabidopsis* plants, but the pathway appears to be suppressed by the invading pathogen in younger plants only (Carella et al., 2015). Based on the data collected in the studies carried out during the program, it appears that ARR takes place in the *T. plicata* - *D. thujina* pathosystem as well. This was observed originally by Søegaard, and was referred to as "physiologically determined resistance" (Søegaard 1969, p. 366). The specific mechanisms underlying ARR in *T. plicata* are unknown.

The comprehensive investigations carried out during this Doctoral project, involved the concomitant analysis of the constitutive and induced resistance mechanisms to *D. thujina* in *T. plicata*, *T. standishii* and *T. standishii* × *plicata* both at the phenotypic and genotypic levels using cutting edge machine learning methodologies. The results produced during the program addressed all of the initial research questions and revealed the apparent involvement of aluminum in plant defense, which has been overlooked in plant pathology. Although the element is toxic to plants, it is also highly toxic to pathogens and has been shown to elicit pathogenesis-related responses in plants via the disruption of calcium signalling and the induction of the phospholipid signalling system. If used as a defense mechanism, aluminum may be detoxified by the plant (Fang-Ma, 2000, Feng-Ma, 2007, Feng-Ma et al., 2001, Guo et al., 2005, Panda et al., 2009) while being deployed against the invading pathogen. This project also showed the relevance of bark storage proteins in defense against pathogens in *Thuja* species. Bark storage proteins have been studied mostly in poplar and *Arabidopsis*, but the evidence produced during the program suggests that those proteins may have defense functions in other taxa as well, or at least in *Thuja* species.

Future research should examine the specific mechanism of action of aluminum in the defense against *D. thujina*. The role of α-thujene and sabinene in resistant *T. plicata* seedlings, and that of citronellyl acetate in clonal *Thuja* sp. lines should be followed up as well. It should be investigated if those terpenes are final or intermediate prod-

ucts that confer resistance to *D. thujina*, and whether or not they have fungicidal or fungistatic properties on *D. thujina*. At the genetic level, the specific NBS-LRR proteins that confer resistance to *D. thujina* in *T. plicata* seedlings should be characterized, as should the specific BSPs related to resistance against the pathogen in *Thuja* sp. clones. The role of dirigent proteins in the defense against *D. thujina* in *Thuja* sp. clonal lines should also be elucidated in future investigations. Finally, resistance markers for resistance to *D. thujina* in *T. plicata* based on single nucleotide polymorphisms (SNPs) could be developed using the *RNA*-Seq samples, especially those produced in Chapters 5-6 considering most of them come from clonal plants. SNP discovery is commonly used in array-based association investigations (La Mantia et al., 2013), as well as in genome-wide association studies (GWAS; Bush and Moore 2012, Hou and Zhao 2013, Korte and Farlow 2013, Manzoni et al. 2018). SNP discovery methodologies based on next generation sequencing data have been developed for species with no reference genomes available (see e.g. Lopez-Maestre et al. 2016, Ojeda et al. 2014) such as the *Thuja* species investigated in this project.

Appendix A

A.1 Plant material used in the investigations carried out during the Doctoral program

Table A.1. Parent information of the *Thuja plicata* clonal lines, full-sib families and self-pollinated seedlings (for five generations) used in the studies carried out during this Doctoral project.

Family/clone ID	Type of material	Used in chapter	CLB Severity[1]	Parent ID	CLB rank[2]	Origin	Latitude	Longitude	Elevation (m)
				Seed parent (female)					
398	Seedlings (full-sib)	2, 4	13.57	220	15	Coast - Vancouver Island	50° 30' 54" N	126° 59' 40" W	120
399	Seedlings (full-sib)	2	9.96	220	15	Coast - Vancouver Island	50° 30' 54" N	126° 59' 40" W	120
525	Seedlings (full-sib)	2, 4	19.16	1426	PS[3]	Mountains - Mainland	49° 58' 25" N	123° 08' 31" W	380
528	Seedlings (full-sib)	2	17.92	1428	PS[3]	Interior	49° 3' 1" N	118° 20' 06" W	1270
582	Seedlings (full-sib)	2	21.29	920	838	Interior	49° 38' 21" N	120° 59' 40" W	1150
583	Seedlings (full-sib)	2, 3, 4	25.76	925	876	Interior	49° 33' 28" N	120° 49' 21" W	1190
685	Seedlings (full-sib)	2, 3, 4	8.32	220	15	Coast - Vancouver Island	50° 30' 54" N	126° 59' 40" W	120
687	Seedlings (full-sib)	2	7.84	232	6	Coast - Mainland	51° 18' 35" N	127° 20' 14" W	110
689	Seedlings (full-sib)	2	7.56	261	33	Coast - Vancouver Island	52° 25' 59" N	127° 41' 24" W	165
8182	Seedlings (full-sib)	2	21.37	261	33	Coast - Vancouver Island	52° 25' 59" N	127° 41' 24" W	165
8255	Seedlings (full-sib)	2, 4	8.06	19	14	Coast - Vancouver Island	50° 24' 39" N	127° 25' 44" W	637
8258	Seedlings (full-sib)	2	9.41	128	794	Coast - Haida Gwaii/Queen Charlotte Islands	52° 27' 0" N	131° 22' 19" W	185
8265	Seedlings (full-sib)	2, 4	28.42	528	814	Interior	51° 49' 55" N	119° 9' 28" W	910
124	Seedlings (5-gen. selfed)	6	-	403	NA	Tahsish River, Vancouver Island	50° 6' N	127° 10' W	60
129	Seedlings (5-gen. selfed)	6	-	13	NA	O'Connell Lake, Vancouver Island	50° 21' N	127° 42' W	122
5382	Clones	5	-	925	NA	Interior	49° 33' 28" N	120° 49' 21" W	1190
5398	Clones	5	-	1409	NA	Coast - Mainland (Kaien Island)	54° 16' 30" N	130° 16' 18" W	55
5412	Clones	5	-	1411	NA	Coast - Haida Gwaii/Queen Charlotte Islands	53° 54' 48" N	132° 05' 08" W	53
				Pollen parent (male)					
398	Seedlings (full-sib)	2, 4	13.57	220	15	Coast - Vancouver Island	50° 30' 54" N	126° 59' 40" W	120
399	Seedlings (full-sib)	2	9.96	261	33	Coast - Vancouver Island	52° 25' 59" N	127° 41' 24" W	165
525	Seedlings (full-sib)	2, 4	19.16	1481	PS[3]	Interior	53° 20' 04" N	120° 18' 52" W	1014
528	Seedlings (full-sib)	2	17.92	1497	PS[3]	Interior	52° 19' 57" N	120° 19' 08" W	1047
582	Seedlings (full-sib)	2	21.29	925	876	Interior	49° 33' 28" N	120° 49' 21" W	1190
583	Seedlings (full-sib)	2, 3, 4	25.76	920	838	Interior	49° 38' 21" N	120° 59' 40" W	1150
685	Seedlings (full-sib)	2, 3, 4	8.32	232	6	Coast - Mainland	51° 18' 35" N	127° 20' 14" W	110
687	Seedlings (full-sib)	2	7.84	261	33	Coast - Vancouver Island	52° 25' 59" N	127° 41' 24" W	165
689	Seedlings (full-sib)	2	7.56	220	15	Coast - Vancouver Island	50° 30' 54" N	126° 59' 40" W	120
8182	Seedlings (full-sib)	2	21.37	415	34	Coast - Mainland	50° 41' 39" N	126° 2' 12" W	183
8255	Seedlings (full-sib)	2, 4	8.06	19	14	Coast - Vancouver Island	50° 24' 39" N	127° 25' 44" W	637
8258	Seedlings (full-sib)	2	9.41	128	794	Coast - Haida Gwaii/Queen Charlotte Islands	52° 27' 0" N	131° 22' 19" W	185
8265	Seedlings (full-sib)	2, 4	28.42	528	814	Interior	51° 49' 55" N	119° 9' 28" W	910
124	Seedlings (5-gen. selfed)	6	-	191	NA	Jervis inlet, Sunshine Coast	50° 7' N	123° 47' W	98
129	Seedlings (5-gen. selfed)	6	-	491	NA	Clayquot Sound, Vancouver Island	49° 27' N	126° 06' W	305
5382	Clones	5	-	1505	NA	Interior	52° 19' 57" N	120° 19' 08" W	1047
5398	Clones	5	-	1450	NA	Coast - Mainland (Kaien Island)	54° 15' 49" N	130° 16' 15" W	25
5412	Clones	5	-	1483	NA	Interior	55° 14' 20" N	128° 03' 07" W	308

[1] Percentage area of foliage blighted. These values were used in Chapter 2 to study the relationship between climate of origin and disease severity.
[2] Score by the British Columbia Ministry of Forests, Lands, Natural Resource Operations and Rural Development. Lower scores refer to populations more resistant to *Didymascella thujina*.
[3] PS: Putatively susceptible to *D. thujina*.

A.2 Split-plot fixed effects model for the Analysis of Variance of individual continuous histological variables measured in Chapter 2

Individual continuous histological variables measured in Chapter 2 were analyzed according to the following statistical model:

$$Y_{ijklm} = \mu + \alpha_i + \beta_{j(i)} + \gamma_{k(j)} + \delta_l + (\beta\delta)_{jl} + (\gamma\delta)_{kl} + \epsilon_{ijklm}$$

Where:

μ = Mean value of the variable of interest.
α_i = Effect of the i^{th} resistance class.
$\beta_{j(i)}$ = Effect of the j^{th} family within the i^{th} resistance class.
$\gamma_{k(j)}$ = Main plot effect (k^{th} seedling within j^{th} family).
δ_l = Effect of the l^{th} branch position per seedling.
$(\alpha\delta)_{il}$ = Effect of the interaction of the l^{th} branch position in the i^{th} resistance class.
$(\beta\delta)_{jl}$ = Effect of the interaction of the l^{th} branch position in the j^{th} family family.
$(\gamma\delta)_{kl}$ = Effect of the interaction of the k^{th} seedling in the l^{th} branch position.
ϵ_{ijklm} = Residual error effect.

Model parameters and mean squares were calculated in R (R Core Team, 2015).

A.3 Split-plot fixed effects model for the Analysis of Variance of individual continuous histological variables measured in Chapters 5 and 6

Individual continuous histological variables measured in Chapters 5 and 6 were analyzed according to the following statistical model:

$$Y_{ijkl} = \mu + \alpha_i + \gamma_{j(i)} + \delta_k + (\alpha\delta)_{ik} + (\gamma\delta)_{jk} + \epsilon_{ijkl}$$

Where:

μ = Mean value of the variable of interest.

α_i = Effect of the i^{th} clonal line.

$\gamma_{j(i)}$ = Main plot effect (j^{th} seedling within i^{th} clonal line).

δ_k = Effect of the k^{th} branch position per seedling.

$(\alpha\delta)_{ik}$ = Effect of the interaction of the k^{th} branch position with the i^{th} clonal line.

$(\gamma\delta)_{jk}$ = Effect of the interaction of the j^{th} seedling with the k^{th} branch position.

ϵ_{ijkl} = Residual error effect.

Model parameters and mean squares were calculated in R (R Core Team, 2015).

A.4 Statistical significance of each factor of the ANOVA carried out on the histological variables studied in Chapter 5

Table A.2. Statistical significance (p-values) of the factors of the split-plot ANOVAs performed on the 12 continuous histological variables studied in Chapter 5 (see also Appendix A.3). *= significant factors at $\alpha = 0.05$; **= significant factors at $\alpha = 0.01$. Pal. mes. th. = palisade mesophyll thickness; Sp. mes. th. = spongy mesophyll thickness; Wh. mes. th. = whole mesophyll thickness; Leaf th. = leaf thickness; Pal. to sp. mes. th. ratio = palisade to spongy mesophyll thickness ratio; Wh. mes. to leaf th. ratio = whole mesophyll to leaf thickness ratio; Lig. cells ep. = percentage of cells in the epidermis with lignified cell walls.

	Cuticle	**Epidermis**	**Pal. mes. th.**	**Sp. mes. th.**	**Wh. mes. th.**	**Leaf th.**	**Leaf width**	**Pal. to sp. mes. th. ratio**	**Wh. mes. to leaf th. ratio**	**Lig. cells ep. (%)**
Subplot										
Line	0.0843	0.0678	0.1010	0.0107*	0.1790	0.2450	0.0826	0.0147*	0.2410	0.7470
Plot										
Crown position	0.1980	0.7360	0.0341*	0.1400	0.3310	0.2560	0.1480	0.00931**	0.9270	0.1130
Line × crown position	0.5260	0.1610	0.7007	0.5280	0.6690	0.4590	0.6560	0.4793	0.8640	0.8130

A.5 Statistical significance of each factor of the ANOVA carried out on the histological variables studied in Chapter 6

Table A.3. Statistical significance (p-values) of the split-plot ANOVAs performed on the 8 continuous histological variables in Chapter 6 that were normal or normalized (see also Appendix A.3). *= significant factors at $\alpha = 0.05$; **= significant factors at $\alpha = 0.01$. Sp. mes. th. = spongy mesophyll thickness; Wh. mes. th. = whole mesophyll thickness; Leaf th. = leaf thickness; Wh. mes. to leaf th. ratio = whole mesophyll to leaf thickness ratio; Lig. cells ep. = percentage of cells in the epidermis with lignified cell walls.

	Cuticle	**Epidermis**	**Sp. mes. th.**	**Wh. mes. th.**	**Leaf th.**	**Leaf width**	**Wh. mes. to leaf th. ratio**	**Lig. cells ep. (%)**
Subplot								
Line	0.1120	0.0004**	0.0204*	0.0824	0.1070	0.0298*	0.0502	0.5350
Plot								
Crown position	0.0540	0.4450	0.0162*	0.0868	0.0880	0.3450	0.5930	0.3810
Line × crown position	0.0080**	0.4410	0.0865	0.3552	0.3440	0.2290	0.7410	0.1070

A.6 Experimental design - Chapter 3

Table A.4. Experimental design of the study in Chapter 3.

Item	Details
Families and conditions	·2 Families. ·2 Conditions (CLB^+, CLB^-). ·3 Replicates per family × condition.
Seedlings' age	·Older than a year when infected. ·About 2 years old when sampled (symptoms had developed in the exposed).
Inoculation technique	Exposure to *Didymascella thujina* in a *Thuja plicata* progeny trial site in Jordan River (British Columbia, Canada).
Infection confirmation	·Disease severity assessment of the infected foliage using colour imaging analysis. ·Scanning electron microscopy study of *D. thujina* spores. ·BLASTn search of the two *D. thujina*'s ITS2 in the assembled transcriptome.
Chemical analyses	Fifty-four variables: cellulose, lignin, fibre, terpenes, total C and N, non-structural carbohydrates and mineral nutrients.
RNA-Seq analyses	Illumina HiSeq 100bp paired-end technology. *In house* made libraries per sample, outsourced to Genome Quebec.

A.7 Experimental design - Chapter 4

Table A.5. Experimental design of the study in Chapter 4.

Experiment	Item	Details
Natural Conditions	Families and conditions	·6 Families. ·2 Conditions (CLB^+ and CLB^-; in separate field sites). ·5 Sampling times (0, 11, 18, 21 and 24 days post deployment, dpd). ·1 pooled sample (3 seedlings) per family × condition × sampling time.
	Seedlings' age	·Older than a year when infected and sampled. ·Older than two years when screened for severity (symptoms had developed in the exposed).
	Inoculation technique	Exposure to *Didymascella thujina* in a *Thuja plicata* progeny trial site in Jordan River (British Columbia, Canada).
	Infection confirmation	Disease severity assessment using colour imaging analysis, scanning electron microscopy.
	Chemical analyses	Fifty-four variables: cellulose, lignin, fibre, terpenes, total C and N, non-structural carbohydrates and mineral nutrients.
Controlled Conditions	Families and conditions	·6 Families. ·2 Conditions (CLB^+ and CLB^-; isolated enviroments withing the same growth chamber). ·4 Sampling times (0, 3, 6 and 9 days post infection, dpi). ·1 pooled sample (3 seedlings) per family × condition × sampling time.
	Seedlings' age	·Older than a year when infected and sampled. ·Older than two years when screened for incidence (symptoms had developed in the exposed).
	Inoculation technique	Using *T. plicata* leaves collected in the field and that were releasing *D. thujina* spores (modified version of Søegaard 1969).
	Infection confirmation	Disease incidence assessment, scanning electron microscopy, BLASTn of *D. thujina*'s ITS2 in the assembled transcriptome.
	Chemical analyses	Fifty-four variables: cellulose, lignin, fibre, terpenes, total C and N, non-structural carbohydrates and mineral nutrients.
	RNA-Seq analyses	·Only from families 398, 583, 685 and 8265 were used. ·Only the real infection condition (CLB^+) was sampled. ·Illumina HiSeq 100bp paired-end technology. *In house* made libraries per sample, outsourced to Genome Quebec.

A.8 Experimental design - Chapter 5

Table A.6. Experimental design of the study in Chapter 5.

Item	Details
Plant material	Three *Thuja plicata* clonal lines (5382, 5398, 5412), each with different resitances to *Didymascella thujina*.
Morphological and histological characterization	·Plant size: collar diameter and height (18 plants per line). ·Leaf toughness: 9 plants per line, old and young foliage. ·Epidermal and cuticle thickness, stomatal density: 3 plants per line, 3 branch positions, 2 leaf sides. ·Leaf and mesohpyll thickness, lignin: 3 plants per line, 3 branch positions.
Conditions, replicates and time points	·2 Conditions (CLB^+ and CLB^-; a single growth chamber with isolated environment per condition). ·4 Sampling times (0, 4, 8 and 12 days post infection, dpi). ·3 plants sampled per line × condition × sampling time.
Inoculation technique	Using *T. plicata* leaves collected in the field and that were releasing *D. thujina* spores (modified version of Søegaard 1969).
Infection confirmation	Disease incidence assessment, scanning electron microscopy, BLASTn of *D. thujina*'s ITS2 in the assembled transcriptome.
Chemical analyses	·Sixty compounds and elements, including lignin, fibre, cellulose, terpenes and mineral nutrients. ·All chemical variables were sampled as stated in the previous item (N=72), except for the minerals. ·Mineral nutrients were sampled only at 0 and 8 dpi (N=36).
RNA-Seq analyses	*In house*-made libraries were outsourced to Genome Quebec for Illumina HiSeq 100bp paired-end sequencing.

A.9 Experimental design - Chapter 6

Table A.7. Experimental design of the study in Chapter 6.

Item	Details
Plant material	·Two *Thuja plicata* seedling lines (selfed for five generations, lines 124 and 129). ·One *Thuja standishii* clonal line (grown from seedlings germinated from wild stand seed obtained from the Japanese Forest Tree Breeding Centre). ·One *T. standishii* × *plicata* clonal line ("Green Giant" Arborvitae - NA 29972; U.S. National Arboretum, Washington DC, USA).
Morphological and histological characterization	·Collar diameter and height: 12 plants per line. ·Leaf toughness: 5 plants per line, old and young foliage. ·Epidermal and cuticle thickness, stomatal density: 3 plants per line, 3 branch positions, 2 leaf sides. ·Leaf and mesohpyll thickness, lignin: 3 plants per line, 3 branch positions.
Conditions, replicates and time points	·2 Conditions (CLB^+ and CLB^-; a single growth chamber with isolated environment per condition). ·3 Sampling times (0, 4 and 8 days post infection, dpi). ·2 plants sampled per line × condition × sampling time.
Inoculation technique	Using *T. plicata* leaves collected in the field and that were releasing *D. thujina* spores (modified version of Søegaard 1969).
Infection confirmation	Disease incidence assessment, scanning electron microscopy, BLASTn of *D. thujina*'s ITS2 in the assembled transcriptome.
Chemical analyses	·Sixty compounds and elements, including lignin, fibre, cellulose, terpenes, and mineral nutrients. ·All chemical variables were sampled as stated in the previous item (N=48), except for the minerals. ·Mineral nutrients were sampled only at 0 and 8 dpi (N=32).
RNA-Seq analyses	Library production and sequencing were outsourced to Genome Quebec (Illumina HiSeq 100bp paired-end technology).

A.10 Custom-made humidity chamber used to perform controlled inoculations of *Thuja plicata* foliage with *Didymascella thujina*

Figure A.1. Custom-made humidity chamber used to carry out controlled inoculations of *Thuja plicata* foliage with *Didymascella thujina*. The cage was made of PVC pipes fully covered with transparent plastic. An irrigation system linked to a tray inside the cage supplied the water used by five Exo Terra® ultrasonic foggers (Rolf C. Hagen Inc., Montreal QC, Canada) to increase the relative humidity above 90% within two days. The excess water was drained by holes punched at the bottom of the cage. During the experiment, the cage remained inside a Conviron growth chamber (Conviron, Winnipeg MB, Canada) set at 12 h darkness at 10°C and 12 h light at 14°C. Temperature and humidity meters were placed inside the cage to monitor those conditions. (Image by Juan A. Aldana).

A.11 Climate variables per parent and family used in Chapter 2

Table A.8. List of the 32 climate variables per parent and family used in Chapter 2 to analyze the relationship between resistance to *Didymascella thujina* and climate of origin of seedlings from 13 *Thuja plicata* full-sib families.

Climate variable
April maximum mean temperature (℃)
April mean temperature (℃)
April precipitation (mm)
August maximum mean temperature (℃)
August mean temperature (℃)
August precipitation (mm)
Autumn degree-days above 5℃
Autumn mean temperature (℃)
Autumn precipitation (mm)
July maximum mean temperature (℃)
July mean temperature (℃)
July precipitation (mm)
June maximum mean temperature (℃)
June mean temperature (℃)
June precipitation (mm)
May maximum mean temperature (℃)
May mean temperature (℃)
May precipitation (mm)
Mean annual precipitation (mm)
Mean annual temperature (℃)
September maximum mean temperature (℃)
September mean temperature (℃)
September precipitation (mm)
Spring degree-days above 5℃
Spring mean temperature (℃)
Spring precipitation (mm)
Summer degree-days above 5℃
Summer heat-moisture index
Summer mean temperature (℃)
Summer precipitation (mm)
Winter degree-days below 5℃
Winter mean minimum temperature (℃)

A.12 Estimated climatic variables of the field site where the 2012 pilot study and the 2013 investigation in Chapter 3 took place

The progeny trial where the 2012 pilot study and the 2013 inoculations were held is located in Jordan River, British Columbia (48° 25' 24.52" N, 124° 1' 27.69" W, elev. 76 m). The pilot study took place between May 2nd and July 18th, 2012, while the experiment referred to in Chapter 3 was performed between May 8th and June 28th, 2013. Weather data for the period when the plants were exposed to *Didymascella thujina* in each year were estimated because no weather loggers or rain collectors were deployed in either of those two field seasons, and there are no weather stations nearby.

Total rain, relative humidity and mean temperature of the infection periods aforementioned were estimated by averaging the values recorded by the weather stations of the John Muir and Port Renfrew elementary schools. Data from both stations were collected from the School-Based Weather Station Network (Weaver and Wiebe, 2016) and used for this analysis because the *Thuja plicata* progeny trial is located between those two schools. Table A.9 summarizes the values of each variable for the 2012 and 2013 infection periods per school station, as well as the estimated values for Jordan River.

Table A.9. Estimated values of selected climate variables in the *Thuja plicata* progeny trial in Jordan River, British Columbia (48° 25' 24.52" N, 124° 1' 27.69" W, elev. 76 m) in the summers of 2012 and 2013.

		2012	**2013**
Length of Exposure	Deployment date to Jordan River	May 2	May 8
	Retrieval date from Jordan River	July 18	June 28
	Total days in the field	77	51
Total Rain	Total rain - Port Renfrew station (mm)	227.2	229.8
	Total rain - John Muir station (mm)	73.1	81.8
	Estimated Total rain received in Jordan River (mm)	150.1	155.8
Relative Humidity	Mean relative humidity - Port Renfrew station (%)	85.43	89.17
	Mean relative humidity - John Muir station (%)	78.89	82.93
	Estimated mean relative humidity in Jordan River (%)	82.16	86.05
Mean Temperature	Mean temperature - Port Renfrew station (℃)	11.2	11.9
	Mean temperature - John Muir station (℃)	11.6	12.3
	Estimated mean temperature in Jordan River (℃)	11.4	12.1

A.13 *Didymascella thujina* spore load and mean temperature in Jordan River (British Columbia) in summer 2014

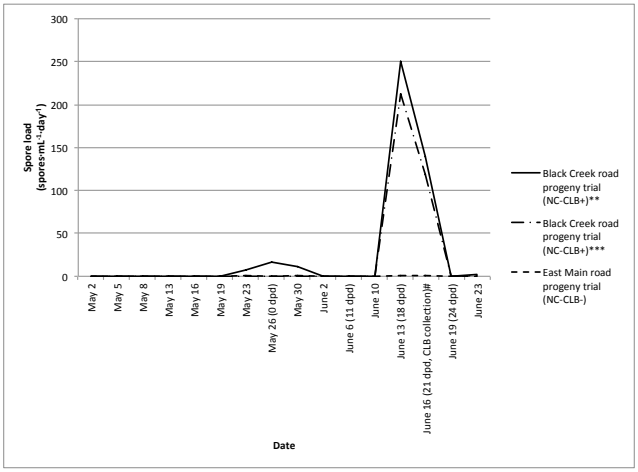

(a)

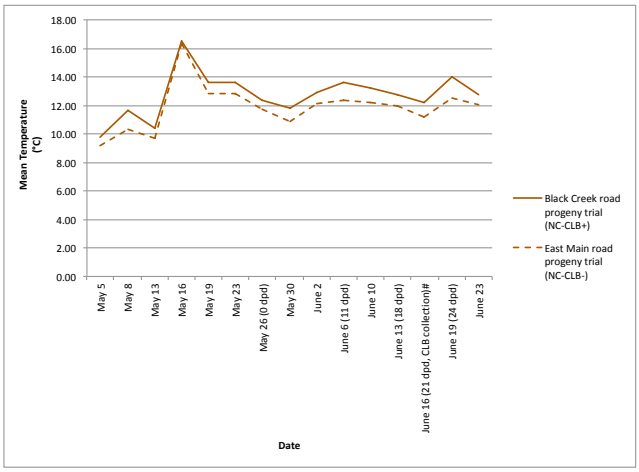

(b)

Figure A.2. *Didymascella thujina* spore load and mean temperature recorded during the Natural Conditions (NC) experiment carried out in 2014 in Jordan River (British Columbia), presented in Chapter 4. *D. thujina* (cedar leaf blight, CLB) was present in the Black Creek road progeny trial (NC-CLB^{+}), and absent in the East Main road progeny trial (NC-CLB^{-}). (a) *D. thujina* spore load on the two sites: ** all spores counted regardless of their germination status; *** germinated spores only. (b) Mean temperature of the two sites.

A.14 *Didymascella thujina* spore load and mean temperature in Jordan River (British Columbia) in summer 2015

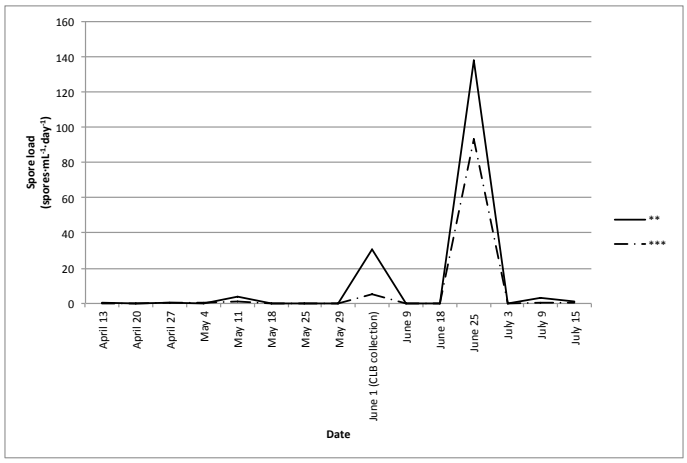

(a)

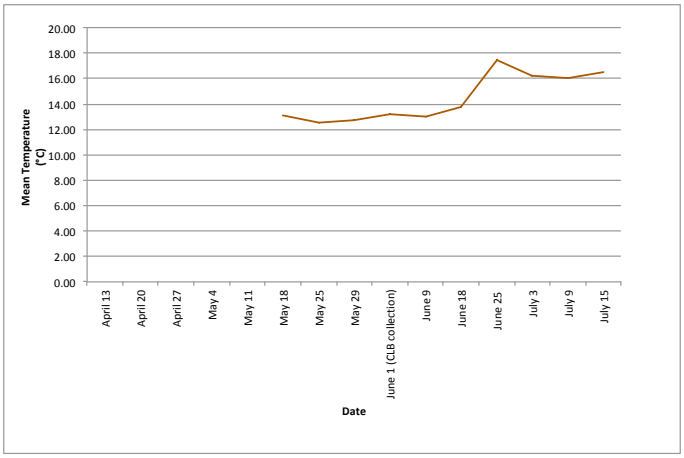

(b)

Figure A.3. *Didymascella thujina* spore load and mean temperature recorded in the *Thuja plicata* progeny trial in Jordan River (British Columbia), where the *D. thujina* inoculum for the experiments presented in Chapters 5 and 6 came from. Data was recorded during the first sporulation season of 2015 (see also Figs. 1.1a - 1.1f). (a) *D. thujina* spore load: ** all spores counted regardless of their germination status; *** germinated spores only. (b) Mean temperature.

A.15 Total rain and mean relative humidity in Jordan River (British Columbia) in summer 2014

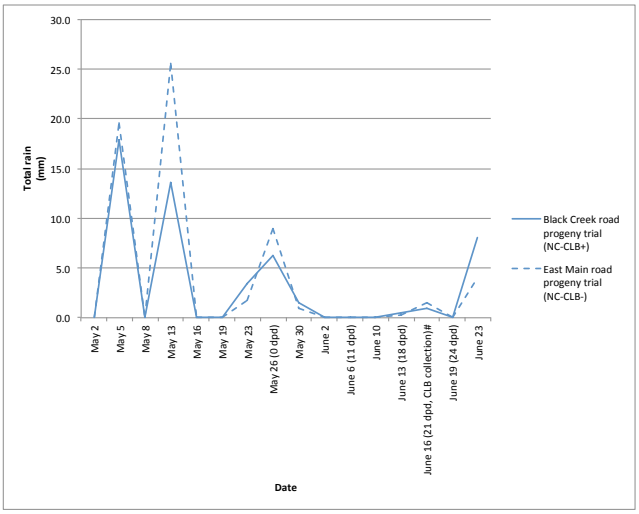

(a)

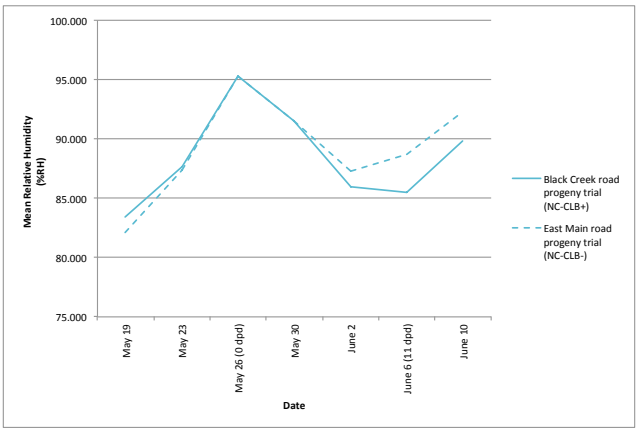

(b)

Figure A.4. Total rain and mean relative humidity recorded during the Natural Conditions (NC) experiment carried out in 2014 in Jordan River (British Columbia), and presented in Chapter 4. *Didymascella thujina* (cedar leaf blight, CLB) was present in the Black Creek road progeny trial (NC-CLB^{+}), and absent in the East Main road progeny trial (NC-CLB^{-}). (a) Total rain on the two sites. (b) Mean relative humidity on the two sites.

A.16 Total rain and mean relative humidity in Jordan River (British Columbia) in summer 2015

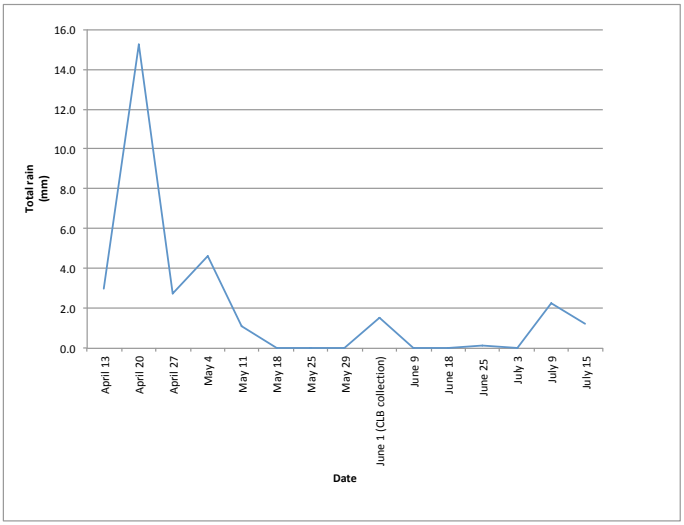

(a)

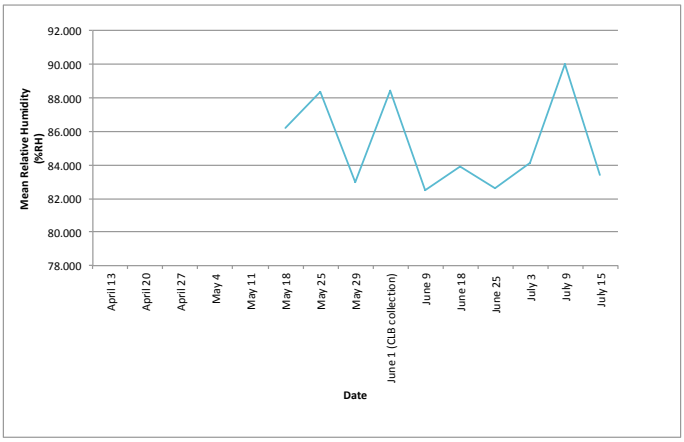

(b)

Figure A.5. Total rain and mean relative humidity recorded in the *Thuja plicata* progeny trial in Jordan River (British Columbia), where the *Didymascella thujina* inoculum for the experiments presented in Chapters 5 and 6 originated. Data was recorded during the first sporulation season of 2015. (a) Total rain. (b) Mean relative humidity.

A.17 Variables transformed for the Pearson correlation analyses in Chapter 2

Table A.10. Variables that were transformed to meet the normality assumption for the Pearson correlation analyses of the evaluation of the relationship between resistance to *Didymascella thujina* and *Thuja plicata* climate of origin in Chapter 2.

Source	Climate variable	Transformation
Female parent	Winter degree-days below 5℃	Cosine
Female parent	June precipitation (mm)	Reciprocal
Female parent	July precipitation (mm)	Reciprocal
Female parent	Autumn mean temperature (℃)	Cosine
Female parent	June maximum mean temperatures (℃)	Reciprocal
Male parent	Winter degree-days below 5℃	Natural logarithm
Male parent	Autumn precipitation (mm)	Square root
Male parent	September precipitation (mm)	Cosine
Male parent	Autumn mean temperature (℃)	Cosine
Male parent	Winter mean minimum temperature (℃)	Sine
Seedling family	Mean annual temperature (℃)	Cosine
Seedling family	May precipitation (mm)	Sine
Seedling family	Autumn mean temperature (℃)	Cosine
Seedling family	Winter mean minimum temperature (℃)	Cosine

A.18 Change point analysis of the random forest output of section 2.3.2.2

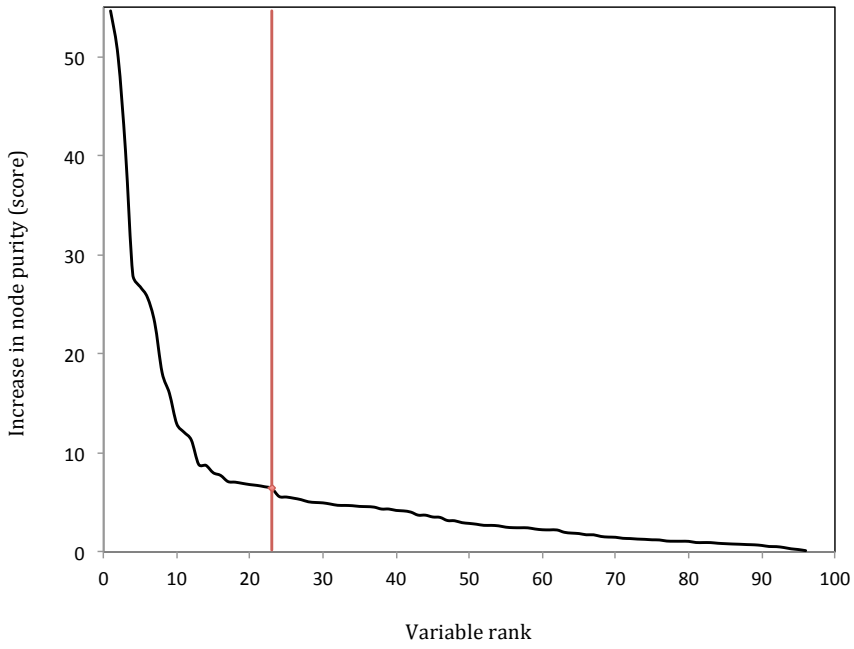

Figure A.6. Change point analysis of the increase in node purity scores output by random forest from 96 climate variables studied as predictors for *D. thujina* severity in seedlings of 13 *T. plicata* families (32 variables per parent and family). The analysis was completed using the changepoint R package with the AMOC method on mean and variance. The top 23 variables were the best predictors according to this analysis (red line).

A.19 Elements and compounds quantified in the study presented in Chapter 3

Table A.11. Elements and compounds quantified in the study presented in Chapter 3

Terpenes	Elements	Acid detergent fibre	Non-structural carbohydrates
Borneol	Al	Lignin	Sugars (as glucose)
Bornyl acetate	B	Cellulose	Starch
Camphene	C	Fibre	
Camphor	Ca		
2-Carene	Cu		
3-Carene	Fe		
β-Caryophylene	K		
1,8-Cineol	Mg		
Citronellene	Mn		
Citronellal	Mo		
Citronellol	N		
Citronellyl acetate	Na		
p-Cymene	P		
Fenchone and terpinolene	S		
Geranyl acetate	Zn		
Geraniol			
α-Humulene			
R-Limonene			
Linalool			
Myrcene			
Ocimene			
α-Phellandrene			
α-Pinene			
β-Pinene			
Pulegone			
Sabinene			
α-Terpinene			
γ-Terpinene			
Terpineol			
α-Thujene			
α-Thujone			
β-Thujone			
Monoterpenes			
Sesqui- and di-terpenes			

A.20 Variable contribution to components 1 to 3 of the principal component analyses of the chemical variables studied in Chapter 4

Table A.12. Variable contribution to components 1 to 3 of the principal component analyses of the chemical variables studied in both the natural conditions and controlled conditions experiments presented in Chapter 4. The top five variables per component are shown in bold.

	Natural conditions experiment			Controlled conditions experiment		
Element/compound	**Component 1**	**Component 2**	**Component 3**	**Component 1**	**Component 2**	**Component 3**
Al	0.139	5.382	0.014	3.240	2.733	0.401
B	0.632	4.780	0.130	3.893	1.476	0.257
C	0.155	5.295	5.050	2.798	0.042	0.871
Ca	0.039	3.259	**8.888**	1.944	3.480	1.058
Cu	0.002	3.922	5.234	0.059	0.093	0.432
Fe	0.067	**5.625**	**6.365**	2.767	**6.187**	0.081
K	2.282	1.788	3.309	**4.759**	1.660	0.044
Mg	0.588	**8.673**	0.894	**4.830**	1.627	0.056
Mn	0.004	4.474	1.461	1.057	0.790	0.058
Mo	0.352	1.329	1.837	1.683	2.655	0.153
N	0.483	0.827	5.627	4.521	1.100	0.015
Na	0.103	**6.458**	4.522	3.802	3.434	0.023
P	1.005	**8.420**	0.680	4.133	1.546	0.080
S	0.006	**9.185**	0.085	2.651	0.040	0.531
Zn	1.128	1.792	2.830	0.265	4.466	0.051
Borneol	0.255	0.113	1.794	0.000	0.390	**13.242**
Bornyl acetate	0.158	1.081	1.515	1.127	0.079	**10.527**
Camphene	1.871	1.216	4.670	0.227	0.950	4.688
Camphor	0.040	0.873	1.396	0.019	1.390	**10.324**
2-Carene	0.000	0.000	0.000	0.000	0.000	0.000
3-Carene	0.058	0.468	0.654	0.110	0.001	0.013
β-Caryophylene	0.566	0.353	0.500	2.286	0.485	0.325
1,8-Cineol	0.000	0.000	0.000	0.001	0.198	**13.778**
Citronellene	0.241	0.089	0.563	0.000	0.000	0.000
Citronellal	0.941	0.049	0.072	1.114	1.441	0.975
Citronellol	0.006	0.100	1.112	0.002	0.264	**14.105**
Citronellyl acetate	1.752	0.077	0.068	0.199	3.719	0.258
p-Cymene	0.475	2.666	**7.281**	1.201	4.413	0.026
Fenchone and terpinolene	2.125	1.897	0.284	**5.801**	0.953	0.549
Geranyl acetate	5.013	0.122	1.240	**4.911**	0.335	0.040
Geraniol	2.699	3.996	1.482	3.888	0.003	0.092
α-Humulene	3.471	0.069	0.057	0.722	1.311	0.584
R-Limonene	**8.123**	0.309	0.421	1.454	**8.110**	0.177
Linalool	0.347	0.000	0.327	0.190	1.989	0.015
Myrcene	**8.253**	0.254	0.078	**4.581**	3.774	0.387
Ocimene	0.000	0.000	0.000	0.281	0.289	0.049
α-Phellandrene	0.000	0.000	0.000	0.000	0.000	0.000
α-Pinene	**8.037**	0.160	0.184	1.580	**6.898**	0.225
β-Pinene	6.325	0.045	0.041	3.611	1.972	0.053
Pulegone	0.010	1.256	0.170	0.002	1.605	9.663
Sabinene	4.655	0.386	0.003	1.536	1.378	1.305
α-Terpinene	0.624	0.437	**6.197**	0.412	0.074	0.186
γ-Terpinene	5.574	0.049	0.756	0.009	4.363	1.379
Terpineol	0.281	0.242	0.493	0.576	0.290	5.278
α-Thujene	**7.558**	0.284	0.111	2.360	**5.177**	0.506
α-Thujone	6.736	0.219	0.190	2.974	3.940	0.000
β-Thujone	3.436	0.047	2.000	2.760	2.252	0.000
Monoterpenes	**8.193**	0.284	0.119	3.768	**5.513**	0.153
Sesqui- and di-terpenes	3.235	0.041	0.006	0.303	2.108	1.283
Fibre	0.003	1.952	**10.192**	2.743	0.046	0.000
Cellulose	0.743	0.172	1.784	0.004	0.004	4.418
Lignin	0.455	3.992	3.492	2.035	0.076	0.725
Sugars (as glucose)	0.647	1.434	2.059	0.400	2.654	0.011
Starch	0.111	4.059	1.763	4.413	0.227	0.552

A.21 Elements and compounds quantified in the studies presented in Chapters 5 and 6

Table A.13. Elements and compounds quantified in the studies presented in Chapters 5 and 6.

Terpenes	Elements	Acid detergent fibre
Borneol	Al	Lignin
Bornyl acetate	B	Cellulose
Camphene	Ca	Fibre
Camphor	Cu	
2-Carene	Fe	
3-Carene	K	
β-Caryophylene	Mg	
1,8-Cineol	Mn	
Citronellene	Mo	
Citronellal	Na	
Citronellol	P	
Citronellyl acetate	S	
p-Cymene	Zn	
Fenchone and terpinolene		
Geranyl acetate		
Geraniol		
α-Humulene		
R-Limonene		
Linalool		
Myrcene		
Ocimene		
α-Phellandrene		
α-Pinene		
β-Pinene		
Pulegone		
Sabinene		
α-Terpinene		
γ-Terpinene		
Terpineol		
α-Thujene		
α-Thujone		
β-Thujone		
Monoterpenes		
Sesqui- and di-terpenes		
α-Gurjunene		
trans-β-Guaiene		
α-Cadinene		
Germacrene-D-4-ol		
Rimulene		
Cembrene		
Sandaracopimarinol		
trans-Ferruginol		
cis-Ferruginol		
Totarol acetate		

A.22 Fixed-effects factorial model for the Analysis of Variance of chemical variables in Chapter 3

Fixed-effects factorial model for the Analysis of Variance of individual chemical variables that were selected using stability selection and change point analyses in Chapter 3. The variables were analyzed according to the following statistical model:

$$Y_{ijk} = \mu + \alpha_i + \beta_j + (\alpha\beta)_{ij} + \epsilon_{ijk}$$

Where:

μ = Mean value of the variable of interest.
α_i = Effect of the i^{th} family.
β_j = Effect of the j^{th} infection treatment.
$(\alpha\beta)_{ij}$ = Effect of the interaction of the i^{th} family in the j^{th} infection treatment.
ϵ_{ijk} = Residual error effect.

Model parameters and mean squares were calculated in R (R Core Team, 2015).

A.23 Mixed-effects factorial model for the Analysis of Variance of chemical variables in Chapter 4

Mixed-effects factorial model for the Analysis of Variance of individual chemical variables that were selected using stability selection and changepoint in both the natural (NC) and controlled conditions (CC) experiments in Chapter 4. Those variables were analyzed according to the following statistical model:

$$Y_{ijkl} = \mu_l + \alpha_k + \beta_i + \tau_j + (\alpha\tau)_{jk} + (\beta\tau)_{ij} + (\alpha\beta\tau)_{ijk} + \Upsilon_{l(k)}$$

Where:

$$\begin{aligned}
\mu_l &= \text{Mean value of the variable of interest in the } l^{th} \text{ family.} \\
\alpha_k &= \text{Effect of the } k^{th} \text{ resistance class.} \\
\beta_i &= \text{Effect of the } i^{th} \text{ infection treatment.} \\
\tau_j &= \text{Effect of the } j^{th} \text{ sampling time.} \\
(\alpha\tau)_{jk} &= \text{Effect of the interaction of the } k^{th} \text{ resistance class in the } j^{th} \text{ sampling time.} \\
(\beta\tau)_{ij} &= \text{Effect of the interaction of the } j^{th} \text{ sampling time in the } i^{th} \text{ infection treatment.} \\
(\alpha\beta\tau)_{ijk} &= \text{Effect of the interaction of the } k^{th} \text{ resistance class in the } j^{th} \text{ sampling time of the } i^{th} \text{ infection treatment.} \\
\Upsilon_{l(k)} &= \text{Random effect of the } l^{th} \text{ family within the } k^{th} \text{ resistance class.}
\end{aligned}$$

The mixed model was fitted to the data using restricted maximum likelihood implemented in R package lme4 (Bates et al., 2015), and statistical significance of the effects was calculated using lmerTest (Kuznetsova et al., 2015).

A.24 Fixed-effects factorial model for the Analysis of Variance of chemical variables in Chapters 5 and 6

Fixed-effects factorial model for the Analysis of Variance of individual chemical variables selected with stability selection and changepoint in Chapters 5 and 6. Selected variables were analyzed according to the following statistical model:

$$Y_{ijkl} = \mu + \alpha_i + \beta_j + \gamma_k + (\alpha\beta)_{ij} + (\alpha\gamma)_{ik} + (\beta\gamma)_{jk} + (\alpha\beta\gamma)_{ijk} + \epsilon_{ijkl}$$

Where:

$$\begin{aligned}
\mu &= \text{Mean value of the variable of interest.} \\
\alpha_i &= \text{Effect of the } i^{th} \text{ plant line.} \\
\beta_j &= \text{Effect of the } j^{th} \text{ time point.} \\
\gamma_k &= \text{Effect of the } k^{th} \text{ infection treatment.} \\
(\alpha\beta)_{ij} &= \text{Effect of the interaction of the } i^{th} \text{ plant line with the } j^{th} \text{ time point.} \\
(\alpha\gamma)_{ik} &= \text{Effect of the interaction of the } i^{th} \text{ plant line with the } k^{th} \text{ infection treatment.} \\
(\beta\gamma)_{jk} &= \text{Effect of the interaction of the } j^{th} \text{ time point with the } k^{th} \text{ infection treatment.} \\
(\alpha\beta\gamma)_{ijk} &= \text{Interaction among all factors.} \\
\epsilon_{ijkl} &= \text{Residual error effect.}
\end{aligned}$$

Model parameters and mean squares were calculated in R (R Core Team, 2015).

A.25 Temporal variation of selected chemical variables from Chapter 4

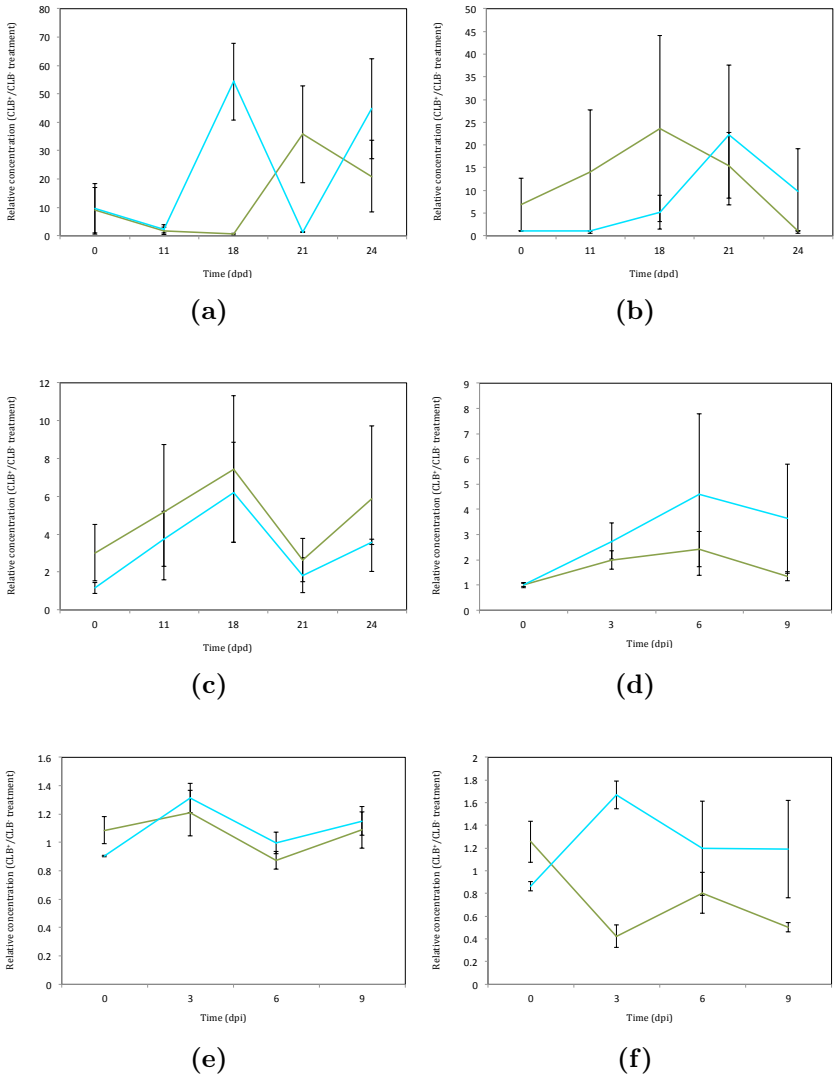

Figure A.7. Temporal variation of the relative concentrations of selected chemical variables in the real infections normalized against mock infections in both experiments carried out in Chapter 4. Variables from the natural conditions experiment: (a) bornyl acetate, (b) camphor, (c) starch. Variables from the controlled conditions experiment: (d) copper, (f) iron, (g) molybdenum. Resistant families in green, susceptible families in cyan. Concentrations are higher in the real infections if the relative concentration (CLB^+/CLB^-) is >1, and higher in the mock infections if <1. dpd = days post deployment, dpi = days post infection.

A.26 Temporal variation of selected chemical variables from Chapter 5

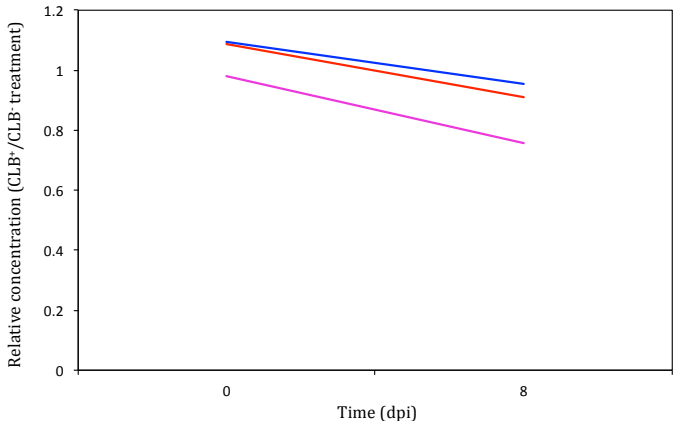

(a)

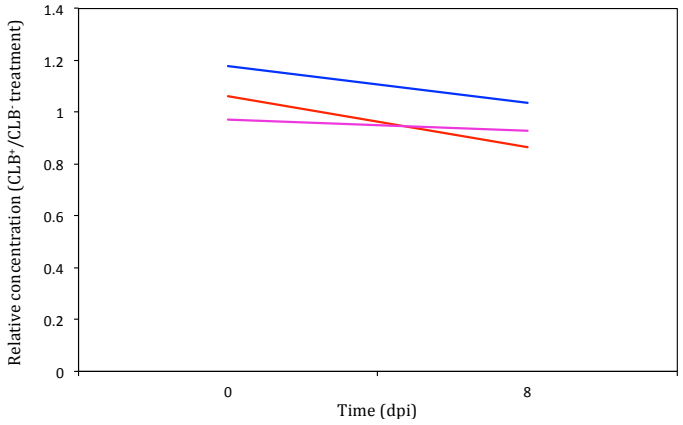

(b)

Figure A.8. Temporal variation of the relative concentrations of selected minerals of *Thuja plicata* in response to *Didymascella thujina* infection as chosen by stability selection in Chapter 5. Clone lines were colour-coded as follows: 5382 in red, 5412 in light purple, and 5398 in blue. (a) Phosphorus, (b) magnesium. Concentrations are higher in the real infections if the relative concentration (CLB^+/CLB^-) is >1, and higher in the mock infections if <1. dpi = days post infection.

A.27 Pipeline used for processing and analyzing the *RNA*-Seq data presented in Chapter 3

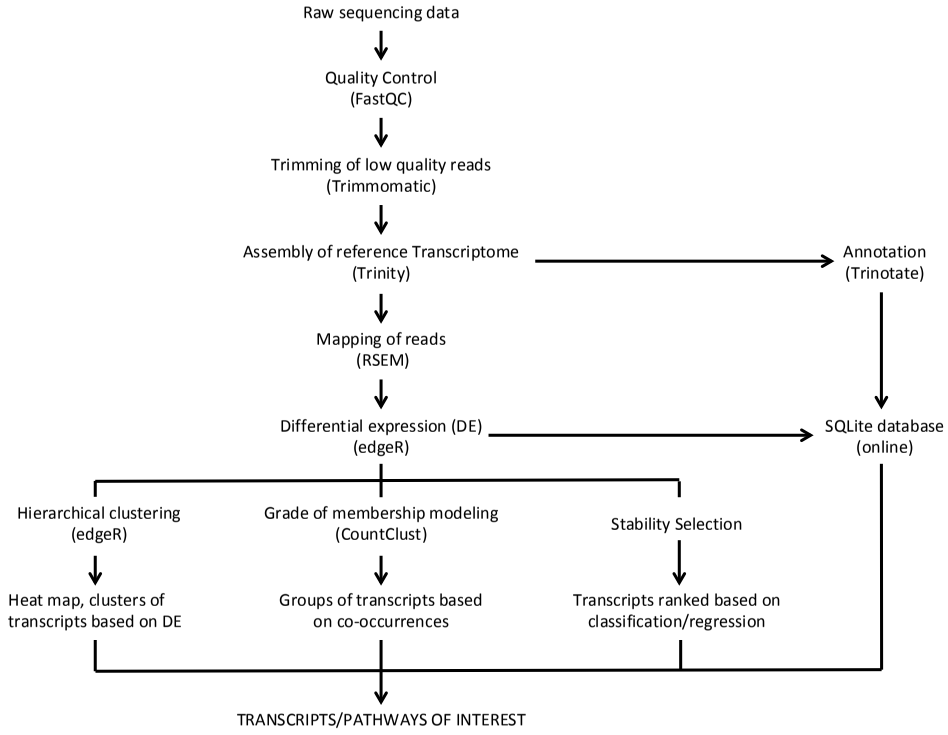

Figure A.9. Pipeline used for processing and analyzing the *RNA*-Seq data presented in Chapter 3.

A.28 Pipeline used for processing and analyzing the *RNA*-Seq data presented in Chapter 4

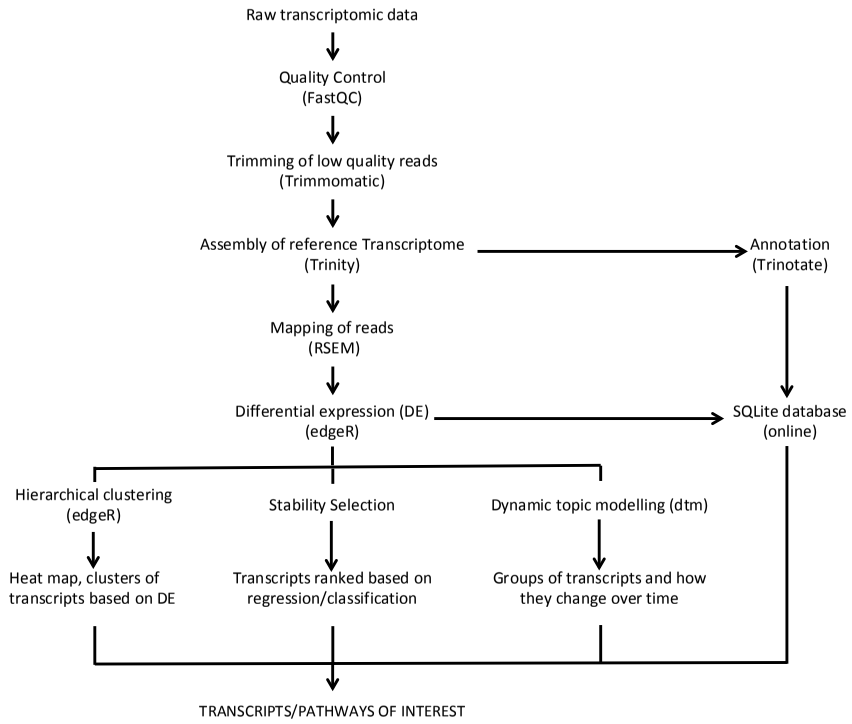

Figure A.10. Pipeline used for processing and analyzing the *RNA*-Seq data presented in Chapter 4.

A.29 Pipeline used for processing and analyzing the *RNA*-Seq data presented in Chapters 5 and 6

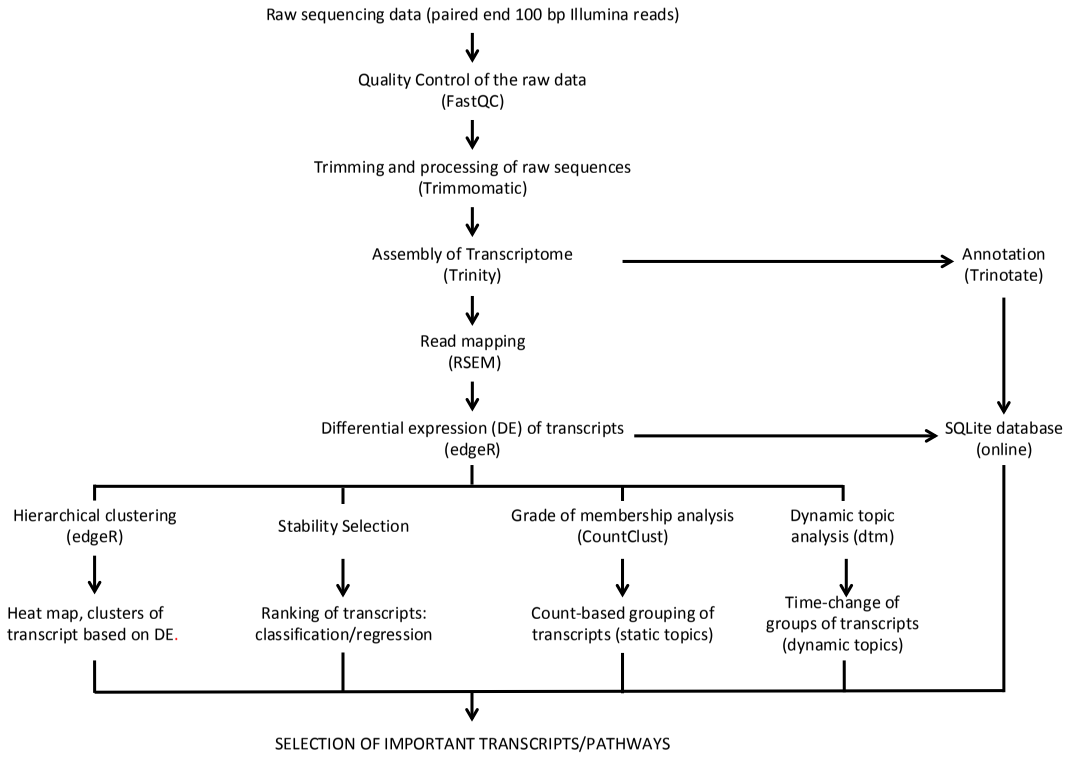

Figure A.11. Pipeline used to process and analyze the *RNA*-Seq data presented in Chapters 5 and 6.

A.30 Statistics of the transcriptomes assembled for the studies in Chapters 3 to 6

Table A.14. Statistics of the transcriptomes assembled for the studies in Chapters 3 to 6 (calculated in PRINSEQ). * = Number of transcriptomic samples used to build the respective assembly.

Chapter	**3**	**4**	**5**	**6**
Sample size (N)*	12	16	72	48
Trinity genes	138,020	93,009	267,664	242,906
Trinity transcripts	173,924	122,588	339,748	311,664
Trinity transcripts with annotations	71,746	51,656	64,889	77,886
Total number of bases	134,254,425	103,775,832	221,595,429	193,615,273
Mean sequence length (bp)	772	847	652	621
Minimum sequence length (bp)	224	224	201	201
Maximum sequence length (bp)	16,325	12,293	17,797	17,893
Mode sequence length (bp (# seqs.))	224 (1,090)	224 (629)	202 (2,071)	201 (1,873)
N50 contig size (bp)	1,315	1,441	1,039	945

A.31 Overall alignment rates of the *RNA*-Seq samples used in Chapter 3

Table A.15. Overall alignment rates of the filtered reads of all libraries used in the gene expression analyses of the experiment presented in Chapter 3.

Family	CLB resistance class	Seedling ID	Condition	Overall alignment rate (%)
583	Susceptible	583-23	CLB^-	96.89
583	Susceptible	583-27	CLB^-	96.81
583	Susceptible	583-33	CLB^-	97.04
685	Resistant	685-24	CLB^-	96.05
685	Resistant	685-27	CLB^-	97.00
685	Resistant	685-34	CLB^-	96.80
583	Susceptible	583-2	CLB^+	95.93
583	Susceptible	583-12	CLB^+	97.19
583	Susceptible	583-17	CLB^+	96.00
685	Resistant	685-1	CLB^+	97.29
685	Resistant	685-4	CLB^+	97.02
685	Resistant	685-18	CLB^+	97.27

A.32 Overall alignment rates of the *RNA*-Seq samples used in Chapter 4

Table A.16. Overall alignment rates of the filtered reads of all libraries used in the gene expression analyses of the experiment presented in Chapter 4.

Family	CLB resistance class	Seedling ID	Time (dpi)	Status	Overall alignment rate (%)
398	Resistant	398-0 dpi	0	Uninfected	97.01
398	Resistant	398-3 dpi	3	Infected	97.36
398	Resistant	398-6 dpi	6	Infected	97.51
398	Resistant	398-9 dpi	9	Infected	96.06
685	Resistant	685-0 dpi	0	Uninfected	96.86
685	Resistant	685-3 dpi	3	Infected	96.94
685	Resistant	685-6 dpi	6	Infected	97.12
685	Resistant	685-9 dpi	9	Infected	97.13
583	Susceptible	583-0 dpi	0	Uninfected	97.24
583	Susceptible	583-3 dpi	3	Infected	96.60
583	Susceptible	583-6 dpi	6	Infected	97.59
583	Susceptible	583-9 dpi	9	Infected	97.01
8265	Susceptible	8265-0 dpi	0	Uninfected	97.33
8265	Susceptible	8265-3 dpi	3	Infected	97.19
8265	Susceptible	8265-6 dpi	6	Infected	97.27
8265	Susceptible	8265-9 dpi	9	Infected	97.36

A.33 Overall alignment rates of the *RNA*-Seq samples used in the mock-infections of Chapter 5

Table A.17. Overall alignment rates of the filtered reads of libraries used in the mock-infection (CLB^-) part of gene expression analyses in Chapter 5.

Line	Time point (dpi)	Sample ID	Overall alignment rate (%)
5382	0	5382-6-0 dpi-Control	95.37
5382	0	5382-9-0 dpi-Control	97.39
5382	0	5382-12-0 dpi-Control	97.45
5382	4	5382-2-4 dpi-Control	97.73
5382	4	5382-5-4 dpi-Control	97.11
5382	4	5382-10-4 dpi-Control	97.38
5382	8	5382-1-8 dpi-Control	97.67
5382	8	5382-8-8 dpi-Control	97.75
5382	8	5382-11-8 dpi-Control	96.59
5382	12	5382-3-12 dpi-Control	97.08
5382	12	5382-4-12 dpi-Control	95.88
5382	12	5382-7-12 dpi-Control	96.99
5398	0	5398-1-0 dpi-Control	97.36
5398	0	5398-3-0 dpi-Control	96.59
5398	0	5398-9-0 dpi-Control	97.26
5398	4	5398-4-4 dpi-Control	97.28
5398	4	5398-8-4 dpi-Control	96.42
5398	4	5398-11-4 dpi-Control	96.24
5398	8	5398-2-8 dpi-Control	97.75
5398	8	5398-5-8 dpi-Control	97.54
5398	8	5398-7-8 dpi-Control	96.50
5398	12	5398-6-12 dpi-Control	97.27
5398	12	5398-10-12 dpi-Control	97.13
5398	12	5398-12-12 dpi-Control	97.20
5412	0	5412-1-0 dpi-Control	97.01
5412	0	5412-9-0 dpi-Control	96.40
5412	0	5412-11-0 dpi-Control	97.30
5412	4	5412-4-4 dpi-Control	97.67
5412	4	5412-6-4 dpi-Control	97.74
5412	4	5412-10-4 dpi-Control	97.25
5412	8	5412-2-8 dpi-Control	97.15
5412	8	5412-3-8 dpi-Control	96.32
5412	8	5412-8-8 dpi-Control	97.20
5412	12	5412-5-12 dpi-Control	97.05
5412	12	5412-7-12 dpi-Control	97.28
5412	12	5412-12-12 dpi-Control	97.44

A.34 Overall alignment rates of the *RNA*-Seq samples used in the real-infections of Chapter 5

Table A.18. Overall alignment rates of the filtered reads of libraries used in the real-infection (CLB^{+}) part of gene expression analyses in Chapter 5.

Line	Time point (dpi)	Sample ID	Overall alignment rate (%)
5382	0	5382-18-0 dpi-Infected	96.41
5382	0	5382-21-0 dpi-Infected	97.48
5382	0	5382-24-0 dpi-Infected	97.22
5382	4	5382-14-4 dpi-Infected	97.21
5382	4	5382-17-4 dpi-Infected	97.54
5382	4	5382-22-4 dpi-Infected	97.50
5382	8	5382-13-8 dpi-Infected	97.41
5382	8	5382-20-8 dpi-Infected	97.18
5382	8	5382-23-8 dpi-Infected	95.78
5382	12	5382-15-12 dpi-Infected	95.35
5382	12	5382-16-12 dpi-Infected	96.81
5382	12	5382-19-12 dpi-Infected	96.73
5398	0	5398-13-0 dpi-Infected	97.37
5398	0	5398-15-0 dpi-Infected	97.35
5398	0	5398-21-0 dpi-Infected	97.58
5398	4	5398-16-4 dpi-Infected	97.28
5398	4	5398-20-4 dpi-Infected	96.43
5398	4	5398-23-4 dpi-Infected	97.17
5398	8	5398-14-8 dpi-Infected	96.67
5398	8	5398-17-8 dpi-Infected	96.84
5398	8	5398-19-8 dpi-Infected	95.96
5398	12	5398-18-12 dpi-Infected	97.26
5398	12	5398-22-12 dpi-Infected	97.29
5398	12	5398-24-12 dpi-Infected	96.61
5412	0	5412-13-0 dpi-Infected	97.11
5412	0	5412-19-0 dpi-Infected	97.39
5412	0	5412-21-0 dpi-Infected	97.17
5412	4	5412-16-4 dpi-Infected	96.33
5412	4	5412-18-4 dpi-Infected	96.08
5412	4	5412-20-4 dpi-Infected	96.88
5412	8	5412-14-8 dpi-Infected	96.58
5412	8	5412-15-8 dpi-Infected	97.19
5412	8	5412-22-8 dpi-Infected	96.67
5412	12	5412-17-12 dpi-Infected	96.91
5412	12	5412-23-12 dpi-Infected	97.20
5412	12	5412-24-12 dpi-Infected	97.12

A.35 Overall alignment rates of the *RNA*-Seq samples used in Chapter 6

Table A.19. Overall alignment rates of the filtered reads of libraries used in the gene expression analyses carried out in Chapter 6. CLB^- = plants in the mock-infections, CLB^+ = plants in the real-infections.

Infection condition	Line	Time (dpi)	Sample ID	Overall alignment rate (%)
CLB^-	*Thuja plicata* 124	0	S5 124-3-0 dpi-Control	98.51
CLB^-	*Thuja plicata* 124	0	S5 124-8-0 dpi-Control	98.50
CLB^-	*Thuja plicata* 124	4	S5 124-2-4 dpi-Control	98.13
CLB^-	*Thuja plicata* 124	4	S5 124-7-4 dpi-Control	98.50
CLB^-	*Thuja plicata* 124	8	S5 124-4-8 dpi-Control	98.27
CLB^-	*Thuja plicata* 124	8	S5 124-6-8 dpi-Control	98.29
CLB^-	*Thuja plicata* 129	0	S5 129-1-0 dpi-Control	98.40
CLB^-	*Thuja plicata* 129	0	S5 129-5-0 dpi-Control	98.20
CLB^-	*Thuja plicata* 129	4	S5 129-3-4 dpi-Control	98.40
CLB^-	*Thuja plicata* 129	4	S5 129-7-4 dpi-Control	98.48
CLB^-	*Thuja plicata* 129	8	S5 129-2-8 dpi-Control	98.44
CLB^-	*Thuja plicata* 129	8	S5 129-6-8 dpi-Control	98.48
CLB^-	*Thuja standishii* × *plicata*	0	hyb-1-0 dpi-Control	98.18
CLB^-	*Thuja standishii* × *plicata*	0	hyb-7-0 dpi-Control	98.05
CLB^-	*Thuja standishii* × *plicata*	4	hyb-3-4 dpi-Control	98.25
CLB^-	*Thuja standishii* × *plicata*	4	hyb-6-4 dpi-Control	98.31
CLB^-	*Thuja standishii* × *plicata*	8	hyb-2-8 dpi-Control	98.19
CLB^-	*Thuja standishii* × *plicata*	8	hyb-5-8 dpi-Control	98.23
CLB^-	*Thuja standishii*	0	T. stand-1-0 dpi-Control	97.67
CLB^-	*Thuja standishii*	0	T. stand-5-0 dpi-Control	97.88
CLB^-	*Thuja standishii*	4	T. stand-2-4 dpi-Control	97.81
CLB^-	*Thuja standishii*	4	T. stand-6-4 dpi-Control	97.93
CLB^-	*Thuja standishii*	8	T. stand-3-8 dpi-Control	97.81
CLB^-	*Thuja standishii*	8	T. stand-7-8 dpi-Control	97.79
CLB^+	*Thuja plicata* 124	0	S5 124-11-0 dpi-Infected	98.38
CLB^+	*Thuja plicata* 124	0	S5 124-16-0 dpi-Infected	98.46
CLB^+	*Thuja plicata* 124	4	S5 124-10-4 dpi-Infected	98.33
CLB^+	*Thuja plicata* 124	4	S5 124-15-4 dpi-Infected	98.28
CLB^+	*Thuja plicata* 124	8	S5 124-12-8 dpi-Infected	98.31
CLB^+	*Thuja plicata* 124	8	S5 124-14-8 dpi-Infected	98.13
CLB^+	*Thuja plicata* 129	0	S5 129-9-0 dpi-Infected	98.28
CLB^+	*Thuja plicata* 129	0	S5 129-13-0 dpi-Infected	98.26
CLB^+	*Thuja plicata* 129	4	S5 129-11-4 dpi-Infected	98.35
CLB^+	*Thuja plicata* 129	4	S5 129-15-4 dpi-Infected	98.19
CLB^+	*Thuja plicata* 129	8	S5 129-10-8 dpi-Infected	98.15
CLB^+	*Thuja plicata* 129	8	S5 129-14-8 dpi-Infected	98.30
CLB^+	*Thuja standishii* × *plicata*	0	hyb-9-0 dpi-Infected	98.03
CLB^+	*Thuja standishii* × *plicata*	0	hyb-16-0 dpi-Infected	98.31
CLB^+	*Thuja standishii* × *plicata*	4	hyb-11-4 dpi-Infected	97.99
CLB^+	*Thuja standishii* × *plicata*	4	hyb-14-4 dpi-Infected	98.24
CLB^+	*Thuja standishii* × *plicata*	8	hyb-10-8 dpi-Infected	98.20
CLB^+	*Thuja standishii* × *plicata*	8	hyb-13-8 dpi-Infected	97.91
CLB^+	*Thuja standishii*	0	T. stand-9-0 dpi-Infected	97.60
CLB^+	*Thuja standishii*	0	T. stand-13-0 dpi-Infected	97.76
CLB^+	*Thuja standishii*	4	T. stand-10-4 dpi-Infected	97.87
CLB^+	*Thuja standishii*	4	T. stand-14-4 dpi-Infected	97.88
CLB^+	*Thuja standishii*	8	T. stand-11-8 dpi-Infected	97.77
CLB^+	*Thuja standishii*	8	T. stand-15-8 dpi-Infected	97.85

A.36 Pearson correlation heat-map of the expression profiles of the samples in Chapter 4

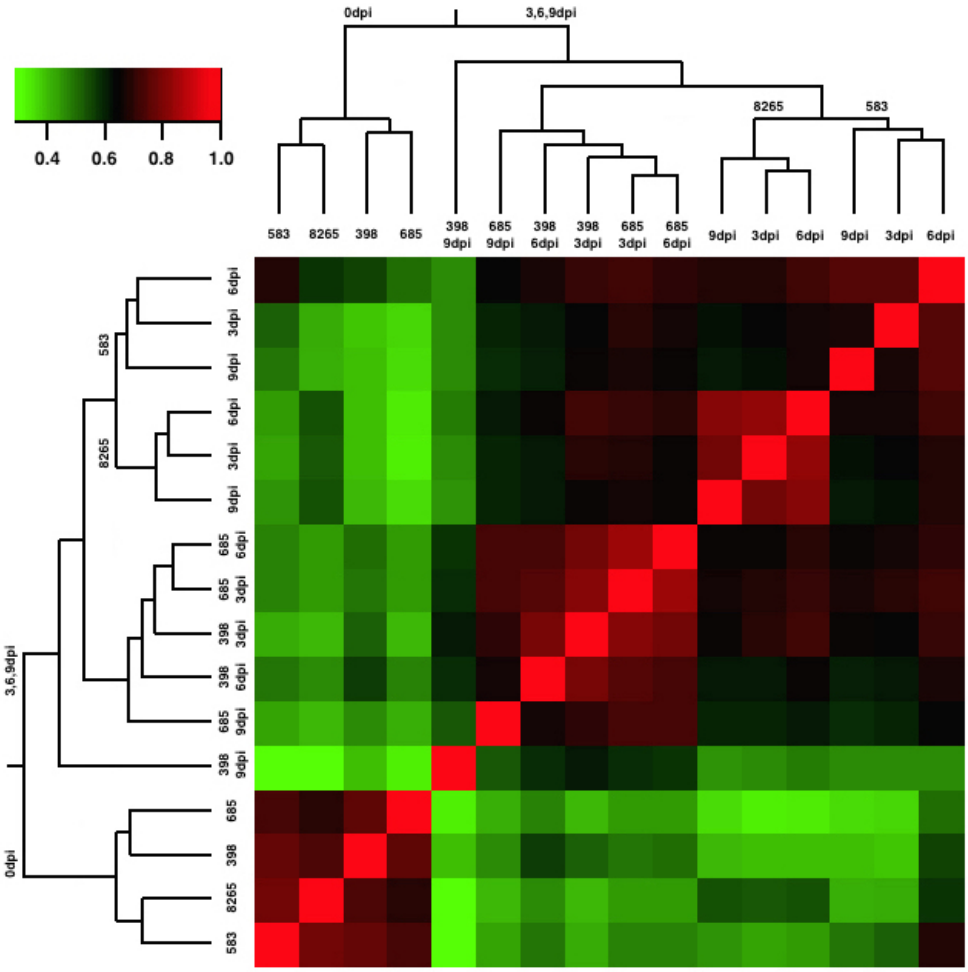

Figure A.12. Pearson correlation heat-map of the expression profiles of the samples in the CC-CLB^{+} treatment used for the gene expression analyses presented in Chapter 4. The samples were hierarchically clustered using Euclidean distance. The labels on the leaves of the clustering trees refer to specific family × time combinations; important nodes were labelled. Notice how the uninfected plants (0 dpi cluster) grouped together regardless of the family, as did the infected seedlings (3, 6, 9 dpi cluster). Susceptible families 583 and 8265 were together in both the uninfected and infected clusters, as were resistant families 398 and 685 (except for sample 398-9 dpi). The top left bar shows the colour coded correlation values (red = high correlation, green = low correlation). dpi = days post infection.

A.37 Pearson correlation heat-map of the expression profiles of the samples in Chapter 5

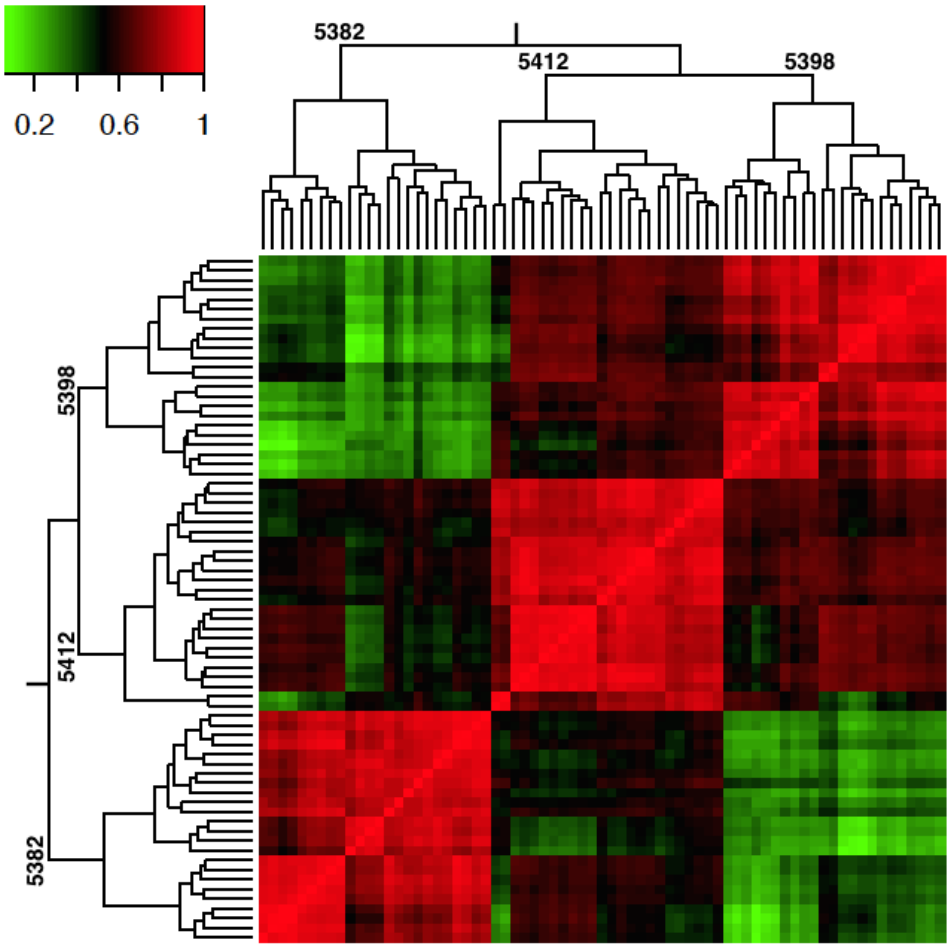

Figure A.13. Pearson correlation heat-map of the expression profiles of the samples used in the experiment presented in Chapter 5. The tree shown was produced using hierarchical clustering with Euclidean distance. Samples from each *Thuja plicata* clonal line grouped "monophyletically" in the clusters shown. Notice that the most resistant lines (5398 and 5412) are clustered together (see also section 5.3.2.2). Correlation values are colour coded according to the top left bar (red = high correlation, green = low correlation).

A.38 Pearson correlation heat-map of the expression profiles of the samples in Chapter 6

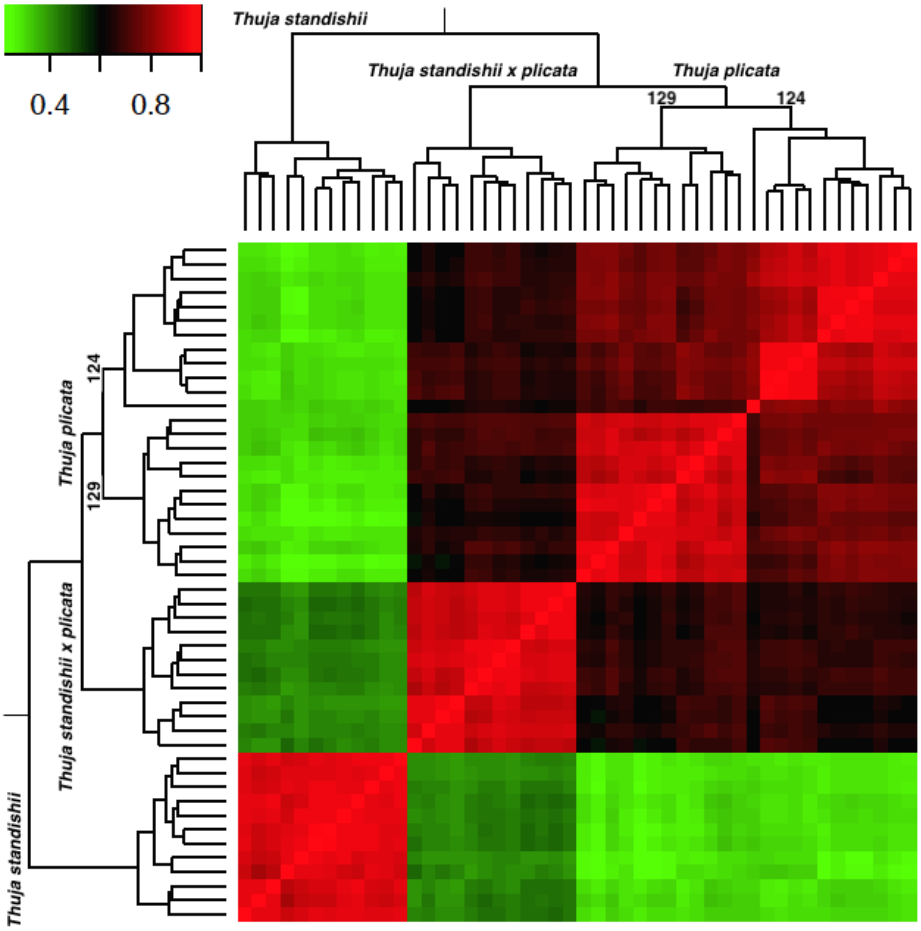

Figure A.14. Pearson correlation heat-map of the expression profiles from two *Thuja plicata* seedling lines (124 and 129), a *Thuja standishii* clonal line, and a *Thuja standishii* × *plicata* clonal line used in the study presented in Chapter 6. Hierarchical clustering of the samples was done with Euclidean distance. Samples from each line grouped together in a "monophyletic" way. Note that both *T. plicata* lines are more correlated to each other than to other lines, and that *T. standishii* × *plicata* samples are more correlated to *T. plicata* lines than to *T. standishii*. Correlations were colour-coded according to the top left bar (green = low correlation, red = high correlation).

A.39 Expression levels of *TRINITY_DN115787-_c0_g2_i1* (catalase-3) - Chapter 5

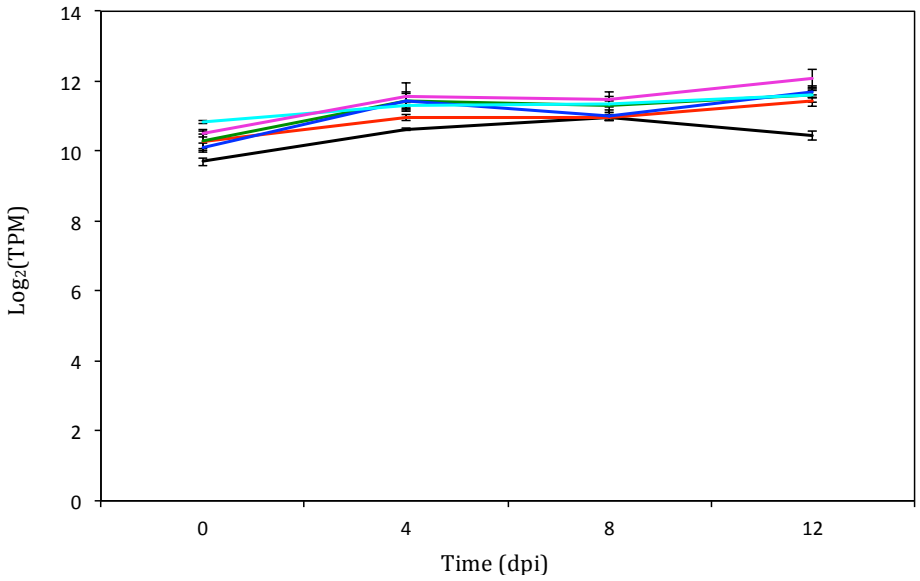

Figure A.15. Expression levels of transcript *TRINITY_DN115787_c0_g2_i1* (catalase-3). Three *Thuja plicata* clonal lines (5382, 5398 and 5412) were real (+) and mock (-) infected with *Didymascella thujina* (cedar leaf blight, CLB) under controlled conditions, and foliar samples taken 0, 4, 8 and 12 days post infection (dpi). The samples were processed for gene expression using the Illumina HiSeq 2000 paired-end technology. Treatments were colour coded as follows: 5382 CLB^- in black, 5382 CLB^+ in red, 5398 CLB^- in green, 5398 CLB^+ in blue, 5412 CLB^- in cyan, and 5412 CLB^+ in magenta. Note that expression levels were similar among treatments. dpi = days post infection.

A.40 Expression levels of *TRINITY_DN4933_c0_g3_i1* (ethylene-responsive transcription factor RAP2-4) - Chapter 5

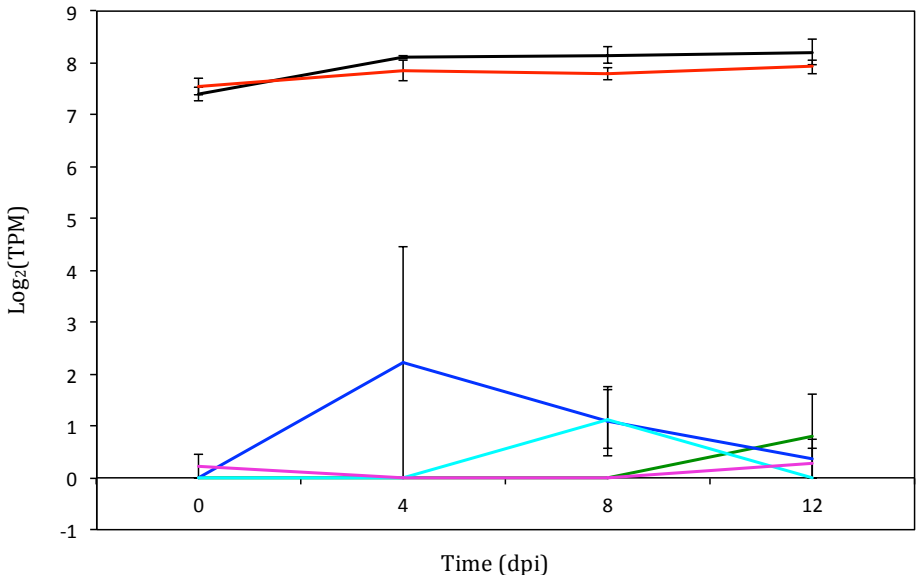

Figure A.16. Expression levels of transcript *TRINITY_DN4933_c0_g3_i1* (ethylene-responsive transcription factor RAP2-4). Three *Thuja plicata* clonal lines (5382, 5398 and 5412) were real (+) and mock (-) infected with *Didymascella thujina* (cedar leaf blight, CLB) under controlled conditions, and foliar samples taken 0, 4, 8 and 12 days post infection (dpi). The samples were processed for gene expression using the Illumina HiSeq 2000 paired-end technology. Treatments were colour coded as follows: 5382 CLB^- in black, 5382 CLB^+ in red, 5398 CLB^- in green, 5398 CLB^+ in blue, 5412 CLB^- in cyan, and 5412 CLB^+ in magenta. Note expression levels were higher in line 5382 than in the other two lines.

A.41 Expression levels of *TRINITY_DN122568_c0_g1_i3* (glyceraldehyde-3-phosphate dehydrogenase B) - Chapter 5

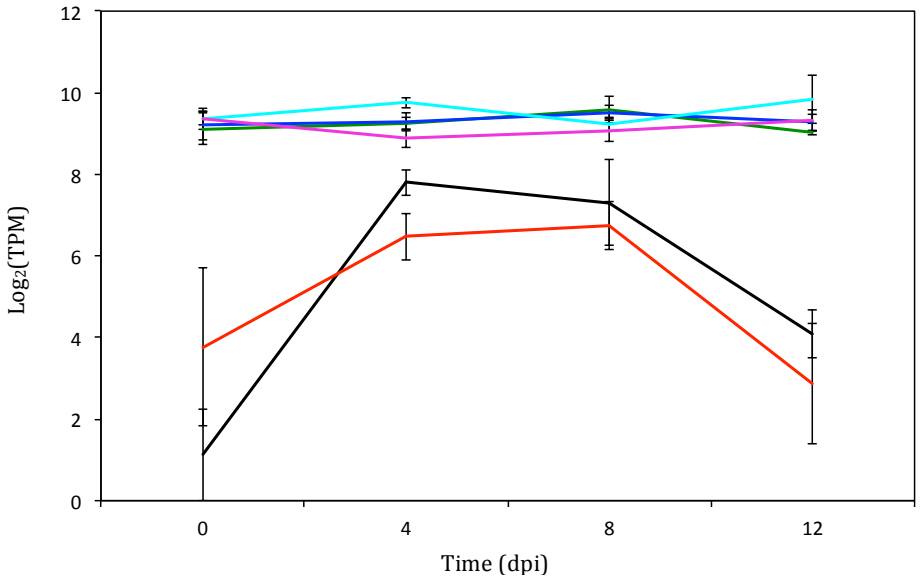

Figure A.17. Expression levels of transcript *TRINITY_DN122568_c0_g1_i3* (glyceraldehyde-3-phosphate dehydrogenase B). Three *Thuja plicata* clonal lines (5382, 5398 and 5412) were real (+) and mock (-) infected with *Didymascella thujina* (cedar leaf blight, CLB) under controlled conditions, and foliar samples taken 0, 4, 8 and 12 days post infection (dpi). The samples were processed for gene expression using the Illumina HiSeq 2000 paired-end technology. Treatments were colour coded as follows: 5382 CLB^- in black, 5382 CLB^+ in red, 5398 CLB^- in green, 5398 CLB^+ in blue, 5412 CLB^- in cyan, and 5412 CLB^+ in magenta. that expression levels were lower in line 5382 in comparison to the other two lines.

A.42 Expression levels of selected transcripts from Chapter 6

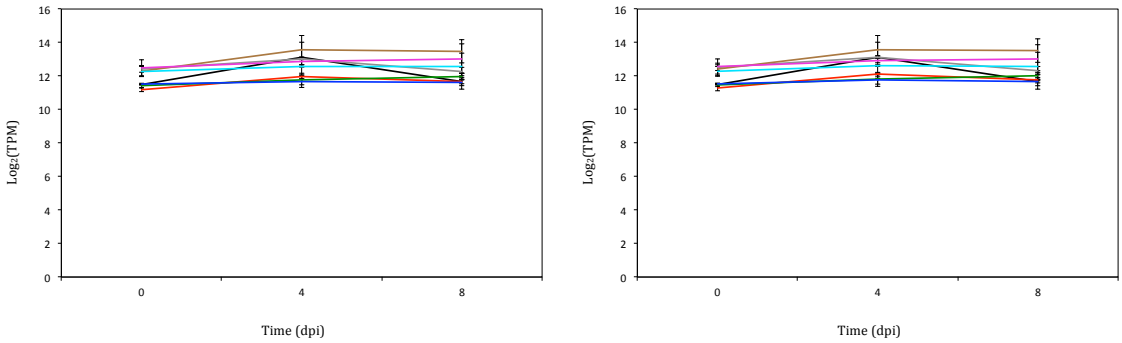

(a) **(b)**

Figure A.18. Expression levels of the two transcripts that were shared among the top ten sequences of the static topics in Table 6.5 of Chapter 6. Two *Thuja plicata* seedling lines (124 and 129), one *Thuja standishii* clonal line, and a *Thuja standishii* × *plicata* clonal line were real (+) and mock (-) infected with *Didymascella thujina* (cedar leaf blight, CLB) in growth chambers at the Bev Glover Growth Facility (University of Victoria, Victoria, British Columbia, Canada). Samples for gene expression analysis using the *RNA*-Seq technique were taken just before inoculation (0 days post infection, dpi), and 4 and 8 dpi. (a) *TRINITY_DN86213_c8_g2_i2* (Uncharacterized protein ORF91), (b) *TRINITY_DN87363_c15_g3_i1* (unknown). Treatments were colour-coded as follows: *T. plicata* 124 CLB^- in black, *T. plicata* 124 CLB^+ in red, *T. plicata* 129 CLB^- in green, *T. plicata* 129 CLB^+ in blue, *T. standishii* CLB^- in cyan, *T. standishii* CLB^+ in magenta, *T. standishii* × *plicata* CLB^- in grey, and *T. standishii* × *plicata* CLB^+ in brown.

A.43 Expression levels of *TRINITY_DN94350_c0_g2_i2* (glutamine synthetase cytosolic isozyme) - Chapter 6

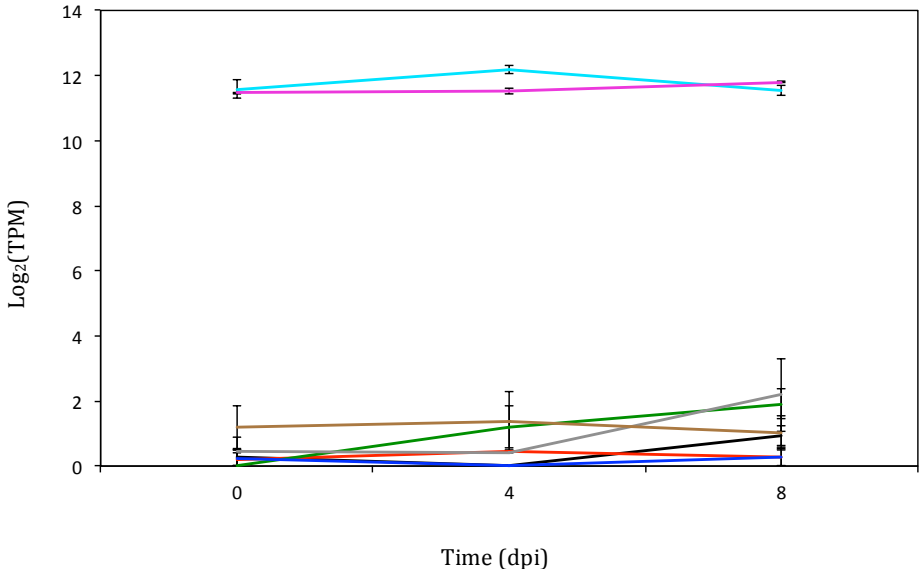

Figure A.19. Expression levels of transcript *TRINITY_DN94350_c0_g2_i2* (glutamine synthetase cytosolic isozyme, see also Table 6.5). One *Thuja standishii* clonal line, two *Thuja plicata* seedling lines (124 and 129), and a *Thuja standishii* × *plicata* clonal line were real (+) and mock (-) infected with cedar leaf blight (CLB, *Didymascella thujina*) under controlled conditions at the Bev Glover Growth Facility (University of Victoria, Victoria, British Columbia, Canada). Foliar samples for differential gene expression analysis using the *RNA*-Seq technology were taken before inoculation (0 days post infection, dpi), and 4 and 8 dpi. Treatments were colour-coded as follows: *T. plicata* 124 CLB^- in black, *T. plicata* 124 CLB^+ in red, *T. plicata* 129 CLB^- in green, *T. plicata* 129 CLB^+ in blue, *T. standishii* CLB^- in cyan, *T. standishii* CLB^+ in magenta, *T. standishii* × *plicata* CLB^- in grey, and *T. standishii* × *plicata* CLB^+ in brown.

A.44 Representative static topics of the *Thuja plicata* lines in Chapter 6

Table A.20. Top ten transcripts of the representative static topics per *Thuja plicata* seedling line in Fig. 6.5. Transcripts shown were organized in a descending manner according to their ϑ probabilities. Annotations were the result of BLASTX searches performed on Swiss-Prot.

Thuja plicata line	Static topic	Transcript	ϑ	E-value	Organism	Annotation	Process	Cellular component
124	4	*TRINITY_DN101197_c2_g1_i5*	0.015966	2×10^{-163}	*Lycopersicon* sp.	Chlorophyll a-b binding protein 1B	Chlorophyll binding	Chloroplast thylakoid membrane
		TRINITY_DN99787_c0_g1_i1	0.014469	0	*Abies* sp.	Pinene synthase		Chloroplast
		TRINITY_DN79613_c1_g1_i1	0.009153	5×10^{-7}	*Picea* sp.	Metallothionein-like protein EMB30	Metal ion binding	
		TRINITY_DN83144_c0_g1_i1	0.008296	4×10^{-150}	*Lycopersicon* sp.	Chlorophyll a-b binding protein 4	Chlorophyll binding	Chloroplast thylakoid membrane
		TRINITY_DN95430_c1_g1_i1	0.007589	0	*Sesamum* sp.	Inositol-3-phosphate synthase	Phospholipid biosynthetic process	Cytoplasm
		TRINITY_DN83187_c1_g2_i1	0.007201	5×10^{-148}	*Pinus* sp.	Cytochrome P450 750A1		
		TRINITY_DN88193_c0_g1_i1	0.006347	0	*Nicotiana* sp.	Oxygen-evolving enhancer protein 1	Photosystem II stabilization	Chloroplast thylakoid membrane
		TRINITY_DN89327_c0_g1_i1	0.005853	2×10^{-139}	*Daucus* sp.	S-adenosylmethionine decarboxylase proenzyme	Spermine biosynthetic process	
		TRINITY_DN85473_c0_g1_i1	0.005658	2×10^{-48}	*Spinacia* sp.	Plastocyanin		Chloroplast
		TRINITY_DN75032_c0_g2_i1	0.005217	2×10^{-46}	*Arabidopsis* sp.	Protein translation factor SUI1 homolog 1	Translation initiation factor activity	
	6	*TRINITY_DN75032_c0_g2_i1*	0.016422	2×10^{-46}	*Arabidopsis* sp.	Protein translation factor SUI1 homolog 1	Translation initiation factor activity	
		TRINITY_DN188465_c0_g1_i1	0.012192	0	*Phaseolus* sp.	Vacuolar-processing enzyme	Cysteine-type peptidase activity	
		TRINITY_DN90395_c0_g1_i1	0.011434	0	*Antirrhinum* sp.	Granule-bound starch synthase 1	Starch biosynthetic process	Chloroplast, amyloplast
		TRINITY_DN86213_c8_g2_i2	0.011123	6×10^{-14}	*Phalaenopsis* sp.	Uncharacterized protein ORF91		Chloroplast
		TRINITY_DN88193_c0_g1_i1	0.010621	0	*Nicotiana* sp.	Oxygen-evolving enhancer protein 1	Photosystem II stabilization	Chloroplast thylakoid membrane
		TRINITY_DN87363_c15_g3_i1	0.00983	NA	No hits	No hits		
		TRINITY_DN101197_c2_g1_i5	0.008179	2×10^{-163}	*Lycopersicon* sp.	Chlorophyll a-b binding protein 1B	Chlorophyll binding	Chloroplast thylakoid membrane
		TRINITY_DN85473_c0_g1_i1	0.007475	2×10^{-48}	*Spinacia* sp.	Plastocyanin		Chloroplast
		TRINITY_DN95406_c1_g1_i2	0.006974	5×10^{-170}	*Pisum* sp.	Cysteine proteinase 15A	Proteolysis	
		TRINITY_DN83144_c0_g1_i1	0.006748	4×10^{-150}	*Lycopersicon* sp.	Chlorophyll a-b binding protein 4	Chlorophyll binding	Chloroplast thylakoid membrane
129	9	*TRINITY_DN188465_c0_g1_i1*	0.021122	0	*Phaseolus* sp.	Vacuolar-processing enzyme	Cysteine-type peptidase activity	
		TRINITY_DN95569_c0_g2_i1	0.014375	0	*Glycine* sp.	Catalase-3	Hydrogen peroxide catabolic process	Cytoplasm
		TRINITY_DN86213_c8_g2_i2	0.013964	6×10^{-14}	*Phalaenopsis* sp.	Uncharacterized protein ORF91		Chloroplast
		TRINITY_DN87363_c15_g3_i1	0.013122	NA	No hits	No hits		
		TRINITY_DN90395_c0_g1_i1	0.012268	0	*Antirrhinum* sp.	Granule-bound starch synthase 1	Starch biosynthetic process	Chloroplast, amyloplast
		TRINITY_DN63359_c0_g1_i1	0.009353	0	*Arabidopsis* sp.	Cysteine proteinase RD21a	Defense response to fungus	Apoplast
		TRINITY_DN88193_c0_g1_i1	0.008824	0	*Nicotiana* sp.	Oxygen-evolving enhancer protein 1	Photosystem II stabilization	Chloroplast thylakoid membrane
		TRINITY_DN95406_c1_g1_i2	0.008815	5×10^{-170}	*Pisum* sp.	Cysteine proteinase 15A	Proteolysis	
		TRINITY_DN87363_c15_g1_i1	0.008662	NA	No hits	No hits		
		TRINITY_DN76822_c2_g2_i1	0.006838	NA	No hits	No hits		
	11	*TRINITY_DN95569_c0_g2_i1*	0.020421	0	*Glycine* sp.	Catalase-3	Hydrogen peroxide catabolic process	Cytoplasm
		TRINITY_DN188465_c0_g1_i1	0.020081	0	*Phaseolus* sp.	Vacuolar-processing enzyme	Cysteine-type peptidase activity	
		TRINITY_DN89327_c0_g1_i1	0.017816	2×10^{-139}	*Daucus* sp.	S-adenosylmethionine decarboxylase proenzyme	Spermine biosynthetic process	
		TRINITY_DN76822_c2_g2_i1	0.016773	NA	No hits	No hits		
		TRINITY_DN79613_c1_g1_i1	0.015164	5×10^{-7}	*Picea* sp.	Metallothionein-like protein EMB30	Metal ion binding	
		TRINITY_DN90395_c0_g1_i1	0.013453	0	*Antirrhinum* sp.	Granule-bound starch synthase 1	Starch biosynthetic process	Chloroplast, amyloplast
		TRINITY_DN86213_c8_g2_i2	0.013257	6×10^{-14}	*Phalaenopsis* sp.	Uncharacterized protein ORF91		Chloroplast
		TRINITY_DN74436_c0_g1_i1	0.013057	2×10^{-88}	*Nepenthes* sp.	Aspartic proteinase nepenthesin-2	Aspartic-type endopeptidase activity	Extracellular region
		TRINITY_DN87363_c15_g3_i1	0.012354	NA	No hits	No hits		
		TRINITY_DN76260_c0_g1_i1	0.010014	1×10^{-29}	*Arabidopsis* sp.	MLP-like protein 423	Defense response	Membrane

A.45 BLASTn results of searches for putative sequences of the DOXP and the α- and β-thujone biosynthesis pathways in Chapter 3

Table A.21. BLASTn results of searches for putative sequences of the DOXP (1-deoxy-D-xylulose-5-phosphate) pathway and the α- and β-thujone biosynthesis pathway of *Thuja plicata* in the assembled transcriptome. The query sequences below were kindly provided by Dr. Dr. Jim Mattsson (Simon Fraser University, Burnaby, British Columbia, Canada). *: Sequences used to find similar genes in the trascriptome that was assembled for the study presented in Chapter 3. The first 15 sequences have not been published; the IDs of the last seven sequences are GenBank accession numbers. **: Top BLASTn hits found in this study's assembly.

Query*	Subject**	Identity (%)	Alignment length	Mismatches	Gap opens	Query start	Query end	Subject start	Subject end	E-value	Bit score
Contig7217 4857 reads, 3226 bases, putative DOXP synthase (Dxs)	*TR31566/c0_g1_i1*	99.78	3206	7	0	1	3206	202	3407	0	5882
Contig37236 101 reads, 610 bases, putative DOXP synthase (Dxs)	*TR10138/c0_g1_i1*	99.47	561	3	0	36	596	561	1	0	1020
Contig1705 23974 reads, 2879 bases, putative DOXP synthase (Dxs) TpDXS1	*TR50643/c0_g1_i1*	100.00	2856	0	0	1	2856	92	2947	0	5275
Contig57623 173 reads, 570 bases, putative DOXP synthase (Dxs)	*TR43001/c0_g1_i1*	100.00	469	0	0	34	502	469	1	0	867
Contig27532 88 reads, 465 bases, putative DOXP synthase (Dxs)	*TR35653/c0_g1_i1*	99.76	416	1	0	50	465	1210	795	0	763
Contig1862 9882 reads, 2142 bases, DOXP reductase (Dxr, IspC)	*TR73363/c0_g1_i1*	100.00	2030	0	0	43	2072	253	2282	0	3749
Contig53446 89 reads, 459 bases, putative DOXP reductase (Dxr, IspC)	*TR72504/c0_g1_i1*	98.52	406	0	3	1	400	318	723	0	712
Contig43584 27 reads, 329 bases, putative DOXP reductase (Dxr, IspC)	*TR17741/c0_g1_i1*	99.31	291	1	1	1	290	291	1	2×10^{-148}	525
Contig6276 1492 reads, 1554 bases, putative 4-diphosphocytidyl-2-C-methyl-D-erythritol synthase (YgbP, IspD)	*TR6224/c0_g1_i1*	99.94	1552	1	0	3	1554	44	1595	0	2861
Contig7676 1982 reads, 1741 bases, putative 4-diphosphocytidyl-2-C-methyl-D-erythritol kinase(YchB, IspE)	*TR52368/c0_g1_i1*	99.60	1732	1	3	1	1732	97	1822	0	3155
Contig3736 2464 reads, 1298 bases, 2-C-methyl-D-erythritol 2,4-cyclodiphosphate synthase (YgbB, IspF)	*TR19649/c0_g1_i2*	100.00	1282	0	0	8	1289	1282	1	0	2368
Contig26378 77 reads, 304 bases, putative 2-C-methyl-D-erythritol 2,4-cyclodiphosphate synthase (YgbB, IspF)	*TR19649/c1_g1_i1*	100.00	178	0	0	127	304	1	178	2×10^{-89}	329
Contig2464 12591 reads, 2637 bases, HMB-PP synthase (GcpE, IspG)	*TR21129/c0_g1_i1*	100.00	2635	0	0	3	2637	58	2692	0	4867
Contig2687 7745 reads, 2036 bases, putative HMB-PP reductase (LytB, IspH)	*TR51331/c0_g1_i1*	99.45	2002	9	2	8	2007	74	2075	0	3635
Contig591 22610 reads, 2507 bases, putative HMB-PP reductase (LytB, IspH)	*TR54761/c7_g2_i1*	99.52	2494	12	0	1	2494	2494	1	0	4540
KC767267	*TR57802/c5_g3_i5*	99.21	1511	12	0	1	1511	1615	105	0	2724
KC767270	*TR52851/c1_g1_i2*	96.40	861	26	4	1	860	1129	273	0	1413
KC767275	*TR57126/c5_g1_i6*	86.52	512	65	3	91	600	639	1148	1×10^{-158}	560
KC767278	*TR22924/c0_g1_i1*	98.67	1426	19	0	10	1435	1	1426	0	2529
KC767279	*TR56505/c0_g1_i1*	100.00	358	0	0	1150	1507	1	358	0	662
KC767280	*TR57111/c2_g1_i1*	88.38	1644	173	9	2	1634	38	1674	0	1962
KC767281	*TR58482/c2_g1_i2*	99.56	1353	6	0	507	1859	1376	24	0	2466

Bibliography

Abrams, M., Kubiske, M., and Mostoller, S. Relating wet and dry year ecophysiology to leaf structure in contrasting temperate tree species. *Ecology*, 75(1):123–133, 1994. doi: 10.2307/1939389.

Acharya, S., Brown, H., Suzuki, A., Nozawa, S., and Itoh, M. Hydroboration of terpenes. V. Isomerization of (+)-sabinene to (+)-α-thujene. Hydroboration of (+)-sabinene and (+)-α-thujene with configurational assignments for the thujanols. *The Journal of Organic Chemistry*, 34(10):3015–3022, 1969.

Achotegui-Castells, A., Rocca, G. D., Llusià, J., Danti, R., Barberini, S., Bouneb, M., Simoni, S., Michelozzi, M., and Peñuelas, J. Terpene arms race in the *Seiridium cardinale - Cupressus sempervirens* pathosystem. *Scientific Reports*, 6:18954, jan 2016. doi: 10.1038/srep18954. Sci Rep. 2016; 6: 18954. Published online 2016 Jan 22.

Adelalu, K., Qu, X.-J., Sun, Y.-X., Deng, T., Sun, H., and Wang, H.-C. Characterization of the complete plastome of western red cedar, *Thuja plicata* (Cupressaceae). *Conservation Genetics Resources*, Dec 2017. doi: 10.1007/s12686-017-0948-1.

Adhikari, B., Savory, E., Vaillancourt, B., Childs, K., Hamilton, J., Day, B., and Buell, C. Expression profiling of *Cucumis sativus* in response to infection by *Pseudoperonospora cubensis*. *PLoS ONE*, 7(4):e34954, 2012.

Afzal, A., Wood, A., and Lightfoot, D. Plant receptor-like serine threonine kinases: roles in signaling and plant defense. *Molecular Plant-Microbe Interactions*, 21(5): 507–517, 2008. doi: 10.1094/MPMI-21-5-0507.

Agrios, G. *Plant Pathology*. Elsevier Academic Press, New York, fifth edition, 2005.

Aharoni, A. and Galili, G. Metabolic engineering of the plant primary-secondary metabolism interface. *Current Opinion in Biotechnology*, 22(2):239–244, 2011. doi: 10.1016/j.copbio.2010.11.004.

Ahmad, S., Veyrat, N., Gordon-Weeks, R., Zhang, Y., Martin, J., Smart, L., Glauser, G., Erb, M., Flors, V., Frey, M., and Ton, J. Benzoxazinoid metabolites regulate innate immunity against aphids and fungi in maize. *Plant Physiology*, 157:317–327, 2011. doi: 10.1104/pp.111.180224.

Ahmad, W., Niaz, A., Kanwal, S., and Rasheed, M. Role of boron in plant growth: a review. *Journal of Agricultural Research*, 47(3):329–338, 2009.

Aitken, S., Yeaman, S., Holliday, J., Wang, T., and Curtis-McLane, S. Adaptation, migration or extirpation: climate change outcomes for tree populations. *Evolutionary Applications*, 1(1):95–111, 2008. doi: 10.1111/j.1752-4571.2007.00013.x.

Alazem, M. and Lin, N.-S. Roles of plant hormones in the regulation of host–virus interactions. *Molecular Plant Pathology*, 16(5):529–540, 2015. doi: 10.1111/mpp.12204.

Alcock, N. *Keithia thujina* Durand: A disease of nursery seedlings of *Thuja plicata*. *Scottish Forestry Journal*, 42(2):77–79, 1928.

Alfaro, R. An induced defense reaction in white spruce to attack by the white pine weevil, *Pissodes strobi*. *Canadian Journal of Forest Research*, 25(10):1725–1730, 1995. doi: 10.1139/x95-186.

Alfaro, R., Borden, J., King, J., Tomlin, E., McIntosh, R., and Bohlmann, J. Mechanisms of Resistance in Conifers Against Shoot Infesting Insects. In Wagner, M., Clancy, K., Lieutier, F., and Paine, T., editors, *Mechanisms and Deployment of Resistance in Trees to Insects*, pages 105–130. Springer Netherlands, 2002.

Allagulova, C., Gimalov, F., Shakirova, F., and Vakhitov, V. The plant dehydrins: structure and putative functions. *Biochemistry (Moscow)*, 68(9):945–951, 2003. doi: 10.1023/A:1026077825584.

Allen, C., Macalady, A., Chenchouni, H., Bachelet, D., McDowell, N., Vennetier, M., Kitzberger, T., Rigling, A., Breshears, D., Hogg, E., Gonzalez, P., Fensham, R., Zhang, Z., Castro, J., Demidova, N., Lim, J.-H., Allard, G., Running, S., Semerci, A., and Cobb, N. A global overview of drought and heat-induced tree mortality reveals emerging climate change risks for forests. *Forest Ecology and Management*, 259(4):660–684, 2010. doi: 10.1016/j.foreco.2009.09.001.

Álvarez-Yepes, D., Gutiérrez-Sánchez, P., and Marín-Montoya, M. Molecular characterization of *potato virus V* (PVV) infecting *Solanum phureja* using next-generation sequencing. *Acta Biológica Colombiana*, 21(3):521–531, sep 2016. doi: 10.15446/abc.v21n3.54712.

Amrine, K., Blanco-Ulate, B., and Cantu, D. Discovery of core biotic stress responsive genes in Arabidopsis by weighted gene co-expression network analysis. *PLoS ONE*, 10(3):e0118731, 2015. doi: 10.1371/journal.pone.0118731.

Andrews, S. FastQC: A quality control tool for high throughput sequence data, version 0.11.2, 2014. URL `http://www.bioinformatics.babraham.ac.uk/projects/fastqc/`.

Anker, C. and Niks, R. Prehaustorial resistance to the wheat leaf rust fungus, *Puccinia triticina*, in *Triticum monococcum* (s.s.). *Euphytica*, 117(3):209–215, 2001.

Antoniw, J., Ritter, C., Pierpoint, W., and van Loon, L. Comparison of three pathogenesis-related proteins from plants of two cultivars of tobacco infected with TMV. *Journal of General Virology*, 47(1):79–87, 1980.

Antos, J., Filipescu, C., and Negrave, R. Ecology of western redcedar (*Thuja plicata*): implications for management of a high-value multiple-use resource. *Forest Ecology and Management*, 375:211–222, 2016. doi: https://doi.org/10.1016/j.foreco.2016.05.043.

Arima, Y., Nakai, Y., Hayakawa, R., and Nishino, T. Antibacterial effect of β-thujaplicin on staphylococci isolated from atopic dermatitis: relationship between changes in the number of viable bacterial cells and clinical improvement in an eczematous lesion of atopic dermatitis. *Journal of Antimicrobial Chemotherapy*, 51 (1):113–122, 2003. doi: 10.1093/jac/dkg037.

Arimura, G.-i., Huber, D., and Bohlmann, J. Forest tent caterpillars (*Malacosoma disstria*) induce local and systemic diurnal emissions of terpenoid volatiles in hybrid poplar (*Populus trichocarpa* $\times$ *deltoides*): cDNA cloning, functional characterization, and patterns of gene expression of (-)-germacrene D synthase, *PtdTPS1*. *The Plant Journal*, 37(4):603–616, 2004.

Arnaud, D. and Hwang, I. A sophisticated network of signaling pathways regulates stomatal defenses to bacterial pathogens. *Molecular Plant*, 8(4):566–581, 2015. doi: 10.1016/j.molp.2014.10.012.

Ashburner, M., Ball, C. A., Blake, J. A., Botstein, D., Butler, H., Cherry, J. M., Davis, A. P., Dolinski, K., Dwight, S. S., Eppig, J. T., Harris, M. A., Hill, D. P., Issel-Tarver, L., Kasarskis, A., Lewis, S., Matese, J. C., Richardson, J. E., Ringwald,

M., Rubin, G. M., and Sherlock, G. Gene Ontology: tool for the unification of biology. *Nature Genetics*, 25(1):25–29, 2000. doi: 10.1038/75556.

Avis, T., Michaud, M., and Tweddell, R. Role of lipid composition and lipid peroxidation in the sensitivity of fungal plant pathogens to aluminum chloride and sodium metabisulfite. *Applied and Environmental Microbiology*, 73(9):2820–2824, May 2007. doi: 10.1128/AEM.02849-06.

Bagamboula, C., Uyttendaele, M., and Debevere, J. Inhibitory effect of thyme and basil essential oils, carvacrol, thymol, estragol, linalool and *p*-cymene towards *Shigella sonnei* and *S. flexneri*. *Food Microbiology*, 21(1):33–42, 2004.

Bajo, J., Santamaría, O., and Diez, J. Cultural characteristics and pathogenicity of *Pestalotiopsis funerea* on *Cupressus arizonica*. *Forest Pathology*, 38(4):263–274, 2008.

Bakker, J. Effects of humidity on stomatal density and its relation to leaf conductance. *Scientia Horticulturae*, 48(3-4):205–212, 1991.

Bal, A., Anand, R., Berge, O., and Chanway, C. Isolation and identification of diazotrophic bacteria from internal tissues of *Pinus contorta* and *Thuja plicata*. *Canadian Journal of Forest Research*, 42(4):807–813, 2012.

Balestrini, R. and Bonfante, P. Cell wall remodeling in mycorrhizal symbiosis: a way towards biotrophism. In Lionetti, V. and Métraux, J.-P., editors, *Frontiers Research Topics: Plant Cell Wall in Pathogenesis, Parasitism and Symbiosis*, pages 116–125. Frontiers Media SA., 2014a. doi: 10.3389/978-2-88919-442-1.

Balestrini, R. and Bonfante, P. Cell wall remodeling in mycorrhizal symbiosis: a way towards biotrophism. *Frontiers in Plant Science*, 5:237, 2014b. doi: 10.3389/fpls.2014.00237.

Barceló, J. and Poschenrieder, C. Fast root growth responses, root exudates, and internal detoxification as clues to the mechanisms of aluminium toxicity and resistance: a review. *Environmental and Experimental Botany*, 48(1):75–92, 2002. doi: 10.1016/S0098-8472(02)00013-8.

Barnes, A. 2016 Economic State of the B.C. Forest Sector. Technical report, Ministry of Forests, Lands, Natural Resource Operations and Rural Development, 2016.

Barrett, L. and Heil, M. Unifying concepts and mechanisms in the specificity of plant-enemy interactions. *Trends in Plant Science*, 17(5):282–292, 2012.

Barton, G. and MacDonald, B. The chemistry and utilization of western red cedar. Catalogue Fo 47-1023, Dept of Fisheries and Forestry, Canadian Forestry Service, Ottawa (Canada), 1971.

Bates, D., Mächler, M., Bolker, B. M., and Walker, S. C. Fitting linear mixed-effects models using lme4. *Journal of Statistical Software*, 67(1):1–48, 2015. doi: 10.18637/jss.v067.i01.

Batistič, O. and Kudla, J. Analysis of calcium signaling pathways in plants. *Biochimica et Biophysica Acta*, 1820(8):1283–1293, aug 2012. doi: 10.1016/j.bbagen.2011.10.012.

Baur, A., Kaufmann, F., Rolli, H., Weise, A., Luethje, R., Berg, B., Braun, M., Baeumer, W., Kietzmann, M., Reski, R., and Gorr, G. A fast and flexible PEG-mediated transient expression system in plants for high level expression of secreted recombinant proteins. *Journal of Biotechnology*, 119(4):332–342, 2005. doi: 10.1016/j.jbiotec.2005.04.018.

Beattie, D. Bioenergetics and Oxidative Metabolism. In Devlin, T., editor, *Textbook of Biochemistry with Clinical Correlations*, pages 529–580, USA, 2006. John Wiley & Sons, Inc.

Bednarek, P. Chemical warfare or modulators of defence responses - the function of secondary metabolites in plant immunity. *Current Opinion in Plant Biology*, 15 (4):407–414, 2012.

Bednarek, P. and Osbourn, A. Plant-microbe interactions: chemical diversity in plant defense. *Science*, 324(5928):746–748, 2009. doi: 10.1126/science.1171661.

Beffa, R., Neuhaus, J., and Meins, F. Physiological compensation in antisense transformants: specific induction of an "ersatz" glucan endo-1,3-β-glucosidase in plants infected with necrotizing viruses. *Proceedings of the National Academy of Sciences of The United States of America*, 90(19):8792–8796, 1993.

Bellincampi, D., Cervone, F., and Lionetti, V. Plant cell wall dynamics and wall-related susceptibility in plant-pathogen interactions. *Frontiers in Plant Science*, 5: 228, 2014. doi: 10.3389/fpls.2014.00228.

Bentz, B., Régnière, J., Fettig, C., Hansen, E., Hayes, J., Hicke, J., Kelsey, R., Negrón, J., and Seybold, S. Climate change and bark beetles of the western United States and Canada: direct and indirect effects. *BioScience*, 60(8):602–613, 2010. doi: 10.1525/bio.2010.60.8.6.

Berg, J., Tymoczko, J., and Stryer, L. *Biochemistry*. W. H. Freeman and Company, New York (USA), sixth edition, 2007.

Berger, S., Sinha, A., and Roitsch, T. Plant physiology meets phytopathology: plant primary metabolism and plant–pathogen interactions. *Journal of Experimental Botany*, 58(15-16):4019–4026, 2007. doi: 10.1093/jxb/erm298.

Berr, A., Ménard, R., Heitz, T., and Shen, W.-H. Chromatin modification and remodelling: a regulatory landscape for the control of *Arabidopsis* defence responses upon pathogen attack. *Cellular Microbiology*, 14(6):829–839, 2012.

Bestwick, C., Brown, I., Bennett, M., and Mansfield, J. Localization of hydrogen peroxide accumulation during the hypersensitive reaction of lettuce cells to *Pseudomonas syringae* pv *phaseolicola*. *The Plant Cell*, 9(2):209–221, 1997. doi: 10.1105/tpc.9.2.209.

Bhadauria, V., Ramsay, L., Bett, K., and Banniza, S. QTL mapping reveals genetic determinants of fungal disease resistance in the wild lentil species *Lens ervoides*. *Scientific Reports*, 7:3231, 2017.

Blanco-Ulate, B., Morales-Cruz, A., Amrine, K., Labavitch, J., Powell, A., and Cantu, D. Genome-wide transcriptional profiling of *Botrytis cinerea* genes targeting plant cell walls during infections of different hosts. In Lionetti, V. and Métraux, J.-P., editors, *Frontiers Research Topics: Plant Cell Wall in Pathogenesis, Parasitism and Symbiosis*, pages 14–29. Frontiers Media SA., 2014a. doi: 10.3389/978-2-88919-442-1.

Blanco-Ulate, B., Morales-Cruz, A., Amrine, K., Labavitch, J., Powell, A., and Cantu, D. Genome-wide transcriptional profiling of *Botrytis cinerea* genes targeting plant cell walls during infections of different hosts. *Frontiers in Plant Science*, 5:435, 2014b. doi: 10.3389/fpls.2014.00435.

Blei, D. M. Probabilistic topic models. *Communications of the ACM*, 55(4):77–84, 2012. ISSN 0001-0782.

Blei, D. M. and Lafferty, J. D. Dynamic Topic Models. In *Proceedings of the 23rd International Conference on Machine Learning*, 2006.

Blei, D. M. and Lafferty, J. D. Topic Models. In Srivastava, A. N. and Sahami, M., editors, *Text Mining: Classification, Clustering, and Applications*, Chapman & Hall/CRC Data Mining and Knowledge Discovery Series, pages 71–94. CRC Press, 2009. ISBN 9781420059458.

Blevins, D. and Lukaszewski, K. Boron in plant structure and function. *Annual Review of Plant Physiology and Plant Molecular Biology*, 49(1):481–500, jun 1998. doi: 10.1146/annurev.arplant.49.1.481.

Boardman, N. Comparative photosynthesis of sun and shade plants. *Annual Review of Plant Physiology*, 28:355–377, 1977. doi: 10.1146/annurev.pp.28.060177.002035.

Bobadilla, R. and Berr, A. Histone Methylation - A Cornerstone for Plant Responses to Environmental Stresses? In Shanker, A. and Shanker, C., editors, *Abiotic and Biotic Stress in Plants: Recent Advances and Future Perspectives*, pages 31–61. InTech, 2016.

Boland, G., Melzer, M., Hopkin, A., Higgins, V., and Nassuth, A. Climate change and plant diseases in Ontario. *Canadian Journal of Plant Pathology*, 26(3):335–350, 2004. doi: 10.1080/07060660409507151.

Bolger, A., Lohse, M., and Usadel, B. Trimmomatic: a flexible trimmer for Illumina sequence data. *Bioinformatics*, 30(15):2114–2120, 2014. doi: 10.1093/bioinformatics/btu170.

Bollenbach, T., Sharwood, R., Gutierrez, R., Lerbs-Mache, S., and Stern, D. The RNA-binding proteins CSP41a and CSP41b may regulate transcription and translation of chloroplast-encoded RNAs in Arabidopsis. *Plant Molecular Biology*, 69 (5):541–552, 2009. doi: 10.1007/s11103-008-9436-z.

Booth, T., Jovanovic, T., Old, K., and Dudzinski, M. Climatic mapping to identify high-risk areas for *Cylindrocladium quinqueseptatum* leaf blight on eucalypts in mainland South East Asia and around the world. *Environmental Pollution*, 108(3): 365–372, 2000. doi: 10.1016/S0269-7491(99)00215-8.

Boudier, B. *Didymascella thujina* principal ennemi du Thuya dans l'ouest de la France. *Phytoma - Defense des cultures*, Novembre:51–56, 1983.

Boudru, M. La rouille des aiguilles du Thuja géant (*Thuja plicata* Don.). *Bulletin de la Société Royale Forestière de Belgique*, 52:69–75, 1945.

Bower, R. and Dunsworth, B. Provenance test of western red cedar on Vancouver Island. In Smith, N., editor, *Western Red Cedar-does it Have a Future? Conference proceedings July 13–14*, pages 131–135, Vancouver, 1987. University of British Columbia Press.

Briat, J.-F., Ravet, K., Arnaud, N., Duc, C., Boucherez, J., Touraine, B., Cellier, F., and Gaymard, F. New insights into ferritin synthesis and function highlight a link between iron homeostasis and oxidative stress in plants. *Annals of Botany*, 105(5): 811–822, 2010. doi: 10.1093/aob/mcp128.

Brini, F., Yamamoto, A., Jlaiel, L., Takeda, S., Hobo, T., Dinh, H., Hattori, T., Masmoudi, K., and Hanin, M. Pleiotropic effects of the wheat dehydrin DHN-5 on stress responses in *Arabidopsis*. *Plant & Cell Physiology*, 52(4):676–688, 2011. doi: 10.1093/pcp/pcr030.

Bronstein, J., Alarcón, R., and Geber, M. The evolution of plant–insect mutualisms. *New Phytologist*, 172(3):412–428, 2006. doi: 10.1111/j.1469-8137.2006.01864.x.

Brown, J., Shipton, W., and White, N. The relationship between hypersensitive tissue and resistance in wheat seedlings infected with *Puccinia graminis tritici*. *Annals of Applied Biology*, 58(2):279–290, 1966.

Brown, J. and Rant, J. Fitness costs and trade-offs of disease resistance and their consequences for breeding arable crops. *Plant Pathology*, 62(S1):83–95, 2013. doi: 10.1111/ppa.12163.

Bruns, E. Fitness Costs of Plant Disease Resistance. In *eLS*, eLS subject area: Plant Science. John Wiley & Sons, Ltd, February 2016.

Buchwald, N. En ny svampesygdom i Danmark. *Didymascella thujina* paa *Thuja plicata*. *Dansk Skovforenings Tidsskrift*, 21:51–59, 1936.

Buerstmayr, H., Lemmens, M., Hartl, L., Doldi, L., Steiner, B., Stierschneider, M., and Ruckenbauer, P. Molecular mapping of QTLs for Fusarium head blight resistance in spring wheat. I. Resistance to fungal spread (type II resistance). *Theoretical and Applied Genetics*, 104(1):84–91, 2002. doi: 10.1007/s001220200009.

Bui, M., Lim, N., Sijacic, P., and Liu, Z. LEUNIG_HOMOLOG and LEUNIG regulate seed mucilage extrusion in *Arabidopsis*. *Journal of Integrative Plant Biology*, 53(5):399–408, 2011. doi: 10.1111/j.1744-7909.2011.01036.x.

Burdekin, D. Needle blight of Western Red Cedar caused by *Didymascella thujina*. Report on forestry research, Forestry Commission, London, 1968.

Burdekin, D. Needle blight of Western Red Cedar caused by *Didymascella thujina*. Report on forestry research, Forestry Commission, London, 1969.

Burdekin, D. and Phillips, D. Chemical control of *Didymascella thujina* on western red cedar in forest nurseries. *Annals of Applied Biology*, 67(1):131–136, 1971.

Burdon, J. and Thrall, P. Coevolution of plants and their pathogens in natural habitats. *Science*, 324(5928):755–756, 2009. doi: 10.1126/science.1171663.

Burdon, R. Genetic diversity and disease resistance: some considerations for research, breeding, and deployment. *Canadian Journal of Forest Research*, 31(4):596–606, 2001. doi: 10.1139/x00-136.

Buschiazzo, E., Ritland, C., Bohlmann, J., and Ritland, K. Slow but not low: genomic comparisons reveal slower evolutionary rate and higher dN/dS in conifers compared to angiosperms. *BMC Evolutionary Biology*, 12:8, 2012. doi: 10.1186/1471-2148-12-8.

Bush, W. and Moore, J. Chapter 11: Genome-wide association studies. *PLoS Computational Biolgy*, 8(12):e1002822, December 2012. 11 pages.

Camacho, C., Coulouris, G., Avagyan, V., Ma, N., Papadopoulos, J., Bealer, K., and Madden, T. L. BLAST+: architecture and applications. *BMC Bioinformatics*, 10:421, 2009.

Camilios-Neto, D., Bonato, P., Wassem, R., Tadra-Sfeir, M., Brusamarello-Santos, L., Valdameri, G., Donatti, L., Faoro, H., Weiss, V., Chubatsu, L., Pedrosa, F., and Souza, E. Dual *RNA*-seq transcriptional analysis of wheat roots colonized by *Azospirillum brasilense* reveals up-regulation of nutrient acquisition and cell cycle genes. *BMC Genomics*, 15:378, 2014. doi: 10.1186/1471-2164-15-378.

Carella, P., Wilson, C., and Cameron, R. Some things get better with age: differences in salicylic acid accumulation and defense signaling in young and mature *Arabidopsis*. *Frontiers in Plant Science*, 5:775, 2015. doi: 10.3389/fpls.2014.00775.

Carson, M., Stuber, C., and Senior, M. Identification and mapping of quantitative trait loci conditioning resistance to southern leaf blight of maize caused by *Cochliobolus heterostrophus* race O. *Phytopathology*, 94(8):862–867, 2004. doi: 10.1094/PHYTO.2004.94.8.862.

Carson, S. and Carson, M. Breeding for resistance in forest trees-a quantitative genetic approach. *Annual Review of Phytopathology*, 27:373–395, 1989. doi: 10.1146/annurev.py.27.090189.002105.

Casazza, A., Rossini, S., Rosso, M., and Soave, C. Mutational and expression analysis of ELIP1 and ELIP2 in *Arabidopsis thaliana*. *Plant Molecular Biology*, 58(1):41–51, 2005. doi: 10.1007/s11103-005-4090-1.

Castillo, F., Hernandez, D., Gallegos, G., Rodriguez, R., and Aguilar, C. Antifungal Properties of Bioactive Compounds from Plants. In Dhanasekaran, D., Thajuddin, N., and Panneerselvam, A., editors, *Fungicides for Plant and Animal Diseases*, pages 81–106. InTech, jan 2012. ISBN 978-953-307-804-5. doi: 10.5772/26598.

Chakraborty, S. and Newton, A. Climate change, plant diseases and food security: an overview. *Plant Pathology*, 60(1):2–14, 2011. doi: 10.1111/j.1365-3059.2010.02411.x.

Chedgy, R., Daniels, C., Kadla, J., and Breuil, C. Screening fungi tolerant to western red cedar (*Thuja plicata* Donn) extractives. Part 1. Mild extraction by ultrasonication and quantification of extractives by reverse-phase HPLC. *Holzforschung*, 61 (2):190–194, 2007a.

Chedgy, R., Morris, P., Morris, Y., and Breuil, C. Black stain of western red cedar (*Thuja plicata* Donn) by *Aureobasidium pullulans*: the role of weathering. *Wood and Fiber Science*, 39(3):472–481, 2007b.

Chen, M.-S. Inducible direct plant defense against insect herbivores: a review. *Insect Science*, 15(2):101–114, 2008.

Chen, X., Wang, Y., and Luo, T. First report of leaf spot caused by *Phoma sorghina* on *Oxalis debilis* in China. *Plant Disease*, 101(6):1047, 2017. doi: 10.1094/PDIS-11-16-1614-PDN.

Cheng, S. and Chang, S. Bioactivity and characterization of exudates from *Cryptomeria japonica* bark. *Wood Science and Technology*, 48(4):831–840, 2014.

Cheng, Y., Kato, N., Wang, W., Li, J., and Chen, X. Two RNA binding proteins, HEN4 and HUA1, act in the processing of AGAMOUS pre-mRNA in *Arabidopsis thaliana*. *Developmental Cell*, 4(1):53–66, 2003. doi: 10.1016/S1534-5807(02)00399-4.

Cheong, Y., Chang, H.-S., Gupta, R., Wang, X., Zhu, T., and Luan, S. Transcriptional profiling reveals novel interactions between wounding, pathogen, abiotic stress, and hormonal responses in Arabidopsis. *Plant Physiology*, 129(2):661–677, 2002. doi: 10.1104/pp.002857.

Chittoor, J., Leach, J., and White, F. Induction of Peroxidase During Defense Against Pathogens. In Datta, S. and Muthukrishnan, S., editors, *Pathogenesis-Related Proteins in Plants*, pages 171–193, Boca Raton, FL., 1999. CRC Press.

Cho, S., Kim, J., Park, J.-A., Eom, T., and Kim, W. Constitutive expression of abiotic stress-inducible hot pepper *CaXTH3*, which encodes a xyloglucan endotransglucosylase/hydrolase homolog, improves drought and salt tolerance in transgenic *Arabidopsis* plants. *FEBS Letters*, 580(13):3136–3144, 2006. doi: 10.1016/j.febslet.2006.04.062.

Christensen, A., Thordal-Christensen, H., Zimmermann, G., Gjetting, T., Lyngkjær, M., Dudler, R., and Schweizer, P. The germinlike protein GLP4 exhibits superoxide dismutase activity and is an important component of quantitative resistance in wheat and barley. *Molecular Plant-Microbe Interactions*, 17(1):109–117, 2004. doi: 10.1094/MPMI.2004.17.1.109.

Coleman, G., Chen, T., Ernst, S., and Fuchigami, L. Photoperiod control of poplar bark storage protein accumulation. *Plant Physiology*, 96(3):686–692, 1991. doi: 10.1104/pp.96.3.686.

Coleman, G., Bañados, M., and Chen, T. Poplar bark storage protein and a related wound-induced gene are differentially induced by nitrogen. *Plant Physiology*, 106 (1):211–215, 1994.

Colhoun, J. Effects of environmental factors on plant disease. *Annual Review of Phytopathology*, 11(1):343–364, 1973. doi: 10.1146/annurev.py.11.090173.002015.

Collard, B., Jahufer, M., Brouwer, J., and Pang, E. An introduction to markers, quantitative trait loci (QTL) mapping and marker-assisted selection for crop improvement: the basic concepts. *Euphytica*, 142(1-2):169–196, 2005.

Cooper, S. and Owen-Smith, N. Effects of plant spinescence on large mammalian herbivores. *Oecologia*, 68(3):446–455, 1986. doi: 10.1007/BF01036753.

Cosgrove, D. Growth of the plant cell wall. *Nature Reviews Molecular Cell Biology*, 6:850–861, 2005.

Culley, D., Horovitz, D., and Hadwiger, L. Molecular characterization of disease-resistance response gene *DRR206-d* from *Pisum sativum* (L.). *Plant Physiology*, 107:301–302, 1995.

Daniels, C. and Russell, J. Analysis of western redcedar (*Thuja plicata* Donn) heartwood components by HPLC as a possible screening tool for trees with enhanced natural durability. *Journal of Chromatographic Science*, 45(5):281–285, 2007.

Daniels, L., Dobry, J., Klinka, K., and Feller, M. Determining year of death of logs and snags of *Thuja plicata* in southwestern coastal British Columbia. *Canadian Journal of Forest Research*, 27(7):1132–1141, 1997.

Das, A., Kamal, S., Shakil, N., Sherameti, I., Oelmüller, R., Dua, M., Tuteja, N., Johri, A., and Varma, A. The root endophyte fungus *Piriformospora indica* leads to early flowering, higher biomass and altered secondary metabolites of the medicinal plant, *Coleus forskohlii*. *Plant Signaling & Behavior*, 7(1):103–112, 2012. doi: 10.4161/psb.7.1.18472.

Das, G. and Varshney, U. Peptidyl-tRNA hydrolase and its critical role in protein biosynthesis. *Microbiology*, 152(8):2191–2195, 2006. doi: 10.1099/mic.0.29024-0.

Daubenmire, R. Nutrient content of leaf litter of trees in the northern Rocky Mountains. *Ecology*, 34(4):786–793, 1953.

Davin, L. and Lewis, N. Dirigent proteins and dirigent sites explain the mystery of specificity of radical precursor coupling in lignan and lignin biosynthesis. *Plant Physiology*, 123(2):453–462, 2000.

de Cremer, K., Mathys, J., Vos, C., Froenicke, L., Michelmore, R., Cammue, B., and de Coninck, B. RNAseq-based transcriptome analysis of *Lactuca sativa* infected by the fungal necrotroph *Botrytis cinerea*. *Plant, Cell and Environment*, 36(11): 1992–2007, apr 2013. doi: 10.1111/pce.12106.

De La Torre, A., Li, Z., Van de Peer, Y., and Ingvarsson, P. Contrasting rates of molecular evolution and patterns of selection among gymnosperms and flowering plants. *Molecular Biology and Evolution*, 34(6):1363–1377, 2017. doi: 10.1093/molbev/msx069.

De Luna, L., Watson, A., and Paulitz, T. Reaction of rice (*Oryza sativa*) cultivars to penetration and infection by *Curvularia tuberculata* and C. *oryzae*. *Plant Disease*, 86(5):470–476, 2002.

de Souza Cândido, E., Soares-Pinto, M., Barbosa-Pelegrini, P., Bergamin-Lima, T., Nascimento-Silva, O., Pogue, R., Grossi-de Sá, M., and Franco, O. Plant storage proteins with antimicrobial activity: novel insights into plant defense mechanisms. *The FASEB Journal*, 25(10):3290–3305, 2011. doi: 10.1096/fj.11-184291.

de Vetten, N., ter Horst, J., van Schaik, H., de Boer, A., Mol, J., and Koes, R. A cytochrome b_5 is required for full activity of flavonoid 3′,5′-hydroxylase, a cytochrome P450 involved in the formation of blue flower colors. *Proceedings of the National Academy of Sciences of The United States of America*, 96(2):778–783, 1999.

de Wit, P., van der Burgt, A., Ökmen, B., Stergiopoulos, I., Abd-Elsalam, K., Aerts, A., Bahkali, A., Beenen, H., Chettri, P., Cox, M., Datema, E., de Vries, R., Dhillon, B., Ganley, A., Griffiths, S., Guo, Y., Hamelin, R., Henrissat, B., Kabir, M., Jashni, M., Kema, G., Klaubauf, S., Lapidus, A., Levasseur, A., Lindquist, E., Mehrabi, R., Ohm, R., Owen, T., Salamov, A., Schwelm, A., Schijlen, E., Sun, H., van den Burg, H., van Ham, R., Zhang, S., Goodwin, S., Grigoriev, I., Collemare, J., and Bradshaw, R. The genomes of the fungal plant pathogens *Cladosporium fulvum* and *Dothistroma septosporum* reveal adaptation to different hosts and lifestyles but also signatures of common ancestry. *PLoS Genetics*, 8(11):e1003088, 2012. doi: 10.1371/journal.pgen.1003088.

De Wolf, E. and Isard, S. Disease cycle approach to plant disease prediction. *Annual Review of Phytopathology*, 45:203–220, 2007. doi: 10.1146/annurev.phyto.44.070505.143329.

Degenhardt, D. and Lincoln, D. Volatile emissions from an odorous plant in response to herbivory and methyl jasmonate exposure. *Journal of Chemical Ecology*, 32(4): 725–743, 2006. doi: 10.1007/s10886-006-9030-2.

Dembitsky, V., Gloriozova, T., and Poroikov, V. Naturally occurring plant isoquinoline N-oxide alkaloids: their pharmacological and SAR activities. *Phytomedicine*, 22(1):183–202, 2015. doi: 10.1016/j.phymed.2014.11.002.

Dennis, J. and Sutherland, J. *Keithia* Blight. In *Seed and seedling Extension Topics*, number 2 in 1, page 15. Province of British Columbia, Ministry of Forests, Victoria, B.C, 1989.

Dennis, R. *Fungi of Southeast England*. Royal Botanic Gardens, Kew, 1995.

Desgagné-Penix, I., Khan, M., Schriemer, D., Cram, D., Nowak, J., and Facchini, P. Integration of deep transcriptome and proteome analyses reveals the components of alkaloid metabolism in opium poppy cell cultures. *BMC Plant Biology*, 10:252, 2010. doi: 10.1186/1471-2229-10-252.

Desmazières, J. Dixième notice sur quelques plantes cryptogames, la plupart inédites, récemment découvertes en France, et que vont paraître en nature dans la collection publiée par l'auteur. *Annales des Sciences Naturelles - Botanique*, 19:335–373, 1843.

Develey-Rivière, M. and Galiana, E. Resistance to pathogens and host developmental stage: a multifaceted relationship within the plant kingdom. *New Phytologist*, 175 (3):405–416, 2007. doi: 10.1111/j.1469-8137.2007.02130.x.

Dey, K. K., Hsiao, C. J., and Stephens, M. Grade of Membership Model and Visualization for *RNA*-seq data using *CountClust*, 2016. URL `https://github.com/kkdey/CountClust`.

Dey, K. K., Hsiao, C. J., and Stephens, M. Visualizing the structure of *RNA*-seq expression data using grade of membership models. *PLoS Genetics*, 13(3):e1006599, 2017. doi: 10.1371/journal.pgen.1006599.

Diamond, A. and Desgagné-Penix, I. Metabolic engineering for the production of plant isoquinoline alkaloids. *Plant Biotechnology Journal*, 14(6):1319–1328, 2016. doi: 10.1111/pbi.12494.

Dickinson, M. *Molecular Plant Pathology*. BIOS Scientific Publishers, New York, 2003.

Dillies, M.-A., Rau, A., Aubert, J., Hennequet-Antier, C., Jeanmougin, M., Servant, N., Keime, C., Marot, G., Castel, D., Estelle, J., Guernec, G., Jagla, B., Jouneau, L., Laloë, D., Le Gall, C., Schaëffer, B., Le Crom, S., Guedj, M., and Jaffrézic, F. A comprehensive evaluation of normalization methods for Illumina high-throughput *RNA* sequencing data analysis. *Briefings in Bioinformatics*, 14(6):671–683, 2013.

Divol, F., Vilaine, F., Thibivilliers, S., Kusiak, C., Sauge, M., and Dinant, S. Involvement of the xyloglucan endotransglycosylase/hydrolases encoded by celery *XTH1* and *Arabidopsis XTH33* in the phloem response to aphids. *Plant, Cell & Environment*, 30(2):187–201, 2007. doi: 10.1111/j.1365-3040.2006.01618.x.

Doehlemann, G., Wahl, R., Horst, R., Voll, L., Usadel, B., Poree, F., Stitt, M., Pons-Kühnemann, J., Sonnewald, U., Kahmann, R., and Kamper, J. Reprogramming a maize plant: transcriptional and metabolic changes induced by the fungal biotroph *Ustilago maydis*. *The Plant Journal*, 56(2):181–195, oct 2008. doi: 10.1111/j.1365-313X.2008.03590.x.

Doehlemann, G., van-der Linde, K., ABmann, D., Schwammbach, D., Hof, A., Mohanty, A., Jackson, D., and Kahmann, R. Pep1, a secreted effector protein of *Ustilago maydis*, is required for successful invasion of plant cells. *PLoS pathogens*, 5(2):e1000290, 2009.

Doležel, J., Bartoš, J., Voglmayr, H., and Greilhuber, J. Nuclear DNA content and genome size of trout and human. *Cytometry Part A*, 51A(2):127–128, 2003. doi: 10.1002/cyto.a.10013.

Domínguez, E., Heredia-Guerrero, J., and Heredia, A. The biophysical design of plant cuticles: an overview. *New Phytologist*, 189(4):938–949, 2011. doi: 10.1111/j.1469-8137.2010.03553.x.

Donahue, J., Alford, S., Torabinejad, J., Kerwin, R., Nourbakhsh, A., Ray, W., Hernick, M., Huang, X., Lyons, B., Hein, P., and Gillaspy, G. The *Arabidop-*

sis thaliana Myo-Inositol 1-Phosphate Synthase1 gene is required for *Myo*-inositol synthesis and suppression of cell death. *The Plant Cell*, 22(3):888–903, 2010. doi: 10.1105/tpc.109.071779.

Donofrio, N. and Delaney, T. Abnormal callose response phenotype and hypersusceptibility to *Peronospora parasitica* in defense-compromised Arabidopsis *nim1-1* and salicylate hydroxylase-expressing plants. *Molecular Plant-Microbe Interactions*, 14 (4):439–450, 2001. doi: 10.1094/MPMI.2001.14.4.439.

Dukes, J., Pontius, J., Orwig, D., Garnas, J., Rodgers, V., Brazee, N., Cooke, B., Theoharides, K., Stange, E., Harrington, R., Ehrenfeld, J., Gurevitch, J., Lerdau, M., Stinson, K., Wick, R., and Ayres, M. Responses of insect pests, pathogens, and invasive plant species to climate change in the forests of northeastern North America: what can we predict? *Canadian Journal of Forest Research*, 39(2): 231–248, 2009. doi: 10.1139/X08-171.

Duplessis, S., Cuomo, C., Lin, Y., Aerts, A., Tisserant, E., Veneault-Fourrey, C., Joly, D., Hacquard, S., Amselem, J., Cantarel, B., Chiu, R., Coutinho, P., Feau, N., Field, M., Frey, P., Gelhaye, E., Goldberg, J., Grabherr, M., Kodira, C., Kohler, A., Kües, U., Lindquist, E., Lucas, S., Mago, R., Mauceli, E., Morin, E., Murat, C., Pangilinan, J., Park, R., Pearson, M., Quesneville, H., Rouhier, N., Sakthikumar, S., Salamov, A., Schmutz, J., Selles, B., Shapiro, H., Tanguay, P., Tuskan, G., Henrissat, B., de Peer, Y. V., Rouzé, P., Ellis, J., Dodds, P., Schein, J., Zhong, S., Hamelin, R., Grigoriev, I., Szabo, L., and Martin, F. Obligate biotrophy features unraveled by the genomic analysis of rust fungi. *Proceedings of the National Academy of Sciences of The United States of America*, 108(22):9166–9171, 2011. doi: 10.1073/pnas.1019315108.

Durand, E. The genus Keithia. *Mycologia*, 5(1):6–11, 1913.

Duressa, D., Soliman, K., Taylor, R., and Senwo, Z. Proteomic analysis of soybean roots under aluminum stress. *International Journal of Plant Genomics*, 2011: 282531, 2011.

Dusabenyagasani, M., Laflamme, G., and Hamelin, R. Nucleotide polymorphisms in three genes support host and geographic speciation in tree pathogens belonging to *Gremmeniella* spp. *Canadian Journal of Botany*, 80(11):1151–1159, 2002. doi: 10.1139/b02-103.

Dushnicky, L., Ballance, G., Sumner, M., and MacGregor, A. The role of lignification as a resistance mechanism in wheat to a toxin-producing isolate of *Pyrenophora tritici-repentis*. *Canadian Journal of Plant Pathology*, 20(1):35–47, 1998.

Ebell, L. Variation in total soluble sugars of conifer tissues with method of analysis. *Phytochemistry*, 8:227–233, 1969.

Ederli, L., Madeo, L., Calderini, O., Gehring, C., Moretti, C., Buonaurio, R., Paolocci, F., and Pasqualini, S. The *Arabidopsis thaliana* cysteine-rich receptor-like kinase CRK20 modulates host responses to *Pseudomonas syringae* pv. *tomato* DC3000 infection. *Journal of Plant Physiology*, 168(15):1784–1794, 2011. doi: 10.1016/j.jplph.2011.05.018.

Elad, Y. and Pertot, I. Climate change impacts on plant pathogens and plant diseases. *Journal of Crop Improvement*, 28(1):99–139, 2014. doi: 10.1080/15427528.2014.865412.

Elliott, M., Broschat, T., Uchida, J., and Simone, G., editors. *Compendium of Ornamental Palm Diseases and Disorders*. American Phytopathological Society (APS) Press, St. Paul, 2004.

Ellis, M. and Ellis, J. *Microfungi on Land Plants: An Identification Handbook*. Richmond Publishing, 2 edition, 1997.

England, J. and Attiwill, P. Changes in leaf morphology and anatomy with tree age and height in the broadleaved evergreen species, *Eucalyptus regnans* F. Muell. *Trees*, 20:79, 2005. doi: 10.1007/s00468-005-0015-5.

Erb, M., Balmer, D., de Lange, E., von Merey, G., Planchamp, C., Robert, C., Röder, G., Sobhy, I., Zwahlen, C., Mauch-Mani, B., and Turlings, T. Synergies and trade-offs between insect and pathogen resistance in maize leaves and roots. *Plant, Cell & Environment*, 34(7):1088–1103, 2011. doi: 10.1111/j.1365-3040.2011.02307.x.

Erickson, F. and Hannig, E. Ligand interactions with eukaryotic translation initiation factor 2: role of the γ-subunit. *The EMBO Journal*, 15(22):6311–6320, 1996.

Falcone-Ferreyra, M., Rius, S., and Casati, P. Flavonoids: biosynthesis, biological functions, and biotechnological applications. *Frontiers in Plant Science*, 2:222, 2012. doi: 10.3389/fpls.2012.00222.

Fäldt, J., Martin, D., Miller, B., Rawat, S., and Bohlmann, J. Traumatic resin defense in Norway spruce (*Picea abies*): methyl jasmonate-induced terpene synthase gene expression, and cDNA cloning and functional characterization of (+)-3-carene synthase. *Plant Molecular Biology*, 51(1):119–133, 2003.

Fan, J. and Doerner, P. Genetic and molecular basis of nonhost disease resistance: complex, yes; silver bullet, no. *Current Opinion in Plant Biology*, 15(4):400–406, 2012. doi: 10.1016/j.pbi.2012.03.001.

Fan, J., Hill, L., Crooks, C., Doerner, P., and Lamb, C. Abscisic acid has a key role in modulating diverse plant-pathogen interactions. *Plant Physiology*, 150(4): 1750–1761, 2009. doi: 10.1104/pp.109.137943.

Fan, S., Grossnickle, S., and Russell, J. Morphological and physiological variation in western redcedar (*Thuja plicata*) populations under contrasting soil water conditions. *Trees-Structure and Function*, 22(5):671–683, 2008.

Fan, S., Jiang, L., Wu, J., Dong, L., Cheng, Q., and Xu, S., P.and Zhang. A novel pathogenesis-related class 10 protein *Gly m 4l*, increases resistance upon *Phytophthora sojae* infection in soybean (*Glycine max* [L.] Merr.). *PLoS ONE*, 10(10): e0140364, 2015. doi: 10.1371/journal.pone.0140364.

Fang-Ma, J. Role of organic acids in detoxification of aluminum in higher plants. *Plant & Cell Physiology*, 41(4):383–390, 2000. doi: 10.1093/pcp/41.4.383.

Feau, N. and Hamelin, R. Say hello to my little friends: how microbiota can modulate tree health. *New Phytologist*, 215(2):508–510, 2017. doi: 10.1111/nph.14649.

Feng-Ma, J. Syndrome of aluminum toxicity and diversity of aluminum resistance in higher plants. *International Review of Cytology*, 264:225–252, 2007.

Feng-Ma, J., Ryan, P., and Delhaize, E. Aluminium tolerance in plants and the complexing role of organic acids. *TRENDS in Plant Science*, 6(6):273–279, june 2001.

Fernandes, G. Plant mechanical defenses against insect herbivory. *Revista Brasileira de Entomologia*, 38(2):421–433, 1994.

Fernández-Magan, F. Nuevos ataques a las Thuyas en los viveros de Galicia. *Anales del Instituto Nacional de Investigaciones Agrarias, Recursos Naturales*, 1:187–199, 1974.

Fernando, A., Ring, F., Lowe, D., and Callan, B. Index of plant pathogens, plant-associated microorganisms, and forest fungi of British Columbia. Information Report BC-X-385, Natural Resources Canada (Pacific Forestry Centre), Victoria, BC, 1999.

Fesel, P. and Zuccaro, A. β-glucan: crucial component of the fungal cell wall and elusive MAMP in plants. *Fungal Genetics and Biology*, 90:53–60, 2016. doi: 10.1016/j.fgb.2015.12.004.

Fichtner, E. *Abiotic Pathogen Suppression: Physiology and Biology of Aluminum Toxicity to Soilborne Fungi*. PhD thesis, North Carolina State University, 2003.

Finn, R. D., Coggill, P., Eberhardt, R. Y., Eddy, S. R., Mistry, J., Mitchell, A. L., Potter, S. C., Punta, M., Qureshi, M., Sangrador-Vegas, A., Salazar, G. A., Tate, J., and Bateman, A. The Pfam protein families database: towards a more sustainable future. *Nucleic Acids Research*, 44(D1):D279–D285, 2016.

Firestone, M., Killham, K., and McColl, J. Fungal toxicity of mobilized soil aluminum and manganese. *Applied and Environmental Microbiology*, 46(3):758–761, 1983.

Fisher, P. and Petrini, O. Fungal saprobes and pathogens as endophytes of rice (*Oryza sativa* L.). *New Phytologist*, 120(1):137–143, 1992. doi: 10.1111/j.1469-8137.1992.tb01066.x.

Fones, H. and Preston, G. The impact of transition metals on bacterial plant disease. *FEMS Microbiology Reviews*, 37(4):495–519, 2013. doi: 10.1111/1574-6976.12004.

Forbes, A. Occurrence of *Keithia thujina* in Ireland. *The Gardeners' Chronicles*, 68: 228–229, 1920.

Forbes, A. *Keithia thujina* in Ireland. *Quarterly Journal of Forestry*, 15:73–75, 1921.

Foster, A., Hall, D., Mortimer, L., Abercromby, S., Gries, R., Gries, G., Bohlmann, J., Russell, J., and Mattsson, J. Identification of genes in *Thuja plicata* foliar terpenoid defenses. *Plant Physiology*, 161(4):1993–2004, 2013. doi: 10.1104/pp.112.206383.

Foster, A., Aloni, R., Fidanza, M., Gries, R., Gries, G., and Mattsson, J. Foliar phase changes are coupled with changes in storage and biochemistry of monoterpenoids in western redcedar (*Thuja plicata*). *Trees*, 30(4):1361–1375, mar 2016. doi: 10.1007/s00468-016-1373-x.

Franceschi, V., Krekling, T., Berryman, A., and Christiansen, E. Specialized phloem parenchyma cells in Norway spruce (Pinaceae) bark are an important site of defense reactions. *American Journal of Botany*, 85(5):601–615, 1998.

Franceschi, V., Krokene, P., Krekling, T., and Christiansen, E. Phloem parenchyma cells are involved in local and distant defense responses to fungal inoculation or bark-beetle attack in Norway spruce (Pinaceae). *American Journal of Botany*, 87 (3):314–326, 2000.

Franceschi, V., Krokene, P., Christiansen, E., and Krekling, T. Anatomical and chemical defenses of conifer bark against bark beetles and other pests. *New Phytologist*, 167(2):353–376, 2005. doi: 10.1111/j.1469-8137.2005.01436.x.

Frank, S. A. Coevolutionary genetics of plants and pathogens. *Evolutionary Ecology*, 7(1):45–75, 1993. doi: 10.1007/BF01237734.

Frank, S. Models of plant-pathogen coevolution. *Trends in Genetics*, 8(6):213–219, 1992. doi: 10.1016/0168-9525(92)90236-W.

Frankel, S. Evaluation of Fungicides to control cedar leaf blight on western red cedar at Humboldt nursery. Forest pest management report 90-01, USDA Forest Service, Pacific Southwest Region, State and Private Forestry, 1990.

Frankel, S. Timing and applications of triadimefon (Bayleton) needed for control of cedar leaf blight on western redcedar at Humboldt nursery. Forest pest management report 91-01, USDA Forest Service, Pacific Southwest Region, State and Private Forestry, 1991.

Frankel, S. Additional studies on rate and number of triadimefon (Bayleton 25% WP) applications needed for control of cedar leaf blight on western redcedar at Humboldt nursery. Forest pest management report 92-02, USDA Forest Service, Pacific Southwest Region, State and Private Forestry, 1992.

Franks, R., Wang, C., Levin, J., and Liu, Z. *SEUSS*, a member of a novel family of plant regulatory proteins, represses floral homeotic gene expression with *LEUNIG*. *Development*, 129:253–263, 2002.

Free, S. J. Chapter Two: Fungal Cell Wall Organization and Biosynthesis. In Friedmann, T., Dunlap, J., and Goodwin, S., editors, *Advances in Genetics*, volume 81, pages 33–82. Academic Press, 2013. doi: 10.1016/B978-0-12-407677-8.00002-6.

Fujita, K., Kambe, R., De Alwis, R., Yagi, T., and Tsutsumi, Y. Airborne monoterpenes emitted from a *Cupressus lusitanica* cell culture induce a signaling cascade that produces β-thujaplicin. *Journal of Chemical Ecology*, 42(8):814–820, 2016. doi: 10.1007/s10886-016-0739-2.

Fujiwara, M., Umemura, K., Kawasaki, T., and Shimamoto, K. Proteomics of Rac GTPase signaling reveals its predominant role in elicitor-induced defense response of cultured rice cells. *Plant Physiology*, 140(2):734–745, 2006. doi: 10.1104/pp.105.068395.

Fulton, L., Batoux, M., Vaddepalli, P., Yadav, W., R.K.and Busch, Andersen, S., Jeong, S., Lohmann, J., and Schneitz, K. *DETORQUEO*, *QUIRKY*, and *ZERZAUST* represent novel components involved in organ development mediated by the receptor-like kinase STRUBBELIG in *Arabidopsis thaliana*. *PLoS Genetics*, 5(1):e1000355, 2009. doi: 10.1371/journal.pgen.1000355.

Fürstenberg-Hägg, J., Zagrobelny, M., and Bak, S. Plant defense against insect herbivores. *International Journal of Molecular Sciences*, 14(5):10242–10297, 2013. doi: 10.3390/ijms140510242.

Gadek, P. and Quinn, C. An analysis of relationships within the Cupressaceae *sensu stricto* based on *rbc*L Sequences. *Annals of the Missouri Botanical Garden*, 80(3):581–586, 1993.

Galindo-González, L. and Deyholos, M. RNA-seq transcriptome response of flax (*Linum usitatissimum* L.) to the pathogenic fungus *Fusarium oxysporum* f. sp. *lini*. *Frontiers in Plant Science*, 7(1766):22 pages, 2016.

Gang, D., Costa, M., Fujita, M., Dinkova-Kostova, A., Wang, H.-B., Burlat, V., Martin, W., Sarkanen, S., Davin, L., and Lewis, N. Regiochemical control of

monolignol radical coupling: a new paradigm for lignin and lignan biosynthesis. *Chemistry & Biology*, 6(3):143–151, 1999.

Gangappa, S. and Botto, J. The multifaceted roles of HY5 in plant growth and development. *Molecular Plant*, 9(10):1353–1365, 2016. doi: 10.1016/j.molp.2016.07.002.

Garrett, K., Dendy, S., Frank, E., Rouse, M., and Travers, S. Climate change effects on plant disease: genomes to ecosystems. *Annual Review of Phytopathology*, 44:489–509, 2006. doi: 10.1146/annurev.phyto.44.070505.143420.

Gees, R. and Hohl, H. Cytological comparison of specific (*R3*) and general resistance to late blight in potato leaf tissue. *Phytopathology*, 78:350–357, 1988.

Geoghegan, I., Steinberg, G., and Gurr, S. The role of the fungal cell wall in the infection of plants. *Trends in Microbiology*, 25(12):957–967, 2017. doi: 10.1016/j.tim.2017.05.015.

Gesell, A., Blaukopf, M., Madilao, L., Yuen, M., Withers, S., Mattsson, J., Russell, J., and Bohlmann, J. The gymnosperm cytochrome P450 CYP750B1 catalyzes stereospecific monoterpene hydroxylation of (+)-sabinene in thujone biosynthesis in western redcedar. *Plant Physiology*, 168(1):94–106, 2015. ISSN 0032-0889.

Ghaffar, M., Norliza, A., Pritchard, J., and Ford-Lloyd, B. Identification of candidate genes involved in brown planthopper resistance in rice using microarray analysis. *Journal of Tropical Agriculture and Food Science*, 44(1):49–62, 2016.

Ghini, R., Hamada, E., and Bettiol, W. Climate change and plant diseases. *Scientia Agricola*, 65(spe):98–107, 2008.

Ghosh, M. Antifungal properties of haem peroxidase from *Acorus calamus*. *Annals of Botany*, 98(6):1145–1153, 2006. doi: 10.1093/aob/mcl205.

Glaubitz, J., El-Kassaby, Y., and Carlson, J. Nuclear restriction fragment length polymorphism analysis of genetic diversity in western redcedar. *Canadian Journal of Forest Research*, 30(3):379–389, 2000.

Goering, H. and Van Soest, P. J. Forage Fiber Analyses (Apparatus, Reagents, Procedures, and Some Applications). In *Agriculture Handbook*, number 379. United States Department of Agriculture, 1970.

Goff, K. and Ramonell, K. The role and regulation of receptor-like kinases in plant defense. *Gene Regulation and Systems Biology*, 1:167–175, 2007.

Gonzalez, D., Bowen, A., Carroll, T., and Conlan, R. S. The transcription corepressor LEUNIG interacts with the histone deacetylase HDA19 and mediator components MED14 (SWP) and CDK8 (HEN3) to repress transcription. *Molecular & Cellular Biology*, 27(15):5306–5315, 2007. doi: 10.1128/MCB.01912-06.

Gonzalez, J. Growth, properties and uses of western red cedar. Special Publication SP-7R, ForIntek Canada Corp., Vancouver, BC, 2004.

González-Fontes, A., Navarro-Gochicoa, M., Camacho-Cristóbal, J., Herrera-Rodríguez, M., Quiles-Pando, C., and Rexach, J. Is Ca^{2+} involved in the signal transduction pathway of boron deficiency? New hypotheses for sensing boron deprivation. *Plant Science*, 217-218:135–139, mar 2014. doi: 10.1016/j.plantsci.2013.12.011.

Goodger, J., Heskes, A., and Woodrow, I. Contrasting ontogenetic trajectories for phenolic and terpenoid defences in *Eucalyptus froggattii*. *Annals of Botany*, 112(4):651–659, 2013. doi: 10.1093/aob/mct010.

Goswami, R., Dong, Y., and Punja, Z. Host range and mycotoxin production by *Fusarium equiseti* isolates originating from ginseng fields. *Canadian Journal of Plant Pathology*, 30(1):155–160, 2008. doi: 10.1080/07060660809507506.

Gou, J.-Y., Yu, X.-H., and Liu, C.-J. A hydroxycinnamoyltransferase responsible for synthesizing suberin aromatics in *Arabidopsis*. *Proceedings of the National Academy of Sciences of The United States of America*, 106(44):18855–18860, 2009. doi: 10.1073/pnas.0905555106.

Grabherr, M. G., Haas, B. J., Yassour, M., Levin, J. Z., Thompson, D. A., Amit, I., Adiconis, X., Fan, L., Raychowdhury, R., Zeng, Q., Chen, Z., Mauceli, E., Hacohen, N., Gnirke, A., Rhind, N., Di Palma, F., Birren, B. W., Nusbaum, C., Lindblad-Toh, K., Friedman, N., and Regev, A. Full-length transcriptome assembly from *RNA*-Seq data without a reference genome. *Nature Biotechnology*, 29(7):644–652, 2011.

Graça, M. and Zimmer, M. Leaf Toughness. In Graça, M., Bärlocher, F., and Gessner, M., editors, *Methods to Study Litter Decomposition: A Practical Guide*, pages 121–125, Dordrecht, 2005. Springer Netherlands. ISBN 978-1-4020-3466-4.

Grattapaglia, D. and Resende, M. Genomic selection in forest tree breeding. *Tree Genetics & Genomes*, 7(2):241–255, 2011. doi: 10.1007/s11295-010-0328-4.

Gray, L., Russell, J., Yanchuk, A., and Hawkins, B. Predicting the risk of cedar leaf blight (*Didymascella thujina*) in British Columbia under future climate change. *Agricultural and Forest Meteorology*, 180:152–163, oct 2013. doi: 10.1016/j.agrformet.2013.04.023.

Green, R. and Klinka, K. A Field Guide for Site Identification and Interpretation for the Vancouver Forest Region. In *Land Management Handbook*, number 28. Ministry of Forests (Research Branch), 1994.

Gregory, C., McBeath, A., and Filipescu, C. An Economic Assessment of the Western Redcedar Industry in British Columbia. Information Report FI-X-017, Canadian Forest Service - Canadian Wood Fibre Centre, Victoria, British Columbia, 2018.

Grossnickle, S. and Russell, J. Yellow-cedar and western redcedar ecophysiological response to fall, winter and early spring temperature conditions. *Annals of Forest Science*, 63(1):1–8, 2006. doi: 10.1051/forest:2005092.

Grossnickle, S. and Russell, J. Physiological variation among western redcedar (*Thuja plicata* Donn ex D. Don) populations in response to short-term drought. *Annals of Forest Science*, 67(5):506, 2010. doi: 10.1051/forest/2010008.

Gudesblat, G., Torres, P., and Vojnov, A. Stomata and pathogens: warfare at the gates. *Plant Signaling & Behavior*, 4(12):1114–1116, 2009.

Guo, Z., Tan, H., Zhu, Z., Lu, S., and Zhou, B. Effect of intermediates on ascorbic acid and oxalate biosynthesis of rice and in relation to its stress resistance. *Plant Physiology and Biochemistry*, 43(10-11):955 –962, 2005. doi: 10.1016/j.plaphy.2005.08.007.

Gupta, S., Rai, A., Kanwar, S., and Sharma, T. Comparative analysis of zinc finger proteins involved in plant disease resistance. *PLoS ONE*, 7(8):e42578, 2012. doi: 10.1371/journal.pone.0042578.

Haas, B. J., Papanicolaou, A., Yassour, M., Grabherr, M., Blood, P. D., Bowden, J., Couger, M. B., Eccles, D., Li, B., Lieber, M., MacManes, M. D., Ott, M., Orvis, J., Pochet, N., Strozzi, F., Weeks, N., Westerman, R., William, T., Dewey, C. N., Henschel, R., LeDuc, R. D., Friedman, N., and Regev, A. *De novo* transcript sequence reconstruction from *RNA*-seq using the Trinity platform for reference generation and analysis. *Nature Protocols*, 8(8):1494–1512, 2013.

Hagel, J. and Facchini, P. Benzylisoquinoline alkaloid metabolism: a century of discovery and a brave new world. *Plant and Cell Physiology*, 54(5):647–672, 2013. doi: 10.1093/pcp/pct020.

Halls, S., Davin, L., Kramer, D., and Lewis, N. Kinetic study of coniferyl alcohol radical binding to the (+)-pinoresinol forming dirigent protein. *Biochemistry*, 43 (9):2587–2595, 2004. doi: 10.1021/bi035959o.

Hamel, F., Breton, C., and Houde, M. Isolation and characterization of wheat aluminum-regulated genes: possible involvement of aluminum as a pathogenesis response elicitor. *Planta*, 205(4):531–538, jun 1998. doi: 10.1007/s004250050352.

Hamelin, R. Molecular Epidemiology of Tree Pathogens. In Jain, S. and Minocha, S., editors, *Molecular Biology of Woody Plants*, volume 2, pages 375–393, 2000.

Hamilton, M., Williams, D., Tilyard, P., Pinkard, E., Wardlaw, T., Glen, M., Vaillancourt, R., and Potts, B. A latitudinal cline in disease resistance of a host tree. *Heredity*, 110:372–379, 2013.

Hammond-Kosack, K. and Jones, J. Plant disease resistance genes. *Annual Review of Plant Physiology and Plant Molecular Biology*, 48:575–607, 1997. doi: 10.1146/annurev.arplant.48.1.575.

Hanin, M., Brini, F., Ebel, C., Toda, Y., Takeda, S., and Masmoudi, K. Plant dehydrins and stress tolerance. *Plant Signaling & Behavior*, 6(10):1503–1509, 2011. doi: 10.4161/psb.6.10.17088.

Hannukkala, A., Kaukoranta, T., Lehtinen, A., and Rahkonen, A. Late-blight epidemics on potato in Finland, 1933-2002; increased and earlier occurrence of epidemics associated with climate change and lack of rotation. *Plant Pathology*, 56 (1):167–176, 2007. doi: 10.1111/j.1365-3059.2006.01451.x.

Hara, Y., Yokoyama, R., Osakabe, K., Toki, S., and Nishitani, K. Function of xyloglucan endotransglucosylase/hydrolases in rice. *Annals of Botany*, 114(6):1309–1318, 2014. doi: 10.1093/aob/mct292.

Hardwick, N. Weather and plant diseases. *Weather*, 57(5):184–190, 2002. doi: 10.1002/wea.6080570507.

Harper, A., McKinney, L., Nielsen, L., Havlickova, L., Li, Y., Trick, M., Fraser, F., Wang, L., Fellgett, A., Sollars, E., Janacek, S., Downie, J., Buggs, R., Kjær, E., and Bancroft, I. Molecular markers for tolerance of European ash (*Fraxinus excelsior*) to dieback disease identified using associative transcriptomics. *Scientific Reports*, 6:19335, 2016.

Harrell Jr., F. E. and Dupont, C. Hmisc: Harrell Miscellaneous, version 3.17-4, 2016. URL `https://cran.r-project.org/web/packages/Hmisc/`.

Hartmann, T. Diversity and variability of plant secondary metabolism: a mechanistic view. *Entomologia Experimentalis et Applicata*, 80(1):177–188, 1996. doi: 10.1111/j.1570-7458.1996.tb00914.x.

Hatano, N. and Hamada, T. Proteome analysis of pitcher fluid of the carnivorous plant *Nepenthes alata*. *Journal of Proteome Research*, 7(2):809–816, 2008. doi: 10.1021/pr700566d.

Hattemer, H. Geographic Variation of Resistance to *Lophodermium pinastri* in Scots Pine. In Gerhold, H., Schreiner, E., McDermott, R., and Winieski, J., editors, *Breeding Pest-Resistant Trees*, pages 97–102, The Pennsylvania State University, University Park, Pennsylvania, August 30 to September 11, 1964 1966. N.A.T.O. and N.S.F. Advanced Study Institute on Genetic Improvement for Disease and Insect Resistance of Forest Trees, Pergamon Press Ltd.

Hau, F. and Rush, M. Preinfectional interactions between *Helminthosporium oryzae* and resistant and susceptible rice plants. *Phytopathology*, 72(3):285–292, 1982.

Hayashi, Y., Yamada, K., Shimada, T., Matsushima, R., Nishizawa, N., Nishimura, M., and Hara-Nishimura, I. A proteinase-storing body that prepares for cell death or stresses in the epidermal cells of Arabidopsis. *Plant and Cell Physiology*, 42(9):894–899, 2001.

Hayden, K., Garbelotto, M., Knaus, B., Cronn, R., Rai, H., and Wright, J. Dual RNA-seq of the plant pathogen *Phytophthora ramorum* and its tanoak host. *Tree Genetics & Genomes*, 10(3):489–502, 2014. doi: 10.1007/s11295-014-0698-0.

Heath, M. Nonhost resistance and nonspecific plant defenses. *Current Opinion in Plant Biology*, 3(4):315–319, 2000. doi: 10.1016/S1369-5266(00)00087-X.

Hebda, R. and Mathewes, R. Holocene history of cedar and native indian cultures of the North American Pacific coast. *Science*, 225(4663):711–713, 1984.

Heldt, H.-W. *Plant Biochemistry*. Elsevier Academic Press, third edition, 2005.

Heldt, H.-W. and Piechulla, B. *Plant Biochemistry*. Elsevier Academic Press, fourth edition, 2010.

Hemetsberger, C., Herrberger, C., Zechmann, B., Hillmer, M., and Doehlemann, G. The *Ustilago maydis* effector Pep1 suppresses plant immunity by inhibition of host peroxidase activity. *PLoS Pathogens*, 8(5):e1002684, 2012. doi: 10.1371/journal.ppat.1002684.

Henry, E., Fung, N., Liu, J., Drakakaki, G., and Coaker, G. Beyond glycolysis: GAPDHs are multi-functional enzymes involved in regulation of ROS, autophagy, and plant immune responses. *PLOS Genetics*, 11(4):e1005199, 2015. doi: 10.1371/journal.pgen.1005199.

Herrera, C. Seed dispersal by vertebrates. In Herrera, C. and Pellmyr, O., editors, *Plant-Animal Interactions: An Evolutionary Approach*, pages 185–209, Oxford, 2002. Blackwell Science Ltd.

Herrmann, M., Vrsanska, M., Jurickova, M., Hirsch, J., Biely, P., and Kubicek, C. The β-D-xylosidase of *Trichoderma reesei* is a multifunctional β-D-xylan xylohydrolase. *Biochemical Journal*, 321(Pt 2):375–381, 1997.

Hirano, S. and Upper, C. Ecology and epidemiology of foliar bacterial plant pathogens. *Annual Review of Phytopathology*, 21:243–270, 1983. doi: 10.1146/annurev.py.21.090183.001331.

Hizume, M. and Fujiwara, M. Fluorescent chromosome banding patterns of several species in the Cupressaceae *sensu stricto*. *Chromosome Botany*, 11(1):1–8, 2016.

Hodge, G. and Dvorak, W. Differential responses of Central American and Mexican pine species and *Pinus radiata* to infection by the pitch canker fungus. *New Forests*, 19(3):241–258, 2000. doi: 10.1023/A:1006613021996.

Hoff, R. Blister Rust Resistance in Western White Pine. In Gerhold, H., Schreiner, E., McDermott, R., and Winieski, J., editors, *Breeding Pest-Resistant Trees*, pages 119–124, The Pennsylvania State University, University Park, Pennsylvania, August 30 to September 11, 1964 1966. N.A.T.O. and N.S.F. Advanced Study Institute on Genetic Improvement for Disease and Insect Resistance of Forest Trees, Pergamon Press Ltd.

Hogg, E. and Bernier, P. Climate change impacts on drought-prone forests in western Canada. *The Forestry Chronicle*, 81(5):675–682, 2005. doi: 10.5558/tfc81675-5.

Holliday, P. *A Dictionary of Plant Pathology*. Cambridge University Press, 1989. ISBN 052133117X.

Hosmani, P., Kamiya, T., Danku, J., Naseer, S., Geldner, N., Guerinot, M., and Salt, D. Dirigent domain-containing protein is part of the machinery required for formation of the lignin-based Casparian strip in the root. *Proceedings of the National Academy of Sciences of The United States of America*, 110(35):14498–14503, 2013. doi: 10.1073/pnas.1308412110.

Hou, L. and Zhao, H. A review of post-GWAS prioritization approaches. *Frontiers in Genetics*, 4:280, 2013. doi: 10.3389/fgene.2013.00280.

Howard, B., Hu, Q., Babaoglu, A., Chandra, M., Borghi, M., Tan, X., He, L., Winter-Sederoff, H., Gassmann, W., Veronese, P., and Heber, S. High-throughput RNA sequencing of Pseudomonas-infected Arabidopsis reveals hidden transcriptome complexity and novel splice variants. *PLoS ONE*, 8(10):e74183, 2013. doi: 10.1371/journal.pone.0074183.

Huang, J.-s. Ultrastructure of bacterial penetration in plants. *Annual Review of Phytopathology*, 24:141–157, 1986. doi: 10.1146/annurev.py.24.090186.001041.

Huber, D. and Bohlmann, J. The Role of Terpene Synthases in the Direct and Indirect Defense of Conifers Against Insect Herbivory and Fungal Pathogens. In Tuzun, S. and Bent, E., editors, *Multigenic and Induced Systemic Resistance in Plants*, pages 296–313. Springer Verlag GMBH, 2005.

Hudgins, J., Krekling, T., and Franceschi, V. Distribution of calcium oxalate crystals in the secondary phloem of conifers: a constitutive defense mechanism? *New Phytologist*, 159(3):677–690, 2003. doi: 10.1046/j.1469-8137.2003.00839.x.

Huerta-Cepas, J., Szklarczyk, D., Forslund, K., Cook, H., Heller, D., Walter, M. C., Rattei, T., Mende, D. R., Sunagawa, S., Kuhn, M., Jensen, L. J., von Mering, C., and Bork, P. eggNOG 4.5: a hierarchical orthology framework with improved functional annotations for eukaryotic, prokaryotic and viral sequences. *Nucleic Acids Research*, 44(D1):D286–D293, 2016.

Hulvey, J., Jr., J. P., Sang, H., Berg, A., and Jung., G. Overexpression of *Sh*CYP51B and *Shatr*D in *Sclerotinia homoeocarpa* isolates exhibiting practical field resistance to a demethylation inhibitor fungicide. *Applied and Environmental Microbiology*, 78(18):6674–6682, 2012.

Hussey, R. Disease-inducing secretions of plant-parasitic nematodes. *Annual Review of Phytopathology*, 27:123–141, 1989. doi: 10.1146/annurev.py.27.090189.001011.

Hutin, C., Nussaume, L., Moise, N., Moya, I., Kloppstech, K., and Havaux, M. Early light-induced proteins protect *Arabidopsis* from photooxidative stress. *Proceedings of the National Academy of Sciences of The United States of America*, 100(8): 4921–4926, 2003.

Ifuku, K., Ishihara, S., Shimamoto, R., Ido, K., and Sato, F. Structure, function, and evolution of the PsbP protein family in higher plants. *Photosynthesis Research*, 98 (1-3):427–437, 2008. doi: 10.1007/s11120-008-9359-1.

Inamori, Y., Shinohara, S., Tsujibo, H., Okabe, T., Morita, Y., Sakagami, Y., Kumeda, Y., and Ishida, N. Antimicrobial activity and metalloprotease inhibition of hinokitiol-related compounds, the constituents of *Thujopsis dolabrata* S. and *Z. hondai* MAK. *Biological & Pharmaceutical Bulletin*, 22(9):990–993, 1999. doi: 10.1248/bpb.22.990.

Inamori, Y., Sakagami, Y., Morita, Y., Shibata, M., Sugiura, M., Kumeda, Y., Okabe, T., Tsujibo, H., and Ishida, N. Antifungal activity of hinokitiol-related compounds on wood-rotting fungi and their insecticidal activities. *Biological & Pharmaceutical Bulletin*, 23(8):995–997, 2000. doi: 10.1248/bpb.23.995.

IPCC [Intergovernmental Panel on Climate Change]. Climate Change 2013: The Physical Science Basis. Contribution of Working Group I to the Fifth Assessment Report of the Intergovernmental Panel on Climate Change. In Stocker, T., Qin, D., Plattner, G.-K., Tignor, M., Allen, S., Boschung, J., Nauels, A., Xia, Y., Bex, V., and Midgley, P., editors, *Summary for Policymakers*, Cambridge, United Kingdom and New York, NY, USA., 2013. Cambridge University Press.

Iqbal, M., Afzal, A., Yaegashi, S., Ruben, E., Triwitayakorn, K., Njiti, V., Ahsan, R., Wood, A., and Lightfoot, D. A pyramid of loci for partial resistance to *Fusarium solani* f. sp. *glycines* maintains *Myo*-inositol-1-phosphate synthase expression in soybean roots. *Theoretical and Applied Genetics*, 105(8):1115–1123, 2002. doi: 10.1007/s00122-002-0987-0.

Ishikawa, H., Matsuura, Y., Yunokihara, R., Mochizuki, R., Kulkarni, A., Suzuki, Y., and Etoh, H. A diterpene, sandaracopimarinol, produced by Japanese cedar and found from the deep seawater pumped up from the Suruga Bay. *Deep Ocean Water Research*, 6(1):47–50, 2005.

Ivanová, H. Comparison of the fungi *Pestalotiopsis funerea* (Desm.) Steyaert and *Truncatella hartigii* (Tubeuf) Steyaert isolated from some species of the genus *Pinus* L. in morphological characteristics of conidia and appendages. *Journal of Forest Science*, 62(6):279–284, 2016.

Jackson, L. Effect of shade on leaf structure of deciduous tree species. *Ecology*, 48 (3):498–499, 1967. doi: 10.2307/1932686.

Janos, D. Vesicular-arbuscular mycorrhizae affect lowland tropical rain forest plant growth. *Ecology*, 61(1):151–162, 1980. doi: 10.2307/1937165.

Jayaraj, J., Anand, A., and Muthukrishnan, S. Pathogenesis-Related Proteins and Their Roles in Resistance to Fungal Pathogens. In Punja, Z., editor, *Fungal Disease Resistance in Plants: Biochemistry, Molecular Biology, and Genetic Engineering*, pages 139–177. Food Products Press, 2004.

Jayaswall, K., Mahajan, P., Singh, G., Parmar, R., Seth, R., Raina, A., Swarnkar, M., Singh, A., Shankar, R., and Sharma, R. Transcriptome analysis reveals candidate genes involved in blister blight defense in tea (*Camellia sinensis* (L) Kuntze). *Scientific Reports*, 6:30412, 2016.

Jensen, A., Leah, R., Chaudhry, B., and Mundy, J. Ribosome Inactivating Proteins: Structure, Function, and Engineering. In Datta, S. and Muthukrishnan, S., editors, *Pathogenesis-Related Proteins in Plants*, pages 235–245, Boca Raton, FL., 1999. CRC Press.

Ji, Z., Zeng, Y., Liang, Y., Qian, Q., and Yang, C. Transcriptomic dissection of the rice–*Fusarium fujikuroi* interaction by RNA-Seq. *Euphytica*, 211(1):123–137, July 2016. doi: 10.1007/s10681-016-1748-5.

Jiang, H.-X., Yang, L.-T., Qi, Y.-P., Lu, Y.-B., Huang, Z.-R., and L.-S.Chen. Root iTRAQ protein profile analysis of two *Citrus* species differing in aluminum-tolerance in response to long-term aluminum-toxicity. *BMC Genomics*, 16:949, 2015. ISSN 1471-2164.

Jokela, J. Incidence and Heritability of *Melampsora* Rust in *Populus deltoides* Bartr. In Gerhold, H., Schreiner, E., McDermott, R., and Winieski, J., editors, *Breeding Pest-Resistant Trees*, pages 111–117, The Pennsylvania State University, University Park, Pennsylvania, August 30 to September 11, 1964 1966. N.A.T.O. and N.S.F. Advanced Study Institute on Genetic Improvement for Disease and Insect Resistance of Forest Trees, Pergamon Press Ltd.

Jones, D. An introduction to plant disease epidemiology. In Jones, D., editor, *The Epidemiology of Plant Diseases*, pages 3–13, Dordrecht, 1998. Springer Netherlands.

Jones, D., Kochian, L., and Gilroy, S. Aluminum induces a decrease in cytosolic calcium concentration in BY-2 tobacco cell cultures. *Plant Physiology*, 116(1): 81–89, 1998. doi: 10.1104/pp.116.1.81.

Joshi, R., Megha, S., Rahman, M., Basu, U., and Kav, N. A global study of transcriptome dynamics in canola (*Brassica napus* L.) responsive to *Sclerotinia sclerotiorum* infection using RNA-Seq. *Gene*, 590(1):57–67, sep 2016. doi: 10.1016/j.gene.2016.06.003.

Judith-Hertz, C. *Systematics and species delimitation in Pestalotia and Pestalotiopsis s.l. (Amphisphaeriales, Ascomycota)*. PhD thesis, Universitätsbibliothek Johann Christian Senckenberg, Frankfurt am Main, 2016.

Kamitani, M., Nagano, A., Honjo, M., and Kudoh, H. RNA-Seq reveals virus–virus and virus-plant interactions in nature. *FEMS Microbiology Ecology*, 92(11):fiw176, 2016.

Kanehisa, M., Furumichi, M., Tanabe, M., Sato, Y., and Morishima, K. KEGG: new perspectives on genomes, pathways, diseases and drugs. *Nucleic Acids Research*, 45(D1):D353–D361, 2017.

Kang, H., Wang, Y., Peng, S., Zhang, Y., Xiao, Y., Wang, D., Qu, S., Li, Z., Yan, S., Wang, Z., Liu, W., Ning, Y., Korniliev, P., Leung, H., Mezey, J., McCouch, S., and Wang, G.-L. Dissection of the genetic architecture of rice resistance to the blast fungus *Magnaporthe oryzae*. *Molecular Plant Pathology*, 17(6):959–972, feb 2016. doi: 10.1111/mpp.12340.

Karasov, T., Horton, M., and Bergelson, J. Genomic variability as a driver of plant-pathogen coevolution? *Current Opinion in Plant Biology*, 18:24–30, 2014. doi: 10.1016/j.pbi.2013.12.003.

Karp, F. and Croteau, R. Evidence that sabinene is an essential precursor of C(3)-oxygenated thujane monoterpenes. *Archives of Biochemistry and Biophysics*, 216 (2):616–624, 1982.

Karp, F., Harris, J., and Croteau, R. Metabolism of monoterpenes: demonstration of the hydroxylation of (+)-sabinene to (+)-*cis*-sabinol by an enzyme preparation from sage (*Salvia officinalis*) leaves. *Archives of Biochemistry and Biophysics*, 256 (1):179–193, 1987.

Katsaruware-Chapoto, R., Mafongoya, P., and Gubba, A. Responses of insect pests and plant diseases to changing and variable climate: a review. *Journal of Agricultural Science*, 9(12):160–168, 2017.

Kawahara, Y., Oono, Y., Kanamori, H., Matsumoto, T., Itoh, T., and Minami, E. Simultaneous *RNA*-seq analysis of a mixed transcriptome of rice and blast fungus interaction. *PLoS ONE*, 7(11):e49423, 2012. doi: 10.1371/journal.pone.0049423.

Keeling, C. and Bohlmann, J. Genes, enzymes and chemicals of terpenoid diversity in the constitutive and induced defence of conifers against insects and pathogens. *New Phytologist*, 170(4):657–675, 2006. doi: 10.1111/j.1469-8137.2006.01716.x.

Keith, L., Velasquez, M., and Zee, F. Identification and characterization of *Pestalotiopsis* spp. causing scab disease of guava, *Psidium guajava*, in Hawaii. *Plant Disease*, 90(1):16–23, 2006. doi: 10.1094/PD-90-0016.

Kessler, A., Halitschke, R., Diezel, C., and Baldwin, I. Priming of plant defense responses in nature by airborne signaling between *Artemisia tridentata* and *Nicotiana attenuata*. *Oecologia*, 148(2):280–292, 2006. doi: 10.1007/s00442-006-0365-8.

Kidd, P., Llugany, M., Poschenrieder, C., Gunsé, B., and Barceló, J. The role of root exudates in aluminium resistance and silicon-induced amelioration of aluminium toxicity in three varieties of maize (*Zea mays* L.). *Journal of Experimental Botany*, 52(359):1339–1352, 2001. doi: 10.1093/jexbot/52.359.1339.

Killick, R. and Eckley, I. changepoint: an R package for changepoint analysis. *Journal of Statistical Software*, 58(3):1–19, 2014.

Kim, M., Jeon, J.-H., Fujita, M., Davin, L., and Lewis, N. The western red cedar (*Thuja plicata*) 8-8' *DIRIGENT* family displays diverse expression patterns and conserved monolignol coupling specificity. *Plant Molecular Biology*, 49(2):199–214, 2002.

Kimball, S. Eukaryotic initiation factor eIF2. *The International Journal of Biochemistry & Cell Biology*, 31(1):25–29, 1999. doi: 10.1016/S1357-2725(98)00128-9.

Kimmons, C., Gwinn, K., and Bernard, E. Nematode reproduction on endophyte-infected and endophyte-free tall fescue. *Plant Disease*, 74(10):757–761, 1990.

Kirik, V., Mathur, J., Grini, P., Klinkhammer, I., Adler, K., Bechtold, N., Herzog, M., Bonneville, J.-M., and Hülskamp, M. Functional analysis of the tubulin-folding cofactor C in *Arabidopsis thaliana*. *Current Biology*, 12(17):1519–1523, 2002. doi: 10.1016/S0960-9822(02)01109-0.

Kleine, T., Kindgren, P., Benedict, C., Hendrickson, L., and Strand, Å. Genome-wide gene expression analysis reveals a critical role for CRYPTOCHROME1 in the response of Arabidopsis to high irradiance. *Plant Physiology*, 144(3):1391–1406, 2007. doi: 10.1104/pp.107.098293.

Klinka, K. and Brisco, D. Silvics and silviculture of coastal western redcedar: a literature review. Special Report Series 11, BC Ministry of Forests and Range, Forest Science Progress, Victoria, British Columbia, 2009.

Klironomos, J., McCune, J., Hart, M., and Neville, J. The influence of arbuscular mycorrhizae on the relationship between plant diversity and productivity. *Ecology Letters*, 3(2):137–141, 2000. doi: 10.1046/j.1461-0248.2000.00131.x.

Kogovšek, P., Pompe-Novak, M., Petek, M., Fragner, L., Weckwerth, W., and Gruden, K. Primary metabolism, phenylpropanoids and antioxidant pathways are regulated in potato as a response to *potato virus Y* infection. *PLoS ONE*, 11(1):e0146135, 2016. doi: 10.1371/journal.pone.0146135.

Köllner, T. G., Held, M., Lenk, C., Hiltpold, I., Turlings, T. C., Gershenzon, J., and Degenhardt, J. A maize (*E*)-β-caryophyllene synthase implicated in indirect defense responses against herbivores is not expressed in most American maize varieties. *The Plant Cell*, 20(2):482–494, feb 2008. doi: 10.1105/tpc.107.051672.

Kope, H. H. and Trotter, D. The use of degree-days to establish biological events for *Didymascella thujina*, a foliar fungal leaf blight of *Thuja plicata* seedlings. In *Seventh International Congress of Plant Pathology (August 9-16), Edinburgh (Scotland)*, 1998a.

Kope, H. H. and Trotter, D. Evaluation of mancozeb and propiconazole to control Keithia leaf blight of container-grown western red cedar. *The Forestry Chronicle*, 74(4):583–587, 1998b.

Kope, H. A method for quantifyng *Keithia* blight on foliage of Western red cedar. Seed and Seedling. In *Seed and Seedling Extension Topics*, number 5 in I, pages 11–12. British Columbia Ministry of Forest, Victoria, British Columbia, 1992.

Kope, H. Fungi Canadenses No. 343: *Didymascella thujina*. *Canadian Journal of Plant Pathology*, 22(4):407–409, 2000.

Kope, H. *Didymascella thujina*. In *Forestry Compendium*, Wallington (UK), 2004. Centre for Agricultural Bioscience International (CABI).

Kope, H. and Dennis, J. *Keithia* blight on Western Red Cedar nursery seedlings. In *Seed and Seedling Extension Topics*, number 5 in I, page 11. British Columbia Ministry of Forest, Victoria, British Columbia, 1992.

Kope, H. and Sutherland, J. *Keithia* blight of western redcedar: effect of styroblock configuration and seedling density on disease severity. In *Seed and seedling Ex-*

tension Topics, number 7 in I, pages 6–7. British Columbia Ministry of Forest, Victoria, British Columbia, 1994a.

Kope, H. and Sutherland, J. *Keithia* blight: review of the disease, and research on container-grown, western redcedar in Brisith Columbia, Canada. In Perrin, R. and Sutherland, J. R., editors, *Diseases and insects in forest nurseries: Dijon (France), October 3-10, 1993*. Institut National de la Recherche Agronomique (INRA), 1994b.

Kope, H., Sutherland, J., and Trotter, D. Influence of cavity size, seedling growing density and fungicide applications on Keithia blight of western redcedar seedling growth and field performance. *New Forests*, 11(2):137–147, 1996a.

Kope, H., Sutherland, J., and Trotter, D. Influence of cavity size, seedling growing density and fungicide applications on Keithia blight of western redcedar seedling growth and field performance. *New Forests*, 11(2):137–147, 1996b.

Kope, H., Ekramoddoullah, A., and Sutherland, J. Analysis of proteins of disease-free and *Didymascella thujina*-infected leaves of western red-cedar (*Thuja plicata*). *Plant Disease*, 82(2):201–212, 1998.

Kordali, S., Cakir, A., Ozer, H., Cakmakci, R., Kesdek, M., and Mete, E. Antifungal, phytotoxic and insecticidal properties of essential oil isolated from Turkish *Origanum acutidens* and its three components, carvacrol, thymol and *p*-cymene. *Bioresource Technology*, 99(18):8788–8795, 2008. doi: 10.1016/j.biortech.2008.04.048.

Korf, R. A synopsis of the Hemiphacidiaceae, a family of the Helotiales (Discomycetes) causing needle-blights of conifers. *Mycologia*, 54(1):12–33, 1962.

Korte, A. and Farlow, A. The advantages and limitations of trait analysis with GWAS: a review. *Plant Methods*, 9:29, 2013. doi: 10.1186/1746-4811-9-29.

Kosová, K., Prášil, I., and Vítámvás, P. Role of Dehydrins in Plant Stress Response. In Pessarakli, M., editor, *Handbook of Plant and Crop Stress*, pages 239–285, Boca Raton, FL., 2010. CRC Press.

Krizek, B., Bequette, C., Xu, K., Blakley, I., Fu, Z., Stratmann, J., and Loraine, A. RNA-seq links the transcription factors AINTEGUMENTA and AINTEGUMENTA-LIKE6 to cell wall remodeling and plant defense pathways. *Plant Physiology*, 171(3):2069–2084, 2016.

Kumar, P., Moreland, D., and Chilton, W. 2H-1,4-benzoxazin-3(4H)-one, an intermediate in the biosynthesis of cyclic hydroxamic acids in maize. *Phytochemistry*, 36(4):893–898, 1994. doi: 10.1016/S0031-9422(00)90458-8.

Kurtz Jr., E. The relation of the characteristics and yield of wax to plant age. *Plant Physiology*, 25(2):269–278, 1950.

Kus, J., Zaton, K., Sarkar, R., and Cameron, R. Age-related resistance in Arabidopsis is a developmentally regulated defense response to *Pseudomonas syringae*. *The Plant Cell*, 14(2):479–490, 2002. doi: 10.1105/tpc.010481.

Kusumi, J., Tsumura, Y., and Tachida, H. Evolutionary rate variation in two conifer species, *Taxodium distichum* (L.) Rich. var. *distichum* (baldcypress) and *Cryptomeria japonica* (Thunb. ex L.f.) D. Don (Sugi, Japanese cedar). *Genes & Genetic Systems*, 90(5):305–315, 2015. doi: 10.1266/ggs.14-00079.

Kuznetsova, A., Brockhoff, P. B., and Christensen, R. H. B. lmerTest: Tests in Linear Mixed Effects Models, version 2.0-25, 2015. URL `https://cran.r-project.org/web/packages/lmerTest/`.

La Mantia, J., Klápště, J., El-Kassaby, Y., Azam, S., Guy, R., Douglas, C., Mansfield, S., and Hamelin, R. Association analysis identifies *Melampsora* × *columbiana* poplar leaf rust resistance SNPs. *PLoS ONE*, 8(11):e78423, 2013. doi: 10.1371/journal.pone.0078423.

La Mantia, J., Unda, F., Douglas, C., Mansfield, S., and Hamelin, R. Overexpression of At*GolS3* and Cs*RFS* in poplar enhances ROS tolerance and represses defense response to leaf rust disease. *Tree Physiology*, 38(3):457–470, 2018. doi: 10.1093/treephys/tpx100.

Lagesen, K., Hallin, P., Rødland, E. A., Stærfeldt, H.-H., Rognes, T., and Ussery, D. W. *RNA*mmer: consistent and rapid annotation of ribosomal *RNA* genes. *Nucleic Acids Research*, 35(9):3100–3108, 2007.

Laine, A. Resistance variation within and among host populations in a plant-pathogen metapopulation: implications for regional pathogen dynamics. *Journal of Ecology*, 92(6):990–1000, 2004. doi: 10.1111/j.0022-0477.2004.00925.x.

Lampl, N., Alkan, N., Davydov, O., and Fluhr, R. Set-point control of RD21 protease activity by AtSerpin1 controls cell death in Arabidopsis. *The Plant Journal*, 74(3): 498–510, 2013. doi: 10.1111/tpj.12141.

Langheinrich, U. and Tischner, R. Vegetative storage proteins in poplar: induction and characterization of a 32- and a 36-kilodalton polypeptide. *Plant Physiology*, 97(3):1017–1025, 1991.

Lanver, D., Müller, A., Happel, P., Schweizer, G., Haas, F., Franitza, M., Pellegrin, C., Reissmann, S., Altmüller, J., Rensing, S., and Kahmann, R. The biotrophic development of *Ustilago maydis* studied by RNA-seq analysis. *The Plant Cell*, 30 (2):300–323, 2018. doi: 10.1105/tpc.17.00764.

Lapin, D. and Van den Ackerveken, G. Susceptibility to plant disease: more than a failure of host immunity. *TRENDS in Plant Science*, 18(10):546–554, 2013. doi: 10.1016/j.tplants.2013.05.005.

Lauvergeat, V., Lacomme, C., Lacombe, E., Lasserre, E., Roby, D., and Grima-Pettenati, J. Two cinnamoyl-CoA reductase (CCR) genes from *Arabidopsis thaliana* are differentially expressed during development and in response to infection with pathogenic bacteria. *Phytochemistry*, 57(7):1187–1195, 2001. doi: 10.1016/S0031-9422(01)00053-X.

Lawrence, S., Cooke, J., Greenwood, J., Korhnak, T., and Davis, J. Vegetative storage protein expression during terminal bud formation in poplar. *Canadian Journal of Forest Research*, 31(6):1098–1103, 2001. doi: 10.1139/x01-028.

Lê, S., Josse, J., and Husson, F. FactoMineR: an R package for multivariate analysis. *Journal of Statistical Software*, 25(1):1–18, 2008. doi: 10.18637/jss.v025.i01.

Leben, C. How plant-pathogenic bacteria survive. *Plant Disease*, 65(8):633–637, 1981.

Lee, M., Liu, Z., Huang, R., and Tong, W. Application of dynamic topic models to toxicogenomics data. *BMC Bioinformatics*, 17(Suppl 13):368, 2016.

Lee, Y., Kim, B., Chong, Y., Lim, Y., and Ahn, J.-H. Cation dependent *O*-methyltransferases from rice. *Planta*, 227(3):641–647, 2008. doi: 10.1007/s00425-007-0646-4.

Leighton, V., Niemeyer, H., and Jonsson, L. Substrate specificity of a glucosyltransferase and an N-hydroxylase involved in the biosynthesis of cyclic hydroxamic acids in Gramineae. *Phytochemistry*, 36(4):887–892, 1994. doi: 10.1016/S0031-9422(00)90457-6.

Leubner-Metzger, G. and Meins Jr., F. Functions and Regulation of Plant β-1,3-Glucanases (PR-2). In Datta, S. and Muthukrishnan, S., editors, *Pathogenesis-Related Proteins in Plants*, pages 49–76, Boca Raton, FL., 1999. CRC Press.

Levin, D. The role of trichomes in plant defense. *The Quarterly Review of Biology*, 48(1):3–15, 1973. doi: 10.1086/407484.

Lewinsohn, E., Gijzen, M., and Croteau, R. Defense mechanisms of conifers: differences in constitutive and wound-induced monoterpene biosynthesis among species. *Plant Physiology*, 96:44–49, 1991a. doi: 10.1104/pp.96.1.44.

Lewinsohn, E., Gijzen, M., Savage, T., and Croteau, R. Defense mechanisms of conifers: relationship of monoterpene cyclase activity to anatomical specialization and oleoresin monoterpene content. *Plant Physiology*, 96(1):38–43, 1991b. doi: 10.1104/pp.96.1.38.

Li, B. and Dewey, C. N. RSEM: accurate transcript quantification from *RNA*-seq data with or without a reference genome. *BMC Bioinformatics*, 12:323, 2011.

Li, B., Ruotti, V., Stewart, R., Thomson, J., and Dewey, C. *RNA*-seq gene expression estimation with read mapping uncertainty. *Bioinformatics*, 26(4):493–500, 2010.

Li, J., Jia, D., and Chen, X. *HUA1*, a regulator of stamen and carpel identities in Arabidopsis, codes for a nuclear RNA binding protein. *The Plant Cell*, 13(10): 2269–2281, 2001. doi: 10.1105/tpc.010201.

Li, L., Lui, Y., Wang, Y., and Lui, G. Studies on the karyotypes of three species and the cytotaxonomy of Thujoideae (Dupressaceae) [sic]. *Acta Botanica Yunnanica*, 18:439–444, 1996.

Li, M., Pu, Y., Yoo, C., and Ragauskas, A. The occurrence of tricin and its derivatives in plants. *Green Chemistry*, 18(6):1439–1454, 2016. doi: 10.1039/C5GC03062E.

Li, N., Zhao, M., Liu, T., Dong, L., Cheng, Q., Wu, J., Wang, L., Chen, X., Zhang, C., Lu, W., Xu, P., and Zhang, S. A novel soybean dirigent gene *GmDIR22* contributes

to promotion of lignan biosynthesis and enhances resistance to *Phytophthora sojae*. *Frontiers in Plant Science*, 8:1185, 2017. doi: 10.3389/fpls.2017.01185.

Liaw, A. and Wiener, M. Classification and regression by randomForest. *R News*, 2 (3):18–22, 2002.

Liberato, J. R., Barreto, R. W., and Shivas, R. G. Leaf-clearing and staining techniques for the observation of conidiophores in the *Phyllactinioideae* (*Erysiphaceae*). *Australasian Plant Pathology*, 34(401-404), 2005.

Lieberei, R. South American leaf blight of the rubber tree (*Hevea* spp.): new steps in plant domestication using physiological features and molecular markers. *Annals of Botany*, 100(6):1125–1142, 2007.

Liepman, A. and Cavalier, D. The cellulose synthase-like A and cellulose synthase-like C families: recent advances and future perspectives. *Frontiers in Plant Science*, 3: 109, 2012. doi: 10.3389/fpls.2012.00109.

Lim, Y., Chedgy, R., Amirthalingam, S., and Breuil, C. Screening fungi tolerant to western red cedar (*Thuja plicata* Donn) extractives. Part 2. Development of a feeder strip assay. *Holzforschung*, 61(2):195–200, 2007.

Lindgren, P., Peet, R., and Panopoulos, N. Gene cluster of *Pseudomonas syringae* pv. "*phaseolicola*" controls pathogenicity of bean plants and hypersensitivity of nonhost plants. *Journal of Bacteriology*, 168(2):512–522, 1986.

Lindner, M., Maroschek, M., Netherer, S., Kremer, A., Barbati, A., Garcia-Gonzalo, J., Seidl, R., Delzon, S., Corona, P., Kolström, M., Lexer, M., and Marchetti, M. Climate change impacts, adaptive capacity, and vulnerability of European forest ecosystems. *Forest Ecology and Management*, 259(4):698–709, 2010. doi: 10.1016/j.foreco.2009.09.023.

Lines, R. Choice of seed origins for the main forest species in Britain: western redcedar. *Forestry Commission Bulletin*, 66:37–38, 1988.

Liscombe, D. and Facchini, P. Evolutionary and cellular webs in benzylisoquinoline alkaloid biosynthesis. *Current Opinion in Biotechnology*, 19(2):173–180, 2008. doi: 10.1016/j.copbio.2008.02.012.

Litvak, M. and Monson, R. Patterns of induced and constitutive monoterpene production in conifer needles in relation to insect herbivory. *Oecologia*, 114(4):531–540, 1998. doi: 10.1007/s004420050477.

Liu, C.-J., Deavours, B., Richard, S., Ferrer, J.-L., Blount, J., Huhman, D., Dixon, R., and Noel, J. Structural basis for dual functionality of isoflavonoid O-methyltransferases in the evolution of plant defense responses. *Plant Cell*, 18 (12):3656–3669, December 2006.

Liu, J., Yang, H., Lu, Q., Wen, X., Chen, F., Peng, L., Zhang, L., and Lu, C. PSBP-DOMAIN PROTEIN1, a nuclear-encoded thylakoid lumenal protein, is essential for photosystem I assembly in *Arabidopsis*. *The Plant Cell*, 24(12):4992–5006, 2012. doi: 10.1105/tpc.112.106542.

Liu, J.-J., Hammett, C., and Sniezko, R. *Pinus monticola* pathogenesis-related gene *PmPR10-2* alleles as defense candidates for stem quantitative disease resistance against white pine blister rust (*Cronartium ribicola*). *Tree Genetics & Genomes*, 9 (2):397–408, 2013. doi: 10.1007/s11295-012-0561-0.

Liu, L., Tang, L., Dong, W., Yao, S., and Zhou, W. An overview of topic modeling and its current applications in bioinformatics. *SpringerPlus*, 5:1608, 2016a. ISSN 2193-1801. doi: 10.1186/s40064-016-3252-8.

Liu, P., Wang, L., Wong, S.-M., and Yue, G. Fine mapping QTL for resistance to VNN disease using a high-density linkage map in Asian seabass. *Scientific Reports*, 6:32122, 2016b.

Liu, X., Vrieling, K., and Klinkhamer, P. Interactions between plant metabolites affect herbivores: a study with pyrrolizidine alkaloids and chlorogenic acid. *Frontiers in Plant Science*, 8:903, 2017. doi: 10.3389/fpls.2017.00903.

Liu, Y., Ahn, J.-E., Datta, S., Salzman, R., Moon, J., Huyghues-Despointes, B., Pittendrigh, B., Murdock, L., Koiwa, H., and Zhu-Salzman, K. *Arabidopsis* vegetative storage protein is an anti-insect acid phosphatase. *Plant Physiology*, 139(3): 1545–1556, November 2005.

Liu, Y.-B., Lu, S.-M., Zhang, J.-F., Liu, S., and Lu, Y.-T. A xyloglucan endotransglucosylase/hydrolase involves in growth of primary root and alters the

deposition of cellulose in *Arabidopsis*. *Planta*, 226(6):1547–1560, 2007. doi: 10.1007/s00425-007-0591-2.

Liu, Z. and Meyerowitz, E. *LEUNIG* regulates *AGAMOUS* expression in *Arabidopsis* flowers. *Development*, 121:975–991, 1995.

Loder, E. Keithia thujina at Leonardslee. *Quarterly Journal of Forestry*, 13:287, 1919.

Lopez-Maestre, H., Brinza, L., Marchet, C., Kielbassa, J., Bastien, S., Boutigny, M., Monnin, D., Filali, A., Carareto, C., Vieira, C., Picard, F., Kremer, N., Vavre, F., Sagot, M.-F., and Lacroix, V. SNP calling from *RNA*-seq data without a reference genome: identification, quantification, differential analysis and impact on the protein sequence. *Nucleic Acids Research*, 44(19):e148, November 2016. doi: 10.1093/nar/gkw655. 13 pages.

Madar, Z., Solel, Z., and Kimchi, M. Pestalotiopsis canker of cypress in Israel. *Phytoparasitica*, 19(1):79–81, 1991. doi: 10.1007/BF02981014.

Maharachchikumbura, S., Guo, L.-D., Chukeatirote, E., Bahkali, A., and Hyde, K. *Pestalotiopsis*-morphology, phylogeny, biochemistry and diversity. *Fungal Diversity*, 50:167–187, 2011. doi: 10.1007/s13225-011-0125-x.

Maharachchikumbura, S., Hyde, K., Groenewald, J., Xu, J., and Crous, P. *Pestalotiopsis* revisited. *Studies in Mycology*, 79:121–186, 2014. doi: 10.1016/j.simyco.2014.09.005.

Maire, R. Champignons Nord-Africains nouveaux ou peu connus, fasc. 3. *Bulletin de la Société d'Histoire Naturelle de l'Afrique du Nord*, 18(5):117–120, 1927.

Major, I. and Constabel, C. Molecular analysis of poplar defense against herbivory: comparison of wound- and insect elicitor-induced gene expression. *New Phytologist*, 172(4):617–635, December 2006. doi: 10.1111/j.1469-8137.2006.01877.x.

Majumder, A., Johnson, M., and Henry, S. 1L-*myo*-Inositol-1-phosphate synthase. *Biochimica et Biophysica Acta*, 1348(1-2):245–256, 1997. doi: 10.1016/S0005-2760(97)00122-7.

Maleck, K., Levine, A., Eulgem, T., Morgan, A., Schmid, J., Lawton, K., Dangl, J., and Dietrich, R. The transcriptome of *Arabidopsis thaliana* during systemic acquired resistance. *Nature Genetics*, 26:403–410, 2000.

Manners, G. and Swan, E. Isolation and structure of a dilignol rhamnoside from the leaves of *Thuja plicata* trees. *Canadian Journal of Chemistry*, 49(22):3607–3611, 1971. doi: 10.1139/v71-603.

Manners, G. and Swan, E. Biosynthesis of two dilignol rhamnosides in leaves of *Thuja plicata* Donn. *Wood and Fiber*, 8(4):218–222, 1977.

Manzoni, C., Kia, D., Vandrovcova, J., Hardy, J., Wood, N., Lewis, P., and Ferrari, R. Genome, transcriptome and proteome: the rise of omics data and their integration in biomedical sciences. *Briefings in Bioinformatics*, 19(2):286–302, 2018. doi: 10.1093/bib/bbw114.

Markovic, D., Nikolic, N., Glinwood, R., Seisenbaeva, G., and Ninkovic, V. Plant responses to brief touching: a mechanism for early neighbour detection? *PLoS ONE*, 11(11):e0165742, 2016. doi: 10.1371/journal.pone.0165742.

Mason, P. and Singer, M. Defensive mixology: combining acquired chemicals towards defence. *Functional Ecology*, 29(4):441–450, 2015. doi: 10.1111/1365-2435.12380.

Massonnet, M., Morales-Cruz, A., Figueroa-Balderas, R., Lawrence, D., Baumgartner, K., and Cantu, D. Condition-dependent co–regulation of genomic clusters of virulence factors in the grapevine trunk pathogen *Neofusicoccum parvum*. *Molecular Plant Pathology*, 19(1):21–34, 2018. doi: 10.1111/mpp.12491.

Matoh, T. Boron in plant cell walls. *Plant and Soil*, 193(1):59–70, 1997. doi: 10.1023/A:1004207824251.

Matsushita, Y.-i., Hwang, Y.-H., Sugamoto, K., and Matsui, T. Antimicrobial activity of heartwood components of sugi (*Cryptomeria japonica*) against several fungi and bacteria. *Journal of Wood Science*, 52(6):552–556, 2006.

Mauch, F., Mauch-Mani, B., and Boller, T. Antifungal hydrolases in pea tissue: ii. inhibition of fungal growth by combinations of chitinase and β-1,3-glucanase. *Plant Physiology*, 88(3):936–942, 1988.

Mauch-Mani, B. and Mauch, F. The role of abscisic acid in plant–pathogen interactions. *Current Opinion in Plant Biology*, 8(4):409–414, 2005.

McKay, S., Hunter, W., Godard, K.-A., Wang, S., Martin, D., Bohlmann, J., and Plant, A. Insect attack and wounding induce traumatic resin duct development and gene expression of (-)-pinene synthase in Sitka spruce. *Plant Physiology*, 133: 368–378, 2003. doi: 10.1104/pp.103.022723.

McKown, A., Guy, R., Quamme, L., Klapste, J., Mantia, J. L., Constabel, C., El-Kassaby, Y., Hamelin, R., Zifkin, M., and Azam, M. Association genetics, geography and ecophysiology link stomatal patterning in *Populus trichocarpa* with carbon gain and disease resistance trade-offs. *Molecular Ecology*, 23(23):5771–5790, 2014. doi: 10.1111/mec.12969.

McLean, R. and Byth, D. Histological studies of the pre-penetration development and penetration of soybeans by rust, *Phakopsora pachyrhizi* Syd. *Australian Journal of Agricultural Research*, 32(3):435–443, 1981.

McMaster, G. and Wilhelm, W. Growing degree-days: one equation, two interpretations. *Agricultural and Forest Meteorology*, 87(4):291–300, 1997. doi: 10.1016/S0168-1923(97)00027-0.

McNeil, M., Bhuiyan, S., Berkman, P., Croft, B., and Aitken, K. Analysis of the resistance mechanisms in sugarcane during sporisorium scitamineum infection using rna-seq and microscopy. *PLoS ONE*, 13(5):e0197840, 2018. doi: 10.1371/journal.pone.0197840.

McQuilken, M. and Hopkins, K. Biology and integrated control of *Pestalotiopsis* on container-grown ericaceous crops. *Pest Management Science*, 60(2):135–142, 2004. doi: 10.1002/ps.792.

Meinshausen, N. and Bühlmann, P. Stability selection. *Journal of the Royal Statistical Society. Series B*, 72(4):417–473, 2010. ISSN 13697412, 14679868.

Menting, J., Scopes, R., and Stevenson, T. Characterization of flavonoid 3′,5′-hydroxylase in microsomal membrane fraction of *Petunia hybrida* flowers. *Plant Physiology*, 106(2):633–642, 1994. doi: 10.1104/pp.106.2.633.

Mersmann, S., Bourdais, G., Rietz, S., and Robatzek, S. Ethylene signaling regulates accumulation of the FLS2 receptor and is required for the oxidative burst contributing to plant immunity. *Plant Physiology*, 154(1):391–400, 2010. doi: 10.1104/pp.110.154567.

Meyer, F., Shuey, L., Naidoo, S., Mamni, T., Berger, D., Myburg, A., van den Berg, N., and Naidoo, S. Dual *RNA*-sequencing of *Eucalyptus nitens* during *Phytophthora cinnamomi* challenge reveals pathogen and host factors influencing compatibility. *Frontiers in Plant Science*, 7:191, 2016. doi: 10.3389/fpls.2016.00191.

Midoro-Horiuti, T., Brooks, E., and Goldblum, R. Pathogenesis-related proteins of plants as allergens. *Annals of Allergy, Asthma & Immunology*, 87(4):261–271, 2001. doi: 10.1016/S1081-1206(10)62238-7.

Miedes, E. and Lorences, E. The implication of xyloglucan endotransglucosylase/hydrolase (XTHs) in tomato fruit infection by *Penicillium expansum* Link. A. *Journal of Agricultural and Food Chemistry*, 55(22):9021–9026, 2007. doi: 10.1021/jf0718244.

Miles, A. *Keithia* on *Thuya plicata*. *The Gardeners' Chronicles*, 73:353, 1922.

Miller, A. and Tanner, J. *Essentials of Chemical Biology: Structure and Dynamics of Biological Macromolecules*. John Wiley & Sons, Ltd, UK, 2008.

Miller, B., Madilao, L., Ralph, S., and Bohlmann, J. Insect-induced conifer defense. White pine weevil and methyl jasmonate induce traumatic resinosis, *de novo* formed volatile emissions, and accumulation of terpenoid synthase and putative octadecanoid pathway transcripts in Sitka spruce. *Plant Physiology*, 137:369–382, 2005. doi: 10.1104/pp.104.050187.

Minic, Z. Physiological roles of plant glycoside hydrolases. *Planta*, 227:723–740, 2008. doi: 10.1007/s00425-007-0668-y.

Minore, D. Western Redcedar – A Literature Review. General Technical Report PNW-150, U.S. Department of Agriculture, Forest Service, Pacific Northwest Forest and Range Experiment Station, Portland, Oregon, February 1983.

Minore, D. *Thuja plicata* Donn ex D. Don (Western Redcedar). In Burns, R. and Honkala, B., editors, *Silvics of North America*, volume 1, Conifers, pages 590–600. Forest Service - United States Department of Agriculture, Washington, D.C., 1990.

Mishra, S., Triptahi, V., Singh, S., Phukan, U., Gupta, M., Shanker, K., and Shukla, R. Wound induced tanscriptional regulation of benzylisoquinoline pathway and characterization of wound inducible PsWRKY transcription factor from *Papaver somniferum*. *PLoS ONE*, 8(1):e52784, 2013. doi: 10.1371/journal.pone.0052784.

Mitchell-Olds, T., Siemens, D., and Pedersen, D. Physiology and costs of resistance to herbivory and disease in *Brassica*. *Entomologia Experimentalis et Applicata*, 80 (1):231–237, 1996. doi: 10.1111/j.1570-7458.1996.tb00925.x.

Moeder, W., Yoshioka, K., and Klessig, D. Involvement of the small GTPase Rac in the defense responses of tobacco to pathogens. *Molecular Plant-Microbe Interactions*, 18(2):116–124, 2005. doi: 10.1094/MPMI-18-0116.

Mohanraj, R. Plant based antibacterial agents. In Mohanraj, R., editor, *Plant Based Medicines*, pages 1–19. Research Signpost, 2014. ISBN 978-81-308-0547-4.

Molina, I., Li-Beisson, Y., Beisson, F., Ohlrogge, J., and Pollard, M. Identification of an Arabidopsis feruloyl-coenzyme A transferase required for suberin synthesis. *Plant Physiology*, 151(3):1317–1328, 2009. doi: 10.1104/pp.109.144907.

Moosavi, M. The effect of gibberellin and abscisic acid on plant defense responses and on disease severity caused by *Meloidogyne javanica* on tomato plants. *Journal of General Plant Pathology*, 83(3):173–184, May 2017. ISSN 1610-739X. doi: 10.1007/s10327-017-0708-9.

Mordue, J. *Pestalotiopsis funerea*. In Institute, C. M., editor, *CMI Descriptions of Pathogenic Fungi and Bacteria No. 514*, Surrey (UK), 1976.

Morita, Y., Matsumura, E., Okabe, T., Fukui, T., Ohe, T., Ishida, N., and Inamori, Y. Biological activity of β-dolabrin, γ-thujaplicin, and 4-acetyltropolone, hinokitiol-related compounds. *Biological & Pharmaceutical Bulletin*, 27(10):1666–1669, 2004. doi: 10.1248/bpb.27.1666.

Morris, E. and Walker, J. Receptor-like protein kinases: the keys to response. *Current Opinion in Plant Biology*, 6(4):339–342, aug 2003. doi: 10.1016/S1369-5266(03)00055-4.

Morris, P. and Stirling, R. Western red cedar extractives associated with durability in ground contact. *Wood Science and Technology*, 46(5):991–1002, 2012. doi: 10.1007/s00226-011-0459-2.

Mortaji, Z. *Cellulose Biosynthesis Inhibitors Modulate Defense Transcripts and Regulate Genes that are Implicated in Cell Wall Re-Structuring in Arabidopsis*. PhD thesis, University of Ontario Institute of Technology, 2011.

Mosblech, A., König, S., Stenzel, I., Grzeganek, P., Feussner, I., and Heilmann, I. Phosphoinositide and inositolpolyphosphate signalling in defense responses of *Arabidopsis thaliana* challenged by mechanical wounding. *Molecular Plant*, 1(2): 249–261, 2008. doi: 10.1093/mp/ssm028.

Mossor-Pietraszewska, T. Effect of aluminium on plant growth and metabolism. *Acta Biochimica Polonica*, 48(3):673–686, 2001.

Mulema, J. and Denby, K. Spatial and temporal transcriptomic analysis of the *Arabidopsis thaliana–Botrytis cinerea* interaction. *Molecular Biology Reports*, 39(4): 4039–4049, 2012. doi: 10.1007/s11033-011-1185-4.

Musolin, D. Insects in a warmer world: ecological, physiological and life-history responses of true bugs (Heteroptera) to climate change. *Global Change Biology*, 13 (8):1565–1585, 2007. doi: 10.1111/j.1365-2486.2007.01395.x.

Nagawa, S., Xu, T., and Yang, Z. RHO GTPase in plants. *Small GTPases*, 1(2): 78–88, 2010. doi: 10.4161/sgtp.1.2.14544.

Neale, D. and Kremer, A. Forest tree genomics: growing resources and applications. *Nature Reviews: Genetics*, 12:111–122, 2011. doi: 10.1038/nrg2931.

Neuhaus, J.-M. Plant Chitinases (PR-3, PR-4, PR-8, PR-11). In Datta, S. and Muthukrishnan, S., editors, *Pathogenesis-Related Proteins in Plants*, pages 77–105, Boca Raton, FL., 1999. CRC Press.

Nussbaum, F. Variation in the airborne fungal spore population of the Tuscarawas valley with respect to microenvironment, time of day, and date. *Ohio Journal of Science*, 90(3):77–86, 1990.

Nzuki, I., Katari, M., Bredeson, J., Masumba, E., Kapinga, F., Salum, K., Mkamilo, G., Shah, T., Lyons, J. B., Rokhsar, D., Rounsley, S., Myburg, A., and Ferguson, M. QTL mapping for pest and disease resistance in cassava and coincidence of some QTL with introgression regions derived from *Manihot glaziovii*. *Frontiers in Plant Science*, 8:1168, 2017. doi: 10.3389/fpls.2017.01168.

Oates, C., Külheim, C., Myburg, A., Slippers, B., and Naidoo, S. The transcriptome and terpene profile of *Eucalyptus grandis* reveals mechanisms of defense against the insect pest, *Leptocybe invasa*. *Plant & Cell Physiology*, 56(7):1418–1428, 2015. doi: 10.1093/pcp/pcv064.

Occhipinti, A. Plant coevolution: evidences and new challenges. *Journal of Plant Interactions*, 8(3):188–196, 2013. doi: 10.1080/17429145.2013.816881.

O'Connell, L. and Ritland, C. Characterization of microsatellite loci in western redcedar (*Thuja plicata*). *Molecular Ecology*, 9(11):1920–1922, 2000.

O'Connell, L., Russell, J., and Ritland, K. Fine-scale estimation of outcrossing in western redcedar with microsatellite assay of bulked DNA. *Heredity*, 93:443–449, 2004.

O'Connell, L., Ritland, K., and Thompson, S. Patterns of post-glacial colonization by western redcedar (*Thuja plicata, Cupressaceae*) as revealed by microsatellite markers. *Botany*, 86(2):194–203, 2008.

Ojeda, D., Dhillon, B., Tsui, C., and Hamelin, R. Single-nucleotide polymorphism discovery in *Leptographium longiclavatum*, a mountain pine beetle-associated symbiotic fungus, using whole-genome resequencing. *Molecular Ecology Resources*, 14 (2):401–410, 2014. doi: 10.1111/1755-0998.12191.

Ojeda Alayon, D., Tsui, C., Feau, N., Capron, A., Dhillon, B., Zhang, Y., Massoumi, A., Boone, C., Carroll, A., Cooke, J., Roe, A., Sperling, F., and Hamelin, R. Genetic and genomic evidence of niche partitioning and adaptive radiation in mountain pine beetle fungal symbionts. *Molecular Ecology*, 26(7):2077–2091, 2017. doi: 10.1111/mec.14074.

Olsen, S., Popper, Z., and Krause, K. Two sides of the same coin: xyloglucan endotransglucosylases/hydrolases in host infection by the parasitic plant *Cuscuta*. *Plant Signaling & Behavior*, 11(3):e1145336, 2016. doi: 10.1080/15592324.2016.1145336.

Orshinsky, A., Hu, J., Opiyo, S., Reddyvari-Channarayappa, V., Mitchell, T., and Boehm, M. RNA-seq analysis of the *Sclerotinia homoeocarpa* – creeping bentgrass pathosystem. *PLoS ONE*, 7(8):e41150, 2012.

Ott, T., van Dongen, J., Günther, C., Krusell, L., Desbrosses, G., Vigeolas, H., Bock, V., Czechowski, T., Geigenberger, P., and Udvardi, M. Symbiotic leghemoglobins are crucial for nitrogen fixation in legume root nodules but not for general plant growth and development. *Current Biology*, 15(6):531–535, 2005. doi: 10.1016/j.cub.2005.01.042.

Ounaroon, A., Decker, G., Schmidt, J., Lottspeich, F., and Kutchan, T. (*R,S*)-Reticuline 7-O-methyltransferase and (*R,S*)-norcoclaurine 6-O-methyltransferase of *Papaver somniferum* – cDNA cloning and characterization of methyl transfer enzymes of alkaloid biosynthesis in opium poppy. *The Plant Journal*, 36(6):808–819, 2003.

Owens, J. and Molder, M. Sexual reproduction in western red cedar (*Thuja Plicata*). *Canadian Journal of Botany*, 58(12):1376–1393, 1980.

Panda, S., Baluska, F., and Matsumoto, H. Aluminum stress signaling in plants. *Plant Signaling & Behavior*, 4(7):592–597, July 2009. doi: 10.4161/psb.4.7.8903.

Pandey, S. and Somssich, I. The role of WRKY transcription factors in plant immunity. *Plant Physiology*, 150(4):1648–1655, may 2009. doi: 10.1104/pp.109.138990.

Panikashvili, D., Shi, J., Schreiber, L., and Aharoni, A. The Arabidopsis *DCR* encoding a soluble BAHD acyltransferase is required for cutin polyester formation and seed hydration properties. *Plant Physiology*, 151(4):1773–1789, 2009. doi: 10.1104/pp.109.143388.

Panter, S. and Jones, D. Age-related resistance to plant pathogens. *Advances in Botanical Research*, 38:251–280, 2002. doi: 10.1016/S0065-2296(02)38032-7.

Parker, D., Beckmann, M., Zubair, H., Enot, D., Caracuel, R., Overy, D., Snowdon, S., Talbot, N., and Draper, J. Metabolomic analysis reveals a common pattern of metabolic re-programming during invasion of three host plant species by *Magnaporthe grisea*. *The Plant Journal*, 59(5):723–737, 2009. doi: 10.1111/j.1365-313X.2009.03912.x.

Parrott, D., Huang, L., and Fischer, A. Downregulation of a barley (*Hordeum vulgare*) leucine-rich repeat, non-arginine-aspartate receptor-like protein kinase reduces expression of numerous genes involved in plant pathogen defense. *Plant Physiology and Biochemistry*, 100:130–140, 2016. doi: 10.1016/j.plaphy.2016.01.005.

Pautasso, M., Döring, T., Garbelotto, M., Pellis, L., and Jeger, M. Impacts of climate change on plant diseases-opinions and trends. *European Journal of Plant Pathology*, 133(1):295–313, 2012. doi: 10.1007/s10658-012-9936-1.

Pawsey, R. The overwintering of *Keithia thujina*, the causal agent for cedar leaf blight. *Transactions of the British Mycological Society*, 40:166–167, jun 1957a.

Pawsey, R. Research on *Keithia thujina*. In *Report on Forest Research*, pages 100–102, London, 1957b.

Pawsey, R. Studies on *Keithia thujina*. In *Report on Forest Research*, page 91, London, 1957c.

Pawsey, R. Research on *Keithia* disease, *Didymascella thujina*. *Report on Forest Research. Forestry Commission, London*, pages 109–111, 1959.

Pawsey, R. An investigation into *Keithia* disease of *Thuja plicata*. *Forestry*, 33(2): 174–186, 1960.

Pawsey, R. Control of *Keithia thujina* Durand by cycloheximide and derivatives. *Nature*, 194(4823):109, 1962a.

Pawsey, R. Rotation sowing of *Thuja* in selected nurseries to avoid infection by *Keithia thujina*. *Quarterly Journal of Forestry*, 52:206–210, 1962b.

Pawsey, R. An investigation of the spore population of the air at Nottingham: II. The results obtained with a Hirst spore trap June-July 1956. *Transactions of the British Mycological Society*, 47(3):357–363, 1964. doi: 10.1016/S0007-1536(64)80008-5.

Pawsey, R. Cycloheximide fungicide trials against *Didymascella thujina* on western red cedar, *Thuja plicata*. *Report on Forest Research. Forestry Commission, London*, pages 141–150, 1965.

Peace, T. Observations on *Keithia thujina* and on the possibility of avoiding attack by growing *Thuja* in isolated nurseries. Report on forest research, Forestry Commission, London, 1955.

Peace, T. The raising of *Thuja* in isolated nurseries to avoid infection by *Keithia thujina*. *Scottish Forestry*, 12:7–10, 1958.

Pelgas, B., Bousquet, J., Meirmans, P., Ritland, K., and Isabel, N. QTL mapping in white spruce: gene maps and genomic regions underlying adaptive traits across pedigrees, years and environments. *BMC Genomics*, 12:145, 2011. doi: 10.1186/1471-2164-12-145.

Pellmyr, O. Pollination by animals. In Herrera, C. and Pellmyr, O., editors, *Plant-Animal Interactions: An Evolutionary Approach*, pages 157–183, Oxford, 2002. Blackwell Science Ltd.

Petersen, O. *Trær og Buske: Diagnoser til dansk frilands-trævækst.* Gyldendal, Kjøbenhavn, 1916.

Petersen, T. N., Brunak, S., von Heijne, G., and Nielsen, H. SignalP 4.0: discriminating signal peptides from transmembrane regions. *Nature Methods*, 8(10):785–786, 2011.

Petre, B., Morin, E., Tisserant, E., Hacquard, S., Silva, C. D., Poulain, J., Poulain, C., Martin, F., Rouhier, N., Kohler, A., and Duplessis, S. *RNA*-seq of early-infected poplar leaves by the rust pathogen *Melampsora larici-populina* uncovers*PtSultr*3;5, a fungal-induced host sulfate transporter. *PLoS ONE*, 7(8):e44408, 2012.

Pettengill, E., Pettengill, J., and Coleman, G. Elucidating the evolutionary history and expression patterns of nucleoside phosphorylase paralogs (vegetative storage proteins) in *Populus* and the plant kingdom. *BMC Plant Biology*, 13:118, 2013. doi: 10.1186/1471-2229-13-118. 17 Pages.

Phillips, D. Needle blight (Didymascella thujina [Dur.] Maire, syn. Keithia thujina Dur.) of Western Red Cedar (Thuja plicata). Technical report, Forestry Commission, London, 1965.

Phillips, D. Needle blight (Didymascella thujina [Dur.] Maire, Keithia thujina Dur.) of Thuja. Technical report, Forestry Commission, London, 1966.

Phillips, D. Needle blight of Western Red Cedar caused by Didymascella thujina (Keithia thujina). Technical report, Forestry Commission, London, 1967.

Phillips, M. and Croteau, R. Resin-based defenses in conifers. *Trends in Plant Science*, 4(5):184–190, 1999. doi: 10.1016/S1360-1385(99)01401-6.

Photita, W., Lumyong, S., Lumyong, P., McKenzie, E., and Hyde, K. Are some endophytes of *Musa acuminata* latent pathogens? *Fungal Diversity*, 16:131–140, 2004.

Phukan, U., Jeena, G., and Shukla, R. WRKY transcription factors: molecular regulation and stress responses in plants. *Frontiers in Plant Science*, 7:760, 2016. doi: 10.3389/fpls.2016.00760.

Placzek, S., Schomburg, I., Chang, A., Jeske, L., Ulbrich, M., Tillack, J., and Schomburg, D. BRENDA in 2017: new perspectives and new tools in BRENDA. *Nucleic Acids Research*, 45(D1):D380–D388, 2017. doi: 10.1093/nar/gkw952.

Plenchette, C., Fortin, J., and Furlan, V. Growth responses of several plant species to mycorrhizae in a soil of moderate P-fertility. *Plant and Soil*, 70(2):199–209, 1983. doi: 10.1007/BF02374780.

Plomion, C., Lalanne, C., Claverol, S., Meddour, H., Kohler, A., Bogeat-Triboulot, M.-B., Barre, A., Le Provost, G., Dumazet, H., Jacob, D., Bastien, C., Dreyer, E., de Daruvar, A., Guehl, J.-M., Schmitter, J.-M., Martin, F., and Bonneu, M. Mapping the proteome of poplar and application to the discovery of drought-stress responsive proteins. *Proteomics*, 6(24):6509–6527, 2006. doi: 10.1002/pmic.200600362.

Poot-Poot, W. and Hernandez-Sotomayor, S. Aluminum stress and its role in the phospholipid signaling pathway in plants and possible biotechnological applications. *IUBMB Life*, 63(10):864–872, sep 2011. doi: 10.1002/iub.550.

Porter, W. Biological studies on western red cedar blight caused by *Keithia thujina* Durand. Interim report, Canada Department of Agriculture, Forest Biology Division, Victoria, BC, 1957.

Prunier, J., Verta, J., and J.J., M. Conifer genomics and adaptation: at the crossroads of genetic diversity and genome function. *New Phytologist*, 209(1):44–62, 2016. doi: 10.1111/nph.13565.

Qu, X.-J., Jin, J.-J., Chaw, S.-M., Li, D.-Z., and Yi, T.-S. Multiple measures could alleviate long-branch attraction in phylogenomic reconstruction of Cupressoideae (Cupressaceae). *Scientific Reports*, 7:41005, 2017. doi: 10.1038/srep41005.

Quesada, T., Gopal, V., Cumbie, W., Eckert, A., Wegrzyn, J., Neale, D., Goldfarb, B., Huber, D., Casella, G., and Davis, J. Association mapping of quantitative disease resistance in a natural population of loblolly pine (*Pinus taeda* L.). *Genetics*, 186 (2):677–686, 2010. doi: 10.1534/genetics.110.117549.

Quinn, J., Burrell, G., and Parkyn, S. Influences of leaf toughness and nitrogen content on in-stream processing and nutrient uptake by litter in a Waikato, New Zealand, pasture stream and streamside channels. *New Zealand Journal of Marine and Freshwater Research*, 34(2):253–271, 2000. doi: 10.1080/00288330.2000.9516931.

R Core Team. *R: A Language and Environment for Statistical Computing*. R Foundation for Statistical Computing, Vienna, Austria, 2015.

Rahman, W., Hameed, N., and Mohd, I. Biflavonyl pigments from *Thuja plicata* (Cupressaceae). *Journal of The Indian Chemical Society*, 49(9):917, 1972.

Rajakani, R., Narnoliya, L., Singh Sangwan, N., Singh Sangwan, R., and Gupta, V. Activated charcoal-mediated *RNA* extraction method for *Azadirachta indica* and plants highly rich in polyphenolics, polysaccharides and other complex secondary compounds. *BMC Research Notes*, 6:125, 2013. doi: 10.1186/1756-0500-6-125.

Rajkumar, A., Qvist, P., Lazarus, R., Lescai, F., Ju, J., Nyegaard, M., Mors, O., Børglum, A., Li, Q., and Christensen, J. Experimental validation of methods for differential gene expression analysis and sample pooling in RNA-seq. *BMC Genomics*, 16:548, jul 2015. doi: 10.1186/s12864-015-1767-y. 8 pages.

Ralph, S., Park, J.-Y., Bohlmann, J., and Mansfield, S. Dirigent proteins in conifer defense: gene discovery, phylogeny, and differential wound- and insect-induced expression of a family of DIR and DIR-like genes in spruce (*Picea* spp.). *Plant Molecular Biology*, 60:21–40, 2006a. doi: 10.1007/s11103-005-2226-y.

Ralph, S., Yueh, H., Friedmann, M., Aeschliman, D., Zeznik, J., Nelson, C., Butterfield, Y., Kirkpatrick, R., Liu, J., Jones, S., Marra, M., Douglas, C., Ritland, K., and Bohlmann, J. Conifer defence against insects: microarray gene expression profiling of Sitka spruce (*Picea sitchensis*) induced by mechanical wounding or feeding by spruce budworms (*Choristoneura occidentalis*) or white pine weevils (*Pissodes strobi*) reveals large-scale changes of the host transcriptome. *Plant, Cell & Environment*, 29(8):1545–1570, 2006b. doi: 10.1111/j.1365-3040.2006.01532.x.

Ramos, L., Narayanan, K., and Jr., R. M. Association of stomatal frequency and morphology in *Lycopersicon* species with resistance to *Xanthomonas campestris* pv. *vesicatoria*. *Plant Pathology*, 41(2):157–164, 1992.

Rengel, Z. Role of calcium in aluminium toxicity. *New Phytologist*, 121(4):499–513, 1992. doi: 10.1111/j.1469-8137.1992.tb01120.x.

Rhouma, A., Chettaoui, M., Krid, S., Elbsir, H., Msallem, M., and Triki., M. Evaluation of susceptibility of an olive progeny (Picholine x Meski) to olive leaf spot disease caused by *Fusicladium oleagineum*. *European Journal of Plant Pathology In press*, 135(1):23–33, Jan 2013. ISSN 1573-8469.

Richards, L., Glassmire, A., Ochsenrider, K., Smilanich, A., Dodson, C., Jeffrey, C., and Dyer, L. Phytochemical diversity and synergistic effects on herbivores. *Phytochemistry Reviews*, 15(6):1153–1166, 2016. doi: 10.1007/s11101-016-9479-8.

Ro, D.-K. and Bohlmann, J. Diterpene resin acid biosynthesis in loblolly pine (*Pinus taeda*): Functional characterization of abietadiene/levopimaradiene synthase (*PtTPS-LAS*) cDNA and subcellular targeting of PtTPS-LAS and abietadienol/abietadienal oxidase (PtAO, CYP720B1). *Phytochemistry*, 67(15):1572–1578, 2006. doi: 10.1016/j.phytochem.2006.01.011.

Ro, D.-K., Arimura, G.-I., Lau, S., Piers, E., and Bohlmann, J. Loblolly pine abietadienol/abietadienal oxidase *PtAO* (CYP720B1) is a multifunctional, multisubstrate cytochrome P450 monooxygenase. *Proceedings of the National Academy of Sciences of The United States of America*, 102(22):8060–8065, 2005.

Roach, C., Hall, D., Zerbe, P., and Bohlmann, J. Plasticity and evolution of (+)-3-carene synthase and (-)-sabinene synthase functions of a Sitka spruce monoterpene synthase gene family associated with weevil resistance. *Journal of Biological Chemistry*, 289(34):23859–23869, 2014. doi: 10.1074/jbc.M114.571703.

Robert, J., Madilao, L., White, R., Yanchuk, A., King, J., and Bohlmann, J. Terpenoid metabolite profiling in Sitka spruce identifies association of dehydroabietic acid, (+)-3-carene, and terpinolene with resistance against white pine weevil. *Botany*, 88(9):810–820, 2010. doi: 10.1139/B10-049.

Robinson, M. D. and Oshlack, A. A scaling normalization method for differential expression analysis of *RNA*-seq data. *Genome Biology*, 11:R25, 2010.

Robinson, M. D., McCarthy, D. J., and Smyth, G. K. edgeR: a bioconductor package for differential expression analysis of digital gene expression data. *Bioinformatics*, 26(1):139–140, 2010.

Rodrigues, C., de Souza, A., Takita, M., Kishi, L., and Machado, M. RNA-seq analysis of *Citrus reticulata* in the early stages of *Xylella fastidiosa* infection reveals auxin-related genes as a defense response. *BMC Genomics*, 14:676, 2013. doi: 10.1186/1471-2164-14-676. 13 Pages.

Ronsheim, M. and Anderson, S. Population-level specificity in the plant-mycorrhizae association alters intraspecific interactions among neighboring plants. *Oecologia*, 128(1):77–84, 2001. doi: 10.1007/s004420000625.

Roose, J., Frankel, L., and Bricker, T. Developmental defects in mutants of the PsbP domain protein 5 in *Arabidopsis thaliana*. *PLoS ONE*, 6(12):e28624, 2011. doi: 10.1371/journal.pone.0028624.

Rorat, T. Plant dehydrins - tissue location, structure and function. *Cellular & Molecular Biology Letters*, 11:536–556, 2006. doi: 10.2478/s11658-006-0044-0.

Rose, R., Rose, C., Omi, S., Forry, K., Durall, D., and Bigg, W. Starch determination by perchloric acid vs enzymes: evaluating the accuracy and precision of six colorimetric methods. *Journal of Agricultural and Food Chemistry*, 39(1):2–11, 1991.

Rosenzweig, C., Iglesias, A., Yang, X., Epstein, P., and Chivian, E. Climate change and extreme weather events: implications for food production, plant diseases, and pests. *Global Change & Human Health*, 2(2):90–104, 2001.

Rostoks, N., Mudie, S., Cardle, L., Russell, J., Ramsay, L., Booth, A., Svensson, J., Wanamaker, S., Walia, H., Rodriguez, E., Hedley, P., Liu, H., Morris, J., Close, T., Marshall, D., and Waugh, R. Genome-wide SNP discovery and linkage analysis in barley based on genes responsive to abiotic stress. *Molecular Genetics and Genomics*, 274(5):515–527, 2005. doi: 10.1007/s00438-005-0046-z.

Roundhill, S., Fineran, B., and Cole, A. Structural aspects of *Ascochyta* blight of lentil. *Canadian Journal of Botany*, 73(3):485–497, 1995.

Rouxel, T. and Balesdent, M.-H. Avirulence Genes. In *Encyclopedia of Life Sciences (ELS)*, ELS subject area: Plant Science, Chichester, January 2010. John Wiley & Sons, Ltd. doi: 10.1002/9780470015902.a0021267.

Ruel, K., Berrio-Sierra, J., Derikvand, M., Pollet, B., Thévenin, J., Lapierre, C., Jouanin, L., and Joseleau, J.-P. Impact of CCR1 silencing on the assembly of lignified secondary walls in *Arabidopsis thaliana*. *New Phytologist*, 184(1):99–113, 2009.

Russell, J. H., Kope, H. H., Ades, P., and Collinson, H. Variation in cedar leaf blight (*Didymascella thujina*) resistance of western redcedar (*Thuja plicata*). *Canadian Journal of Forest Research*, 37(10):1978–1986, 2007. doi: 10.1139/X07-034.

Russell, J. and Ferguson, D. Preliminary results from five generations of a western redcedar (*Thuja plicata*) selection study with self-mating. *Tree Genetics & Genomes*, 4(3):509–518, 2008.

Russell, J. and Yanchuk, A. Breeding for Growth Improvement and Resistance to Multiple Pests in *Thuja plicata*. In Sniezko, R., Yanchuk, A., Kliejunas, J., Palmieri, K., Alexander, J., and Frankel, S., editors, *Proceedings of the fourth international workshop on the genetics of host-parasite interactions in forestry: Disease and insect resistance in forest trees*, pages 40–44, Albany (CA): Pacific Southwest Research Station, 2012. Forest Service, U.S. Department of Agriculture.

Russell, J., Burdon, R., and Yanchuk, A. Inbreeding depression and variance structures for height and adaptation in self- and outcross *Thuja plicata* families in varying environments. *Forest Genetics*, 10(3):171–184, 2003. ISSN 1335-048X.

Ruuhola, T., Leppänen, T., Julkunen-Tiitto, R., Rantala, M., and Lehto, T. Boron fertilization enhances the induced defense of silver birch. *Journal of Chemical Ecology*, 37(5):460–471, apr 2011. doi: 10.1007/s10886-011-9948-x.

Ruzin, S. E. *Plant Microtechnique and Microscopy*. Oxford University Press, Oxford, 1999.

Sakagami, Y., Inamori, Y., Isoyama, N., Tsujibo, H., Okabe, T., Morita, Y., and Ishida, N. Phytogrowth-inhibitory activities of β-dolabrin and γ-thujaplicin, hinokitiol-related compounds and constituents of *Thujopsis dolabrata* Sieb. et Zucc.

var *hondai* MAKINO. *Biological & Pharmaceutical Bulletin*, 23(5):645–648, 2000. doi: 10.1248/bpb.23.645.

Sakalidis, M., Feau, N., Dhillon, B., and Hamelin, R. Genetic patterns reveal historical and contemporary dispersal of a tree pathogen. *Biological Invasions*, 18(6):1781–1799, 2016. doi: 10.1007/s10530-016-1120-7.

Saladié, M., Rose, J., Cosgrove, D., and Catalá, C. Characterization of a new xyloglucan endotransglucosylase/hydrolase (XTH) from ripening tomato fruit and implications for the diverse modes of enzymic action. *The Plant Journal*, 47:282–295, 2006. doi: 10.1111/j.1365-313X.2006.02784.x.

Salinari, F., Giosuè, S., Tubiello, F., Rettori, A., Rossi, V., Spanna, F., Rosenzweig, C., and Gullino, M. Downy mildew (*Plasmopara viticola*) epidemics on grapevine under climate change. *Global Change Biology*, 12(7):1299–1307, 2006. doi: 10.1111/j.1365-2486.2006.01175.x.

Sangwan, N., Farooqi, A., Shabih, F., and Sangwan, R. Regulation of essential oil production in plants. *Plant Growth Regulation*, 34(1):3–21, 2001.

Šarac, Z., Matejić, J., Stojanović-Radić, Z., Veselinović, J., Džamić, A., Bojović, S., and Marin, P. Biological activity of *Pinus nigra* terpenes—evaluation of FtsZ inhibition by selected compounds as contribution to their antimicrobial activity. *Computers in Biology and Medicine*, 54:72–78, 2014.

Sarup, P., Bala, S., and Kamboj, S. Pharmacology and phytochemistry of oleogum resin of *Commiphora wightii* (Guggulu). *Scientifica*, 2015:138039, 2015. doi: 10.1155/2015/138039.

Sauter, J. and van Cleve, B. Biochemical, immunochemical, and ultrastructural studies of protein storage in poplar (*Populus* × *canadensis* 'robusta') wood. *Planta*, 183(1):92–100, 1991.

Scheel, D. and Nuernberger, T. Signal Transduction in Plant Defense Responses to Fungal Infection. In Punja, Z., editor, *Fungal Disease Resistance in Plants: Biochemistry, Molecular Biology, and Genetic Engineering*, pages 1–30. Food Products Press, 2004.

Scheer, M., Grote, A., Chang, A., Schomburg, I., Munaretto, C., Rother, M., Söhngen, C., Stelzer, M., Thiele, J., and Schomburg, D. BRENDA, the enzyme information system in 2011. *Nucleic Acids Research*, 39(suppl 1):D670–D676, 2011. doi: 10.1093/nar/gkq1089.

Schenk, P., Kazan, K., Wilson, I., Anderson, J., Richmond, T., Somerville, S., and Manners, J. Coordinated plant defense responses in *Arabidopsis* revealed by microarray analysis. *Proceedings of the National Academy of Sciences of The United States of America*, 97(21):11655–11660, 2000.

Schmieder, R. and Edwards, R. Quality control and preprocessing of metagenomic datasets. *Bioinformatics*, 27(6):863–864, 2011.

Schneck, C. *Ausländische Wald-und Parkbäume*, volume Zweite. Paul Parey, Berlin, 1939.

Schneider, C. A., Rasband, W. S., and Eliceiri, K. W. NIH Image to ImageJ: 25 years of image analysis. *Nature Methods*, 9(7):671–675, 07 2012.

Schoch, C., Seifert, K., Huhndorf, S., Robert, V., Spouge, J., Levesque, W., C.A.and Chen, and Fungal Barcoding Consortium. Nuclear ribosomal internal transcribed spacer (ITS) region as a universal DNA barcode marker for *Fungi*. *Proceedings of the National Academy of Sciences of The United States of America*, 109(16):6241–6246, 2012. doi: 10.1073/pnas.1117018109.

Scholthof, K.-B. The disease triangle: pathogens, the environment and society. *Nature Reviews Microbiology*, 5:152–156, 12 2007.

Schomburg, D. and Stephan, D. trans-Cinnamate 4-monooxygenase. In Schomburg, D. and Stephan, D., editors, *Enzyme Handbook*, volume 8, pages 441–444, Berlin, Heidelberg, 1994. Springer-Verlag Berlin Heidelberg. ISBN 978-3-642-57942-4.

Schwartz, H., Otto, K., and Gent, D. Relation of temperature and rainfall to development of *Xanthomonas* and *Pantoea* leaf blights of onion in Colorado. *Plant Disease*, 87(1):11–14, 2003. doi: 10.1094/PDIS.2003.87.1.11.

SEQC/MAQC-III Consortium. A comprehensive assessment of *RNA*-seq accuracy, reproducibility and information content by the Sequencing Quality Control Consortium. *Nature Biotechnology*, 32(9):903–914, aug 2014. doi: 10.1038/nbt.2957.

Serrano, M., Coluccia, F., Torres, M., L'Haridon, F., and Métraux, J.-P. The cuticle and plant defense to pathogens. *Frontiers in Plant Science*, 5:274, 2014. doi: 10.3389/fpls.2014.00274.

Shalev, T., Yuen, M., Gesell, A., Yuen, A., Russell, J. H., and Bohlmann, J. An annotated transcriptome of highly inbred *Thuja plicata* (Cupressaceae) and its utility for gene discovery of terpenoid biosynthesis and conifer defense. *Tree Genetics & Genomes*, 14(3):35, 2018. doi: 10.1007/s11295-018-1248-y.

Shang, H.-Y., Li, Z.-H., Dong, M., Adams, R., Miehe, G., Opgenoorth, L., and Mao, K.-S. Evolutionary origin and demographic history of an ancient conifer (*Juniperus microsperma*) in the Qinghai-Tibetan Plateau. *Scientific Reports*, 5:10216, 2015.

Sharma, N., Sharma, K., Gaur, R., and Gupta, V. Role of chitinase in plant defense. *Asian Journal of Biochemistry*, 6(1):29–37, 2011.

Sharma, P. *Plant Pathology*. Alpha Science International, Oxford, 2006.

Sharma, S. and Dietz, K.-J. The significance of amino acids and amino acid-derived molecules in plant responses and adaptation to heavy metal stress. *Journal of Experimental Botany*, 57(4):711–726, 2006. doi: 10.1093/jxb/erj073.

Sharmin, S., Azam, M., Islam, M., Sajib, A., Mahmood, N., Hasan, A., Ahmed, R., Sultana, K., and Khan, H. Xyloglucan endotransglycosylase/hydrolase genes from a susceptible and resistant jute species show opposite expression pattern following *Macrophomina phaseolina* infection. *Communicative & Integrative Biology*, 5(6): 598–606, 2012. doi: 10.4161/cib.21422.

Sherwood, R. Pathological anatomy of *Dactylis glomerata* infected by *Stagonospora arenaria*. *Phytopathology*, 72(1):146–150, 1981.

Sherwood, R. Anatomical and physiological mechanisms of resistance to brown leaf spot in smooth bromegrass. *Crop Science*, 36(2):239–242, 1996.

Shibata, Y., Kawakita, K., and Takemoto, D. Age-related resistance of *Nicotiana benthamiana* against hemibiotrophic pathogen *Phytophthora infestans* requires both ethylene- and salicylic acid-mediated signaling pathways. *Molecular Plant-Microbe Interactions*, 23(9):1130–1142, 2010. doi: 10.1094/MPMI-23-9-1130.

Shimada, Y., Nakano-Shimada, R., Ohbayashi, M., Okinaka, Y., Kiyokawa, S., and Kikuchi, Y. Expression of chimeric P450 genes encoding flavonoid-3′,5′-hydroxylase in transgenic tobacco and petunia plants. *FEBS Letters*, 461(3):241–245, 1999. doi: 10.1016/S0014-5793(99)01425-8.

Shindo, T., Misas-Villamil, J., Hörger, A., Song, J., and van der Hoorn, R. A role in immunity for Arabidopsis cysteine protease RD21, the ortholog of the tomato immune protease C14. *PLoS ONE*, 7(1):e29317, 2012. doi: 10.1371/journal.pone.0029317.

Silva, S. Aluminium toxicity targets in plants. *Journal of Botany*, 2012:219462, 2012. doi: 10.1155/2012/219462.

Simko, I., Atallah, A., Ochoa, O., Antonise, R., Galeano, C., Truco, M., and Michelmore, R. Identification of QTLs conferring resistance to downy mildew in legacy cultivars of lettuce. *Scientific Reports*, 3:2875, 2013.

Singh, D., Kumar, T., Gupta, V., and Chaturvedi, P. Antimicobial activity of some promising plant oils, molecules and formulations. *Indian Journal of Experimental Biology*, 50(10):714–717, 2012.

Sitaraman, J., Bui, M., and Liu, Z. *LEUNIG_HOMOLOG* and *LEUNIG* perform partially redundant functions during Arabidopsis embryo and floral development. *Plant Physiology*, 147(2):672–681, 2008. doi: 10.1104/pp.108.115923.

Smirnov, O., Kosyan, A., Kosyk, O., and Taran, N. Response of phenolic metabolism induced by aluminium toxicity in *Fagopyrum esculentum* Moench. plants. *Ukrainian Biochemical Journal*, 87(6):129–135, 2015. doi: 10.15407/ubj87.06.129.

Smit, F. and Dubery, I. Cell wall reinforcement in cotton hypocotyls in response to a *Verticillium dahliae* elicitor. *Phytochemistry*, 44(5):811–815, 1997. doi: 10.1016/S0031-9422(96)00595-X.

Smith, A., Pinkard, E., Hunter, G., Wingfield, M., and Mohammed, C. Anatomical variation and defence responses of juvenile *Eucalyptus nitens* leaves to *Mycosphaerella* leaf disease. *Australasian Plant Pathology*, 35(6):725–731, 2006.

Smith, P. and Atkins, C. Purine biosynthesis. Big in cell division, even bigger in nitrogen assimilation. *Plant Physiology*, 128(3):793–802, 2002. doi: 10.1104/pp.010912.

Sniezko, R. and Koch, J. Breeding trees resistant to insects and diseases: putting theory into application. *Biological Invasions*, 19(11):3377–3400, 2017. doi: 10.1007/s10530-017-1482-5.

Soanes, D., Chakrabarti, A., Paszkiewicz, K., Dawe, A., and Talbot, N. Genome-wide transcriptional profiling of appressorium development by the rice blast fungus *Magnaporthe oryzae*. *PLoS Pathogens*, 8(2):e1002514, 2012. doi: 10.1371/journal.ppat.1002514.

Søegaard, B. Resistance tests against infection by *Didymascella* thujina (Durand) Maire in *Thuja plicata* Lamb. In *8th International Congress in Botany*, pages 120–122, Paris, 1954.

Søegaard, B. Leaf Blight Resistance in *Thuja*: Experiments on Resistance to Attack by *Didymascella thujina* (Dur.) Maire (*Keithia thujina*) on *Thuja plicata* Lamb. In Veterinary, R. and College, A., editors, *Royal Veterinary and Agricultural College Yearbook*, pages 30–48, Copenhagen, 1956.

Søegaard, B. Variation and Inheritance of Resistance to Attack by *Didymascella thujina* in Western Red Cedar and Related Species. In Gerhold, H., Schreiner, E., McDermott, R., and Winieski, J., editors, *Breeding Pest-Resistant Trees*, pages 83–87, The Pennsylvania State University, University Park, Pennsylvania, August 30 to September 11, 1964 1966. N.A.T.O. and N.S.F. Advanced Study Institute on Genetic Improvement for Disease and Insect Resistance of Forest Trees, Pergamon Press Ltd.

Søegaard, B. Resistensundersøgelse hos *Thuja*. *Særtryk af Det forstlige Forsøgsvæsen i Danmark beretning nr. 245*, 31(3):279–398, 1969.

Sonah, H., Deshmukh, R., and Bélanger, R. Computational prediction of effector proteins in fungi: opportunities and challenges. *Frontiers in Plant Science*, 7:126, feb 2016. doi: 10.3389/fpls.2016.00126.

Song, Y., Cao, M., Xie, L., Liang, X., Zeng, Y., R.S.and Su, Huang, J., Wang, R., and Luo, S. Induction of DIMBOA accumulation and systemic defense responses

as a mechanism of enhanced resistance of mycorrhizal corn (*Zea mays* L.) to sheath blight. *Mycorrhiza*, 21(8):721–731, 2011. doi: 10.1007/s00572-011-0380-4.

Sousa, M., Tavares, R., Gerós, H., and Lino-Neto, T. First report of *Hakea sericea* leaf infection caused by *Pestalotiopsis funerea* in Portugal. *Plant Pathology*, 53(4): 535–535, 2004. doi: 10.1111/j.1365-3059.2004.01042.x.

Spanu, P. The genomics of obligate (and nonobligate) biotrophs. *Annual Review of Phytopathology*, 50(1):91–109, 2012. doi: 10.1146/annurev-phyto-081211-173024.

Spittlehouse, D. and Stewart, R. Adaptation to climate change in forest management. *BC Journal of Ecosystems and Management*, 4(1):1, 2003.

Sridhar, V., Surendrarao, A., Gonzalez, D., Conlan, R., and Liu, Z. Transcriptional repression of target genes by LEUNIG and SEUSS, two interacting regulatory proteins for *Arabidopsis* flower development. *Proceedings of the National Academy of Sciences of The United States of America*, 101(31):11494–11499, 2004. doi: 10.1073/pnas.0403055101.

Srinivasan, K. and Muthumary, J. Taxol production from *Pestalotiopsis* sp an endophytic fungus Isolated from *Catharanthus roseus*. *Journal of Ecobiotechnology*, 1 (1):028–031, 2009.

Stakman, E. Relation between *Puccinia graminis* and plants highly resistant to its attack. *Journal of Agricultural Research*, 4(3):193–200, 1915.

Stein, E., Molitor, A., Kogel, K.-H., and Waller, F. Systemic resistance in *Arabidopsis* conferred by the mycorrhizal fungus *Piriformospora Indica* requires jasmonic acid signaling and the cytoplasmic function of NPR1. *Plant and Cell Physiology*, 49 (11):1747–1751, 2008. doi: 10.1093/pcp/pcn147.

Steinborn, K., Maulbetsch, C., Priester, B., Trautmann, S., Pacher, T., Geiges, B., Küttner, F., Lepiniec, L., Stierhof, Y.-D., Schwarz, H., Jürgens, G., and Mayer, U. The *Arabidopsis PILZ* group genes encode tubulin-folding cofactor orthologs required for cell division but not cell growth. *Genes & Development*, 16(8):959–971, 2002. doi: 10.1101/gad.221702.

Stewart, H. *Cedar: Tree of Life to the Northwest Coast Indians*. Douglas and McIntyre, Vancouver, 1984.

Steyaert, R. Contribution à l'étude monographique de Pestalotia de Not. et Monochaetia Sacc. (Truncatella gen. nov. et Pestalotiopsis gen. nov.). *Bulletin du Jardin botanique de l'État a Bruxelles*, 19(3):285–347, 1949.

Stirling, R., Sturrock, R., and Braybrooks, A. Fungal decay of western redcedar wood products- a review. *International Biodeterioration & Biodegradation*, 125: 105 – 115, 2017. doi: 10.1016/j.ibiod.2017.09.001.

Strobel, G., Li, J., Ford, E., Worapong, J., Baird, G., and Hess, W. *Pestalotiopsis jesteri*, sp. nov. an endophyte from *Fragraea bodenii*, a common plant in the southern highlands of Papua New Guinea. *Mycotaxon*, 76:257–266, 2000.

Sturrock, R., Frankel, S., Brown, A., Hennon, P., Kliejunas, J., Lewis, K., Worrall, J., and Woods, A. Climate change and forest diseases. *Plant Pathology*, 60(1): 133–149, 2011. doi: 10.1111/j.1365-3059.2010.02406.x.

Sudha, G. and Ravishankar, G. Involvement and interaction of various signaling compounds on the plant metabolic events during defense response, resistance to stress factors, formation of secondary metabolites and their molecular aspects. *Plant Cell, Tissue and Organ Culture*, 71(3):181–212, 2002. doi: 10.1023/A:1020336626361.

Sulaiman, C. and Balachandran, I. Total phenolics and total flavonoids in selected Indian medicinal plants. *Indian Journal of Pharmaceutical Sciences*, 74(3):258–260, 2012.

Sun, C., Palmqvist, S., Olsson, H., Borén, M., Ahlandsberg, S., and Jansson, C. A novel WRKY transcription factor, SUSIBA2, participates in sugar signaling in barley by binding to the sugar-responsive elements of the *iso1* promoter. *The Plant Cell*, 15:2076–2092, 2003. doi: 10.1105/tpc.014597.

Sun, C., Höglund, A.-S., Olsson, H., Mangelsen, E., and Jansson, C. Antisense oligodeoxynucleotide inhibition as a potent strategy in plant biology: identification of SUSIBA2 as a transcriptional activator in plant sugar signalling. *The Plant Journal*, 44(1):128–138, 2005. doi: 10.1111/j.1365-313X.2005.02515.x.

Sun, X.-L., Yu, Q.-Y., Tang, L.-L., Ji, W., Bai, X., Cai, H., Liu, X.-F., Ding, X.-D., and Zhu, Y.-M. *GsSRK*, a G-type lectin S-receptor-like serine/threonine protein kinase, is a positive regulator of plant tolerance to salt stress. *Journal of Plant Physiology*, 170(5):505–515, 2013. doi: 10.1016/j.jplph.2012.11.017.

Susi, H. and Laine, A.-L. The effectiveness and costs of pathogen resistance strategies in a perennial plant. *Journal of Ecology*, 103(2):303–315, 2015. doi: 10.1111/1365-2745.12373.

Szwacka, M., Tykarska, T., Wisniewska, A., Kuras, M., Bilski, H., and Malepszy, S. Leaf morphology and anatomy of transgenic cucumber lines tolerant to downy mildew. *Biologia Plantarum*, 53(4):697–701, 2009.

Taiz, L., Zeiger, E., Møller, I., and Murphy, A., editors. *Plant Physiology and Development*. Sinauer Associates, Inc., Publishers, Sunderland, Massachusetts, U.S.A., sixth edition, 2015.

Takagi, I. and Sato, T. A rapid process for embedding plant tissues in Quetol 651 epoxy resin for electron microscopy. *Journal of Electron Microscopy*, 28(2):141–144, 1979.

Talley, S., Coley, P., and Kursar, T. The effects of weather on fungal abundance and richness among 25 communities in the intermountain west. *BMC Ecology*, 2:7, 2002. doi: 10.1186/1472-6785-2-7.

Tang, D., Ade, J., Frye, C., and Innes, R. Regulation of plant defense responses in Arabidopsis by EDR2, a PH and START domain-containing protein. *The Plant Journal*, 44(2):245–257, 2005. doi: 10.1111/j.1365-313X.2005.02523.x.

Taniguti, L., Schaker, P., Benevenuto, J., Peters, L., Carvalho, G., Palhares, A., Quecine, M., Nunes, F., Kmit, M., Wai, A., Hausner, G., Aitken, K., Berkman, P., Fraser, J., Moolhuijzen, P., Coutinho, L., Creste, S., Vieira, M., Kitajima, J., and Monteiro-Vitorello, C. Complete genome sequence of *Sporisorium scitamineum* and biotrophic interaction transcriptome with sugarcane. *PLoS ONE*, 10(6):e0129318, 2015. doi: 10.1371/journal.pone.0129318.

Tariq, M. and Mott, C. The significance of boron in plant nutrition and environment-a review. *Journal of Agronomy*, 6(1):1–10, 2007.

Taylor, R., Herms, D., Cardina, J., and Moore, R. Climate change and pest management: unanticipated consequences of trophic dislocation. *Agronomy*, 8(1):7, 2018.

Teixeira, P., Thomazella, D., Reis, O., do Prado, P., do Rio, M., Fiorin, G., José, J., Costa, G., Negri, V., Mondego, J., Mieczkowski, P., and Pereira, G. High-resolution transcript profiling of the atypical biotrophic interaction between *Theobroma cacao* and the fungal pathogen *Moniliophthora perniciosa*. *The Plant Cell*, 26(11):4245–4269, nov 2014. doi: 10.1105/tpc.114.130807.

Telford, A., Cavers, S., Ennos, R., and Cottrell, J. Can we protect forests by harnessing variation in resistance to pests and pathogens? *Forestry*, 88(1):3–12, 2015. doi: 10.1093/forestry/cpu012.

The Gene Ontology Consortium. Gene Ontology consortium: going forward. *Nucleic Acids Research*, 43(D1):D1049–D1056, 2015.

The UniProt Consortium. UniProt: a hub for protein information. *Nucleic Acids Research*, 43(D1):D204–D212, 2015.

The UniProt Consortium. UniProt: the universal protein knowledgebase. *Nucleic Acids Research*, 45(D1):D158–D169, 2017.

Thordal-Christensen, H., Zhang, Z., Wei, Y., and Collinge, D. Subcellular localization of H_2O_2 in plants. H_2O_2 accumulation in papillae and hypersensitive response during the barley-powdery mildew interaction. *The Plant Journal*, 11(6):1187–1194, 1997. doi: 10.1046/j.1365-313X.1997.11061187.x.

Tichtinsky, G., Vanoosthuyse, V., Cock, J., and Gaude, T. Making inroads into plant receptor kinase signalling pathways. *TRENDS in Plant Science*, 8(5):231–237, may 2003. doi: 10.1016/S1360-1385(03)00062-1.

Tohge, T., Watanabe, M., Hoefgen, R., and Fernie, A. Shikimate and phenylalanine biosynthesis in the green lineage. *Frontiers in Plant Science*, 4:Article 62, 2013. doi: 10.3389/fpls.2013.00062.

Tomlin, E., Antonejevic, E., Alfaro, R., and Borden, J. Changes in volatile terpene and diterpene resin acid composition of resistant and susceptible white spruce leaders exposed to simulated white pine weevil damage. *Tree Physiology*, 20(16): 1087–1095, 2000. doi: 10.1093/treephys/20.16.1087.

Torre, S., Fjeld, T., Gislerød, H., and Moe, R. Leaf anatomy and stomatal morphology of greenhouse roses grown at moderate or high air humidity. *Journal of the American Society for Horticultural Science*, 128(4):598–602, 2003.

Trapnell, C., Williams, B. A., Pertea, G., Mortazavi, A., Kwan, G., van Baren, M. J., Salzberg, S. L., Wold, B. J., and Pachter, L. Transcript assembly and quantification by *RNA*-seq reveals unannotated transcripts and isoform switching during cell differentiation. *Nature Biotechnology*, 28(5):511–515, 2010.

Tremblay, A., Hosseini, P., Alkharouf, N., Li, S., and Matthews, B. Gene expression in leaves of susceptible *Glycine max* during infection with *Phakopsora pachyrhizi* using next generation sequencing. *Sequencing*, 2011:827250, 2011.

Trotter, D., Shrimpton, G., and Kope, H. The Effects of *Keithia* Blight on Outplanting Performance of Western Redcedar Container Seedlings at Two Reforestation Sites in British Columbia-Preliminary Results. In *Proceedings of the Forest Nursery Association of B.C. August 1994*, Moscow, Idaho., 1994.

Tsiri, D., Graikou, K., Pobłocka-Olech, L., Krauze-Baranowska, M., Spyropoulos, C., and Chinou, I. Chemosystematic value of the essential oil composition of *Thuja* species cultivated in Poland-antimicrobial activity. *Molecules*, 14(11):4707–4715, 2009.

Tsuchiya, T. and Eulgem, T. *EMSY-like* genes are required for full *RPP7*-mediated race-specific immunity and basal defense in *Arabidopsis*. *Molecular Plant-Microbe Interactions*, 24(12):1573–1581, 2011.

Tsuwamoto, R., Fukuoka, H., and Takahata, Y. *GASSHO1* and *GASSHO2* encoding a putative leucine-rich repeat transmembrane-type receptor kinase are essential for the normal development of the epidermal surface in Arabidopsis embryos. *The Plant Journal*, 54(1):30–42, 2008. doi: 10.1111/j.1365-313X.2007.03395.x.

Tu, Y., Liu, F., Guo, D., Fan, L., Zhu, Z., Xue, Y., Gao, Y., and Guo, M. Molecular characterization of flavanone 3-hydroxylase gene and flavonoid accumulation in two chemotyped safflower lines in response to methyl jasmonate stimulation. *BMC Plant Biology*, 6:132, 2016. doi: 10.1186/s12870-016-0813-5.

Ulferts, S., Delventhal, R., Splivallo, R., Karlovsky, P., and Schaffrath, U. Abscisic acid negatively interferes with basal defence of barley against *Magnaporthe oryzae*. *BMC Plant Biology*, 15:7, 2015. doi: 10.1186/s12870-014-0409-x.

Uma, B., Rani, T., and Podile, A. Warriors at the gate that never sleep: non-host resistance in plants. *Journal of Plant Physiology*, 168(18):2141–2152, 2011. doi: 10.1016/j.jplph.2011.09.005.

Underwood, W., Melotto, M., and He, S. Role of plant stomata in bacterial invasion. *Cellular Microbiology*, 9(7):1621–1629, 2007. doi: 10.1111/j.1462-5822.2007.00938.x.

van Loon, L. Occurence and Properties of Plant Pathogenesis-Related Proteins. In Datta, S. and Muthukrishnan, S., editors, *Pathogenesis-Related Proteins in Plants*, pages 1–19, Boca Raton, FL., 1999. CRC Press.

van Loon, L. and van Strien, E. The families of pathogenesis-related proteins, their activities, and comparative analysis of PR-1 type proteins. *Physiological and Molecular Plant Pathology*, 55(2):85–97, aug 1999. doi: 10.1006/pmpp.1999.0213.

van Loon, L., Pierpoint, W., Boller, T., and Conejero, V. Recommendations for naming plant pathogenesis-related proteins. *Plant Molecular Biology Reporter*, 12 (3):245–264, sep 1994. doi: 10.1007/BF02668748.

Vance, C., Heichel, G., Barnes, D., Bryan, J., and Johnson, L. Nitrogen fixation, nodule development, and vegetative regrowth of alfalfa (*Medicago sativa* L.) following harvest. *Plant Physiology*, 64(1):1–8, 1979. doi: 10.1104/pp.64.1.1.

Vasse, J., de Billy, F., Camut, S., and Truchet, G. Correlation between ultrastructural differentiation of bacteroids and nitrogen fixation in alfalfa nodules. *Journal of Bacteriology*, 172(8):4295–4306, 1990.

Vegni, G. and Ferro, G. Control of *Didymascella (Keithia) thujina* dieback of *Thuja* with zineb. *Rivista di Patologia Vegetale (Serie III)*, 4(2):171–176, 1964.

Veitch, H. The Coniferæ of Japan. *Journal of the Royal Horticultural Society of London*, XIV:18–33, 1892.

Velazhahan, R., Datta, S., and Muthukrishnan, S. The PR-5 Family: Thaumatin-Like Proteins. In Datta, S. and Muthukrishnan, S., editors, *Pathogenesis-Related Proteins in Plants*, pages 107–129, Boca Raton, FL., 1999. CRC Press.

Vialle, A., Feau, N., Frey, P., Bernier, L., and Hamelin, R. Phylogenetic species recognition reveals host-specific lineages among poplar rust fungi. *Molecular Phylogenetics and Evolution*, 66(3):628–644, 2013. doi: 10.1016/j.ympev.2012.10.021.

Vidhyasekaran, P. *Fungal Pathogenesis in Plants and Crops: Molecular Biology and Host Defense Mechanisms*. Taylor & Francis, second edition, 2008.

Villar, A., Mares, M., Rios, J., Canton, E., and Gobernado, M. Antimicrobial activity of benzylisoquinoline alkaloids. *Pharmazie*, 42(4):248–250, 1987.

Viruega, J., Roca, L., Moral, J., and Trapero, A. Factors affecting infection and disease development on olive leaves inoculated with *Fusicladium oleagineum*. *Plant Disease*, 95(9):1139–1146, 2011. doi: 10.1094/PDIS-02-11-0126.

Voet, D. and Voet, J. *Biochemistry*. John Wiley & Sons, Inc., USA, third edition, 2004.

Voigt, C. Callose-mediated resistance to pathogenic intruders in plant defense-related papillae. *Frontiers in Plant Science*, 5:168, 2014. doi: 10.3389/fpls.2014.00168.

von Rudloff, E. and Lapp, M. Populational variation in the leaf oil terpene composition of western red cedar, *Thuja plicata*. *Canadian Journal of Botany*, 57(5): 476–479, 1979.

von Rudloff, E., Lapp, M., and Yeh, F. Chemosystematic study of *Thuja plicata*: multivariate analysis of leaf oil terpene composition. *Biochemical Systematics and Ecology*, 16(2):119–125, 1988.

Vorwerk, S., Schiff, C., Santamaria, M., Koh, S., Nishimura, M., Vogel, J., Somerville, C., and Somerville, S. *EDR2* negatively regulates salicylic acid-based defenses and cell death during powdery mildew infections of *Arabidopsis thaliana*. *BMC Plant Biology*, 7:35, 2007. doi: 10.1186/1471-2229-7-35.

Vourc'h, G., Martin, J.-L., Duncan, P., Escarré, J., and Clausen, T. Defensive adaptations of *Thuja plicata* to ungulate browsing: a comparative study between mainland and island populations. *Oecologia*, 126(1):84–93, jan 2001. doi: 10.1007/s004420000491.

Vourc'h, G., Russell, J., and Martin, J.-L. Linking deer browsing and terpene production among genetic identities in *Chamaecyparis nootkatensis* and *Thuja plicata* (Cupressaceae). *Journal of Heredity*, 93(5):370–376, 2002.

Wagner, G., Kin, K., and Lynch, V. Measurement of m*RNA* abundance using *RNA*-seq data: RPKM measure is inconsistent among samples. *Theory in Biosciences*, 131(4):281–285, 2012.

Walker, M., Tehseen, M., Doblin, M., Pettolino, F., Wilson, S., Bacic, A., and Golz, J. The transcriptional regulator LEUNIG_HOMOLOG regulates mucilage release from the Arabidopsis testa. *Plant Physiology*, 156(1):46–60, 2011. doi: 10.1104/pp.111.172692.

Wallace, H. *Nematode Ecology and Plant Disease*. Edward Arnold, London, 1973.

Wang, T., Hamann, A., Spittlehouse, D., and Carroll, C. Locally downscaled and spatially customizable climate data for historical and future periods for North America. *PLoS ONE*, 11(6):e0156720, 2016a. doi: 10.1371/journal.pone.0156720.

Wang, T., Wang, Z., Xia, F., and Su, Y. Local adaptation to temperature and precipitation in naturally fragmented populations of *Cephalotaxus oliveri*, an endangered conifer endemic to China. *Scientific Reports*, 6:25031, 2016b.

Wang, Y., Nowak, G., Culley, D., Hadwiger, L., and Fristensky, B. Constitutive expression of pea defense gene *DRR206* confers resistance to blackleg (*Leptosphaeria maculans*) disease in transgenic canola (*Brassica napus*). *Molecular Plant-Microbe Interactions*, 12(5):410–418, 1999.

Wang, Y., Bouchabke-Coussa, O., Lebris, P., Antelme, S., Soulhat, C., Gineau, E., Dalmais, M., Bendahmane, A., Morin, H., Mouille, G., Legée, F., Cézard, L., Lapierre, C., and Sibout, R. LACCASE5 is required for lignification of the *Brachypodium distachyon* culm. *Plant Physiology*, 168(1):192–204, 2015. ISSN 0032-0889.

Wang, Y.-N., Tang, L., Hou, Y., Wang, P., Yang, H., and Wei, C.-L. Differential transcriptome analysis of leaves of tea plant (*Camellia sinensis*) provides comprehensive insights into the defense responses to *Ectropis oblique* attack using RNA-seq [sic]. *Functional & Integrative Genomics*, 16(4):383–398, 2016c.

Weaver, A. and Wiebe, E. School-Based Weather Station Network, 2016. URL `http://www.victoriaweather.ca`.

Wei, J., Xu, T., Guo, L., Liu, A., Zhang, Y., and Pan, X. Endophytic *Pestalotiopsis* species associated with plants of *Podocarpaceae*, *Theaceae* and *Taxaceae* in southern China. *Fungal Diversity*, 24:55–74, 2007.

Weir, J. *Keithia thujina*. The cause of a serious leaf disease of western red cedar. *Phytopathology*, 6:360–363, 1916.

Welz, H. and Geiger, H. Genes for resistance to northern corn leaf blight in diverse maize populations. *Plant Breeding*, 119(1):1–14, 2000. doi: 10.1046/j.1439-0523.2000.00462.x.

Wen, Z., Berenbaum, M., and Schuler, M. Inhibition of CYP6B1-mediated detoxification of xanthotoxin by plant allelochemicals in the black swallowtail (*Papilio polyxenes*). *Journal of Chemical Ecology*, 32(3):507–522, 2006.

Werner, A. and Witte, C.-P. The biochemistry of nitrogen mobilization: purine ring catabolism. *Trends in Plant Science*, 16(7):381–387, 2011. doi: 10.1016/j.tplants.2011.03.012.

Westerink, N., Joosten, M., and de Wit, P. Fungal (A)Virulence Factors at the Crossroads of Disease Susceptibility and Resistance. In Punja, Z., editor, *Fungal Disease Resistance in Plants: Biochemistry, Molecular Biology, and Genetic Engineering*, pages 93–137. Food Products Press, 2004.

Westermann, A., Gorski, S., and Vogel, J. Dual RNA-seq of pathogen and host. *Nature Reviews Microbiology*, 10:618–630, 2012.

Western Red Cedar Export Association. Western Red Cedar and it's uses. Technical report, Western Red Cedar Export Association, Vancouver, BC, 2004.

Wetzel, S., Demmers, C., and Greenwood, J. S. Seasonally fluctuating bark proteins are a potential form of nitrogen storage in three temperate hardwoods. *Planta*, 178 (3):275–281, 1989. doi: 10.1007/BF00391854.

White, T., Adams, W., and Neale, D. *Forest Genetics*. CABI Publishing, Wallingford (Oxfordshire, UK), 2007.

Wiik, L. and Ewaldz, T. Impact of temperature and precipitation on yield and plant diseases of winter wheat in southern Sweden 1983-2007. *Crop Protection*, 28(11): 952–962, 2009. doi: 10.1016/j.cropro.2009.05.002.

Wilcox, P., Amerson, H., Kuhlman, E., Liu, B.-H., O'Malley, D., and Sederoff, R. Detection of a major gene for resistance to fusiform rust disease in loblolly pine by genomic mapping. *Proceedings of the National Academy of Sciences of The United States of America*, 93(9):3859–3864, 1996. doi: 10.1073/pnas.93.9.3859.

Williams, C. *Conifer Reproductive Biology*. Springer Netherlands, 2009.

Williams, R., Spencer, J., and Rice-Evans, C. Flavonoids: antioxidants or signalling molecules? *Free Radical Biology & Medicine*, 36(7):838–849, 2004. doi: 10.1016/j.freeradbiomed.2004.01.001.

Wink, M. Evolution of secondary metabolites in legumes (Fabaceae). *South African Journal of Botany*, 89:164–175, 2013. doi: 10.1016/j.sajb.2013.06.006.

Wittstock, U. and Gershenzon, J. Constitutive plant toxins and their role in defense against herbivores and pathogens. *Current Opinion in Plant Biology*, 5(4):300–307, 2002. doi: 10.1016/S1369-5266(02)00264-9.

Wojtasik, W., Kulma, A., Dymińska, L., Hanuz, J., Czemplik, M., and Szopa, J. Evaluation of the significance of cell wall polymers in flax infected with a pathogenic strain of *Fusarium oxysporum*. *BMC Plant Biology*, 16:75, 2016. doi: 10.1186/s12870-016-0762-z.

Woods, A., Martín-García, J., Bulman, L., Vasconcelos, M., Boberg, J., Porta, N. L., Peredo, H., Vergara, G., Ahumada, R., Brown, A., and Diez, J. Dothistroma needle blight, weather and possible climatic triggers for the disease's recent emergence. *Forest Pathology*, 46(5):443–452, jan 2016. doi: 10.1111/efp.12248.

Wright, E., Rivera, M., and Flynn, M. First report of *Pestalotiopsis guepini* and *Glomerella cingulata* on blueberry in Buenos Aires (Argentina). *EPPO Bulletin*, 28(1-2):219–220, 1998. doi: 10.1111/j.1365-2338.1998.tb00725.x.

Wu, H., Ying, C., and Muir, J. Effect of geographic variation and jack pine introgression on disease and insect resistance in lodgepole pine. *Canadian Journal of Forest Research*, 26(5):711–726, 1996.

Xu, L., Zhu, L., Tu, L., Liu, L., Yuan, D., Jin, L., Long, L., and Zhang., X. Lignin metabolism has a central role in the resistance of cotton to the wilt fungus *Verticillium dahliae* as revealed by RNA-seq-dependent transcriptional analysis and histochemistry. *Journal of Experimental Botany*, 62(15):5607–5621, 2011.

Ye, D.-Y., Qi, Y.-H., Cao, S.-F., Wei, B.-Q., and Zhang, H.-S. Histopathology combined with transcriptome analyses reveals the mechanism of resistance to *Meloidogyne incognita* in *Cucumis metuliferus*. *Journal of Plant Physiology*, 212:115–124, 2017. doi: 10.1016/j.jplph.2017.02.002.

Yeats, T. and Rose, J. The formation and function of plant cuticles. *Plant Physiology*, 163(1):5–20, 2013. doi: 10.1104/pp.113.222737.

Yeh, F. Isozyme variation of *Thuja plicata* (Cupressaceae) in British Columbia. *Biochemical Systematics and Ecology*, 16(4):373–377, 1988.

Yeh, Y.-H., Chang, Y.-H., Huang, P.-Y., Huang, J.-B., and Zimmerli, L. Enhanced Arabidopsis pattern-triggered immunity by overexpression of cysteine-rich receptor-like kinases. *Frontiers in Plant Science*, 6:322, 2015. doi: 10.3389/fpls.2015.00322.

Yoshida, K. Histology of current shoots of Japanese cedar (*Cryptomeria japonica* D. Don) inoculated with *Cercospora sequoiae* Ellis & Everhart. *Journal of Forest Research*, 3(1):49–53, 1998.

Yoshikuni, Y., Martin, V., Ferrin, T., and Keasling, J. Engineering cotton (+)-δ-cadinene synthase to an altered function: germacrene D-4-ol synthase. *Chemistry & Biology*, 13(1):91–98, 2006. doi: 10.1016/j.chembiol.2005.10.016.

Young, N. QTL mapping and quantitative disease resistance in plants. *Annual Review of Phytopathology*, 34:479–501, 1996. doi: 10.1146/annurev.phyto.34.1.479.

Yu, K., Gong, B., Lee, M., Liu, Z., Xu, J., Perkins, R., and Tong, W. Discovering functional modules by topic modeling *RNA*-seq based toxicogenomic data. *Chemical Research in Toxicology*, 27(9):1528–1536, 2014. PMID: 25083553.

Yuan, G., Liao, T., Tan, H., Li, Q., and Lin, W. First report of leaf spot caused by *Phoma sorghina* on tobacco in China. *Plant Disease*, 100(8):1790, 2016.

Yuan, J., Huang, L., Zhou, N., Wang, H., and Niu, G. Fractionation of inorganic phosphorus and aluminum in red acidic soil and the growth of *Camellia oleifera*. *HortScience*, 52(9):1293–1297, 2017.

Zahran, H. *Rhizobium*-legume symbiosis and nitrogen fixation under severe conditions and in an arid climate. *Microbiology and Molecular Biology Reviews*, 63(4):968–989, 1999.

Ze-ping, J. and Huo-ran, W. Taxonomy of the Cupressaceae: subfamilies, tribes and genera. *Acta Phytotaxonomica Sinica*, 35(3):236–248, 1997.

Zhang, B. and Horvath, S. A general framework for weighted gene co-expression network analysis. *Statistical Applications in Genetics and Molecular Biology*, 4(1): 17, 2005.

Zhang, J., Zheng, H., Li, Y., Li, H., Liu, X., Qin, H., Dong, L., and Wang, D. Coexpression network analysis of the genes regulated by two types of resistance responses to powdery mildew in wheat. *Scientific Reports*, 6:23805, 2016.

Zhang, J., Klopfenstein, N., and Peterson, G. Genetic variation in disease resistance of *Juniperus virginiana* and *J. scopulorum* grown in eastern Nebraska. *Silvae Genetica*, 46(1):11–16, 1997.

Zhang, X., Han, X., Shi, R., Yang, G., Qi, L., Wang, R., and Li, G. Arabidopsis cysteine-rich receptor-like kinase 45 positively regulates disease resistance to *Pseudomonas syringae*. *Plant Physiology and Biochemistry*, 73(Supplement C):383–391, 2013. doi: 10.1016/j.plaphy.2013.10.024.

Zhang, Y.-M., Tan, N.-H., Lu, Y., Chang, Y., and Jia, R.-R. Chamobtusin A, a novel skeleton diterpenoid alkaloid from *Chamaecyparis obtusa* cv. *tetragon*. *Organic Letters*, 9(22):4579–4581, 2007. doi: 10.1021/ol702087h.

Zhou, M., Hu, Q., Li, Z., Li, D., Chen, C.-F., and Luo, H. Expression of a novel antimicrobial peptide Penaeidin4-1 in creeping bentgrass (*Agrostis stolonifera* L.) enhances plant fungal disease resistance. *PLoS ONE*, 6(9):e24677, 2011. doi: 10.1371/journal.pone.0024677.

Zhu, B. and Coleman, G. Phytochrome-mediated photoperiod perception, shoot growth, glutamine, calcium, and protein phosphorylation influence the activity of the poplar bark storage protein gene promoter (bspA). *Plant Physiology*, 126(1): 342–351, 2001. doi: 10.1104/pp.126.1.342.

Zinsou, V., Wydra, K., Ahohuendo, B., and Schreiber, L. Leaf waxes of cassava (*Manihot esculenta* Crantz) in relation to ecozone and resistance to *Xanthomonas* blight. *Euphytica*, 149(1-2):189–198, 2006.

Züst, T. and Agrawal, A. Trade-offs between plant growth and defense against insect herbivory: an emerging mechanistic synthesis. *Annual Review of Plant Biology*, 68: 513–534, 2017.

Zvereva, A. and Pooggin, M. Silencing and innate immunity in plant defense against viral and non-viral pathogens. *Viruses*, 4(11):2578–2597, 2012.

Zyprian, E., Ochßner, I., Schwander, F., Šimon, S., Hausmann, L., Bonow-Rex, M., Moreno-Sanz, P., Grando, M. S., Wiedemann-Merdinoglu, S., Merdinoglu, D., Eibach, R., and Töpfer, R. Quantitative trait loci affecting pathogen resistance and ripening of grapevines. *Molecular Genetics and Genomics*, 291(4):1573–1594, 2016.